NEUTRALIZING ANTIBODIES IN THE PREVENTION AND TREATMENT OF COVID-19

EDITED BY: Peter Chen and Raymund Razonable
PUBLISHED IN: Frontiers in Immunology

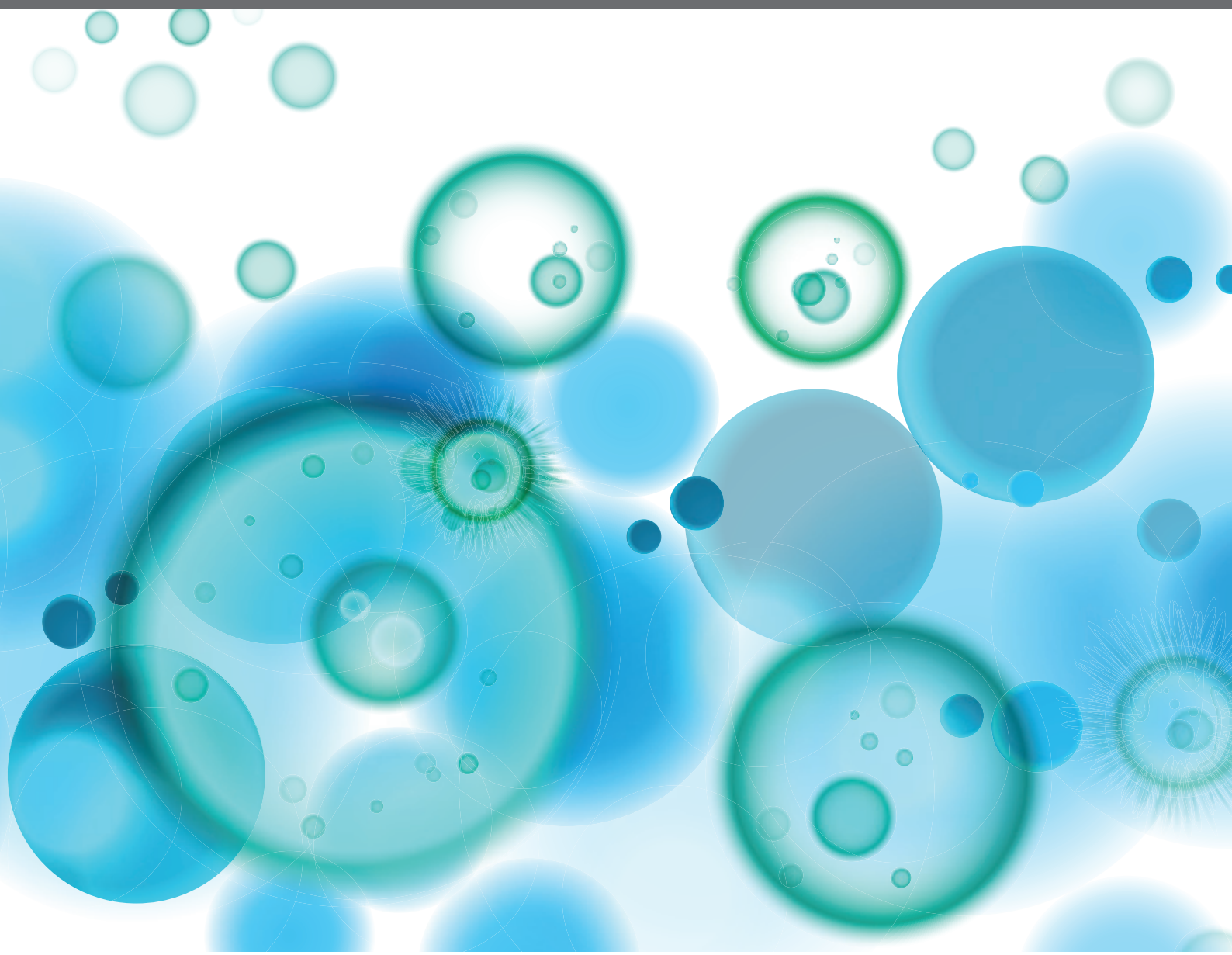

frontiers Research Topics

ISSN 1664-8714
ISBN 978-2-88976-429-7
DOI 10.3389/978-2-88976-429-7

About Frontiers

Frontiers is more than just an open-access publisher of scholarly articles: it is a pioneering approach to the world of academia, radically improving the way scholarly research is managed. The grand vision of Frontiers is a world where all people have an equal opportunity to seek, share and generate knowledge. Frontiers provides immediate and permanent online open access to all its publications, but this alone is not enough to realize our grand goals.

Frontiers Journal Series

The Frontiers Journal Series is a multi-tier and interdisciplinary set of open-access, online journals, promising a paradigm shift from the current review, selection and dissemination processes in academic publishing. All Frontiers journals are driven by researchers for researchers; therefore, they constitute a service to the scholarly community. At the same time, the Frontiers Journal Series operates on a revolutionary invention, the tiered publishing system, initially addressing specific communities of scholars, and gradually climbing up to broader public understanding, thus serving the interests of the lay society, too.

Dedication to Quality

Each Frontiers article is a landmark of the highest quality, thanks to genuinely collaborative interactions between authors and review editors, who include some of the world's best academicians. Research must be certified by peers before entering a stream of knowledge that may eventually reach the public - and shape society; therefore, Frontiers only applies the most rigorous and unbiased reviews.
Frontiers revolutionizes research publishing by freely delivering the most outstanding research, evaluated with no bias from both the academic and social point of view. By applying the most advanced information technologies, Frontiers is catapulting scholarly publishing into a new generation.

What are Frontiers Research Topics?

Frontiers Research Topics are very popular trademarks of the Frontiers Journals Series: they are collections of at least ten articles, all centered on a particular subject. With their unique mix of varied contributions from Original Research to Review Articles, Frontiers Research Topics unify the most influential researchers, the latest key findings and historical advances in a hot research area! Find out more on how to host your own Frontiers Research Topic or contribute to one as an author by contacting the Frontiers Editorial Office: frontiersin.org/about/contact

NEUTRALIZING ANTIBODIES IN THE PREVENTION AND TREATMENT OF COVID-19

Topic Editors:
Peter Chen, Department of Medicine, Cedars-Sinai Medical Center, United States
Raymund Razonable, Mayo Clinic, United States

Citation: Chen, P., Razonable, R., eds. (2022). Neutralizing Antibodies in the Prevention and Treatment of COVID-19. Lausanne: Frontiers Media SA.
doi: 10.3389/978-2-88976-429-7

Table of Contents

05 ***Editorial: Neutralizing Antibodies in the Prevention and Treatment of COVID-19***
Raymund R. Razonable and Peter Chen

07 ***Use of Outpatient-Derived COVID-19 Convalescent Plasma in COVID-19 Patients Before Seroconversion***
Oliver F. Wirz, Katharina Röltgen, Bryan A. Stevens, Suchitra Pandey, Malaya K. Sahoo, Lorna Tolentino, Michelle Verghese, Khoa Nguyen, Molly Hunter, Theo Thomas Snow, Abhay Raj Singh, Catherine A. Blish, Jennifer R. Cochran, James L. Zehnder, Kari C. Nadeau, Benjamin A. Pinsky, Tho D. Pham and Scott D. Boyd

16 ***Sensitivity of SARS-CoV-2 Variants to Neutralization by Convalescent Sera and a VH3-30 Monoclonal Antibody***
Shuai Yue, Zhirong Li, Yao Lin, Yang Yang, Mengqi Yuan, Zhiwei Pan, Li Hu, Leiqiong Gao, Jing Zhou, Jianfang Tang, Yifei Wang, Qin Tian, Yaxing Hao, Juan Wang, Qizhao Huang, Lifan Xu, Bo Zhu, Pinghuang Liu, Kai Deng, Li Wang, Lilin Ye and Xiangyu Chen

23 ***SARS-CoV-2 mRNA Vaccines Elicit Different Responses in Immunologically Naïve and Pre-Immune Humans***
David Forgacs, Hyesun Jang, Rodrigo B. Abreu, Hannah B. Hanley, Jasper L. Gattiker, Alexandria M. Jefferson and Ted M. Ross

33 ***Isolation and Characterization of Mouse Monoclonal Antibodies That Neutralize SARS-CoV-2 and Its Variants of Concern Alpha, Beta, Gamma and Delta by Binding Conformational Epitopes of Glycosylated RBD With High Potency***
Sabrina Mariotti, Antonio Capocefalo, Maria Vincenza Chiantore, Angelo Iacobino, Raffaela Teloni, Maria Laura De Angelis, Alessandra Gallinaro, Maria Franca Pirillo, Martina Borghi, Andrea Canitano, Zuleika Michelini, Melissa Baggieri, Antonella Marchi, Paola Bucci, Paul F. McKay, Chiara Acchioni, Silvia Sandini, Marco Sgarbanti, Fabio Tosini, Antonio Di Virgilio, Giulietta Venturi, Francesco Marino, Valeria Esposito, Paola Di Bonito, Fabio Magurano, Andrea Cara, Donatella Negri and Roberto Nisini

49 ***Rapid Assessment of Binding Affinity of SARS-COV-2 Spike Protein to the Human Angiotensin-Converting Enzyme 2 Receptor and to Neutralizing Biomolecules Based on Computer Simulations***
Damiano Buratto, Abhishek Saxena, Qun Ji, Guang Yang, Sergio Pantano and Francesco Zonta

61 ***Effectiveness of Regdanvimab Treatment in High-Risk COVID-19 Patients to Prevent Progression to Severe Disease***
Ji Yeon Lee, Jee Young Lee, Jae-Hoon Ko, Miri Hyun, Hyun Ah Kim, Seongcheol Cho, Yong Dae Lee, Junghoon Song, Seunghwan Shin and Kyong Ran Peck

70 ***The Global Epidemic of the SARS-CoV-2 Delta Variant, Key Spike Mutations and Immune Escape***
Dandan Tian, Yanhong Sun, Jianming Zhou and Qing Ye

77 ***Endogenous Antibody Responses to SARS-CoV-2 in Patients With Mild or Moderate COVID-19 Who Received Bamlanivimab Alone or Bamlanivimab and Etesevimab Together***
Lin Zhang, Josh Poorbaugh, Michael Dougan, Peter Chen, Robert L. Gottlieb, Gregory Huhn, Stephanie Beasley, Montanea Daniels, Thi Ngoc Vy Trinh, Melissa Crisp, Joshua Joaquin Freitas, Peter Vaillancourt, Dipak R. Patel, Ajay Nirula, Nicole L. Kallewaard, Richard E. Higgs and Robert J. Benschop

87 ***A Potent and Protective Human Neutralizing Antibody Against SARS-CoV-2 Variants***
Sisi Shan, Chee Keng Mok, Shuyuan Zhang, Jun Lan, Jizhou Li, Ziqing Yang, Ruoke Wang, Lin Cheng, Mengqi Fang, Zhen Qin Aw, Jinfang Yu, Qi Zhang, Xuanling Shi, Tong Zhang, Zheng Zhang, Jianbin Wang, Xinquan Wang, Justin Jang Hann Chu and Linqi Zhang

101 ***Convalescent Plasma Treatment in Patients With Covid-19: A Systematic Review and Meta-Analysis***
Anselm Jorda, Manuel Kussmann, Nebu Kolenchery, Jolanta M. Siller-Matula, Markus Zeitlinger, Bernd Jilma and Georg Gelbenegger

110 ***Is Better Standardization of Therapeutic Antibody Quality in Emerging Diseases Epidemics Possible?***
Sanda Ravlić, Ana Hećimović, Tihana Kurtović, Jelena Ivančić Jelečki, Dubravko Forčić, Anamarija Slović, Ivan Christian Kurolt, Željka Mačak Šafranko, Tatjana Mušlin, Dina Rnjak, Ozren Jakšić, Ena Sorić, Gorana Džepina, Oktavija Đaković Rode, Kristina Kujavec Šljivac, Tomislav Vuk, Irena Jukić, Alemka Markotić and Beata Halassy

122 ***Single-Domain Antibodies Efficiently Neutralize SARS-CoV-2 Variants of Concern***
Irina A. Favorskaya, Dmitry V. Shcheblyakov, Ilias B. Esmagambetov, Inna V. Dolzhikova, Irina A. Alekseeva, Anastasia I. Korobkova, Daria V. Voronina, Ekaterina I. Ryabova, Artem A. Derkaev, Anna V. Kovyrshina, Anna A. Iliukhina, Andrey G. Botikov, Olga L. Voronina, Daria A. Egorova, Olga V. Zubkova, Natalia N. Ryzhova, Ekaterina I. Aksenova, Marina S. Kunda, Denis Y. Logunov, Boris S. Naroditsky and Alexandr L. Gintsburg

131 ***Considerations for the Feasibility of Neutralizing Antibodies as a Surrogate Endpoint for COVID-19 Vaccines***
Jianyang Liu, Qunying Mao, Xing Wu, Qian He, Lianlian Bian, Yu Bai, Zhongfang Wang, Qian Wang, Jialu Zhang, Zhenglun Liang and Miao Xu

145 ***Humoral Immune Response Diversity to Different COVID-19 Vaccines: Implications for the "Green Pass" Policy***
Immacolata Polvere, Alfredina Parrella, Lucrezia Zerillo, Serena Voccola, Gaetano Cardinale, Silvia D'Andrea, Jessica Raffaella Madera, Romania Stilo, Pasquale Vito and Tiziana Zotti

frontiers | Frontiers in Immunology

EDITORIAL
published: 31 May 2022
doi: 10.3389/fimmu.2022.938069

Editorial: Neutralizing Antibodies in the Prevention and Treatment of COVID-19

Raymund R. Razonable[1] *and Peter Chen*[2*]

[1] Division of Public Health, Infectious Diseases and Occupational Medicine, Department of Medicine, Mayo Clinic, Rochester, MN, United States, [2] Department of Medicine, Women's Guild Lung Institute, Cedars-Sinai Medical Center, Los Angeles, CA, United States

Keywords: SARS – CoV – 2, neutralizing antibodies, COVID-19 vaccines, COVID-19 Therapeutics, Convalescent plasma (CP) therapy

Editorial on the Topic

Neutralizing Antibodies in the Prevention and Treatment of COVID-19

The COVID-19 therapeutic landscape rapidly evolved throughout the course of the SARS-CoV-2 pandemic. However, the ingenuity of our community quickly coalesced to identify novel ways to combat this deadly disease. One prime example is the infusion of anti-SARS-CoV-2 neutralizing antibodies as passive immunity to treat high-risk COVID-19 patients who are vulnerable to severe outcomes. Initially, convalescent plasma obtained from volunteers who have recovered from SARS-CoV-2 infections was used as a potential therapy for COVID-19 patients. Next, the rapid development of anti-SARS-CoV-2 monoclonal antibodies was added to our COVID-19 therapeutic armamentarium and was a stunning example of how contemporary technology can lead to discovery and validations of novel therapeutics. Neutralizing antibodies also play a key role in the immunity conferred by SARS-CoV-2 vaccines. Indeed, COVID-19 vaccination stimulates the production of high titers of neutralizing antibodies, which largely mediates the effect of infection prevention. Unfortunately, RNA viruses, such as SARS-CoV-2, are prone to mutations, and accordingly, SARS-CoV-2 variants have emerged that have developed resistance to neutralizing antibody therapies. As such, continued is needed to identify, develop and improve neutralizing antibodies in prevention and treatment of COVID-19. This Topic is a collection of pertinent studies that contribute to our understanding of the benefits of neutralizing antibody therapies in COVID-19 and develops tools for their improvement.

Convalescent plasma gained traction as a therapy for SARS-CoV-2 infections in the early days of the pandemic. The concept was that neutralizing antibodies in the plasma of individuals who have recovered from COVID-19 could be passively transferred to newly-infected individuals to reduce their viral load and alter the course of the infection towards clinical improvement and recovery. Initial retrospective cohort studies suggested benefit with the infusion of high-titer convalescent plasma particularly when given early in the hospital course. Subsequently, data from randomized controlled trials emerged as the pandemic progressed that muddled the support for its use as a therapy for those infected with SARS-CoV-2. Indeed, the meta-analysis by Jorda et al. finds that convalescent plasma had no benefit as a therapy in COVID-19. This conclusion was also reached by the NIH and IDSA (Infectious Disease Society of America) who do not recommend giving convalescent plasma to hospitalized COVID-19 patients. However, the US FDA currently continues to allow for the use of high titer convalescent plasma under emergency use

OPEN ACCESS

Edited and reviewed by:
Denise L. Doolan, James Cook University, Australia

***Correspondence:**
Peter Chen
peter.chen@cshs.org

Specialty section:
This article was submitted to Vaccines and Molecular Therapeutics, a section of the journal Frontiers in Immunology

Received: *06 May 2022*
Accepted: *11 May 2022*
Published: *31 May 2022*

Citation:
Razonable RR and Chen P (2022) Editorial: Neutralizing Antibodies in the Prevention and Treatment of COVID-19. Front. Immunol. 13:938069. doi: 10.3389/fimmu.2022.938069

authorization (EUA) for immunocompromised patients *early* in the course for COVID-19, even in the outpatient setting. Wirz et al. provides insight to the benefits of early use of convalescent plasma into patients infected with SARS-CoV-2; Only patients transfused before seroconversion, which *de facto* equates to early in the disease course, had demonstratable increase in plasma anti-SARS-CoV-2 antibody levels. Additionally, Yue et al. found the neutralizing ability of convalescent plasma is attenuated if collected prior to the emergence of variants of concern and is another consideration when choosing this treatment modality.

Monoclonal antibodies (mAb), another treatment from the passive transfer of neutralizing antibodies, were the next iteration of SARS-CoV-2 therapies that first obtained FDA EUA in November 2020. Lee et al. provide evidence for Regdanvimab as a mAb treatment to prevent progression to severe disease in high-risk patients. In the US, the FDA had granted emergency use authorizations for bamlanivimab, bamlanivimab-etesevimab, casirivimab-indevimab, sotrovimab, and bebtelovimab at various time points. However, their longevity has been short-lived because of the emergence of SARS-CoV-2 variants of concern (VOC) with mutations of the spike protein at the binding epitope can lead to resistance (Yue et al. and Tian et al.) Thus, the work by Shan et al. that identified a mAb that binds a conserved epitope in the receptor binding domain of the spike protein on the SARS-CoV-2 virus is pertinent due to the ability to potentially resist new VOCs that may emerge. Favorskaya et al. develop dimeric molecules that potently neutralize SARS-CoV-2 and decreases the chance of resistance to VOCs. Moreover, Mariotti et al. present a murine model to isolate and characterize mAbs that could help identify future mAbs for therapeutics and diagnostics. Additionally, Buratto et al. developed an *in silico* method to identify the binding affinity of the ACE2 receptor to the spike protein providing a platform to study SARS-CoV-2 mutations and help future development of neutralizing antibodies. A theoretical concern for mAbs was that treatment in SARS-CoV-2 infections would suppress the natural immunity from infection, but the findings of Zhang et al. dispelled this notion by showing sufficient maturation of anti-SARS-CoV-2 humoral immunity despite mAb treatment.

Finally, the development of vaccinations was another major breakthrough in our COVID-19 fight. Interestingly, Forgacs et al. show that the SARS-CoV-2 infection behaves as an antigenic boost that can augment the immunogenic response after COVID-19 vaccinations. The protective effect is largely mediated by the production of neutralizing antibodies, but several of the papers in this Topic discuss the need for standardized methods to evaluate efficacy that may not be fully represented by neutralizing antibody levels (Liu et al., Ravlić et al., Polvere et al.). The articles in this Topic highlights the collective efforts of our scientists around the world in developing antibody-based therapies for the prevention and treatment of COVID-19.

AUTHOR CONTRIBUTIONS

All authors listed have made a substantial, direct, and intellectual contribution to the work and approved it for publication.

FUNDING

This work was supported by R01HL155759 (PC), R01HL137076 (PC), and an intramural grant at Mayo Clinic (RR).

Conflict of Interest: Topic Editor RR received grants from Regeneron, Gilead, and Roche, for research purposes. Topic Editors PC received grants from Regeneron, Gilead, and Eli Lilly.

Publisher's Note: All claims expressed in this article are solely those of the authors and do not necessarily represent those of their affiliated organizations, or those of the publisher, the editors and the reviewers. Any product that may be evaluated in this article, or claim that may be made by its manufacturer, is not guaranteed or endorsed by the publisher.

frontiers in Immunology

ORIGINAL RESEARCH
published: 14 September 2021
doi: 10.3389/fimmu.2021.739037

Use of Outpatient-Derived COVID-19 Convalescent Plasma in COVID-19 Patients Before Seroconversion

Oliver F. Wirz[1], Katharina Röltgen[1], Bryan A. Stevens[1], Suchitra Pandey[1,2], Malaya K. Sahoo[1], Lorna Tolentino[2], Michelle Verghese[1], Khoa Nguyen[1], Molly Hunter[3], Theo Thomas Snow[4], Abhay Raj Singh[4], Catherine A. Blish[5,6], Jennifer R. Cochran[7], James L. Zehnder[1], Kari C. Nadeau[4,8], Benjamin A. Pinsky[1,5], Tho D. Pham[1,2†] and Scott D. Boyd[1,4*†]*

[1] Department of Pathology, Stanford University School of Medicine, Stanford, CA, United States, [2] Stanford Blood Center, Palo Alto, CA, United States, [3] ATUM, Newark, CA, United States, [4] Sean N. Parker Center for Allergy and Asthma Research, Stanford, CA, United States, [5] Department of Medicine, Division of Infectious Diseases and Geographic Medicine, Stanford University, Stanford, CA, United States, [6] Chan Zuckerberg Biohub, San Francisco, CA, United States, [7] Department of Bioengineering, Stanford University, Stanford, CA, United States, [8] Department of Medicine, Division of Pulmonary, Allergy and Critical Care Medicine, Stanford University, Stanford, CA, United States

OPEN ACCESS

Edited by:
Raymund Razonable,
Mayo Clinic, United States

Reviewed by:
Eizo Takashima,
Ehime University, Japan
Dapeng Zhou,
Tongji University, China

***Correspondence:**
Scott D. Boyd
sboyd1@stanford.edu
Tho D. Pham
thopham@stanford.edu

†These authors have contributed equally to this work

Specialty section:
This article was submitted to Vaccines and Molecular Therapeutics, a section of the journal Frontiers in Immunology

Received: 09 July 2021
Accepted: 24 August 2021
Published: 14 September 2021

Citation:
Wirz OF, Röltgen K, Stevens BA, Pandey S, Sahoo MK, Tolentino L, Verghese M, Nguyen K, Hunter M, Snow TT, Singh AR, Blish CA, Cochran JR, Zehnder JL, Nadeau KC, Pinsky BA, Pham TD and Boyd SD (2021) Use of Outpatient-Derived COVID-19 Convalescent Plasma in COVID-19 Patients Before Seroconversion. Front. Immunol. 12:739037. doi: 10.3389/fimmu.2021.739037

Background: Transfusion of COVID-19 convalescent plasma (CCP) containing high titers of anti-SARS-CoV-2 antibodies serves as therapy for COVID-19 patients. Transfusions early during disease course was found to be beneficial. Lessons from the SARS-CoV-2 pandemic could inform early responses to future pandemics and may continue to be relevant in lower resource settings. We sought to identify factors correlating to high antibody titers in convalescent plasma donors and understand the magnitude and pharmacokinetic time course of both transfused antibody titers and the endogenous antibody titers in transfused recipients.

Methods: Plasma samples were collected up to 174 days after convalescence from 93 CCP donors with mild disease, and from 16 COVID-19 patients before and after transfusion. Using ELISA, anti-SARS-CoV-2 Spike RBD, S1, and N-protein antibodies, as well as capacity of antibodies to block ACE2 from binding to RBD was measured in an *in vitro* assay. As an estimate for viral load, viral RNA and N-protein plasma levels were assessed in COVID-19 patients.

Results: Anti-SARS-CoV-2 antibody levels and RBD-ACE2 blocking capacity were highest within the first 60 days after symptom resolution and markedly decreased after 120 days. Highest antibody titers were found in CCP donors that experienced fever. Effect of transfused CCP was detectable in COVID-19 patients who received high-titer CCP and had not seroconverted at the time of transfusion. Decrease in viral RNA was seen in two of these patients.

Conclusion: Our results suggest that high titer CCP should be collected within 60 days after recovery from donors with past fever. The much lower titers conferred by transfused antibodies compared to endogenous production in the patient underscore the importance of providing CCP prior to endogenous seroconversion.

Keywords: SARS-CoV-2, COVID-19, convalescent plasma for COVID-19 therapy, humoral immune response, antiviral antibodies

HIGHLIGHTS

High-titer convalescent plasma can be collected from low-severity outpatients with history of fever and typically within 60 days after symptom cessation. High-titer convalescent plasma should be adminstered to COVID-19 patients before endogenous seroconversion occurs.

INTRODUCTION

The COVID-19 pandemic is exacting a terrible toll on societies and health systems worldwide. Transfusion of COVID-19 convalescent plasma (CCP) containing anti-SARS-CoV-2 antibodies may have therapeutic benefit for COVID-19 patients until more efficacious therapeutics are widely available. CCP is also used as a source for purifying SARS-CoV-2-specific immunoglobulins for more standardized antibody treatment regimens (e.g. anti-coronavirus hyperimmune intravenous immunoglobulin). In the United States, vaccines and therapeutic monoclonal antibodies have been given emergency use authorization by the Food and Drug Administration (FDA), but logistical and financial limitations may limit the use of these interventions, especially in low- and middle-income countries, favoring the continued use of patient-derived antibody-based therapies such as CCP. It is therefore crucial to assess the magnitude and stability of serological responses in CCP donors and define an ideal timeframe for CCP donation. While some studies show SARS-CoV-2-specific B cells and detectable levels of SARS-CoV-2-specific antibodies for several months after infection (1–3), others have shown that antibody levels begin to decrease as early as one month after symptom onset, especially in less severely ill outpatients (4, 5). Although CCP efficacy in all COVID-19 patients is equivocal (6–8), recent studies suggest that high-titer CCP administered to patients early in disease course may be protective (9–12), a practice also recently recommended by the FDA (13). Since the majority of SARS-CoV-2-infected individuals, and hence also potential CCP donors, are mildly ill outpatients, we have sought to determine the patient characteristics associated with higher antibody titers in these individuals. Prior studies have lacked detailed time course data for analyzing the kinetics of antibodies derived from CCP in recipients, and for comparing the therapeutic antibody quantities to those derived from the patient's own humoral immune response early during the disease course, to better understand the potential benefits of early transfusion.

METHODS

Clinical Specimens

Venipuncture blood samples from 93 COVID-19 convalescent plasma (CCP) donors from the San Francisco Bay Area in California who donated CCP at Stanford Blood Center from 4/14/2020 to 8/25/2020, as well as from 16 COVID-19 patients admitted to Stanford Hospital were collected in sodium heparin- or K_2EDTA-coated vacutainers and plasma was used for serology testing, N-antigenemia testing, and rRT-PCR detection of RNAemia. Plasma samples were stored at 4°C (short-term) or -80°C (long-term). For three transfused COVID-19 patients, the sampling timepoints were not ideal to assess whether the transfused CCP influenced the recipient's plasma antibody levels (shown in **Supplementary Figure 1**). Retrospective chart review was performed on all COVID-19 patients admitted to Stanford Hospital. This study was approved by the Stanford University Institutional Review Board (Protocols IRB-48973, IRB-55689, and IRB-13952). All patients were transfused CCP as a part of the National Convalescent Plasma Expanded Access Protocol sponsored by the Mayo Clinic and approved by the Stanford University Institutional Review Board (Protocol IRB-56100).

ELISA to Detect Anti-SARS-CoV-2 Antibodies in Plasma Samples

The ELISA protocol used in the present study was described by Röltgen et al. (4). In brief, ELISA plates were coated with SARS-CoV-2 spike RBD, S1, or N protein at a concentration of 0.1 μg per well (0.025 μg per well for the N protein IgG assay). Plasma samples from CCP donors and COVID-19 patients were incubated at a dilution of 1:100 for 1 hour. Anti-SARS-CoV-2 IgA, IgG, and IgM antibodies were detected using HRP (horseradish peroxidase) conjugated goat anti-human IgG (γ-chain specific, catalog no. 62-8420, Thermo Fisher, 1:5,000 dilution), IgM (μ-chain specific, catalog no. A6907, Sigma, 1:5,000 dilution), or IgA (α-chain specific, catalog no. P0216, Agilent, 1:2,000 dilution). Development was done using 3,3′,5,5′-Tetramethylbenzidine (TMB) substrate and optical density (OD) at 450 nm was measured with a microplate reader and blank values were subtracted from values obtained for plasma samples. Seroconversion for each isotype/protein assay was defined as values above mean ELISA ODs of 94 negative control samples from healthy blood donors collected before the pandemic plus three times their standard deviation (mean + 3 SD). All samples were tested twice in independent experiments.

Competition ELISA to Detect Antibodies That Block Binding of ACE2 to RBD

The protocol for the competition ELISA procedure used here was recently described by Röltgen et al. (4) In brief, plates were coated with SARS-CoV-2 spike RBD protein and then incubated with plasma samples at a dilution of 1:10 for 1 hour at room temperature. Then, recombinant ACE2 joined to a mouse IgG2a Fc (ACE2-mFc) at 0.5 µg/mL was added to the plasma sample for another 45 minutes. After washing, RBD-ACE2-mFc was detected using horseradish peroxidase conjugated anti-mouse IgG. ELISA plates were developed and measured as described above. A positive and a negative quality control (Access SARS-CoV-2 IgG QC, QC1-QC2, catalog no. C58964, Beckman Coulter) was included on each plate. OD values were converted to '*% ACE2 blocking*' using the following formula: *% ACE2 blocking* = 100*(1-(sample OD - 0.2)/(QC1 OD – 0.2)), taking into account the background noise of the assay of 0.2 which was determined by testing negative control plasma samples that were collected before the pandemic. All samples were tested two times in independent experiments.

Real-Time PCR for Detection of SARS-CoV-2 RNA in Plasma Samples

The protocol for detection of SARS-CoV-2 RNA in plasma was performed based on a published rRT-PCR assay targeting the envelope (*E*) gene (14, 15). RNA was isolated from 400 µL of EDTA-anticoagulated plasma using Qiagen EZ1 Virus Mini Kit v2.0 (Qiagen German-town, MD). Ct values of positive tests with this assay normally range from Ct <20 to 45 cycles. Testing of plasma samples with a Ct value of 40 or higher were tested again to ensure reproducibility of the positive result. No viral culture was performed as part of this study, therefore, presence of SARS-CoV-2 in tested plasma was defined as RNAemia.

Antigen Detection

SARS-CoV-2 nucleocapsid antigen was quantified using S-PLEX Direct Detection Assay, S-PLEX SARS-CoV-2 N Kit (Catalog #K150ADHS, Meso Scale Discovery [MSD], Rockville, MD), according to manufacturer's protocol. Raw signal was converted to a concentration based on linear regression to the 7-point calibration curve. Cut off for positivity was calculated as the mean value of 40 pre-pandemic plasma samples plus three times the standard deviation.

Statistics

GraphPad Prism version 8.4.1 software (GraphPad Software, San Diego, California, USA) was used to visualize data, analyze for differences in antibody responses and N-antigenemia levels between different timepoints to carry out linear regression of % RBD-ACE2 blocking and antibody titers. Ordinary one-way ANOVA test and Kruskal-Wallis test with Dunn's multiple comparison test was used to compare more than two groups when samples either followed, or did not follow Gaussian distribution, respectively. Unpaired t-test was used to compare IgG levels and % RBD-ACE2 blocking in samples from symptom positive *versus* negative patients, while no correction for multiple comparison was performed. Goodness of fit for linear regression analyses was reported as the coefficient of determination (R2). Correlation between antibody OD450 values, RNAemia, and RBD-ACE2 blocking assay OD450 values were calculated as Spearman correlations with the R cor function. Two-sided tests with $p<0.05$ were considered as statistically significant.

RESULTS

Time After Recovery and Symptoms Correlate to Humoral Immune Response in Mildly Ill COVID-19 Convalescent Plasma Donors

We studied the SARS-CoV-2-specific humoral immune response in 172 CCP samples collected from 93 non-hospitalized outpatients (**Table 1**). In contrast to earlier studies (4, 5), samples were collected up to 174 days after convalescence. We measured IgM, IgA, and IgG levels in the plasma of these donors against the SARS-CoV-2 Spike S1 region, receptor binding domain (RBD) and nucleocapsid antigen (N) using laboratory-developed ELISAs. Anti-RBD titers decreased with time after symptom cessation (**Figure 1A**). Antibody levels were highest in CCP donations collected within two months after symptom resolution and were markedly decreased after 120 days (**Figure 1B**). Similarly, antibody titers waned with time for anti-S1 (**Supplementary Figure 2**). Analysis of individual donors with four or more donation timepoints clearly revealed that antibody signals consistently decreased over time (**Supplementary Figure 3**).

Viral spike RBD interaction with human angiotensin-converting enzyme 2 (ACE2) initiates SARS-CoV-2 entry into host cells. We performed an RBD-ACE2 blocking ELISA to measure the functional activity of plasma antibodies to block RBD-ACE2 interaction. CCP donor anti-RBD IgG levels were positively correlated to RBD-ACE2 blocking capacity and all

TABLE 1 | Non-hospitalized CCP donor demographics and clinical characteristics.

Characteristics		n = 93
Age, median (IQR)		48 (35-56)
Sex	Female	28 (30.1%)
	Male	65 (69.9%)
Symptom, N of individuals (% present)	Fever	70 (75.3 %)
	Cough	55 (59.1 %)
	Body ache	36 (38.7 %)
	Lethargy/Tiredness/Fatigue	29 (31.2 %)
	Loss of smell/taste	20 (21.5 %)
	Headache	19 (20.4 %)
	Dyspnea	18 (19.4 %)
Number of timepoints, N of individuals (% present)	1 timepoint	55 (59.1%)
	2 timepoints	18 (19.4%)
	3 timepoints	8 (8.6%)
	4 timepoints	8 (8.6%)
	>4 timepoints	4 (4.3%)

CCP, COVID-19 convalescent plasma; IQR, interquartile range. The 12 samples from six hospitalized CCP donors, as well as three samples from donors with no symptom description, were excluded.

samples with titers of at least 1:1600 exhibited RBD-ACE2 blocking activity, while only a subset of samples with lower titers showed RBD-ACE2 blocking activity (**Figure 1C**). We also measured anti-RBD IgM and IgA titers, which showed weaker correlations to RBD-ACE2 blocking (**Figures 1D, E**). Similarly, RBD-ACE2 blocking capacity was significantly higher in CCP samples collected within 60 days post symptom (**Figure 1F**). Together, this further emphasized the importance of CCP donations early after recovery.

Identifying CCP donor factors associated with high antibody titers would contribute to more efficient donor recruitment strategies. We therefore explored whether certain symptoms reported in our cohort of mildly ill outpatients (**Table 1**) correlated with anti-RBD IgG levels (**Figure 1G**) and

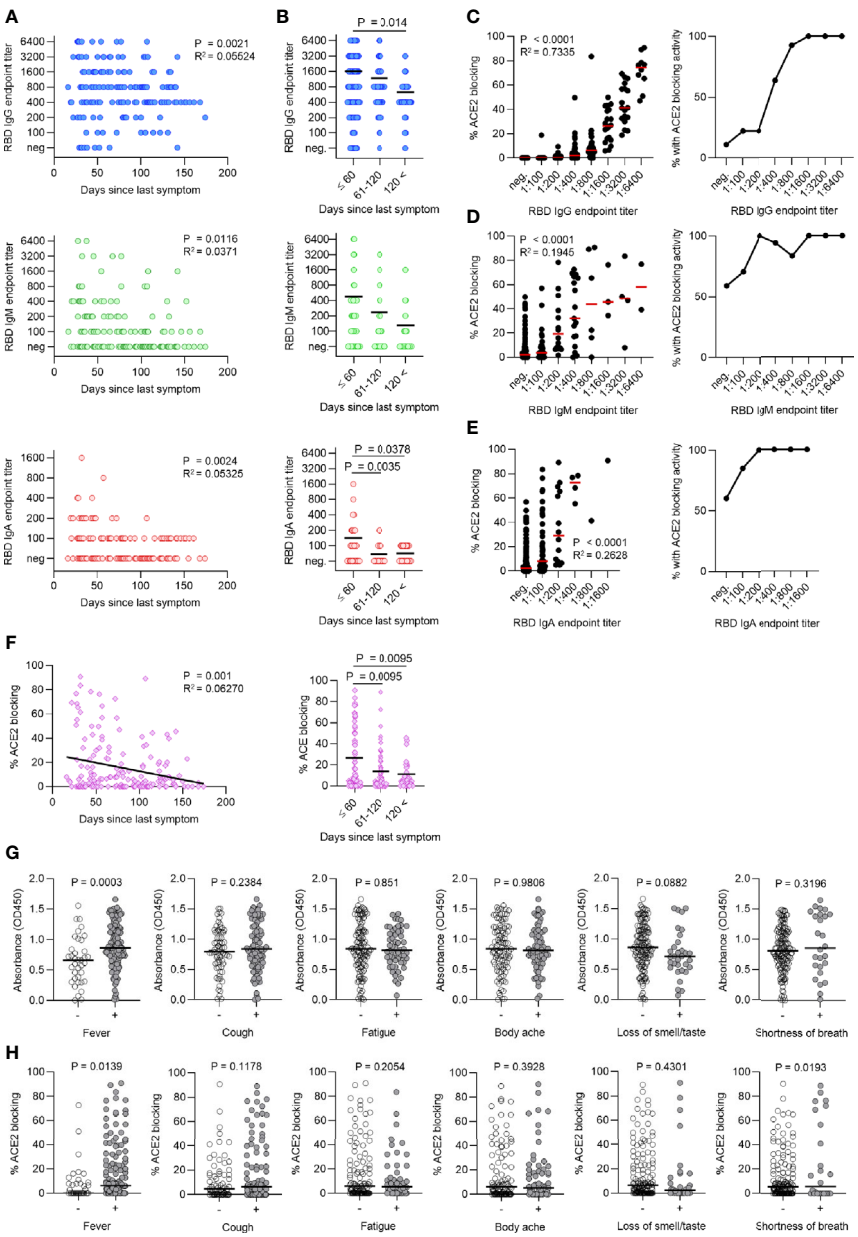

FIGURE 1 | Time after recovery and symptoms correlate to humoral immune response in mildly ill COVID-19 convalescent plasma donors. **(A)** Titers of SARS-CoV-2 RBD-specific IgG, IgM, and IgA in the plasma of 93 COVID-convalescent plasma (CCP) donors (172 individual samples) decrease over time after symptom cessation. **(B)** Antibody titers begin to decrease after 120 days. **(C–E)** Titers of IgG **(C)**, IgM **(D)**, and IgA **(E)** were correlated to RBD-ACE2 blocking activity (in %, left panel). The percentage of cases with any detectable RBD-ACE2 blocking activity is shown for each titer (right panel). **(F)** RBD-ACE2 blocking capacity (in %) over time shown for all cases (left panel) and separated in bins of 60 days (right panel). **(G, H)** Comparison of RBD-specific IgG titers **(G)** (Absorbance, OD450) and RBD-ACE2 blocking activity **(H)** in symptom positive *versus* negative cases for most common reported symptoms.

TABLE 2 | Demographics and clinical characteristics of 16 CCP-treated COVID-19 patients.

Characteristics		Admitted, non-ICU (n = 4)	Admitted, ICU (n = 8)	Admitted, ICU, Deceased (n = 4)
Patient number		1, 13, 15, 16	4, 7, 8, 9, 10, 11, 12, 14	2, 3, 5, 6
Age, mean		49	51	61
Sex (%)	Female	3 (75)	2 (25)	1 (25)
	Male	1 (25)	6 (75)	3 (75)
Symptom, N of individuals (% present)	Dyspnea	3 (75)	6 (75)	2 (50)
	Fever	2 (50)	5 (62.5)	2 (50)
	Cough	3 (75)	2 (25)	3 (75)
	GI	3 (75)	3 (37.5)	1 (25)
	Myalgia	2 (50)	2 (25)	1 (25)
	Chills	2 (50)	1 (12.5)	1 (25)
	Fatigue	0 (0)	1 (12.5)	1 (25)
	Confusion	0 (0)	2 (25)	0 (0)
	Headache	1 (25)	0 (0)	0 (0)
Comorbidities, N of individuals (% present)	Obesity	2 (50)	4 (50)	1 (25)
	Diabetes mellitus	2 (50)	4 (50)	3 (75)
	Hypertension	1 (25)	5 (62.5)	4 (100)
	Asthma	1 (25)	2 (25)	0 (0)
Mechanical ventilation (%)		0 (0)	4 (50)	4 (100)
Admission, days post symptoms, mean		5	4	7
Length of hospital stay, mean		13	29	38
CCP therapy, days post symptoms, mean		7	8	8
Seroconverted before CCP therapy, N of individuals (%)		2 (50)	6 (75)	4 (100)

CCP, COVID-19 convalescent plasma; ICU, intensive care unit.

RBD-ACE2 blocking capacity (**Figure 1H**). Interestingly, fever was the only symptom that distinguished CCP donors with higher levels of anti-RBD IgG and RBD-ACE2 blocking activity (**Figures 1G, H**). Similarly, increased anti-S1 and anti-N IgG antibodies were found in patients with fever (data not shown).

SARS-CoV-2-Specific Antibody Levels, Viral N-Antigenemia and RNAemia in COVID-19 Patients Before and After Convalescent Plasma Therapy

Several reports showed the benefits of CCP transfusions at early times during the disease course for patients infected with SARS-CoV-2 (9–12, 16), likely because CCP was transfused before these patients seroconverted. We therefore aimed to understand the patients' immune response at the time of transfusion, analyze potential immediate biological effect of CCP transfusions, and compare these to the endogenous response. To address this, we measured anti-SARS-CoV-2 antibodies, RBD-ACE2 blocking functional antibody levels, viral RNAemia and N-antigenemia in a group of 16 COVID-19 inpatients prior to CCP transfusion and daily for up to one week thereafter (Patient information, **Table 2**). Increases in antibody levels one day after CCP transfusion were observed in four COVID-19 patients who had not yet seroconverted and who received CCP units with high levels of specific IgG antibodies (**Figure 2A**). Anti-RBD IgG antibody titer increased immediately after the transfusion, followed by a plateau or slight decrease; we attribute this serological response to the CCP transfusion.

In contrast, CCP was transfused in nine patients either near the timepoint of anti-RBD IgG seroconversion (**Figure 2B**), or who already developed high antibody titers and RBD-ACE2 blocking activity (**Figure 2C**). Here, it is difficult to separate the serological effect of the transfused CCP from the patients' own response. For three patients, the sampling timepoints were not suitable to assess whether the transfused CCP influenced the recipient's plasma antibody levels (**Supplementary Figure 1**). Similar results were found when we measured titers of antibodies specific for Spike S1 region and N-antigen in these patients (**Supplementary Figure 4**). With the plasma dilution used in our experiment, two patients reached maximal RBD-ACE2 blocking activity between one and two weeks after symptom onset, as a result of their own serological response.

With the aim to assess an effect of the transfused plasma, N-antigen and viral RNA levels in the blood were measured to estimate viral load. N-antigenemia was found in 93.75% (15/16) and RNAemia in 75% (12/16) of patients (**Figure 2**, **Supplementary Figure 1**). Inversely correlating with their serological responses, N-antigenemia and RNAemia were reduced in all patients over the course of their illness (**Figure 2**, **Supplementary Figure 1**). Interestingly, two patients (1 and 14) who received CCP before seroconversion showed reduced RNAemia immediately following CCP transfusion (**Figure 2A**), potentially supporting efficacy of early CCP administration. Over the course of the study period, N-antigenemia was becoming undetectable for 40% (6/15) of the patients while RNAemia resolved in 75% (9/12) of previously positive patients. The persistence of low levels of declining viral RNA and protein in the blood of seroconverted patients could be due to the antibodies not yet having achieved the concentrations needed to fully bind and opsonize the remaining viral proteins in the body. Antibody titers negatively correlated to N-antigen levels in these patients (**Supplementary Figure 5A**) and level of N-antigen at timepoint of transfusion distinguished hospitalized patients where CCP was given before seroconversion (**Supplementary Figure 5B**).

DISCUSSION

Here, we studied the immune response to SARS-CoV-2 infection in mildly ill outpatients that donated COVID-19 convalescent plasma (CCP). High titer plasma important for transfusion was mainly found within 60 days after symptom cessation and in patients that had fever. Furthermore, we analyzed whether transfused CCP can be detected and has a direct effect on viral antigens and viral RNA levels in 16 hospitalized COVID-19 patients. An effect was found only in those individuals that did not seroconvert yet.

Logistical and financial limitations may still limit the use of vaccines and therapeutic monoclonal antibodies, especially in low- and middle-income countries, favoring the continued use of patient-derived antibody-based therapies such as CCP. Here, we aimed to identify donor factors associated with high antibody titers to improve CCP donor recruitment strategies. For this,

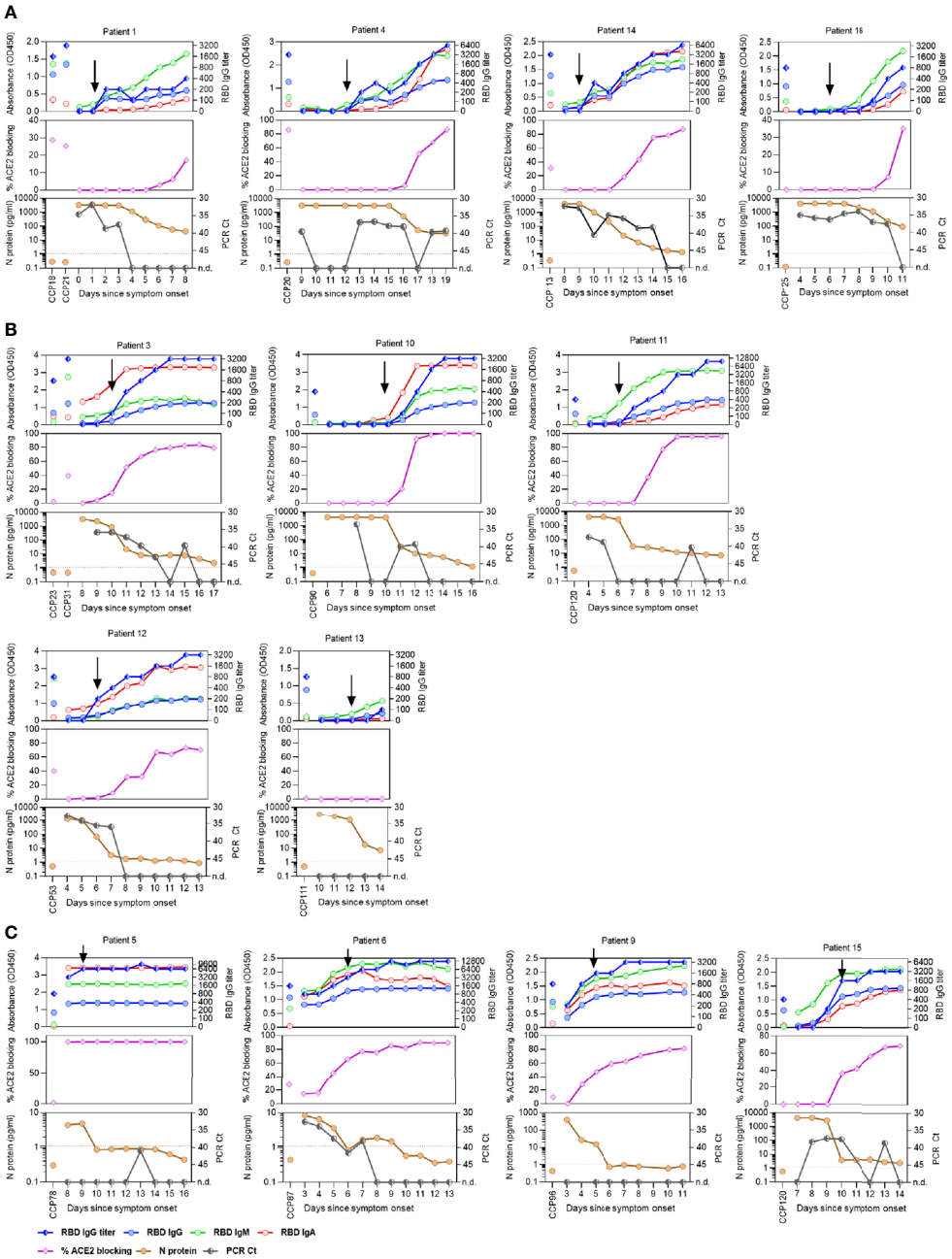

FIGURE 2 | SARS-CoV-2-specific antibody titers, viral N-antigenemia and RNAemia in COVID-19 patients before and after convalescent plasma therapy. Absorbance level of SARS-CoV-2 RBD-specific IgG, IgM, and IgA (1:100 diluted plasma samples), titer of RBD-specific IgG, ACE2 blocking activity (in %), as well as levels of N-antigenemia, and RNAemia are shown for patients that received COVID-19 convalescent plasma (CCP) before **(A)**, during **(B)**, or after seroconversion **(C)**. Timepoints of CCP transfusion are indicated by black arrows.

we first assessed titers of SARS-CoV-2 Spike-RBD, -S1, and N-specific antibodies in relation to symptom cessation.

Antibody titers continuously waned after symptoms ended with most marked decrease after 120 days. Our data indicated that CCP collected within 60 days after symptom resolution is most likely to maximize antibody levels for transfusion. While we studied mildly ill outpatient which make up the majority of SARS-CoV-2 infected individuals and hence potential blood donors, a similar timeframe for collecting high titer plasma was also suggested for more severely ill patients (17). In addition, we also measured the functional activity of antibodies to block RBD-ACE2 interaction. Results from the here used RBD-ACE2 blocking assay closely correlate with a SARS-CoV-2 pseudotyped virus neutralization assay (4). RBD-ACE2 blocking

activity was found in all plasma units with an anti-RBD IgG titer of at least 1:1600. This is concordant with a recent study where similar IgG titers were associated with efficient virus neutralization (5). Since anti-RBD antibodies of IgM and IgA isotypes showed weaker correlation to RBD-ACE2 blocking activity, we concluded that anti-RBD IgG titers were the best correlate for virus-neutralizing activity.

In our donor cohort consisting of mildly ill outpatients, we found that fever was the only symptom correlating to higher antibody levels. While dyspnea was relatively rare among our studied cohort (19.4%), a recent study including CCP donors that were more severely ill found increased antibody levels among patients with dyspnea (5).

Several trials have studied the benefit of high titer CCP transfusions on COVID-19 outcome with median duration of symptoms at day of transfusion ranging from 3 to 30 days (10, 18–20). The importance of transfusions at early times during the disease course has been noted for patients infected with SARS-CoV-2 (9–12, 16), and also for SARS-CoV (21). The benefits from CCP transfusion are likely to be greatest for patients who have not yet seroconverted, if the patient's endogenous neutralizing antibody response is greater in magnitude than the transfused antibody quantity. It is therefore critically important to understand the patients' immune response at the time of transfusion, analyze the immediate biological effect of CCP transfusions, and compare these to the endogenous response. Sampling COVID-19 patients before and daily up to one week after the CCP transfusion allowed to detect transfused antibodies in four of the studied COVID-19 patients that did not seroconvert yet. At later times afterwards, a rapid increase in antibody levels was seen, very likely reflecting the patients' own endogenous antibody production and seroconversion. At the same time when we observed the endogenous antibody increase, N-antigenemia and RNAemia resolved in most patients. While the four patients who received CCP before seroconversion recovered from COVID-19, our analysis was not designed to evaluate the efficacy of CCP transfusions. These findings, however, are in line with previous studies showing reduced fatal disease outcomes when CCP was administered early after symptom onset and before seroconversion (10, 11, 16, 21). In contrast, little clinical effect was seen when CCP was transfused more than 14 days after symptom onset (12, 18, 22, 23), likely because at this timepoint the patients already seroconverted with high antibody levels (4). The data are consistent with a role for early CCP administration as a bridging therapy until the patient mounts their own humoral immune response. Standardized serological testing, as opposed to temporal assessment of symptomatology, would be a more mechanistically supported approach to determine patient eligibility for CCP administration.

Limitations of this study include the relatively low number of CCP-treated COVID-19 patients and non-seroconverted patients at time of transfusion. Because most patients seroconvert during infection, the small volume of a unit of CCP (200-300 ml) compared to total plasma volume of patients make it difficult to detect increases in specific antibodies after transfusion in seroconverted patients. We note that we studied outpatient CCP donors, who may have had lower antibody levels compared to inpatients (4).

In this study, we demonstrated that anti-SARS-CoV-2 antibody levels and RBD-ACE2 blocking ability in plasma from outpatient donors were highest within the first two months after symptom resolution, strongly favoring CCP collection early after donor recovery. Donors who had fever during infection had elevated anti-SARS-CoV-2 antibody levels; this criterion may help CCP donor outreach strategies to identify donors with high antibody levels. We showed that increased antibody levels after CCP transfusion were only detected in patients who had not seroconverted at the time of administration, providing a mechanistic basis that could explain why the clinical benefit of CCP therapy appears to be greatest in recipients who are treated soon after symptom onset. In our view, transfusion prior to the patient's own seroconversion should be considered the relevant clinical goal, informed by rapid serological testing in evaluating the potential benefit of convalescent plasma transfusion in individual patients. This study was performed before the widespread occurrence of viral variants. As new variants continue to emerge, the inter- and intra-strain effectiveness of CCP transfusion should be assessed. Further efforts should be directed at studying the efficacy of CCP administration in COVID-19 patients who have already seroconverted but are still early in the disease course. Use of CCP in immunocompromised patients warrants further study, as this group may stand to benefit the most from the treatment (24, 25).

DATA AVAILABILITY STATEMENT

The original contributions presented in the study are included in the article/**Supplementary Material**. Further inquiries can be directed to the corresponding authors.

ETHICS STATEMENT

The studies involving human participants were reviewed and approved by Stanford University Institutional Review Board. Written informed consent for participation was not required for this study in accordance with the national legislation and the institutional requirements.

AUTHOR CONTRIBUTIONS

OW, TP, and SB conceptualized and designed the study. OW, KR, MS, MV, and KN performed the experiments. OW, KR, BS, SP, MS, LT, MV, KN, TS, and AS collected data and/or contributed samples/reagents or EHR processing methods. CB, JC, JZ, KN, and BP provided intellectual contributions throughout the study. OW and TP performed statistical analyses. OW, TP, and SB analyzed the data. OW, KR, TP, and SB wrote the manuscript. All authors contributed to the article and approved the submitted version.

FUNDING

This work was supported by NIH/NIAID R01AI127877 (SB), NIH/NIAID R01AI130398 (SB), NIH 1U54CA260517 (SB), an endowment to S.D.B. from the Crown Family Foundation, an Early Postdoc. Mobility Fellowship Stipend to OW from the Swiss National Science Foundation (SNSF), and a Coulter COVID-19 Rapid Response Award to JC and SB. This work was also supported by MesoScale Diagnostics (MSD), who provided the S-PLEX SARS-CoV-2 N Kits, BioTek 405 Select automated 96-well plate washer, and MESO® SECTOR S 600 Reader used in this study. MSD had no role in study design, data collection and analysis, decision to publish, or preparation of the manuscript.

ACKNOWLEDGMENTS

The authors thank Dana Anderson for helpful advice about protein production, and the ATUM Bio team for optimization, production and providing of antigens.

SUPPLEMENTARY MATERIAL

The Supplementary Material for this article can be found online at: https://www.frontiersin.org/articles/10.3389/fimmu.2021.739037/full#supplementary-material

Supplementary Figure 1 | Measurements in three additional COVID-19 patients. Titers of SARS-CoV-2 RBD-specific IgG, IgM, and IgA, RBD-specific IgG titers, RBD-ACE2 blocking activity (in %), as well as levels of N-antigenemia, and RNAemia are shown for three patients for whom available sample timepoints were not suitable to assess whether the patients had seroconverted before CCP transfusion. Timepoint(s) of CCP transfusion are indicated by black arrows.

Supplementary Figure 2 | Titers of SARS-CoV-2 RBD-specific, S1-specific and N-specific IgG, IgM, and IgA antibodies. Titers of SARS-CoV-2 RBD-specific, S1-specific and N-specific IgG, IgM, and IgA antibodies (Absorbance at OD450) plotted *versus* timepoint post symptom cessation.

Supplementary Figure 3 | Titers of SARS-CoV-2 RBD-specific, S1-specific and N-specific IgG, IgM, and IgA antibodies for individual donors with multiple timepoints. Titers of SARS-CoV-2 RBD-specific, S1-specific and N-specific IgG, IgM, and IgA antibodies (Absorbance at OD450) plotted versus timepoint post symptom cessation for a selection of donors with > 3 samples.

Supplementary Figure 4 | SARS-CoV-2 S1/N-specific antibody titers in COVID-19 patients who received convalescent plasma. Levels of SARS-CoV-2 S1/N-specific IgG, IgM, and IgA antibodies (Absorbance at OD450) are shown for patients who received COVID-convalescent plasma (CCP) before **(A)**, during **(B)**, or after seroconversion **(C)**. **(D)** Shows three patients for whom available sample timepoints were not suitable to assess if patients already seroconverted before CCP transfusion. Timepoint(s) of CCP transfusion indicated by black arrow.

Supplementary Figure 5 | N-antigenemia levels negatively correlate with developing immune response. **(A)** Viral N-antigenemia levels for all samples from COVID-19 patients correlated with (from left to right) RBD-specific IgG titers, RBD-specific IgG Absorbance OD450, N-specific IgG Absorbance OD450, and RBD-ACE2 blocking capacity. Reduced N-antigenemia in samples correlated with developing immune response. **(B)** Levels of N-antigenemia in collected plasma from COVID-19 patients distinguished patients that received CCP before, during or after seroconversion.

REFERENCES

1. Wajnberg A, Amanat F, Firpo A, Altman DR, Bailey MJ, Mansour M, et al. Robust Neutralizing Antibodies to SARS-CoV-2 Infection Persist for Months. *Science* (2020) 370(6521):1227–30. doi: 10.1126/science.abd7728
2. Dan JM, Mateus J, Kato Y, Hastie KM, Yu ED, Faliti CE, et al. Immunological Memory to SARS-CoV-2 Assessed for Up to 8 Months After Infection. *Science* (2021) 371(6529):eabf4063. doi: 10.1126/science.abf4063
3. Ogega CO, Skinner NE, Blair PW, Park HS, Littlefield K, Ganesan A, et al. Durable SARS-CoV-2 B Cell Immunity After Mild or Severe Disease. *J Clin Invest* (2021) 131(7):e145516. doi: 10.1172/JCI145516
4. Röltgen K, Powell AE, Wirz OF, Stevens BA, Hogan CA, Najeeb J, et al. Defining the Features and Duration of Antibody Responses to SARS-CoV-2 Infection Associated With Disease Severity and Outcome. *Sci Immunol* (2020) 5: eabe0240. doi: 10.1126/sciimmunol.abe0240
5. Salazar E, Kuchipudi SV, Christensen PA, Eagar T, Yi X, Zhao P, et al. Convalescent Plasma Anti-SARS-CoV-2 Spike Protein Ectodomain and Receptor-Binding Domain Igg Correlate With Virus Neutralization. *J Clin Invest* (2020) 130:6728–38. doi: 10.1172/JCI141206
6. Casadevall A, Joyner MJ, Pirofski L-A. A Randomized Trial of Convalescent Plasma for COVID-19 - Potentially Hopeful Signals. *JAMA* (2020) 324:455–7. doi: 10.1001/jama.2020.10218
7. Correction to Data in Trial of Convalescent Plasma Treatment for COVID-19. *Jama* (2020) 324:519. doi: 10.1001/jama.2020.13216
8. Gharbharan A, Jordans CCE, Geurtsvankessel C, den Hollander JG, Karim F, Mollema FPN, et al. Effects of potent neutralizing antibodies from convalescent plasma in patients hospitalized for severe SARS-CoV-2 infection. *Nat Commun*. (2021) 12(1):3189. doi: 10.1038/s41467-021-23469-2
9. Salazar E, Christensen PA, Graviss EA, Nguyen DT, Castillo B, Chen J, et al. Significantly Decreased Mortality in a Large Cohort of Coronavirus Disease 2019 (COVID-19) Patients Transfused Early With Convalescent Plasma Containing High-Titer Anti-Severe Acute Respiratory Syndrome Coronavirus 2 (SARS-CoV-2) Spike Protein Igg. *Am J Pathol* (2021) 191:90–107. doi: 10.1016/j.ajpath.2020.10.008
10. Libster R, Pérez Marc G, Wappner D, Coviello S, Bianchi A, Braem V, et al. Early High-Titer Plasma Therapy to Prevent Severe Covid-19 in Older Adults. *N Engl J Med* (2021) 384(7):610–8. doi: 10.1056/NEJMoa2033700
11. Joyner MJ, Senefeld JW, Klassen SA, Mills JR, Johnson PW, Theel ES, et al. Effect of Convalescent Plasma on Mortality Among Hospitalized Patients With COVID-19: Initial Three-Month Experience. *medRxiv* (2020). 2020.08.12.20169359. doi: 10.1101/2020.08.12.20169359
12. Xia X, Li K, Wu L, Wang Z, Zhu M, Huang B, et al. Improved Clinical Symptoms and Mortality Among Patients With Severe or Critical COVID-19 After Convalescent Plasma Transfusion. *Blood* (2020) 136:755–9. doi: 10.1182/blood.2020007079
13. The U.S. Food and Drug Administration (FDA). *EUA Fact Sheet for Health Care Providers COVID-19 Convalescent Plasma* (2021). Available at: https://www.fda.gov/news-events/fda-brief/fda-brief-fda-updates-emergency-use-authorization-covid-19-convalescent-plasma-reflect-new-data (Accessed 18 February 2021).
14. Hogan CA, Sahoo MK, Pinsky BA. Sample Pooling as a Strategy to Detect Community Transmission of SARS-CoV-2. *JAMA* (2020) 323:1967–9. doi: 10.1001/jama.2020.5445
15. Corman VM, Landt O, Kaiser M, Molenkamp R, Meijer A, Chu DK, et al. Detection of 2019 Novel Coronavirus (2019-nCoV) by Real-Time RT-PCR. *Euro Surveill* (2020) 25:2000045. doi: 10.2807/1560-7917.ES.2020.25.3.2000045
16. Hegerova L, Gooley TA, Sweerus KA, Maree C, Bailey N, Bailey M, et al. Use of Convalescent Plasma in Hospitalized Patients With COVID-19: Case Series. *Blood* (2020) 136:759–62. doi: 10.1182/blood.2020006964
17. Gontu A, Srinivasan S, Salazar E, Nair MS, Nissly RH, Greenawalt D, et al. Limited Window for Donation of Convalescent Plasma With High Live-Virus Neutralizing Antibody Titers for COVID-19 Immunotherapy. *Commun Biol* (2021) 4:267. doi: 10.1038/s42003-021-01813-y
18. Li L, Zhang W, Hu Y, Tong X, Zheng S, Yang J, et al. Effect of Convalescent Plasma Therapy on Time to Clinical Improvement in Patients With Severe

and Life-Threatening COVID-19: A Randomized Clinical Trial. *JAMA* (2020) 324:1–11. doi: 10.1001/jama.2020.10044
19. Agarwal A, Mukherjee A, Kumar G, Chatterjee P, Bhatnagar T, Malhotra P. Convalescent Plasma in the Management of Moderate Covid-19 in Adults in India: Open Label Phase II Multicentre Randomised Controlled Trial (PLACID Trial). *BMJ* (2020) 371:m3939. doi: 10.1136/bmj.m3939
20. Simonovich VA, Burgos Pratx LD, Scibona P, Beruto MV, Vallone MG, Vázquez C, et al. A Randomized Trial of Convalescent Plasma in Covid-19 Severe Pneumonia. *N Engl J Med* (2021) 384:619–29. doi: 10.1056/NEJMoa2031304
21. Cheng Y, Wong R, Soo YO, Wong WS, Lee CK, Ng MH, et al. Use of Convalescent Plasma Therapy in SARS Patients in Hong Kong. *Eur J Clin Microbiol Infect Dis* (2005) 24:44–6. doi: 10.1007/s10096-004-1271-9
22. Duan K, Liu B, Li C, Zhang H, Yu T, Qu J, et al. Effectiveness of Convalescent Plasma Therapy in Severe COVID-19 Patients. *Proc Natl Acad Sci USA* (2020) 117:9490–6. doi: 10.1073/pnas.2004168117
23. Zeng QL, Yu ZJ, Gou JJ, Li GM, Ma SH, Zhang GF, et al. Effect of Convalescent Plasma Therapy on Viral Shedding and Survival in Patients With Coronavirus Disease 2019. *J Infect Dis* (2020) 222:38–43. doi: 10.1093/infdis/jiaa228
24. Fung M, Nambiar A, Pandey S, Aldrich JM, Teraoka J, Freise C, et al. Treatment of Immunocompromised COVID-19 Patients With Convalescent Plasma. *Transpl Infect Dis* (2020) 23:e13477. doi: 10.1111/tid.13477
25. Truong TT, Ryutov A, Pandey U, Yee R, Goldberg L, Bhojwani D, et al. Increased Viral Variants in Children and Young Adults With Impaired Humoral Immunity and Persistent SARS-CoV-2 Infection: A Consecutive Case Series. *EBioMedicine* (2021) 67:103355. doi: 10.1016/j.ebiom.2021.103355

Conflict of Interest: SB has consulted for Regeneron, Sanofi, and Novartis on topics unrelated to this study, and owns stock in AbCellera. KN reports grants from National Institute of Allergy and Infectious Diseases (NIAID), Food Allergy Research & Education (FARE), End Allergies Together (EAT); National Heart, Lung, and Blood Institute (NHLBI), and National Institute of Environmental Health Sciences (NIEHS). KN is Director of the FARE and World Allergy Organization (WAO) Center of Excellence at Stanford University; Advisor at Cour Pharmaceuticals; Cofounder of Before Brands, Alladapt, Latitude, and IgGenix; National Scientific Committee member for the Immune Tolerance Network (ITN) of NIAID; recipient of a Research Sponsorship from Nestle; Consultant and Advisory Board Member at Before Brands, Alladapt, IgGenix, NHLBI, and ProBio; and Data and Safety Monitoring Board member at NHLBI. CB is on the board of Catamaran Bio. Author MH was employed by company ATUM.

The remaining authors declare that the research was conducted in the absence of any commercial or financial relationships that could be construed as a potential conflict of interest.

Publisher's Note: All claims expressed in this article are solely those of the authors and do not necessarily represent those of their affiliated organizations, or those of the publisher, the editors and the reviewers. Any product that may be evaluated in this article, or claim that may be made by its manufacturer, is not guaranteed or endorsed by the publisher.

frontiers in Immunology

ORIGINAL RESEARCH
published: 23 September 2021
doi: 10.3389/fimmu.2021.751584

Sensitivity of SARS-CoV-2 Variants to Neutralization by Convalescent Sera and a VH3-30 Monoclonal Antibody

Shuai Yue[1†], Zhirong Li[1†], Yao Lin[1†], Yang Yang[1,2†], Mengqi Yuan[3], Zhiwei Pan[1], Li Hu[1], Leiqiong Gao[1], Jing Zhou[1], Jianfang Tang[1], Yifei Wang[1], Qin Tian[1], Yaxing Hao[1], Juan Wang[4], Qizhao Huang[1], Lifan Xu[1], Bo Zhu[5], Pinghuang Liu[3], Kai Deng[6,7], Li Wang[1*], Lilin Ye[1*] and Xiangyu Chen[1,5*]*

[1] Institute of Immunology, Third Military Medical University, Chongqing, China, [2] Department of Stomatology, Daping Hospital and Research Institute of Surgery, Third Military Medical University, Chongqing, China, [3] College of Veterinary Medicine, China Agricultural University, Beijing, China, [4] Department of Emergency Medicine, Southwest Hospital, Third Military Medical University, Chongqing, China, [5] Institute of Cancer, Xinqiao Hospital, Third Military Medical University, Chongqing, China, [6] Institute of Human Virology, Key Laboratory of Tropical Disease Control of Ministry of Education, Zhongshan School of Medicine, Sun Yat-sen University, Guangzhou, China, [7] Infectious Diseases Institute, Guangzhou Eighth People's Hospital, Guangzhou Medical University, Guangzhou, China

OPEN ACCESS

Edited by:
Peter Chen,
Cedars-Sinai Medical Center,
United States

Reviewed by:
Quanxin Long,
Chongqing Medical University, China
Osaretin Emmanuel Asowata,
Population Council, United States

***Correspondence:**
Kai Deng
dengkai6@mail.sysu.edu.cn
Li Wang
liwang118@tmmu.edu.cn
Lilin Ye
yelilinlcmv@tmmu.edu.cn
Xiangyu Chen
chenxiangyutmmu@163.com

[†]These authors have contributed equally to this work

Specialty section:
This article was submitted to Vaccines and Molecular Therapeutics, a section of the journal Frontiers in Immunology

Received: 01 August 2021
Accepted: 06 September 2021
Published: 23 September 2021

Citation:
Yue S, Li Z, Lin Y, Yang Y, Yuan M, Pan Z, Hu L, Gao L, Zhou J, Tang J, Wang Y, Tian Q, Hao Y, Wang J, Huang Q, Xu L, Zhu B, Liu P, Deng K, Wang L, Ye L and Chen X (2021) Sensitivity of SARS-CoV-2 Variants to Neutralization by Convalescent Sera and a VH3-30 Monoclonal Antibody. Front. Immunol. 12:751584. doi: 10.3389/fimmu.2021.751584

The severe acute respiratory syndrome coronavirus 2 (SARS-CoV-2) has caused a global pandemic of novel coronavirus disease (COVID-19). Though vaccines and neutralizing monoclonal antibodies (mAbs) have been developed to fight COVID-19 in the past year, one major concern is the emergence of SARS-CoV-2 variants of concern (VOCs). Indeed, SARS-CoV-2 VOCs such as B.1.1.7 (UK), B.1.351 (South Africa), P.1 (Brazil), and B.1.617.1 (India) now dominate the pandemic. Herein, we found that binding activity and neutralizing capacity of sera collected from convalescent patients in early 2020 for SARS-CoV-2 VOCs, but not non-VOC variants, were severely blunted. Furthermore, we observed evasion of SARS-CoV-2 VOCs from a VH3-30 mAb 32D4, which was proved to exhibit highly potential neutralization against wild-type (WT) SARS-CoV-2. Thus, these results indicated that SARS-CoV-2 VOCs might be able to spread in convalescent patients and even harbor resistance to medical countermeasures. New interventions against these SARS-CoV-2 VOCs are urgently needed.

Keywords: COVID-19, SARS-CoV-2 variants, neutralizing mAb, convalescent sera, antibody response

INTRODUCTION

As the causative agent of COVID-19, SARS-CoV-2 has caused a global pandemic with more than 211.28 million cases and 4.42 million fatalities as of August 24, 2021 (1). The SARS-CoV-2 utilizes its spike (S) protein, including the surface subunit S1 and the transmembrane subunit S2, for receptor binding and virus entry. Specifically, the S1 domain binds to the cellular receptor angiotensin-converting enzyme 2 (ACE2) *via* its receptor binding domain (RBD). The engagement of ACE2 with RBD further leads to the shedding of S1 subunit from S2 subunit, which promotes S2-mediated virus–host membrane fusion and virus entry (2, 3). Given the critical

role of RBD protein in initiating SARS-CoV-2 infection, it becomes one primary target of neutralizing antibodies elicited by both natural infection and vaccination (4–6).

However, one major concern is the emergence of SARS-CoV-2 variants of concern (VOCs), in particular, with mutation(s) located in the RBD region (7, 8). These SARS-CoV-2 VOCs threaten efforts to contain the COVID-19 pandemic and include B.1.1.7 (N501Y in RBD) (9), B.1.351 (K417N, E484K, and N501Y in RBD) (10), P.1 (K417T, E484K and N501Y in RBD) (11), and B.1.617.1 (L452R and E484Q in RBD) (12). Indeed, these SARS-CoV-2 VOCs harbor transmission advantage over non-VOC variants and account more than 90% of currently sequenced SARS-CoV-2 viruses (8). To address the potential neutralization escape caused by these mutations in RBD, we analyzed the binding activity and neutralizing capacity of serum collected from a cohort of convalescent patients with different clinical symptoms in early 2020 against SARS-CoV-2 VOCs as well as non-VOC variants. In addition, we profiled the neutralizing capacity of one previously reported VH3-30 monoclonal antibody (mAb) against SARS-CoV-2 VOCs and non-VOC variants.

MATERIALS AND METHODS

Human Samples

We enrolled a cohort of 28 convalescent COVID-19 patients with severe (n = 11), moderate (n = 9), and mild/asymptomatic (n = 8) symptoms upon being admitted to Guangzhou Eighth People's Hospital. All COVID-19 patients were positive for SARS-CoV-2 virus RNA qPCR test upon hospital admission. COVID-19 patients were diagnosed as severe when meeting at least one of the following conditions: (1) RR ≥ 30/min, (2) PaO2/FiO2 ≤ 300 mmHg, (3) SpO2 ≤ 93%, and (4) imageological evidence of significant progress (>50%) in 24–48 h. COVID-19 patients with moderate symptoms were diagnosed by respiratory symptoms, fever, and imageological evidence of pneumonia. The mild COVID-19 patients were diagnosed by inapparent clinical symptoms and no imageological evidence of pneumonia. The asymptomatic COVID-19 patients were those who show no clinical symptoms. These patients were enrolled 15 to 32 days after symptom onset (January to March 2020); the medium age was 58 [43–64, interquartile range (IQR)] years; 60.7% were female; serum was collected from patients during convalescence and the time between symptom onset to serum sample collection was 23 (15–32, IQR) days. Healthy control subjects were six adult participants in the study. All the healthy control subjects were negative for SARS-CoV-2 virus RNA qPCR test upon blood-sampling collection (**Supplementary Table S1**). Sera were collected from blood without sodium citrate treatment and stored in aliquots at −80°C. The study received IRB approvals at Guangzhou Eighth People's Hospital (KE202001134).

Enzyme Linked Immunosorbent Assay

Fifty nanograms of SARS-CoV-2 RBD proteins of WT strain (Sino Biological, 40592-V08H), B.1.1.7 (Sino Biological, 40592-V08H82), P.1 (Sino Biological, 40592-V08H86), B.1.351 (Sino Biological, 40592-V08H85), and B.1.617.1 (Sino Biological, 40592-V08H88) as well as RBD proteins with point mutation such as W436R (Sino Biological, 40592-V08H9), F342L (Sino Biological, 40592-V08H6), V483A (Sino Biological, 40592-V08H5), K458R (Sino Biological, 40592-V08H7), A435S (Sino Biological, 40592-V08H4), N354D (Sino Biological, 40592-V08H2), G476S (Sino Biological, 40592-V08H8), and V367F (Sino Biological, 40592-V08H1) in 50 µl PBS per well was coated on ELISA plates overnight at 4°C. Then, the ELISA plates were blocked for 1 h with blocking buffer (5% FBS plus 0.05% Tween 20). Next, fivefold serially diluted mAbs or fivefold serially diluted patient sera were added to each well in 50 µl of blocking buffer for 1 h. After washing with PBST, the bound antibodies were incubated with anti-human IgG HRP detection antibody (Bioss Biotech) for 45 min, followed by washing with PBST and then reacting with TMB (Beyotime). The ELISA plates were allowed to react for 5 min and then stopped by 1 M H_2SO_4 stop buffer. The optical density (OD) value was determined at 450 nm. Concentration for 50% of maximal effect (EC_{50}) was calculated by using nonlinear regression.

ELISA-Based Receptor-Binding Inhibition Assay

Two hundred nanograms of hACE2 protein (Sino Biological, 10108-H05H) in 50 µl PBS per well was coated on ELISA plates overnight at 4°C. Then, the ELISA plates were blocked for 1 h with blocking buffer (5% FBS plus 0.05% Tween 20); meanwhile, threefold serial diluted mAbs or twofold diluted patient sera were incubated with 0.2 µg/ml SARS-CoV-2 RBD protein for 1 h. Then, the incubated mixtures were added to ELISA plates and allowed to develop for 1 h, followed by PBST washing and anti-His HRP antibody (Sino Biological, 105327-MM02T-H) incubating for 45 min. Next, the ELISA plates were washed with PBST and added with TMB (Beyotime). After 5 min, the ELISA plates were stopped and determined at 450 nm. The half maximal inhibitory concentration (IC_{50}) was determined by using four-parameter logistic regression.

SARS-CoV-2 Pseudovirus Neutralization Assay

For neutralization experiments, SARS-CoV-2 pseudotype particles were pre-incubated with serial diluted convalescent sera or mAbs for 1 h at 37°C. Then, hACE2-expressing HEK-293T (hACE2/293T) cells were incubated with the mixtures overnight and then cultured with fresh media. At 48 h after the mixture incubation, the luciferase activity of SARS-CoV-2 typed pseudovirus-infected hACE2/293T cells were measured by a luciferase reporter assay kit (Promega, E1910).

Statistics

The SARS-CoV-2 RBD antibody titers, the virus neutralizing function of the sera belonging to patients, and the virus neutralizing function of mAb 32D4 were compared with the one-way ANOVA test. p-values less than 0.05 were defined as statistically significant. GraphPad Prism version 6.0 software was used for statistical analysis.

RESULTS

Reduced Titer of Sera Antibodies Specific for SARS-CoV-2 VOC RBD in Individuals Recovered From WT SARS-CoV-2 Infection

Firstly, we examined the binding activity of antibodies that specifically bind to the RBD protein of WT SARS-CoV-2 strain and the mutated RBD proteins of SARS-CoV-2 VOCs (including B.1.1.7, B.1.351, P.1, and B.1.617.1) (**Figure 1A**) in the convalescent sera of WT SARS-CoV-2-infected patients (early 2020) by IgG ELISA. Notably, we found a significantly lower binding activity of antibodies specific for B.1.351, P.1, and B.1.617.1 RBDs but not B.1.1.7 RBD when compared to those of the WT one in the group of convalescent COVID-19 patients with severe illness (**Figure 1B**). This feature was less pronounced when extended to convalescent COVID-19 patients with moderate or mild/asymptomatic illness (**Figures 1C–E**), which might be due to the suboptimal tonic RBD-specific antibodies in these patients (4, 13). Consistently, binding ability of convalescent sera from COVID-19 patients with severe illness against SARS-CoV-2 VOCs, albeit blunted, was superior to those of COVID-19 patients with moderate or mild/asymptomatic illness (**Supplementary Figures S1A–E**). Therefore, these results suggest a crucial role of residues N501, E484, L452, and K417 in epitope regions of high-affinity antibodies specific for SARS-CoV-2 RBD.

Reduced Neutralization Against SARS-CoV-2 VOCs by Convalescent Sera Elicited by WT SARS-CoV-2 Infection

We then assessed the neutralizing capacity of convalescent sera from WT SARS-CoV-2-infected patients with severe illness by ELISA-based RBD-ACE2 binding inhibition assays and pseudovirus neutralization assays as previously described (4, 14). Neutralization against B.1.1.7 by convalescent sera was slightly less efficient as compared to that against WT (**Figures 1F, G**), which might be due to higher ACE2 binding ability observed in B.1.1.7 (**Figure 1H**). However, the neutralizing potency of convalescent sera against B.1.351, P.1, and B.1.617.1 was significantly reduced when compared to that against WT (**Figures 1F, G**). Given the comparable ACE2

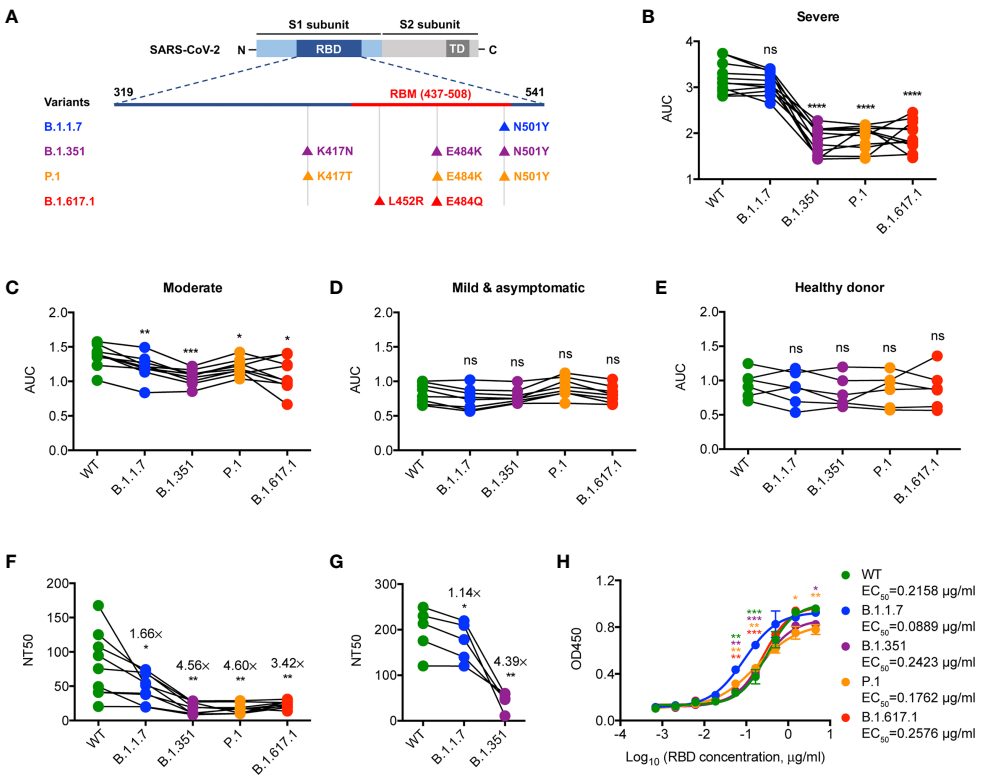

FIGURE 1 | Neutralization of SARS-CoV-2 VOCs by convalescent sera. **(A)** Schematic diagram showing the location of mutations of SARS-CoV-2 VOCs in the context of RBD protein domain. RBD, receptor binding domain; RBM, receptor binding motif; TD, transmembrane domain. **(B–E)** ELISA binding assay of COVID-19 convalescent patient sera **(B–D)** or healthy donor sera **(E)** to ELISA plate coating of RBD proteins of SARS-CoV-2 and its mutated variants as indicated. AUC, area under the curve. **(F)** COVID-19 convalescent patient serum-mediated inhibition of indicated RBD proteins binding to ACE2 protein by ELISA. NT50, neutralizing titer 50. **(G)** COVID-19 convalescent patient serum-mediated neutralization of indicated SARS-CoV-2 pseudoviruses. NT50, neutralizing titer 50. **(H)** ELISA binding assay of ACE2 to indicated RBD proteins. EC_{50}, concentration for 50% of maximal effect. The data are representative of at least two independent experiments. $^{*}p < 0.05$, $^{**}p < 0.01$, $^{***}p < 0.001$, and $^{****}p < 0.0001$. Not significant, ns. Error bars in **(H)** indicate SD.

binding ability between WT and VOCs (including B.1.351, P.1, and B.1.617.1) (**Figure 1H**), the noticeable resistance of these VOCs to convalescent sera was likely caused by the lack of binding ability to the RBD with E484K, L452R, and K417N/T mutations (**Figure 1B**). Thus, SARS-CoV-2 VOCs may partially evade the neutralization by antibodies elicited by the WT strain infection.

Similar Binding Activity and Neutralizing Capacity of Convalescent Sera for SARS-CoV-2 Non-VOC Variants

Considering a substantial transmission disadvantage of SARS-CoV-2 non-VOC variants in the COVID-19 pandemic (15), we next sought to analyze the neutralizing potency of convalescent sera against non-VOC variants with a different RBD mutation, including F342L, N354D, V367F, A435S, W436R, K458R, G476S, and V483A (**Figure 2A**). We found it of particular interest that the binding and neutralizing ability of specific antibodies in convalescent serum for the RBD of SARS-CoV-2 non-VOC were not weaker than those for the WT RBD (**Figures 2B, C**). This finding indicates minimal influences of these mutations to the neutralizing activity of SARS-CoV-2 RBD-targeted mAbs and also excludes the possibility that the SARS-CoV-2 pandemic shifts to these non-VOC variants.

Neutralization Sensitivity of a VH3-30 mAb 32D4 to SARS-CoV-2 Variants

Finally, we set out to determine the neutralizing capacity of 32D4 mAb on these SARS-CoV-2 variants. The 32D4 mAb, isolated from memory B cells of WT SARS-CoV-2-infected patients, is one of the first identified human neutralizing mAbs that target SARS-CoV-2 RBD (14). As analyzed by IMGT (16), the 32D4 mAb is encoded by the IGHV3-30 gene (**Figure 3A**), which is one of the most enriched IGHV genes used by RBD-targeting antibodies and thus characterizes one binding mode of RBD-targeting antibodies (17). As shown, the 32D4 mAb showed high binding affinity for SARS-CoV-2 VOCs, with EC_{50} values of 0.0207 μg/ml for B.1.1.7, 0.0153 μg/ml for B.1.351, and 0.0161 μg/ml for P.1 (**Figure 3B**). However, the binding affinity of 32D4 for B.1.617.1 was severely blunted and the EC_{50} value was increased to 1.9450 μg/ml (**Figure 3B**), indicative of a key role of the residue L452 for the 32D4 binding epitope. Besides, 32D4 was less effective in inhibiting B.1.1.7, B.1.351, and P.1 to engage with ACE2 as compared to the WT one and completely failed to block interaction between B.1.617.1 and ACE2 as evidenced by functional ELISA assays (**Figure 3C**). Consistently, neutralization of mAb 32D4 against SARS-CoV-2 B.1.351 pseudoviruses was also blunted (**Figure 3D**). Along with our finding, recent studies also found that the neutralizing activity of several mAbs, including those being approved or in the late clinical stage, was abolished by SARS-CoV-2 VOCs (8, 18–20). In contrast, the binding and neutralizing ability of 32D4 mAb for SARS-CoV-2 non-VOC variants were largely unaffected (**Figures 3E, F**). Thus, these results suggest that neutralizing mAb targeting the SARS-CoV-2 WT protein sequence might be re-examined whether they are suitable as prophylaxis or treatment for individuals infected with SARS-CoV-2 VOCs.

DISCUSSION

The circulating SARS-CoV-2 VOCs, including B.1.1.7, B.1.351, P.1, and B.1.617.1, have taken a major toll on the global control of the COVID-19 pandemic. Indeed, accumulating evidence suggested reduced

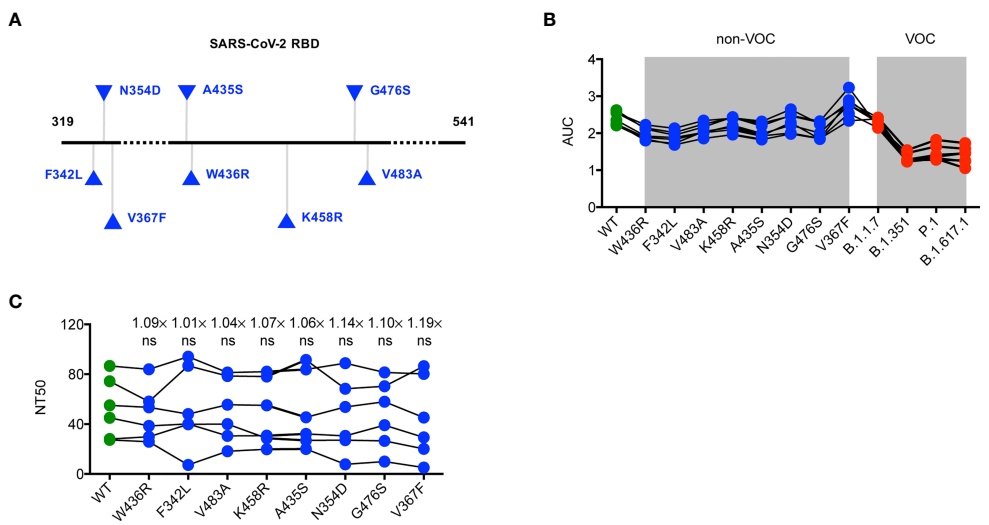

FIGURE 2 | Neutralization of SARS-CoV-2 non-VOC variants by convalescent sera. **(A)** Schematic diagram presenting the location of mutations of non-VOC variants in the context of RBD protein domain. **(B)** ELISA binding assay of sera originated from COVID-19 patients with severe illness to ELISA plate coating of RBD proteins of WT RBD and its mutated variants as indicated. **(C)** COVID-19 convalescent patient serum-mediated inhibition of indicated RBD proteins binding to ACE2 protein by ELISA. The data are representative of at least two independent experiments. Not significant, ns.

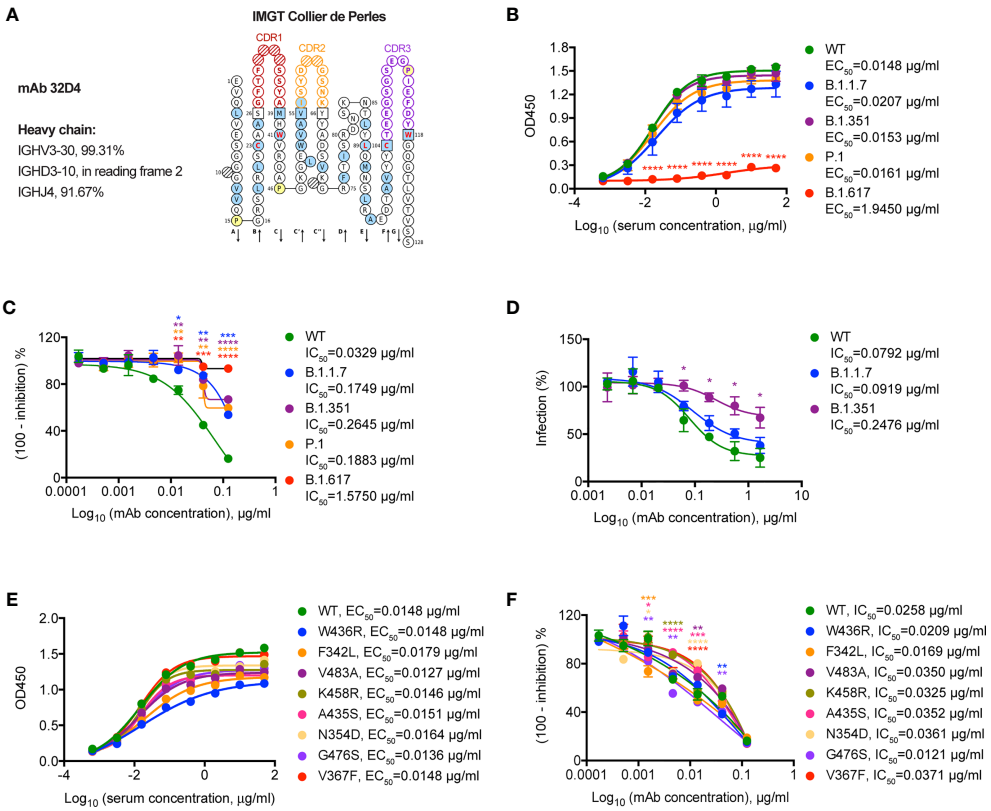

FIGURE 3 | Neutralization of SARS-CoV-2 variants by a VH3-30 mAb 32D4. **(A)** IMGT Collier de Perles for 32D4. **(B)** ELISA binding assay of mAb 32D4 to RBD proteins of WT and VOCs. EC_{50}, concentration for 50% of maximal effect. **(C)** ELISA analysis of mAb 32D4-mediated inhibition of WT and VOC RBD proteins binding to ACE2 protein. IC_{50}, half maximal inhibitory concentration. **(D)** 32D4-mediated neutralization of indicated SARS-CoV-2 pseudoviruses. IC_{50}, half maximal inhibitory concentration. **(E)** ELISA binding assay of mAb 32D4 to RBD proteins of WT and non-VOC variants. EC_{50}, concentration for 50% of maximal effect. **(F)** ELISA analysis of mAb 32D4-mediated inhibition of WT and non-VOC RBD proteins binding to ACE2 protein. IC_{50}, half maximal inhibitory concentration. $^{*}p < 0.05$, $^{**}p < 0.01$, $^{***}p < 0.001$, and $^{****}p < 0.0001$. The data are representative of at least two independent experiments. Error bars in **(B–D, F)** indicate SD.

neutralization against SARS-CoV-2 VOCs by convalescent sera elicited by SARS-CoV-2 D614G variant (20, 21) or SARS-CoV-2 B.1.1.117 variant (22), sera from mRNA-1273- or BNT162b2-vaccinated individuals (5, 20, 21, 23), and FDA-approved neutralizing mAbs (8, 18). In the study, we also found attenuated neutralization capacity against SARS-CoV-2 VOCs, especially B.1.351, P.1, and B.1.617.1, by sera collected from convalescent patients in the early 2020 or by a VH3-30 mAb 32D4 isolated from the memory B cells of these convalescent patients.

Neutralization resistance of B.1.1.7 to convalescent sera and mAb 32D4 was not noticeable as compared to that of other VOCs in our study. This dichotomous neutralization resistance was also reported by other studies (24, 25) and seems paradoxical to the increased affinity between the B.1.1.7 RBD with a single N501Y mutation and ACE2 observed in our study and previous studies (17, 26). However, we and another group (23) found that SARS-CoV-2-specific mAbs show partial or complete loss of binding to RBD with E484K substitution but not N501Y substitution. Besides, diminished neutralization capacity of convalescent sera and neutralizing mAbs was mainly caused by single mutation at residue E484 but not N501 (18, 23, 25). Thus, RBD E484 residue is a crucial binding site for mAbs and VOCs with mutation at E484 (E484K for B.1.351 and P.1; E484Q for B.1.617.1) show enhanced neutralization resistance.

The VH3-30 gene is one of the most-enriched IGHV genes used by RBD-targeting neutralizing mAbs elicited by natural infection (17, 27) and vaccination (28). SARS-CoV-2-specific neutralizing mAbs with VH3-30 gene, exemplified by REGN10987 (17, 29), C002 (17), and 32D4 in the study, are characterized by a similar binding mode to some extent (17, 30) and consequent mutational escape of SARS-CoV-2 variants. REGN10987 is suggested to be escaped by SARS-CoV-2 variants with mutations ranging from N439 to N453 within RBD, especially K444Q and V445A (31). The L452 residue is a key recognizing site for C002 (17). Here, we also found the losing binding and neutralization of 32D4 to B.1.617.1 variant with L452R substitution. In addition to B.1.617.1, other VOCs (e.g., B.1.1.7, B.1.351, and P.1) also partially escape neutralization by 32D4. The mechanism underlying the escape of VOCs to 32D4-mediated neutralization awaits further structural analysis.

Convalescent plasma or sera transfusion has been highlighted as a promising therapy in fighting newly emerged viral infections. Indeed, transfusion of convalescent plasma harvested from recovered COVID-19 patients is reported to be beneficial in treating critically ill patients with SARS-CoV-2 infection (32–35). Given the neutralization resistance of SARS-CoV-2 VOCs to convalescent sera collected from individuals infected with WT SARS-CoV-2 infection in early 2020, transfusion of these convalescent sera might not be suitable in treating COVID-19 patients infected with SARS-CoV-2 VOCs. Consistently, Cele et al. found that the B.1.351 variant was poorly neutralized by plasma from individuals infected with non-VOC B.1.1.117 (22). By contrast, cross-neutralization of non-VOC B.1.1.117 by plasma from those infected with B.1.351 was more effective (22). These results suggest the potential neutralization of plasma from SARS-CoV-2 VOC-infected individuals to WT, other VOCs, and non-VOC variants, which awaits further investigation.

As with other RNA viruses such as influenza and HIV, SARS-CoV-2 is also characterized by antigenic drift (17). In addition to E484K, L452R, and K417N/T mutations, numerous RBD mutations (including F342L, N354D, V367F, A435S, W436R, K458R, G476S, and V483A) have also been detected in non-VOC variants (36, 37). Though these RBD mutants show significantly increased affinity to hACE2 (36, 37), we found largely unaffected neutralizing potencies of convalescent sera and mAb 32D4 against SARS-CoV-2 variants with relevant RBD mutation. These results might explain the rare cases of these non-VOC variants during the COVID-19 pandemic and further indicated a crosstalk between human host immune pressure and SARS-CoV-2 variant selection.

Taken together, our study presents the comparison of sensitivity of SARS-CoV-2 VOC and non-VOC variants to neutralization by convalescent sera and a VH3-30 mAb from convalescent patients in the early 2020. Although these results are based on functional ELISA assays and pseudovirus assays and await confirmation with authentic SARS-CoV-2, the ELISA/pseudovirus assays have been proven to be free of biosafety issue but as reliable as the canonical plaque assay with authentic SARS-CoV-2 (4, 38–41). The results suggest that SARS-CoV-2 VOCs might be able to spread in convalescent patients and even harbor resistance to medical countermeasures. Indeed, we observed evasion of SARS-CoV-2 VOCs from the 32D4 mAb, which was proved to exhibit highly potential neutralization against WT SARS-CoV-2. Thus, containment of these SARS-CoV-2 VOCs by medical interventions (e.g., next-generation vaccines, pan-neutralizing mAbs) is in urgent need.

DATA AVAILABILITY STATEMENT

The original contributions presented in the study are included in the article/**Supplementary Material**. Further inquiries can be directed to the corresponding authors.

ETHICS STATEMENT

The studies involving human participants were reviewed and approved by Guangzhou Eighth People's Hospital (KE202001134). The patients/participants provided their written informed consent to participate in this study.

AUTHOR CONTRIBUTIONS

SY, ZL, YL, YY, and MY performed the experiments. ZP, LH, LG, JZ, JT, YW, QT, YH, JW, QH, and LX assisted in processing patient samples. XC designed the study, analyzed the data, and wrote the paper with LY, LW, KD, PL, SY, and BZ. XC and LY supervised the study. All authors contributed to the article and approved the submitted version.

FUNDING

This work was supported by grants from the National Natural Science Fund for Distinguished Young Scholars (No. 31825011 to LY) and the National Natural Science Foundation of China (No. 31900643 to QH).

SUPPLEMENTARY MATERIAL

The Supplementary Material for this article can be found online at: https://www.frontiersin.org/articles/10.3389/fimmu.2021.751584/full#supplementary-material

Supplementary Figure 1 | Antibody responses to RBD proteins of WT and VOCs in patients recovered from different COVID-19 illness. **(A–E)** ELISA binding assay of COVID-19 convalescent patient sera and healthy donor sera to ELISA plate coating of RBD proteins of WT **(A)**, B.1.1.7 **(B)**, B.1.351 **(C)**, P.1 **(D)** and B.1.617.1 **(E)**. AUC, area under the curve. $^{*}P < 0.05$, $^{**}P < 0.01$, $^{***}P < 0.001$ and $^{****}P < 0.0001$. Not significant, ns. Error bars in **(A–E)** indicate SEM.

REFERENCES

1. WHO. *World Health Organization. Weekly Epidemiological Update on COVID-19 - 24 August 2021* (2021). Available at: https://www.who.int/publications/m/item/weekly-epidemiological-update-on-covid-19—24-august-2021.
2. Wrapp D, Wang N, Corbett KS, Goldsmith JA, Hsieh CL, Abiona O, et al. Cryo-EM Structure of the 2019-Ncov Spike in the Prefusion Conformation. *Science* (2020) 367:1260–3. doi: 10.1126/science.abb2507
3. Yan R, Zhang Y, Li Y, Xia L, Guo Y, Zhou Q. Structural Basis for the Recognition of SARS-CoV-2 by Full-Length Human ACE2. *Science* (2020) 367:1444–8. doi: 10.1126/science.abb2762
4. Chen X, Pan Z, Yue S, Yu F, Zhang J, Yang Y, et al. Disease Severity Dictates SARS-CoV-2-Specific Neutralizing Antibody Responses in COVID-19. *Signal Transduct Target Ther* (2020) 5:180. doi: 10.1038/s41392-020-00301-9
5. Edara VV, Norwood C, Floyd K, Lai L, Davis-Gardner ME, Hudson WH, et al. Infection- and Vaccine-Induced Antibody Binding and Neutralization of the B.1.351 SARS-CoV-2 Variant. *Cell Host Microbe* (2021) 29:516–521.e513. doi: 10.1016/j.chom.2021.03.009
6. Gaebler C, Wang Z, Lorenzi JCC, Muecksch F, Finkin S, Tokuyama M, et al. Evolution of Antibody Immunity to SARS-CoV-2. *Nature* (2021) 591 (7851):639–44. doi: 10.1038/s41586-021-03207-w

7. Plante JA, Mitchell BM, Plante KS, Debbink K, Weaver SC, Menachery VD. The Variant Gambit: COVID-19's Next Move. *Cell Host Microbe* (2021) 29 (4):508–15. doi: 10.1016/j.chom.2021.02.020
8. Corti D, Purcell LA, Snell G, Veesler D. Tackling COVID-19 With Neutralizing Monoclonal Antibodies. *Cell* (2021) 184(12):3086–08. doi: 10.1016/j.cell.2021.05.005
9. Davies NG, Abbott S, Barnard RC, Jarvis CI, Kucharski AJ, Munday JD, et al. Estimated Transmissibility and Impact of SARS-CoV-2 Lineage B.1.1.7 in England. *Science* (2021) 372(6538):eabg3055. doi: 10.1126/science.abg3055
10. Tegally H, Wilkinson E, Giovanetti M, Iranzadeh A, Fonseca V, Giandhari J, et al. Detection of a SARS-CoV-2 Variant of Concern in South Africa. *Nature* (2021) 592:438–43. doi: 10.1038/s41586-021-03402-9
11. Faria NR, Mellan TA, Whittaker C, Claro IM, Candido DDS, Mishra S, et al. Genomics and Epidemiology of the P.1 SARS-CoV-2 Lineage in Manaus, Brazil. *Science* (2021) 372:815–21. doi: 10.1126/science.abh2644
12. Cherian S, Potdar V, Jadhav S, Yadav P, Gupta N, Das M, et al. SARS-CoV-2 Spike Mutations, L452R, E484Q and P681R, in the Second Wave of COVID-19 in Maharashtra, India. *Microorganisms* (2021) 9(7):1542. doi: 10.3390/microorganisms9071542
13. Sokal A, Chappert P, Barba-Spaeth G, Roeser A, Fourati S, Azzaoui I, et al. Maturation and Persistence of the Anti-SARS-CoV-2 Memory B Cell Response. *Cell* (2021) 184(5):1201–13.e14. doi: 10.1101/2020.11.17.385252
14. Chen X, Li R, Pan Z, Qian C, Yang Y, You R, et al. Human Monoclonal Antibodies Block the Binding of SARS-CoV-2 Spike Protein to Angiotensin Converting Enzyme 2 Receptor. *Cell Mol Immunol* (2020) 17:647–9. doi: 10.1038/s41423-020-0426-7
15. Volz E, Mishra S, Chand M, Barrett JC, Johnson R, Geidelberg L, et al. Transmission of SARS-CoV-2 Lineage B.1.1.7 in England: Insights From Linking Epidemiological and Genetic Data. *medRxiv* (2021). doi: 10.1101/2020.12.30.20249034
16. Giudicelli V, Brochet X, Lefranc MP. IMGT/V-QUEST: IMGT Standardized Analysis of the Immunoglobulin (IG) and T Cell Receptor (TR) Nucleotide Sequences. *Cold Spring Harb Protoc* (2011) 2011:695–715. doi: 10.1101/pdb.prot5633
17. Yuan M, Huang D, Lee CD, Wu NC, Jackson AM, Zhu X, et al. Structural and Functional Ramifications of Antigenic Drift in Recent SARS-CoV-2 Variants. *Science* (2021) 373(6556):818–23. doi: 10.1101/2021.02.16.430500
18. Chen RE, Zhang X, Case JB, Winkler ES, Liu Y, VanBlargan LA, et al. Resistance of SARS-CoV-2 Variants to Neutralization by Monoclonal and Serum-Derived Polyclonal Antibodies. *Nat Med* (2021) 27(4):717–26. doi: 10.1038/s41591-021-01294-w
19. Hu J, Peng P, Wang K, Fang L, Luo FY, Jin AS, et al. Emerging SARS-CoV-2 Variants Reduce Neutralization Sensitivity to Convalescent Sera and Monoclonal Antibodies. *Cell Mol Immunol* (2021) 18:1061–3. doi: 10.1038/s41423-021-00648-1
20. Hoffmann M, Arora P, Groß R, Seidel A, Hörnich BF, Hahn AS, et al. SARS-CoV-2 Variants B.1.351 and P.1 Escape From Neutralizing Antibodies. *Cell* (2021) 184 (9):2384–93.e12. doi: 10.1016/j.cell.2021.03.036
21. Hoffmann M, Hofmann-Winkler H, Krüger N, Kempf A, Nehlmeier I, Graichen L, et al. SARS-CoV-2 Variant B.1.617 is Resistant to Bamlanivimab and Evades Antibodies Induced by Infection and Vaccination. *Cell Rep* (2021) 36(3):109415. doi: 10.1016/j.celrep.2021.109415
22. Cele S, Gazy I, Jackson L, Hwa SH, Tegally H, Lustig G, et al. Escape of SARS-CoV-2 501y.V2 From Neutralization by Convalescent Plasma. *Nature* (2021) 593:142–6. doi: 10.1038/s41586-021-03471-w
23. Collier DA, De Marco A, Ferreira I, Meng B, Datir RP, Walls AC, et al. Sensitivity of SARS-CoV-2 B.1.1.7 to mRNA Vaccine-Elicited Antibodies. *Nature* (2021) 593:136–41. doi: 10.1038/s41586-021-03412-7
24. Planas D, Bruel T, Grzelak L, Guivel-Benhassine F, Staropoli I, Porrot F, et al. Sensitivity of Infectious SARS-CoV-2 B.1.1.7 and B.1.351 Variants to Neutralizing Antibodies. *Nat Med* (2021) 27(5):917–24. doi: 10.1101/2021.02.12.430472
25. Wang P, Nair MS, Liu L, Iketani S, Luo Y, Guo Y, et al. Antibody Resistance of SARS-CoV-2 Variants B.1.351 and B.1.1.7. *Nature* (2021) 593:130–5. doi: 10.1038/s41586-021-03398-2
26. Starr TN, Greaney AJ, Hilton SK, Ellis D, Crawford KHD, Dingens AS, et al. Deep Mutational Scanning of SARS-CoV-2 Receptor Binding Domain Reveals Constraints on Folding and ACE2 Binding. *Cell* (2020) 182:1295–310.e1220. doi: 10.1016/j.cell.2020.08.012
27. Robbiani DF, Gaebler C, Muecksch F, Lorenzi JCC, Wang Z, Cho A, et al. Convergent Antibody Responses to SARS-CoV-2 in Convalescent Individuals. *Nature* (2020) 584:437–42. doi: 10.1038/s41586-020-2456-9
28. Wang Z, Schmidt F, Weisblum Y, Muecksch F, Barnes CO, Finkin S, et al. mRNA Vaccine-Elicited Antibodies to SARS-CoV-2 and Circulating Variants. *Nature* (2021) 592(7855):616–22. doi: 10.3410/f.739524179.793585051
29. Hansen J, Baum A, Pascal KE, Russo V, Giordano S, Wloga E, et al. Studies in Humanized Mice and Convalescent Humans Yield a SARS-CoV-2 Antibody Cocktail. *Science* (2020) 369:1010–4. doi: 10.1126/science.abd0827
30. Barnes CO, Jette CA, Abernathy ME, Dam KA, Esswein SR, Gristick HB, et al. SARS-CoV-2 Neutralizing Antibody Structures Inform Therapeutic Strategies. *Nature* (2020) 588:682–7. doi: 10.1038/s41586-020-2852-1
31. Starr TN, Greaney AJ, Addetia A, Hannon WW, Choudhary MC, Dingens AS, et al. Prospective Mapping of Viral Mutations That Escape Antibodies Used to Treat COVID-19. *Science* (2021) 371:850–4. doi: 10.1126/science.abf9302
32. Arnold Egloff SA, Junglen A, Restivo JS, Wongskhaluang M, Martin C, Doshi P, et al. Convalescent Plasma Associates With Reduced Mortality and Improved Clinical Trajectory in Patients Hospitalized With COVID-19. *J Clin Invest* (2021) 151788. doi: 10.1172/JCI151788
33. Li L, Zhang W, Hu Y, Tong X, Zheng S, Yang J, et al. Effect of Convalescent Plasma Therapy on Time to Clinical Improvement in Patients With Severe and Life-Threatening COVID-19: A Randomized Clinical Trial. *JAMA* (2020) 324:460–70. doi: 10.1001/jama.2020.10044
34. Shen C, Wang Z, Zhao F, Yang Y, Li J, Yuan J, et al. Treatment of 5 Critically Ill Patients With COVID-19 With Convalescent Plasma. *JAMA* (2020) 323:1582–9. doi: 10.1001/jama.2020.4783
35. Simonovich VA, Burgos Pratx LD, Scibona P, Beruto MV, Vallone MG, Vázquez C, et al. A Randomized Trial of Convalescent Plasma in Covid-19 Severe Pneumonia. *N Engl J Med* (2021) 384:619–29. doi: 10.1056/NEJMoa2031304
36. Ou J, Zhou Z, Dai R, Zhang J, Zhao S, Wu X, et al. V367F Mutation in SARS-CoV-2 Spike RBD Emerging During the Early Transmission Phase Enhances Viral Infectivity Through Increased Human ACE2 Receptor Binding Affinity. *J Virol* (2021) 95:e0061721. doi: 10.1128/JVI.00617-21
37. Koyama T, Weeraratne D, Snowdon JL, Parida L. Emergence of Drift Variants That May Affect COVID-19 Vaccine Development and Antibody Treatment. *Pathogens* (2020) 9. doi: 10.20944/preprints202004.0024.v1
38. Cao Y, Su B, Guo X, Sun W, Deng Y, Bao L, et al. Potent Neutralizing Antibodies Against SARS-CoV-2 Identified by High-Throughput Single-Cell Sequencing of Convalescent Patients' B Cells. *Cell* (2020) 182:73–84.e16. doi: 10.1016/j.cell.2020.05.025
39. Ju B, Zhang Q, Ge J, Wang R, Sun J, Ge X, et al. Human Neutralizing Antibodies Elicited by SARS-CoV-2 Infection. *Nature* (2020) 9(5):324. doi: 10.3390/pathogens9050324
40. Shi R, Shan C, Duan X, Chen Z, Liu P, Song J, et al. A Human Neutralizing Antibody Targets the Receptor-Binding Site of SARS-CoV-2. *Nature* (2020) 584:120–4. doi: 10.1038/s41586-020-2381-y
41. Wan J, Xing S, Ding L, Wang Y, Gu C, Wu Y, et al. Human-IgG-Neutralizing Monoclonal Antibodies Block the SARS-CoV-2 Infection. *Cell Rep* (2020) 32:107918. doi: 10.1016/j.celrep.2020.107918

Conflict of Interest: The authors declare that the research was conducted in the absence of any commercial or financial relationships that could be construed as a potential conflict of interest.

frontiers in Immunology

ORIGINAL RESEARCH
published: 27 September 2021
doi: 10.3389/fimmu.2021.728021

SARS-CoV-2 mRNA Vaccines Elicit Different Responses in Immunologically Naïve and Pre-Immune Humans

David Forgacs[1], *Hyesun Jang*[1], *Rodrigo B. Abreu*[1], *Hannah B. Hanley*[1], *Jasper L. Gattiker*[1], *Alexandria M. Jefferson*[1] *and Ted M. Ross*[1,2*]

[1] Center for Vaccines and Immunology, University of Georgia, Athens, GA, United States, [2] Department of Infectious Diseases, University of Georgia, Athens, GA, United States

As the COVID-19 pandemic continues, the authorization of vaccines for emergency use has been crucial in slowing down the rate of infection and transmission of the SARS-CoV-2 virus that causes COVID-19. In order to investigate the longitudinal serological responses to SARS-CoV-2 natural infection and vaccination, a large-scale, multi-year serosurveillance program entitled SPARTA (SARS SeroPrevalence and Respiratory Tract Assessment) was initiated at 4 locations in the U.S. The serological assay presented here measuring IgG binding to the SARS-CoV-2 receptor binding domain (RBD) detected antibodies elicited by SARS-CoV-2 infection or vaccination with a 95.5% sensitivity and a 95.9% specificity. We used this assay to screen more than 3100 participants and selected 20 previously infected pre-immune and 32 immunologically naïve participants to analyze their antibody binding to RBD and viral neutralization (VN) responses following vaccination with two doses of either the Pfizer-BioNTech BNT162b2 or the Moderna mRNA-1273 vaccine. Vaccination not only elicited a more robust immune reaction than natural infection, but the level of neutralizing and anti-RBD antibody binding after vaccination is also significantly higher in pre-immune participants compared to immunologically naïve participants ($p<0.0033$). Furthermore, the administration of the second vaccination did not further increase the neutralizing or binding antibody levels in pre-immune participants ($p=0.69$). However, ~46% of the immunologically naïve participants required both vaccinations to seroconvert.

Keywords: SARS-CoV-2, coronavirus, vaccination, immunization, pre-immune, neutralization, antibody response

OPEN ACCESS

Edited by:
Peter Chen,
Cedars-Sinai Medical Center, United States

Reviewed by:
Roopali Rajput,
National Institute of Tuberculosis and Respiratory Diseases, India
Jose Alejandro Chabalgoity,
University of the Republic, Uruguay

***Correspondence:**
Ted M. Ross
tedross@uga.edu

Specialty section:
This article was submitted to Vaccines and Molecular Therapeutics, a section of the journal Frontiers in Immunology

Received: *20 June 2021*
Accepted: *13 September 2021*
Published: *27 September 2021*

Citation:
Forgacs D, Jang H, Abreu RB, Hanley HB, Gattiker JL, Jefferson AM and Ross TM (2021) SARS-CoV-2 mRNA Vaccines Elicit Different Responses in Immunologically Naïve and Pre-Immune Humans. Front. Immunol. 12:728021. doi: 10.3389/fimmu.2021.728021

INTRODUCTION

In December 2019, individuals linked to an animal market in Wuhan, China presented with what was initially described as atypical pneumonia. Bronchoalveolar lavage fluid collected from hospitalized individuals contained a novel coronavirus detected by Illumina and Nanopore sequencing and electron microscopy (1). This novel coronavirus, SARS-CoV-2, is a member of the Betacoronavirus genus in the Coronaviridae family (2). Four main structural proteins make up

the SARS-CoV-2 virion: nucleocapsid proteins surround the positive strand RNA genome, membrane proteins connect the membrane to the nucleocapsid, envelope proteins facilitate budding and detachment from the host cell, and spike proteins are involved in host receptor binding (3). Similar to the closely related SARS virus that caused a 2003 outbreak, SARS-CoV-2 targets the ACE2 receptor located on the surface of the host cells (4–7).

Since its initial identification, SARS-CoV-2 spread rapidly and resulted in a global pandemic. According to the World Health Organization, there is a cumulative burden of over 168 million confirmed cases and 3.5 million deaths as of May 28, 2021. In order to effectively combat the ongoing pandemic, a combination of targeted interventions and effective vaccines are required in conjunction with a deeper understanding of the elicited immune responses. The SARS-CoV-2 spike protein has been used as the primary antigen in several vaccines authorized for emergency use (EUA) by the U.S. Food and Drug Administration (FDA) (8–10). The spike protein is highly immunogenic, and is able to elicit a wide array of serological and cellular responses (11, 12). Many neutralizing antibodies isolated from convalescent human sera specifically target the 223 amino acid receptor binding domain (RBD; amino acids 319-541) of the 1273 amino acid spike protein (13, 14). Therefore, RBD-directed antibodies are a suitable predictor of both serological binding and neutralizing potential (13, 15–17).

In December 2020, two mRNA-based vaccines received EUA in the U.S. Both the Pfizer-BioNTech BNT162b2 vaccine (2x 30μg doses 21 days apart) and the Moderna mRNA-1273 vaccine (2x 100μg doses 28 days apart) contain mRNA coding for the full-length spike protein (8, 9). These vaccines are delivered intramuscularly in a positively charged lipid nanoparticle to enhance host cell uptake (8, 9). Following endocytosis and endosomal escape, the mRNA is translated into protein by the host cells. Two proline mutations in the C-terminal S2 fusion machinery were inserted into the pre-fusion spike protein conformation to more closely mimic the intact virus (18–20). When displayed by antigen-presenting cells (APCs), the spike protein stimulates a similar immune response to antigens presented over the course of a natural infection (21). In human trials, both vaccines reported 95% efficacy in healthy adults in preventing symptomatic infection by SARS-CoV-2 (8, 9). Full immunization is achieved 14 days following the second vaccination (9, 22). However, it is yet to be determined how quickly serological immunity wanes or what the exact nature of the memory response is upon re-exposure to the virus.

In order to explore these questions, our group initiated a large-scale longitudinal surveillance program entitled SPARTA to investigate the durability and effectiveness of immune responses to SARS-CoV-2 infection, re-infection, and vaccination. Blood was collected for the analysis of serological and cellular immune responses, and saliva was collected to test for the presence of SARS-CoV-2 viral RNA by nucleic acid amplification test (NAAT). Many SPARTA participants belong to high-risk groups prioritized for receiving early vaccination.

Here, we present validation for our serological assays used for SPARTA, as well as data tracking SARS-CoV-2-specific antibody levels in 32 immunologically naïve and 20 previously infected pre-immune participants going through vaccination by measuring both anti-RBD antibody binding *via* indirect ELISA, and viral neutralization (VN) using the USA-WA1/2020 SARS-CoV-2 strain. We also demonstrated how the effect of a single vaccination differs in immunologically naïve and pre-immune participants. While most researchers focus only on using ELISA or surrogate virus pseudo-neutralization assays as a substitute for VN with varying results (23–29), we felt it was not only important to demonstrate the capacity of antibodies to bind to a SARS-CoV-2-derived protein, but also to assess *in vitro* protection against infectious SARS-CoV-2 virus by analyzing the potential of serum antibodies to limit virus-mediated cytopathic effects.

MATERIALS AND METHODS

Ethics Statement and the Role of the Funding Source

The study procedures, informed consent, and data collection documents were reviewed and approved by the WIRB-Copernicus Group Institutional Review Board (WCG IRB #202029060) and the University of Georgia. The funding sources had no role in sample collection nor the decision to submit the paper for publication.

SPARTA Participant Selection

Eligible volunteers between the ages of 18 and 90 years old (y.o.) were recruited and enrolled with written informed consent beginning March, 2020. Participants in the SPARTA program were enrolled at four locations: Athens, GA, Augusta, GA, Los Angeles, CA, and Memphis, TN in the U.S., and blood and saliva samples were collected monthly. Participants were predominantly people in high-risk groups, such as health-care workers, first responders, the elderly, and university employees and students receiving in-person tuition. Exclusion criteria included being younger than 18 years old, weighing less than 110 lbs, being pregnant, being cognitively impaired, or having anemia or a blood-borne infectious condition such as hepatitis C or HIV. As of May 28, 2021, 3124 participants were enrolled in the study and enrollment is ongoing. 69.9% of the participants identified as female and 29.2% identified as male. The mean age was 43.7 years (range 18-90). 76.4% of the participants self-identified as White/Caucasian, 11.7% as Black/African-American, 8.1% as Asian, and 3.8% as other or multiple.

Of those participants, 40 were chosen based on their vaccination and infection status as well as serum availability, and assorted into age and vaccine-matched groups based on the presence of SARS-CoV-2 infection prior to vaccination. At the pre-vaccination timepoint, 20 of them were categorized as immunologically naïve to SARS-CoV-2, and reported no specific COVID-19 symptoms, never had a positive NAAT result, and tested negative for RBD-specific IgG antibodies

with concentrations below our experimentally determined threshold of 1.139μg/mL [see under *ROC analysis* heading] (**Table S1A**). The other 20 participants were immunologically pre-immune due to a previous SARS-CoV-2 infection prior to vaccination and reported COVID-19 symptoms, positive NAAT, and/or antibody concentrations above the threshold (**Table S1B**).

Serum samples were collected from 8 of the 20 pre-immune participants between the two vaccinations. In contrast, mid-vaccine serum was collected from only one of the 20 matched immunologically naïve participants. Therefore, an additional 12 immunologically naïve participants were selected who had a mid-vaccine timepoint, in order to statistically compare how a single vaccine dose affects antibody levels in immunologically naïve and pre-immune individuals (**Table S1C**). The mean age across all 52 participants was 45 y.o. (SD = 15.7, range = 24-72), with 57.7% female (n=30) and 42.3% male (n=22). 79% of the participants received the Pfizer-BioNTech BNT162b2 vaccine (n=41), while 21% received the Moderna mRNA-1273 vaccine (n=11) between December 18, 2020 and February 18, 2021.

Blood Collection and Processing

BD Vacutainer serum separation venous blood collection tubes (BD, Franklin Lakes, NJ, USA) containing whole blood were centrifuged at 2500 rpm for 10 min. After centrifugation, the supernatant serum layer was isolated and heat inactivated in a 56°C water bath for 45 min to disable any infectious SARS-CoV-2 virus (30). Serum was thereafter stored at -80°C.

Enzyme-Linked Immunosorbent Assay (ELISA)

Immulon® 4HBX plates (Thermo Fisher Scientific, Waltham, MA, USA) were coated with 100 ng/well of recombinant SARS-CoV-2 RBD protein in PBS overnight at 4°C in a humidified chamber. Plates were blocked with blocking buffer made with 2% bovine serum albumin (BSA) Fraction V (Thermo Fisher Scientific, Waltham, MA, USA) and 1% gelatin from bovine skin (Sigma-Aldrich, St. Louis, MO, USA) in PBS/0.05% Tween20 (Thermo Fisher Scientific, Waltham, MA, USA) at 37°C for 90 min. Serum samples from the participants were initially diluted 1:50 and then further serially diluted 1:3 in blocking buffer to generate a 4-point binding curve (1:50, 1:150, 1:450, 1:1350), and subsequently incubated overnight at 4°C in a humidified chamber. Plates were washed 5 times with PBS/0.05% Tween20 and IgG antibodies were detected using horseradish peroxidase (HRP)-conjugated goat anti-human IgG detection antibody (Southern Biotech, Birmingham, AL, USA) at a 1:4,000 dilution and incubated for 90 min at 37°C. Plates were then washed 5 times with PBS/0.05% Tween20 prior to development with 100μL of 0.1% 2,2'-azino-bis(3-ethylbenzothiazoline-6-sulphonic acid) (ABTS, Bioworld, Dublin, OH, USA) solution with 0.05% H_2O_2 for 18 minutes at 37°C. The reaction was terminated with 50μL of 1% (w/v) SDS (VWR International, Radnor, PA, USA). Colorimetric absorbance was measured at 414nm using a PowerWaveXS plate reader (Biotek, Winooski, VT, USA). All samples and controls were run in duplicate and the mean of the two blank-adjusted optical density (OD) values were used in downstream analyses. IgG equivalent concentrations were calculated based on a 7-point standard curve generated by a human IgG reference protein (Athens Research and Technology, Athens, GA, USA), and verified on each plate using human sera with known concentrations.

ROC Analysis and Threshold Determination Using a Validation Cohort

In order to distinguish between antibody positive and negative participants, ROC (receiver operating characteristic) analysis was performed on a validation cohort comprised of 22 NAAT-confirmed positive and 49 pre-pandemic human sera. Serum from NAAT-confirmed positive participants were obtained from samples intended to be discarded from a central Georgia hospital in May and June 2020, before SARS-CoV-2 vaccines became available. They were all between the ages of 22 and 60 (mean = 43.5 y.o.) with a nearly even female (n=11) to male ratio (n=10) with one participant whose gender was unknown (**Table S2**). All participants tested positive for the presence of SARS-CoV-2 viral RNA collected *via* nasopharyngeal swab by NAAT 9-74 days prior to the blood draw. In addition, the presence of any COVID-19 symptoms the participants had experienced at the time of the NAAT were recorded (**Table S2**). These symptoms included, but were not limited to fever, cough, chills, loss of taste or smell, and shortness of breath. The pre-pandemic sera were collected between 2013 and 2018. The threshold between positives and negatives was chosen at the antibody concentration corresponding to the most similar sensitivity and specificity values, in order to balance false positive and false negative rates. Linear regression and correlation analyses were applied to test the relationship between anti-RBD IgG antibody concentrations (ELISA) and VN endpoint titers. All analyses were performed using GraphPad Prism 9.1.1 (RRID:SCR_002798).

Viral Neutralization Assay

All research activities using infectious SARS-CoV-2 virus occurred in a Biosafety Level 3 (BSL-3) laboratory in the Animal Health Research Center at the University of Georgia (Athens, GA, USA). The USA-WA1/2020 SARS-CoV-2 strain (NCBI accession number: PRJNA717311) was propagated as previously described (31). 50μl of two-fold serially diluted serum (1:5–1:640 or 1:50–1:6400 depending on the magnitude of antibody binding concentration and vaccination status) was incubated with the SARS-CoV-2 virus (100 TCID50/50μl) for 1 h at 37°C. The serum-virus mixture was then transferred to Vero E6 cells in 96-well cell culture plates. The plates were observed for 3 days for cytopathic effects (CPEs), such as the aggregation and detachment of cells. The VN endpoint titer was determined as the reciprocal of the highest dilution that completely inhibited CPE formation. All neutralization titers were represented as the average of the five replicates.

Statistical Comparison of Participant Groups

Statistical difference between pre-, mid-, and post-vaccination timepoints for both the immunologically naïve and the infected

cohorts were determined using a paired *t*-test, while the difference between the post-vaccination timepoints of immunologically naïve and infected participants was determined using an unpaired *t*-test. The pre-vaccination timepoints occurred at least 1 day prior to receiving the first dose of an mRNA vaccine (mean = 32.6 days, range = 1–99 days), mid-vaccination timepoints occurred between the administration of the two vaccinations (mean = 13.5 days, range = 4-26 days), while post-vaccination timepoints occurred a minimum of 14 days after the administration of the second dose of the same mRNA vaccine (mean = 28.8 days, range = 4–51 days). Statistical analyses were performed using GraphPad 9.1.1, and statistical significance was represented by $^{*}p<0.05$, $^{**}p<0.01$, $^{***}p<0.001$, and $^{****}p<0.0001$.

RESULTS

In order to establish the threshold value between participants with positive and negative RBD-binding IgG antibody levels, a ROC analysis based on serum from the validation cohort of 49 pre-pandemic negative participants and 22 confirmed NAAT positive, non-vaccinated participants was performed. The threshold between negative and positive anti-RBD IgG antibody concentrations was set at 1.139μg/mL, yielding a sensitivity of 95.5% and a specificity of 95.9% (**Figures 1A, B**).

Further investigation into this validation cohort demonstrated that VN was absent in all participants with anti-RBD IgG antibody concentrations below the threshold, while all participants above the threshold showed some level of VN (**Figure 2A**), and there was a strong correlation between ELISA binding and VN (r=0.9125, $p<0.0001$). Similarly, a strong positive relationship was observed between the antibody binding and neutralization levels for all timepoints of the 53 SPARTA participants from this study (r=0.9359, $p<0.0001$) (**Figure 2B**).

Using the experimentally determined threshold of 1.139μg/mL, 40 age-matched and vaccine-matched participants were selected, 20 of whom were immunologically naïve to SARS-CoV-2 prior to receiving a complete mRNA vaccine regimen, while the other 20 were pre-immune with signs of prior SARS-CoV-2 infection before vaccination. None of the immunologically naïve participants had any documented history of COVID-19, while 16 out of the 20 participants in the pre-immune group have reported COVID-19 symptoms or a positive NAAT. The remaining 4 were asymptomatic but had elevated RBD IgG antibody titers (**Tables S1A, B**).

VN of the pre-vaccination and post-vaccination serum samples collected from these 40 participants demonstrated that vaccinations significantly increased the VN titer of both immunologically naïve and pre-immune participants ($p<0.0001$) (**Figure 3A**). Interestingly, after vaccination, the neutralizing antibody titer of pre-immune individuals was significantly higher than the neutralizing antibody titer of immunologically naïve individuals ($p<0.0001$) (**Figure 3A**). The post-vaccination neutralization titers for immunologically naïve participants ranged from 1:5–1:400, while the post-vaccination neutralization titers in pre-immune participants ranged from 1:400–1:3200. The highest tested VN titer was 1:6400, but all participants demonstrated some level of CPE at this dilution point.

Similarly, there were significant increases in RBD-binding antibody concentrations due to vaccination in both the immunologically naïve and pre-immune groups ($p<0.0001$) (**Figure 3B**). The difference in post-vaccination antibody concentrations between immunologically naïve and pre-immune participants was less pronounced than demonstrated by VN titers, but antibody concentrations were still significantly

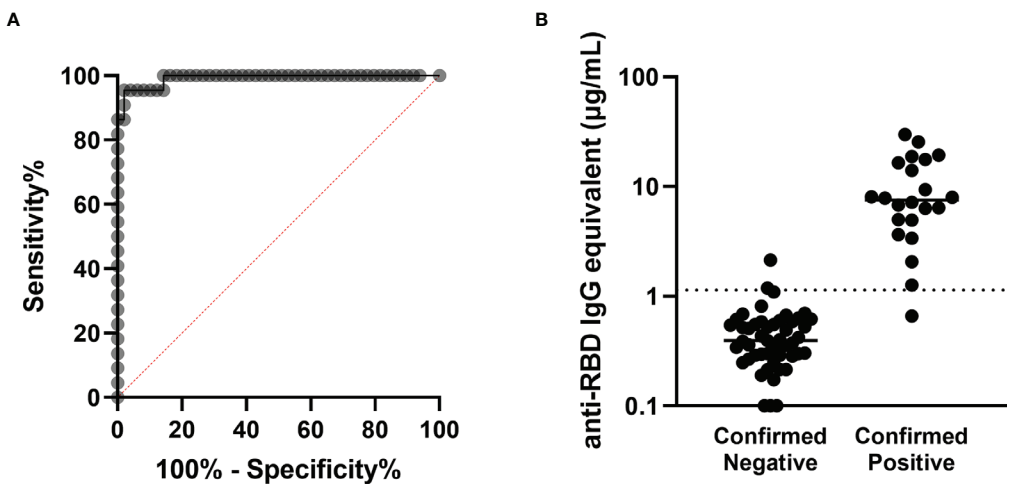

FIGURE 1 | Determination of the antibody concentration threshold based on the validation cohort. **(A)** ROC analysis based on the 22 confirmed positive and 49 confirmed negative sera comprising the validation cohort. The area under the curve is 0.9917 ($^{****}p < 0.0001$), and the sensitivity and specificity of this assay were determined to be 95.5% and 95.9% respectively, with the threshold between negative and positive set at 1.139μg/mL. **(B)** Anti-RBD antibody concentrations are shown for each participant in the validation cohort, sorted into negatives and positives based on prior confirmed COVID-19 status. The threshold is marked with the horizontal dotted line.

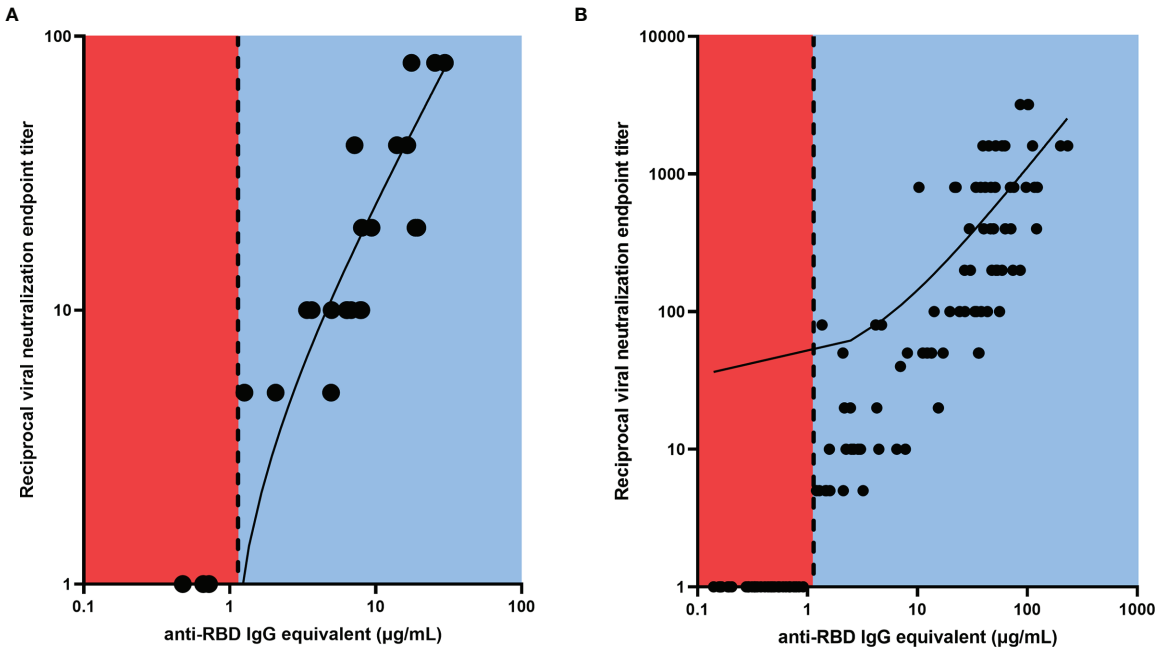

FIGURE 2 | Linear regression between RBD-binding IgG antibody concentration and reciprocal VN endpoint titer. There was a strong positive relationship between antibody binding and VN titer for **(A)** the validation cohort (r = 0.9125, ****p < 0.0001), and **(B)** the SPARTA cohort (r = 0.9359, ****p < 0.0001). The vertical dotted line represents the threshold between negative and positive antibody concentrations, determined by the ROC analysis. No participants below the threshold demonstrated any neutralizing activity, while all participants above the threshold showed some level of VN. In order to represent the values on a logarithmic scale, lack of neutralization was reported as 1.

higher in pre-immune participants (p=0.0033) (**Figure 3B**). Additionally, post-vaccination antibody levels for naïve participants were significantly higher than the antibody levels elicited by natural infection, as shown in both neutralizing (p<0.0001) and binding (p<0.0001) antibody concentrations.

Eight of the 20 participants in the age-matched pre-immune cohort had serum collected between the first and the second vaccinations (**Table S1B**). These timepoints ranged between 4 and 16 days after the first vaccination with a mean of 10.8 days (SD = 4.6). These previously infected participants had a significant increase in both VN titers (p=0.002) and RBD-binding IgG antibody concentrations (p=0.03) following the first vaccination, but there was no further significant change in RBD-binding or neutralizing antibody titers following the second vaccination (p=0.69) (**Figures 4A, B**).

Only one of the 20 naïve participants from the age-matched cohort had available samples collected between the two vaccinations (**Table S1A**). Therefore, an additional 12 participants were selected that had samples collected 9–26 days after the first vaccination (mean = 15.8 days, SD = 5.3 days), but prior to the second vaccination. Overall, there was a significant increase in neutralizing and RBD-binding antibody titers following both the first (p=0.0074 and p=0.02 respectively) and second vaccinations (p=0.0006 and p=0.0001 respectively) (**Figures 4C, D**). However, 46% of these participants (n=6) had no detectable neutralizing activity or anti-RBD IgG antibodies after the administration of the first vaccination (mean = 12 days after the first vaccination, SD = 3.7 days, range = 9–18 days). These participants only seroconverted after receiving the second vaccination. The remaining participants (54%, n=7) exhibited a low level of positive neutralizing and binding antibody levels following the first vaccination (mean = 19 days after the first day, SD = 4.3 days, range = 12–26 days). There was a significant rise in neutralizing and anti-RBD IgG antibody levels following the second vaccination (p=0.023 and p=0.009 respectively).

DISCUSSION

Accurately tracking serological responses in people infected with or vaccinated against SARS-CoV-2 is critical in assessing the effectiveness of the induced immunity, which can subsequently inform public health decisions. Following SARS-CoV-2 infection, there is an expansion of B and T cells directed at various antigens in the virus, especially the receptor binding domain of the highly immunogenic spike protein (13, 15–17). Currently, COVID-19 vaccines authorized in the U.S. include the spike protein as the vaccine antigen that elicits protective immunity (8, 9). In this study, we examined the serological responses elicited by immunologically naïve or previously infected pre-immune individuals who were subsequently vaccinated with mRNA-based COVID-19 vaccines.

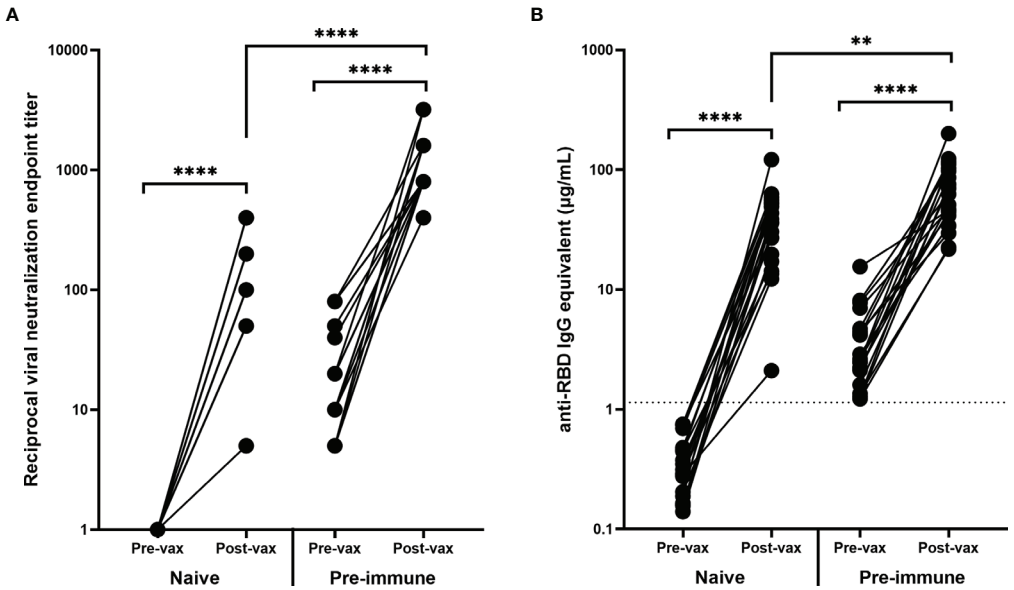

FIGURE 3 | Antibody response before and after vaccination. Vaccination significantly increased the **(A)** VN and **(B)** RBD-binding antibody levels of all participants regardless of pre-vaccination naïve (n = 20) or pre-immune (n = 20) status (****$p < 0.0001$). The post-vaccination VN and anti-RBD IgG levels for participants who were pre-immune prior to vaccination were significantly higher (****$p < 0.0001$ and **$p < 0.01$ respectively). Post-vaccination timepoints took place a minimum of 14 days after the administration of the second mRNA vaccination. In order to represent the values on a logarithmic scale, lack of neutralization was reported as 1.

RBD was chosen over the full-length spike protein as the antigenic target for binding assay to determine antibody positive responses. Anti-RBD antibodies have lower cross-reactivity and background binding by ELISA compared to anti-spike antibodies. This results in a higher overall sensitivity and specificity for the assay. While the full-length spike protein has a larger number of epitopes that antibodies can bind which may correspond to higher antibody titers, other groups indicated that most individuals tested positive or negative for both anti-RBD and anti-spike antibodies with few individuals testing positive for one but not the other (32, 33). Similarly, our validation cohort showed that anti-RBD and anti-spike antibody results were congruent.

Serological protection conferred by vaccination was significantly more robust compared to antibodies induced by natural viral infection. Both total anti-RBD IgG binding, as well as *in vitro* neutralizing activity were stronger in vaccinated subjects (34). The immune system may respond more efficiently to a single protein during vaccination, allowing for a more focused immune response to fewer epitopes, compared to the array of viral proteins and epitopes present during natural infection. Moreover, vaccination elicited higher antibody titers in participants who were pre-immune to SARS-CoV-2 compared to those who were immunologically naïve. This robust and immediate recall of high affinity antibodies may be attributed to memory B cell mediated processes (35), similar to immune responses shown in other infectious agents (36, 37), as well as in antibody binding to SARS-CoV-2 (35, 38) and in neutralization assays performed using a pseudo-typed virus displaying SARS-CoV-2 spike protein (23). These findings highlight the importance of vaccination, especially in light of reports of short-term protection and abundant cases of reinfections after antibodies elicited by natural infection (39, 40).

A single vaccination with an mRNA vaccine was sufficient to significantly increase the neutralization titer in humans previously infected with SARS-CoV-2 (41). Anti-RBD antibody binding and VN supported the conclusion that all 8 pre-immune participants examined in this study had a significant increase in antibody levels prior to the administration of the second vaccination with no further significant change in antibody levels after the second vaccination. Not only did the first vaccination yield a more significant rise in antibody levels in pre-immune participants compared to immunologically naïve participants, pre-immune individuals had a more rapid rise following the first vaccination, with some individuals experiencing a significant increase in antibody titer in just 4 days after the first vaccination. Such a rapid increase in IgG levels in serum so soon after vaccination most likely indicates a memory cell-driven response that was recalled from a prior natural infection (42–44).

Immunologically naïve participants could be categorized into two groups: individuals that seroconverted before the second vaccination, and those who did not seroconvert until after the second vaccination. This is likely due to the timing of the blood collection. In general, serum samples collected earlier after the first vaccination (average = 12 days, range = 9-18 days) had no change in antibody levels, while participants with later blood collections (average = 19 days, range = 12-26 days) tended to have an increase in antibody titers. There was a significant positive correlation between the number of days

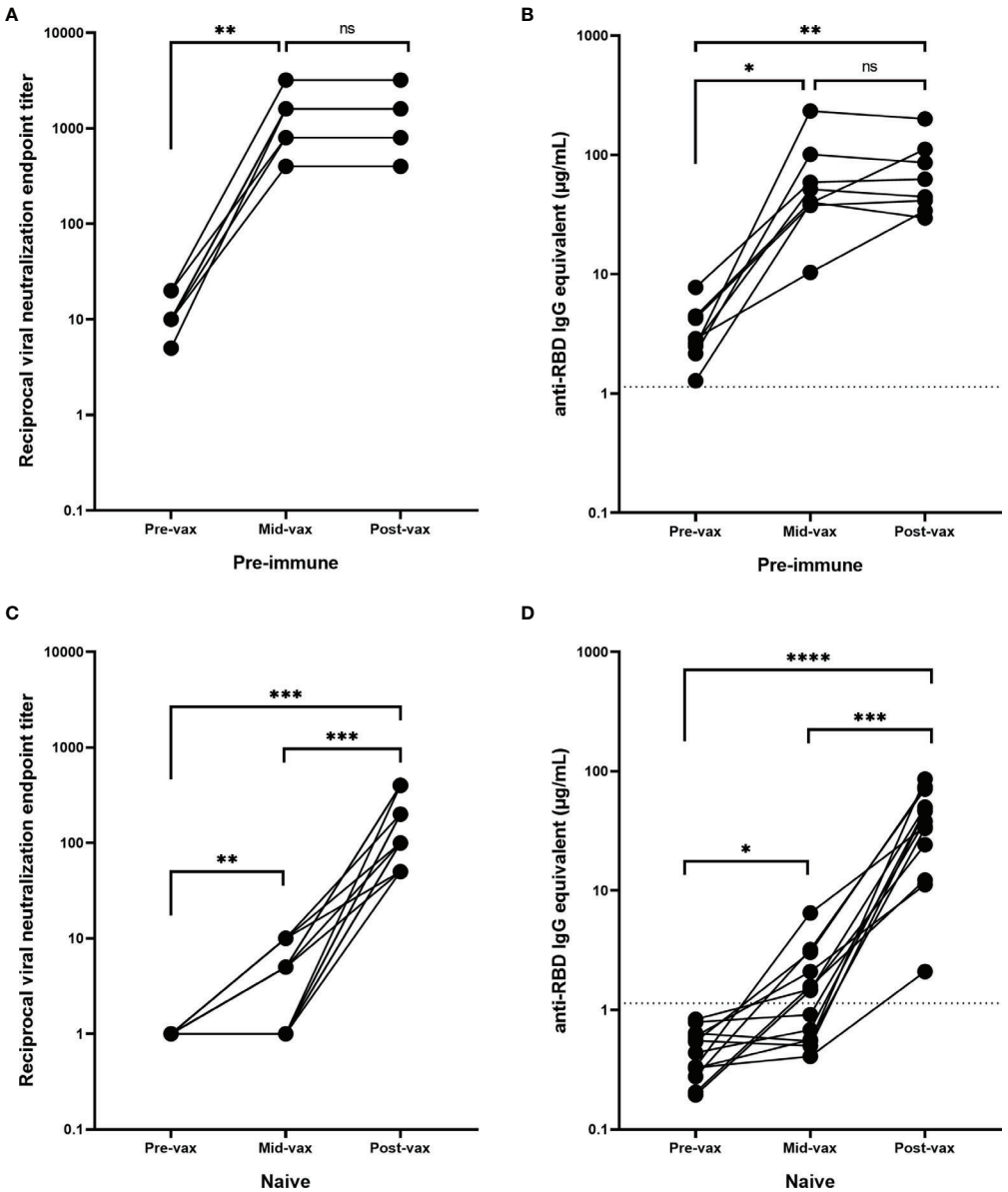

FIGURE 4 | Antibody response during vaccination. Pre-immune participants (n = 8) with serum obtained between the two mRNA vaccinations (mid-vax) have demonstrated a significant increase in **(A)** neutralizing (**p = 0.002) and **(B)** anti-RBD antibody levels (*p = 0.03) before the second vaccination was administered, and there was no significant change (ns) in antibody titer in response to the second vaccination (p = 0.69). Immunologically naïve participants (n = 13) with serum obtained between the two mRNA vaccinations have demonstrated a significant increase in **(C)** neutralizing (***p = 0.0005), and **(D)** binding antibody levels (****p < 0.0001). Six of them showed no neutralizing activity before the second vaccination was administered. While the other 7 showed a significant increase (**p = 0.0074) and exhibited a low level of neutralization even after the first vaccination, the second vaccination was still crucial in boosting antibody levels (***p = 0.0006). In order to represent the values on a logarithmic scale, lack of neutralization was reported as 1.

after the first vaccination that the serum was taken and the antibody level (**Figures S1A, B**), while the same trend was less apparent in infected participants (**Figures S1C, D**). Other research groups have shown similar trends because later serum collections allowed additional time for the immune system to mount a *de novo* response to the vaccine antigens (45). However, there was no correlation between the number of days after the second vaccination and the titer level amongst immunologically naïve (**Figures S1E, F**) or pre-immune participants (**Figures S1G, H**).

Even though there was no significant change in antibody levels in pre-immune participants in response to the second vaccination, delaying or even skipping the second vaccination may have unknown, long-term effects that have not yet been explored. The longevity of antibodies or the quantity and quality of the memory B cells could be impaired compared to

participants who received a full vaccine regimen, and there could be additional long-term advantages for fully vaccinated participants even when short-term serological benefits are not immediately apparent.

The limitations of this study included having a range of time points for serum collection as opposed to a pre-determined number of days after vaccination. Also, there was only one of the 20 immunologically naïve participants with serum collected between vaccinations in the age matched cohort, necessitating the addition of 12 non-age matched participants with available serum in order to increase the power of our study. In addition, the diversity of our naïve and pre-immune cohorts was low due to the low number of vaccinated participants available at the time of study, most of whom were Caucasian.

Overall, this study validated a robust ELISA assay for detecting SARS-CoV-2 anti-RBD IgG antibody binding with high sensitivity and specificity in human sera. Using a set of serum samples collected from 20 immunologically naïve and 20 pre-immune age-matched and vaccine-matched participants, it was demonstrated that vaccination with SARS-CoV-2 mRNA vaccines elicits higher serological binding and neutralizing antibody levels than non-vaccinated individuals who were naturally infected. Furthermore, a single vaccination was sufficient to boost pre-immune participants and the second vaccination did not further increase their antibody levels. In immunologically naïve participants, ~50% of participants had no significant rise in antibody titers until after the administration of the second vaccination, while the other half whose titers started to rise prior to the second vaccination were significantly boosted further by receiving the second vaccination. Future studies will assess the longevity and magnitude of anti-RBD and neutralizing antibody titers after vaccination between immunologically naïve and pre-immune individuals.

DATA AVAILABILITY STATEMENT

The original contributions presented in the study are included in the article/**Supplementary Material**. Further inquiries can be directed to the corresponding author.

ETHICS STATEMENT

The studies involving human participants were reviewed and approved by Western Institutional Review Board. The patients/participants provided their written informed consent to participate in this study.

AUTHOR CONTRIBUTIONS

DF was responsible for the conceptualization, methodology, validation, formal analysis, investigation, writing, and editing of the manuscript. HJ was responsible for the methodology, validation, investigation, writing, and editing of the manuscript. RA was responsible for the methodology, validation, and editing of the manuscript. HH was responsible for the resources, writing, and editing of the manuscript. JG was responsible for the investigation and writing of the manuscript. AJ was responsible for the validation and investigation of the study. TR was responsible for the conceptualization, resources, project administration, funding acquisition, writing, and editing of the manuscript. All authors contributed to the article and approved the submitted version.

FUNDING

This study was funded, in part, by the University of Georgia (US) (UGA-001), and by the National Institute of Allergy and Infectious Diseases (NIAID), a component of the U.S. National Institutes of Health (NIH), Department of Health and Human Services, under contract 75N93019C00052. In addition, TR is supported by the Georgia Research Alliance as an eminent scholar (GRA-001).

ACKNOWLEDGMENTS

The authors would like to thank the SPARTA collection and processing teams in Athens and Augusta, GA, as well as Debbie Bratt for program coordination. The authors also thank Katie Mailloux, Jasmine Burris, Omar Hamwy, Hua Shi, Naveen Gokanapudi, Lillian Buescher, Patrick Fagan, Brittany Baker, Charlotte Bolle, Courtney Briggs, Tejal Hill, Jordan Byrne, and Lauren Howland for technical assistance. We acknowledge the staff at the Animal Health Research Center at the University of Georgia for the upkeep and maintenance of the BSL-3 facilities. The recombinant proteins were produced by Jeffrey Ecker, Spencer Pierce, Ethan Cooper, and the team in the Center for Vaccines and Immunology protein production core. We would also like to thank all participants enrolled in the study, as well as Dr. Brad Phillips, Kimberly Schmitz, and the entire staff at the University of Georgia Clinical and Translational Research Unit (CTRU) for assistance in collecting samples in the SPARTA program. The CTRU was supported by the National Center for Advancing Translational Sciences of the National Institutes of Health under Award Number UL1TR002378.

SUPPLEMENTARY MATERIAL

The Supplementary Material for this article can be found online at: https://www.frontiersin.org/articles/10.3389/fimmu.2021.728021/full#supplementary-material

REFERENCES

1. Zhu N, Zhang D, Wang W, Li X, Yang B, Song J, et al. A Novel Coronavirus From Patients With Pneumonia in China, 2019. *N Engl J Med* (2020) 382:727–33. doi: 10.1056/NEJMoa2001017
2. Gorbalenya AE, Baker SC, Baric RS, de Groot RJ, Drosten C, Gulyaeva AA, et al. The Species Severe Acute Respiratory Syndrome-Related Coronavirus: Classifying 2019-Ncov and Naming it SARS-CoV-2. *Nat Microbiol* (2020) 5:536–44. doi: 10.1038/s41564-020-0695-z
3. Chen Y, Liu Q, Guo D. Emerging Coronaviruses: Genome Structure, Replication, and Pathogenesis. *J Med Virol* (2020) 92:418–23. doi: 10.1002/jmv.25681
4. Li W, Moore MJ, Vasilieva N, Sui J, Wong SK, Berne MA, et al. Angiotensin-Converting Enzyme 2 Is a Functional Receptor for the SARS Coronavirus. *Nature* (2003) 426:450–4. doi: 10.1038/nature02145
5. Lan J, Ge J, Yu J, Shan S, Zhou H, Fan S, et al. Structure of the SARS-CoV-2 Spike Receptor-Binding Domain Bound to the ACE2 Receptor. *Nature* (2020) 581:215–20. doi: 10.1038/s41586-020-2180-5
6. Huang Y, Yang C, Xu X-F, Xu W, Liu S-W. Structural and Functional Properties of SARS-CoV-2 Spike Protein: Potential Antivirus Drug Development for COVID-19. *Acta Pharmacol Sin* (2020) 41:1141–9. doi: 10.1038/s41401-020-0485-4
7. Hoffmann M, Kleine-Weber H, Schroeder S, Krüger N, Herrler T, Erichsen S, et al. SARS-CoV-2 Cell Entry Depends on ACE2 and TMPRSS2 and is Blocked by a Clinically Proven Protease Inhibitor. *Cell* (2020) 181:271–80.e8. doi: 10.1016/j.cell.2020.02.052
8. Polack FP, Thomas SJ, Kitchin N, Absalon J, Gurtman A, Lockhart S, et al. Safety and Efficacy of the BNT162b2 mRNA COVID-19 Vaccine. *N Engl J Med* (2020) 383:2603–15. doi: 10.1056/NEJMoa2034577
9. Baden LR, El Sahly HM, Essink B, Kotloff K, Frey S, Novak R, et al. Efficacy and Safety of the mRNA-1273 SARS-CoV-2 Vaccine. *N Engl J Med* (2021) 384:403–16. doi: 10.1056/NEJMoa2035389
10. Meo SA, Bukhari IA, Akram J, Meo AS, Klonoff DC. COVID-19 Vaccines: Comparison of Biological, Pharmacological Characteristics and Adverse Effects of Pfizer/BioNTech and Moderna Vaccines. *Eur Rev Med Pharmacol Sci* (2021) 25:1663–9. doi: 10.26355/eurrev_202102_24877
11. Zhao J, Zhao S, Ou J, Zhang J, Lan W, Guan W, et al. COVID-19: Coronavirus Vaccine Development Updates. *Front Immunol* (2020) 11:602256. doi: 10.3389/fimmu.2020.602256
12. Henderson R, Edwards RJ, Mansouri K, Janowska K, Stalls V, Gobeil SMC, et al. Controlling the SARS-CoV-2 Spike Glycoprotein Conformation. *Nat Struct Mol Biol* (2020) 27:925–33. doi: 10.1038/s41594-020-0479-4
13. Ravichandran S, Coyle EM, Klenow L, Tang J, Grubbs G, Liu S, et al. Antibody Signature Induced by SARS-CoV-2 Spike Protein Immunogens in Rabbits. *Sci Transl Med* (2020) 12:eabc3539. doi: 10.1126/scitranslmed.abc3539
14. Zeng Q, Huang G, Li Y, Xu Y. Tackling COVID19 by Exploiting Pre-Existing Cross-Reacting Spike-Specific Immunity. *Mol Ther* (2020) 28:2314–5. doi: 10.1016/j.ymthe.2020.09.035
15. Ju B, Zhang Q, Ge J, Wang R, Sun J, Ge X, et al. Human Neutralizing Antibodies Elicited by SARS-CoV-2 Infection. *Nature* (2020) 584:115–9. doi: 10.1038/s41586-020-2380-z
16. Zost SJ, Gilchuk P, Case JB, Binshtein E, Chen RE, Nkolola JP, et al. Potently Neutralizing and Protective Human Antibodies Against SARS-CoV-2. *Nature* (2020) 584:443–9. doi: 10.1038/s41586-020-2548-6
17. Perera RA, Mok CK, Tsang OT, Lv H, Ko RL, Wu NC, et al. Serological Assays for Severe Acute Respiratory Syndrome Coronavirus 2 (SARS-CoV-2), March 2020. *Eurosurveillance* (2020) 25:2000421. doi: 10.2807/1560-7917.ES.2020.25.16.2000421
18. Walsh EE, Frenck RWJr., Falsey AR, Kitchin N, Absalon J, Gurtman A, et al. Safety and Immunogenicity of Two RNA-Based COVID-19 Vaccine Candidates. *N Engl J Med* (2020) 383:2439–50. doi: 10.1056/NEJMoa2027906
19. Xia X. Domains and Functions of Spike Protein in SARS-CoV-2 in the Context of Vaccine Design. *Viruses* (2021) 13:109. doi: 10.3390/v13010109
20. Wrapp D, Wang N, Corbett KS, Goldsmith JA, Hsieh C-L, Abiona O, et al. Cryo-EM Structure of the 2019-Ncov Spike in the Prefusion Conformation. *Science* (2020) 367:1260–3. doi: 10.1126/science.abb2507
21. Heine A, Juranek S, Brossart P. Clinical and Immunological Effects of mRNA Vaccines in Malignant Diseases. *Mol Cancer* (2021) 20:52. doi: 10.1186/s12943-021-01339-1
22. Thompson MG, Burgess JL, Naleway AL, Tyner HL, Yoon SK, Meece J, et al. Interim Estimates of Vaccine Effectiveness of BNT162b2 and mRNA-1273 COVID-19 Vaccines in Preventing SARS-CoV-2 Infection Among Health Care Personnel, First Responders, and Other Essential and Frontline Workers-Eight US Locations, December 2020-March 2021. *MMWR Morb Mortal Wkly Rep* (2021) 70:495–500. doi: 10.15585/mmwr.mm7013e3
23. Goel RR, Apostolidis SA, Painter MM, Mathew D, Pattekar A, Kuthuru O, et al. Distinct Antibody and Memory B Cell Responses in SARS-CoV-2 Naïve and Recovered Individuals Following mRNA Vaccination. *Sci Immunol* (2021) 6:eabi6950. doi: 10.1126/sciimmunol.abi6950
24. Johnson M, Wagstaffe HR, Gilmour KC, Mai AL, Lewis J, Hunt A, et al. Evaluation of a Novel Multiplexed Assay for Determining IgG Levels and Functional Activity to SARS-CoV-2. *J Clin Virol* (2020) 130:104572. doi: 10.1016/j.jcv.2020.104572
25. Pısıl Y, Shida H, Miura T. A Neutralization Assay Based on Pseudo-Typed Lentivirus With SARS CoV-2 Spike Protein in ACE2-Expressing CRFK Cells. *Pathogens* (2021) 10:153. doi: 10.3390/pathogens10020153
26. von Rhein C, Scholz T, Henss L, Kronstein-Wiedemann R, Schwarz T, Rodionov RN, et al. Comparison of Potency Assays to Assess SARS-CoV-2 Neutralizing Antibody Capacity in COVID-19 Convalescent Plasma. *J Virol Methods* (2021) 288:114031. doi: 10.1016/j.jviromet.2020.114031
27. Rathe JA, Hemann EA, Eggenberger J, Li Z, Knoll ML, Stokes C, et al. SARS-CoV-2 Serologic Assays in Control and Unknown Populations Demonstrate the Necessity of Virus Neutralization Testing. *J Infect Dis* (2021) 223:1120–31. doi: 10.1093/infdis/jiaa797
28. Ebinger JE, Fert-Bober J, Printsev I, Wu M, Sun N, Prostko JC, et al. Antibody Responses to the BNT162b2 mRNA Vaccine in Individuals Previously Infected With SARS-CoV-2. *Nat Med* (2021) 27:981–4. doi: 10.1038/s41591-021-01325-6
29. Stamatatos L, Czartoski J, Wan Y-H, Homad LJ, Rubin V, Glantz H, et al. mRNA Vaccination Boosts Cross-Variant Neutralizing Antibodies Elicited by SARS-CoV-2 Infection. *Science* (2021) 372:1413–8. doi: 10.1126/science.abg9175
30. Pastorino B, Touret F, Gilles M, de Lamballerie X, Charrel RN. Heat Inactivation of Different Types of SARS-CoV-2 Samples: What Protocols for Biosafety, Molecular Detection and Serological Diagnostics? *Viruses* (2020) 12:735. doi: 10.3390/v12070735
31. Jureka A, Silvas J, Basler C. Propagation, Inactivation, and Safety Testing of SARS-CoV-2. *Viruses* (2020) 12:622. doi: 10.3390/v12060622
32. Premkumar L, Segovia-Chumbez B, Jadi R, Martinez DR, Raut R, Markmann A, et al. The Receptor Binding Domain of the Viral Spike Protein Is an Immunodominant and Highly Specific Target of Antibodies in SARS-CoV-2 Patients. *Sci Immunol* (2020) 5:eabc8413. doi: 10.1126/sciimmunol.abc8413
33. Amanat F, Stadlbauer D, Strohmeier S, Nguyen THO, Chromikova V, McMahon M, et al. A Serological Assay to Detect SARS-CoV-2 Seroconversion in Humans. *Nat Med* (2020) 26:1033–6. doi: 10.1038/s41591-020-0913-5
34. Edara VV, Hudson WH, Xie X, Ahmed R, Suthar MS. Neutralizing Antibodies Against SARS-CoV-2 Variants After Infection and Vaccination. *JAMA* (2021) 325:1896–8. doi: 10.1001/jama.2021.4388
35. Abu Jabal K, Ben-Amram H, Beiruti K, Batheesh Y, Sussan C, Zarka S, et al. Impact of Age, Ethnicity, Sex and Prior Infection Status on Immunogenicity Following a Single Dose of the BNT162b2 mRNA COVID-19 Vaccine: Real-World Evidence From Healthcare Workers, Israel, December 2020 to January 2021. *Eurosurveillance* (2021) 26:2100096. doi: 10.2807/1560-7917.ES.2021.26.6.2100096
36. Luabeya AKK, Kagina BMN, Tameris MD, Geldenhuys H, Hoff ST, Shi Z, et al. First-In-Human Trial of the Post-Exposure Tuberculosis Vaccine H56: IC31 in Mycobacterium Tuberculosis Infected and non-Infected Healthy Adults. *Vaccine* (2015) 33:4130–40. doi: 10.1016/j.vaccine.2015.06.051
37. Hussein J, Zewdie M, Yamuah L, Bedru A, Abebe M, Dagnew AF, et al. A Phase I, Open-Label Trial on the Safety and Immunogenicity of the Adjuvanted Tuberculosis Subunit Vaccine H1/IC31® in People Living in a TB-Endemic Area. *Trials* (2018) 19:24. doi: 10.1186/s13063-017-2354-0

38. Krammer F, Srivastava K, Alshammary H, Amoako AA, Awawda MH, Beach KF, et al. Antibody Responses in Seropositive Persons After a Single Dose of SARS-CoV-2 mRNA Vaccine. *N Engl J Med* (2021) 384:1372–4. doi: 10.1056/NEJMc2101667
39. Babiker A, Marvil CE, Waggoner JJ, Collins MH, Piantadosi A. The Importance and Challenges of Identifying SARS-CoV-2 Reinfections. *J Clin Microbiol* (2021) 59:e02769–20. doi: 10.1128/JCM.02769-20
40. Cromer D, Juno JA, Khoury D, Reynaldi A, Wheatley AK, Kent SJ, et al. Prospects for Durable Immune Control of SARS-CoV-2 and Prevention of Reinfection. *Nat Rev Immunol* (2021) 21:395–404. doi: 10.1038/s41577-021-00550-x
41. Lustig Y, Nemet I, Kliker L, Zuckerman N, Yishai R, Alroy-Preis S, et al. Neutralizing Response Against Variants After SARS-CoV-2 Infection and One Dose of BNT162b2. *N Engl J Med* (2021) 384:2453–4. doi: 10.1056/NEJMc2104036
42. Kurosaki T, Kometani K, Ise W. Memory B Cells. *Nat Rev Immunol* (2015) 15:149–59. doi: 10.1038/nri3802
43. Crotty S, Aubert RD, Glidewell J, Ahmed R. Tracking Human Antigen-Specific Memory B Cells: A Sensitive and Generalized ELISPOT System. *J Immunol Methods* (2004) 286:111–22. doi: 10.1016/j.jim.2003.12.015
44. Seifert M, Küppers R. Human Memory B Cells. *Leukemia* (2016) 30:2283–92. doi: 10.1038/leu.2016.226
45. Hall VJ, Foulkes S, Saei A, Andrews N, Oguti B, Charlett A, et al. COVID-19 Vaccine Coverage in Health-Care Workers in England and Effectiveness of BNT162b2 mRNA Vaccine Against Infection (SIREN): A Prospective, Multicentre, Cohort Study. *Lancet* (2021) 397:1725–35. doi: 10.1016/S0140-6736(21)00790-X

Author Disclaimer: The content is solely the responsibility of the authors and does not necessarily represent the official views of the NIH.

Conflict of Interest: The authors declare that the research was conducted in the absence of any commercial or financial relationships that could be construed as a potential conflict of interest.

Publisher's Note: All claims expressed in this article are solely those of the authors and do not necessarily represent those of their affiliated organizations, or those of the publisher, the editors and the reviewers. Any product that may be evaluated in this article, or claim that may be made by its manufacturer, is not guaranteed or endorsed by the publisher.

frontiers in Immunology

ORIGINAL RESEARCH
published: 26 October 2021
doi: 10.3389/fimmu.2021.750386

Isolation and Characterization of Mouse Monoclonal Antibodies That Neutralize SARS-CoV-2 and Its Variants of Concern Alpha, Beta, Gamma and Delta by Binding Conformational Epitopes of Glycosylated RBD With High Potency

*Sabrina Mariotti[1†], Antonio Capocefalo[2†], Maria Vincenza Chiantore[1†], Angelo Iacobino[1†], Raffaela Teloni[1], Maria Laura De Angelis[3], Alessandra Gallinaro[4], Maria Franca Pirillo[4], Martina Borghi[1], Andrea Canitano[4], Zuleika Michelini[4], Melissa Baggieri[1], Antonella Marchi[1], Paola Bucci[1], Paul F. McKay[5], Chiara Acchioni[1], Silvia Sandini[1], Marco Sgarbanti[1], Fabio Tosini[1], Antonio Di Virgilio[6], Giulietta Venturi[1], Francesco Marino[7], Valeria Esposito[7], Paola Di Bonito[1], Fabio Magurano[1], Andrea Cara[4], Donatella Negri[1] and Roberto Nisini[1]**

[1] Dipartimento di Malattie infettive, Istituto Superiore di Sanità, Roma, Italy, [2] Dipartimento Sicurezza alimentare, nutrizione e sanità pubblica veterinaria, Istituto Superiore di Sanità, Roma, Italy, [3] Dipartimento di Oncologia e Medicina Molecolare, Istituto Superiore di Sanità, Roma, Italy, [4] Centro nazionale per la salute globale, Istituto Superiore di Sanità, Roma, Italy, [5] Department of Infectious Disease, Imperial College, London, United Kingdom, [6] Centro per la sperimentazione ed il benessere animale, Istituto Superiore di Sanità, Roma, Italy, [7] Centro nazionale per il controllo e la valutazione dei farmaci, Istituto Superiore di Sanità, Roma, Italy

Antibodies targeting Receptor Binding Domain (RBD) of SARS-CoV-2 have been suggested to account for the majority of neutralizing activity in COVID-19 convalescent sera and several neutralizing antibodies (nAbs) have been isolated, characterized and proposed as emergency therapeutics in the form of monoclonal antibodies (mAbs). However, SARS-CoV-2 variants are rapidly spreading worldwide from the sites of initial identification. The variants of concern (VOC) B.1.1.7 (Alpha), B.1.351 (Beta), P.1 (Gamma) and B.1.167.2 (Delta) showed mutations in the SARS-CoV-2 spike protein potentially able to cause escape from nAb responses with a consequent reduction of efficacy of vaccines and mAbs-based therapy. We produced the recombinant RBD (rRBD) of SARS-CoV-2 spike glycoprotein from the Wuhan-Hu 1 reference sequence in a mammalian system, for mice immunization to isolate new mAbs with neutralizing activity. Here we describe four mAbs that were able to bind the rRBD in Enzyme-Linked Immunosorbent Assay and the transmembrane full-length spike protein expressed in HEK293T cells by flow cytometry assay. Moreover, the mAbs recognized the RBD in supernatants of SARS-CoV-2 infected VERO E6 cells by Western Blot under non-reducing condition or in supernatants of cells infected with lentivirus pseudotyped for spike protein, by immunoprecipitation assay. Three out of four mAbs lost their binding efficiency to completely N-deglycosylated rRBD

OPEN ACCESS

Edited by:
Raymund Razonable, Mayo Clinic, United States

Reviewed by:
Hans De Haard, argenx BVBA, Belgium
Marc Paul Girard, Université Paris Diderot, France

***Correspondence:**
Roberto Nisini
roberto.nisini@iss.it

[†]These authors have contributed equally to this work

Specialty section:
This article was submitted to Vaccines and Molecular Therapeutics, a section of the journal Frontiers in Immunology

Received: *30 July 2021*
Accepted: *11 October 2021*
Published: *26 October 2021*

Citation:
Mariotti S, Capocefalo A, Chiantore MV, Iacobino A, Teloni R, De Angelis ML, Gallinaro A, Pirillo MF, Borghi M, Canitano A, Michelini Z, Baggieri M, Marchi A, Bucci P, McKay PF, Acchioni C, Sandini S, Sgarbanti M, Tosini F, Di Virgilio A, Venturi G, Marino F, Esposito V, Di Bonito P, Magurano F, Cara A, Negri D and Nisini R (2021) Isolation and Characterization of Mouse Monoclonal Antibodies That Neutralize SARS-CoV-2 and Its Variants of Concern Alpha, Beta, Gamma and Delta by Binding Conformational Epitopes of Glycosylated RBD With High Potency. Front. Immunol. 12:750386. doi: 10.3389/fimmu.2021.750386

and none was able to bind the same recombinant protein expressed in *Escherichia coli*, suggesting that the epitopes recognized by three mAbs are generated by the conformational structure of the glycosylated native protein. Of particular relevance, three mAbs were able to inhibit Wuhan SARS-CoV-2 infection of VERO E6 cells in a plaque-reduction neutralization test and the Wuhan SARS-CoV-2 as well as the Alpha, Beta, Gamma and Delta VOC in a pseudoviruses-based neutralization test. These mAbs represent important additional tools for diagnosis and therapy of COVID-19 and may contribute to the understanding of the functional structure of SARS-CoV-2 RBD.

Keywords: SARS-COV-2 variants, neutralizing monoclonal antibodies, epitopes expression, therapy, diagnosis, pathogenesis

INTRODUCTION

An outbreak of severe transmittable pneumonia, later referred to as COVID-19 (COronaVIrus Disease 19), was first described in China in late 2019 (1). The disease resulted in high occurrences of fatal pneumonia with clinical symptoms resembling those of severe acute respiratory syndrome coronavirus (SARS-CoV) infections observed during the 2002-2004 SARS epidemic. Symptoms included persistent fever, chills/rigor, myalgia, malaise, dry cough, headache and dyspnea (2). The causative pathogen was identified as a novel coronavirus, initially designated 2019-nCoV and subsequently SARS-CoV-2 (3). SARS-CoV-2 has been able to spread rapidly worldwide since it is transmitted efficiently from human to human, even prior to the onset of symptoms, *via* droplets/aerosol from coughing or sneezing, or direct contact (4). In March of 2020, the World Health Organization officially declared COVID-19 as a pandemic. The emergence of virus variants of concern (VOC) with increased infectivity (Alpha, B.1.1.7; Beta, B.1.351; Gamma, P.1 and Delta, B.1.617.2) greatly contributed to the rise of infections (5) that, as of early October 2021 counted around 233,2 million confirmed cases with over 4.7 million deaths worldwide (https://covid19.who.int/). The pandemic is having a devastating impact on the global economy and public health systems worldwide. Therefore, in addition to safe and highly protective vaccines against SARS-CoV-2 and its VOC, monoclonal antibodies (mAbs), able to recognize and neutralize SARS-CoV-2 to be employed as new diagnostic tools and efficacious therapeutic approaches are still urgently needed.

SARS-CoV-2 is an enveloped virus with a positive single-stranded capped and polyadenylated RNA genome of about 30 kb. SARS-CoV-2 belongs to betacoronavirus genus in the *Coronaviridae* family. The genome has at least 10 open reading frames (ORF), ORF1a and ORF1b, produced by ribosomal frameshifting code for two long polyproteins, pp1a and pp1b, processed in 16 non-structural proteins (ns1-ns16) comprising the viral enzymes the RNA dependent RNA polymerase (RdRp) and two viral proteases (PL proteinase, 3CL). The non-structural proteins rearrange rough endoplasmic reticulum and Golgi compartments membranes into double-membrane vesicles where viral replication and transcription occur (viral factory). The entire replication cycle takes place in the cytoplasm. One-third of the genome encodes, in the order, four main structural proteins: spike (S), envelope (E), membrane (M) and nucleocapsid (N) proteins. Several small accessory proteins (ORF 3A,3B, 6, 7a, 7b, 8, 9a, 9b, 10) are coded in this region, some with important functions for the virus life cycle (6–8).

SARS-CoV-2 utilizes the transmembrane S glycoprotein to form homotrimers, protruding from the coronavirus particle surface, to mediate entry into host cells *via* the angiotensin-converting enzyme 2 (ACE2) receptor (9). The role of the Receptor Binding Domain (RBD) in the S protein suggests that immunization with this protein domain could induce antibodies (Abs) able to block virus binding and fusion thus neutralizing virus infection (10–12).

The RBD folds independently into a globular structure away from the rest of the S protein and exists in two different conformations as part of the trimer: "open" and "closed". In the "open" state, it can bind ACE2, mostly by amino acid (aa) residues within a short segment called the Receptor Binding Motif (RBM). Many studies have shown that subunit protein antigens based on the RBD can elicit neutralizing antibodies (nAbs) against SARS-CoV (11–15). In this study, we produced SARS-CoV-2 recombinant RBD (rRBD) by expressing polyhistidine-tagged proteins in prokaryotic and eukaryotic systems and immunized mice with the protein produced in eukaryotic cells to induce RBD-specific antibody response. Spleen from mouse showing high humoral specific immune responses was isolated for the production of mAbs. We fully characterized four mAbs that showed a potent specific binding to the RBD and three of them were endowed with a strong capacity of neutralize SARS-CoV-2 and its VOC Alpha, Beta, Gamma and Delta.

MATERIALS AND METHODS

Expression and Purification of rRBD

DNA sequence encoding the RBD (residue 318-538) was amplified by PCR from a mammalian cell codon optimized synthetic DNA sequence (Genescript Leiden, the Netherlands) encoding the ectodomain of SARS-CoV-2 spike protein Wuhan-Hu-1 isolate (NCBI Reference Sequence: NC_045512.2). Primer pair included an HindIII restriction site in the 5′ forward primer

in frame with the murine Ig κ-chain leader sequence (5'-TTAAGCTTCAGGGTGCAGCCAACCGAGT-3', HindIII site underlined) and an XhoI restriction site in the 3′ end reverse primer (5'-TTCTCGAGAGCACTTGTTCTTCACCAGATT-3', XhoI site underlined) in frame with the polyhistidine tag of the plasmid pSecTag2HygroA (Invitrogen, Thermo Fisher Scientific) to produce pIgkRBD318-538.

Expression of rRBD was carried out in HEK293T cells grown in high glucose (4.5 g/l glucose) Advanced Dulbecco's modified Eagle's medium (Advanced DMEM, Thermo Fisher Scientific, MA, USA) supplemented with 10% fetal bovine serum (FBS, Gibco, Thermo Fisher Scientific), kanamycin (100 units/ml, Gibco) and 2 mM of L-glutamine (Gibco) incubated at 37°C and 5% CO_2. Transfection was carried out using polyethylenimine (PEI) transfection reagent (Sigma). Briefly, cells were seeded overnight at $1x10^7$ cells in 175 cm^2 flasks in 50 ml of Advanced DMEM containing 2% FBS. The culture medium was then removed and replaced with 45 ml of Ham's F-12 Nutrient Mixture (F-12, Gibco) and transfected with 5 ml of Opti-MEM Reduced-Serum Medium (Gibco) containing 85 μg of DNA plasmid and 85 μl of PEI (0.5 mg/ml). Three days post-transfection, the culture supernatant was harvested, clarified by centrifugation, filtered and stored at 4°C. Protein purification was performed using Ni-NTA Agarose (Qiagen, Hilden, Germany) according to the manufacturer's recommendations with minor modifications. Briefly, 100 ml of supernatant from rRBD-HEK293T transfected cells were combined to 100 ml of 2X Binding buffer (0.2 M sodium phosphate, 300 mM NaCl, 20 mM imidazole and 0.1% Tween 20, pH 8.0) and 1 ml of 50% slurry Ni-NTA agarose. The binding mix was incubated with gently agitation overnight at 4°C, loaded onto the column and ran by automated system. Column was washed with 100 ml of wash buffer (0.1 M sodium phosphate, 300 mM NaCl, 20 mM imidazole and 0.1% Tween 20, pH 8.0) and rRBD was eluted with 5 ml of elution buffer (0.1 M sodium phosphate, 300 mM NaCl, 250 mM imidazole and 0.05% Tween 20, pH 8.0) in ten different fractions. By SDS-PAGE analysis, fractions were selected then pooled and dialyzed in PBS buffer.

The theoretical mass of the HEK293T rRBD protein, deduced from the amino acid sequence, is 29.1 kDa.

For procaryotic expression in *Escherichia coli* (*E. coli*), DNA sequence encoding the RBD (residue 319-541) was amplified by PCR with the opportune primers (forward 5'-GCG CGGATCCAGGGTGCAGCCTACCGAATCAAT-3' and reverse 5'-GCGCAAGCTTGAAGTTCACGCACTTGTTCTTGACC-3') by using a codon optimized SARS-CoV-2 spike template DNA, obtained by *de novo* gene synthesis (Genescript) and cloned into BamHI/HindIII restriction sites of pQE30 (Qiagen). rRBD containing RGS(H)6 tag at N-terminus was purified by Ni-NTA (Qiagen) affinity chromatography using a denaturing protocol to optimize the yield and HisTRAP High Performance columns (Cytiva, Sweden AB). The theoretical mass of the *E. coli* rRBD protein, deduced from the amino acid sequence, is 26 kDa.

SDS-PAGE and Western Blot (WB) Analysis

For the analysis of intracellular proteins, cell pellets were treated with 40 μl of cell extraction buffer (50 mM Tris-HCl, 250 mM NaCl, 1% NP-40; pH 7.4). Protein samples were lysed in SDS-loading buffer containing 50 mM Tris-HCl, pH 6.8, 3% SDS, 50% glycerol, 0.5% bromophenol blue, with or without 5% β-mercaptoethanol (βME). Samples were heated at 95°C for 5 min and loaded onto 7.5%, 4-20% or 4-15% gradient mini-PROTEAN TGX precast gels (Biorad). To monitor protein purification, gels were stained by SimplyBlueTMSafeStain (Novex, LifeTechnologies). For rRBD protein quantification gels were stained by fluorescent protein stain (Krypton Protein Stain, Thermo Scientific, USA) according to the manufacturer's instructions using known amounts of bovine serum albumin (BSA) as standard. Gels were analyzed using ChemiDoc MP Imaging System (Biorad) and Image Lab Software (Image Lab 6.0.1). rRBD proteins resolved by SDS-PAGE were transferred onto polyvinylidene difluoride (PVDF) membrane (Thermo Fisher Scientific). The membranes were blocked with 3% skim milk in Tris-Buffer Saline and 0.05% Tween 20 (TBS-T) before incubation with anti-Tetra-His and anti-RGSHHHH mAbs (QIAGEN) for 1 h at room temperature. Immune complexes were detected with horseradish peroxidase (HRP)-conjugated goat anti-mouse immunoglobulin G (IgG) secondary antibody (Abcam, Cambridge, UK) for 1 h at room temperature. Signals were detected using either Crescendo Western HRP chemiluminescent substrate (Millipore, Burlington, MA, USA) or TMB colorimetric substrates (Vector, Burlingame, CA). SDS-PAGE in non-reducing condition was performed by resolving 100 ng of rRBD or virus infected VERO E6 cells (Cercopithecus aethiops derived epithelial kidney, ATCC CRL-1586) supernatant containing $1x10^6$ SARS-CoV-2 Plaque Forming Units (PFU)/ml denatured in SDS loading buffer without βME, followed by WB using anti-Tetra His (Qiagen) or anti-RBD mAbs.

N-Deglycosylation of rRBD

N-deglycosylation of HEK293T-produced rRBD was performed using the peptide-N (4)-(N-acetyl-β-D-glucosaminyl) asparagine amidase F (PNGase F; Roche, Basel, Switzerland) according to manufacturer's conditions. Briefly, rRBD was denatured for 10 min at 95°C, followed by the addition of PNGase F (1U/50 ng) and incubation a 37°C. Deglycosylated samples were diluted in SDS-loading buffer and incubated at 60°C for 15 min, then analyzed by SDS-PAGE followed by WB using anti-Tetra His mAb (Qiagen). In non-reducing reaction conditions, rRBD was treated with PNGase F in the presence of 2% SDS, diluted in SDS-loading buffer without βME and resolved in SDS-PAGE followed by WB using anti-His and anti-RBD mAbs.

Plasmid Construction

Plasmid pSpike-C3 expressing the wild type codon optimized SARS-CoV-2 spike ORF (Wuhan-Hu-1, GenBank: NC_045512.2) containing a 21 aa deletion at the cytoplasmic tail (delta21) of the spike protein has been already described (16). Plasmid pSpike-FurPPC3 expresses the wild type codon optimized SARS-CoV-2 spike, contains a 21 aa deletion at the cytoplasmic tail (delta21) and was stabilized by the introduction of 2 prolines at aa positions 986 and 987 and by mutation at the furin site (RRAR into GSAS). pSpike-UKC3, pSpike-SAC3 and pSpike-BRC3 plasmids express the Alpha variant (lineage

B.1.1.7), the Beta variant (lineage B.1.351) and the Gamma variant (lineage P.1) Spike ORFs, respectively, with a 21 aa deletion at the cytoplasmic tail. Plasmid pSpike-INd19 expresses the Delta variant (lineage B.1.617.2) spike ORF with a 19 aa deletion at the cytoplasmic tail. The Alpha variant B.1.1.7 pSpike-UKC3 used in these studies contained the following mutations: del69-70HV, del145Y, N501Y, A570D, D614G, P681H, T716I, S982A, D1118H. The Beta variant B.1.351 pSpike-SAC3 used in these studies contained the following mutations: L18F, D80A, D215G, del242-244LAL, R246I, K417N, E484K, N501Y, D614G, A701V. The Gamma variant P1 pSpike-BRC3 used in these studies contained the following mutations: L18F, T20N, P26S, D138Y, R190S, K417T, E484K, N501Y, D614G, H655Y, T1027I. The Delta variant B.1.617.2 pSpike-INd19 used in these studies contained the following mutations: T19R, del157-157, L452R, T484K, D614G, P681R, D950N.

For construction of pRetro-hACE2, a retroviral transfer vector expressing the human ACE2 receptor for SARS-CoV-2, a SpeI/BamHI fragment of DNA was removed from hACE2 plasmid (Addgene plasmid #1786) and inserted into XbaI/ BamHI restriction sites of pQCXIN retroviral transfer vector plasmid (Clontech).

Production of Lentiviral (LV) and Retroviral Vectors

293T Lenti-X cells (Clontech, Mountain View, CA, USA) were used for production of LV-Luc pseudotyped with Spike variants by transient transfection as previously described (16). Briefly, 293T Lenti-X cells ($3.5x10^6$ cells) were seeded on 10 cm Petri dishes (Corning Incorporated - Life Sciences, Oneonta, NY, USA) and transiently transfected with plasmids pGAE-LucW, pADSIV3+ and the pseudotyping plasmid (pSpike-C3, pSpike-UKC3, pSpike-SAC3, pSpike-BRC3, pSpike-INd19 and control phCMV-VSV.G) using the JetPrime transfection kit (Polyplus Transfection Illkirch, France) following the manufacture's recommendations using a 1:2:1 ratio (transfer vector: packaging plasmid: spike plasmid). At 48 h post transfections, culture supernatants containing the LV-Luc pseudotypes (LV-Luc/Spike-C3, LV-Luc/Spike-UKC3, LV-Luc/Spike-SAC3, LV-Luc/SpikeBRC3, LV-Luc/SpikeINd19 and LV-Luc/VSV.G) were collected and stored in 1 ml aliquots at -80°C until use.

Packaging Phoenix-AMPHO (ATCC) cell line was used for production of retroviral particles expressing hACE2 (Retro-hACE2). Briefly, cells were transiently transfected with the pRetro-hACE2 plasmid at 80% confluence in a 6 cm dish, by the calcium phosphate method. Cell medium (4 ml of DMEM, high glucose, Euroclone, supplemented with 10% FBS, glutamine and antibiotics) was replaced just before transfection, adding chloroquine (Sigma-Aldrich Merck KGaA) to a final concentration of 25 μM. Medium was further replaced 24 h after transfection and again 8 h later (this time with 2.5 ml only). After an additional 24 h, medium, containing retroviruses, was collected and centrifuged at 500 x g for 10 minutes (to pull down cells in suspension and cellular debris). After centrifugation, 2 ml of medium was carefully collected (to avoid disturbing the pellet) and used to transduce the murine melanoma cell line B16-F10 (ICLC, Genoa, Italy).

Binding of rRBD to B16-F10 Cells Expressing hACE2

B16-F10 cells were transduced with Retro-hACE2 in the presence of 8 μg/ml Polybrene (Merck KGaA, Darmstadt, Germany). After 24 h of transduction, cells were seeded in B16-F10 growing medium after cell centrifugation at 400 x g for 10 min. Selection with 800 μg/ml of the antibiotic G418 (Sigma-Aldrich, St. Louis, MO, USA) was started 5 days later. After 5 passages, B16-hACE2 cells were incubated with mouse anti-hACE2 antibody (MAB5676-Millipore) followed by goat-anti-mouse PE (Biolegend) and hACE2 positive cells were sorted by FACSaria (Becton-Dickinson, Franklin Lakes, NJ, USA) and maintained with half dose of antibiotic. B16-F10 and B16-hACE2 cells were incubated with 100 μl of HEK293T rRBD (1 μg) for 30 min on ice. After three washes to remove unbound protein, the cells were incubated with the anti-Tetra-His mAb (Biorad) diluted 1:250 for 30 min on ice. Then, an anti-mouse IgG FITC-labeled, diluted 1:250 was added for 30 min on ice. After washes, the cell-associated fluorescence was measured by Beckman Coulter Gallios flow cytometer equipped with Kaluza Software (Beckman Coulter, Brea, CA, USA).

For blocking experiment, 1 μg of rRBD was preincubated or not with 2 μg/ml of anti-RBD mAbs for 30 min at 37°C in 100 μl of PBS+1%FBS. Then, the mixture was added to 50000 B16-F10 and B16-hACE2 cells for 30 min on ice. After 2 washes, 100 μl of anti-Tetra-His mouse mAb (Qiagen) diluted 1:250 was added and incubated for 30 min on ice followed by 30 min on ice incubation with an anti-mouse IgG FITC-labeled (Biolegend, diluted 1:250). After washes the cell-associated fluorescence was measured by Gallios cytometer (Beckman Coulter. Brea, CA, USA).

Size Exclusion High-Performance Liquid Chromatography (SE-HPLC)

The chromatographic analysis of rRBD was performed with an Alliance Waters e2695 HPLC system (Waters Corporation, Milford, Massachusetts) controlled by the Empower software. SE-HPLC analysis was performed isocratically (with a constant concentration of the mobile phase) at room temperature using a Tosoh bioscience guard-column TSK gel SWXL (40 × 6 mm) and a Tosoh bioscience HPLC column TSK gel G3000SWXL (300 x 7.8 mm, 5 μm). The mobile phase consisted of 100 mM phosphate buffer with 100 mM Na_2SO_4, at pH 7.2. The flow rate was 0.5 ml/min and the total analysis time was 35 min. The protein was injected without any dilution/pretreatment and the injection volume was 175 μl. A Bio-Rad's Gel Filtration Standard (mixture of molecular weight markers ranging from 1,350 to 670,000 Da) was used as calibrator. The elution was monitored with a PDA 2998 Waters set at 214 nm (17).

Mice Immunization

Six-week-old female pathogen-free BALB/c mice were obtained from Charles River Laboratories (Calco, LC, Italy) and housed in

the Istituto Superiore di Sanità. All animal protocols and procedures were performed in accordance with European Union guidelines and Italian legislation (DL26/2014) and have been approved by the Italian Ministry of Healthy and reviewed by the Service for Animal Welfare at ISS (Protocol n. 670/2020-PR of July 21st, 2020). Mice were immunized with a subcutaneous injection on both sides of lower anterior abdomen on days 0, 14 and 28. Five μg of HEK293T rRBD in 50 μl were mixed with an equal volume of emulsified complete Freund's adjuvant (Millipore-Sigma) for priming or with incomplete Freund's adjuvant (Millipore-Sigma) for boosts respectively, immediately prior to administration. Blood samples were collected on days 0 (pre-immunization) and at day 42 (2 weeks after the third immunization) by retro-orbital collection, centrifuged and sera stored at -20°C until analyzed. The collected sera were tested by *in-house* ELISA for the determination of anti-RBD specific antibody titres in order to identify the high responder mouse. The selected mouse received a final boost of 5 μg of HEK293T rRBD in the absence of adjuvant by intravenous injection. Three days later the mouse was sacrificed, splenocytes were prepared by mechanical disruption and passage through cell strainers (BD Pharmingen, San Diego, CA, USA) and resuspended in RPMI 1640 (Euroclone) containing 10% FBS (Gibco), 100 units/ml of kanamycin (Gibco), non-essential aminoacids (Gibco), 1 mM sodium pyruvate (Gibco) (complete RPMI medium) with the addition of 25 mM Hepes buffer solution (Euroclone).

Hybridoma Fusion and Isolation of Specific mAb-Producing Clones

Mouse myeloma cell line SP2 (ATCC. Manassas, VA, USA) was cultured in complete RPMI medium. Spleen cells isolated from the selected mouse were incubated with 5 ml lysis buffer on ice for 5 min. After washing, splenocytes were resuspended into serum-free RPMI supplemented with 25 mM Hepes and counted. SP2 cells were then mixed with the splenocytes, centrifuged at 1000 rpm for 10 min and slowly resuspended with 1 ml of polyethilenglycol (PEG, Sigma-Aldrich). Then, 7 ml of complete RPMI medium supplemented with 25 mM of Hepes was slowly added, the cells centrifuged, and the pellet resuspended in complete RPMI medium containing hypoxanthine, aminopterin and thymidine (HAT, Sigma-Aldrich). After fusion, cells were cultured in 96 well plate flat bottom (Corning) for 14 days at 37°C with 5% CO_2 and the resultant fused growing cell lines were selected by microscope examination, transferred to individual wells in new 96-well plates and expanded in complete RPMI with HAT. Hybridomas were screened for antigen specificity of produced Abs by ELISA. The selected polyclonal Ab-producing hybridomas were single-cell-cloned by limiting dilution in the presence of $5x10^4$ cells/well feeder splenocytes in 96 well flat bottom plate in complete RPMI medium with HAT for 12 days. The growing clones were tested for antigen specificity by ELISA and those producing mAbs specific for RBD expanded in static T75 flasks (Corning) in serum free medium DCCM2 (Biological Industries) supplemented with kanamycin, hypoxanthine and thymidine (HT, Sigma-Aldrich).

Monoclonal Antibody Purification

The clones producing mAbs specific for SARS-CoV-2 RBD were expanded and the mAbs purified and concentrated by using chromatography cartridges protein G columns (Thermo Fisher). Briefly, the protein G column was washed with PBS, then 30 ml of mAb culture supernatant was diluted 1:1 in PBS and passed over the column. Finally, the bound mAb was eluted with 0.1 M glycine pH 2.5 and the pH immediately neutralized with 1 M Tris pH 7.9 before dialysis with PBS. The concentration of purified mAbs was evaluated by NanoPhotometer (Implen, Münich, DE) spectrophotometer at 280 nm and expressed as μg/ml.

Human Sera

Pseudonymized sera from healthy or COVID-19 convalescent volunteers who gave their informed consent to donate blood for research purposes and to participate to the collaborative study between Istituto Superiore di Sanità and Italian Air Force entitled: "*Valutazione della performance analitica di un test antigenico per il rilevamento di SARS-CoV-2, confronto con un test di screening molecolare*" were heat-inactivated at 56°C for 30 minutes and frozen until use.

ELISA

rRBD was plated o/n at 4°C on high binding flat-bottom 96-well polystyrene plates (Greiner Bio-One, Rainbach, Austria) at 0.5 μg/ml (50 μl/well) in sodium bicarbonate (pH 9.0) buffer. Then plates were washed with PBS+0.5% Tween 20 and incubated with 200 μl/well of a blocking solution (postcoat) of PBS containing 2% BSA (w/v) for 1 h at RT. Then, 50 μl of serum or hybridoma supernatants diluted in blocking buffer were incubated for 3 h at 37°C, followed by washing. Goat anti-mouse IgG alkaline phosphatase (PA)-conjugated (Southern Biotech, Birmingham, AL, USA) or mouse anti-human IgG PA-conjugated (Invitrogen) (1:1000 in blocking buffer) were incubated for 1 h at 37°C. After washes, PA substrate (Sigma) was added, the enzymatic reaction stopped by 3N NaOH and absorbance (405 nm) measured by Varioskan Flash reader (Thermo Fisher Scientific). Results were considered positive when the optical density (OD) obtained with the mAbs was three times greater than the negative control. The subclass of isolated mAbs was identified using enzyme-conjugated anti-mouse subclass specific antibody (anti-IgG1, IgG2a, IgG2b, IgG3; Southern Biotech)

For competitive ELISA, plate was coated with 0.5 μg/ml of HEK293T rRBD o/n and after 1 h of incubation with the postcoat solution, 50 μl/well of a mixture of fixed R590 and R64 mAbs concentration (0.02 μg/ml) and two-fold dilutions (starting form 1:25) of human sera were added and incubated 3 h at 37°C. Sera from convalescent COVID-19 patients with known titers of neutralizing antibodies (nAbs) and sera from healthy subjects were tested. Then, goat anti-mouse IgG PA-conjugated antibody (1:1000; Southern Biotech) was added for 1 h at 37°C, followed by development of enzymatic reaction.

Evaluation of the mAbs Binding Capacity by Flow Cytometry

To analyze the binding of anti-RBD mAbs to the native trimeric spike, HEK293T cells transfected with pSpike plasmids

expressing the transmembrane wild-type S protein of SARS-CoV-2 Wuhan or VOC were collected by trypsinization. After washing, $1x10^5$ cells per polypropylene tube were incubated for 30 min on ice with 100 µl of anti-RBD mAbs at serial concentrations (starting from 0.4 µg/ml) diluted with PBS+1% FBS or with murine IgG1 negative control mAb (SinoBiological, USA). Anti-S2 (40590-T62 SinoBiological, USA) antibody was used as a positive control of spike expression, as described above. After two washes to remove unbound mAbs, a goat anti-mouse IgG FITC-labeled (Southern Biotech, Birmingham, AL, USA) mAb was added (dilution 1:250) and incubated 30 minutes on ice. Rabbit anti-S2 (40590-T62 SinoBiological, USA) antibody followed by a donkey anti-rabbit FITC-labeled mAb (Biolegend, San Diego, CA, USA) was used as a positive control of spike expression. After two washes, the cells were resuspended with PBS+1%FBS and their associated fluorescence measured by flow cytometry by acquiring $2x10^4$ events in a large forward and side scatter-based gate by using a Beckman Coulter Gallios with Kaluza Software (Beckman Coulter).

Immunoprecipitation (IP)

Immunoprecipitation of LV pseudotyped with pSpike-FurPPC3 (LV-FurPPC3) or with VSV.G (LV-VSV.G) as negative control was performed using Dynabeads Protein G (Thermo Fisher), according to the manufacturer's instructions. Briefly, purified mAbs R590 and R64 were conjugated to protein G beads for 30 min at room temperature. Beads were washed twice in IP buffer (20 mM Tris-HCl pH 7.4, 150 mM NaCl, 0.1% NP-40) and incubated with Lenti-X cell supernatant containing pseudotyped LV in IP buffer for 2 hours at room temperature. After washing three times in IP buffer, beads were eluted with SDS-loading buffer at 95°C for 10 min. Immunoprecipitation was analyzed by SDS-PAGE followed by WB using an anti-S1 mAb (MA5-36247, Thermo Fischer).

Pseudovirus Titration and Neutralization Assay

Preparations of LV-Luc Wuhan, Alpha, Beta, Gamma and Delta pseudotypes (LV-Luc/Spike-C3, LV-Luc/Spike-UKC3, LV-Luc/Spike-SAC3, LV-Luc/SpikeBRC3 and LV-Luc/SpikeINd19) were titered in VERO E6 cells seeded in a 96-well plate (View plate, PerkinElmer) at a density of 20000 cells/well. After 48 h, luciferase expression was determined by the britelite plus Reporter Gene Assay System (PerkinElmer) and measured with a Varioskan luminometer (Thermo Fisher). Dilutions providing 150000-200000 relative luminescence units (RLU) were used in the neutralization assay. Briefly, mAb serial 2-fold dilutions starting from 20 µg/ml were incubated in duplicate with the Wuhan, Alpha, Beta, Gamma and Delta LV-Luc pseudoviruses for 30 min at 37°C in 96-deep well plates (Resnova, Genzano di Roma, Italy), and thereafter added to VERO E6 cells seeded in a 96-well View plate at a density of 20000 cells/well. Virus-only and cell-only controls were included. After 48 h, luciferase expression was determined by the britelite plus Reporter Gene Assay System (PerkinElmer). RLU data points were converted to a percentage neutralization value, calculated relative to virus-only controls. Results are expressed as inhibitory concentration (IC) 50 corresponding to the mAb concentration giving 50% inhibition of infection (neutralization) compared to the virus control wells (16).

Virus Propagation

VERO E6 cells were grown in Dulbecco's modified Eagle's medium (DMEM, Gibco) supplemented with 2.5% heat-inactivated Fetal Calf Serum (FCS), 100 units/ml penicillin, 100 µg/ml streptomycin, 2 mM L-glutamine, 1 mM sodium pyruvate, and 1x non-essential amino acids (Gibco).

Viral isolate BetaCov/Italy/CDG1/2020|EPI ISL 412973|2020-02-20 (GISAID accession ID: EPI_ISL_412973) was propagated by inoculation of 70% confluent VERO E6 cells in 75 cm^2 cell culture flasks. Cells were observed for cytopathic effect every 24 h. Stocks of SARS-CoV-2 virus were harvested at 72 h post infection, and supernatants were collected, clarified, aliquoted, and stored at -80°C. Infectious virus titer was determined as PFU. For some experiments of WB and IP, SARS-CoV-2 virus was inactivated at 56°C for 30 minutes.

Plaque Reduction Neutralization Test (PRNT)

Method used for PRNT was essentially the same as previously described (18). The viral stocks of SARS-CoV-2 were titred three times by semi-log10 dilutions by plaque forming assay. Then serial 2-fold dilutions (starting from 5µg/ml) of purified mAbs were incubated with 80 PFU of SARS-CoV-2 at the final volume of 600 µl at 4°C overnight. The mixtures were added in duplicates to confluent monolayers of VERO E6 cells, grown in 12-well plates and incubated at 37°C in a humidified 5% CO_2 atmosphere for 60 min. Then, 4 ml/well of a medium containing 2% Gum Tragacanth (Sigma Aldrich) + MEM 2.5% FCS were added. Plates were left at 37°C with 5% CO_2. After 3 days, the overlay was removed, and the cell monolayers were washed with PBS to completely remove the overlay medium. Cells were stained with a crystal violet 1.5% alcoholic solution. The presence of SARS-CoV-2 virus–infected cells was indicated by the formation of plaques. The IC50 was determined as the highest dilution of serum resulting in 50% ($PRNT_{50}$) reduction of plaques as compared to the virus control.

Statistical Analysis

For neutralization and ELISA experiments technical duplicates or triplicates were performed. All of the statistical analyses were performed using the GraphPad Prism software v9 (GraphPad Software, San Diego, CA, USA) (16). The IC50 were calculated with a non-linear regression method. The EC_{50} were calculated by non-linear regression analysis of log10 of serum dilution plotted versus absorbance at 405 nm. Statistical analysis of data in figure 2A and 3A were performed using the non-parametric Mann-Whitney 2-sided *U*-test and the Kruskal-Wallis multiple comparison test. The p values < 0.05 were considered significant.

RESULTS

Characteristics of the Produced rRBD

Based on the solved structure provided by Walls et al. (9), the sequence of the RBD covering amino acids from F318 to C538 (**Figure 1A**) was selected for expression of a secreted His-tagged

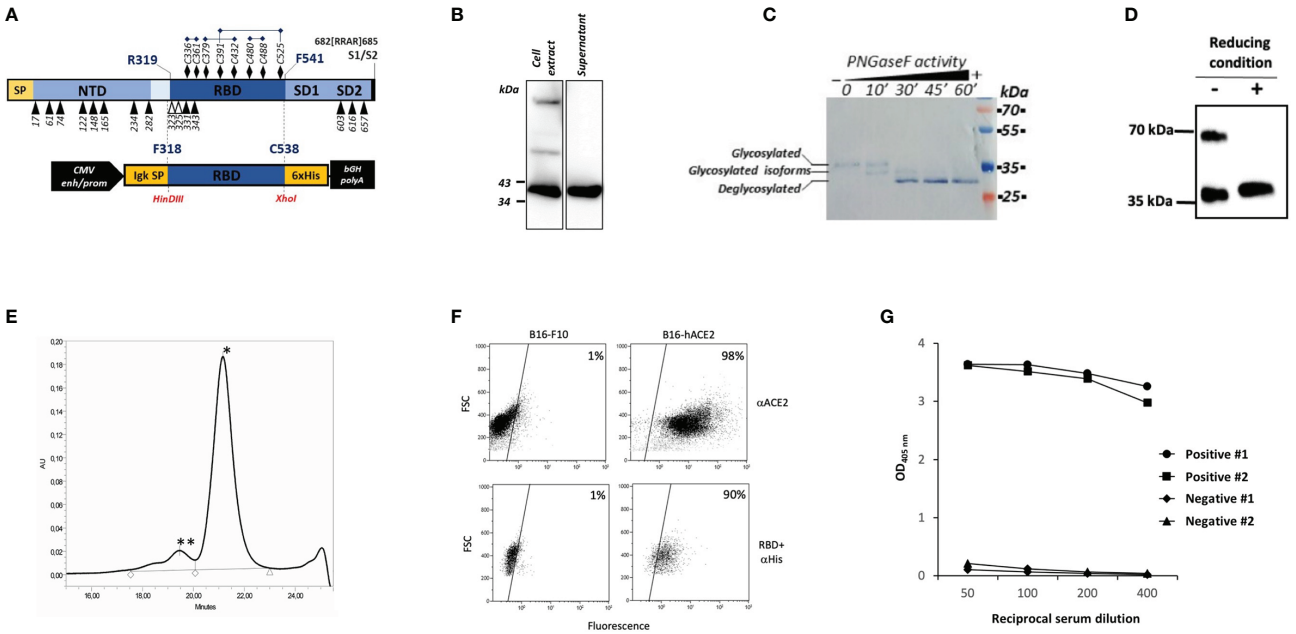

FIGURE 1 | Production and characterization of HEK293T rRBD. **(A)** Diagram of SARS-CoV-2 S1 domain and of the rRBD expression cassette in pIgkRBD$_{318\text{-}538}$ SARS-CoV-2 plasmid vector. Functional elements are indicated: SP (signal peptide), NTD (N-terminal domain), RBD, SD1 and SD2 (subdomain 1 and 2), CMV enh/prom (human cytomegalovirus immediate early enhancer/promoter), Igk SP (murine Ig κ-chain leader sequence), 6xHis (polyhistidine tag) and bGH polyA (bovine growth hormone polyadenylation signal). N-glycosylation and O-glycosylation sites are indicated by black and white respectively triangles. Cysteine residues are indicated by black diamond and disulfide bonds are reported. **(B–D)** WB characterization of rRBD using an anti-Tetra His mAb. **(B)** Detection of rRBD in the cell extract and in the supernatant of transfected HEK293T cells. **(C)** Purified rRBD was denatured and digested with PNGase F in a time-dependent manner. The positions of glycosylated, deglycosylated and glycosylated isoforms of rRBD are indicated. **(D)** rRBD was denatured in SDS-loading buffer without βME or with βME. **(E)** SE-HPLC chromatogram of rRBD. The retention time suggests an approximate molecular mass of less than ~40 kDa (*) corresponding to the monomeric form and another molecular mass of >150 kDa (**) corresponding to the aggregate multimeric structure. **(F)** rRBD binding to ACE2 receptor by flow cytometry. In the upper panels B16-F10 or B16 cells expressing human ACE2 receptor (B16-hACE2) were stained with anti-ACE2 mouse mAb and goat anti-mouse IgG PE-conjugated as secondary antibody. In the lower panel cells were incubated with rRBD and then stained with an anti-histidine mouse mAb revealed with goat anti-mouse FITC-conjugated mAb. The numbers indicate the percentages of positive cells. Each panel from **(B–F)** shows a representative experiment repeated at least two times. **(G)** Binding of serial dilution of human serum from two COVID-19 positive and two negative subjects on rRBD coated to the ELISA plate. Graph reports results obtained by two out of seven positive and seven negative subjects.

protein from human HEK293T cells and then analyzed by SDS-PAGE and WB. As shown in figure 1B, rRBD was well detected in both the cell lysate and the supernatant of transiently transfected HEK293T cells as a band of approximatively 35 kDa. This result contrasts with the predicted molecular mass of 29.1 kDa calculated on the basis of rRBD amino acid sequence but could be explained by post-translational modifications that occur in mammalian cells. Indeed, two N-glycosylations and one O-glycosylation have been described at SARS-CoV-2 RBD N-terminal region (19) (**Figure 1B**). To verify the role of N-glycosylation on rRBD electrophoretic mobility, we analyzed by WB the molecular weight of rRBD before and after the enzymatic treatment with the glydosidase PNGase F. The time-dependent decrease of the observed rRBD molecular mass in correlation with PNGase F exposure, confirmed the presence of N-linked glycosylations in the rRBD (**Figure 1C**).

To evaluate the role of cysteine residues in disulfide bonds formation and the potential presence of RBD multimeric structures, we compared the mobility of rRBD on SDS-PAGE under reducing and non-reducing conditions. Notably, rRBD in the absence of reducing agents ran as two different bands (**Figure 1D**), as previously observed by Farnos et al. (20). This data confirms that the unfolded state of rRBD is constrained by the native disulfide bonds and indicates that in the folded state multimeric structures can be formed (20). This conclusion is supported by SE-HPLC analysis showing that purified rRBD exists mainly as a monomer, with a small fraction of rRBD producing aggregates, as shown by the presence of two different peaks in the chromatogram (**Figure 1E**). The rRBD preparations used for all the experiments were checked for quantitative analysis by Krypton stained SDS-PAGE that always showed the absence of contaminants (**Supplementary Figure S1**)

We next evaluated the ability of rRBD to bind the hACE2 receptor on B16-hACE2 cells, the B16-F10 murine cell line stably transduced with hACE2, as a measure for assessing the structural integrity and the correct folding of the protein. An anti-hACE2 mAb confirmed that hACE2 was expressed on the surface of B16-hACE2 cells (**Figure 1F**) and we could show that rRBD binds to B16-hACE2 cells but not to control B16-F10 cells, demostrating that the produced recombinant protein maintains

the functional properties of the viral RBD, namely its capacity to bind human ACE2.

Finally, we used previously screened sera from normal controls or COVID-19 convalescent individuals with known levels of anti-RBD specific Abs to test the antigenic properties of produced recombinant protein. Only sera from patients with anti-SARS-CoV-2 Abs bound to rRBD (**Figure 1G**). These results confirm that our purified recombinant protein retains native structure and preserves the antigenic properties of the SARS-CoV-2 spike RBD.

Binding Characteristics of RBD Specific mAbs

Mice were immunized with rRBD expressed in mammalian HEK293T cells to generate specific Abs. Sera from immunized mice were screened for RBD binding by ELISA, and the mouse with the highest titers of serum-specific IgG was sacrificed and splenocytes were fused with a mouse myeloma. Hybridomas secreting anti-RBD Ab were cloned by limiting dilutions to obtain monoclonal cultures. Four monoclonal hybridomas were selected and the secreted mAbs R64, R71, R196 and R590 were purified on protein G columns from the culture supernatant and their chracteristics were tested by ELISA, flow cytometry, WB, IP and functional assays. The selected mAbs were IgG1 (data not shown) and bound HEK293T rRBD in the ELISA (**Figure 2A**). The half maximal effective concentration (EC_{50}) required for all mAbs to bind HEK293T rRBD glycoprotein falls below 100 ng/ml (**Figure 2A**): in particular R590, R71 and R196 were characterized by high binding affinity (EC_{50}: 8.66, 10.07 and 17.99 ng/ml respectively), while R64 shows the lowest affinity (EC_{50}: 70.96 ng/ml).

We confirmed the mAb ability to bind RBD also when this protein domain is part of the homotrimeric spike complex exposed on the surface of transfected HEK293T cells (**Figure 2B**). An anti-S2 mAb was used to determine the percentage of fully transfected HEK293T cells. As shown in figure 2B, the four mAbs recognized the trimeric spike glycoprotein (**Figure 2B**) showing a different efficiency of binding in terms of mean fluorescence intensity (**Figure 2C**): R590=R64>R71>R196. Interestingly, at low doses the mAbs were still able to stain all the transfected cells (**Figure 2D**).

mAbs Recognize Conformational Epitopes of the Glycosylated RBD

In the attempt to characterize the epitopes recognized by our mAbs, we first compared their reactivity to the rRBD produced in HEK293T or to rRBD produced in a prokaryotic expression system. To this end, the RBD domain was produced in *E. coli* as His-tagged fusion protein that ran as a ~26 kDa single band in WB and Coomassie staining (**Supplementary Figure S2**). This prokaryotic expression system is normally inefficient in disulfide bonds formation when recombinant proteins are expressed in

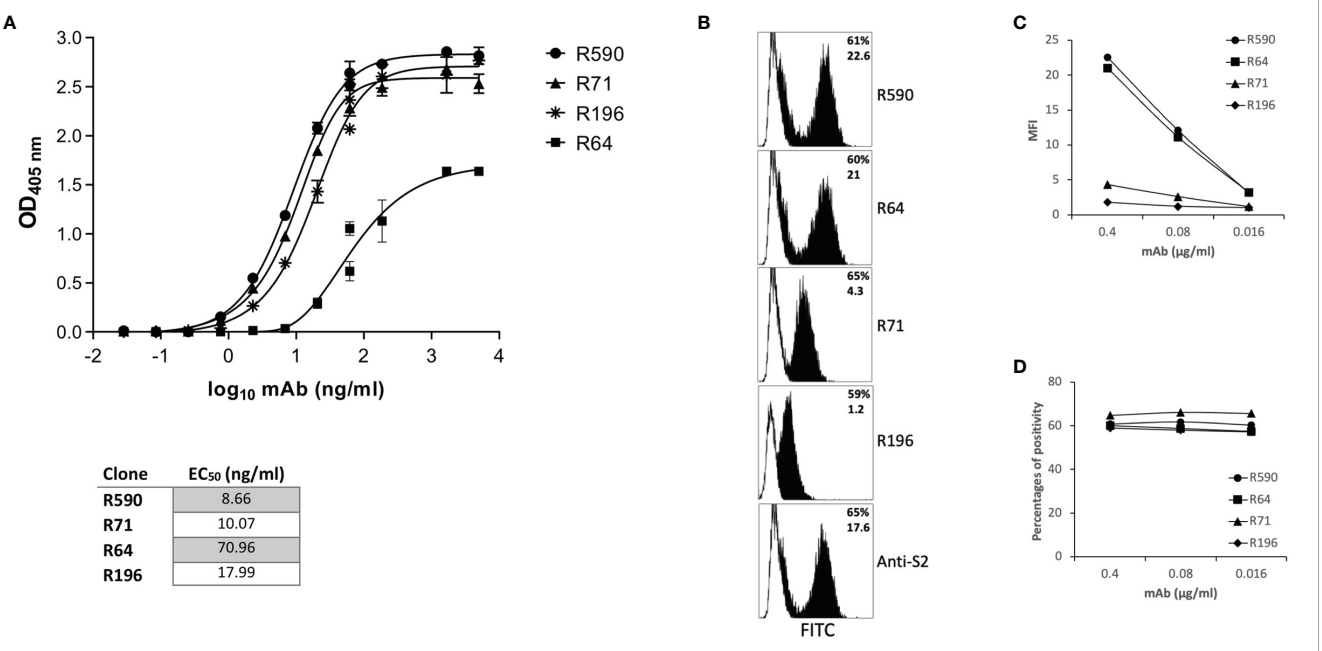

Clone	EC_{50} (ng/ml)
R590	8.66
R71	10.07
R64	70.96
R196	17.99

FIGURE 2 | Characterization of anti-RBD mAbs. **(A)** ELISA-binding affinity of purified mAbs to rRBD produced in mammalian expression system. Error bars indicate standard deviations of technical triplicates from a representative experiment repeated twice. Table indicates the EC_{50} of isolated mAbs. **(B–D)** HEK293T cells transfected with plasmid coding for wild type transmembrane homotrimeric spike (pSpike-C3) were incubated with anti-RBD mAbs at 0.4 µg/ml (**B**, black histograms) or with murine IgG1 control mAb (**B**, white histograms) or with serial dilution of mAbs starting from 0.4 µg/ml **(C, D)** followed by staining with anti-mouse FITC-conjugated mAb before analysis by flow cytometry. An anti-S2 mAb was used as control to determine the percentage of transfection. In **(B)** the upper numbers indicate the percentages of positive cells, lower numbers indicate mean fluorescence intensity. In **(C)** mean fluorescence intensity (MFI) of staining is shown. In **(D)** percentages of positive stained cells is shown. A representative experiment of three is shown.

the cytoplasm as inclusion bodies (21) that require denaturing agents for solubilization. Indeed, the produced *E. coli* rRBD ran as a single band in both reducing and non-reducing conditions (data not shown). Sera of immunized mice were able to bind both the HEK293T and *E. coli* rRBD proteins in ELISA, although the rRBD produced in *E. coli* was recognized with low efficiency. On the contrary, all the tested mAbs were shown to bind the HEK293T rRBD, but not the *E. coli* rRBD (**Figure 3A**). Interestingly, none of our mAbs recognized the rRBD produced in both HEK293T and *E. coli* expression systems in WB under reducing and denaturing conditions (data not shown). These data suggest that immunization with HEK293T rRBD results in a small fraction of antibody recognizing linear epitopes and a larger array of IgG, which includes our mAbs, that are likely to recognize discontinuous epitopes (22). To evaluate the role of disulfide bonds in the generation of conformational epitopes, we tested the reactivity of our mAbs to the HEK293T rRBD in WB following SDS-PAGE under either reducing or non-reducing conditions (**Figure 3B**). As expected, none of mAbs recognized the rRBD in reducing conditions, but mAbs R71, R196, R590, and to a lesser extent R64, bound HEK293T rRBD in the absence of reducing agents. The role of disulfide bonds in the generation of the relevant epitopes was confirmed by the observation that R71, R196 and R590, but not R64, recognized both the full-length spike and the cleaved S1 domain present in the heat inactivated supernatant of SARS-CoV-2 infected VERO E6 cells only in non-reducing conditions (**Figure 3C**). To ascertain whether the absence of binding with mAb R64 could be ascribed to alteration of protein conformation due to the experimental conditions that included the use of SDS (23), we performed an immunoprecipitation assay using LV pseudotyped with SARS-CoV-2 spike protein. As shown in **Figure 3D**, R64 as well as R590, used as a positive control, were able to immunoprecipitate the SARS-CoV-2 pseudovirus, but not the VSV.G psudotyped LV, indicating that R64 binds RBD of SARS-CoV-2 in its native, unmodified conformation.

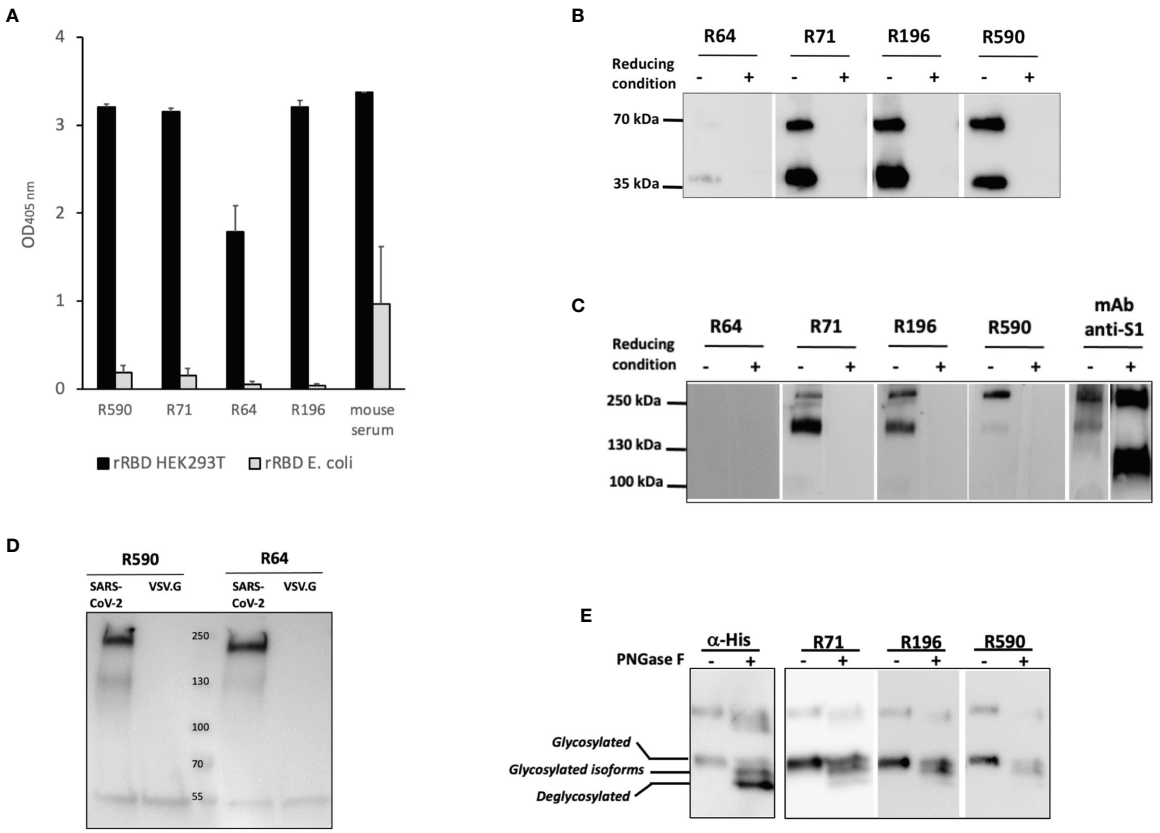

FIGURE 3 | Binding of mAbs to RBD requires disulfide bonds and glycosylation. **(A)** Binding of mAbs to rRBD produced in mammalian (RBD HEK) or prokaryotic (RBD *E. coli*) expression system evaluated by ELISA. Serum from a mouse immunized with rRBD HEK was used as positive control of antigenicity. Error bars indicate standard deviations of technical duplicates from a representative experiment repeated three times. **(B, C)** rRBD **(B)** or VERO E6 cell supernatant containing $1x10^6$ SARS-CoV-2 PFU/ml **(C)** were denatured without (non-reducing condition) or with (reducing condition) βME and resolved on SDS-PAGE followed by WB using R64, R71, R196 and R590 mAbs. Anti-S1 mAb was used as positive control. **(D)** HEK293T cell supernatant containing lentiviral vector pseudotyped with pSpike-FurPPC3 (SARS-CoV-2) was incubated with mAbs R590 and R64 conjugated to protein G. Lentiviral vector pseudotyped with VSV.G (VSV.G) was used as negative control. Immunoprecipitation was analyzed by SDS-PAGE followed by WB using anti-S1 mAb. **(E)** rRBD N-deglycosylation was performed in denatured, non-reducing conditions and revealed using α-His mAb and R71, R196 and R590. The positions of glycosylated, deglycosylated and glycosylated isoforms of rRBD are reported. Each panel from **(B–E)** shows a representative experiment repeated at least two times.

To better characterize the binding of mAbs to HEK293T rRBD, we analyzed the involvement of glycosylation. N-glycosylations have been described on residues N-331 and N-343 of the spike RBD (19) and we have shown (**Figure 1C**) that HEK293T rRBD shares the co-translational N-glycosylation described for the SARS-CoV-2 spike protein. **Figure 3E** shows that R71, R196 and R590 lose the binding efficiency to the fully de-glycosylated form of rRBD, indicating that these mAbs do not bind linear, but conformational epitopes of the glycosylated protein.

Three mAbs Show SARS-CoV-2 Neutralization Capacity

The selected mAbs were evaluated for their ability to prevent the binding of RBD to its receptor ACE2 by using B16-hACE2 cells in a flow cytometry blocking experiment. Pre-incubation of rRBD with mAbs R590 or R64 showed a drastic reduction of its binding to ACE2 receptor (**Figure 4A**, upper panels). This binding inhibition was not observed after the pre-incubation with R196 and R71 even if RBD-mAbs immunocomplexes were bound to the receptor as shown using anti-mouse IgG mAb (**Figure 4A**, lower panels), proving that these mAbs bind epitopes outside the RBM and not involved in ACE2 interaction.

The ability of our mAbs to neutralize SARS-CoV-2 was evaluated using two experimental approaches. The neutralization potential against the authentic virus was evaluated by PRNT using SARS-CoV-2 isolated from COVID-19 patients. mAbs R590 and R64, and to a lesser extent R71, were endowed with a strong neutralization capacity that correlated with the efficiency of binding to the native protein on cell surface, while R196 was not neutralizing. R590 showed the highest potency against the authentic virus (IC50: 0.08 μg/ml) followed by R64, while R71 showed limited neutralizing capacity (IC50 = 0.312 and 1.25 μg/ml, respectively) (**Figure 4B**, left panel). In contrast, the mAb R196, did not show any virus neutralization under these experimental conditions (data not shown). The neutralizing activity of the mAbs was also evaluated using a pseudovirus neutralization assay, based on LV expressing Luciferase and pseudotyped with SARS-CoV-2 spike (LV-Luc/Spike) (16) (**Figure 4B**, right panel). As expected, the IC50 values are slightly different from those calculated by a PRNT assay; however, the relative neutralizing potency among the mAbs was confirmed. Indeed, R590 was the most potent nAb with the lowest IC50 compared to R64 and R71 (IC50 = 0.045, 0.474 and 2.157 μg/ml, respectively), while R196 mAb was not able to neutralize the pseudovirus (data not shown).

The mAbs R590, R64 and R71 Bind SARS-CoV-2 Trimeric Spike Belonging to Major VOC and Neutralize the Corresponding Pseudoviruses

With the worldwide progression of COVID-19 pandemic, several new SARS-CoV-2 variants containing mutations in the spike protein have been isolated, showing increased infectivity and ability to cause disease in susceptible individuals. Clinical studies were designed to define whether immunization with vaccines based on the original SARS-CoV-2 Wuhan-Hu-1 spike sequence may be sufficiently protective against these VOC (24–26). Moreover, mAbs developed for diagnostic or therapeutic purposes may not be useful for individuals infected with these variants and/or affected by COVID-19 (27). First, we measured the ability of the neutralizing RBD-specific R590, R71 and R64 mAbs to bind their epitopes expressed on the surface of HEK293T cells transfected with plasmids coding for the trimeric spike with the original (Wuhan-Hu-1) protein sequence and with the sequences of the Alpha, Beta, Gamma and Delta variants. The three SARS-CoV-2 nAbs recognized the original native spike protein as well as the four main variants (**Figure 5A**). Importantly, the mAbs R590, R64 and R71 inhibited the infection of VERO E6 cells with all the variant strains in the pseudovirus neutralization assay (**Figure 5B**), indicating a broad neutralizing activity of these mAbs.

Sera of Patients With nAbs Generated During Natural SARS-CoV-2 Infection Compete for the Same Epitopes Recognized by Our Neutralizing mAbs

We asked whether the same conformation and glycosylated structure of the epitopes recognized by our neutralizing mAbs may be relevant for the *in vivo* generation of nAbs in SARS-CoV-2 infected individuals. We selected sera from COVID-19 convalescent patients showing high SARS-CoV-2 neutralizing capacity or from individuals with no measurable neutralizing activity to test whether these sera were able to compete for the same neutralizing epitope(s) recognized by mAbs R590 and R64. **Figure 6** shows that increasing concentration of neutralizing sera from COVID-19 patients progressively reduced the binding of the mixture of mAbs R590 and R64 to coated rRBD, while non neutralizing sera were ineffective to prevent the binding of our nAbs to rRBD. These data indicate that convalescent COVID-19 patients developed nAbs that compete for the same epitopes recognized by our neutralizing mAbs, suggesting that conformational and epitopes of the glycosylated RBD are crucial for SARS-CoV-2 infectivity.

DISCUSSION

An unprecedented global effort to counteract the COVID-19 pandemic started in early 2020 to identify appropriate public health strategies and to develop drugs, vaccines and nAbs against SARS-CoV-2 (28, 29). COVID-19 is still a public health threat to societies since the complexity of mass vaccination programs, the lack of effective drugs to specifically treat SARS-CoV-2 infected individuals (30–32) and the emergence of VOC predict that virus circulation may last for years (33). A more detailed and broad understanding of the molecular mechanisms underlying the pathogenesis of COVID-19 will have significant implications for developing countermeasures against the virus with particular emphasis to drug discovery, diagnosis and more effective and safe vaccine design (34). The SARS-CoV-2 spike protein is a high glycosylated transmembrane protein assembled as a homotrimer on the virus surface, with three S1 subunits containing the RBD sitting on the top of a trimeric membrane fusion envelope-anchored S2 subunits (35). Residues 319-541 of the spike protein

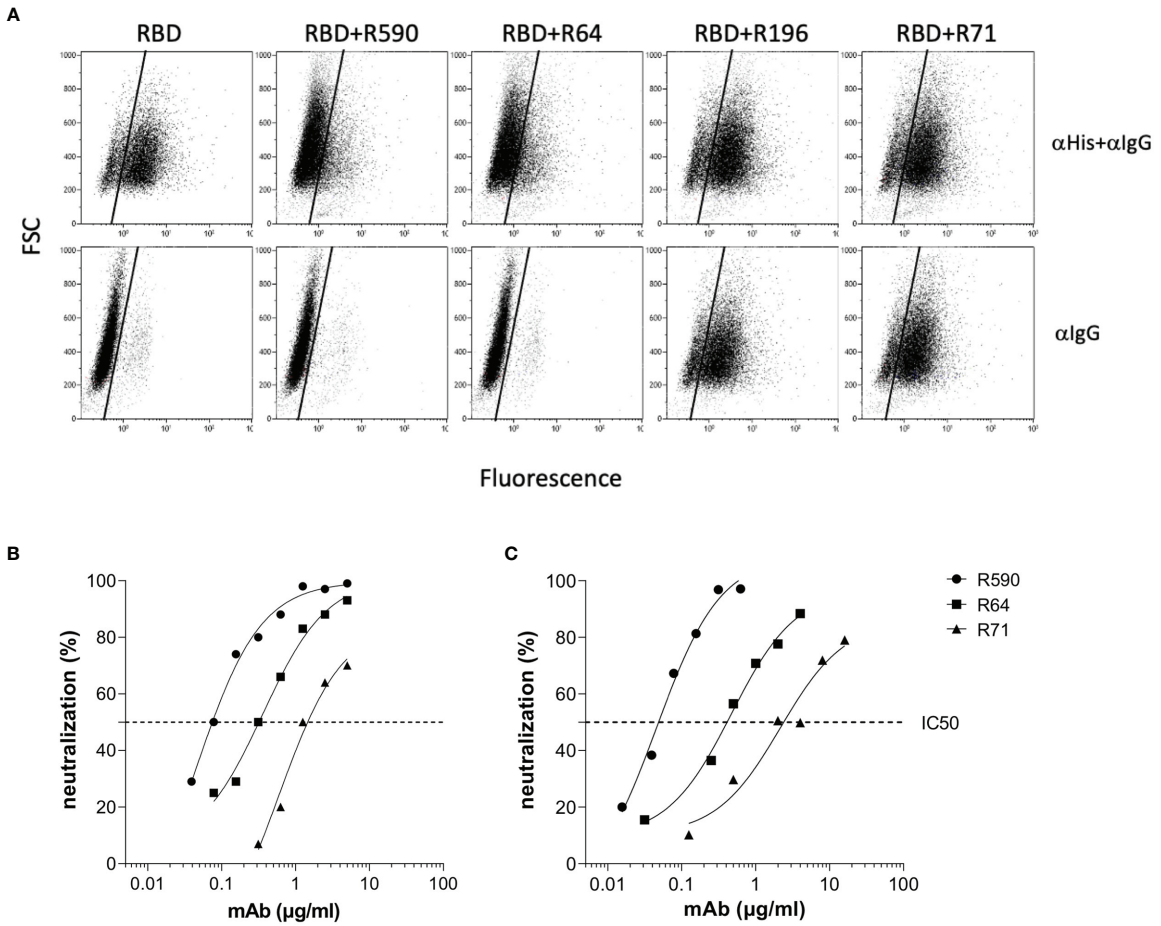

FIGURE 4 | mAb inhibition of RBD-ACE2 binding and neutralization activity against Wuhan SARS-CoV-2. **(A)** B16-hACE2 cells were incubated with rRBD alone or with rRBD pre-incubated with isolated mAbs. In the upper panels the ACE2-RBD binding was quantified by measuring the signal given by an α-His mAb revealed with a FITC-conjugated α-mouse IgG mAb (αHis+αIgG). In the lower panels, after rRBD incubation, an α-mouse IgG FITC-conjugated mAb was added in order to reveal anti-RBD mAbs bound to the hACE2 receptor. A representative experiment of two is shown. **(B)** Neutralization curves of anti-RBD mAbs against SARS-CoV-2 by PRNT or **(C)** spike pseudotyped LV neutralization assay. Data are representative of one experiment out of three with two technical replicates.

correspond to the RBD, the domain that interacts with the ACE2 receptor of target cells. The RBD undergoes hinge-like conformational movements and constantly switches between an open conformational state (RBD standing-up position) for receptor binding and a closed conformational state (RBD lying-down position). A complex topology corresponds to this dynamism including several co-translational modifications by reason of nine cysteine residues (eight of them forming disulfide bonds) (36), two N-glycosylations at sites N331 and N343 and at least one O-glycosylation at Thr323 and a possible O-glycosylation at Ser325 (19, 35, 37). All these modifications have a relevant role on the spike protein correct folding, dynamics and stability, but glycosylation of RBD seems to be not determinant for its interaction whit ACE2 receptor, since a refolded non-glycosylated rRBD produced in *E. coli* was shown by surface plasmon resonance to bind the receptor (38).

In this study, considering the key role of RBD in viral life cycle, we immunized mice with a rRBD produced in eukaryotic system to establish and characterize novel RBD-specific mouse mAbs. We isolated mAbs that showed extremely potent RBD binding activity and a broad neutralization activity, demonstrated by their ability to block efficiently the infection of SARS-CoV-2 and its major VOC. The performance of these mAbs, including their ability to interact with infectious virus, was probably dependent on the quality of the rRBD used to immunize mice. In fact, we showed that the produced rRBD was correctly folded, N-glycosylated, suitable to interact with ACE2 receptor expressing cells, and recognized by sera of vaccinees and COVID-19 convalescent patients, thus confirming that our HEK293T rRBD reproduced the structural antigenic and functional characteristics of RBD present in native spike protein. We showed that mAbs R590, R64, R71 and R196 do not recognize the *E. coli* rRBD which exposes only linear epitopes as it was produced in denaturing conditions. On the contrary, mAbs react with HEK293T rRBD in ELISA and in WB following SDS-PAGE run under non-reducing conditions. The

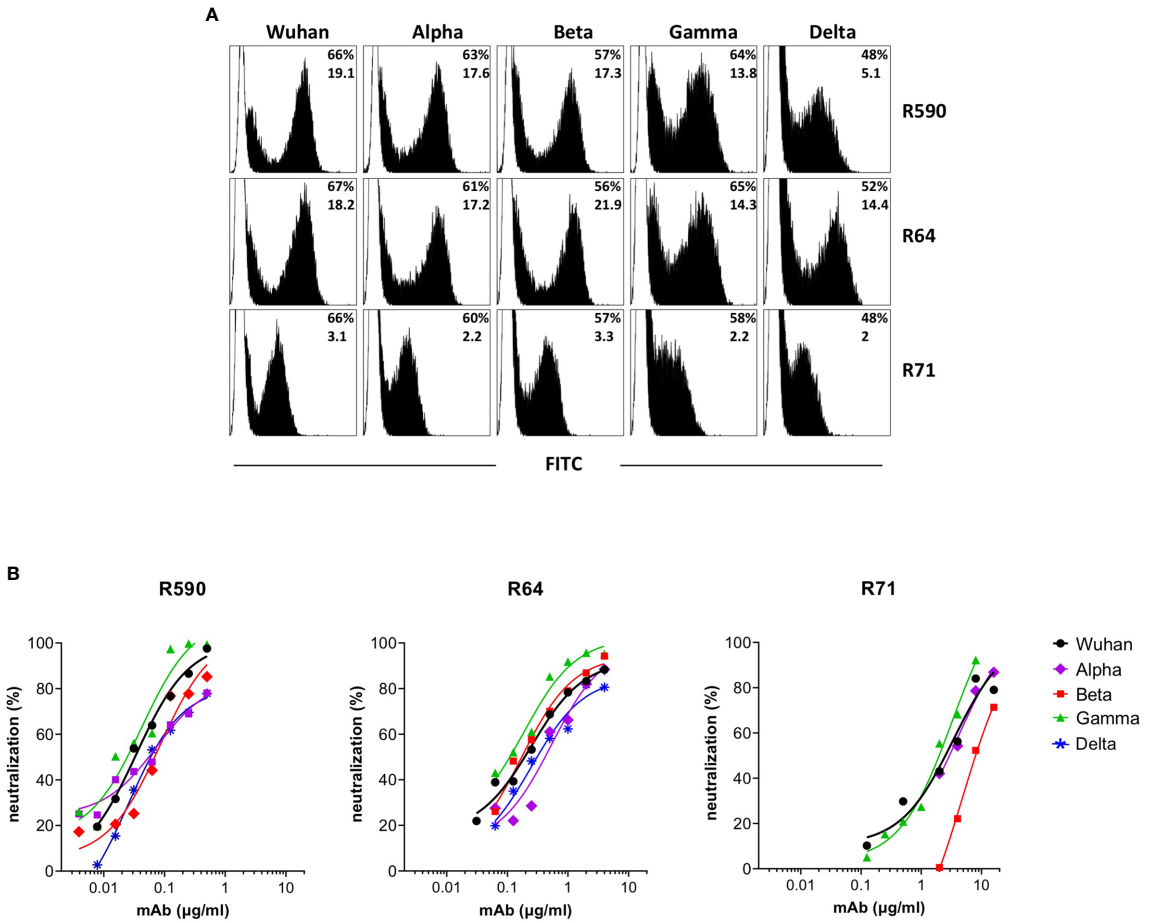

FIGURE 5 | Binding and neutralization potency of anti-RBD mAbs against Wuhan and VOC. **(A)** HEK293T cells transfected with plasmid coding for wild type transmembrane homotrimeric spike of Wuhan or VOC were stained with R590, R71, R64 neutralizing anti-RBD mAbs (black histograms), or with murine IgG1 control mAb (white histograms) followed by goat anti-mouse FITC-conjugated mAb and analysed by flow cytometry. The upper numbers indicate the percentages of positive cells, lower numbers indicate mean fluorescence intensity. A representative experiment is shown. **(B)** Neutralization curves obtained by using LV pseudotyped with spike of Wuhan or its Alpha, Beta, Gamma and Delta VOC testing serial dilutions of isolated R590, R64 and R71 mAbs. Data are mean representative of three independent experiments each with two technical replicates.

tridimensional configuration of proteins permits the generation of conformational epitopes formed from discontinuous antigenic determinants and it is largely dependent on disulfide bridges integrity (22). Therefore, reducing agents, such as βME, breaking disulfide bonds can affect the structure of conformational epitopes. Moreover, the mAbs R590, R71 and R196 lose their binding efficiency when HEK293T rRBD is fully N-de-glycosylated. Several plausible mechanisms can be envisaged to speculate how glycosylation could influence antibody binding (39). Glycans could be directly recognized by the antibody or may modify the conformation of the epitope. It is unlikely that our mAbs recognize a glycan antigen, since in this case their reactivity would not be lost altering the conformation of the protein with βME. A possible explanation is that N-glycosylation does not induce significant changes in protein structure, but decreases protein dynamics, leading to an increase in protein stability (40). The consequent conformational equilibrium of the antigen determinant may amplify the binding affinity of the specific antibody (41). Overall, these results suggest that our mAbs recognize conformational, but not linear epitopes on glycosylated RBD. This conclusion is in line with the data reported by Li Y et al. who demonstrated that RBD does not expose linear epitopes (42). Therefore, we did not map the epitopes recognized by our mAbs using a linear peptide library, whereas we attempted to define their binding and functional interactions with RBD. The antibodies R590 and R64 blocked the interaction of HEK293T rRBD with human ACE2 and neutralized infection of VERO E6 using both infectious SARS-CoV-2 and a pseudovirus based on LV expressing Luciferase and pseudotyped with SARS-CoV-2 spike. Instead, R196 and R71 were unable to inhibit the binding of HEK293T rRBD to ACE2 and while R196 was not able to block virus infection in the neutralization assays, R71 showed neutralization activity at high concentration with a mechanism that conceivably does not involve the RBD-ACE2 interaction. In addition, even if all mAbs recognized the native

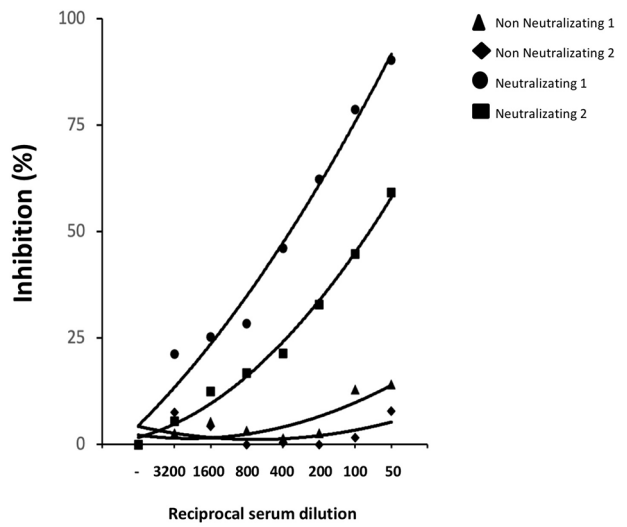

FIGURE 6 | Competition immune-enzymatic assay. Increasing amounts of human serum from two COVID-19 patients with nAbs or two healthy subjects were mixed with a fixed amount of neutralizing R590 and R64 mAbs to perform a competitive ELISA. The reduction of the mAbs binding to HEK293T rRBD was measured as absorbance reduction and considered dependent on nAb concentration in sera. Results are expressed as percentage of inhibition compared to the maximum binding of R590 and R64 in the absence of the human anti-RBD neutralizing serum as competitor. Results from two representative neutralizing sera out seven and two non-neutralizing out of six are shown.

form of the protein expressed on the HEK293T transfected cells, only R590, R71 and R196 but not R64 were able to bind the S1 region of inactivated SARS-CoV-2 supernatants of infected VERO E6 cells in a WB after SDS-PAGE run in non-reducing conditions. Interestingly, R64 immunoprecipitated the spike protein present on lentiviral pseudoviruses, suggesting that the epitope recognized by R64 is susceptible to any structural modification of the spike protein, including those caused by the SDS used for PAGE analysis (21). Based on all these data, we hypothesize that these anti-RBD mAbs bind to different epitopes on RBD: the two different epitopes recognized by R590 and R64 are likely located in the receptor binding site involved in the ACE2 interaction, while the two different epitopes recognized by R71 and R196 are located outside RBM (43).

It is worth noting that mAbs R590, R71 and R196 showed a high binding potency in ELISA and mAbs R590 and R64 also showed a high neutralizing efficiency. This is not surprising, since our mAbs were generated in mice following a prime-boosts schedule with a total of four immunizations at 14 days intervals to favor the affinity maturation of specific antibodies. A similar approach was followed for the isolation of specific human mAbs from vaccinated individuals (44) and differs from approaches based on the isolation of mAbs from convalescent donors, who experienced an antigenic challenge in the limited time-frame of the acute phase of the disease (45–48), that require a larger screening to identify mAbs with high potency.

Of particular interest, and in contrast to many described nAbs (27, 49–51), R590, R64 and R71showed the remarkable capacity to neutralize the major SARS-CoV-2 VOC (Alpha, Beta, Gamma and Delta) in a pseudovirus-based neutralization assay. This result indicates that the rRBD used for immunization exposes epitopes shared by the Wuhan-Hu-1 strains and its VOC. Viral variants must preserve the capacity to infect cells: since the interaction of RBD with the cellular receptor ACE2 is a crucial step in viral entry and infectivity, we may hypothesize that mutations in the RBD sequence, that hamper the generation of the conformational epitopes recognized by mAbs R590 and R64, may also affect the viral fitness reducing the capacity of SARS-CoV-2 to infect cells. Noteworthily, we showed that sera from COVID-19 patients who developed nAbs compete for the binding of our neutralizing mAbs to HEK293T rRBD, suggesting that conformational epitopes of glycosylated RBD are crucial for SARS-CoV-2 infectivity. Since mAbs R590 and R64 also neutralize SARS-CoV-2 VOC, a simple competition ELISA performed using these mAbs would predict whether COVID-19 convalescent or vaccinated individuals developed antibodies able to neutralize SARS-CoV-2 and its VOC. Lastly, the observation that immunization with our HEK293T rRBD induced antibodies neutralizing SARS-CoV-2 and its variants encourages its use for the development of a pan-SARS-CoV-2 subunit vaccine.

This study has some limitations: we did not test the reactivity of our mAbs with SARS-CoV-1, MERS-CoV or other common human coronaviruses and we could not precisely map the conformational epitopes that they recognized using cryo-microscopy, crystal studies, mutagenesis, or other techniques. Also, we did not evaluate the neutralizing activity of mAbs R590 and R64 *in vivo* in animal models. Should animal models confirm the neutralizing activity of these mAbs, the sequence of the immunoglobulin genes of the respective monoclonal hybridoma will easily permit the generation of humanized monoclonal antibodies that would increase the arsenal of "super-antibodies" in the fight against SARS-CoV-2 and its VOC (52).

In conclusion, beside possible implications for the therapy of COVID-19 patients if humanized, the described mAbs can be used for basic research activities to dissect the molecular mechanism of the virus life-cycle by investigating the expression profile and subcellular localization of spike glycoprotein during viral entry, replication, packaging and budding. Moreover, these mAbs could serve as valuable tools for the antigenic diagnosis of COVID-19 or for distinguishing individuals with high titers of nAbs in a simple ELISA format. Therefore, our mAbs may contribute to the advancement in basic and translational research and would accelerate the discovery of drugs targeting virus transmission.

DATA AVAILABILITY STATEMENT

The raw data supporting the conclusions of this article will be made available by the authors, without undue reservation.

ETHICS STATEMENT

Ethical review and approval was not required for the study on human participants in accordance with the local legislation and institutional requirements. The patients/participants provided their written informed consent to participate in this study. The animal study was reviewed and approved by National Committee for the Protection of Animals Used for Scientific Purposes established by the Animal Care and Welfare Department, Italian Health Ministry.

AUTHOR CONTRIBUTIONS

SM, AntC, MC, AI, RT, FT, and PDB: production, purification and characterization of recombinant proteins. SM, RT, AI, and AV: mice immunization, hybridoma production and mAb screening. SM, RT, MC, AntC, and AI: purification and characterization of mAb. MBa, AM, PB, FaM, and ZM: SARS-CoV-2 culture and virus neutralization assay. AndC, MP, AG, PM, and ACar: production of plasmids, lentiviral and retroviral vectors. MBo, AG, MA, and DN: pseudo-virus neutralization assay. CA, SS, MS, and PDB: genetic studies and plasmids design. GV: generation of B16-hACE2 cells. FrM and VE: size exclusion chromatography. RN, SM, AntC, MC, PDB, FaM, MS, ACar, and DN conceived the study and RN, SM, AntC, MC, ACar, and DN wrote the manuscript. All authors contributed to the article and approved the submitted version.

FUNDING

This work was funded, and the publication fee was provided by ISS intramural funds, NATO grant #G5817. In addition, this project has received funding from the European Union's Horizon 2020 research and innovation program under grant agreement no. 681137 (EAVI2020).

ACKNOWLEDGMENTS

Authors would like to thank Robin J. Shattock for plasmids and Massimo Sanchez and Valentina Tirelli for cell sorting.

SUPPLEMENTARY MATERIAL

The Supplementary Material for this article can be found online at: https://www.frontiersin.org/articles/10.3389/fimmu.2021.750386/full#supplementary-material

Supplementary Figure S1 | Quantification of rRBD produced in mammalian system. **(A)** Increasing volumes of purified rRBD and known amounts of BSA were resolved on SDS-PAGE. The gel was stained using Krypton fluorescent protein stain. **(B)** Lane profiling of total protein signal showing a cross-section view of each lane rotated 90 degrees. Area of green peaks above the lane is proportional to the amount of protein and its value is reported. Rf, current relative front value. Intensity (Int), average intensity value. * indicate the amount of BSA used to build a standard curve; ** indicate the calculated amount of rRBD based on the BSA standard curve.

Supplementary Figure S2 | rRBD production in *E. coli* coli expression system. **(A)** Schematic representation of RBD construct in *E. coli* expression vector. RBD fragment was inserted into BamHI/HindIII restriction sites of pQE30 vector's multi cloning site (MCS), in frame with the ATG and 6xHis tag. **(B)** Protein purity was analyzed by SDS-PAGE followed by staining with Coomassie blue. Protein identity was confirmed by WB using the anti-RGSHHHH antibody. One of three independent experiments is shown.

REFERENCES

1. Zhu N, Zhang D, Wang W, Li X, Yang B, Song J, et al. A Novel Coronavirus From Patients With Pneumonia in China, 2019. *N Engl J Med* (2020) 382 (8):727–33. doi: 10.1056/NEJMoa2001017
2. Wang D, Hu B, Hu C, Zhu F, Liu X, Zhang J, et al. Clinical Characteristics of 138 Hospitalized Patients With 2019 Novel Coronavirus-Infected Pneumonia in Wuhan, China. *JAMA* (2020) 323(11):1061–9. doi: 10.1001/jama.2020.1585
3. Coronaviridae Study Group of the International Committee on Taxonomy of V. The Species Severe Acute Respiratory Syndrome-Related Coronavirus: Classifying 2019-Ncov and Naming It SARS-CoV-2. *Nat Microbiol* (2020) 5 (4):536–44. doi: 10.1038/s41564-020-0695-z
4. Kimball A, Hatfield KM, Arons M, James A, Taylor J, Spicer K, et al. Asymptomatic and Presymptomatic SARS-CoV-2 Infections in Residents of a Long-Term Care Skilled Nursing Facility - King County, Washington, March 2020. *MMWR Morb Mortal Wkly Rep* (2020) 69(13):377–81. doi: 10.15585/mmwr.mm6913e1
5. Abdool Karim SS, de Oliveira T. New SARS-CoV-2 Variants - Clinical, Public Health, and Vaccine Implications. *N Engl J Med* (2021) 384(19):1866–8. doi: 10.1056/NEJMc2100362
6. Li X, Geng M, Peng Y, Meng L, Lu S. Molecular Immune Pathogenesis and Diagnosis of COVID-19. *J Pharm Anal* (2020) 10(2):102–8. doi: 10.1016/j.jpha.2020.03.001
7. Davidson AD, Williamson MK, Lewis S, Shoemark D, Carroll MW, Heesom KJ, et al. Characterisation of the Transcriptome and Proteome of SARS-CoV-2 Reveals a Cell Passage Induced in-Frame Deletion of the Furin-Like Cleavage Site From the Spike Glycoprotein. *Genome Med* (2020) 12(1):68. doi: 10.1186/s13073-020-00763-0
8. Kim D, Lee JY, Yang JS, Kim JW, Kim VN, Chang H. The Architecture of SARS-CoV-2 Transcriptome. *Cell* (2020) 181(4):914–21.e10. doi: 10.1016/j.cell.2020.04.011
9. Walls AC, Park YJ, Tortorici MA, Wall A, McGuire AT, Veesler D. Structure, Function, and Antigenicity of the SARS-CoV-2 Spike Glycoprotein. *Cell* (2020) 183(6):1735. doi: 10.1016/j.cell.2020.11.032
10. Su S, Du L, Jiang S. Learning From the Past: Development of Safe and Effective COVID-19 Vaccines. *Nat Rev Microbiol* (2021) 19(3):211–9. doi: 10.1038/s41579-020-00462-y
11. Ju B, Zhang Q, Ge J, Wang R, Sun J, Ge X, et al. Human Neutralizing Antibodies Elicited by SARS-CoV-2 Infection. *Nature* (2020) 584(7819):115–9. doi: 10.1038/s41586-020-2380-z
12. Byrnes JR, Zhou XX, Lui I, Elledge SK, Glasgow JE, Lim SA, et al. Competitive SARS-CoV-2 Serology Reveals Most Antibodies Targeting the Spike Receptor-Binding Domain Compete for ACE2 Binding. *mSphere* (2020) 5 (5):1–11. doi: 10.1128/mSphere.00802-20
13. Choi YK, Cao Y, Frank M, Woo H, Park SJ, Yeom MS, et al. Structure, Dynamics, Receptor Binding, and Antibody Binding of the Fully Glycosylated Full-Length SARS-CoV-2 Spike Protein in a Viral Membrane. *J Chem Theory Comput* (2021) 17(4):2479–87. doi: 10.1021/acs.jctc.0c01144
14. Pramanick I, Sengupta N, Mishra S, Pandey S, Girish N, Das A, et al. Conformational Flexibility and Structural Variability of SARS-CoV2 S Protein. *Structure* (2021) 29(8):834–45.e5. doi: 10.1016/j.str.2021.04.006

15. Carnell GW, Ciazynska KA, Wells DA, Xiong X, Aguinam ET, McLaughlin SH, et al. SARS-CoV-2 Spike Protein Stabilized in the Closed State Induces Potent Neutralizing Responses. *J Virol* (2021) 95(15):e0020321. doi: 10.1128/JVI.00203-21
16. Dispinseri S, Secchi M, Pirillo MF, Tolazzi M, Borghi M, Brigatti C, et al. Neutralizing Antibody Responses to SARS-CoV-2 in Symptomatic COVID-19 Is Persistent and Critical for Survival. *Nat Commun* (2021) 12(1):2670. doi: 10.1038/s41467-021-22958-8
17. Fekete S, Beck A, Veuthey JL, Guillarme D. Theory and Practice of Size Exclusion Chromatography for the Analysis of Protein Aggregates. *J Pharm BioMed Anal* (2014) 101:161–73. doi: 10.1016/j.jpba.2014.04.011
18. Magurano F, Baggieri M, Marchi A, Rezza G, Nicoletti L, Group C-S. SARS-CoV-2 Infection: The Environmental Endurance of the Virus can be Influenced by the Increase of Temperature. *Clin Microbiol Infect* (2021) 27(2):289.e5–7. doi: 10.1016/j.cmi.2020.10.034
19. Watanabe Y, Allen JD, Wrapp D, McLellan JS, Crispin M. Site-Specific Glycan Analysis of the SARS-CoV-2 Spike. *Science* (2020) 369(6501):330–3. doi: 10.1126/science.abb9983
20. Farnos O, Venereo-Sanchez A, Xu X, Chan C, Dash S, Chaabane H, et al. Rapid High-Yield Production of Functional SARS-CoV-2 Receptor Binding Domain by Viral and Non-Viral Transient Expression for Pre-Clinical Evaluation. *Vaccines (Basel)* (2020) 8(4):1-20. doi: 10.3390/vaccines8040654
21. Graumann K, Premstaller A. Manufacturing of Recombinant Therapeutic Proteins in Microbial Systems. *Biotechnol J* (2006) 1(2):164–86. doi: 10.1002/biot.200500051
22. Ferdous S, Kelm S, Baker TS, Shi J. Martin ACR. B-Cell Epitopes: Discontinuity and Conformational Analysis. *Mol Immunol* (2019) 114:643–50. doi: 10.1016/j.molimm.2019.09.014
23. Krainer G, Hartmann A, Bogatyr V, Nielsen J, Schlierf M, Otzen DE. SDS-Induced Multi-Stage Unfolding of a Small Globular Protein Through Different Denatured States Revealed by Single-Molecule Fluorescence. *Chem Sci* (2020) 11(34):9141–53. doi: 10.1039/d0sc02100h
24. Krause PR, Fleming TR, Longini IM, Peto R, Briand S, Heymann DL, et al. SARS-CoV-2 Variants and Vaccines. *N Engl J Med* (2021) 385(2):179–86. doi: 10.1056/NEJMsr2105280
25. Karim SSA. Vaccines and SARS-CoV-2 Variants: The Urgent Need for a Correlate of Protection. *Lancet* (2021) 397(10281):1263–4. doi: 10.1016/S0140-6736(21)00468-2
26. Stankov MV, Cossmann A, Bonifacius A, Dopfer-Jablonka A, Ramos GM, Godecke N, et al. Humoral and Cellular Immune Responses Against SARS-CoV-2 Variants and Human Coronaviruses After Single BNT162b2 Vaccination. *Clin Infect Dis* (2021). doi: 10.1093/cid/ciab555
27. Liu Z, VanBlargan LA, Bloyet LM, Rothlauf PW, Chen RE, Stumpf S, et al. Landscape Analysis of Escape Variants Identifies SARS-CoV-2 Spike Mutations That Attenuate Monoclonal and Serum Antibody Neutralization. *bioRxiv* (2020). doi: 10.1101/2020.11.06.372037
28. Niu L, Wittrock KN, Clabaugh GC, Srivastava V. Cho MW. A Structural Landscape of Neutralizing Antibodies Against SARS-CoV-2 Receptor Binding Domain. *Front Immunol* (2021) 12:647934. doi: 10.3389/fimmu.2021.647934
29. Matricardi PM, Dal Negro RW, Nisini R. The First, Holistic Immunological Model of COVID-19: Implications for Prevention, Diagnosis, and Public Health Measures. *Pediatr Allergy Immunol* (2020) 31(5):454–70. doi: 10.1111/pai.13271
30. Callaway E. The Race for Coronavirus Vaccines: A Graphical Guide. *Nature* (2020) 580(7805):576–7. doi: 10.1038/d41586-020-01221-y
31. Riva L, Yuan S, Yin X, Martin-Sancho L, Matsunaga N, Pache L, et al. Discovery of SARS-CoV-2 Antiviral Drugs Through Large-Scale Compound Repurposing. *Nature* (2020) 586(7827):113–9. doi: 10.1038/s41586-020-2577-1
32. Gandhi RT, Lynch JB, Del Rio C. Mild or Moderate Covid-19. *N Engl J Med* (2020) 383(18):1757–66. doi: 10.1056/NEJMcp2009249
33. Kissler SM, Tedijanto C, Goldstein E, Grad YH, Lipsitch M. Projecting the Transmission Dynamics of SARS-CoV-2 Through the Postpandemic Period. *Science* (2020) 368(6493):860–8. doi: 10.1126/science.abb5793
34. Chapman AP, Tang X, Lee JR, Chida A, Mercer K, Wharton RE, et al. Rapid Development of Neutralizing and Diagnostic SARS-COV-2 Mouse Monoclonal Antibodies. *Sci Rep* (2021) 11(1):9682. doi: 10.1038/s41598-021-88809-0
35. Zhao P, Praissman JL, Grant OC, Cai Y, Xiao T, Rosenbalm KE, et al. Virus-Receptor Interactions of Glycosylated SARS-CoV-2 Spike and Human ACE2 Receptor. *Cell Host Microbe* (2020) 28(4):586–601 e6. doi: 10.1016/j.chom.2020.08.004
36. Shrimal S, Cherepanova NA, Gilmore R. Cotranslational and Posttranslocational N-Glycosylation of Proteins in the Endoplasmic Reticulum. *Semin Cell Dev Biol* (2015) 41:71–8. doi: 10.1016/j.semcdb.2014.11.005
37. Zhang S, Go EP, Ding H, Anang S, Kappes JC, Desaire H, et al. Analysis of Glycosylation and Disulfide Bonding of Wild-Type SARS-CoV-2 Spike Glycoprotein. *bioRxiv* (2021). doi: 10.1101/2021.04.01.438120
38. He Y, Qi J, Xiao L, Shen L, Yu W, Hu T. Purification and Characterization of the Receptor-Binding Domain of SARS-CoV-2 Spike Protein From Escherichia Coli. *Eng Life Sci* (2021) 21(6):453–60. doi: 10.1002/elsc.202000106
39. Lisowska E. The Role of Glycosylation in Protein Antigenic Properties. *Cell Mol Life Sci* (2002) 59(3):445–55. doi: 10.1007/s00018-002-8437-3
40. Lee HS, Qi Y, Im W. Effects of N-Glycosylation on Protein Conformation and Dynamics: Protein Data Bank Analysis and Molecular Dynamics Simulation Study. *Sci Rep* (2015) 5:8926. doi: 10.1038/srep08926
41. Movahedin M, Brooks TM, Supekar NT, Gokanapudi N, Boons GJ, Brooks CL. Glycosylation of MUC1 Influences the Binding of a Therapeutic Antibody by Altering the Conformational Equilibrium of the Antigen. *Glycobiology* (2017) 27(7):677–87. doi: 10.1093/glycob/cww131
42. Li Y, Ma ML, Lei Q, Wang F, Hong W, Lai DY, et al. Linear Epitope Landscape of the SARS-CoV-2 Spike Protein Constructed From 1,051 COVID-19 Patients. *Cell Rep* (2021) 34(13):108915. doi: 10.1016/j.celrep.2021.108915
43. Barnes CO, Jette CA, Abernathy ME, Dam KA, Esswein SR, Gristick HB, et al. SARS-CoV-2 Neutralizing Antibody Structures Inform Therapeutic Strategies. *Nature* (2020) 588(7839):682–7. doi: 10.1038/s41586-020-2852-1
44. Bernasconi NL, Traggiai E, Lanzavecchia A. Maintenance of Serological Memory by Polyclonal Activation of Human Memory B Cells. *Science* (2002) 298(5601):2199–202. doi: 10.1126/science.1076071
45. Andreano E, Nicastri E, Paciello I, Pileri P, Manganaro N, Piccini G, et al. Extremely Potent Human Monoclonal Antibodies From COVID-19 Convalescent Patients. *Cell* (2021) 184(7):1821–35.e16. doi: 10.1016/j.cell.2021.02.035
46. Jones BE, Brown-Augsburger PL, Corbett KS, Westendorf K, Davies J, Cujec TP, et al. The Neutralizing Antibody, LY-CoV555, Protects Against SARS-CoV-2 Infection in Nonhuman Primates. *Sci Transl Med* (2021) 13(593). doi: 10.1126/scitranslmed.abf1906
47. Graham C, Seow J, Huettner I, Khan H, Kouphou N, Acors S, et al. Neutralization Potency of Monoclonal Antibodies Recognizing Dominant and Subdominant Epitopes on SARS-CoV-2 Spike Is Impacted by the B.1.1.7 Variant. *Immunity* (2021) 54(6):1276–89.e6. doi: 10.1016/j.immuni.2021.03.023
48. Liu H, Wu NC, Yuan M, Bangaru S, Torres JL, Caniels TG, et al. Cross-Neutralization of a SARS-CoV-2 Antibody to a Functionally Conserved Site Is Mediated by Avidity. *Immunity* (2020) 53(6):1272–80 e5. doi: 10.1016/j.immuni.2020.10.023
49. Chen RE, Zhang X, Case JB, Winkler ES, Liu Y, VanBlargan LA, et al. Resistance of SARS-CoV-2 Variants to Neutralization by Monoclonal and Serum-Derived Polyclonal Antibodies. *Nat Med* (2021) 27(4):717–26. doi: 10.1038/s41591-021-01294-w
50. Hoffmann M, Hofmann-Winkler H, Krüger N, Kempf A, Nehlmeier I, Graichen L, et al. SARS-CoV-2 Variant B.1.617 Is Resistant to Bamlanivimab and Evades Antibodies Induced by Infection and Vaccination. *Cell Rep* (2021) 36(9):1–9. doi: 10.1101/2021.05.04.442663
51. Chen RE, Winkler ES, Case JB, Aziati ID, Bricker TL, Joshi, et al. *In Vivo* Monoclonal Antibody Efficacy Against SARS-CoV-2 Variant Strains. *Nature* (2021) 596(7870):103–8. doi: 10.1038/s41586-021-03720-y
52. Dolgin E. 'Super-Antibodies' Could Curb COVID-19 and Help Avert Future Pandemics. *Nat Biotechnol* (2021) 39(7):783–5. doi: 10.1038/s41587-021-00980-x

Conflict of Interest: The authors declare that the research was conducted in the absence of any commercial or financial relationships that could be construed as a potential conflict of interest.

this article, or claim that may be made by its manufacturer, is not guaranteed or endorsed by the publisher.

frontiers in Immunology

ORIGINAL RESEARCH
published: 11 November 2021
doi: 10.3389/fimmu.2021.730099

Rapid Assessment of Binding Affinity of SARS-COV-2 Spike Protein to the Human Angiotensin-Converting Enzyme 2 Receptor and to Neutralizing Biomolecules Based on Computer Simulations

*Damiano Buratto[1], Abhishek Saxena[1], Qun Ji[1], Guang Yang[1], Sergio Pantano[1,2] and Francesco Zonta[1]**

[1] Shanghai Institute for Advanced Immunochemical Studies, ShanghaiTech University, Shanghai, China, [2] Institut Pasteur de Montevideo, Montevideo, Uruguay

SARS-CoV-2 infects humans and causes Coronavirus disease 2019 (COVID-19). The S1 domain of the spike glycoprotein of SARS-CoV-2 binds to human angiotensin-converting enzyme 2 (hACE2) *via* its receptor-binding domain, while the S2 domain facilitates fusion between the virus and the host cell membrane for entry. The spike glycoprotein of circulating SARS-CoV-2 genomes is a mutation hotspot. Some mutations may affect the binding affinity for hACE2, while others may modulate S-glycoprotein expression, or they could result in a virus that can escape from antibodies generated by infection with the original variant or by vaccination. Since a large number of variants are emerging, it is of vital importance to be able to rapidly assess their characteristics: while changes of binding affinity alone do not always cause direct advantages for the virus, they still can provide important insights on where the evolutionary pressure is directed. Here, we propose a simple and cost-effective computational protocol based on Molecular Dynamics simulations to rapidly screen the ability of mutated spike protein to bind to the hACE2 receptor and selected neutralizing biomolecules. Our results show that it is possible to achieve rapid and reliable predictions of binding affinities. A similar approach can be used to perform preliminary screenings of the potential effects of S-RBD mutations, helping to prioritize the more time-consuming and expensive experimental work.

Keywords: COVID-19, SARS-CoV-2, Spike-RBD, human ACE2, binding affinity, neutralizing antibodies, protein-protein interaction, molecular dynamics

OPEN ACCESS

Edited by:
Peter Chen,
Cedars-Sinai Medical Center,
United States

Reviewed by:
Srinivasa Reddy Bonam,
Institut National de la Santé et de la Recherche Médicale (INSERM),
France
Jean-Luc Pellequer,
UMR5075 Institut de Biologie Structurale (IBS), France

***Correspondence:**
Francesco Zonta
fzonta@shanghaitech.edu.cn

Specialty section:
This article was submitted to Vaccines and Molecular Therapeutics, a section of the journal Frontiers in Immunology

Received: *24 June 2021*
Accepted: *25 October 2021*
Published: *11 November 2021*

Citation:
Buratto D, Saxena A, Ji Q, Yang G, Pantano S and Zonta F (2021) Rapid Assessment of Binding Affinity of SARS-COV-2 Spike Protein to the Human Angiotensin-Converting Enzyme 2 Receptor and to Neutralizing Biomolecules Based on Computer Simulations. Front. Immunol. 12:730099. doi: 10.3389/fimmu.2021.730099

INTRODUCTION

Severe acute respiratory syndrome coronavirus-2 (SARS-CoV-2) causes pneumonia/severe respiratory infection in humans called Coronavirus disease 2019 (COVID-19). The first cases of COVID-19 were reported in December 2019 from Wuhan, China (1). At the moment of writing this manuscript, SARS-CoV-2 infection is reported in ~180 million people resulting in ~5 million deaths (2). SARS-CoV-2 is an enveloped virus belonging to a diverse subgenus sarbecovirus within the Betacoronaviruses, a lineage of viruses that use bats as reservoirs and can be transmitted into other mammals (3–8). SARS-CoV-2 is genetically distinct from severe acute respiratory syndrome coronavirus (SARS-CoV) and Middle East respiratory syndrome coronavirus (MERS-CoV). Its closest known relative is Bat CoV RaTG13 (4–6), with 96.3% of gene identity. The single-stranded RNA genome of SARS-CoV-2 encodes Spike (S), Envelope (E), Membrane (M), and Nucleocapsid (N) structural proteins (5). The Spike (S) glycoprotein comprising S1 and S2 subdomains interacts with human angiotensin-converting enzyme 2 (hACE2) present primarily on pneumocytes/lung immune cells for attachment (*via* S1 c-terminal receptor-binding domain S-RBD), fusion, and virus entry into the host cell (*via* S2) (9–12). S-RBD also has a role in cross-species transmission and evolution of SARS-CoV-2 (8, 12–15). It is also the major immune determinant of a human neutralizing immune response upon natural infection and vaccination (16–19). Although S-RBD plays a critical role in viral infectivity and transmission, it is highly variable among sarbecoviruses and possibly a hotspot of complex selective pressure which shapes SARS-CoV-2 evolution (8, 20–22). Recombination events in the genome contribute to CoVs evolution, and recombination breakpoints are evident in the SARS-CoV-2 genome at the beginning and end of the S-RBD (6, 9, 23). Mutations within the S-RBD can increase affinity for ACE2, transmissibility, and mediate immune escape (8, 24–28).

Computer simulations have been widely used to provide important insight into the role of mutations within the S-RBD. Molecular dynamics (MD) simulations-based analyses show some of the earliest known S-RBD mutations (F342L, N352D/D364Y, V367F, W436R, and V483A) can increase binding affinities and favor hACE2 interaction (29–31). Another study on the B.1.135 (K417N/E484K/N501Y) variant suggests that while N501Y alone could improve the binding affinity, the other two mutations reduced it, possibly causing a non-net change in binding properties (26). In agreement with this hypothesis, experimental mutational scanning suggest that N501Y/N501T slightly increase hACE2 binding while K417N/K417T enhance S-RBD expression, and E484K did not cause any significant phenotypic change (8).

In this paper, we report a computational protocol to rapidly assess the binding affinity of the S-RBD to the hACE2 receptor. We applied our method on some early reported mutations (G476S, V483A, H519Q, and H520), the triple mutant B.1.135 K417N/E484K/N501Y, first isolated in South Africa – beta variant, and triple mutant P.1 K417T/E484K/N501Y, first isolated in Brazil – gamma variant, investigating their effect at the molecular level. Our results suggest that none of the mutations causes an essential increase of the K_D/IC_{50} properties of the Spike protein. Still, we observe a significant, albeit small, decrease of binding affinity for the two triple mutants. However, we observe a more marked reduction of the binding of spike protein to an artificial neutralizing nanobody caused by E484K, a mutation found in several variants of concern and which has been reported to produce a virus able to escape neutralizing antibodies (32–35).

MATERIAL AND METHODS

Molecular Modeling and Dynamics

The model of the reference type (RT) variant Covid-19 RBD in complex with hACE2 receptor was derived by the X-RAY crystal structure PDBID 6LZG (36). All the mutants of the Covid-19 S-RBD were created starting from this model using CHIMERA (37). Each model was solvated with TIP3P water, containing Cl- and K+ ions at a concentration of ~0.15 M to mimic the physiological ionic strength. After solvation, the total number of atoms for each system was around 1.7×10^5.

MD simulations were carried on using the Gromacs 2018 package (38) and the Amber14SB force field (39), following simulation protocols similar to those we used in our previous works (40–43). Specifically, after energy minimization, we performed 200 ps of Simulated Annealing to allow side chains to equilibrate after each mutation is introduced. We then performed two short simulations lasting 100 ps, first in the NVT and then in the NPT ensembles, both with positional restraints (being the position restraint constant $k_{pr} = 1000 \frac{KJ}{mol \cdot nm^2}$) on the heavy atoms of the protein. Finally, we performed equilibrium MD simulation under periodic boundary conditions at constant pressure for 50 ns. Analyses were performed only on the last 25 ns after equilibration, as explained in the Results section. Temperature T and pressure P were kept constant during the equilibrium MD simulation, at 300 K and 1 atm, respectively, using the Berendsen thermostat and barostat (44). Fast smooth Particle–Mesh Ewald summation (45) was used for long-range electrostatic interactions, with a cut-off of 1.0 nm for the direct interactions. Each simulation was performed in five identical replicas: while classical MD simulations are in principle deterministic, parallel computing algorithms currently implemented in MD software can produce different trajectories. Nevertheless, experimental structures represent a thermodynamic average. Hence, replicating the simulations allows to check the results consistency and reduce the risk of being trapped by entropic barriers, thus improving the sampling of the configuration space available.

Binding Free Energy Computations

To produce fast and reliable predictions of the binding free energy, we use the PRODIGY web server (46, 47), which has been designed for this purpose. The results are then compared with those obtained with MM-PBSA (an acronym for Molecular Mechanics – Poisson Boltzmann and Surface Area continuum

solvation approximation method), a more standard methodology, widely used in the field (48, 49). Binding free energies are calculated as ensemble averages over the configuration space explored by the five different replicas. To speed up the calculation, while maintaining a meaningful set of configurations for the energy calculations, we clustered the configuration space sampled by the various MD trajectories after equilibration (i.e., the last 25 ns each of the five replicas) according to their root mean square deviation (RMSD), and calculate the binding energy using one representative for 60 bigger clusters, being the clustering distance 1.2 Å. The final result is then obtained as the average of the free energy computed for each of these configurations. The results obtained by the two methods show correlation (R=0.82, **Supplementary Figure 1**). However, the PRODIGY webserver is considerably faster than the MM-PBSA calculations (~50 times faster than our local MD-dedicated GPU cluster - this figure can be much higher if parallel computational resources are not available). Furthermore, it requires a much easier set-up so that the calculation can be performed by less experienced investigators.

From the binding free energy difference, it is possible to estimate the change in binding affinity using thermodynamics theory, according to the expression (50): $RT\Delta\ln(K_D) = \Delta\Delta G_{Exp}$. The results computed with the PRODIGY webserver show correlation with experimental data (**Supplementary Figure 2**).

Recombinant Production of SARS-CoV-2 S-RBD Mutants and hACE2

Reference SARS-CoV-2 S-RBD (nt 22,517 – 23,185; MN908947) and hACE2-ECD (aa19 – aa617; Uniprot Q9BYF1) coding gene fragments were obtained by chemical synthesis. S-RBD reference gene with C-terminus hexahistidine tag was cloned in *5'NotI/3'BamHI* restriction sites of pSCSTa plasmid under the control of CMV promoter and used to generate mutant constructs (G476S, V483A, H519Q, and A520S) by oligonucleotide-mediated PCR mutagenesis. All S-RBD proteins were transiently produced in FreeStyle 293f cells (Invitrogen). Culture supernatant containing protein was bound to Ni-NTA resin (Yeason Biotech), eluted with 500 mM imidazole in 20 mM HEPES/500 mM NaCl, buffer exchanged to 1x PBS and further cleaned by size exclusion chromatography using Superdex 200 10/300 column (GE Healthcare) on AKTA Avant150 FPLC system. The Human ACE2 gene was cloned into unique *SfiI* restriction sites in pFUSE-mIgG2A-Fc2 plasmid (Invivogen) under the control of a hEF1-HTLV-1 promoter and produced like S-RBD proteins. Culture supernatant containing hACE2-ECD-mFc was bound to Mabselect resin (GE Healthcare), eluted by Pierce IgG elution buffer (Thermo Scientific), and buffer exchanged to 1x PBS. All recombinant proteins were resolved on 4 – 12% gradient SDS-PAGE to ascertain purity and correct size.

Experimental Determination of the Binding Affinities Between S-RBD Variants and ACE2 Receptor

Maxisorp ELISA wells were coated with 200 nM S-RBD reference/mutant protein overnight at 4°C, blocked with 2% (w/v) skimmed milk at room temperature for 1 hour (h). To determine EC_{50} values, hACE2-ECD dilutions (two-fold; 250 nM – 0.015 nM) were added to the designated wells and incubated at room temperature for 1 h. To determine IC_{50} values, hACE2-ECD at predetermined EC_{50} concentration (for respective S-RBD reference/mutant) was mixed with the cognate S-RBD protein (two-fold dilution; 1000 – 0.487 nM) and incubated at room temperature for 1 h before being added to the designated S-RBD reference/mutant coated and blocked wells. The binding was detected with 1:1000 diluted anti-mouse IgG (Fc specific) PO labeled secondary antibody (Cell Signalling Technologies).

The kinetics of S-RBD – hACE2-ECD interaction was analyzed by biolayer interferometry (BLI) using the Octet Red96 system (PALL ForteBio). HIS1K dip and read optical sensors (PALL ForteBio) were used to detect non-specific binding with the highest concentration of hACE2-ECD used in the assay, and passed sensors were subsequently loaded with 1000 nM S-RBD reference/mutant protein to reach a loading threshold of ~0.5 nm. Human ACE2-ECD dilutions (two-fold; 2500 – 312.5 nM) were used as an analyte to measure *KD*. Reference sensors with no load and reference well with only 1x kinetics buffer were used as controls.

Statistical Analysis

Statistical analysis of ELISA data was done using Prism software version 8.00 (GraphPad). EC_{50} and IC_{50} values were determined by nonlinear regression analysis, by fitting log (agonist concentration) vs. response and log (inhibitor concentration) *vs.* normalized response, respectively.

The IC_{50} binding curves (column means) were analyzed by two-way ANOVA with Dunnett's multiple comparison tests. The biolayer interferometry (BLI) binding curves were generated and K_D were determined by fitting the curves globally and analyzed by the 1:1 model using Pall Forte Bio Octet Data Analysis Software version 10.0. The K_D values of three replicates so obtained were compared by two-way ANOVA with Tukey's multiple comparison tests using Prism software version 8.00 (GraphPad).

Binding free energies were computed from the representative configuration of the 60 more populated cluster. Values on **Tables 1**, **2** are presented as averages and standard errors of the mean. The errors for the variation of binding affinity were computed with the error propagation formula, p-values were obtained using the Student t-test. Box plots were draw using Python and the Seaborn package.

RESULTS

Sampling of the Interaction Between the S-RBD and the hACE2 Receptor

A reliable computation of the binding free energy between two proteins should take into account the possibility of their dynamical rearrangement and extensive sampling (50). X-ray structures can be considered as faithful representations of the energy minima, but cannot take into account a very important

TABLE 1 | Table of computed ΔG and ΔΔG ($\Delta G_{variant} - \Delta G_{RT}$).

	ΔG kcal/mol	$\sigma_{\Delta G}$ kcal/mol	ΔΔG kcal/mol	p-value
Reference Type	-12.02	0.06	–	–
G476S	-11.40	0.08	0.61	$7.8*10^{-8}$
V483A	-12.15	0.08	-0.13	0.21
H519Q	-12.18	0.08	-0.17	0.11
A520S	-11.88	0.08	0.13	0.19
N501Y E484K K417N	-11.11	0.07	0.90	$3.7*10^{-16}$
K417N	-11.97	0.08	0.05	0.62
N501Y E484K K417T	-11.03	0.09	0.98	$3.3*10^{-15}$
K417T	-11.84	0.07	0.17	0.08
N501Y	-11.63	0.08	0.39	$2.5*10^{-4}$
E484K	-12.10	0.08	-0.09	0.41

*The table reports averages, standard error of the mean and p-values of the difference between the binding affinities of S-RBD and hACE2 receptor. The relative binding affinity **ΔΔG** use the RT as reference.*

contribution to their binding affinity, i.e., the temperature effects on the two interacting proteins. Furthermore, when introducing a mutation in a structural model, it is likely that the local structure will not be well equilibrated. For both these reasons, we performed MD simulations of each possible pairs of spike-hACE2 receptor proteins. Each simulation was repeated in five different replicas to further improve the configurational sampling and reducing the probability of being trapped in local minima (see Methods section).

Analysis of the root mean square deviation (RMSD - **Supplementary Figure 3**) of the various trajectories shows that the S-RBD finds its equilibrium position on average after 25 ns. For this reason, we decided to carry on the following analysis on the second half of each trajectory.

From the dynamic point of view, all the different variants behave similarly. Analysis of the contact maps between the two proteins reveals that in the RT variant, the interaction is mainly mediated by residues Lys417, Tyr449, Leu455, Phe456, Ala475, Phe 486, Asn487, Tyr489, Gln493, Gly496, Gln498, Thr500, Asn501, Gly502 and Tyr505 (interaction probability higher than 90% along the trajectory, see **Figure 1**, **Supplementary Figures 4**, **5**). No significant difference is observed between the RT and the single point mutations G476S, V483A, H519Q, A520S. It is worth noticing that only the first two mutants are in proximity of the binding region, while the other two are far from it, and we do not expect to see any effect on the binding to the hACE2 receptor caused by them.

When looking at the two triple mutants, we can observe that mutations of Lys417 and Asp501 are slightly more impactful in affecting the interaction between the spike protein and the hACE2 receptor. Lys417 forms a salt bridge with Asp30 of hACE2, which is abolished upon lysine mutation to asparagine or threonine. The change from asparagine to tyrosine in position 501 forces a different arrangement of the spike protein residues Tyr499 and Gly496, affecting their interactions with Asp38, Gln32, and Lys353 of the hACE2 (**Figure 1** and **Supplementary Figure 5**). Since Glu48 does not interact with the hACE2 receptor in the RT, its mutation to lysine does not produce critical differences in the contact map.

In agreement with these observations, root mean square fluctuations (RMSF) show no evident changes in the dynamical behavior of the complex, especially in the contact region (**Figure 2**).

Rapid Evaluation of Binding Free Energy Between the S-RBD and the hACE2 Receptor

In principle, binding free energy estimates can be computed from each of the configurations obtained from MD simulations. However, the computational cost for repeating the calculation on all of them would be extremely high, especially if we use standard methodology like MM-PBSA. Moreover, MD trajectories may be highly correlated on the short time scale. Hence, to ensure we are considering a wide variety of configurations, we clustered them using a 0.12 nm RMSD cutoff, and we computed the binding free energy only for one representative in each of the 60 bigger clusters. The final estimate is obtained as the average of the 60 representative configuration.

To further reduce the time of computation of the binding free energy, we decided to use the PRODIGY web server (46), which

TABLE 2 | Table of computed ΔG and ΔΔG ($\Delta G_{gamma\ variant} - \Delta G_{RT}$) to neutralizing proteins.

	ΔG kcal/mol	$\sigma_{\Delta G}$ kcal/mol	ΔΔG kcal/mol	p-value
RT - nanoBody (7JVB)	-10.36	0.09	–	–
Gamma - nanoBody (7JVB)	-9.13	0.06	1.23	$3.0*10^{-17}$
RT - miniprotein (7JZM)	-9.19	0.05	–	–
Gamma - miniprotein (7JZM)	-9.06	0.05	0.13	0.06
RT - miniprotein (7JZU)	-9.92	0.06	–	–
Gamma - miniprotein (7JZU)	-9.70	0.04	0.23	$1.1*10^{-3}$

*The table reports averages, error of the mean and p-values of the difference between the binding affinities of gamma variant S-RBD and different neutralizing proteins. The relative binding affinity **ΔΔG** use the RT as reference.*

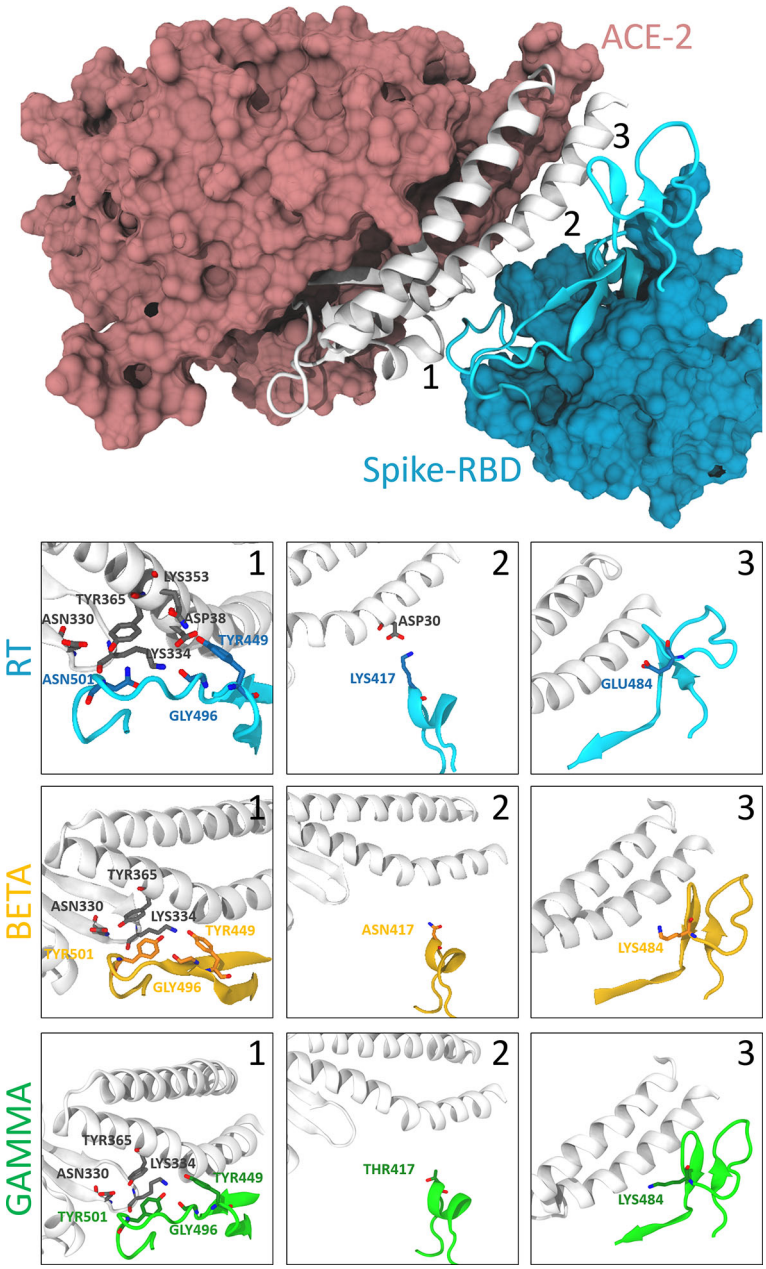

FIGURE 1 | Interactions between the spike protein and the hACE2 receptor. The top panel shows the binding between the S-RBD region of the RT and the hACE2 receptor. The interaction interface is shown in cartoon representation (white for hACE2 and cyan for S-RBD), while the rest of the protein is represented according to its surface (pink for hACE2 and light blue for S-RBD). The bottom panels show the differences between RT (cyan), beta (orange), and gamma (green) variants in correspondence with the position of the three S-RBD mutations (labeled with numbers 1-3 in the top panel). Relevant residues are shown with their side-chain representation in these panels. One can notice how residue Asn501 is at the center of a rich pattern of interactions, which is altered after its mutation to Tyr. On the other hand, Lys417 of the S-RBD interacts only with the Asp30 of the hACE2, and this interaction is broken after its modification to a non-basic amino acid. Finally, Glu484 does not show any critical interactions, and this does not change with the mutants.

produces results comparable with MM-PBSA calculations, being at the same time much less computationally expensive.

Results are reported in **Figure 3** and **Table 1** (free energy differences with the RT).

None of the mutants show a significantly improved binding affinity, while mutants G476S, N501Y (alpha variant), and the two triple mutants (beta and gamma variants) show a significantly decreased binding affinity ($P<<0.05$) with a binding energy difference of 0.6 ± 0.8 kcal/mol, 0.4 ± 0.8 kcal/mol, 0.9 ± 0.7 kcal/mol, and 1.0 ± 0.8 kcal/mol respectively. These results are compatible with similar studies on the triple mutants (26, 51). All the other mutants show no significant

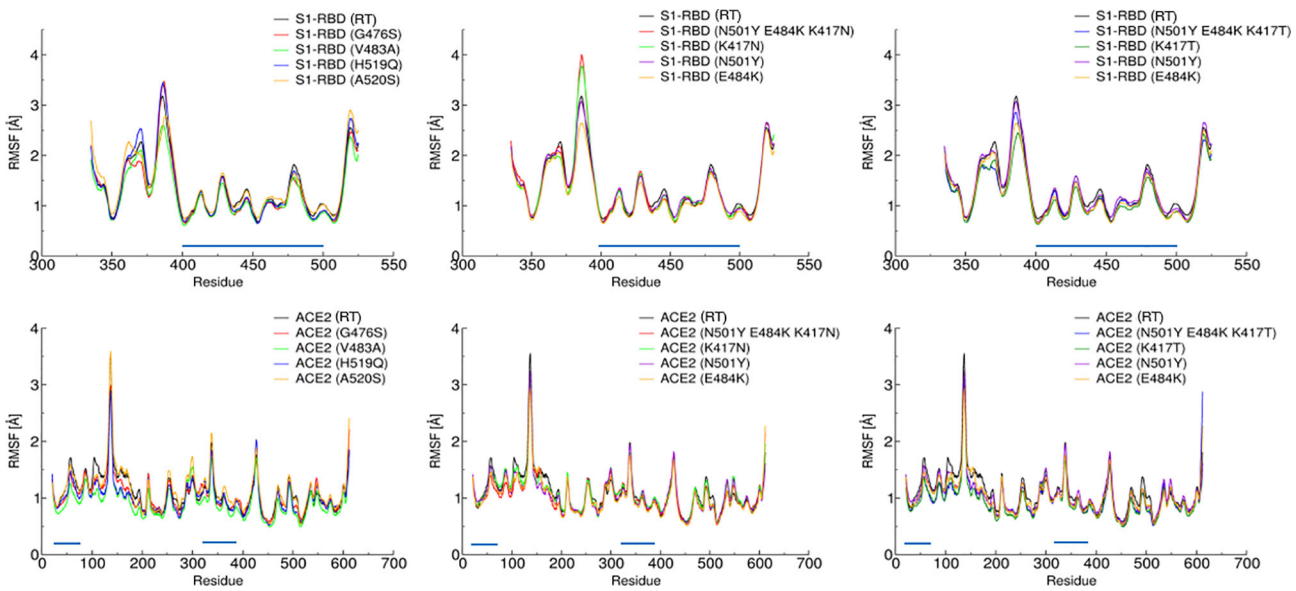

FIGURE 2 | Root Mean Square Fluctuation of the S-RBD variants (top panels) and hACE2 receptor (bottom panels) vs. residue index. The graphs are divided into three different panels for better readability. Amino acids belonging to the contact region are indicated by a blue line parallel to the x-axis. A direct comparison between the various trajectories reveals that the dynamic behavior of the complex S-RBD/hACE2 is not significantly affected by these mutations.

differences (P>0.08). However, in all the cases the changes are small (less than 1kcal/mol), and the binding affinity changes are predicted to be within a 5-fold range.

Mutation E484K Reduces the Binding Affinity of the S Protein to a Potent Neutralizing Nanobody

To test whether spike mutations can result in a virus that is able to escape immune response, we explored the effect of the mutation present in the gamma variant on the binding affinity of the highly specific nanobody Nb20 (PDB ID 7JVB) reported by Xiang et al. (52). We also tested different kinds of neutralizing molecules, i.e., the highly specific miniproteins LCB1/LCB3 (PDB ID 7JZU and 7JZM respectively) designed by Cao et al. (53), using the same method described in the previous section. Our calculations revealed that the affinity of the nanobody to the gamma variant is significantly decreased when compared to the RT, with a difference in the binding energy of 1.2 ± 0.1 kcal/mol, which translates into approximately a 7.5-fold decrease of binding affinity. This may be in agreement with the significant

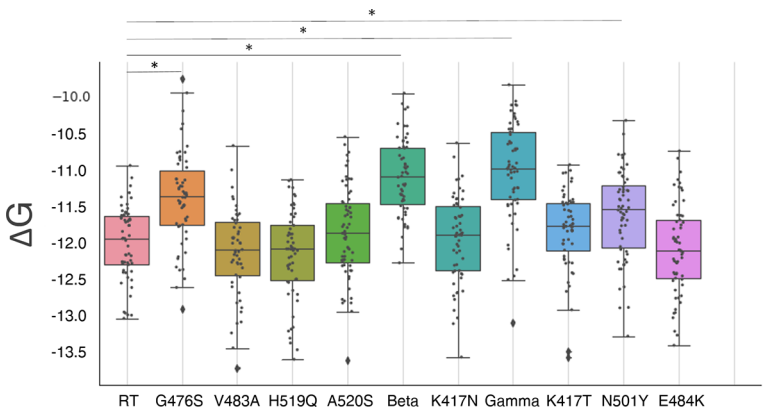

FIGURE 3 | Box plots of the distribution of S-RBD and hACE2 receptor binding free energy. A boxplot is constructed of two parts, a box and a set of whiskers. The box is drawn from the first quartile (Q_1, the median of the lower half of the dataset) to the third quartile (Q_3, the median of the upper half of the dataset) with a horizontal line drawn in the middle to denote the median. The whiskers are drawn from the upper/lower quartile to the largest/lowest data point excluding any outliers. The outliers are shown with black diamonds. Statistically different distributions are indicated with a (*) symbol. G476 mutant, alpha (N501Y), beta, and gamma variants show a worse binding affinity. However, the differences in absolute value are small.

reduction in binding affinity reported for this nanobody against the E484K mutation (54). The interaction of the miniproteins LCB1 and LCB3 with the gamma variant shows a small increase of 0.13 ± 0.06 kcal/mol (P=0.06) and 0.23 ± 0.07 kcal/mol (P<<0.05) in the binding affinity (**Figure 4** and **Table 2**).

A detailed analysis of the nanobody-S-RBD complex trajectory shows that the change in binding energy is primarily due to mutation E484K. Residue GLU484, indeed, is located inside a positively charged pocket and stably interacts with the side chain of two arginines and a tyrosine (Arg97, Arg31, and Tyr104 – **Figure 5**). These interactions are clearly disrupted by the mutation E484K that inverts the residue charge, forcing it out of the pocket. On the other hand, there are no notable differences in the interaction of the two miniproteins between the RT and gamma variants.

Experimental Validation of Computational Results on Single Point Variants

To validate the computational predictions, we performed an experimental comparative binding analysis using direct-binding and competitive ELISA experiments to determine EC_{50}/IC_{50} values for S-RBD – hACE2-ECD interaction. This analysis is limited to single-point variants. To determine EC_{50} values of hACE-ECD binding to S-RBD reference/mutants, respective titration curves were generated using hACE-ECD dilutions on immobilized S-RBD protein (**Figure 6A**). Human ACE-ECD had a higher EC_{50} against S-RBD reference (23.75 nM) in comparison to the mutants (11.48 – 19.86 nM); however, this difference was only 1.19 to 2.06-fold. To determine IC_{50} of S-RBD – hACE2-ECD interaction, competitive binding reactions were set up by mixing hACE-ECD at a predetermined EC_{50} with dilutions of respective S-RBD protein. Human ACE-ECD bound to S-RBD mutants with a slightly higher IC_{50} (slightly lower apparent affinity) than S-RBD reference. We observed a statistically significant difference in the binding affinity of G476S ($p=0.002$) and A520S ($p=0.007$) S-RBD mutants compared to the reference (**Figure 6B**). However, consistent with the trend observed in EC_{50} values, the fold difference in IC_{50} for S-RBD reference/mutants was low (1.09 to 1.31). See **Table 3** for a summary of the results.

To further validate the binding trend obtained by ELISA IC_{50} values, biolayer interferometry (BLI) kinetics experiments were performed by loading HIS1K sensors with S-RBD reference/mutants at a concentration of 1000 nM, and hACE-ECD (two-fold dilutions; 2500 – 312.5 nM) was used as analyte. Consistent with ELISA IC_{50} trend, the calculated equilibrium dissociation constants (K_D) range for S-RBD – hACE-ECD interaction was narrow (Ref – 46.3 ± 1.28 nM, G476S – 65.1 ± 1.17 nM, V483A 57.7 ± 0.96 nM, H519Q 53.4 ± 0.94 nM, and A520S 55.4 ± 1.05 nM) (**Figures 6C–G**). A statistically significant difference was observed in the K_D values of G476S and V483A, compared to reference S-RBD. Furthermore, like EC_{50} and IC_{50}, the K_D values differed on an average from 1.11 to 1.39-fold from the S-RBD reference. Further, the on (K_{ON} = 9.86 x 10^3 to 1.11 x 10^4 1/Ms) and off-rates (K_{DIS} = 4.57 x 10^{-4} to 6.68 x 10^{-4} 1/s) were largely similar for all S-RBD samples. The binding behavior of selected S-RBD mutants seems less likely to modulate S-RBD – hACE-ECD interaction. The experiments were performed in three replicas and results are summarized in **Table 4**.

Comparison with computational estimates can be done using the formula $\Delta\Delta G_{Exp} = RT\Delta\ln(K_D)$(see method Section) where K_D is the average obtained from the 3 replicas. The correlation between the two set of data is R=0.996 (**Supplementary Figure 2**) showing that our method is able to achieve a qualitative correct prediction of the effect of the mutations on the binding affinity.

DISCUSSION

In this paper, we performed an *in silico* screening of a selected number of SARS-COV2 variants and calculated the binding affinity between S-RBD and the hACE2 receptor. Results of the simulations, in agreement with experimental observations, do not show remarkable differences in the expected K_D for any of the variants. In some cases, variants show even a worsened affinity.

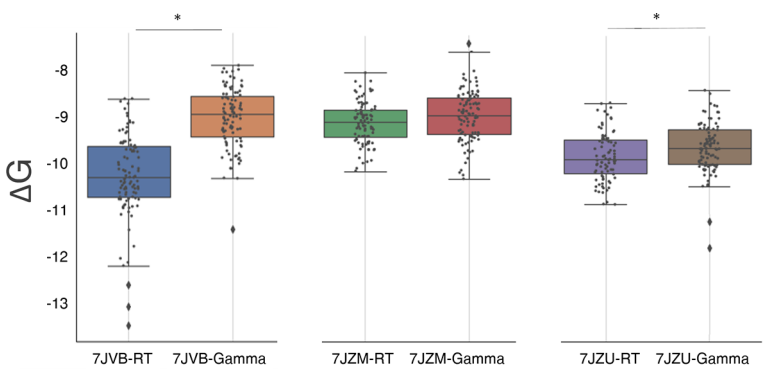

FIGURE 4 | Box plots of the distribution of S-RBD and neutralizing molecules binding free energy (see **Figure 3** for the box plot description). The three plots compare the binding free energy of the RT and the gamma variant to three neutralizing molecules (described in the text). Statistically different distributions are indicated with a (*) symbol.

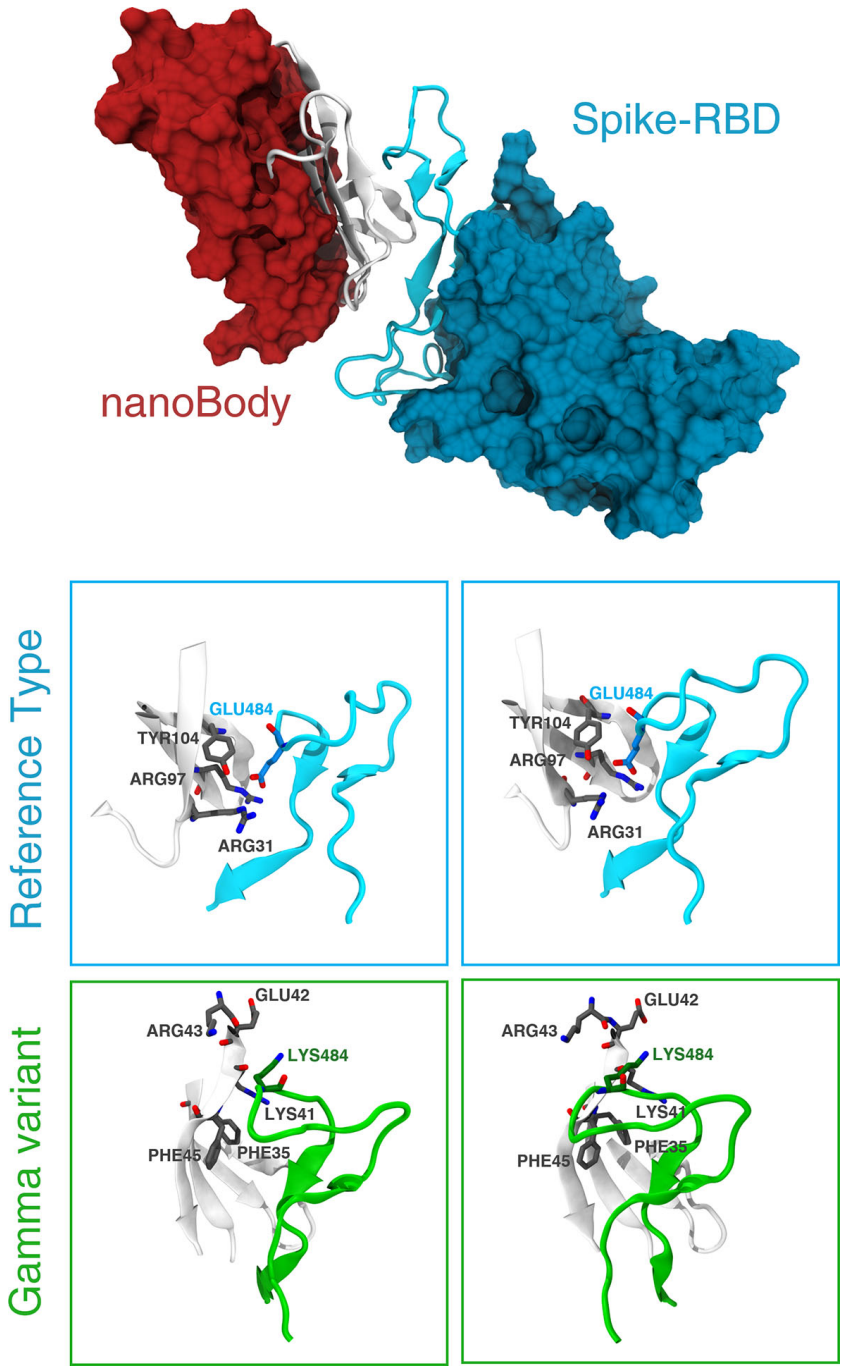

FIGURE 5 | Details of the interaction between the nanobody and the gamma variant. The top panel shows the binding between the S-RBD region of the RT and the neutralizing nanobody Nb20. The interface of interaction is shown in cartoon representation (white for the Nb20 and cyan for S-RBD), while the rest of the protein is represented according to its surface (red for Nb20 and blue for S-RBD). The bottom panels show the differences between RT (cyan) and gamma variant (green) in stereographic representation. The positively charged Arg31 recognizes the negatively charged Glu484 in S-RBD in Nb20. This bond is clearly broken after the E484K mutation.

However, variations in K_D not necessarily translate into a higher infectivity of the virus. Many different effects might be in play, and even mutations far from the binding site can improve the virus's fitness. The D614G mutation constitutes a clear example. This variant introduced a mutation far away from the ACE2 interaction domain and displaced the original variant isolated in Wuhan worldwide in a couple of months. Similar effects have been recently reported for other mutations away from the recognition domain (55).

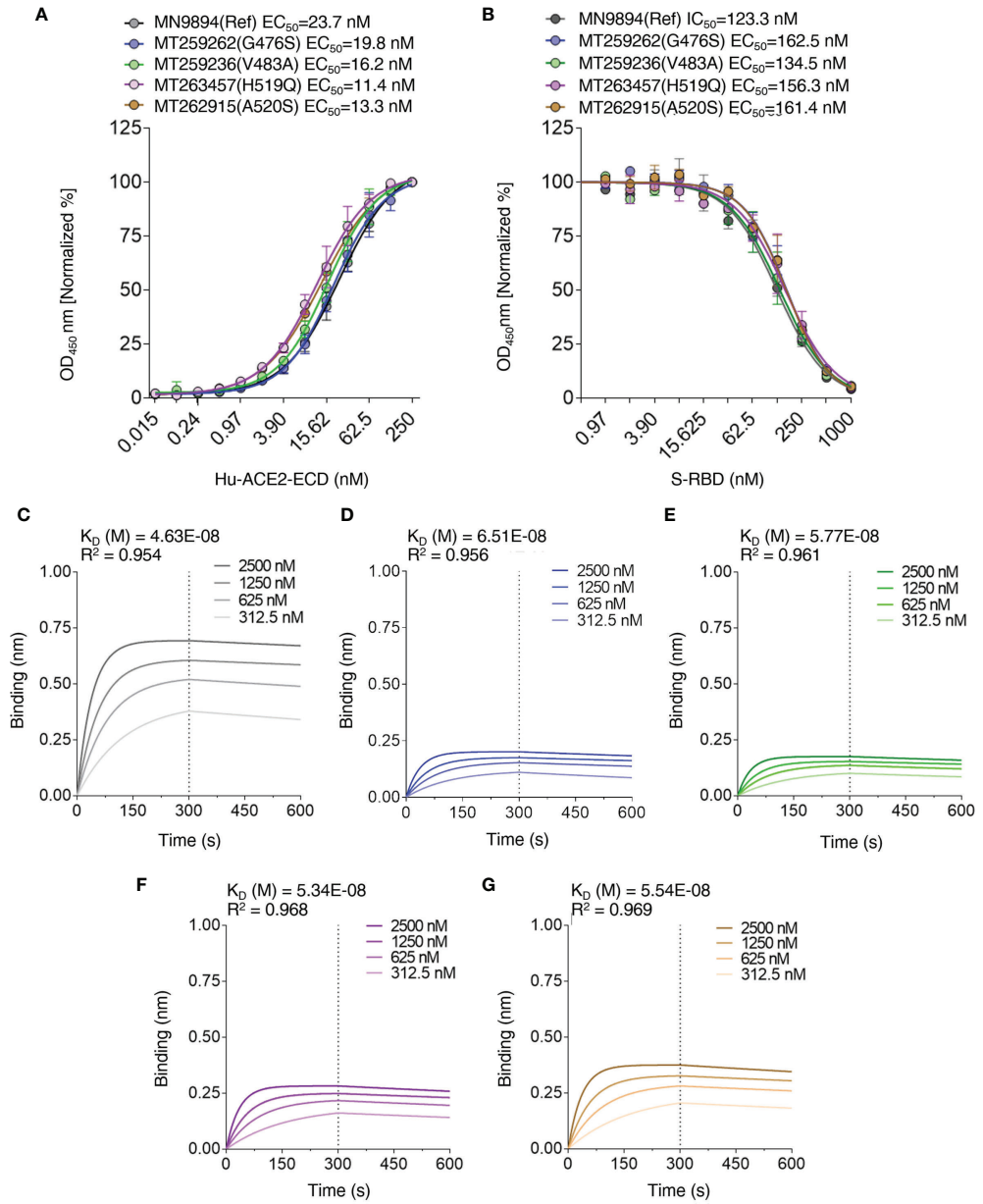

FIGURE 6 | Interaction profiles of S-RBD reference/mutants and hACE2-ECD. **(A)** *EC50* values of S-RBD – hACE2-ECD interaction were determined by direct binding ELISA using titration curves with hACE2-ECD dilutions, and **(B)** *IC50* values of S-RBD – hACE2-ECD interaction were determined by competitive ELISA using titration curves with S-RBD dilutions and hACE2-ECD at a predetermined *EC50*. Biolayer interferometry was used to generate association and dissociation curves of S-RBD – hACE2-ECD interaction for S-RBD reference **(C)**, G476S **(D)**, V483A **(E)**, H519Q **(F)**, and A520S **(G)**; legends represent the nanomolar (nM) concentration of hACE2-ECD and K_D values are depicted.

TABLE 3 | ELISA binding profiles of S-RBD reference/mutants and hACE2-ECD.

	EC_{50} nM	EC_{50} Error (± SD)	IC_{50} nM	IC_{50} Error (± SD)
Ref	23.7	1.05	123.21	1.05
G476S	19.86	1.07	162.55	1.04
V483A	16.25	1.07	134.58	1.06
H519Q	11.48	1.07	156.31	1.06
A520S	13.39	1.07	161.43	1.04

Geometric mean EC_{50} (double replicates; n=3 independent experiments) and IC_{50} (double replicates; n=2 independent experiments) values of S-RBD reference/mutants and hACE2-ECD interaction are tabulated with standard error of the mean (± SD).

TABLE 4 | Kinetics profiles of S-RBD reference/mutants and hACE2-ECD.

	K_D (M)	K_D Error	K_{ON} (1/Ms)	K_{ON} Error	K_{DIS} (1/s)	K_{DIS} Error	Full R^2
Rep-1							
Ref	4.63E-08	1.34E-09	9.86E+03	6.19E+01	4.57E-04	1.29E-05	0.9543
G476S	6.51E-08	1.32E-09	1.03E+04	6.39E+01	6.68E-04	1.29E-05	0.9565
V483A	5.77E-08	1.11E-09	1.11E+04	6.40E+01	6.39E-04	1.18E-05	0.9618
H519Q	5.34E-08	1.05E-09	1.07E+04	5.63E+01	5.71E-04	1.08E-05	0.9688
A520S	5.54E-08	1.14E-09	9.91E+03	5.24E+01	5.49E-04	1.09E-05	0.9694
Rep-2							
Ref	4.62E-08	1.21E-09	1.10E+04	7.04E+01	5.08E-04	1.29E-05	0.95
G476S	6.32E-08	1.03E-09	1.29E+04	7.96E+01	8.17E-04	1.23E-05	0.9544
V483A	4.78E-08	8.25E-10	1.39E+04	7.82E+01	6.65E-04	1.09E-05	0.9606
H519Q	4.96E-08	8.50E-10	1.30E+04	6.94E+01	6.45E-04	1.05E-05	0.965
A520S	5.42E-08	9.59E-10	1.16E+04	6.15E+01	6.30E-04	1.07E-05	0.9672
Rep-3							
Ref	4.16E-08	1.12E-09	1.21E+04	8.07E+01	5.03E-04	1.32E-05	0.9428
G476S	5.70E-08	9.72E-10	1.42E+04	9.33E+01	8.11E-04	1.28E-05	0.9459
V483A	4.50E-08	7.97E-10	1.53E+04	9.34E+01	6.91E-04	1.15E-05	0.9522
H519Q	4.58E-08	8.27E-10	1.44E+04	8.49E+01	6.60E-04	1.13E-05	0.9554
A520S	4.96E-08	9.09E-10	1.29E+04	7.26E+01	6.38E-04	1.11E-05	0.9607

Experimental K_D values in molar (M) concentration, association rate constant [K_{ON} (1/Ms)], and dissociation rate constant [K_{DIS} (1/s)] with error generated while fitting the binding curves from three replicates for S-RBD reference/mutants and hACE2-ECD interaction are tabulated.

Notwithstanding, the K_D remains a key factor to be analyzed. This is the reason why we think our contribution can be helpful to other researchers working in the design and identification of miniproteins and nanobodies against SARS-CoV-2 (52, 54, 56, 57). Having a preliminary screening of the effect of mutations on the binding affinity can help save time and other resources, especially during emergency situations, like the one we are experiencing in the current pandemic.

The great diffusion of newer virus variants (58) suggests an evolutionary advantage due to the mutations, even though their affinity is not significantly changed. Several recent studies indicate that these mutations could lead to immune escape (32–35).

To have an idea on how immune escape could happen at molecular level, we analyzed MD trajectories and computed the binding free energy of the gamma variant bound to a highly specific nanobody. We found that the affinity is indeed reduced by 1.2 kcal/mol and that this change is due mainly to the E484K mutation. This mutation can be found in several emerging SARS-COV-2 variants, and was shown to affect the binding of antibodies significantly. In other words, the virus can trade its ability to tightly bind to the hACE2 receptor in exchange for becoming more elusive to specific antibodies.

While this mechanism cannot be generalized for the whole antibody population, we can see that position 484 is a good mutation spot for the virus, from an evolutionary point of view, since this residue only interacts with neutralizing antibodies and not with the hACE2 receptor. Indeed, other mutations have also been found in this position, such as the E484Q in the kappa variant. Spreading of similar variants could escape the antibody recognition and could require a periodical update of vaccines and monoclonal antibodies used in clinical applications to avoid a potential loss of efficacy (34).

On the other hand, synthetic miniproteins that have been designed to mimic the structure of the hACE2 receptor, the natural binder for the S protein, are less affected by the mutation, and they still can work as bait.

It is worth to notice that the absolute values of the binding energies calculated may depend on some of the computational details chosen (namely, force field, water models, specific methods to calculate binding energies, etc.). However, our method is able to achieve a qualitatively correct prediction of the effect of mutations at the protein-protein interface. Indeed, we obtained a high correlation with analogous values calculated using the MM-PBSA and with experimental results (**Supplementary Figure 1**).

In summary, our work demonstrated that molecular simulations can be used to rapidly screen the effect of SARS-COVID-2 mutations, in particular concerning their ability to bind the hACE2 receptor or neutralizing molecules. This kind of analysis could be of primary importance as a preliminary screening and to produce working hypotheses that can help to prioritize the experimental study on the virus mutations.

DATA AVAILABILITY STATEMENT

The raw data supporting the conclusions of this article will be made available by the authors upon request, without undue reservation.

AUTHOR CONTRIBUTIONS

DB built structural models and performed molecular dynamics simulations. QJ produced S-RBD and hACE2-ECD proteins and performed binding experiments by ELISA and BLI. DB, QJ, AS, GY, SP, and FZ analyzed data. DB, AS, and FZ wrote the first draft of the manuscript. FZ and SP wrote the final version of the manuscript. AS and GY supervised wet-lab experiments. FZ and SP supervised computational studies. All authors contributed to editing and approved the final draft.

FUNDING

This work was supported by the National Science Foundation of China (Grant No. 31770776 to FZ) and by FOCEM (MERCOSUR Structural Convergence Fund, COF 03/11 to SP).

SUPPLEMENTARY MATERIAL

The Supplementary Material for this article can be found online at: https://www.frontiersin.org/articles/10.3389/fimmu.2021.730099/full#supplementary-material

Supplementary Figure 1 | Correlation between binding free energy computed by MM-PBSA and the PRODIGY webserver.

Supplementary Figure 2 | Comparison of binding affinity computed using the PRODIGY webserver and available experimental data. Binding affinities ratios are obtained from the dissociation constant using the formula: $RT\Delta \ln(K_D) = \Delta\Delta G_{Exp}$. (top) Table containing K_D, and $\Delta\Delta G$, $\Delta\Delta G_{Exp}$ and standard error of the mean computed using the RT as reference. (bottom) Correlation between binding affinity computed using PRODIGY and $\Delta\Delta G_{Exp}$.

Supplementary Figure 3 | Root mean square deviations (RMSD) of the complex S-RBD hACE2 receptor simulation. We report here only one (randomly chosen) of the five trajectory replicas produced for data analysis. All other simulations produce similar results.

Supplementary Figure 4 | Details of the interaction of the RT S-RBD and hACE2 receptor. For clarity, the figure is split into two different regions, which are spatially separated **(A, B)**. Lys417 interacts only with Asp30. Tyr449 and Gln498 share an interaction with Asn38 and Gln42 side chains. Leu455 and Phe456 are inside a pocket of charged amino acids and interact with the main chain of Asp30, Lys31, and Thr27. Phe486 is inside a hydrophobic pocket formed by Phe28, Leu79, and Phe83. Asn487 interacts with the polar side chain of Gln24. Gln493 is within a charged pocket and interacts with the side chains of Lys31, Glu35, and His34. Thr500 shares an interaction with the polar side chain of Tyr41 and the charged side chains of Asp355 and Arg357. Asn501 is inside a charged pocket but interacts to some extent with Tyr41 and Lys353. Tyr505 establishes an interaction with Glu35 and Arg393.

Supplementary Figure 5 | Maps of the contact between different variants of S-RBD and hACE2 receptor. The x-axis of the matrix represents S-RBD residues, while the y axis represents hACE2 receptor residues. The color represents the probability of interaction along the whole set of trajectories and goes from white (0%) to blue (100%).

REFERENCES

1. Fan W, Zhao S, Yu B, Chen Y-M, Wang W, Song Z-G, et al. A New Coronavirus Associated With Human Respiratory Disease in China. *Nature* (2020) 579(7798):265–9. doi: 10.1038/s41586-020-2008-3
2. WHO. *Coronavirus (COVID-19) Dashboard*. Available at: https://covid19.who.int/.
3. Jie C, Fang L, Zheng-Li S. Origin and Evolution of Pathogenic Coronaviruses. *Nat Rev Microbiol* (2019) 17:181–92. doi: 10.1038/s41579-018-0118-9
4. Peng Z, Yang X-L, Wang X-G, Hu B, Zhang L, Zhang W, et al. A Pneumonia Outbreak Associated With a New Coronavirus of Probable Bat Origin. *Nature* (2020) 579:270–3. doi: 10.1038/s41586-020-2012-7
5. Roujian L, Zhao X, Li J, Niu P, Yang B, Wu H, et al. Genomic Characterisation and Epidemiology of 2019 Novel Coronavirus: Implications for Virus Origins and Receptor Binding. *Lancet* (2020) 395:565–74. doi: 10.1016/S0140-6736(20)30251-8
6. Xiaojun L, Giorgi EE, Marichannegowda MH, Foley B, Xiao C, Kong X-P, et al. Emergence of SARS-CoV-2 Through Recombination and Strong Purifying Selection. *Sci Adv* (2020) 6(27):eabb9153. doi: 10.1126/sciadv.abb9153
7. Meagan B, Eric D, Ralph B. SARS-CoV and Emergent Coronaviruses: Viral Determinants of Interspecies Transmission. *Curr Opin Virol* (2011) 1:624–34. doi: 10.1016/j.coviro.2011.10.012
8. Starr TN, Greaney AJ, Hilton SK, Ellis D, Crawford KHD, Dingens AS, et al. Deep Mutational Scanning of SARS-CoV-2 Receptor Binding Domain Reveals Constraints on Folding and ACE2 Binding. *Cell* (2020) 182:1295–310. doi: 10.1016/j.cell.2020.08.012
9. Alexandra CW, Park Y-J, Tortorici MA, Wall A, McGuire AT, Veesler D. Structure, Function, and Antigenicity of the SARS-CoV-2 Spike Glycoprotein. *Cell* (2020) 181:281–92. doi: 10.1016/j.cell.2020.02.058
10. Wrapp D, Wang N, Corbett KS, Goldsmith JA, Hsieh C-L, Abiona O, et al. Cryo-EM Structure of the 2019-Ncov Spike in the Prefusion Conformation. *Science* (2020) 367:1260–3. doi: 10.1126/science.abb2507
11. Hoffmann M, Kleine-Weber H, Schroeder S, Krüger N, Herrler T, Erichsen S, et al. SARS-CoV-2 Cell Entry Depends on ACE2 and TMPRSS2 and Is Blocked by a Clinically Proven Protease Inhibitor. *Cell* (2020) 181:271–80. doi: 10.1016/j.cell.2020.02.052
12. Letko M, Marzi A, Munster V. Functional Assessment of Cell Entry and Receptor Usage for SARS-CoV-2 and Other Lineage B Betacoronaviruses. *Nat Microbiol* (2020) 5:562–9. doi: 10.1038/s41564-020-0688-y
13. Wu K, Peng G, Wilken M, Geraghty RJ, Li F. Mechanisms of Host Receptor Adaptation by Severe Acute Respiratory Syndrome Coronavirus. *J Biol Chem* (2012) 287:8904–11. doi: 10.1074/jbc.M111.325803
14. Frieman M, Yount B, Agnihothram S, Page C, Donaldson E, Roberts A, et al. Molecular Determinants of Severe Acute Respiratory Syndrome Coronavirus Pathogenesis and Virulence in Young and Aged Mouse Models of Human Disease. *J Virol* (2012) 86:884–97. doi: 10.1128/JVI.05957-11
15. Ren W, Qu X, Li W, Han Z, Yu M, Zhou P, et al. Difference in Receptor Usage Between Severe Acute Respiratory Syndrome (SARS) Coronavirus and SARS-Like Coronavirus of Bat Origin. *J Virol* (2008) 82:1899–907. doi: 10.1128/JVI.01085-07
16. Chandrashekar A, Liu J, Martinot AJ, McMahan K, Mercado NB, Peter L, et al. SARS-CoV-2 Infection Protects Against Rechallenge in Rhesus Macaques. *Science* (2020) 369:812–7. doi: 10.1126/science.abc4776
17. Salazar E, Kuchipudi SV, Christensen PA, Eagar T, Yi X, Zhao P, et al. Convalescent Plasma Anti-SARS-CoV-2 Spike Protein Ectodomain and Receptor-Binding Domain IgG Correlate With Virus Neutralization. *J Clin Invest* (2020) 130:6728–38. doi: 10.1172/JCI141206
18. Qiang M, Ma P, Li Y, Liu H, Harding A, Min C, et al. Potent SARS-CoV-2 Neutralizing Antibodies Selected From a Human Antibody Library Constructed Decades Ago. *BioRxiv* (2020). doi: 10.1101/2020.11.06.370676
19. Kyriakidis NC, López-Cortés A, Vásconez González E, Barreto Grimaldos A, Ortiz Prado E. SARS-CoV-2 Vaccines Strategies: A Comprehensive Review of Phase 3 Candidates. *NPJ Vaccines* (2021) 6:28.2021. doi: 10.1038/s41541-021-00292-w
20. Demogines A, Farzan M, Sawyer SL. Evidence for ACE2-Utilizing Coronaviruses (CoVs) Related to Severe Acute Respiratory Syndrome CoV in Bats. *J Virol* (2012) 86:6350–3. doi: 10.1128/JVI.00311-12
21. Frank HK, Enard D, Boyd SD. Exceptional Diversity and Selection Pressure on SARS-CoV and SARS-CoV-2 Host Receptor in Bats Compared to Other Mammals. *bioRxiv* (2020) 2020.04.20.051656. doi: 10.1101/2020.04.20.051656
22. MacLean OA, Lytras S, Singer JB, Weaver S, Kosakovsky Pond SL, Robertson DL. Evidence of Significant Natural Selection in the Evolution of SARS-CoV-2 in Bats, Not Humans. *bioRxiv* (2020) 2020.05.28.122366. doi: 10.1101/2020.05.28.122366
23. Li F. Structure, Function, and Evolution of Coronavirus Spike Proteins. *Annu Rev Virol* (2016) 3:237–61. doi: 10.1146/annurev-virology-110615-042301
24. Rees-Spear C, Muir L, Griffith SA, Heaney J, Aldon Y, Snitselaar JL, et al. The Effect of Spike Mutations on SARS-CoV-2 Neutralization. *Cell Rep* (2021) 34:108890. doi: 10.1016/j.celrep.2021.108890
25. Fratev F. The N501Y and K417N Mutations in the Spike Protein of SARS-CoV-2 Alter the Interactions With Both Hace2 and Human Derived Antibody: A Free Energy of Perturbation Study. *bioRxiv* (2021) 20201223424283. doi: 10.1101/2020.12.23.424283
26. Cheng H, Krieger JM, Kaynak B, Arditi M, Bahar I. Impact of South African 501.V2 Variant on SARS-CoV-2 Spike Infectivity and Neutralization: A Structure-

Based Computational Assessment. *bioRxiv* (2021) 2020.01.10.426143. doi: 10.1101/2021.01.10.426143
27. Li Q, Wu J, Nie J, Zhang L, Hao H, Liu S, et al. The Impact of Mutations in SARS-CoV-2 Spike on Viral Infectivity and Antigenicity. *Cell* (2020) 182:1284–94. doi: 10.1016/j.cell.2020.07.012
28. Garcia-Beltran WF, Lam EC, St Denis K, Nitido AD, Garcia ZH, Hauser BM, et al. Multiple SARS-CoV-2 Variants Escape Neutralization by Vaccine-Induced Humoral Immunity. *Cell* (2021) S0092-8674(21):2372–83. doi: 10.1016/j.cell.2021.03.013
29. Zou J, Yin J, Fang L, Yang M, Wang T, Wu W, et al. Computational Prediction of Mutational Effects on SARS-CoV-2 Binding by Relative Free Energy Calculations. *J Chem Inf Model* (2020) 60:5794–802. doi: 10.1021/acs.jcim.0c00679
30. Ou J, Zhou Z, Dai R, Zhang J, Lan W, Zhao S, et al. Emergence of RBD Mutations in Circulating SARS-CoV-2 Strains Enhancing the Structural Stability and Human ACE2 Receptor Affinity of the Spike Protein. *bioRxiv* (2020) 2020.03.15.991844. doi: 10.1101/2020.03.15.991844
31. Saha P, Majumder R, Srivastava AK, Mandal M, Sarkar S. Mutations in Spike Protein of SARS-CoV-2 Modulate Receptor Binding, Membrane Fusion and Immunogenicity: An Insight Into Viral Tropism and Pathogenesis of COVID-19. *chemrxiv* (2020) 12320567. doi: 10.26434/chemrxiv.12320567
32. Altmann DM, Reynolds CJ, Boyton RJ. SARS-CoV-2 Variants: Subversion of Antibody Response and Predicted Impact on T Cell Recognition. *Cell Rep Med* (2021) 2:100286. doi: 10.1016/j.xcrm.2021.100286
33. Wang P, Nair MS, Liu L, Iketani S, Lou Y, Guo Y, et al. Antibody Resistance of SARS-CoV-2 Variants B.1.351 and B.1.1.7. *Nature* (2021) 593:130–5. doi: 10.1038/s41586-021-03398-2
34. Wang Z, Schmidt F, Weisblum Y, Muecksch F, Barnes CO, Finkin S, et al. mRNA Vaccine-Elicited Antibodies to SARS-CoV-2 and Circulating Variants. *Nature* (2021) 592:616–22. doi: 10.1038/s41586-021-03324-6
35. Collier DA, De Marco A, Ferreira IATM, Meng B, Datir RP, Walls AC, et al. Sensitivity of SARS-CoV-2 B.1.1.7 to mRNA Vaccine-Elicited Antibodies. *Nature* (2021) 593:136–41. doi: 10.1038/s41586-021-03412-7
36. Wang Q, Zhang Y, Wu L, Niu S, Song C, Zhang Z, et al. Structural and Functional Basis of SARS-CoV-2 Entry by Using Human Ace2. *Cell* (2020) 181:894–904.e899. doi: 10.1016/j.cell.2020.03.045
37. Pettersen EF, Goddard TD, Huang CC, Couch GS, Greenblatt DM, Meng EC, et al. UCSF Chimera–a Visualization System for Exploratory Research and Analysis. *J Comput Chem* (2004) 25:1605–12. doi: 10.1002/jcc.20084
38. Pronk S, Páll S, Schulz R, Larsson P, Bjelkmar P, Apostolov R, et al. GROMACS 4.5: A High-Throughput and Highly Parallel Open Source Molecular Simulation Toolkit. *Bioinformatics* (2013) 29:845–54. doi: 10.1093/bioinformatics/btt055
39. Maier JA, Martinez C, Kasavajhala K, Wickstrom L, Hauser KE. Ff14sb: Improving the Accuracy of Protein Side Chain and Backbone Parameters From Ff99sb. *J Chem Theory Comput* (2015) 11:3696–713. doi: 10.1021/acs.jctc.5b00255
40. Ziraldo G, Buratto D, Kuang Y, Xu L, Carrer A, Nardin C, et al. A Human-Derived Monoclonal Antibody Targeting Extracellular Connexin Domain Selectively Modulates Hemichannel Function. *Front Physiol* (2019) 10:392. doi: 10.3389/fphys.2019.00392
41. Zonta F, Buratto D, Crispino G, Carrer A, Bruno F, Yang G, et al. Cues to Opening Mechanisms From in Silico Electric Field Excitation of Cx26 Hemichannel and *In Vitro* Mutagenesis Studies in HeLa Transfectans. *Front Mol Neurosci* (2018) 11:170. doi: 10.3389/fnmol.2018.00170
42. Zonta F, Girotto G, Buratto D, Crispino G, Morgan A, Abdulhadi K, et al. The P.Cys169Tyr Variant of Connexin 26 is Not a Polymorphism. *Hum Mol Genet* (2015) 24:2641–8. doi: 10.1093/hmg/ddv026
43. Zonta F, Mammano F, Torsello M, Fortunati N, Orian L, Polimeno A. Role of Gamma Carboxylated Glu47 in Connexin 26 Hemichannel Regulation by Extracellular Ca(2)(+): Insight From a Local Quantum Chemistry Study. *Biochem Biophys Res Commun* (2014) 445:10–5. doi: 10.1016/j.bbrc.2014.01.063
44. Berendsen HJC, Postma JPM, van Gunsteren WF, Dinola A, Haak JR. Molecular Dynamics With Coupling to an External Bath. *J Chem Phys* (1984) 81:3684–90. doi: 10.1063/1.448118
45. Darden T, York D, Pedersen L. Particle Mesh Ewald: An N · Log(N) Method for Ewald Sums in Large Systems. *J Chem Phys* (1993) 98:10089–93. doi: 10.1063/1.464397
46. Xue LC, Rodrigues JP, Kastritis PL, Bonvin AM, Vangone A. PRODIGY: A Web Server for Predicting the Binding Affinity of Protein-Protein Complexes. *Bioinformatics* (2016) 32:3676–8. doi: 10.1093/bioinformatics/btw514
47. Vangone A, Bonvin AM. Contacts-Based Prediction of Binding Affinity in Protein-Protein Complexes. *Elife* (2015) 4:e07454. doi: 10.7554/eLife.07454
48. Kollman PA, Massova I, Reyes C, Kuhn B, Huo S, Chong L, et al. Calculating Structures and Free Energies of Complex Molecules: Combining Molecular Mechanics and Continuum Models. *Acc Chem Res* (2000) 33:889–97. doi: 10.1021/ar000033j
49. Wang E, Sun H, Wang J, Wang Z, Liu H, Zhang JZH, et al. End-Point Binding Free Energy Calculation With MM/PBSA and MM/GBSA: Strategies and Applications in Drug Design. *Chem Rev* (2019) 119:9478–508. doi: 10.1021/acs.chemrev.9b00055
50. Cournia Z, Allen B, Sherman W. Relative Binding Free Energy Calculations in Drug Discovery: Recent Advances and Practical Considerations. *J Chem Inf Model* (2017) 57:2911–37. doi: 10.1021/acs.jcim.7b00564
51. Villoutreix BO, Calvez V, Marcelin AG, Khatib AM. In Silico Investigation of the New UK (B.1.1.7) and South African (501y.V2) SARS-CoV-2 Variants With a Focus at the ACE2-Spike RBD Interface. *Int J Mol Sci* (2021) 22:695. doi: 10.3390/ijms22041695
52. Xiang Y, Nambulli S, Xiao Z, Liu H, Sang Z, Duprex WP, et al. Versatile and Multivalent Nanobodies Efficiently Neutralize SARS-CoV-2. *Science* (2020) 370:1479–84. doi: 10.1126/science.abe4747
53. Cao L, Goreshnik I, Coventry B, Case JB, Miller L, Kozodoy L, et al. *De Novo* Design of Picomolar SARS-CoV-2 Miniprotein Inhibitors. *Science* (2020) 370:426–31. doi: 10.1126/science.abd9909
54. Sun D, Sang Z, Kim J, Xiang Y, Cohen T, Belford AK, et al. Potent Neutralizing Nanobodies Resist Convergent Circulating Variants of SARS-CoV-2 by Targeting Diverse and Conserved Epitopes. *Nat Commun* (2021) 12:4676. doi: 10.1038/s41467-021-24963-3
55. Gonzalez-Puelma J, Aldridge J, Montes de Oca M, Pinto M, Uribe-Paredes R, Fernández-Goycoolea J, et al. Mutation in a SARS-CoV-2 Haplotype From Sub-Antarctic Chile Reveals New Insights Into the Spike's Dynamics. *Viruses* (2021) 13(5):883. doi: 10.3390/v13050883
56. Valenzuela Nieto G, Jara R, Watterson D, Modhiran N, Amarilla AA, Himelreichs J, et al. Potent Neutralization of Clinical Isolates of SARS-CoV-2 D614 and G614 Variants by a Monomeric, Sub-Nanomolar Affinity Nanobody. *Sci Rep* (2021) 11:3318. doi: 10.1038/s41598-021-82833-w
57. Guttler T, Aksu M, Dickmanns A, Stegmann KM, Gregor K, Rees R, et al. Neutralization of SARS-CoV-2 by Highly Potent, Hyperthermostable, and Mutation-Tolerant Nanobodies. *EMBO J* (2021) 40:e107985. doi: 10.15252/embj.2021107985
58. Mahase E. Covid-19: What New Variants Are Emerging and How Are They Being Investigated? *BMJ* (2021) 372:n158. doi: 10.1136/bmj.n158

Conflict of Interest: The authors declare that the research was conducted in the absence of any commercial or financial relationships that could be construed as a potential conflict of interest.

frontiers in Immunology

ORIGINAL RESEARCH
published: 23 November 2021
doi: 10.3389/fimmu.2021.772320

Effectiveness of Regdanvimab Treatment in High-Risk COVID-19 Patients to Prevent Progression to Severe Disease

Ji Yeon Lee[1†], Jee Young Lee[2†], Jae-Hoon Ko[3†], Miri Hyun[1], Hyun Ah Kim[1], Seongcheol Cho[2], Yong Dae Lee[2], Junghoon Song[2], Seunghwan Shin[2‡] and Kyong Ran Peck[3*‡]*

[1] Division of Infectious Diseases, Department of Internal Medicine, Keimyung University Dongsan Hospital, Keimyung University School of Medicine, Daegu, South Korea, [2] Department of Internal Medicine, Seoul Red Cross Hospital, Seoul, South Korea, [3] Division of Infectious Diseases, Department of Medicine, Samsung Medical Center, Sungkyunkwan University School of Medicine, Seoul, South Korea

OPEN ACCESS

Edited by:
Raymund Razonable,
Mayo Clinic, United States

Reviewed by:
Sang-Oh Lee,
University of Ulsan, South Korea
Osaretin Emmanuel Asowata,
Population Council, United States

***Correspondence:**
Seunghwan Shin
sshhissh@gmail.com
Kyong Ran Peck
krpeck@skku.edu

[†]These authors have contributed equally to this work and share first authorship

[‡]These authors have contributed equally to this work

Specialty section:
This article was submitted to Vaccines and Molecular Therapeutics, a section of the journal Frontiers in Immunology

Received: 07 September 2021
Accepted: 08 November 2021
Published: 23 November 2021

Citation:
Lee JY, Lee JY, Ko J-H, Hyun M, Kim HA, Cho S, Lee YD, Song J, Shin S and Peck KR (2021) Effectiveness of Regdanvimab Treatment in High-Risk COVID-19 Patients to Prevent Progression to Severe Disease. Front. Immunol. 12:772320. doi: 10.3389/fimmu.2021.772320

Objective: To evaluate clinical effectiveness of regdanvimab, a monoclonal antibody agent for treating coronavirus 2019 (COVID-19).

Methods: A retrospective cohort study was conducted at two general hospitals during the study period of December 2020 to May 2021. Mild COVID-19 patients with risk factors for disease progression admitted to the hospitals within seven days of symptom onset were enrolled and followed until discharge or referral. Multivariate analyses for disease progression were conducted in the total and propensity score (PS)-matched cohorts.

Results: A total of 778 mild COVID-19 patients were included and classified as the regdanvimab (n = 234) and supportive care (n = 544) groups. Significantly fewer patients required O_2 supplementation *via* nasal prong in the regdanvimab group (8.1%) than in the supportive care group (18.4%, $P < 0.001$). The decreased risk for O_2 support by regdanvimab treatment was noticed in the multivariate analysis of the total cohort (HR 0.570, 95% CI 0.343–0.946, $P = 0.030$), but it was not statistically significant in the PS-matched cohort ($P = 0.057$). Progression to severe disease was also significantly lower in the regdanvimab group (2.1%) than in the supportive care group (9.6%, $P < 0.001$). The significantly reduced risk for progression to severe disease by regdanvimab treatment was observed in the analysis of both the total cohort (HR 0.262, 95% CI 0.103–0.667, $P = 0.005$) and PS-matched cohort (HR 0.176, 95% CI 0.060–0.516, $P = 0.002$). Potential risk factors for progression were investigated in the supportive care group and $SpO_2 < 97\%$ and CRP elevation >1.5 mg/dL were common risk factors for O_2 support and progression to severe disease. Among the patients with any of these factors, regdanvimab treatment was associated with decreased risk for progression to severe disease with slightly lower HR (HR 0.202, 95% CI 0.062–0.657, $P = 0.008$) than that of the total cohort.

Conclusion: Regdanvimab treatment was associated with a decreased risk of progression to severe disease.

Keywords: Regdanvimab, monoclonal antibody, COVID-19, progression, outcome

INTRODUCTION

The coronavirus disease 2019 (COVID-19) pandemic is ongoing and has caused more than four million deaths as of October 2021 (1). Among the therapeutic agents tested against COVID-19, neutralizing monoclonal antibody (mAb) agents against severe acute respiratory syndrome coronavirus 2 (SARS-CoV-2) were found to decrease viral loads and prevent disease progression of mild COVID-19 (2–9). On September 2021, US National Institutes of Health recommended use of anti-SARS-CoV-2 mAb regimens, including casirivimab/imdevimab (Regeneron Pharmaceuticals Inc., NY, USA), bamlanivimab/etesevimab (Eli Lilly and Company, IN, USA), and sotrovimab (GlaxoSmithKline LLC, NC, USA), to treat non-hospitalized patients with mild to moderate COVID-19 who are at high risk of clinical progression (10). In the phase III trial, casirivimab/imdevimab decreased viral load faster than placebo, and COVID-19-related hospitalization or death from any causes were significantly reduced both in 2400mg and 1200mg arm (relative risk reduction of 71.3% and 70.4%, respectively) (7). Bamlanivimab/etesevimab also exhibited significant reduction of COVID-19-related hospitalization or death from any causes (relative risk difference, 70%) (9), and sotrovimab reduced COVID-19 progression risk by 85% (8).

Regdanvimab (CT-P59, Celltrion Inc, Incheon, Republic of Korea), a mAb agent against SARS-CoV-2, was approved by the Korea Ministry of Food and Drug Safety for the treatment of mild COVID-19 patients with risk factors for progression on February 5, 2021 based on the results of *in-vitro* study and the interim data of a phase II/III clinical trial (6, 11), and was reviewed by European Medicines Agency on March 2, 2021 for the support of national decisions on early use (12). In that trial, the incidence of severe COVID-19 cases requiring inpatient treatment was reduced by 54% among all COVID-19 patients and 68% among patients with moderate COVID-19 older than age 50. The time for clinical recovery was 5.4 days in the regdanvimab group, which was reduced by 3.4 days compared to 8.8 days in the placebo group (13). The approval in Korea was conditioned on the success of a phase III clinical trial, which was reported to meet its endpoints in June 2021 (14). To evaluate the clinical response to regdanvimab in the real world, we conducted a retrospective cohort study evaluating the pre- and post-periods of regdanvimab treatment.

METHODS

Study Design and Population

This retrospective cohort study was conducted at two general hospitals designated for the care of mild and moderate COVID-19 patients between December 2020 and May 2021. The diagnosis of COVID-19 was made using the real-time polymerase chain reaction (RT-PCR) test for SARS-CoV-2. During the study period, most of mild COVID-19 patients were hospitalized at general COVID-19 designated hospitals, and worsening COVID-19 patients with O_2 requirements of more than 5L per min *via* nasal prong or facial mask were referred to tertiary care centers. Regdanvimab was administered intravenously with the dose of 40mg/kg during hospitalization. Because regdanvimab was approved for administration within seven days of symptom onset, mild COVID-19 patients with any risk factors for disease progression who were admitted to the hospitals within seven days of symptom onset were screened. Mild COVID-19 was defined as COVID-19 patients who did not require O_2 supplement at admission (SpO_2 > 94% in room air). The risk factors for disease progression were 1) age ≥ 60 years, 2) cardiovascular disease, 3) chronic respiratory disease, 4) diabetes mellitus, 5) hypertension, and 6) radiologic evidence of pneumonia. Patients without any COVID-19 related symptoms, those without risk factors for progression, those admitted more than seven days after symptom onset, those referred to other hospitals before disease progression or recovery, and those who received regdanvimab more than seven days after symptom onset were excluded from the cohort. Attending physicians of both hospitals prescribed regdanvimab for the indicated patients after the drug became available on February 2021. Most of COVID-19 patients admitted from February to May 2021 received regdanvimab treatment if indicated, while those admitted from December 2020 to February 2021 did not receive the drug. There was an overlap period on February 2021. The enrolled patients were classified into the regdanvimab group or the supportive care group, and the clinical outcomes of the patients were followed until the day of discharge or referral. This study was approved by the Institutional Review Board of Samsung Medical Center (IRB no. 2021-07-079).

Data Collection and Outcome Assessment

Baseline characteristics and epidemiologic information were collected from the electronic medical records. Clinical status at admission was evaluated using SpO_2, radiologic evidence for pneumonia, complete blood count, chemistry profile, and C-reactive protein (CRP) levels. The initial cycle threshold (Ct) values of the RT-PCR at diagnosis (nasopharyngeal swab) were also collected. Ordinal disease severity scores were used to evaluate prognosis (**Supplementary Materials**) (15). The primary endpoints assessed were requiring O_2 support *via* nasal prong (severity score 3) and a composite outcome indicating progression to severe disease (severity scores 4 to 8,

including referral to a tertiary care hospital due to increasing O_2 requirements). Requiring other treatment modalities including remdesivir, steroids, and antibiotics, and the length of hospital stay among patients who recovered without referral were compared as secondary outcomes.

Statistical Analysis

To compare clinical factors, either the Student's *t*-test or Mann–Whitney U test was used for continuous variables, and the Chi-square or Fisher's exact test was used for categorical variables. The Kaplan-Meier method and long-rank test was used to calculate the 21-day probability of disease progression. Cox proportional hazard models were used to evaluate potential risk factors for disease progression within 21 days. All collected factors relevant to outcomes were evaluated in univariate analyses, and statistically significant factors were included in the multivariate analyses. When a continuous variable was statistically significant in the univariate analysis, it was converted into a categorical variable using interquartile ranges, the receiver operating characteristic (ROC) curve, or known normal limits, and the variable with the highest hazard ratio was included in the multivariate analysis. We used a propensity score (PS) matching method with the nearest neighbor matching algorithm and a 1:1 ratio without replacement to adjust potential confounders (16). A logistic regression analysis was performed to calculate the PS in a logistic model, and prognostic covariates reported from previous reports and those identified from the present cohort were included in that PS model (**Supplementary Materials**) (17–19). All *P*-values were two-tailed, and those <0.05 were considered statistically significant. IBM SPSS Statistics version 20.0 (IBM, Armonk, NY, USA) and R software (version 4.1.0 with packages; the R Project for Statistical Computing, Vienna, Austria) were used for all statistical analyses.

RESULTS

Baseline Characteristics of Mild COVID-19 Patients With Risk Factors for Progression

During the study period, 1872 mild COVID-19 patients were admitted to the two general hospitals designated for COVID-19 patient care (**Figure 1**). After excluding 1094 patients, 778 patients with risk factors for progression to severe disease who were admitted within seven days of symptom onset were included. The patients were classified into regdanvimab (n = 234) and supportive care (n = 544) groups. The supportive care group were diagnosed from November 26, 2020 to February 28, 2021, while the regdanvimab group were diagnosed from February 11 to May 31, 2021. The baseline characteristics of the patients are presented in **Table 1**. Patients in the regdanvimab group were younger (51.8 ± 14.3 years) than those in the supportive care group (56.2 ± 15.3 years, $P < 0.001$). Patients in the regdanvimab group were admitted earlier (2.8 ± 2.0 days from symptom onset) than those in the supportive care group (3.5 ± 2.2 days, $P < 0.001$). The average values of the initial laboratory tests were within normal ranges, except for CRP (1.6 ± 2.6 mg/dL). The CRP level was significantly lower in the regdanvimab group (1.2 ± 1.7 mg/dL) than in the supportive care group (1.7 ± 2.9 mg/dL, $P = 0.001$).

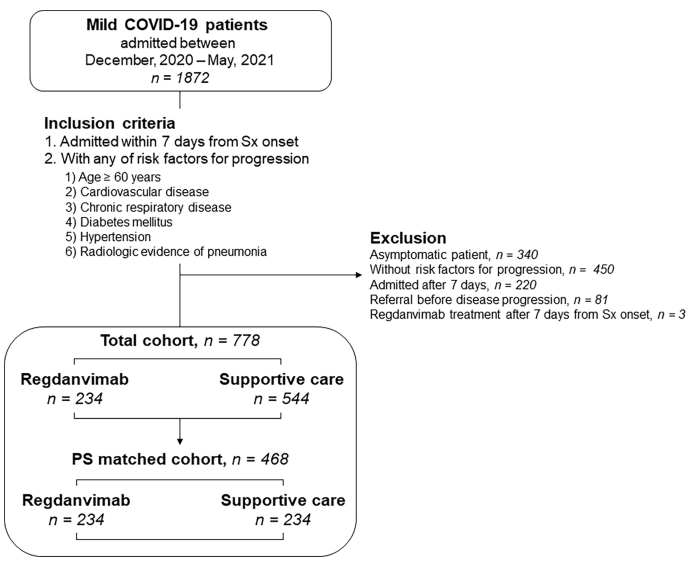

FIGURE 1 | Patient selection for the retrospective cohort. Mild COVID-19 patients admitted to two hospitals designated for COVID-19 patient care were screened. High-risk patients who were admitted within 7 days of symptom onset were included. The effects of regdanvimab treatment were evaluated using multivariate analyses in the total cohort and in propensity score–matched cohorts developed to adjust for potential confounders. COVID-19, coronavirus disease 2019; Sx, symptom; PS, propensity score.

TABLE 1 | Baseline characteristics of the regdanvimab and supportive care groups.

Variables	Regdanvimab (n = 234)	Supportive care (n = 544)	*P* value
Demographics			
Age, years	51.8 ± 14.3	56.2 ± 15.3	<0.001
Male sex	130 (55.6)	267 (49.1)	0.101
BMI	25.2 ± 3.6	24.8 ± 3.6	0.112
Sx onset to admission, days	2.8 ± 2.0	3.5 ± 2.2	<0.001
Initial presentation			
Initial Ct value (NP swab, RdRp)	19.2 ± 6.4	19.9 ± 5.7	0.160
Pneumonia	168 (71.8)	354 (65.1)	0.068
SIRS	47 (20.1)	95 (17.5)	0.418
SpO_2	97.2 ± 1.0	97.3 ± 1.2	0.748
Initial laboratory tests			
WBC count,/μL	4749.4 ± 1505.4	4812.3 ± 1535.9	0.599
Lymphocyte count,/μL	1202.1 ± 460.9	1264.3 ± 720.8	0.224
Platelet count, $x10^3$/μL	199.7 ± 61.3	191.8 ± 66.0	0.116
Total bilirubin, mg/dL	0.62 ± 0.3	0.59 ± 0.2	0.155
Albumin, g/dL	4.5 ± 0.3	4.4 ± 0.3	0.002
AST, IU/L	32.7 ± 18.5	33.3 ± 19.6	0.704
ALT, IU/L	33.7 ± 23.6	32.9 ± 24.9	0.668
BUN, mg/dL	13.5 ± 4.0	14.4 ± 4.9	0.004
Creatinine, mg/dL	0.8 ± 0.2	0.9 ± 0.3	0.287
CPK, IU/L	128.3 ± 185.7	127.5 ± 165.2	0.953
LDH, IU/L	388.7 ± 100.9	398.0 ± 121.3	0.265
CRP, mg/dL	1.2 ± 1.7	1.7 ± 2.9	0.001
Underlying diseases*			
Cardiovascular disease	22 (9.4)	54 (9.9)	0.896
Respiratory disease	8 (3.4)	35 (6.4)	0.122
Diabetes mellitus	40 (17.1)	91 (16.7)	0.917
Hypertension	79 (33.8)	182 (33.5)	0.934
Liver disease	4 (1.7)	7 (1.3)	0.647
Renal disease	1 (0.4)	3 (0.6)	0.824
Charlson Comorbidity Index	0 (0–1)	0 (0–1)	0.176

*Data are expressed as the number (%) of patients, mean ± SD, or median (IQR) unless indicated otherwise. *There were no immunocompromised patients, such as hematology/oncology patients, organ transplant recipients, or HIV-infected patients.*

BMI, body mass index; Sx, symptom; Ct, cycle threshold; NP, nasopharyngeal; RdRp, RNA-dependent RNA polymerase; SIRS, systemic inflammatory response syndrome; SpO_2, saturation of percutaneous oxygen; WBC, white blood cell; AST, aspartate aminotransferase; ALT, alanine aminotransferase; BUN, blood urea nitrogen; CPK, creatine phosphokinase; LDH, lactate dehydrogenase; CRP, C-reactive protein; HIV, human immunodeficiency virus.

Treatment and Outcomes of the Cohort Patients

The treatment and outcomes of the regdanvimab and supportive care groups are summarized in **Table 2**. Patients in the regdanvimab group received regdanvimab treatment an average of 4.0 days after symptom onset and 2.2 days after admission. No patient in the regdanvimab group received remdesivir, but three in the supportive care group did (0.6%). Significantly less patients received steroid treatment in the regdanvimab group (9.8%) than in the supportive care group (19.1%, $P = 0.001$). Other immune modulators, such as baricitinib or tocilizumab, were not administered for the study population and no one participated in other clinical trials for therapeutics. No patient in the regdanvimab group received antibiotics treatment, but 73 patients (13.4%) in the supportive care group did ($P < 0.001$).

After admission, significantly less patients required O_2 supplementation *via* nasal prong in the regdanvimab group (8.1%) than in the supportive care group (18.4%, $P < 0.001$). When O_2 support free survival was calculated using the Kaplan-Meier method, significantly fewer patients required O_2 support in the regdanvimab group than in the supportive care group ($P < 0.001$, **Figure 2A**). Significantly less patients progressed to severe disease in the regdanvimab group (2.1%) than in the supportive care group (9.6%, $P < 0.001$). When progression-free survival for severe disease was calculated using the Kaplan-Meier method, significantly fewer patients progressed to severe disease in the regdanvimab group than in the supportive care group ($P < 0.001$, **Figure 2B**). Significantly more patients were discharged after recovery without referral to tertiary care centers in the regdanvimab group (97.9%) than in the supportive care group (90.8%, $P < 0.001$), and the hospital stays were also shorter in the regdanvimab group (median 11.0 days, interquartile range (IQR) 9.0–12.5 days) than the supportive care group (median 12.0 days, IQR 10.0–15.0 days, $P < 0.001$).

Univariate and Multivariate Analyses for 21-Day Disease Progression Probability in Total Cohort

To identify potential confounding factors for O_2 support *via* nasal prong and progression to severe disease, univariate and multivariate analyses were conducted (**Supplementary Tables 1**, **2**). In the

TABLE 2 | Treatment and outcomes of the regdanvimab and supportive care groups.

Variables	Regdanvimab (n = 234)	Supportive care (n = 544)	*P* value
Regdanvimab			
Regdanvimab treatment	234 (100.0))	0 (0.0)	NA
Interval from symptom onset to regdanvimab, days	4.0 ± 1.8	NA	NA
Interval from admission to regdanvimab, days	2.2 ± 1.5	NA	NA
Remdesivir, steroids, and antibiotics*			
Remdesivir treatment	0 (0.0)	3 (0.6)	0.255
Interval from admission to remdesivir, days	NA	5.7 ± 4.0	NA
Steroid treatment	23 (9.8)	104 (19.1)	0.001
Interval from admission to steroids, days	2.8 ± 2.4	4.0 ± 3.5	0.119
Antibiotic treatment	0 (0.0)	73 (13.4)	<0.001
Interval from admission to antibiotics, days	NA	4.3 ± 3.7	NA
Outcome measures			
O_2 supplementation *via* nasal prong	19 (8.1)	100 (18.4)	<0.001
Interval from admission to nasal prong, days	2.0 (2.0–4.0)	3.0 (2.0–5.0)	0.129
Composite outcome for progression to severe disease	5 (2.1)	52 (9.6)	<0.001
Interval from admission to composite outcome, days	5.0 (2.5–7.5)	5.0 (3.0–8.0)	0.691
O_2 supplement *via* facial mask	1 (0.4)	12 (2.2)	0.076
Interval from admission to facial mask, days	10.0 (10.0–10.0)	6.5 (5.0–7.8)	0.154
O_2 supplement *via* HFNC	0 (0.0)	8 (1.5)	0.062
Interval from admission to HFNC, days	NA	7.0 (6.0–8.8)	NA
Referral to tertiary care center†	5 (2.1)	49 (9.0)	<0.001
Interval from admission to referral, days	5.0 (2.5–7.5)	5.0 (3.0–8.0)	0.664
Live discharge after recovery without referral	229 (97.9)	494 (90.8)	<0.001
Interval from admission to discharge, days	11.0 (9.0–12.5)	12.0 (10.0–15.0)	<0.001
In-hospital mortality during follow-up period‡	0 (0.0)	1 (0.2)	0.512

*Data are expressed as the number (%) of patients or mean ± SD unless indicated otherwise. *Other immune modulators, such as baricitinib or tocilizumab, were not administered for the study population and no one participated in other clinical trials for therapeutics. †‡One patient in the supportive care group could not be referred to a tertiary care center due to insufficient capacity; that patient received mechanical ventilation support and died. ‡Outcome of patient was followed until discharge or referral. Final outcomes of referred patients were not collected. NA, not applicable; HFNC, high flow nasal cannula.*

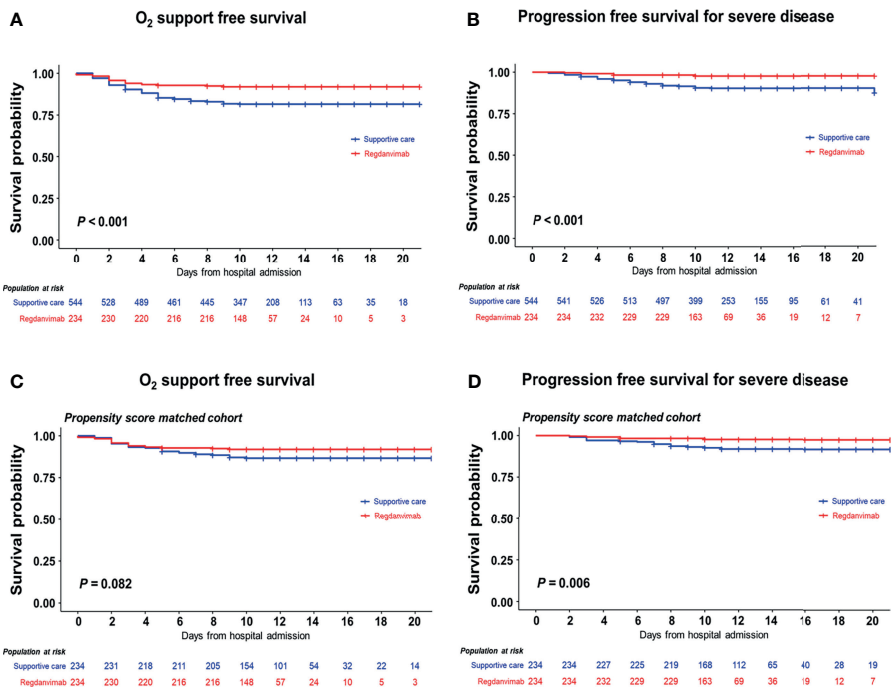

FIGURE 2 | Progression-free survival analysis in the total and propensity score–matched cohorts. The 21-day probabilities for composite outcomes 1 **(A)** and 2 **(B)** were evaluated in the total cohort, and the regdanvimab group showed clinical benefit for both outcomes. Statistically significant benefits were also found in the propensity score–matched cohort for composite outcomes 1 **(C)** and 2 **(D)**.

multivariate analysis, regdanvimab treatment was significantly associated with a decreased risk for O_2 support *via* nasal prong (HR 0.570, 95% CI 0.343–0.946, $P = 0.030$; **Table 3**). Age ≥ 70 years, SpO_2 < 97%, thrombocytopenia, creatinine level, CRP elevation > 1.5 mg/dL, cardiovascular disease, and hypertension were associated with an increased risk for O_2 support. The risk for progression to severe disease was also significantly decreased with regdanvimab treatment (HR 0.262, 95% CI 0.103–0.667, $P = 0.005$). SpO_2 < 97% and CRP elevation > 1.5 mg/dL were associated with an increased risk for progression to severe disease.

To investigate potential risk factors for progression of the study population in the absence of the regdanvimab effect, analyses were conducted in the supportive care group (**Supplementary Tables 3**, **4**). Among the variables found to be significant in the univariate analyses, SpO_2 < 97% and CRP elevation >1.5 mg/dL remained significant risk factors in the multivariate analyses for O_2 support and progression to severe disease. When the total cohort was classified into a higher-risk group (patients with SpO_2 < 97% or CRP > 1.5 mg/dL, n = 319) and a lower-risk group (patients without either of those two risk factors, n = 459), a significantly higher proportion of the patients in the higher-risk group required O_2 supplementation (28.5%) and progressed to severe disease (14.4%), compared with those in the low-risk group (6.1%, and 2.4%, respectively, both $P < 0.001$). In the multivariate analyses of the high-risk group, regdanvimab treatment was associated with decreased risk for progression to severe disease with slightly lower HR (HR 0.202, 95% CI 0.062–0.657, $P = 0.008$) than that of the total cohort (**Supplementary Table 5**).

To identify risk factors for regdanvimab failure, analyses were conducted in the regdanvimab group (**Supplementary Tables 6**, **7**). In the multivariate analysis, age ≥ 60 years, time from symptom onset to admission, SpO_2 < 97%, and thrombocytopenia were associated with an increased risk for O_2 support, but only systemic inflammatory response syndrome (SIRS) was associated with an increased risk for progression to severe disease.

Analysis of a PS-Matched Cohort

A PS-matched cohort was developed with 1:1 ratio, and 234 patients in the supportive care group were matched to 234 patients in the regdanvimab group. The baseline characteristics of the matched cohort were statistically balanced (**Supplementary Table 8**). In the multivariate analysis, regdanvimab treatment was not significantly associated with a decreased risk for O_2 support *via* nasal prong (HR 0.548, 95% CI 0.301–0.999, $P = 0.050$), but it was significantly associated with a decreased risk for progression to severe disease (HR 0.176, 95% CI 0.060–0.516, $P = 0.002$; **Table 4** and **Supplementary Tables 9**, **10**). These findings were also observed in the survival analysis using the Kaplan-Meier method (**Figures 2C, D**).

DISCUSSION

Passive immunization using mAb products require healthcare resources for intravenous administration to mild COVID-19 patients (10). To overcome such limitation, casirivimab/imdevimab added indication for subcutaneous injection based on a phase I trial (20). In the Republic of Korea, mAb agents are practically applicable to mild COVID-19 patients with risk factors for progression because those patients are managed at general hospitals where intravenous administration is available (21, 22). After the conditioned approval of regdanvimab on February 17, 2021, several COVID-19-designated hospitals began actively administering regdanvimab to indicated patients. To date, regdanvimab has been widely administered

TABLE 3 | Multivariate analysis of 21-day disease progression probability.

Factors for disease progression	O_2 support		Progression to severe disease	
	HR (95% CI)	*P* value	HR (95% CI)	*P* value
Age ≥ 70 years	2.024 (1.322–3.099)	0.001	1.106 (0.576–2.123)	0.763
Male sex	0.947 (0.609–1.472)	0.808	1.560 (0.792–3.074)	0.199
BMI	1.037 (0.985–1.091)	0.166		
BMI ≥ 25			1.555 (0.889–2.721)	0.122
Sx onset to admission, days	1.062 (0.963–1.170)	0.230		
SpO_2 < 97%*	2.970 (2.018–4.372)	<0.001	2.697 (1.545–4.708)	<0.001
Neutrophil > 3500/μL	1.321 (0.878–1.990)	0.182	1.283 (0.717–2.297)	0.402
Thrombocytopenia (<150 x10^3/μL)	2.103 (1.402–3.155)	<0.001	1.720 (0.958–3.087)	0.069
Albumin < 4.0 g/dL	1.379 (0.851–2.234)	0.192	1.574 (0.750–3.303)	0.230
Creatinine, mg/dL	2.394 (1.141–5.023)	0.021	2.028 (0.681–6.041)	0.204
CPK, IU/L			1.001 (1.000–1.002)	0.199
CPK elevation (>250 IU/L)	1.144 (0.659–1.988)	0.632		
LDH elevation (>400 IU/L)	1.326 (0.880–1.999)	0.177	0.920 (0.513–1.650)	0.780
CRP elevation (>1.5 mg/dL)	2.742 (1.779–4.225)	<0.001	2.414 (1.292–4.509)	0.006
Cardiovascular disease	1.703 (1.020–2.845)	0.042		
Hypertension	1.564 (1.054–2.322)	0.027	1.403 (0.792–2.486)	0.246
Regdanvimab treatment	0.570 (0.343–0.946)	0.030	0.262 (0.103–0.667)	0.005

**Median value of total cohort.*

HR, hazard ratio; CI, confidence interval; BMI, body mass index; Sx, symptom; SpO_2, saturation of percutaneous oxygen; CPK, creatine phosphokinase; LDH, lactate dehydrogenase; CRP, C-reactive protein.

TABLE 4 | Multivariate analysis of 21-day disease progression probability of the PS-matched cohort.

Factors for disease progression	O_2 support		Progression to severe disease	
	HR (95% CI)	*P* value	HR (95% CI)	*P* value
Age ≥ 70 years	1.120 (0.507-2.476)	0.779		
Sx onset to admission, days	1.233 (1.052–1.445)	0.010		
SIRS	1.699 (0.885–3.262)	0.111		
SpO_2 < 97%*	3.847 (2.111–7.011)	<0.001	2.829 (1.186–6.747)	0.019
Thrombocytopenia (<150 x10^3/μL)	2.864 (1.563–5.250)	<0.001	1.909 (0.814–4.478)	0.003
Albumin < 4.0 g/dL	1.875 (0.752–4.679)	0.178		
BUN elevation (>19 mg/dL)	1.490 (0.628–3.535)	0.366		
LDH, IU/L			1.004 (1.001–1.008)	0.025
LDH elevation (>400 IU/L)	1.813 (0.984–3.339)	0.056		
CRP elevation (>5 mg/dL)	3.613 (1.569–8.319)	0.003	5.881 (1.843–18.771)	0.003
Cardiovascular disease	3.456 (1.617–7.385)	0.001		
Diabetes mellitus	1.684 (0.874–3.243)	0.119		
Hypertension	1.546 (0.853–2.802)	0.151		
Regdanvimab treatment	0.548 (0.301–0.999)	0.050	0.176 (0.060–0.516)	0.002

**Median value of total cohort.*

HR, hazard ratio; CI, confidence interval; Sx, symptom; SpO_2, saturation of percutaneous oxygen; BUN, blood urea nitrogen; LDH, lactate dehydrogenase; CRP, C-reactive protein.

in Korean COVID-19 designated hospitals, but the data from clinical trials of regdanvimab have not been published as a full scientific article yet (13). As evaluation of the clinical efficacy of treatment modalities in a real-world setting would be especially necessary for drugs under emergency use authorizations (4), we conducted the present retrospective cohort study for scientific background for COVID-19 management.

Of note, in the multivariate analyses of the total cohort and PS-matched cohort, regdanvimab treatment was significantly associated with a decreased risk of progression to severe disease. Although a reduced risk for requiring O_2 supplementation was not statistically significant in the PS-matched cohort, a tendency favoring the regdanvimab group was noticed, consistent with the analysis of the total cohort. The need for other treatment modalities, including remdesivir, steroids, and antibiotics, was significantly lower in the regdanvimab group, and the length of hospital stay among patients who recovered without referral was also shorter in the regdanvimab group than in the supportive care group. These findings consistently indicate that regdanvimab treatment offers clinical benefit for high-risk patients. Because most mild to moderate COVID-19 patients of the Republic of Korea are managed at designated general hospitals, these primary outcomes of the present study are not identical with those of clinical trials conducted for non-hospitalized COVID-19 patients (4, 7, 9). The clinical status of COVID-19 patients who require O_2 supplementation in the present study would be similar or slightly more severe than those who require hospitalization in those trials, though indications for hospitalization were not clearly presented (4, 7, 9). Since those clinical trials did not evaluated progression to severe disease as an outcome value, the finding of the present study would additionally support effectiveness of mAb agents for mild to moderate COVID-19 patients.

However, the progression rate in this study population was low (18.4% for O_2 supplement and 9.6% for progression to severe disease in the supportive care group), because regdanvimab treatment is approved for early COVID-19 patients who have relatively broad risk factors for disease progression. The proportion of COVID-19-related hospitalization was much lower in the clinical trials of other mAb agents for non-hospitalized patients (control arms, 3.2–7.0%) (7, 9). To figure out whether a high-risk subgroup might gain more benefit from regdanvimab treatment, we investigated the common risk factors for progression in our analyses of the total cohort and supportive care group. Among the various clinical variables, SpO_2 < 97% and CRP level > 1.5 mg/dL were common risk factors for progression, and the progression rate in the higher-risk sub-group (of patients with either of those factors) was 28.5% for O_2 supplementation and 14.4% for progression to severe disease. Meanwhile, in the lower-risk sub-group (of patients without any of these two factors), progression rates to O_2 supplement and to severe disease were 6.1% and 2.4% respectively, which were similar to those treated with regdanvimab. Adding those factors to the treatment guidelines could increase the cost-effectiveness, but a certain proportion of patients would lose their treatment opportunity. The appropriate indication for mAb treatment thus needs to be adjusted based on the outbreak situation and healthcare resources.

Although only five patients in the regdanvimab group (2.1%) progressed to severe disease, we also conducted multivariate analyses to identify the risk factors for regdanvimab failure. It was difficult to find consistent factors between the two primary endpoints, but the statistically significant factors of late admission, decreased oxygenation, thrombocytopenia, and SIRS might be associated with progressed disease. The time interval between symptom onset to admission or regdanvimab treatment was associated with O_2 supplementation, consistent with previous cohort study conducted at USA (4), but administration time interval was not associated with progression to severe disease in the present cohort. These findings suggest that early administration of regdanvimab would be important, but other unmeasured factors may have stronger association with regdanvimab failure. Since potential

virulence factors associated with viral mutation was not evaluated in the present analysis, a larger cohort study with viral sequencing needs to be conducted to clearly elucidate the factors involved in regdanvimab failure.

The present study has several limitations. First, we retrospectively evaluated patients before and after regdanvimab became available. Even though the management in the outbreak setting could be different, it is less likely because study population were admitted at early time point after symptoms onset and managed at the same hospital. During the study period, management for mild COVID-19 patients did not change, and the community-based spread of SARS-CoV-2 variants of concerns (VOCs) was not significant in the Republic of Korea (23). The two hospitals participated in the present study have been dedicated for mild and moderate COVID-19 patient care since the first (March 2020) and second (June 2020) domestic outbreak, respectively, and the medical resources and management protocols were well-stabilized before the start of present study (December 2020). Nevertheless, basic demographic factors such as age, sex, and underlying disease could be variable according to the outbreak situation and seasons. To overcome that limitation, we enrolled a control group more than two times larger than the regdanvimab group in a short period and performed multivariate analyses and PS matching. Second, the cohort study was conducted in two general hospitals, and outcomes after patients were referred to tertiary care centers could not be investigated. During hospitalization at these general hospitals, only one patient in the supportive care group died who could not be referred to a tertiary care center due to insufficient capacity. A large, nation-wide cohort study is needed to evaluate the final outcomes of patients whose disease progressed despite regdanvimab treatment. Last, although the study patients were confirmed with COVID-19 with SARS-CoV-2 RT-PCR, whole genome sequencing (WGS) to detect viral mutation was not performed. Although the effectiveness of mAbs could be different against VOCs, VOCs were not dominant during the study period in the Republic of Korea. The healthcare authority selectively performed WGS to detect viral mutation for risk groups such as immigrants from VOC-endemic countries and individuals exposed to VOCs. In the present cohort, only one case in the regdanvimab group was reported to be infected with alpha variant. Although he progressed to severe disease despite regdanvimab treatment, it was difficult to interpret the impact of a single case of VOC. Follow-up studies against VOCs need to be conducted during a VOC-dominant outbreak period with sequencing of entire study population.

In conclusion, in a retrospective cohort study evaluating high-risk COVID-19 patients, regdanvimab treatment within seven days of symptom onset was associated with decreased risk of progression to severe disease.

DATA AVAILABILITY STATEMENT

The original contributions presented in the study are included in the article/**Supplementary Material**. Further inquiries can be directed to the corresponding authors.

ETHICS STATEMENT

The studies involving human participants were reviewed and approved by Samsung Medical Center. Written informed consent for participation was not required for this study in accordance with the national legislation and the institutional requirements.

AUTHOR CONTRIBUTIONS

JiL, JeL, J-HK, SS, and KP contributed to the conceptualization. JiL, JeL, J-HK, MH, HK, SC, YDL, JS, and SS, and KP contributed to the investigation. J-HK and SS contributed to the statistical analysis. KP contributed to the supervision. J-HK, SS, and KP contributed to the writing, review, and editing. All authors contributed to the article and approved the submitted version.

FUNDING

This work was supported by Research Program funded by the Korea Disease Control and Prevention Agency (#2021-ER1906-00).

SUPPLEMENTARY MATERIAL

The Supplementary Material for this article can be found online at: https://www.frontiersin.org/articles/10.3389/fimmu.2021.772320/full#supplementary-material

REFERENCES

1. WHO. *WHO Coronavirus (COVID-19) Dashboard* (2021). Available at: https://covid19.who.int/ (Accessed 19 October, 2021).
2. Group A-TL-CS. A Neutralizing Monoclonal Antibody for Hospitalized Patients With Covid-19. *N Engl J Med* (2020) 384(10):905–14. doi: 10.1056/NEJMoa2033130
3. Weinreich DM, Sivapalasingam S, Norton T, Ali S, Gao H, Bhore R, et al. REGN-COV2, a Neutralizing Antibody Cocktail, in Outpatients With Covid-19. *N Engl J Med* (2020) 384(3):238–51. doi: 10.1056/NEJMoa2035002
4. Verderese JP, Stepanova M, Lam B, Racila A, Kolacevski A, Allen D, et al. Neutralizing Monoclonal Antibody Treatment Reduces Hospitalization for Mild and Moderate COVID-19: A Real-World Experience. *Clin Infect Dis* (2021). doi: 10.1093/cid/ciab579

5. Chen P, Nirula A, Heller B, Gottlieb RL, Boscia J, Morris J, et al. SARS-CoV-2 Neutralizing Antibody LY-CoV555 in Outpatients With Covid-19. *N Engl J Med* (2021) 384(3):229–37. doi: 10.1056/NEJMoa2029849
6. Kim C, Ryu DK, Lee J, Kim YI, Seo JM, Kim YG, et al. A Therapeutic Neutralizing Antibody Targeting Receptor Binding Domain of SARS-CoV-2 Spike Protein. *Nat Commun* (2021) 12(1):288. doi: 10.1038/s41467-020-20602-5
7. Weinreich DM, Sivapalasingam S, Norton T, Ali S, Gao H, Bhore R, et al. REGEN-COV Antibody Combination and Outcomes in Outpatients With Covid-19. *N Engl J Med* (2021). doi: 10.1056/NEJMoa2108163
8. FDA. *Fact Sheet For Healthcare Providers Emergency Use Authorization (EUA) Of Sotrovimab* (2021). Available at: https://www.fda.gov/media/149534/download (Accessed October 19, 2021).
9. Dougan M, Nirula A, Azizad M, Mocherla B, Gottlieb RL, Chen P, et al. Bamlanivimab Plus Etesevimab in Mild or Moderate Covid-19. *N Engl J Med* (2021) 385(15):1382–92. doi: 10.1056/NEJMoa2102685
10. NIH. *COVID-19 Treatment Guidelines, Anti-SARS-CoV-2 Monoclonal Antibodies* (2021). Available at: https://www.covid19treatmentguidelines.nih.gov/therapies/anti-sars-cov-2-antibody-products/anti-sars-cov-2-monoclonal-antibodies/ (Accessed October 19, 2021).
11. MFDS. *Approval of Regdanvimab for the Treatment of COVID-19, February 5, 2021* (2021). Available at: https://www.mfds.go.kr/brd/m_99/view.do?seq=45029&srchFr=&srchTo=&srchWord=&srchTp=&itm_seq_1=0&itm_seq_2=0&multi_itm_seq=0&company_cd=&company_nm=&page=1 (Accessed May 5, 2021).
12. EMA. *EMA Review of Regdanvimab for COVID-19 to Support National Decisions on Early Use* (2021). Available at: https://www.ema.europa.eu/en/news/ema-review-regdanvimab-covid-19-support-national-decisions-early-use (Accessed July 21, 2021).
13. Kim SB, Kim J, Huh K, Choi WS, Kim YJ, Joo EJ, et al. Korean Society of Infectious Diseases/National Evidence-Based Healthcare Collaborating Agency Recommendations for Anti-SARS-CoV-2 Monoclonal Antibody Treatment of Patients With COVID-19. *Infect Chemother* (2021) 53(2):395–403. doi: 10.3947/ic.2021.0304
14. arena Ct. *Celltrion's Covid-19 Drug Regdanvimab Meets Phase III Endpoints* (2021). Available at: https://www.clinicaltrialsarena.com/news/celltrion-regdanvimab-phaseiii-data/ (Accessed July 11, 2021).
15. Sung HK, Kim JY, Heo J, Seo H, Jang Ys, Kim H, et al. Clinical Course and Outcomes of 3,060 Patients With Coronavirus Disease 2019 in Korea, January–May 2020. *J Korean Med Sci* (2020) 35(30):e280. doi: 10.3346/jkms.2020.35.e280
16. Rosenbaum PR, Rubin DB. Reducing Bias in Observational Studies Using Subclassification on the Propensity Score. *J Am Stat Assoc* (1984) 79 (387):516–24. doi: 10.1080/01621459.1984.10478078
17. Suh HJ, Lee E, Park S-W. Clinical Characteristics of COVID-19: Risk Factors for Early Oxygen Requirement After Hospitalization. *J Korean Med Sci* (2021) 36(19):e139. doi: 10.3346/jkms.2021.36.e139
18. Wolff D, Nee S, Hickey NS, Marschollek M. Risk Factors for Covid-19 Severity and Fatality: A Structured Literature Review. *Infection* (2021) 49(1):15–28. doi: 10.1007/s15010-020-01509-1
19. Moon SS, Lee K, Park J, Yun S, Lee YS, Lee DS. Clinical Characteristics and Mortality Predictors of COVID-19 Patients Hospitalized at Nationally-Designated Treatment Hospitals. *J Korean Med Sci* (2020) 35(36):e328. doi: 10.3346/jkms.2020.35.e328
20. FDA. *Fact Sheet For Health Care Providers Emergency Use Authorization Of REGEN-COV*. Available at: https://www.fda.gov/media/145611/download (Accessed October 19, 2021).
21. Yoon YK, Lee J, Kim SI, Peck KR. A Systematic Narrative Review of Comprehensive Preparedness Strategies of Healthcare Resources for a Large Resurgence of COVID-19 Nationally, With Local or Regional Epidemics: Present Era and Beyond. *J Korean Med Sci* (2020) 35(44):e387. doi: 10.3346/jkms.2020.35.e387
22. Peck KR. Early Diagnosis and Rapid Isolation: Response to COVID-19 Outbreak in Korea. *Clin Microbiol Infect* (2020) 26(7):805–7. doi: 10.1016/j.cmi.2020.04.025
23. KDCA. *Regular Situation Report for COVID-19, June 1, 2021* (2021). Available at: https://www.kdca.go.kr/board/board.es?mid=a20501010000&bid=0015&list_no=713505&cg_code=&act=view&nPage=39 (Accessed October 19, 2021).

Conflict of Interest: The authors declare that the research was conducted in the absence of any commercial or financial relationships that could be construed as a potential conflict of interest.

frontiers in Immunology

REVIEW
published: 30 November 2021
doi: 10.3389/fimmu.2021.751778

The Global Epidemic of the SARS-CoV-2 Delta Variant, Key Spike Mutations and Immune Escape

Dandan Tian, Yanhong Sun, Jianming Zhou and Qing Ye *

National Clinical Research Center for Child Health, National Children's Regional Medical Center, The Children's Hospital, Zhejiang University School of Medicine, Hangzhou, China

During the COVID-19 pandemic, SARS-CoV-2 variants have emerged and spread worldwide. The Delta (B.1.617.2) variant was first reported in India in October 2020 and was classified as a "variant of concern (VOC)" by the WHO on 11 May, 2021. Compared to the wild-type strain, several studies have shown that the Delta variant is more transmissible and has higher viral loads in infected samples. COVID-19 patients infected with the Delta variant have a higher risk of hospitalization, intensive care unit (ICU) admission, and mortality. The Delta variant is becoming the dominant strain in many countries around the world. This review summarizes and analyses the biological characteristics of key amino acid mutations, the epidemic characteristics, and the immune escape of the Delta variant. We hope to provide scientific reference for the monitoring and prevention measures of the SARS-CoV-2 Delta variant and the development strategy of a second-generation vaccine.

Keywords: COVID-19, SARS-CoV-2 variants, mutations, vaccine, immune escape

OPEN ACCESS

Edited by:
Raymund Razonable, Mayo Clinic, United States

Reviewed by:
Gabriel M. Gutierrez, Leidos, United States
Hanna-Mari Baldauf, Ludwig Maximilian University of Munich, Germany

***Correspondence:**
Qing Ye
qingye@zju.edu.cn

Specialty section:
This article was submitted to Vaccines and Molecular Therapeutics, a section of the journal Frontiers in Immunology

Received: *02 August 2021*
Accepted: *08 November 2021*
Published: *30 November 2021*

Citation:
Tian D, Sun Y, Zhou J and Ye Q (2021) The Global Epidemic of the SARS-CoV-2 Delta Variant, Key Spike Mutations and Immune Escape. Front. Immunol. 12:751778. doi: 10.3389/fimmu.2021.751778

1 INTRODUCTION

Over the last two decades, SARS -CoV-2 has been the third coronavirus known to cause severe acute respiratory disease in humans, following SARS-CoV in 2003 and MERS-CoV in 2012 (1–3). Coronavirus disease 2019 (COVID-19) caused by severe acute respiratory syndrome coronavirus 2 (SARS-CoV-2) has a deleterious impact on health services and the global economy (4–6). As of 8 October 2021, COVID-19 has spread rapidly to more than 200 countries, and there have been 236,599,025 confirmed cases of COVID-19, including 4,831,486 deaths (www.who.int).

At the end of January 2020, the D614G mutation, which turns aspartic acid (Asp) into glycine (Gly) at site 614 of the spike protein, was first discovered in the UK and quickly became the dominant epidemic strain in the world, attracting widespread attention (7, 8). The established nomenclature systems for naming and tracking SARS-CoV-2 genetic lineages by Nextstrain, GISAID (https://www.gisaid.org/), and Pango are currently in use by scientists. The SARS-CoV-2 variants were classified as "variant of concern (VOCs)" and "Variant of Interest, VOI)" by the WHO. At present, Alpha B.1.1.7 (known as 20I/501Y.V1, VOC 202012/01) (9), Beta B.1.351 (known as 501Y.V2) (10), Gamma P.1 (known as 501Y.V3) (11) and Delta B.1.617.2 (known as 478K.V1) (12) are defined as "variants of concern (VOCs)" by the WHO. Several studies have indicated that the Delta variant has higher transmissibility (13–15) and immune evasion than the early original virus strain and the other three VOCs. COVID-19 patients infected with Delta have a

higher risk of hospitalization, ICU admission, and mortality (16–18). The Delta is becoming a prominent global strain globally, which has brought new challenges to the prevention and control of the COVID-19 pandemic.

1.1 The Biological Characteristics of Key Amino Acid Mutations in the Spike Protein of the SARS-CoV-2 Delta Variant

SARS-CoV-2 invades host cells by binding the spike protein to angiotensin-converting enzyme-2 (ACE2) (19–21). The SARS-CoV-2 spike protein is cleaved by furin into the S1 subunit and S2 subunit. The S1 subunit consists of an N-terminal domain (NTD) and a receptor-binding domain (RBD) and is responsible for binding to the host-cell ACE2 receptor. In comparison, the S2 subunit includes the trimeric core of the protein and is responsible for membrane fusion. The spike protein is the dominant neutralization target of monoclonal antibodies (mAbs), convalescent plasma, and vaccines (22–24). Therefore, mutations in the S protein affect the transmissibility, pathogenicity, and immune escape of SARS-CoV-2 variants. The Delta variant has accumulated nine amino acid mutations (T19R, G142D, FR156▪157del, R158G, L452R, T478K, D614G, P681R, D950N) in the spike protein (25).

1.1.1 L452R

The L452R mutation is located in the receptor-binding motif (RBM) region in the RBD region, containing residues that bind to ACE2 (26–28). Analysis of the SARS-CoV-2 spike protein revealed that the L452 residue does not directly contact the ACE2 receptor (29). Instead, L452, together with F490 and L492, forms a hydrophobic patch on the surface of the spike RBD. The L452R mutation may cause structural changes in this region that stabilize the interaction between the spike protein and the host cell's ACE2 receptor, leading to increasing infectivity (26, 30). Deng X et al. observed that the entry efficiency into host cells of stable pseudoviruses carrying the L452R mutation was 6.7-22.5-fold higher in 293T cells and 5.8-14.7-fold higher in human airway lung organoids (HAOs) compared to D614G alone (293T cells and HAOs can stably express ACE2) (26). These results indicated that L452R mutation could increase the binding affinity of the spike protein to the host-cell receptor ACE2.

Wilhelm A et al. (31) found that authentic SARS-CoV-2 variants harboring L452R had reduced susceptibility to convalescent and vaccine-elicited sera and mAbs. Compared to B.1, the neutralization activity of convalescent sera against Delta was reduced by 5.33-fold. The neutralization activity of sera elicited by the mRNA vaccine against Delta was 2-fold weaker than B.1. In contrast to Kappa, authentic SARS-CoV-2 variants harboring L452R have a substantial resistance against imdevimab and bamlanivimab. Even at high concentrations, imdevimab was not effective against Delta, indicating high resistance. However, neutralization of Delta was moderately reduced with the clinically approved combination of casirivimab/imdevimab (31). In addition, another pseudovirus simulation showed that the L452R mutation could enhance the immune escape ability of the virus against convalescent plasma (32) and monoclonal antibodies (SARS2-01, SARS2-02, LY-CoV555, SARS2-32, X593, P2B2F6) (33).

1.1.2 T478K

Compared with the other two B.1.617 lineages (B.1.617.1 and B.1.617.3), Delta (B.1.617.2) does not have the E484Q mutation but has a unique T478K mutation (25). An in silico molecular dynamics study on the protein structure of spike has predicted that the T478K mutation, substituting a non-charged amino acid (threonine) with a positive one (lysine), may significantly alter the electrostatic surface of the protein and increase steric hindrance of the spike protein. These factors could enhance the binding affinity of RBD to ACE2 and enhance the ability of the virus to invade the host cell (34). Similarly, *in vitro* cell culture studies have shown that the Delta variant carrying T478K is more likely to undergo secondary mutation in a low titer antibody environment, leading to the failure of host antibody immunization (34).

1.1.3 P681R

Interestingly, the P681R mutation in the S protein of the B.1.617 lineage is unique and newly identified in VOCs. The P681R mutation is located at the furin cleavage site (FCS; residues RRAR positioned between 682-5), and the cleavage of this region is the key to host cell entry (35). Several analyses have found that the P681R mutation affects viral replication dynamics and potentially determines the B.1.617 variants (36–38). Pseudoviruses carrying the P681R mutation showed that this mutation significantly increased the level of the cleaved S2 subunit and the level of the cleaved S2 subunit of the D614G/P681R mutation was significantly higher than that of D614G alone. *In vitro*, cell culture experiments revealed that the size of floating syncytia in the D614G/P681R mutant-infected culture was significantly larger than that in the D614G mutant-infected cell culture (39). These data suggested that the P681R mutation facilitates furin-mediated cleavage of the SARS-CoV-2 S protein, accelerates viral fusion, and promotes cell-cell infection.

In addition, the neutralization analyses of pseudoviruses showed that three monoclonal antibodies against RBD had 1.5-fold (1.2 ~2.65) decreased neutralization activity by against pseudoviruses with the D614G/P681R mutation. The neutralizing activity assay using the 19 sera elicited by the BNT162b2 vaccine (two doses) showed that pseudoviruses carrying the D614G/P681R mutation are significantly resistant to the vaccine-induced NAbs compared to the D614G pseudoviruses (39). These results suggested that the P681R mutation generated resistance to some mAbs and sera elicited by mRNA vaccines.

Stefano Pascarella et al. (40) reported that the surface electrostatic potential (EP) of the RBD of the spike protein is markedly increased. This is particularly noticeable in the Delta variant, which shows multiple replacements from neutral or negatively charged amino acids to positively charged amino acids. The EP in the spike protein of the Delta variant includes the uncharged and hydrophobic residue of Leu452 changing to the positively charged residue Arg and the neutral residue Thr

changing to the positively charged Lys at position 478. The positive electrostatic potential can favor the interaction between the B.1.617.2+ RBD and the negatively charged ACE2, increasing the binding affinity of RBD to ACE2 receptor, thus conferring a potential increase in the virus transmission.

The above studies suggested that L452R, T478K, and P681R are the three key mutations of the SARS-CoV-2 Delta variant. These mutations increased transmissibility and generated immune escape of the Delta variant, as shown in **Figure 1**.

1.2 Delta Variant: More Transmissible, Shorter Incubation Period, Higher Viral Loads

Epidemiological investigation showed that the incubation period (the period of time from infection to illness onset) after infection with the Delta variant was 2-3 days, which was shorter than that of the wild-type strain (3-7 days). The basic reproductive number (R0, the infected person can transmit the pathogen to several other people) of the Delta variant (R0:4.04~5.0) was higher than that of the wild-type strain (R0:2.2~3.77). In addition, the generation time (GT, the interval between infection of the primary case and secondary cases) was 2.9 days (95% CI: 2.4–3.3), which was much shorter than the wild-type strain (2.9 *vs.* 5.7). It has been reported that the fifth generation of cases emerged just ten days after the first case was infected with the Delta variant (41–43).

One preprint from CDC Guangdong Province, China, had reported that the viral loads of patients infected with the Delta variant (n=62, Ct =24.00, IQR:19.00~29.00) were 1260-fold higher than those of the wild-type strain (n=63, Ct=34.31, IQR:31.00~36.00) when PCR was first used to detect SARS-CoV-2. Moreover, the number of patients infected with the Delta variant containing the viral loads > 6x105 copies/mL in oropharyngeal swabs was significantly higher than that of the wild-type strain when the viruses were first detected (80.65% *vs.* 19.05%) (44). In addition, the mean time of virus turning negative after the Delta variant infection was 13~15 days, which was much longer than that of wild-type strains of 7~9 d (45).

Moreover, epidemiological studies from Guangzhou also showed that patients infected with the Delta variant could spread in a short time even if individuals did not converse when sharing toilets or eat in the same space (46–48). Similarly, a follow-up case in Australia showed that a driver

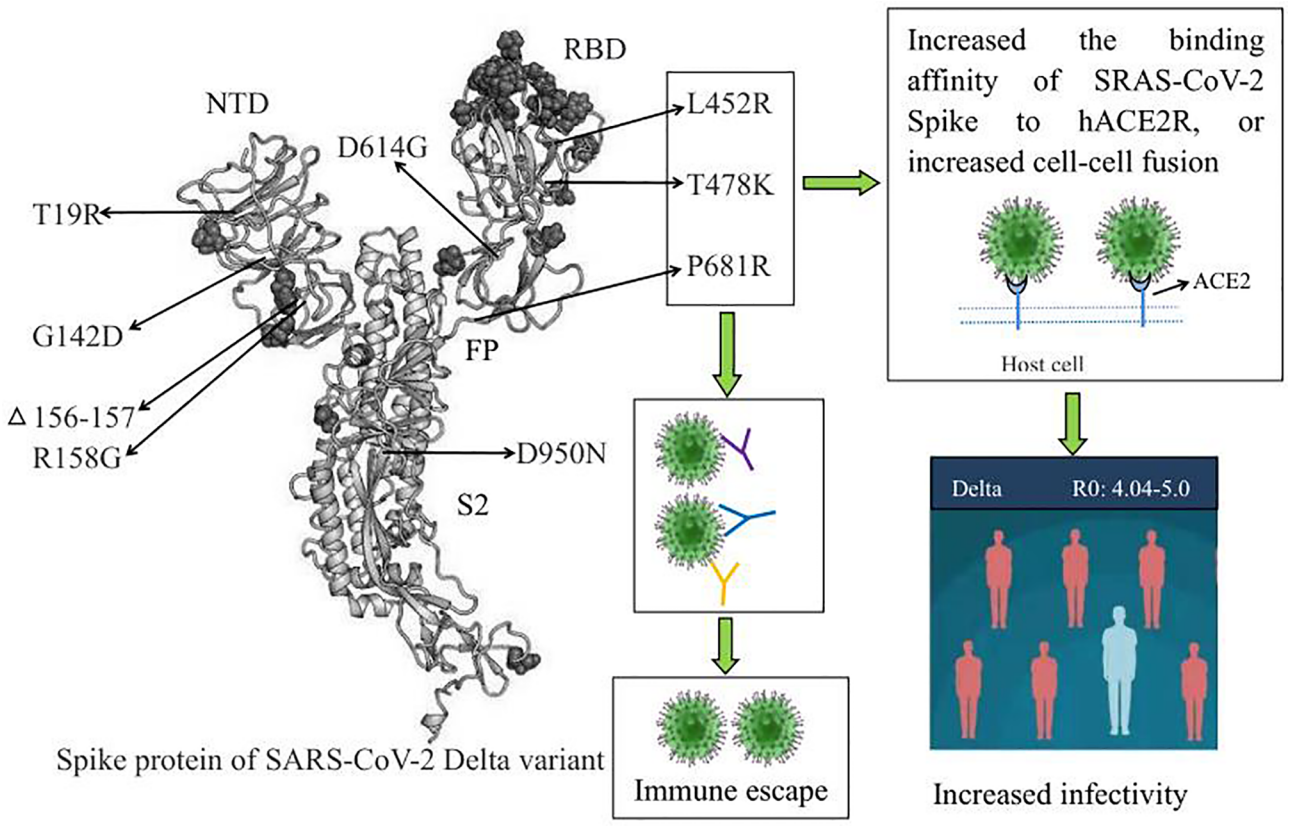

FIGURE 1 | The biological characteristics of key amino acid mutations in the Spike protein of the SARS-CoV-2 Delta variant. L452R, T478K, and P681R are the three key amino acid mutations of the Delta variant, and these mutations increased transmissibility and generated immune escape of the Delta variant. RBD, receptor binding domain; NTD, N-terminal domain; ACE2, angiotensin-converting enzyme-2.

infected with the Delta variant was on the road, in a shopping mall, or in a cafe at the same time as three patients; virus transmission occurred despite a distance of only 10-60 cm (49). This suggests that the Delta variant may spread through aerosol in addition to the respiratory tract and close contact, leading to enhanced interpersonal transmission ability.

These data indicated that the Delta variant has higher transmissibility and a shorter incubation period. Patients infected with the Delta variant had higher viral loads (Ct value was less than 30).

1.3 The Delta Variant Is Becoming the Dominant Epidemic Strain in Many Countries Around the World

Delta (B.1.617.2) was first reported in India in October 2020 (12). Ram VS et al. reported that in India, the second wave started in March 2021, and they became the first country to report 400 000 cases per day by the end of April, and the emerged new Delta variant has played as a key infectious agent (50). The Delta variant has been linked to a resurgence of COVID-19 in Nepal and southeast Asia. Delta seems to be around 60% more transmissible than the already highly infectious Alpha variant (B.1.1.7) identified in the UK in late 2020 (51). From 20 to 27 May 2021, the total confirmed cases infected with the Delta variant increased from 3424 to 6959 in the UK (52, 53). Public Health England's weekly coronavirus data on circulating variants showed 29,892 new cases of the Delta variant in the UK in the week (as of 9 June 2021), bringing the total number of cases of the Delta variant detected to 42,323 (54, 55).

According to nationwide sampling conducted by the genomics company Helix in San Mateo, California, Delta is rising fast, while Alpha fell from more than 70% of cases in late April to around 42% by mid-June 2021 (51). Since mid-June 2021, a sharp increase in COVID-19 cases has been observed in Israel, attributed to the Delta variant, which by mid-July 2021 constituted more than 95% of sequenced virus isolates in Israel (56, 57).

The first local infection of the Delta variant was identified in Guangzhou, Guangdong Province, China, on 21 May 2021 (44). From 21 May to 23 June 2021, the Delta variant caused epidemics in Guangzhou, Maoming, Foshan, Zhanjiang, and Shenzhen in Guangdong Province, China (46, 47). These results suggested that the Delta variant is becoming the dominant epidemic strain in many countries worldwide.

1.4 Delta Variant Has a Higher Risk of Hospital Admission, ICU Admission, and Mortality

Many clinical studies have reported that critical COVID-19 illness caused by infection with the wild-type strain includes acute respiratory distress syndrome; coagulopathies (58); septic shock; and multiple organ injuries, including liver injury (59), kidney injury (60), heart injury (61), and gastrointestinal symptoms (62). Preliminary data from Britain and Scotland showed that the hospitalization rate of patients infected with the Delta variant was 2-fold higher than that with Alpha (51). In Canada, a retrospective cohort study (63) showed that compared to non-VOC SARS-CoV-2 strains, the adjusted elevation in risk associated with N501Y-positive variants (B1.1.17, B.1.351 and P.1) was 59% (49-69%) for hospitalization, 105% (82-134%) for ICU admission, and 61% (40-87%) for death. Moreover, the adjusted risk of patients infected with the Delta variant was 120% (93-153%) for hospitalization, 287% (198-399%) for ICU admission, and 137% (50-230%) for death, which was significantly higher than N501Y-positive VOC variants, as shown in **Table 1**. In addition, the odds ratios (OR) for hospitalization, ICU admission, and death with Delta variant were as high as 2.20 (95% CI:1.93-2.53), 3.87 (95% CI:1.5-3.3), and 2.37 (95% CI:1.50-3.30), respectively (63). Similarly, the hazard ratios (HRs) of hospitalization for patients infected with the Delta variant was higher than that for patients infected with the wild-type strain in Scotland and in Singapore, with HRs:1.85 (95% CI:1.39-2.47) and HRs: 4.90 (95% CI:1.43-30.78), respectively (64). These studies showed that the risk of patients' hospitalization, ICU admission, and mortality after Delta infection was higher than N501Y-positive VOC variants (B1.1.17, B.1.351, and P.1) and the wild-type strain, increasing the risk of severe COVID-19 disease.

TABLE 1 | The epidemiological characteristics of the SARS-CoV-2 Delta variant.

WHO label	Delta
Pango lineage	B.1.617.2
Next strain	S:478K
GISAID clade	G/478K.V1
Amino acid mutations in the spike protein	T19R, G142D, FR156-157del, R158G, L452R, T478K, D614G, P681R, D950N (25)
Higher transmissibility	around 60% more transmissible than Alpha variant (51)
Higher risk of hospitalization, ICU admission, and mortality	the risk of patients infected with the Delta variant was 120% (93-153%) for hospitalization, 287% (198-399%) for ICU admission, and 137% (50-230%) for death, In Canada (63)
Immune escape	Resistance to partial mAbs, convalescent plasma, and partial vaccine
Shorter incubation period	2-3 days (Delta) *vs*. 3-7 days (Wild-type strain) (41–43)
Viral loads of patients infected with Delta when PCR first used to detect SARS-CoV-2	1260-fold higher than the wild-type strain (44)
The basic reproductive number: R0	4.04 ~ 5.0 (Delta) *vs*. 2.2~3.77 (Wild-type strain) (41–43)
The longer mean time of virus turning negative after the Delta variant infection	13~15 days (Delta) *vs*. 7-9 days (Wild-type strain) (45)

R0: The basic reproductive number.

1.5 Immune Escape From the Neutralization Activity of the Monoclonal Antibodies (mAbs) and Convalescent Plasma

It has been reported that the neutralization activity of 30% (6/20) of mAbs against the Delta variant was reduced more than 5-fold compared with that of the wild-type strain. In addition, the neutralization activity of 45% and 5% of convalescent plasma against Delta was reduced by approximately 3-10-fold and >10-fold, respectively (65, 66). Interestingly, the neutralization assay found that the neutralizing activity of convalescent plasma from individuals infected with the P.1 and B.1.351 variants against Delta was entirely lost, suggesting that individuals infected with B.1.351 and P.1 may be at risk of reinfection with the Delta variant (66).

1.6 Vaccine Efficacy Against Delta Variant

In Israel, two doses of the Pfizer vaccine (mRNA vaccine) can reduce symptomatic infections by 94%, related hospitalization by 87%, severe cases by 92%, and the risk of Delta infection by 79% (66, 67). In England, compared with patients infected with Delta who were not vaccinated, the risk of symptomatic infection caused by the Delta variant was decreased by 33%, and the hospitalization rate decreased by 75% three weeks after the first dose of the AstraZeneca or Pfizer vaccine. The effectiveness of the second dose of the AstraZeneca and Pfizer vaccines against Delta infection was increased by 60% and 88%, respectively. The hospitalization rate of patients infected with Delta who received two doses of the AstraZeneca and Pfizer vaccines was decreased by 92% and 96%, respectively (68–70).

The Delta variant can cause breakthrough infections in vaccinated populations in Guangzhou. The effectiveness evaluation of inactivated-virus vaccines-Sinovac/CoronaVac against the Delta variant during the epidemic in Guangdong showed that the efficacy of Sinovac/CoronaVac to prevent close contact infection was 69%, the efficacy of Sinovac/CoronaVac to prevent the development of symptomatic COVID-19 was 73%, and the efficacy of Sinovac/CoronaVac to prevent severe COVID-19 cases was 95% (45, 71).

All of these data revealed that, although the Delta variant presents partial immune escape, the mRNA vaccine (AstraZeneca and Pfizer vaccine) and inactivated-virus vaccines (Sinovac/CoronaVac) still have a protective effect against the Delta variant.

The severity of COVID-19 is mainly related to hosting factors, especially cellular immune responses in patients. Patients with mild COVID-19 and recovered patients with severe COVID-19 exhibit a normal humoral and a T cell-mediated immune response to effectively eliminate the virus (72). Vaccines induce neutralizing antibodies against the SARS-CoV-2 and induce a T cell response against the virus. Animal experiments have shown that a single intramuscular injection of the RNA-vaccine in mice elicited robust production of anti–SARS-CoV-2 S protein IgG antibody isotypes indicative of a type 1 T helper cell response. A prime/boost regimen induced potent T cell responses in mice, including antigen-specific responses in the lung and spleen (73). Another study showed that a single prime RNA- vaccine vaccination in mice led to robust neutralizing antibodies and produced a strong viral antigen-specific CD8+ T lymphocyte response (74). Moreover, several clinical studies have shown that individuals with prior infection can enhance T cell immunity against VOCs after one dose of mRNA vaccines (75, 76). mRNA vaccines generate antigen-specific T cells in a coordinated immune response, and vaccine-induced T cells resemble durable memory cells primed by infection (75, 76). These findings suggest that RNA vaccine-induced T cell responses are also involved in antiviral effects and neutralizing antibodies.

2 CONCLUSIONS

This review describes the biological characteristics of the L452R, T478K, and P681R mutations of the Delta variant spike protein. These mutations impact Delta variant biological behavior, including increased transmissibility and immune evasion. COVID-19 patients infected with Delta have a higher risk of hospitalization and ICU admission than patients infected with other VOCs (B1.1.17, B.1.351, and P.1) and wild-type strains. The Delta variant may be the most transmissible VOC and is becoming the main epidemic variant in many countries worldwide.

AUTHOR CONTRIBUTIONS

DT conceived and wrote the manuscript and prepared figures. YS and JZ contributed to the data collection and prepared the table. QY conceived and contributed to the modification and revision of the manuscript. All authors contributed to this article and approved the submitted versions.

REFERENCES

1. Su S, Wong G, Shi W, Liu J, Lai A, Zhou J, et al. Epidemiology, Genetic Recombination, and Pathogenesis of Coronaviruses. *Trends Microbiol* (2016) 24:490–502. doi: 10.1016/j.tim.2016.03.003
2. Graham RL, Baric RS. Recombination, Reservoirs, and the Modular Spike: Mechanisms of Coronavirus Cross-Species Transmission. *J Virol* (2010) 84:3134–46. doi: 10.1128/JVI.01394-09
3. Lee N, Hui D, Wu A, Chan P, Cameron P, Joynt GM, et al. A Major Outbreak of Severe Acute Respiratory Syndrome in Hong Kong. *N Engl J Med* (2003) 348:1986–94. doi: 10.1056/NEJMoa030685
4. Zaki AM, van Boheemen S, Bestebroer TM, Osterhaus AD, Fouchier RA. Isolation of a Novel Coronavirus From a Man With Pneumonia in Saudi Arabia. *N Engl J Med* (2012) 367:1814–20. doi: 10.1056/NEJMoa1211721
5. Tsang KW, Ho PL, Ooi GC, Yee WK, Wang T, Chan-Yeung M, et al. A Cluster of Cases of Severe Acute Respiratory Syndrome in Hong Kong. *N Engl J Med* (2003) 348:1977–85. doi: 10.1056/NEJMoa030666
6. Zhou P, Yang XL, Wang XG, Hu B, Zhang L, Zhang W, et al. A Pneumonia Outbreak Associated With a New Coronavirus of Probable Bat Origin. *Nature* (2020) 579:270–3. doi: 10.1038/s41586-020-2012-7
7. Korber B, Fischer WM, Gnanakaran S, Yoon H, Theiler J, Abfalterer W, et al. Tracking Changes in SARS-CoV-2 Spike: Evidence That D614G Increases

Infectivity of the COVID-19 Virus. *CELL* (2020) 182:812–27. doi: 10.1016/j.cell.2020.06.043
8. Groves DC, Rowland-Jones SL, Angyal A. The D614G Mutations in the SARS-CoV-2 Spike Protein: Implications for Viral Infectivity, Disease Severity and Vaccine Design. *Biochem Biophys Res Commun* (2021) 538:104–7. doi: 10.1016/j.bbrc.2020.10.109
9. Leung K, Shum MH, Leung GM, Lam TT, Wu JT. Early Transmissibility Assessment of the N501Y Mutant Strains of SARS-CoV-2 in the United Kingdom, October to November 2020. *Euro Surveill* (2021) 26:2002106. doi: 10.2807/1560-7917.ES.2020.26.1.2002106
10. Makoni M. South Africa Responds to New SARS-CoV-2 Variant. *Lancet* (2021) 397:267. doi: 10.1016/S0140-6736(21)00144-6
11. Faria NR, Mellan TA, Whittaker C, Claro IM, Candido D, Mishra S, et al. Genomics and Epidemiology of the P.1 SARS-CoV-2 Lineage in Manaus, Brazil. *SCIENCE* (2021) 372:815–21. doi: 10.1126/science.abh2644
12. Singh J, Rahman SA, Ehtesham NZ, Hira S, Hasnain SE. SARS-CoV-2 Variants of Concern Are Emerging in India. *Nat Med* (2021) 27:1131–3. doi: 10.1038/s41591-021-01397-4
13. Callaway E. Delta Coronavirus Variant: Scientists Brace for Impact. *Nature* (2021) 595:17–8. doi: 10.1038/d41586-021-01696-3
14. Despres HW, Mills MG, Shirley DJ, Schmidt MM, Huang ML, Jerome KR, et al. Quantitative Measurement of Infectious Virus in SARS-CoV-2 Alpha, Delta and Epsilon Variants Reveals Higher Infectivity (Viral Titer:RNA Ratio) in Clinical Samples Containing Thedelta and Epsilon Variants. (2021). doi: 10.1101/2021.09.07.21263229. medRxiv preprint 2021 Sep 20.
15. Challen R, Dyson L, Overton CE. Early Epidemiological Signatures of Novel SARS-CoV-2 Variants: Establishment of B.1.617.2 in England. *medRxiv* (2021). doi: 10.1101/2021.06.05.21258365
16. Funk T, Pharris A, Spiteri G, Bundle N, Melidou A, Carr M, et al. Characteristics of SARS-CoV-2 Variants of Concern B.1.1.7, B.1.351 or P.1: Data From Seven EU/EEA Countries, Weeks 38/2020 to 10/2021. *Euro Surveill* (2021) 26:2100348. doi: 10.2807/1560-7917.ES.2021.26.16.2100348
17. Sheikh A, McMenamin J, Taylor B, Jamal S, Khubaib M, Kohli S, et al. SARS-CoV-2 Delta VOC in Scotland: Demographics, Risk of Hospital Admission, and Vaccine Effectiveness. *Lancet* (2021) 397:2461–2. doi: 10.1016/S0140-6736(21)01358-1
18. Fisman DN, Bogoch I, Lapointe-Shaw L, McCready J, Tuite AR. Risk Factors Ssociated With Mortality Among Residents With Coronavirus Disease 2019 (COVID-19) in Long-Term Care Facilities in Ontario, Canada. *JAMA* (2020) 3:e2015957. doi: 10.1001/jamanetworkopen.2020.15957
19. Lu R, Zhao X, Li J, Niu P, Yang B, Wu H, et al. Genomic Characterisation and Epidemiology of 2019 Novel Coronavirus: Implications for Virus Origins and Receptor Binding. *Lancet* (2020) 395:565–74. doi: 10.1016/S0140-6736(20)30251-8
20. Pachetti M, Marini B, Benedetti F, Giudici F, Mauro E, Storici P, et al. Emerging SARS-CoV-2 Mutation Hot Spots Include a Novel RNA-Dependent-RNA Polymerase Variant. *J Transl Med* (2020) 18:179. doi: 10.1186/s12967-020-02344-6
21. Hoffmann M, Kleine-Weber H, Schroeder S, Kruger N, Herrler T, Erichsen S, et al. SARS-CoV-2 Cell Entry Depends on ACE2 and TMPRSS2 and Is Blocked by a Clinically Proven Protease Inhibitor. *Cell* (2020) 181:271–80. doi: 10.1016/j.cell.2020.02.052
22. Lan J, Ge J, Yu J, Shan S, Zhou H, Fan S, et al. Structure of the SARS-CoV-2 Spike Receptor-Binding Domain Bound to the ACE2 Receptor. *Nature* (2020) 581:215–20. doi: 10.1038/s41586-020-2180-5
23. Fehr AR, Perlman S. Coronaviruses: An Overview of Theirreplication and Pathogenesis. *Methods Mol Biol* (2015) 1282:1–23. doi: 10.1007/978-1-4939-2438-7_1
24. Volz E, Hill V, McCrone JT, Price A, Jorgensen D, O'Toole A, et al. Evaluating the Effects of SARS-CoV-2 Spike Mutation D614G on Transmissibility and Pathogenicity. *Cell* (2021) 184:64–75. doi: 10.1016/j.cell.2020.11.020
25. Harvey WT, Carabelli AM, Jackson B, Gupta RK, Thomson EC, Harrison EM, et al. SARS-CoV-2 Variants, Spike Mutations and Immune Escape. *Nat Rev Microbiol* (2021) 19:409–24. doi: 10.1038/s41579-021-00573-0
26. Deng X, Garcia-Knight MA, Khalid M, Servellita V, Wang C, Morris MK, et al. Transmission, Infectivity, and Antibody Neutralization of an Emerging SARS-CoV- 2 Variant in California Carrying a L452R Spike Protein Mutation. *medRxiv preprint* (2021). doi: 10.1101/2021.03.07.21252647
27. Tchesnokova V, Kulakesara H, Larson L, Bowers V, Rechkina E, Kisiela D, et al. Acquisition of the L452R Mutation in the ACE2-Binding Interface of Spike Protein Triggers Recent Massive Expansion of SARS-CoV-2 Variants. *bioRxiv* (2021) 11:2021.02.22.432189. doi: 10.1101/2021.02.22.432189
28. Zhang W, Davis BD, Chen SS, Sincuir Martinez JM, Plummer JT, Vail E. Emergence of a Novel SARS-Cov-2 Variant in Southern California. *JAMA* (2021) 325:1324–6. doi: 10.1001/jama.2021.1612
29. Yadav PD, Mohandas S, Shete AM, Nyayanit DA, Gupta N. *SARS CoV-2 Variant B.1.617.1 Is Highly Pathogenic in Hamstersthan B.1 Variant*. bioRxiv preprint. doi: 10.1101/2021.05.05.442760.
30. Chen J, Wang R, Wang M, Wei GW. Mutations Strengthened SARS-Cov-2 Infectivity. *J Mol Biol* (2020) 432:5212–26. doi: 10.1016/j.jmb.2020.07.009
31. Wilhelm A, Toptan T, Pallas C, Wolf T, Goetsch U, Gottschalk R, et al. Antibody-Mediated Neutralization of Authentic SARS-Cov-2 B.1.617 Variants Harboring L452R and T478K/E484Q. *Viruses* (2021) 13:1693. doi: 10.3390/v13091693
32. Li Q, Wu J, Nie J, Zhang L, Hao H, Liu S, et al. The Impact of Mutations in SARS-CoV-2 Spike on Viral Infectivity and Antigenicity. *Cell* (2020) 182:1284–94. doi: 10.1016/j.cell.2020.07.012
33. Liu Z, VanBlargan LA, Bloyet LM, Rothlauf PW, Chen RE, Stumpf S, et al. Landscape Analysis of Escape Variants Identifies SARS-CoV-2 Spike Mutations That Attenuate Monoclonal and Serum Antibody Neutralization. *bioRxiv* (2020). doi: 10.1101/2020.11.06.372037
34. Di Giacomo S, Mercatelli D, Rakhimov A, Giorgi FM. Preliminary Report on Severe Acute Respiratory Syndrome Coronavirus 2 (SARS-CoV-2) Spike Mutation T478K. *J Med Virol* (2021) 93:5638–43. doi: 10.1002/jmv.27062
35. Shang J, Wan Y, Luo C, Ye G, Geng Q, Auerbach A, et al. Cell Entry Mechanisms of SARS-CoV-2. *Proc Natl Acad Sci USA* (2020) 117:11727–34. doi: 10.1073/pnas.2003138117
36. Peacock TP, Goldhill DH, Zhou J, Baillon L, Frise R, Swann OC, et al. The Furin Cleavage Site in the SARS-CoV-2 Spike Protein Is Required for Transmission in Ferrets. *Nat Microbiol* (2021) 6:899–909. doi: 10.1038/s41564-021-00908-w
37. Johnson BA, Xie X, Bailey AL, Kalveram B, Lokugamage KG, Muruato A, et al. Loss of Furin Cleavage Site Attenuates SARS-CoV-2 Pathogenesis. *Nature* (2021) 591:293–9. doi: 10.1038/s41586-021-03237-4
38. PHE. *Public Health England. "3 June 2021 Risk Assessment for SARS-CoV- 2 Variant: Delta (VOC-21APR-02, B.1.617.2)"* (2021). Available at: https://assets.publishing.service.gov.uk/government/uploads/system/uploads/attachment_data/file/991135/3_June_2021_Risk_assessment_for_SARS-CoV-2_variant_DELTA.pdf.
39. Saito A, Nasser H, Uriu K, Kosugi Y, Irie T, Shirakawa K, et al. SARS-CoV-2 Spike P681R Mutation Enhances and Accelerates Viral Fusion. *bioRxiv preprint* (2021). doi: 10.1101/2021.06.17.448820
40. Pascarella S, Ciccozzi M, Zella D, Bianchi M, Benetti F, Benvenuto D, et al. SARS-CoV-2 B.1.617 Indian Variants: Are Electrostatic Potential Changes Responsible for a Higher Transmission Rate? *J Med Virol* (2021) 93:6551–6. doi: 10.1002/jmv.27210
41. D'Arienzo M, Coniglio A. Assessment of the SARS-Cov-2 Basic Reproduction Number, R0, Based on the Early Phase of COVID-19 Outbreak in Italy. *Biosaf Health* (2020) 2:57–9. doi: 10.1016/j.bsheal.2020.03.004
42. Sanche S, Lin YT, Xu C, Romero-Severson E, Hengartner K, Ke R, et al. High Contagiousness and Rapid Spread of Severe Acute Respiratory Syndrome Coronavirus 2. *Emerg Infect Dis* (2020) 26:1470–7. doi: 10.3201/eid2607.200282
43. Zhou T, Liu Q, Yang Z, Liao J, Yang K, Bai W, et al. Preliminary Prediction of the Basic Reproduction Number of the Wuhan Novel Coronavirus 2019-nCoV. *J Evid Based Med* (2020) 13:3–7. doi: 10.1111/jebm.12376
44. Li B, Deng A, Li K, Hu Y, Li Z, Xiong Q, et al. Viral Infection and Transmission in a Large, Well-Traced Outbreak Caused by the SARS-CoV-2 Delta Variant. *medRxiv Preprint* (2021). doi: 10.1101/2021.07.07.21260122
45. Shi Q, Gao X, Hu B. Research Progress on Characteristics, Epidemiology and Control Measure of SARS-CoV-2 Delta VOC. *Chin J Nosocomiol* (2021) 3:1–5. doi: 10.11816/cn.ni.2021-211664
46. Zhang M, Xiao J, Deng A, Zhang Y, Zhuang Y, Hu T, et al. Transmission Dynamics of an Outbreak of the COVID-19 Deltavariant B.1.617.2 — Guangdong Province, China, May–June 2021. *China CDC Weekly* (2021) 3:584. doi: 10.46234/ccdcw2021.148

47. Li Z, Nie K, Li K, Hu Y, Song Y, Kang M, et al. Genome Characterization of the First Outbreak of COVID-19 Delta Variant B.1.617.2 -Guangzhou City, Guangdong Province, China, May 2021. *China CDC Weekly* (2021) 3:587. doi: 10.46234/ccdcw2021.151
48. *14 Seconds to Get Infected With Delta? Contact Screen Exposure! Five or Six Generations Can Be Passed in 10 Days!*. Available at: https://m.thepaper.cn/baijiahao_13267433.
49. Alex M, Luca S, Giorgio B, Lidia M. Increased Close Proximity Airborne Transmission of the SARS-CoV-2 Delta Variant. *Sci Total Environ* (2021) 6:151499. doi: 10.1016/j.scitotenv.2021.151499
50. Ram VS, Babu GR, Prabhakaran D. COVID-19 Pandemic in India. *Eur Heart J* (2020) 41:3874–6. doi: 10.1093/eurheartj/ehaa493
51. Callaway E. Delta Coronavirus Variant: Scientists Brace for Impact. *Nature* (2021) 595:17–8. doi: 10.1038/d41586-021-01696-3
52. Public Health England. *Covid-19 Variants: Genomically Confirmed Case Numbers* (2021). Available at: https://www.gov.uk/government/publications/covid-19-variants-genomically-confirmed-case-numbers/variants-distribution-of-cases-data.
53. Public Health England. *Covid-19 Variants: Genomically Confirmed Case Numbers* (2021). Available at: https://www.gov.uk/government/publications/covid-19-variants-genomically-confirmed-case-numbers.
54. Public Health England. *Covid-19 Variants: Genomically Confirmed Case Numbers* (2021). Available at: https://www.gov.uk/government/publications/covid-19-variants-genomically-confirmed-case-numbers.
55. Public Health England. *Covid-19 Variants: Genomically Confirmed Case Numbers* (2021). Available at: https://www.gov.uk/government/publications/covid-19-variants-genomically-confirmed-case-numbers.
56. Ministry of Health. *Israel COVID-19 Data Tracker*. Jerusalem: Ministry of Health. Available at: https://www.gov. il/en/departments/guides/information-corona (Accessed 16 Aug 2021).
57. Pnina S, Neta SZ, Orna M, Bat-Sheva G, Michal C. Nosocomial Outbreak Caused by the SARS-CoV-2 Delta Variant in a Highly Vaccinated Population, Israel, July 2021. *Euro Surveill* (2021) 26:pii=2100822. doi: 10.2807/1560-7917.ES.2021.26.39.2100822
58. Liu Y, Gao W, Guo W, Guo Y, Shi M, Dong G, et al. Prominent Coagulation Disorder Is Closely Related to Inflammatory Response and Could be as a Prognostic Indicator for ICU Patients With COVID-19. *J Thromb Thrombolysis* (2020) 50:825–32. doi: 10.1007/s11239-020-02174-9
59. Tian D, Ye Q. Hepatic Complications of COVID-19 and Its Treatment. *J Med Virol* (2020) 92:1818–24. doi: 10.1002/jmv.26036
60. Han X, Ye Q. Kidney Involvement in COVID-19 and Its Treatments. *J Med Virol* (2021) 93:1387–95. doi: 10.1002/jmv.26653
61. Ye Q, Lu D, Shang S, Wang J, Fu J, Mao J, et al. Crosstalk Between Coronavirus Disease 2019 and Cardiovascular Disease and Its Treatment. *ESC Heart Fail* (2020) 7:3464–72. doi: 10.1002/ehf2.12960
62. Ye Q, Wang B. The Mechanism and Treatment of Gastrointestinal Symptoms in Patients With COVID-19. *Am J Physiol Gastrointestinal Liver Physiol* (2020) 319:245–52. doi: 10.1152/ajpgi.00148.2020
63. David NF, Tuite AR. Progressive Increase in Virulence of Novel SARS-CoV-2 Variants in Ontario, Canada. *bioRxiv* (2021). doi: 10.1101/2021.07.05.21260050
64. Sheikh A, Mcmenamin J, Taylor B, Jamal S, Khubaib M, Kohli S, et al. SARS-CoV-2 Delta VOC in Scotland: Demographics, Risk of Hospital Admission, and Vaccine Effectiveness. *Lancet* (2021) 397:2461–2. doi: 10.1016/S0140-6736(21)01358-1
65. Edara VV, Lai L, Sahoo MK, Floyd K, Sibai M, Solis D, et al. Infection and Vaccine-Induced Neutralizing Antibody Responses to the SARS-CoV-2 B.1.617.1 Variant. *bioRxiv* (2021). doi: 10.1101/2021.05.09.443299
66. Liu C, Ginn HM, Dejnirattisai W, Supasa P, Wang B, Tuekprakhon A, et al. Reduced Neutralization of SARS-CoV-2 B.1.617 by Vaccine and Convalescent Serum. *Cell* (2021) 184:4220–36. doi: 10.1016/j.cell.2021.06.020
67. Lustig Y, Zuckerman N, Nemet I, Atari N, Kliker L, Regev-Yochay G, et al. Neutralising Capacity Against Delta (B.1.617.2) and Other Variants of Concern Following Comirnaty (BNT162b2, Biontech/Pfizer) Vaccination in Health Care Workers, Israel. *Euro Surveill* (2021) 26:2100557. doi: 10.2807/1560-7917.ES.2021.26.26.2100557
68. Dagan N, Barda N, Kepten E, Miron O, Perchik S, Katz MA, et al. BNT162b2 mRNA Covid-19 Vaccine in a Nationwide Mass Vaccination Setting. *N Engl J Med* (2021) 384(15):1412–23. doi: 10.1056/NEJMoa2101765
69. Wall EC, Wu M, Harvey R, Kelly G, Warchal S, Sawyer C, et al. Neutralising Antibody Activity Against SARS-CoV-2 Vocs B.1.617.2 and B.1.351 by BNT162b2 Vaccination. *Lancet* (2021) 397:2331–3. doi: 10.1016/S0140-6736(21)01290-3
70. Adam D. What Scientists Know About New, Fast-Spreading Coronavirus Variants. *Nature* (2021) 594:19–20. doi: 10.1038/d41586-021-01390-4
71. World Health Organization. *Evidence Assessment: Sinovac/Coronavac COVID-19 Vaccine*. Available at: https://www.the paper.cn/news Detail_forward_13323339.
72. Zhou X, Ye Q. Cellular Immune Response to COVID-19 and Potential Immune Modulators. *Front Immunol* (2021) 12:646333. doi: 10.3389/fimmu.2021.646333
73. Erasmus JH, Khandhar AP, O'Connor MA, Walls AC, Hemann EA, Murapa P, et al. An Alphavirus-Derived Replicon RNA Vaccine Induces SARS-CoV-2 Neutralizing Antibody and T Cell Responses in Mice and Nonhuman Primates. *Sci Transl Med* (2020) 12:eabc9396. doi: 10.1126/scitranslmed.abc9396
74. Alwis R, Gan ES, Chen S, Leong YS, Tan HC, Zhang SL, et al. A Single Dose of Self-Transcribing and Replicating RNA-Based SARS-CoV-2 Vaccine Produces Protective Adaptive Immunity in Mice. *Mol Ther* (2021) 29:1970–83. doi: 10.1016/j.ymthe.2021.04.001
75. Reynolds CJ, Pade C, Gibbons JM, Butler DK, Otter AD, Menacho K, et al. Prior SARS-CoV-2 Infection Rescues B and T Cell Responses to Variants After First Vaccine Dose. *Science* (2021) 30:eabh1282. doi: 10.1126/science.abh1282
76. Schramm R, Jäckle AC, Rivinius R, Fischer B, Müller B, Boeken U, et al. Poor Humoral and T–Cell Response to Two–Dose SARS–CoV–2 Messenger RNA Vaccine BNT162b2 in Cardiothoracic Transplant Recipients. *Clin Res Cardiol* (2021) 110:1142–9. doi: 10.1007/s00392-021-01880-5

Conflict of Interest: The authors declare that the research was conducted in the absence of any commercial or financial relationships that could be construed as a potential conflict of interest.

frontiers in Immunology

ORIGINAL RESEARCH
published: 09 December 2021
doi: 10.3389/fimmu.2021.790469

Endogenous Antibody Responses to SARS-CoV-2 in Patients With Mild or Moderate COVID-19 Who Received Bamlanivimab Alone or Bamlanivimab and Etesevimab Together

*Lin Zhang[1†], Josh Poorbaugh[1†], Michael Dougan[2], Peter Chen[3], Robert L. Gottlieb[4,5], Gregory Huhn[6], Stephanie Beasley[1], Montanea Daniels[1], Thi Ngoc Vy Trinh[1], Melissa Crisp[1], Joshua Joaquin Freitas[1], Peter Vaillancourt[1], Dipak R. Patel[1], Ajay Nirula[1], Nicole L. Kallewaard[1], Richard E. Higgs[1] and Robert J. Benschop[1]**

[1] Lilly Research Laboratories, Eli Lilly and Company, Indianapolis, IN, United States, [2] Massachusetts General Hospital and Harvard Medical School, Boston, MA, United States, [3] Department of Medicine, Women's Guild Lung Institute, Cedars-Sinai Medical Center, Los Angeles, CA, United States, [4] Department of Internal Medicine, Center for Advanced Heart and Lung Disease, Baylor University Medical Center, Dallas, TX, United States, [5] Baylor Scott & White Research Institute, Dallas, TX, United States, [6] The Ruth M. Rothstein CORE Center, Cook County Health, Chicago, IL, United States

Background: Neutralizing monoclonal antibodies (mAbs) to SARS-CoV-2 are clinically efficacious when administered early, decreasing hospitalization and mortality in patients with mild or moderate COVID-19. We investigated the effects of receiving mAbs (bamlanivimab alone and bamlanivimab and etesevimab together) after SARS-CoV-2 infection on the endogenous immune response.

Methods: Longitudinal serum samples were collected from patients with mild or moderate COVID-19 in the BLAZE-1 trial who received placebo (n=153), bamlanivimab alone [700 mg (n=100), 2800 mg (n=106), or 7000 mg (n=98)], or bamlanivimab (2800 mg) and etesevimab (2800 mg) together (n=111). A multiplex Luminex serology assay measured antibody titers against SARS-CoV-2 antigens, including SARS-CoV-2 protein variants that evade bamlanivimab or etesevimab binding, and SARS-CoV-2 pseudovirus neutralization assays were performed.

Results: The antibody response in patients who received placebo or mAbs had a broad specificity. Titer change from baseline against a receptor-binding domain mutant (Spike-RBD E484Q), as well as N-terminal domain (Spike-NTD) and nucleocapsid protein (NCP) epitopes were 1.4 to 4.1 fold lower at day 15-85 in mAb recipients compared with placebo. Neutralizing activity of day 29 sera from bamlanivimab monotherapy cohorts against both spike E484Q and beta variant (B.1.351) were slightly reduced compared with placebo (by a factor of 3.1, p=0.001, and 2.9, p=0.002, respectively). Early viral load correlated with the subsequent antibody titers of the native, unmodified humoral response (p<0.0001 at Day 15, 29, 60 and 85 for full-length spike).

OPEN ACCESS

Edited by:
Ingo Drexler, Heinrich Heine University, Germany

Reviewed by:
Shan Su, New York Blood Center, United States
Catarina E. Hioe, Icahn School of Medicine at Mount Sinai, United States

***Correspondence:**
Robert J. Benschop
rbenschop@lilly.com

†These authors have contributed equally to this work and share first authorship

Specialty section:
This article was submitted to Vaccines and Molecular Therapeutics, a section of the journal Frontiers in Immunology

Received: *06 October 2021*
Accepted: *18 November 2021*
Published: *09 December 2021*

Citation:
Zhang L, Poorbaugh J, Dougan M, Chen P, Gottlieb RL, Huhn G, Beasley S, Daniels M, Ngoc Vy Trinh T, Crisp M, Freitas JJ, Vaillancourt P, Patel DR, Nirula A, Kallewaard NL, Higgs RE and Benschop RJ (2021) Endogenous Antibody Responses to SARS-CoV-2 in Patients With Mild or Moderate COVID-19 Who Received Bamlanivimab Alone or Bamlanivimab and Etesevimab Together. Front. Immunol. 12:790469. doi: 10.3389/fimmu.2021.790469

Conclusions: Patients with mild or moderate COVID-19 treated with mAbs develop a wide breadth of antigenic responses to SARS-CoV-2. Small reductions in titers and neutralizing activity, potentially due to a decrease in viral load following mAb treatment, suggest minimal impact of mAb treatment on the endogenous immune response.

Keywords: serology, antibodies, immune response, COVID-19, bamlanivimab, etesevimab

INTRODUCTION

Coronavirus disease 2019 (COVID-19) is caused by the novel human pathogen severe acute respiratory syndrome coronavirus 2 (SARS-CoV-2) and has resulted in widespread global morbidity and mortality (1).

The host immune response continues to be the best defense against SARS-CoV-2 (2). While both innate and adaptive immune processes are important, the humoral response against the virus remains critical (3, 4). Healthy individuals exposed to SARS-CoV-2 mount a robust immune response involving the production of anti-SARS-CoV-2 antibodies against a wide variety of SARS-CoV-2 epitopes across the nucleocapsid protein (NCP) and the spike protein (5). Virus-neutralizing antibodies are primarily directed to the receptor-binding domain (RBD) of the spike protein, however some neutralizing epitopes reside within the N-terminal domain (NTD) (6, 7). While individuals who recover from COVID-19 develop robust immunoglobulin G antibody responses against SARS-CoV-2 that can persist for at least 3-5 months after infection (8, 9), waning titers and plasma neutralizing abilities over time have been reported (10–12).

Several neutralizing monoclonal antibodies (mAbs) have been developed to treat COVID-19. Two such antibodies, bamlanivimab and etesevimab, bind to the RBD region of the spike protein and have been shown to reduce nasopharyngeal viral load in patients with mild or moderate COVID-19 and prevent progression of COVID-19 leading to hospitalization or death (13, 14). The efficacy of these mAbs can be reduced by mutations within the RBD spike protein, such as at residue E484, which negatively impacts bamlanivimab binding (13, 15).

Studies are necessary to assess the potential effect treatment with neutralizing mAbs has on the specificity, magnitude, and duration of the endogenous antibody response to SARS-CoV-2 infection. Using serum samples collected from patients with mild or moderate COVID-19 enrolled in the BLAZE–1 trial who received placebo, bamlanivimab alone, or bamlanivimab and etesevimab together, we performed longitudinal analyses of antibody responses to SARS-CoV-2 infection. We examined the binding and neutralization activity of sera to SARS-CoV-2 viral proteins and assessed the relationship between early viral load and antibody titers.

MATERIALS AND METHODS

Convalescent Serum Samples

Samples were obtained from individuals infected with SARS-CoV-2 who received placebo, bamlanivimab (700, 2800, or 7000 mg), or bamlanivimab (2800 mg) and etesevimab (2800 mg) together in the phase 2 portion of the BLAZE-1 trial (NCT04427501) as described previously (13). All donors provided written informed consent. Treatment was administered within three days of the first positive SARS-CoV-2 test sample collection. Serum samples were collected longitudinally at time of enrollment [baseline (prior to infusion)] and on day 3, day 15, day 29, day 60, and day 85 after infusion. Prior to use in each assay, serum samples were centrifuged for 5 minutes at 10000 x *g* to pellet any debris.

Luminex Multiplexing

Luminex xMAP technology is an established, multiplex, flow cytometry-based platform that allows the simultaneous quantitation of many protein analytes in a single reaction (16). Antigen-coated microspheres were used to detect and quantitate endogenous antibodies against multiple viral proteins simultaneously (**Table 2**). The method was performed essentially as previously described (17). Briefly, patient serum samples were titrated (1:800 – 1:8E9) in phosphate buffered saline-high salt solution (PBS-HS; 0.01 M PBS, 1% [bovine serum albumin] BSA, 0.02% Tween, 300 mM NaCl) and combined with Luminex MAGPlex microspheres coupled with either SARS-CoV-2 or RBD mutant proteins. Diluted serum samples and microsphere solution were incubated for 90 minutes at room temperature, followed by a 60-minute incubation with the detector phycoerythrin-conjugated anti-IgG Fc-specific antibody (#109-115-098, Jackson Labs). Washed beads were then resuspended in a PBS-1% BSA solution and read using a Luminex FlexMAP 3D System with xPONENT Software.

Pseudovirus Production and Characterization

E484K and E484Q mutagenesis reactions were performed using the QuickChange Lightning Site-Directed Mutagenesis Kit (Agilent #210519) using a template of a spike mammalian expression vector based on the Wuhan sequence (Genbank MN908947.3) with a deletion of the C-terminal 19 amino acids. For the beta variant (B.1.351) pseudovirus a consensus sequence representative of lineage was synthesized and incorporated by Gibson cloning. Pseudoviruses bearing mutant spike proteins were produced using the delta-G-luciferase recombinant Vesicular Stomatitis Virus (rVSV) system (KeraFast EH1025-PM, Whitt 2010). Briefly, 293T cells were transfected with individual mutant spike expression plasmids, and 16-20 hours later, transfected cells were infected with VSV-G-pseudotyped delta-G luciferase rVSV, and 16-20 hours thereafter conditioned culture medium was harvested, clarified by centrifugation at 1320 g for 10 minutes at 4°C, aliquoted and

stored frozen at -80°C. Relative luciferase reporter signal read-out was determined by luciferase assay (Promega E2650) of extracts from VeroE6 cells infected with serially-diluted virus. Luciferase activity was measured on a PerkinElmer EnVision 2104 Multilabel Reader.

Pseudovirus Neutralization Assays

Neutralization assays were carried out essentially as described previously (18). Serum antibodies were diluted 4-fold in negative serum and 10-point 3-fold titrations in 25% negative serum were performed in 384 well polystyrene plates in duplicate using a Beckman (Biomek i5) liquid handler. Positive and negative control antibodies and an unrelated control (hIgG1 isotype) were tested in a 10-point, 3-fold serial dilution starting at 8 μg/mL, 2 μg/mL and 8 μg/mL, respectively, in 25% negative serum. An empirically pre-determined fixed amount of pseudovirus (Wuhan, E484Q, E484K, or the B.1.351 spike) was dispensed by WDII liquid dispenser on titrated serum antibodies and controls and pre-incubated for 20 minutes at 37°C. Following pre-incubation, the virus-antibody complexes were transferred by Biomek i5 to 8,000/well VeroE6 cells in white, opaque, tissue culture treated 384W plates, and incubated for 16-20 hours at 37°C. Control wells included virus only (no antibody; 14 replicates) and cells only (14 replicates). Following infection, cells were lysed with Promega BrightGlo and luciferase activity was measured on the Biotek Synergy Neo2 Multimode Reader.

Viral Load Determination

Viral load was measured by nasopharyngeal swab followed by quantitative RT-PCR reaction (13, 19). Viral load data is based on the cycle threshold and calculated as an arbitrary unit. The primer sequences for the RT-PCR assay have been reported previously (20).

Statistical Analysis

Titer is commonly defined as the smallest dilution above the cut point or the dilution factor at the cut point based on an interpolation of assay values that straddle the cut point (21). In the serology assay, we used the latter method to calculate the titers (cut point for full-length spike, spike-RBD, spike-NTD, and NCP was set as 3, and cut point for spike-RBD E484Q was set as 1000). If the maximum signal of a titration curve is less than the cut point, then the titer is imputed as 800 (smallest dilution). The samples were run in three batches in the Luminex serology assay, and batch effect was included as a fixed effect in the statistical model for downstream analysis.

The treatment effects on titers were compared based on change from baseline in $\log_{10}$ titer at different time points. Mixed-model repeated-measure analysis with unstructured covariance matrix (2-sided test with α level of 0.05) was used to conduct the significance testing. Treatment group, visit day, treatment × visit interaction, and batch effect were included as fixed effects in the model. Adjustments for multiple testing were not conducted; therefore, the findings should be interpreted as exploratory. The statistical analyses were performed with R software (version 4.0.3) (22). Spearman correlations between viral load (at baseline and visit day 3) and $\log_{10}$ titer fold change from baseline (at visit day 3, 15, 29, 60, and 85) were computed. Since most samples from the same patient were processed in the same batch, batch has minimum impact on this correlation.

To calculate IC50 titer of data from the pseudovirus neutralization assay, a 4-parameter logistic function was used to estimate the absolute IC50 based on 1/dilution factor (bottom is fixed at 0). If a sample has less than 50% neutralization over observed concentration range or a poor fit (the standard error of the IC50 is not estimable, majority of which has less than 50% neutralization over observed concentration range, or the estimated IC50 is larger than the maximum 1/dilution factor), its IC50 titer was imputed to 0.125 (twice the maximum 1/dilution factor). For the pseudovirus neutralization assay analysis, treatment effects (compared to placebo) were compared based on $\log_{10}$ 1/IC50 titer using a non-parametric Steel's Test using JMP® (v14.1).

RESULTS

Patient Characteristics

Serum samples were obtained from patients with mild or moderate COVID-19 enrolled in the BLAZE–1 trial who received placebo, bamlanivimab (700 mg, 2800 mg, or 7000 mg), or bamlanivimab (2800 mg) and etesevimab (2800 mg) together. Baseline demographics and clinical characteristics of patients enrolled in the BLAZE-1 study have previously been reported (13). Among the placebo cohort, no patient reported an immunocompromised condition and 3 patients (1.96%) reported receiving immunosuppressive treatment at baseline, while among recipients of bamlanivimab alone or bamlanivimab and etesevimab together 6 patients (1.45%) reported immunocompromised condition and 10 patients (2.41%) reported receiving immunosuppressive treatment at baseline. A total of 568 patients provided serum samples, 560 samples were collected at baseline, and postbaseline samples were collected at days 3, 15, 29, 60, and 85 (**Table 1**). Patients had mild to moderate COVID-19, defined per US Food and Drug Administration guidance (23), with symptoms including but not limited to fever, cough, sore throat, malaise, headache, muscle pain, gastrointestinal symptoms, or shortness of breath with exertion. A total of 440 patients (77.5%) had mild COVID-19 at baseline, while 128 (22.5%) had moderate COVID-19 at baseline. Means of viral load at baseline were 6.3 (standard deviation [SD] 2.2) and 6.9 (SD 2.0) for patients with mild and moderate COVID-19, respectively. Participants were recruited into the study during the summer of 2020, prior to the widespread emergence of many of the SARS-CoV-2 variants of interest/concern such as the Alpha, Beta, Gamma, and Delta variants. Genotypic analysis of the SARS-CoV-2 virus present in baseline samples confirm absence of these SARS-CoV-2 variants in this cohort, with the majority of infecting viruses containing the D614G substitution in spike found in the B.1 pangolin lineages.

Antibody Responses to SARS-CoV-2

A multiplex assay using the Luminex platform was performed to determine the magnitude and specificity of antibody responses to SARS-CoV-2. Antibody titers against four different SARS-CoV-2

TABLE 1 | Number of patients in the BLAZE-1 study that provided serum samples at each timepoint.

Treatment	Baseline	Day 3	Day 15	Day 29	Day 60	Day 85
Placebo	152	140	124	126	125	120
Bamlanivimab 700 mg	99	93	90	86	82	84
Bamlanivimab 2800 mg	104	100	90	91	91	92
Bamlanivimab 7000 mg	97	91	89	86	77	80
Bamlanivimab (2800 mg) and etesevimab (2800 mg) together	108	98	95	96	91	80

Patients received placebo, bamlanivimab alone (700, 2800, or 7000 mg), or bamlanivimab (2800 mg) and etesevimab (2800 mg) together.

spike versions (the full-length spike protein bearing the D614G substitution, the Spike-RBD, the RBD carrying the E484Q alteration, or the NTD) and the nucleocapsid protein (NCP) (**Table 2**) were calculated using serum samples obtained from each cohort. Since bamlanivimab does not bind significantly to Spike RBD with alterations at residue E484 (15, 24), and as the epitopes for bamlanivimab and etesevimab lie within the spike RBD (25, 26), titers against Spike RBD E484Q, NTD, or NCP proteins solely reflect the endogenous antibody response. Titers against the full-length spike protein and the Spike-RBD, were greater among cohorts that received bamlanivimab monotherapy (all doses), as anticipated (27), and bamlanivimab and etesevimab together compared with the placebo cohort, reflecting detection of bamlanivimab and/or etesevimab (**Figure 1**). Tracking the endogenous antibody responses against SARS-CoV-2 proteins, titers were generally lowest at baseline, with levels increasing over time and peaking around day 29 followed by slight declines in titers through day 85. The same patterns for Spike RBD E484Q, the NTD, and NCP titers were observed in the mAb-receiving cohorts. In the placebo cohort, least square means of titers against the SARS-CoV-2 viral proteins at day 85 were reduced 1.4 to 1.7 fold from day 29. Similar reductions were observed for the cohorts treated with mAbs: among the bamlanivimab monotherapy cohorts, least square means of titers against Spike-NTD and NCP at day 85 was reduced 1.3 to 1.5 fold and 1.6 to 1.7 fold, respectively, from day 29. Treatment with bamlanivimab and etesevimab together resulted in 1.3 and 1.6 fold reductions in least square means of titers against Spike-NTD and NCP at day 85 from day 29.

Effect of mAb Treatment on Endogenous Antibody Titers

Next, we calculated the titer change from baseline at day 3, 15, 29, 60, and 85 against the Spike-NTD and NCP (i.e., proteins that bind neither bamlanivimab nor etesevimab), as well as Spike-RBD E484Q (a mutation that negatively impacts bamlanivimab binding) (**Figure 2**). Compared to placebo, treatment with bamlanivimab monotherapy resulted in an attenuated increase in antibody titer changes from baseline from day 15 through day 85 against Spike-E484Q (ranging from 2.0 to 2.9 fold across bamlanivimab doses and time points), Spike-NTD (ranging from 2.5 to 4.1 fold), and NCP (ranging from 1.4 to 2.2 fold) (**Figure 2**). Similarly, among recipients of bamlanivimab and etesevimab administered together, an attenuated increase in antibody titer changes from baseline from day 15 through day 85 against both Spike-NTD (ranging from 2.9 to 3.7 fold) and NCP (ranging from 2.5 to 3.4 fold) were observed compared with placebo.

mAb Treatment Effect on Neutralization of SARS-CoV-2 Pseudoviruses

To probe the functionality of the polyclonal antibody response, we tested a randomly selected subset (stratified by treatment group) of the day 29 serum samples for neutralization activity. SARS-CoV-2 viral neutralization was measured using a vesicular stomatitis virus (VSV)-based pseudovirus (18, 28). We assessed IC50 titers of serum samples against three different pseudoviruses, containing the E484Q or E484K substitutions in spike, as well as

TABLE 2 | Details on SARS-CoV-2 proteins.

		Serology Assays	
Protein	**SARS-CoV-2 Sequence Length (AA)**	**Backbone**	**Expression**
Full-length Spike (with D614G)	1195 (14-1208)	Wuhan WT spike	CHO
Spike-RBD	199 (329-527)	Wuhan RBD	CHO
Spike-RBD E484Q	223 (319-541)	Wuhan RBD	CHO
Spike-NTD	294 (14-307)	Wuhan NTD	CHO
NCP	419 (1-419)	Wuhan NCP	CHO
		Pseudovirus Assays	
E484Q	1256 (1-1256)	Wuhan spike	NA
E484K	1256 (1-1256)	Wuhan spike	NA
B.1.351	1253 (1-241; 245-1256)	Wuhan spike with (L18F,D80A,D215G,del242-244, K417N,E484K, N501Y,D614G, A701V)	NA

CHO, Chinese hamster ovary cells; NA, not applicable; NCP, nucleocapsid protein; NTD, N-terminal domain; RBD, receptor-binding domain; WT, wild-type.

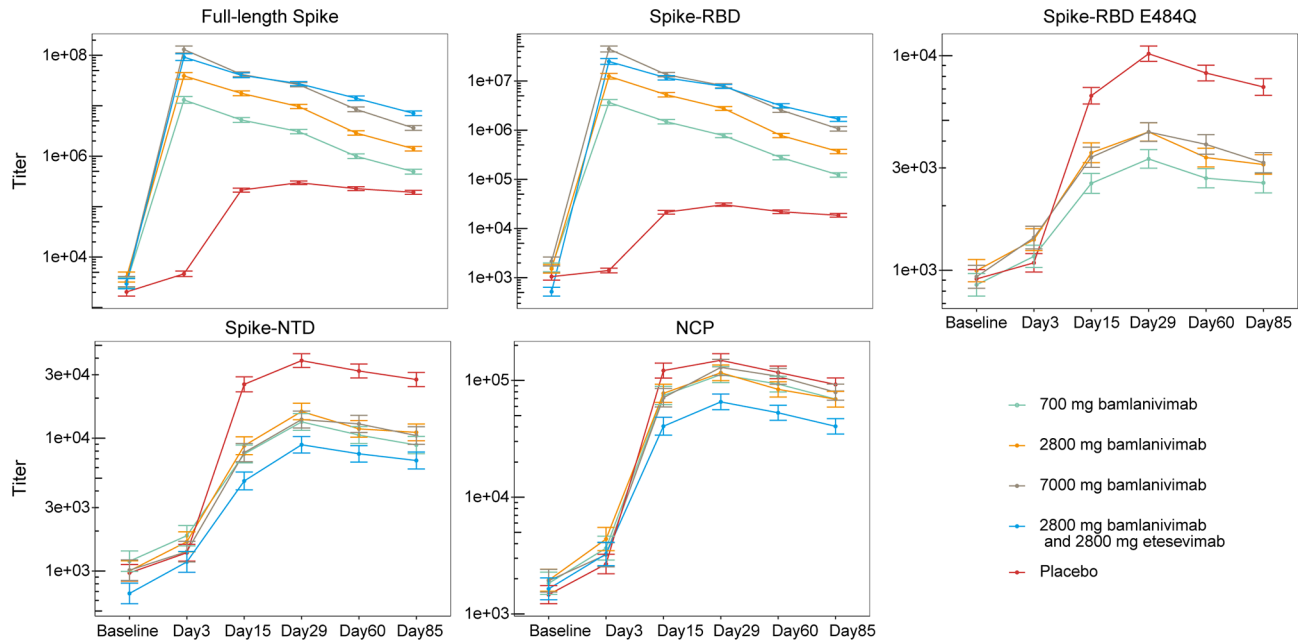

FIGURE 1 | Antibody responses to SARS-CoV-2 viral proteins among patients treated with bamlanivimab monotherapy, bamlanivimab and etesevimab together, and placebo. Least squares means (± SE) were plotted across visit days for different treatment groups. The full-length spike protein carries the D614G substitution. Titers against Spike-RBD E484Q not shown for cohort receiving bamlanivimab and etesevimab together as etesevimab binds to this mutant protein. The number of samples at each timepoint are outlined in **Table 1**. RBD, Receptor binding domain; NCP, Nucleocapsid protein; NTD, N-terminal domain; SE, Standard error.

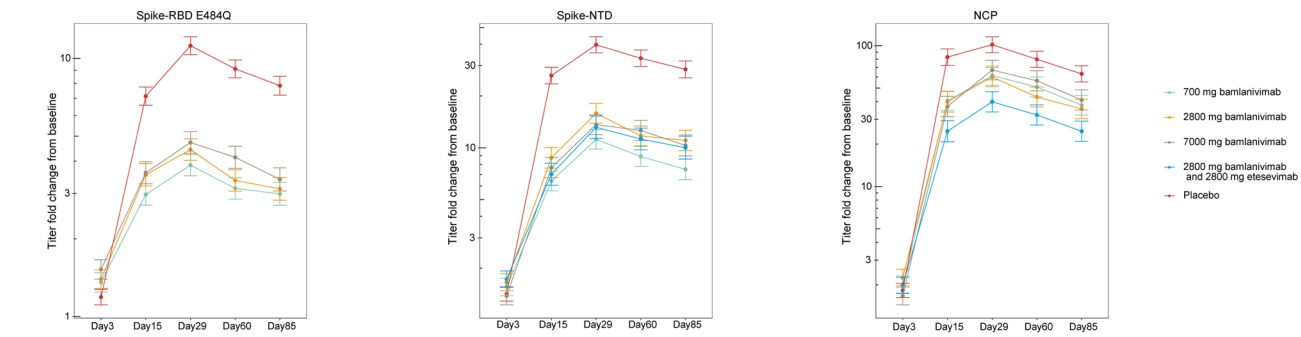

Fold change in mAb treatment vs placebo, p-value

	day 15	day 29	day 60	day 85
bamlanivimab				
700 mg	-2.4 p<0.0001	-2.9 p<0.0001	-2.9 p<0.0001	-2.6 p<0.0001
2800 mg	-2.0 p<0.0001	-2.5 p<0.0001	-2.7 p<0.0001	-2.5 p<0.0001
7000 mg	-2.0 p<0.0001	-2.4 p<0.0001	-2.2 p<0.0001	-2.3 p<0.0001

Fold change in mAb treatment vs placebo, p-value

	day 15	day 29	day 60	day 85
bamlanivimab				
700 mg	-4.1 p<0.0001	-3.5 p<0.0001	-3.7 p<0.0001	-3.8 p<0.0001
2800 mg	-3.0 p<0.0001	-2.5 p<0.0001	-2.8 p<0.0001	-2.6 p<0.0001
7000 mg	-3.4 p<0.0001	-2.9 p<0.0001	-2.6 p<0.0001	-2.8 p<0.0001
bamlanivimab 2800 mg and etesevimab 2800 mg	-3.7 p<0.0001	-3.0 p<0.0001	-2.9 p<0.0001	-2.9 p<0.0001

Fold change in mAb treatment vs placebo, p-value

	day 15	day 29	day 60	day 85
bamlanivimab				
700 mg	-2.0 p=0.0006	-1.7 p=0.013	-1.6 p=0.029	-1.7 p=0.013
2800 mg	-2.1 p=0.0007	-1.7 p=0.009	-1.9 p=0.003	-1.8 p=0.005
7000 mg	-2.2 p=0.0001	-1.5 p=0.044	-1.4 p=0.095	-1.5 p=0.041
bamlanivimab 2800 mg and etesevimab 2800 mg	-3.4 P<0.0001	-2.5 p<0.0001	-2.5 p<0.0001	-2.6 p<0.0001

FIGURE 2 | Treatment effect of bamlanivimab monotherapy or bamlanivimab and etesevimab together at days 3, 15, 29, 60 and 85. Least squares means (± SE) of fold changes from baseline were plotted across visit days for different treatment groups: green= 700 mg bamlanivimab, orange= 2800 mg bamlanivimab, gray = 7000 mg bamlanivimab, blue= 2800 mg bamlanivimab and 2000 mg etesevimab, and red = placebo. Titers against Spike-RBD E484Q not shown for cohort receiving bamlanivimab and etesevimab together as etesevimab binds to this mutant protein. The number of samples at each timepoint are outlined in **Table 1**. RBD, Receptor binding domain; NCP, Nucleocapsid protein; NTD, N-terminal domain; SE, Standard error.

the beta-variant (B.1.351) which contains E484K and K417N substitutions that have been shown to significantly reduce the binding of both bamlanivimab and etesevimab (29). Bamlanivimab treatment (all dose levels pooled) resulted in significantly smaller neutralization of spike E484Q pseudovirus compared with placebo (p=0.001) with the median of the bamlanivimab group 3.1-fold lower compared to the median of the placebo group. Similar neutralization activity was observed against the Spike E484K pseudovirus (data not shown). As anticipated, treatment with bamlanivimab and etesevimab together resulted in significantly increased neutralization of spike E484Q pseudovirus compared with placebo (p<0.0001) with the median of the bamlanivimab and etesevimab together group 15.2-fold higher compared to the median of the placebo group, due to the presence of etesevimab in the serum (**Figure 3**). Treatment with bamlanivimab alone or bamlanivimab and etesevimab together reduced sera neutralization against the beta variant B.1.351 compared with placebo (**Figure 3**). Reciprocal IC50 values were slightly lower in both bamlanivimab monotherapy (p=0.002) and bamlanivimab and etesevimab together (p=0.019) treatment arms compared with placebo with medians 2.9 and 2.3-fold lower than placebo median, respectively.

Early Viral Load Predicts Antibody Titer

Next, we explored whether the amount of SARS-CoV-2 nasopharyngeal viral load impacts the magnitude of the endogenous, pharmacologically unmodified antibody response. Viral load was measured by nasopharyngeal swab followed by quantitative reverse transcriptase–polymerase chain reaction (13). Using serum samples provided by patients in the placebo cohort, we investigated the relationship between early viral load at baseline and the $\log_{10}$ change from baseline in antibody titer against the full-length spike and NCP at days 3, 15, 29, 60, and 85 (**Figure 4**). Patients with higher viral loads at baseline showed greater fold increases in antibody titers against the full-length spike and the NCP proteins on day 15 (r=0.47, r=0.43, respectively; p<0.0001) and day 29 (r=0.49, r=0.39, respectively; p<0.0001) when antibody responses peaked (but not on day 3 when most titers were below the detection limit), indicating that baseline viral load determines the magnitude of the humoral response. These relationships between early viral load and antibody titers against the full-length spike and the NCP proteins persisted to day 60 (r=0.49, r=0.37, respectively; p<0.0001) and day 85 (r=0.43, r=0.3 respectively; p<0.001). Similar relationships were observed between antibody titers and viral loads at day 3 (data not shown).

DISCUSSION

This study provides a comprehensive assessment of the effects of mAb treatment on endogenous antibody responses to SARS-CoV-2 infection.

We found that patients produce a wide breath of serological responses against SARS-CoV-2 epitopes regardless of mAb treatment, with responses durable through to 85 days. To explore the effects on endogenous responses among mAb recipients, we utilized the finding that SARS-CoV-2 variants carrying mutations in the RBD of the spike protein have the potential to evade mAb treatment (15, 23, 29, 30). As the E484 residue is a key contact within the epitope of bamlanivimab (25), E484K and E484Q substitutions greatly attenuate binding of bamlanivimab; however, binding of etesevimab persists, due to its distinct binding epitope (13). Therefore, we examined changes in antibody titers against the Spike-RBD E484Q protein, in addition to titers against proteins that lie outside of the epitopes of both bamlanivimab and etesevimab (Spike-NTD and NCP). We found that mAb treatment resulted in smaller increases in anti-SARS-CoV-2 endogenous antibody titers (1.4 to 4.1 fold) as compared to placebo, with some being statistically significant. Despite these small reductions,

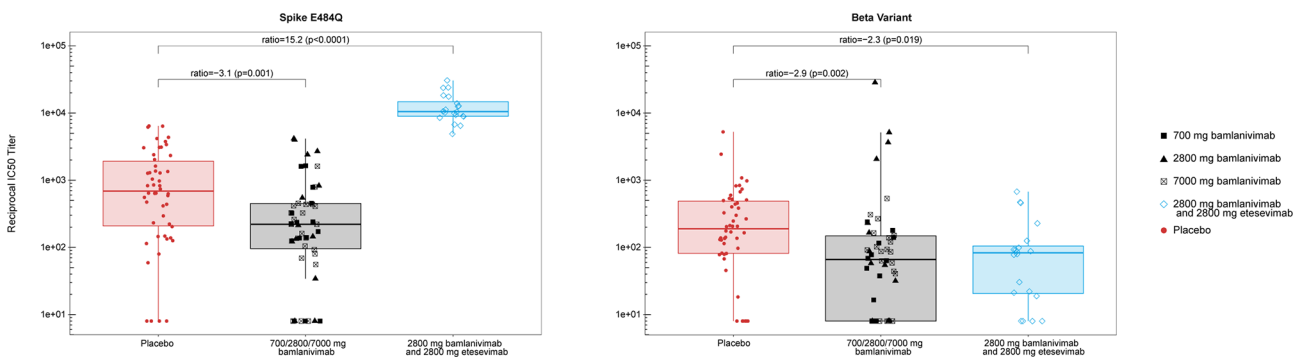

FIGURE 3 | Neutralization activity of serum samples against spike E484Q and beta variant (B.1.351) at day 29. Each data point represents the reciprocal IC50 titer from serum samples collected from an individual patient. Median of the reciprocals of IC50 titers against the spike E484Q were 225, 213, and 220, for sera collected from the bamlanivimab 700, 2800, and 7000 mg cohorts, respectively. Median of the reciprocals of the IC50 titers against beta (B.1.351) were 49, 87, and 86, for sera collected from the bamlanivimab 700, 2800, and 7000 mg cohorts, respectively. Boxes and horizontal bars denote the interquartile range (IQR) and the median reciprocal IC50 titer, respectively. The whiskers are equal to the maximum and minimum values below or above the median at 1.5 times the IQR. Ratio = median in bamlanivimab or bamlanivimab and etesevimab vs median in placebo. p = p-value from non-parametric Steel's test.

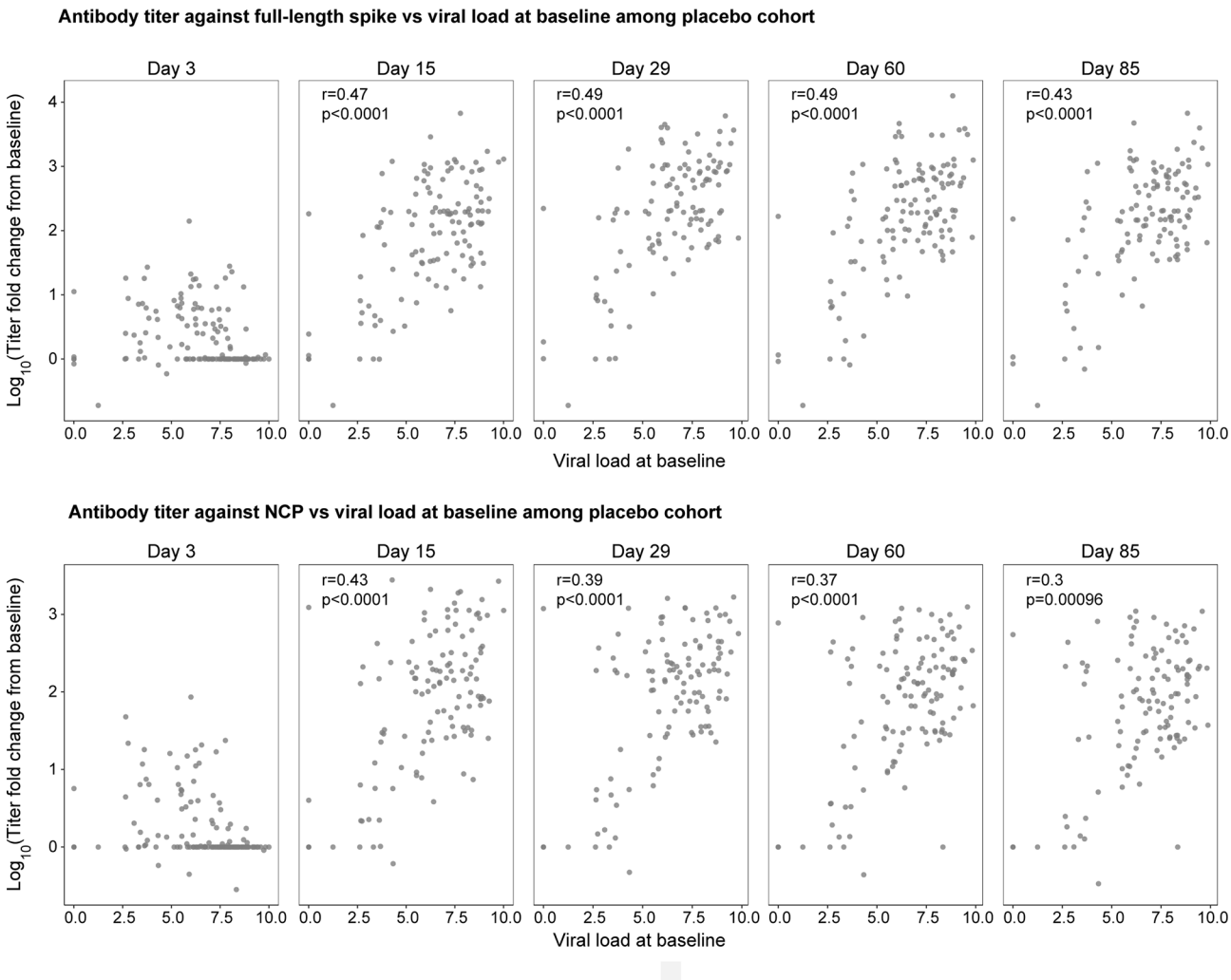

FIGURE 4 | The natural history relationship between viral load at baseline (x-axis) and the fold change in antibody titer against the full-length spike (top panel) and NCP (bottom panel) from baseline to day 3, 15, 29, 60, and 85 in the placebo cohort. 42% and 54% of patients were sero-negative at both baseline and day 3 for full-length spike and NCP, respectively. r is the spearman correlation between viral load and log of titer fold change from baseline; p is the p-value associated with spearman correlation test.

antibody titers among mAb recipients showed comparable patterns to the placebo group from baseline to day 85. Clinical relevance of these slightly lower titers is not known. Further, it remains to be seen whether mAb-treated patients and placebo-treated patients possess equal levels of protection upon SARS-CoV-2 re-exposure. The effect of mAb treatment on memory responses (including T and B cells) also remains unknown. Importantly, the level of exogenously administered antibody is much higher than the titer of endogenous anti-spike antibodies, so patients who receive mAb treatment have an overall greater ability to neutralize virus.

To assess the effects of mAb treatment on the spectrum of epitopes neutralized, we measured IC50 titers against Spike E484Q, Spike E484K, and the beta variant (B.1.351). The latter is a variant of concern and has two key mutations in the RBD of spike, E484K and the K417N, and can escape both bamlanivimab and etesevimab recognition and neutralization *in vitro* (15, 31). We found that serum samples collected from patients who received bamlanivimab treatment were slightly less effective in neutralizing spike E484Q and beta variant compared with placebo (by a factor of 3.1 and 2.9, respectively). As noted before, it is unknown whether these small reductions are clinically meaningful.

Finally, we investigated the relationship between the early viral load and endogenous antibody titers over time within the placebo cohort. The results show that individuals with lower viral loads at baseline generate lower antibody titers at later time points (i.e. from day 15 and beyond), suggesting that early viral load determines the magnitude of the subsequent antibody response. This finding, taken together with findings

from previous reports showing that mAb treatment administered early during infection reduces SARS-CoV-2 viral load (13, 19), suggest that the reductions in endogenous antibody titers among mAb recipients may be due to reduced early viral load as a result of the efficacy of mAb treatment. In addition, bamlanivimab is an IgG1 and may also inhibit endogenous B cell activation through engagement of FcγRIIb, though we do not know the level of contribution of this relative to the effect of decreased viral antigen exposure. As mean viral load at baseline was similar across treatment groups (13), the observed effects on endogenous antibody responses can be attributed to mAb-dependent reductions in viral load following treatment. Importantly, this reduction in endogenous antibody responses does not slow viral clearance during acute SARS-CoV-2 infection; indeed, viral decay is significantly accelerated among patients administered bamlanivimab alone or bamlanivimab and etesevimab together (13, 19). This finding may have implications for optimal timing of SARS-CoV-2 vaccination following recovery from COVID-19 as a result of neutralizing mAb therapy.

Taken together, the similarity in breadth and duration of response between the placebo and mAb treatment cohorts suggest that a similar immune response was induced upon SARS-CoV-2 infection, but that the magnitude of endogenous antibody production was attenuated presumably due to the reduction in antigen exposure (as suggested by reduced viral load) achieved by mAb treatment.

This study has several limitations. First, it is not yet known whether the risk to reinfection with SARS-CoV-2 is similar for mAb-treated patients and placebo-treated patients. Second, since mAb treatment resulted in a small effect on endogenous antibody production, we hypothesize that treatment may also impact vaccine-induced antibody responses. However, this remains to be evaluated in future dedicated studies. Third, we could not evaluate changes to antibody titers for additional SARS-CoV-2 variants, nor wild-type spike/RBD proteins in this study due to drug interference. Other groups have found that the polyclonal immune response for some individuals has at least a proportion that is directed at the E484 position (32). By using the drug tolerant E484Q/K spike-RBDs in this investigation, we may be underestimating the overall endogenous spike immune response. Fourth, we assessed the impact of just two mAbs (bamlanivimab alone or bamlanivimab and etesevimab together) on the endogenous immune response, and therefore we do not know the effect of other mAbs on the immune response. However, we hypothesize similar results, as those mAbs also reduce viral load upon administration (33).

In conclusion, this research identified that mAb therapy for COVID-19 infection does not abolish the endogenous immune response against SARS-CoV-2, but instead results in only minor attenuations of titer and neutralization capacity. We hypothesize that these minor changes pose very low risk for patients in terms of reinfection and long-term immune protection.

DATA AVAILABILITY STATEMENT

The original contributions presented in the study are included in the article/supplementary material. Further inquiries can be directed to the corresponding author.

ETHICS STATEMENT

This study (BLAZE-1 ClinicalTrials.gov number, NCT04427501) was conducted in accordance with the Declaration of Helsinki and Council for International Organizations of Medical Sciences International Ethical Guidelines, and applicable International Council for Harmonization Good Clinical Practice Guidelines, laws, and regulations. The protocol was reviewed and approved by the ethics committees of all participating centers, and patients provided written informed consent before study entry.

AUTHOR CONTRIBUTIONS

LZ, JP, RLG, and RB conceptualized the study. LZ, JP, MDo, SB, TN, MC, JF, PV, DP, AN, NK, and RB contributed to the study design. JP, MDo, PC, GH, RLG, SB, MDa, TNVT, MC, and DP contributed to data acquisition. LZ, JP, GH, MD, RLG, SB, MDa, DP, AN, NK, RH, and RB contributed to data interpretation. LZ, JP, RLG, MDa, SB, TN, MC, and RH analyzed the data. LZ, JP, MDo, PV, NK, and RB contributed to the writing of this paper. All authors revised the manuscript. All authors read and approved the final version for submission.

FUNDING

This work was supported by Eli Lilly and Company.

ACKNOWLEDGMENTS

We wish to thank Paul Anderson and Liliana Weber for providing expert automation support and feedback for the neutralization assay, and Ina Hughes and Saleema Hassanali for assistance with pseudovirus neutralization assay development. We thank Jeffrey Boyles for the generation of the SARS-CoV-2 protein reagents used to generate the Luminex serology assay. We thank Angela O'Sullivan, PhD, medical writer and employee of Eli Lilly and Company, for writing and editorial support. Bamlanivimab emerged from the collaboration between Eli Lilly and Company and AbCellera Biologics to create antibody therapies for the prevention and treatment of COVID-19. Eli Lilly and Company developed the antibody after it was discovered by AbCellera Biologics and scientists at the National Institute of Allergy and Infectious Diseases Vaccine Research Center. Etesevimab emerged from the collaboration between Eli Lilly and Company, and Junshi Biosciences.

REFERENCES

1. *WHO Coronavirus (COVID-19) Dashboard*. Available at: https://covid19.who.int/ (Accessed 28 October, 2021).
2. Chowdhury MA, Hossain N, Kashem MA, Shahid MA, Alam A. Immune Response in COVID-19: A Review. *J Infect Public Health* (2020) 13(11):1619–29. doi: 10.1016/j.jiph.2020.07.001
3. Scourfield DO, Reed SG, Quastel M, Alderson J, Bart VM, Teijeira Crespo A, et al. The Role and Uses of Antibodies in COVID-19 Infections: A Living Review. *Oxford Open Immunol* (2021) 2(1):iqab003. doi: 10.1093/oxfimm/iqab003
4. Corbett KS, Flynn B, Foulds KE, Francica JR, Boyoglu-Barnum S, Werner AP, et al. Evaluation of the mRNA-1273 Vaccine Against SARS-CoV-2 in Nonhuman Primates. *N Engl J Med* (2020) 383(16):1544–55. doi: 10.1056/NEJMoa2024671
5. Sette A, Crotty S. Adaptive Immunity to SARS-CoV-2 and COVID-19. *Cell* (2021) 184(4):861–80. doi: 10.1016/j.cell.2021.01.007
6. Suthar MS, Zimmerman MG, Kauffman RC, Mantus G, Linderman SL, Hudson WH, et al. Rapid Generation of Neutralizing Antibody Responses in COVID-19 Patients. *Cell Rep Med* (2020) 1(3):100040. doi: 10.1016/j.xcrm.2020.100040
7. Cerutti G, Guo Y, Zhou T, Gorman J, Lee M, Rapp M, et al. Potent SARS-CoV-2 Neutralizing Antibodies Directed Against Spike N-Terminal Domain Target a Single Supersite. *Cell Host Microbe* (2021) 29(5):819–33.e7. doi: 10.1016/j.chom.2021.03.005
8. Rodda LB, Netland J, Shehata L, Pruner KB, Morawski PA, Thouvenel CD, et al. Functional SARS-CoV-2-Specific Immune Memory Persists After Mild COVID-19. *Cell* (2021) 184(1):169–83. e17. doi: 10.1016/j.cell.2020.11.029
9. Wajnberg A, Amanat F, Firpo A, Altman DR, Bailey MJ, Mansour M, et al. Robust Neutralizing Antibodies to SARS-CoV-2 Infection Persist for Months. *Science* (2020) 370(6521):1227–30. doi: 10.1126/science.abd7728
10. Gaebler C, Wang Z, Lorenzi JC, Muecksch F, Finkin S, Tokuyama M, et al. Evolution of Antibody Immunity to SARS-CoV-2. *Nature* (2021) 591(7851):639–44. doi: 10.1038/s41586-021-03207-w
11. Seow J, Graham C, Merrick B, Acors S, Pickering S, Steel KJ, et al. Longitudinal Observation and Decline of Neutralizing Antibody Responses in the Three Months Following SARS-CoV-2 Infection in Humans. *Nat Microbiol* (2020) 5(12):1598–607. doi: 10.1038/s41564-020-00813-8
12. Muecksch F, Wise H, Batchelor B, Squires M, Semple E, Richardson C, et al. Longitudinal Serological Analysis and Neutralizing Antibody Levels in Coronavirus Disease 2019 Convalescent Patients. *J Infect Dis* (2021) 223(3):389–98. doi: 10.1093/infdis/jiaa659
13. Gottlieb RL, Nirula A, Chen P, Boscia J, Heller B, Morris J, et al. Effect of Bamlanivimab as Monotherapy or in Combination With Etesevimab on Viral Load in Patients With Mild to Moderate COVID-19: A Randomized Clinical Trial. *Jama* (2021) 325(7):632–44. doi: 10.1001/jama.2021.0202
14. Dougan M, Nirula A, Azizad M, Mocherla B, Gottlieb RL, Chen P, et al. Bamlanivimab Plus Etesevimab in Mild or Moderate Covid-19. *N Engl J Med* (2021) 385(15):1382–92. doi: 10.1056/NEJMoa2102685
15. Starr TN, Greaney AJ, Dingens AS, Bloom JD. Complete Map of SARS-CoV-2 RBD Mutations That Escape the Monoclonal Antibody LY-CoV555 and its Cocktail With LY-Cov016. *Cell Rep Med* (2021) 2(4):100255. doi: 10.1016/j.xcrm.2021.100255
16. Elshal MF, McCoy JP. Multiplex Bead Array Assays: Performance Evaluation and Comparison of Sensitivity to ELISA. *Methods* (2006) 38(4):317–23. doi: 10.1016/j.ymeth.2005.11.010
17. Chen P, Datta G, Li YG, Chien J, Price K, Chigutsa E, et al. First in Human Study of Bamlanivimab in a Randomized Trial of Hospitalized Patients With COVID-19. *Clin Pharmacol Ther* (2021) 110:1467–77. doi: 10.1002/cpt.2405
18. Nie J, Li Q, Wu J, Zhao C, Hao H, Liu H, et al. Establishment and Validation of a Pseudovirus Neutralization Assay for SARS-CoV-2. *Emerg Microbes Infect* (2020) 9(1):680–6. doi: 10.1080/22221751.2020.1743767
19. Chen P, Nirula A, Heller B, Gottlieb RL, Boscia J, Morris J, et al. SARS-CoV-2 Neutralizing Antibody LY-CoV555 in Outpatients With Covid-19. *N Engl J Med* (2020) 384(3):229–37. doi: 10.1056/NEJMoa2029849
20. *Emergency Use Authorization (EUA) Summary Lilly SARS-CoV-2 Assay*. Available at: https://www.fda.gov/media/140543/download (Accessed 28 October, 2021).
21. Shankar G, Arkin S, Cocea L, Devanarayan V, Kirshner S, Kromminga A, et al. Assessment and Reporting of the Clinical Immunogenicity of Therapeutic Proteins and Peptides—Harmonized Terminology and Tactical Recommendations. *AAPS J* (2014) 16(4):658–73. doi: 10.1208/s12248-014-9599-2
22. Team RC. *R: A Language and Environment for Statistical Computing*. Vienna, Austria: R foundation for Statistical Computing (2013).
23. US Food and Drug Administration. *COVID-19: Developing Drugs and Biological Products for Treatment or Prevention Guidance for Industry*. Vienna, Austria: R Foundation for Statistical Computing. Available at: https://www.fda.gov/media/137926/download (Accessed 28 October, 2021).
24. Hoffmann M, Arora P, Groß R, Seidel A, Hörnich BF, Hahn AS, et al. SARS-CoV-2 Variants B. 1.351 and P. 1 Escape From Neutralizing Antibodies. *Cell* (2021) 184(9):2384–93.e12. doi: 10.1016/j.cell.2021.03.036
25. Jones BE, Brown-Augsburger PL, Corbett KS, Westendorf K, Davies J, Cujec TP, et al. The Neutralizing Antibody, LY-CoV555, Protects Against SARS-CoV-2 Infection in Nonhuman Primates. *Sci Trans Med* (2021) 13(593):eabf1906. doi: 10.1126/scitranslmed.abf1906
26. Shi R, Shan C, Duan X, Chen Z, Liu P, Song J, et al. A Human Neutralizing Antibody Targets the Receptor-Binding Site of SARS-CoV-2. *Nature* (2020) 584(7819):120–4. doi: 10.1038/s41586-020-2381-y
27. Chigutsa E, O'Brien L, Ferguson-Sells L, Long A, Chien J. Population Pharmacokinetics and Pharmacodynamics of the Neutralizing Antibodies Bamlanivimab and Etesevimab in Patients With Mild to Moderate COVID-19 Infection. *Clin Pharmacol Ther* (2021) 110(5):1302–10. doi: 10.1002/cpt.2420
28. Dogan M, Kozhaya L, Placek L, Gunter C, Yigit M, Hardy R, et al. SARS-CoV-2 Specific Antibody and Neutralization Assays Reveal the Wide Range of the Humoral Immune Response to Virus. *Commun Biol* (2021) 4(1):1–13. doi: 10.1038/s42003-021-01649-6
29. US Food and Drug Administration. *Fact Sheet for Health Care Providers Emergency Use Authorization (EUA) of Bamlanivimab and Etesevimab* . Available at: https://www.fda.gov/media/145802/download (Accessed 28 October, 2021).
30. Wang P, Nair MS, Liu L, Iketani S, Luo Y, Guo Y, et al. Antibody Resistance of SARS-CoV-2 Variants B.1.351 and B.1.1.7. *Nature* (2021) 593(7857):130–5. doi: 10.1038/s41586-021-03398-2
31. Stamatatos L, Czartoski J, Wan Y-H, Homad LJ, Rubin V, Glantz H, et al. mRNA Vaccination Boosts Cross-Variant Neutralizing Antibodies Elicited by SARS-CoV-2 Infection. *Science* (2021) 372(6549):1413–8. doi: 10.1126/science.abg9175
32. Greaney AJ, Starr TN, Barnes CO, Weisblum Y, Schmidt F, Caskey M, et al. Mapping Mutations to the SARS-CoV-2 RBD That Escape Binding by Different Classes of Antibodies. *Nat Commun* (2021) 12(1):4196. doi: 10.1038/s41467-021-24435-8
33. Weinreich DM, Sivapalasingam S, Norton T, Ali S, Gao H, Bhore R, et al. REGN-COV2, a Neutralizing Antibody Cocktail, in Outpatients With Covid-19. *N Engl J Med* (2021) 384(3):238–51. doi: 10.1056/NEJMoa2035002

Conflict of Interest: Authors LZ, JP, SB, MDa, TNVT, MC, JF, PV, DP, AN, NK, RH, and RB are all employees and shareholders of Eli Lilly and Company. MDo reports receiving grants from Eli Lilly and Company, and Novartis; and receiving consulting fees from Moderna, Tillotts, SQZ, AzurRx, Partner Therapeutics, and ORIC Pharmaceuticals; and has Neoleukin Therapeutics stock. PC reports receiving consulting fees from Eli Lilly and Company and Gilead; and receiving payment or honoraria from Rockpointe, Frontier Collaborative, CME Outfitter, and Physician Education Resource. RG reports receiving consulting fees from Eli Lilly and Company, GSK Pharmaceuticals, and Gilead Sciences; and receiving payment or honoraria from Gilead Sciences. GH reports receiving grants from Eli Lilly and company, Gilead, Viiv, Janssen, and Proteus; receiving consulting fees from Gilead, Viiv, and Janssen; and receiving payment or honoraria from Rockpointe, CME Outfitter, Simply Speaking, and Clinical Care Options.

The authors declare that this study received funding from Eli Lilly and Company. The funder had the following involvement with the study: study design, data analysis, decision to publish, and preparation of the manuscript.

the publisher, the editors and the reviewers. Any product that may be evaluated in this article, or claim that may be made by its manufacturer, is not guaranteed or endorsed by the publisher.

frontiers in Immunology

ORIGINAL RESEARCH
published: 13 December 2021
doi: 10.3389/fimmu.2021.766821

A Potent and Protective Human Neutralizing Antibody Against SARS-CoV-2 Variants

Sisi Shan[1†], Chee Keng Mok[2,3†], Shuyuan Zhang[4†], Jun Lan[4†], Jizhou Li[5†], Ziqing Yang[1], Ruoke Wang[1], Lin Cheng[6], Mengqi Fang[1], Zhen Qin Aw[2,3,7], Jinfang Yu[4], Qi Zhang[1], Xuanling Shi[1], Tong Zhang[8], Zheng Zhang[6], Jianbin Wang[5], Xinquan Wang[4*], Justin Jang Hann Chu[2,3,7*] and Linqi Zhang[1,9,10*]*

[1] NexVac Research Center, Comprehensive AIDS Research Center, Center for Infectious Disease Research, Beijing Advanced Innovation Center for Structural Biology, School of Medicine, Tsinghua University, Beijing, China, [2] Biosafety Level 3 Core Facility, Yong Loo Lin School of Medicine, National University of Singapore, Singapore, Singapore, [3] Laboratory of Molecular RNA Virology and Antiviral Strategies, Department of Microbiology and Immunology, Yong Loo Lin School of Medicine, National University of Singapore, Singapore, Singapore, [4] The Ministry of Education Key Laboratory of Protein Science, Beijing Advanced Innovation Center for Structural Biology, Beijing Frontier Research Center for Biological Structure, Collaborative Innovation Center for Biotherapy, School of Life Sciences, Tsinghua University, Beijing, China, [5] School of Life Sciences, Tsinghua-Peking Center for Life Sciences, Tsinghua University, Beijing, China, [6] Institute for Hepatology, National Clinical Research Center for Infectious Disease, Shenzhen Third People's Hospital, The Second Affiliated Hospital, School of Medicine, Southern University of Science and Technology, Shenzhen, China, [7] Infectious Disease Translation Research Programme, Yong Loo Lin School of Medicine, National University of Singapore, Singapore, Singapore, [8] Beijing Youan Hospital, Capital Medical University, Beijing, China, [9] Institute of Biopharmaceutical and Health Engineering, Tsinghua Shenzhen International Graduate School, Tsinghua University, Shenzhen, China, [10] Institute of Biomedical Health Technology and Engineering, Shenzhen Bay Laboratory, Shenzhen, China

As severe acute respiratory syndrome coronavirus 2 (SARS-CoV-2) variants continue to emerge and spread around the world, antibodies and vaccines to confer broad and potent neutralizing activity are urgently needed. Through the isolation and characterization of monoclonal antibodies (mAbs) from individuals infected with SARS-CoV-2, we identified one antibody, P36-5D2, capable of neutralizing the major SARS-CoV-2 variants of concern. Crystal and electron cryo-microscopy (cryo-EM) structure analyses revealed that P36-5D2 targeted to a conserved epitope on the receptor-binding domain of the spike protein, withstanding the three key mutations—K417N, E484K, and N501Y—found in the variants that are responsible for escape from many potent neutralizing mAbs, including some already approved for emergency use authorization (EUA). A single intraperitoneal (IP) injection of P36-5D2 as a prophylactic treatment completely protected animals from challenge of infectious SARS-CoV-2 Alpha and Beta. Treated animals manifested normal body weight and were devoid of infection-associated death up to 14 days. A substantial decrease of the infectious virus in the lungs and brain, as well as reduced lung pathology, was found in these animals compared to the controls. Thus, P36-5D2 represents a new and desirable human antibody against the current and emerging SARS-CoV-2 variants.

Keywords: SARS-CoV-2, variants of concern, human neutralizing antibody, *in vivo* protection, epitope

OPEN ACCESS

Edited by:
Peter Chen,
Cedars-Sinai Medical Center,
United States

Reviewed by:
Kwok Yung Yuen,
The University of Hong Kong,
Hong Kong SAR, China
Chang-Han Lee,
Seoul National University, South Korea

***Correspondence:**
Jianbin Wang
jianbinwang@tsinghua.edu.cn
Xinquan Wang
xinquanwang@mail.tsinghua.edu.cn
Justin Jang Hann Chu
miccjh@nus.edu.sg
Linqi Zhang
zhanglinqi@tsinghua.edu.cn

†These authors have contributed equally to this work

Specialty section:
This article was submitted to Vaccines and Molecular Therapeutics, a section of the journal Frontiers in Immunology

Received: *30 August 2021*
Accepted: *15 November 2021*
Published: *13 December 2021*

Citation:
Shan S, Mok CK, Zhang S, Lan J, Li J, Yang Z, Wang R, Cheng L, Fang M, Aw ZQ, Yu J, Zhang Q, Shi X, Zhang T, Zhang Z, Wang J, Wang X, Chu JJH and Zhang L (2021) A Potent and Protective Human Neutralizing Antibody Against SARS-CoV-2 Variants. Front. Immunol. 12:766821. doi: 10.3389/fimmu.2021.766821

INTRODUCTION

As the severe acute respiratory syndrome coronavirus 2 (SARS-CoV-2) continues to rage around the world, multiple variants have emerged and spread rapidly. Currently, four major variants of concern (VOCs) have been designated: Alpha (B.1.1.7), initially identified in the UK; Beta (B.1.351) in South Africa; Gamma (P.1) in Brazil; and Delta (B.1.617.2) in India (1–7). These VOCs are not only rapidly displacing local SARS-CoV-2 variants but are also carrying mutations in the N-terminal domain (NTD) and receptor-binding domain (RBD) on the spike protein that are critical for interactions with the ACE2 receptor and neutralizing antibodies (8–21). Conserved among variants Alpha, Beta, and Gamma, the N501Y mutation was previously shown to enhance the binding affinity to ACE2 (22, 23). The Beta and Gamma variants each has three mutation sites in common within the RBD region—K417N/T, E484K, and N501Y—which change their antigenic profiles. The Delta variant contains the unique L452R and T478K mutations while sharing a common mutation with the Alpha and Gamma variants at P681 near the furin cleavage site. Various deletion mutants in the NTD have also been identified, such as 69-70del and Y144del in Alpha and 242-244del in Beta. Mutations in other spike regions were also identified, and some are located in or proximal to major S protein antigenic sites and, therefore, may adversely affect the antibody neutralization induced by natural infection or through vaccination (12–14, 24). Serum from individuals vaccinated with the Moderna or Pfizer mRNA vaccine demonstrated a nearly eightfold reduction in virus neutralization capability to the Beta variant and fivefold to the Gamma variant, while retaining similar neutralizing activity to the Alpha variant compared to the wild-type virus (11, 19). The chimpanzee adenovirus-based vaccine, ChAdOx1 nCoV-19, given to individuals as a two-dose regimen failed to protect against mild to moderate coronavirus disease 2019 (COVID-19) caused by the Beta variant (25).

We and others have previously reported the isolation and characterization of several hundred RBD-specific mAbs from individuals infected with SARS-CoV-2 (26–35), some of which have been approved for emergency use authorization (EUA) or under active clinical development. Through structure and functional characterization, the RBD-specific antibodies were classified into four major categories (8, 10): class I antibodies, which are encoded by the *VH3-53* gene segment with short CDRH3 loops, block ACE2 and bind only to "up" RBDs; class II neutralizing antibodies include ACE2-blocking neutralizing antibodies that bind both "up" and "down" RBDs and can contact adjacent RBDs; class III neutralizing antibodies bind outside the ACE2 site and recognize both "up" and "down" RBDs; and class IV neutralizing antibodies, which do not block ACE2 and bind only to "up" RBDs. Most class I mAbs were largely disrupted by the K417N/T mutation and class II mAbs by the E484K mutation. Class III and IV mAbs were relatively less affected by the escape mutants (12–14). Fortunately, by screening multiple mAbs from convalescent or vaccinated individuals, a few broad and potent neutralizing antibodies directed to RBD were identified to neutralize or to *in vivo* protect against selected VOCs (19, 20, 36–39). These neutralizing antibodies may contribute to the residual serum neutralizing activity against SARS-CoV-2 VOCs in these individuals.

Here, we report on the isolation and characterization of a broad, potent, and protective antibody, P36-5D2, isolated from a SARS-CoV-2 convalescent individual and capable of neutralizing the major VOCs such as the Alpha, Beta, and Gamma variants. Through crystal and electron cryo-microscopy (cryo-EM) structure analyses, P36-5D2 was found to target a conserved epitope on the RBD of the spike protein, bypassing the three key mutations (K417N, E484K, and N501Y) responsible for immune escape from many potent neutralizing mAbs (12–14). P36-5D2 also demonstrated impressive protection in a transgenic mouse model against infection with either the SARS-CoV-2 Alpha or Beta variant. Treated animals demonstrated a substantial decrease in infectious virus load in the lungs and brain and reduced lung pathology compared to the control animals. Thus, P36-5D2 serves as an important reference for the development of next-generation antibody therapies against SARS-CoV-2 infection.

RESULTS

P36-5D2 Shows Broad and Potent Neutralizing Activity Against Pseudotyped and Infectious SARS-CoV-2

We used flow cytometry to isolate memory B cells that recognized the fluorescence-labeled SARS-CoV-2 spike trimer as previously described (28). A total of 70 mAbs were able to bind to the SARS-CoV-2 spike, eight of which demonstrated neutralizing ability against the SARS-CoV-2 pseudovirus and infectious virus (**Table 1**, **Supplementary Figures S1A, B**). Four mAbs—P36-1A3, P36-1B7, P36-5D2, and P74-6D2—showed stronger neutralizing activity, with respective IC_{50} values of 0.015, 0.025, 0.053, and 0.025 μg/ml against pseudovirus (**Table 1**, **Supplementary Figure S1A**). The remaining four—P33-1F1, P33-3C5, P36-1C5, and P36-8F2—had relatively weaker neutralizing potency, with IC_{50} values ranging from 0.037 to 39.6 μg/ml, and failed to reach 90% neutralizing activity even at the highest concentration of 50 μg/ml (**Table 1**, **Supplementary Figure S1A**). The control and representative mAbs from each class, REGN10933 (class I), CB6 (class I), BD368-2 (class II), and REGN10987 (class III), were RBD-specific and showed comparable neutralizing activity to that reported (26, 27, 32). Another control NTD-specific mAb, 4A8 (40), had an IC_{50} of 0.115 μg/ml, but failed to reach 90% neutralization. Comparable neutralizing potency was also found for the eight isolated mAbs against the infectious SARS-CoV-2 wild-type (WT) strain (**Table 1**, **Supplementary Figure S1B**).

To evaluate the neutralizing breadth of the top 4 neutralizing mAbs, we used the established panel of pseudoviruses including three of the most challenging SARS-CoV-2 VOCs, Alpha, Beta, and Gamma, as well as single mutants derived from the three

TABLE 1 | Binding capacity, neutralizing activity, and gene family analysis of eight monoclonal antibodies (mAbs) isolated from individuals infected with SARS-CoV-2 and five published representative mAbs.

mAb name	Pseudovirus (μg/ml)		Infectious virus (μg/ml)		Binding to RBD		Heavy chain			Kappa chain or Lambda chain		
	IC50	IC90	IC50	IC90	KD (nM)	Comepting w/ ACE2	IGHV	CDR3 lengh	SHM%	IGK(L)V	CDR3 lengh	SHM%
P33-1F1	39.679	>50	27.918	>50	n.a.	n.a.	3-13*01	14	1.37	K 1-39*01	10	0.70
P33-3C5	0.037	>50	0.151	>50	n.a.	n.a.	1-24*01	14	1.70	L 2-14*01	10	0.34
P36-1A3	0.015	0.101	0.029	0.320	2.33	+++	3-66*01	9	1.02	K 1-9*01	8	0.00
P36-1B7	0.025	0.305	0.096	1.388	7.37	+++	3-66*01	11	0.68	K 1-9*01	10	0.00
P36-1C5	0.142	>50	0.154	>50	n.a.	n.a.	3-7*01	23	1.69	L 3-1*01	9	0.36
P36-5D2	0.053	0.910	0.060	0.513	6.91	+	1-3*01	15	0.68	K 1-5*01	9	0.71
P36-8F2	23.487	>50	22.476	>50	n.a.	n.a.	3-13*01	22	0.34	K 1-39*01	10	0.00
P74-6D2	0.025	0.302	0.075	1.260	4.11	+++	1-18*01	10	1.37	K 1-33*01	8	0.36
REGN10933(class I)	0.006	0.046	n.a.	n.a.	<0.01	+++	3-11*01	13	n.a.	K 1-33*01	9	n.a.
CB6(class I)	0.015	0.136	n.a.	n.a.	0.26	+++	3-66*01	13	n.a.	K 1-39*01	11	n.a.
BD368-2(class II)	0.004	0.023	n.a.	n.a.	0.07	+++	3-23*01	18	n.a.	K 2-28*01	9	n.a.
REGN10987(class III)	0.006	0.046	n.a.	n.a.	<0.01	+++	3-30*01	13	n.a.	L 2-14*03	10	n.a.
4A8(NTD)	0.115	>50	n.a.	n.a.	n.a.	n.a.	1-24*01	21	n.a.	K 2-24*01	9	n.a.

IC50 represents the half-maximal concentration and IC90 the 90% inhibitory concentration in the pseudovirus and infectious SARS-CoV-2 neutralization assay. Antibody binding to RBD was presented either by K_D or by competing with ACE2, in which +++ indicates >70% competition, ++ means 50%–70%, + denotes 20%–50%, and – indicates <20% competition. The program IMGT/V-QUEST was applied to analyze the gene germline, CDR3 length, and somatic hypermutation (SHM). The CDR3 length was calculated from the amino acid sequences. The SHM frequency was calculated from the mutated nucleotides.

RBD, receptor-binding domain; IGHV, immunoglobulin heavy-chain variable region gene; n.a. not available.

VOCs (20). As shown in **Figure 1A**, **Supplementary Figure S2**, P36-5D2 was the most broad and potent against all the pseudotyped VOCs and variants tested, as was the class III control REGN10987. In contrast, P36-1B7, like the class I mAb CB6, was substantially impacted by the SARS-CoV-2 Alpha, Beta, and Gamma variants, largely due to K417N/T and N501Y mutations. P74-6D2 demonstrated reduced or loss of neutralizing activities to the three VOCs, which was largely attributed to E484K, similar to the class II control mAb BD368-2 and the class I control mAb REGN10933. P36-1A3 appeared to be heavily affected by N501Y and K417-E484K-N501Y mutations. Furthermore, the neutralizing patterns against these pseudotyped VOCs and variants correlated well with their binding avidity to cell surface-expressed VOCs and the mutant spike proteins (**Figure 1B**, **Supplementary Figure S3**). This result suggested that a compromised binding avidity is a major escape mechanism.

Subsequently, we evaluated the neutralizing ability of P36-5D2 against the infectious SARS-CoV-2 WT, Alpha, and Beta. Consistent with that from pseudoviruses, P36-5D2 showed broad neutralizing activity to all three infectious viruses, with IC_{50} values of 0.060, 0.051, and 0.034 μg/ml against the SARS-CoV-2 WT, Alpha, and Beta respectively (**Figure 1C**). The dissociation constant (K_D) of P36-5D2 with the SARS-CoV-2 RBD was 6.91 nM, measured using surface plasmon resonance (SPR), which was similar to those of P36-1A3, P36-1B7, and P74-6D2 (**Supplementary Figure S1B**). Through competition analysis measured by SPR, we found that P36-5D2 partially competed while P36-1A3, P36-1B7, and P74-6D2 completely competed with ACE2 for binding to RBD (**Supplementary Figure S1C**). Competition among the four mAbs further showed that P36-5D2 recognized a less overlapping epitope, while the other three strongly competed among each other (**Supplementary Figures S1D, E**). These results indicated that P36-5D2 recognized a different epitope from those by the other three mAbs.

P36-5D2 Binds to a Highly Conserved Epitope on RBD and Avoids Three Key Mutant Residues (K417N, E484K, and N501Y)

To reveal the molecular basis of the broad and potent neutralizing activity of P36-5D2, we determined the crystal structure of its antigen-binding fragment (Fab) bound to the RBD-3M carrying the K417N, E484K, and N501Y mutations initially identified in the SARS-CoV-2 Beta variant. At a resolution of 3.1 Å, we found that P36-5D2 recognized an epitope consisting of 11 residues (T345, R346, L441, K444, V445, G446, G447, Y449, N450, T470, and F490) on RBD, devoid of the three key mutant residues K417N, E484K, and N501Y that facilitated escape from the neutralization of many mAbs, including some approved for EUA (**Figure 2A**). Over 99.5% conservation was found at all these sites among the 1.96 million spike sequences in the GISAID EpiCoV database collected from December 2019 to July 2021. The paratope of P36-5D2 consisted of nine heavy-chain residues—T30 and T31 of HCDR1; G54 and K59 of HCDR2; and R103, Q105, F106, D107, and Y108 of HCDR3—as well as six light-chain residues: W32 of LCDR1; D50 of LCDR2; and Y91, N92, G93, and Y94 of LCDR3 (**Figure 2B**). At the binding interface, R346 of the RBD had salt bridge interaction with D107 of HCDR3 and D50 of LCDR2, and K444, G446, and N450 had hydrogen bond interactions with residues Y91 of LCDR3 and K59, F106, and D107 of HCDR2 and HCDR3 (**Figures 2C, D** and **Supplementary Table S2**). Based on the binding specificity, P36-5D2 was closest to the class III RBD-targeting mAbs, including REGN10987, S309, C110, and C135 (8, 27, 30, 41).

A

Fold changes in IC50	WT	WT D614G	Alpha (B.1.1.7)	Beta (B.1.351)	Gamma (P.1)	K417N	K417T	E484K	N501Y	417N/484K/501Y
		variants			RBD					
P36-5D2	+1.0	+2.1	+1.4	+1.7	+2.1	+1.8	-1.1	-1.3	+2.3
P36-1B7	+1.0	BDL	BDL	BDL	BDL	-426.5	-1.3	BDL	BDL
P74-6D2	+1.0	-3.7	BDL	BDL	+1.6	+1.6	BDL	+1.4	BDL
P36-1A3	+1.0	-7.8	BDL	BDL	-1.9	-1.5	+2.2	-2.5	BDL
REGN10933(class I)	+1.0	+1.9	-9.9	-7.0	-1.0	-3.0	-5.4	+1.3	-14.8
CB6(class I)	+1.0	-14.2	BDL	BDL	BDL	-80.0	-1.8	-4.2	BDL
BD368-2(class II)	+1.0	+1.5	BDL	BDL	+1.7	+1.0	BDL	+1.1	BDL
REGN10987(class III)	+1.0	+1.2	+1.1	+1.8	+1.5	-1.1	-2.0	-1.2	+1.9

B

Fold changes in surface binding	WT	WT D614G	Alpha (B.1.1.7)	Beta (B.1.351)	Gamma (P.1)	K417N	K417T	E484K	N501Y	417N/484K/501Y
		variants			RBD					
P36-5D2	+1.0	+2.8	-1.2	+1.1	+2.5	+2.5	-1.6	-1.3	-1.5
P36-1B7	+1.0	-156.5	BDL	-166.4	-22.8	-3.3	-2.4	-34.6	-9.9
P74-6D2	+1.0	+2.2	-22.3	-10.8	+2.1	+2.4	-7.6	+1.2	-4.4
P36-1A3	+1.0	+2.7	-54.5	-98.5	+1.1	-2.0	+1.2	-1.5	-784.4
REGN10933(class I)	+1.0	+1.2	-3.2	-3.3	+1.4	+1.5	-1.5	-1.6	-4.0
CB6(class I)	+1.0	+2.7	-76.3	-266.4	BDL	-38.7	-1.4	-1.4	-332.2
BD368-2(class II)	+1.0	+1.3	-569.1	BDL	+1.7	+1.5	BDL	+1.4	BDL
REGN10987(class III)	+1.0	-1.2	-1.1	-1.2	+1.6	+1.5	-1.5	-1.4	-1.4

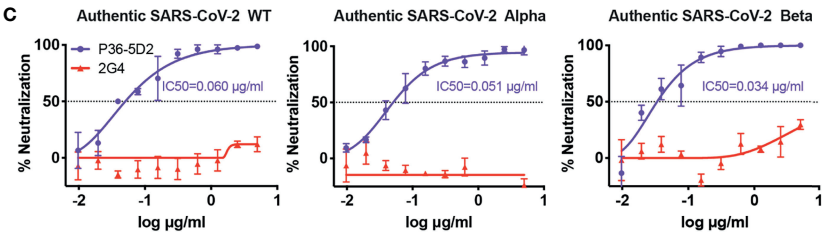

FIGURE 1 | P36-5D2 shows broad and potent neutralizing and binding spectrum against pseudotyped and infectious SARS-CoV-2. P36-5D2, P36-1B7, P74-6D2, and P36-1A3 were the top 4 isolated neutralizing monoclonal antibodies (mAbs) against severe acute respiratory syndrome coronavirus 2 (SARS-CoV-2) from infected individuals. Published representative receptor-binding domain (RBD)-specific mAbs included REGN10933 (class I), CB6 (class I), BD356-2 (class II), and REGN10987 (class III). The neutralizing and binding ability of mAbs against pseudotyped SARS-CoV-2, including Alpha (B.1.1.7), Beta (B.1.351), and Gamma (P.1), and the respective mutations derived from the three variants of concern (VOCs) were evaluated. Values indicate the fold changes in half-maximal inhibitory concentrations (IC_{50}) **(A)** and the mean fluorescence intensity (MFI) relative to that of wild-type (WT) D614G **(B)**. The IC_{50} of antibodies against WT D614G are listed in **(A)**. The *minus symbol* represents increased resistance and the *plus sign* indicates increased sensitivity. IC_{50} or MFI highlighted in *red* indicates that resistance increased at least threefold; in *blue*, sensitivity increased at least threefold. *BDL* (below detection limit) represents the highest concentration of mAbs that failed to reach 50% potency in neutralization activity or mAbs that failed to bind the cell surface-expressed SARS-CoV-2 variants. Results are presented as the mean value from three independent experiments. **(C)** Neutralization of P36-5D2 against the infectious SARS-CoV-2 WT, Alpha, and Beta variants. 2G4 is the negative control antibody specific for Ebola virus glycoprotein (EBOV GP). Experiments were performed in triplicate, and all data were presented as the means ± SEM.

The P36-5D2 epitope overlapped more with that of REGN10987 and C110 than with S309 and C135 (**Figures 2E–H**). All these five class III mAbs shared two residues, R346 and L441, among their epitopes. Interestingly, P36-5D2, C110, and C135 had light-chain variable regions all derived from germline *IGKV 1-5*, indicating a selective preference for the particular germline gene during the development of this class of mAbs from different infected individuals.

We went further to determine the cryo-EM structures of the P36-5D2 Fab bound to the SARS-CoV-2 spike trimer at 3.7-Å resolution (**Figure 2I**). In one model, P36-5D2 Fabs bound two "up" RBDs and one "down" RBD. In the other model, P36-5D2 Fabs bound two "down" RBDs and one "up" RBD of the spike trimer. Consistent with the crystal structure analysis, the cryo-EM structure clearly demonstrated that the mutant residues K417N, E484K, and N501Y were not involved in the P36-5D2 epitope. Furthermore, P36-5D2 and ACE2 only had two overlapping residues at G446 and Y447, which was sufficient to exert spatial hindrance in disrupting the interaction between ACE2 and RBD. These results collectively revealed the highly conserved nature of the P36-5D2 epitope and provided a molecular basis for its broad and potent neutralizing activity against all the SARS-CoV-2 VOCs and mutant strains tested here.

Next, we conducted a single-site alanine scanning mutagenesis for the 11 epitope residues within the P36-5D2 epitope to identify the key residues that mediate RBD binding. All 11 mutated spikes were successfully expressed on the surface of human embryonic kidney (HEK) 293T cells and can bind to the cellular receptor ACE2 (**Figures 3A, B, E**). Among the mutated residues, R346A, K444A, G446A, and N450A resulted in a near loss of P36-5D2 binding (**Figures 3A, C**). Two resides, K444A and V445A, also resulted in a substantial reduction in REGN10987 binding (**Figure 3D**), consistent with the epitope residues defined by structural analysis. Furthermore, among the 11 pesudoviruses bearing alanine mutated spikes, nine were able to confer resistance to P36-5D2, while the remaining two (L441A and T470A) had a relatively weaker impact

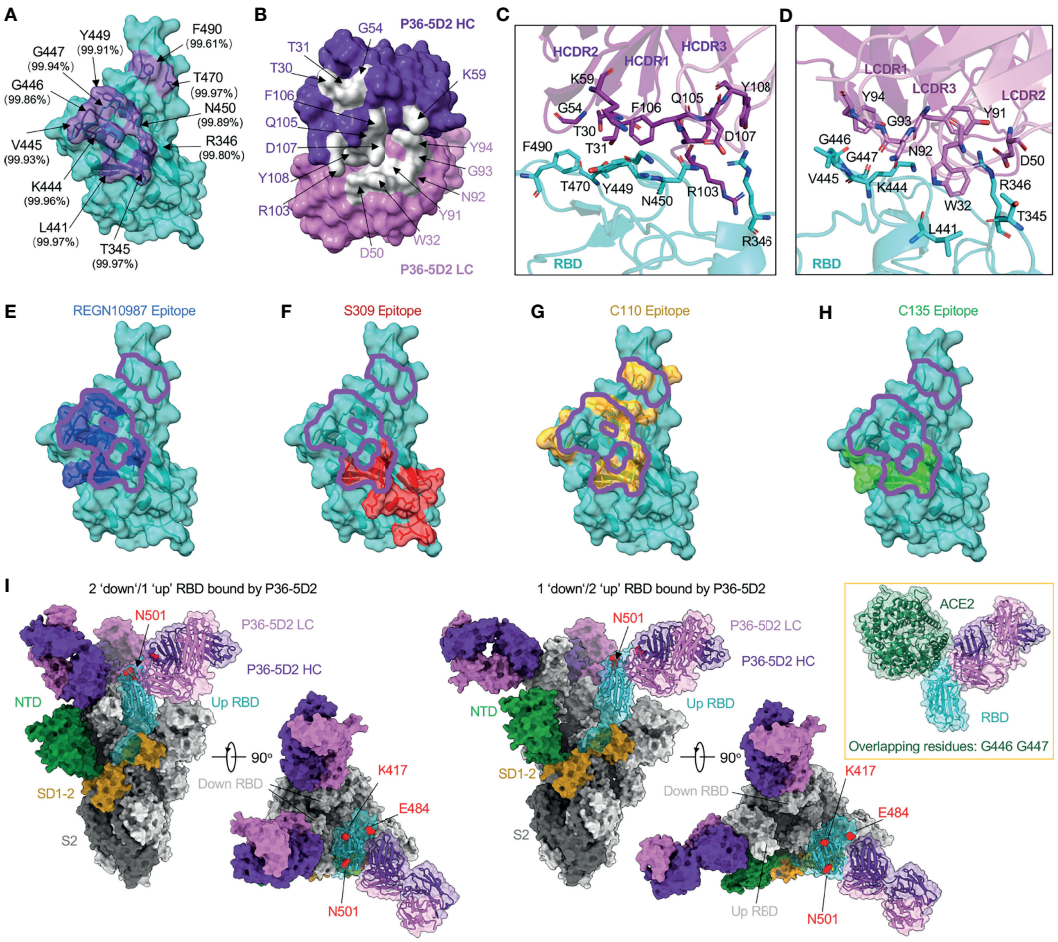

FIGURE 2 | P36-5D2 binds to a highly conserved epitope on the receptor-binding domain (RBD) and avoids three key mutant residues: K417N, E484K, and N501Y. **(A)** The epitope of P36-5D2 (*purple*) is highlighted on the surface of severe acute respiratory syndrome coronavirus 2 (SARS-CoV-2) RBD-3M carrying K417T, E484K, and N501Y (*cyan*) (PDB: 7FJC). RBD-3M residues on the epitope are labeled. The percentages show the conservation at these positions observed in the GISAID EpiCoV database by aligning 1,959,333 sequences of the SARS-CoV-2 spike from December 2019 to July 2021. **(B)** The paratope of P36-5D2 (*sliver*) is highlighted on heavy chain (*purple*) and light chain (*pink*). Antibody residues are labeled in *purple* or *pink* depending on their origin from heavy or light chain. **(C, D)** Interaction between P36-5D2 Fab and SARS-CoV-2 RBD-3M. **(E–H)** Listed class III mAbs Fab fragments are superposed onto P36-5D2/RBD-3M crystal structure. REGN10987, S309, C110, and C135 are reference class III mAbs. The epitopes of these antibodies were assigned by selection of any RBD residue within 4 Å of any antibody residue. The epitope of REGN10987 (PDB: 6XDG) is colored in *blue*, S309 (PDB: 7JX3) in *red*, C110 (PDB: 7K8V) *yellow*, C135 (PDB: 7K8Z) *green*, and P36-5D2 in *purple*. **(I)** Electron cryo-microscopy (cryo-EM) for the P36-5D2 Fab and SARS-CoV-2 spike complex (*left*, 3.65 Å; *right*, 3.69 Å) reveals the binding of P36-5D2 Fab to both "up" and "down" RBDs. P36-5D2/RBD-3M crystal structure shown as cartoon superposed onto one protomer of P36-5D2/spike cryo-EM structure. The spike is shown as a molecular surface, with one protomer RBD colored *cyan*, NTD *green*, SD1-2 *yellow*, and S2 *gray*. The *top view* shows that P36-5D2 avoids residues K417, E484, and N501, which are shown as *red-colored spheres*. *Inset*: structure superposition showing clashes between ACE2 (PDB: 6MOJ; *green*) and P36-5D2 Fab. Overlapping residues shared between P36-5D2 and ACE2 are listed below.

(**Figure 3F**). These results suggested that the levels of binding to the surface-expressed spikes could not be accounted for during the entire neutralization of P36-5D2.

P36-5D2 Protects K18-hACE2 Mice From Infectious SARS-CoV-2 Alpha or Beta Infection

Thereafter, we evaluated the prophylactic potential of P36-5D2 against infectious SARS-CoV-2 Alpha or Beta infection in a well-established hACE2 transgenic mouse model (42, 43). The entire experimental protocol and assays conducted to evaluate the protection capability of P36-5D2 are outlined in **Figure 4A**. Briefly, 12 K18-hACE2 mice were IP administered with P36-5D2 at a dose of 10 mg/kg body weight a day before the intranasal (IN) challenge with 10^3 plaque-forming units (PFU) SARS-CoV-2 Alpha or Beta variant. The mice were monitored for 14 days to record their body weight and symptoms. Half of them were euthanized at 4 days post-infection (dpi) to obtain the right lung and brain for viral titration and the left lung for histological staining (**Figure 4A**).

For SARS-CoV-2 Alpha infection, P36-5D2-treated animals maintained relatively stable body weights with 100% survival,

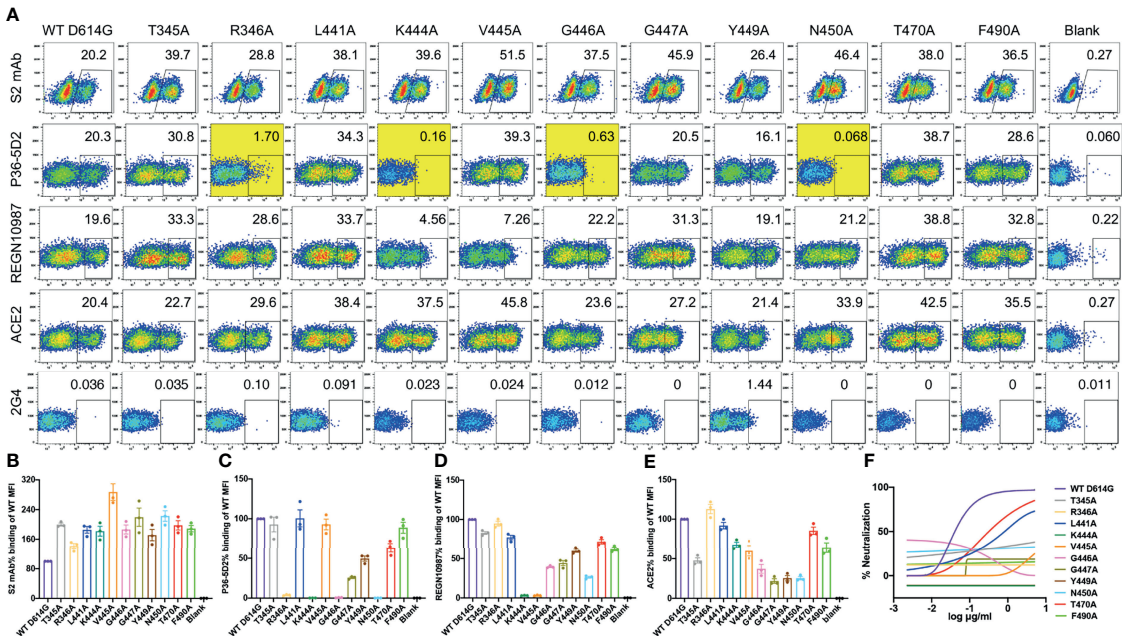

FIGURE 3 | Impact of single alanine mutated residues on P36-5D2 binding and neutralization. **(A)** Wild-type and single alanine mutated spike were expressed on the surface of HEK 293T cells, incubated with P36-5D2, REGN10987, or ACE2, followed by staining with anti-human IgG Fc phycoerythrin (PE) or anti-His PE, and analyzed by FACS. For each panel, the *X*-axis means tested antibody or ACE2 binding PE/FITC and the *Y*-axis means side-scattered light (SSC). The gated cell percentages are shown. **(B)** The S2 monoclonal antibody (mAb) is a positive control antibody used for spike expression normalization. **(C–E)** The relative mean fluorescence intensity (MFI) of mAbs or ACE2 binding was determined by comparing the total MFI in the selected gate between the spike variants and WT D614G. 2G4 targeting Ebola virus glycoprotein (EBOV GP) is a negative control mAb. *NC* denotes HEK 293T cells with mock transfection. Alanine mutated residues completely destroying P36-5D2 binding are highlighted in *yellow*. Data are presented as the mean ± SEM from three independent experiments. **(F)** Impact of single alanine mutated residues on pseudovirus neutralization sensitivity to P36-5D2. Results are presented as the mean value from three independent experiments.

whereas those without treatment suffered drastic loss of body weight starting from 5 dpi and reached humane endpoint at 7 dpi (**Figures 4B, C**). The viral titers found at 4 dpi for the untreated group were on average $3.3 \times 10^5 \pm 1.5 \times 10^5$ PFU/tissue and brain $7.2 \times 10^5 \pm 10^6$ PFU/tissue. In contrast, the P36-5D2-treated group showed minimum detectable levels of viruses in the lung and brain tissues (**Figures 4F, G**). To assess the extent of lung damage and pulmonary inflammation of the virus infection, we performed histopathological analysis on the lung sections using hematoxylin and eosin (H&E) staining. The untreated group infected by the SARS-CoV-2 Alpha variant revealed evidence of moderate to severe lung damage and inflammation with marked infiltration of inflammatory cells such as granulocytes. In contrast, in the P36-5D2 group, the lung tissue remained intact and well defined (**Figure 4J**).

For SARS-CoV-2 Beta infection, the untreated group exhibited progressive body weight loss from 3 to 5 dpi, and all succumbed to infection by 5 dpi. These results indicated that the disease progressed faster and with greater severity caused by SARS-CoV-2 Beta as compared to SARS-CoV-2 Alpha infection. Yet, P36-5D2 still conferred complete protection and the mice maintained stable body weights, except for one mouse experiencing a slight decline with mild symptoms at 6 dpi and recovering by 8 dpi (**Figures 4D, E**). In the untreated group, the viral titers found at 4 dpi were on average 789 ± 420 PFU/tissue and brain $7.0 \times 10^4 \pm 10^5$ PFU/tissue. The prophylactic use of P36-5D2 against the SARS-CoV-2 Beta variant was able to reduce lung viral titers for 2 logs compared to that in the control animals. The brain titers of the P36-5D2 group were undetectable, except for one mouse (**Figures 4H, I**). Evaluation of H&E staining revealed that the lung sections from the untreated group infected by the Beta variant showed similar histopathological changes to those infected by the Alpha variant, with severe inflammatory infiltrates and edema. In contrast, in the P36-5D2 group, there was no damage or pulmonary inflammation in lung tissues (**Figure 4K**). These results strongly indicate the broad and potent neutralizing activity of P36-5D2 against the SARS-CoV-2 Alpha and Beta variants *in vivo via* prophylactic interventions.

DISCUSSION

We report here the structural and functional characterization of the human neutralizing antibody P36-5D2 isolated from SARS-CoV-2 convalescent individuals. Compared to many other isolated human mAbs, the most outstanding and unique feature of P36-5D2 is its breadth and potency against the SARS-CoV-2 Alpha, Beta, and Gamma variants, as well as mutant viruses derived from the variants. Passive delivery of

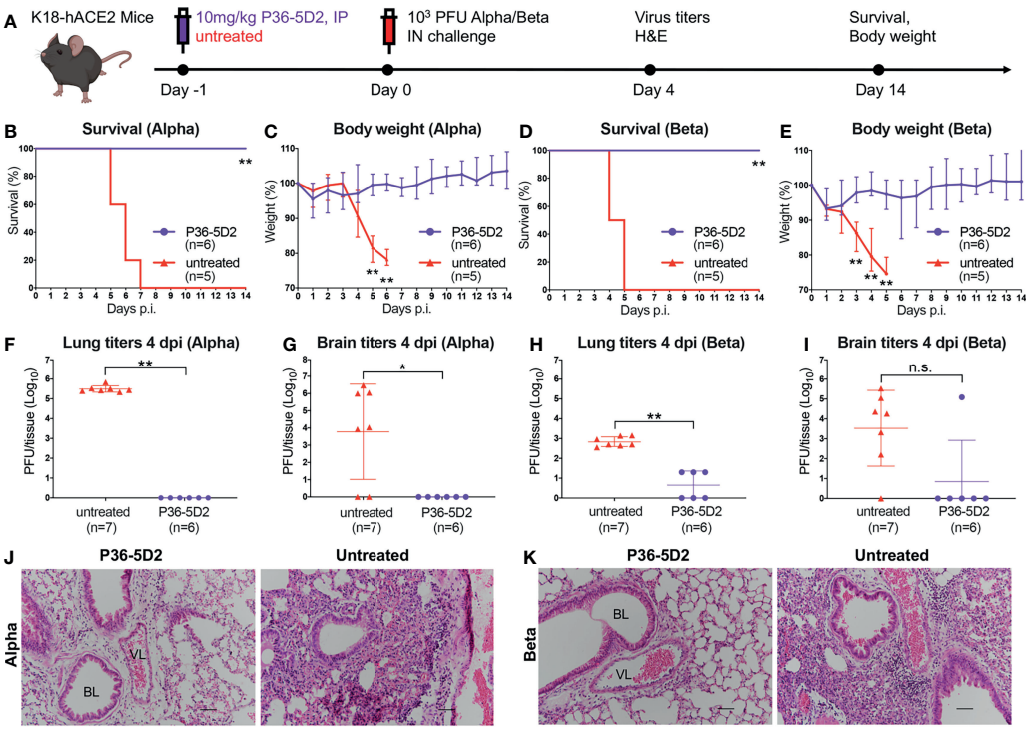

FIGURE 4 | Efficacy of P36-5D2 prophylaxis against the infectious severe acute respiratory syndrome coronavirus 2 (SARS-CoV-2) Alpha or Beta variant in K18-hACE-2 mice. **(A)** Experimental schedule for antibody prophylaxis. Eight-week-old K18-hACE2 transgenic female mice were administered 10 mg/kg of P36-5D2 intraperitoneally or untreated 1 day prior to challenge with 10^3 plaque-forming units (PFU) infectious SARS-CoV-2 Alpha or Beta *via* the intranasal route. **(B–E)** The survival percentage **(B, D)** and body weight **(C, E)** were recorded daily after infection until the occurrence of death or until the experimental end point at 14 days post-infection (dpi) (P36-5D2, $n = 6$; untreated, $n = 5$). Mice were sacrificed at 4 dpi for virus titer analysis (P36-5D2, $n = 6$; untreated, $n = 7$). **(F–I)** Lung titers **(F, H)** and brain titers **(G, I)** were tested by plaque assays in lung and brain tissue homogenates. The PFU per tissue were compared between groups in $\log_{10}$-transformed units. All data are presented as the mean ± SEM. Analysis of a two-tailed unpaired *t*-test was used. $^*p < 0.05$, $^{**}p < 0.01$. *n.s.*, not significant. **(J, K)** H&E staining of lung sections from P36-5D2-injected or untreated mice at 4 dpi. *VL*, vascular lumen; *BL*, bronchiolar lumen. *Scale bars*, 50 mm. Each image is representative of each group.

P36-5D2 protected K18-hACE2 mice from infection with the SARS-CoV-2 Alpha or Beta variant and significantly reduced the viral loads in both the lungs and brain. Crystal and cryo-EM structural analyses showed that P36-5D2 recognized a highly conserved epitope on RBD, which is accessible in both "up" and "down" conformations and able to withstand the mutated residues K417N, E484K, and N501Y that compromised many neutralizing mAbs, including some approved for EUA. Recently, Hastie and colleagues conducted a comprehensive study to map the landscape of neutralizing epitopes on the RBD of SARS-CoV-2 (44). A total of 186 RBD-directed antibodies with potential therapeutic use were categorized into seven core "communities" (RBD-1 to RBD-7) based on their distinct footprints and broad competition profiles. RBD-1, RBD-2, and RBD-3 antibodies targeted the receptor-binding surface, while RBD-4 and RBD-5 antibodies bound to the outer face of RBD. RBD-6 and RBD-7 antibodies, on the other hand, bound to the inner face of RBD. In this context, P36-5D2 would fall into the community of RBD-5 antibodies together with REGN10987 and S309. Consistent with what we have found here, RBD-5 antibodies showed broad resistance to the SARS-CoV-2 variants, suggesting that this community of antibodies binds to the conserved epitopes across all variants. Similar to REGN10987 and S309, P36-5D2 barely competed with ACE2 for binding to RBD, suggesting that their mechanism of neutralization may involve immunoglobulin G (IgG)-mediated spike crosslinking on virions, steric hindrance, or aggregation of virions (41). Nevertheless, these results indicated that we have identified a broad and potent neutralizing antibody capable of overcoming the major circulating SARS-CoV-2 variants. P36-5D2 and the epitope it recognized may serve as an important reference for the development of next-generation antibody therapies and vaccines against SARS-CoV-2 infection.

A couple of points need to be highlighted here. Firstly, despite the rapid emergence and spread of the SARS-CoV-2 variants, infected and convalescent individuals can generate and produce RBD-specific antibodies with impressive breadth and potency. The number and relative proportion of such antibodies appeared to be small, but they may contribute substantially to the remaining serum neutralizing activity to the variants in recovered or vaccinated individuals, particularly after boosting with mRNA vaccines (24, 45, 46). Comprehensive characterization of this class of antibodies will provide us with deeper insights into their ontogeny and potential ways of inducing broader and more

effective protection against the circulating and future variants. Secondly, although many of the current SARS-CoV-2 variants bear mutations in the RBD, the identification of P36-5D2 has revealed the existence of a highly conserved sequence and structure on RBD that could potentially be used to trigger more broad and potent immune responses, avoiding the current prevalent mutations in dampening the immune responses generated during natural infection and vaccination. This would require preferentially exposing the conserved regions on RBD while minimizing the receptor-binding motif that is commonly recognized during infection and vaccination. How to achieve this design and, more importantly, to realize the desired immune response will surely be a big challenge. However, recent advances in structure-based vaccine design through understanding of the antigen–antibody interaction will certainly offer new possibilities for this highly anticipated outcome. The identification of P36-5D2, as well as other similar mAbs (19, 20, 36–39), represents the first but important step for us to achieve the ultimate goal of developing a universal vaccine against all SARS-CoV-2 variants and beyond.

MATERIALS AND METHODS

Study Approval

This study received approval from the Research Ethics Committee of Beijing Youan Hospital, China (LL-2020-039-K) and Shenzhen Third People's Hospital (2020-084). The research was conducted in strict accordance with the rules and regulations of the Chinese Government for the protection of human subjects. The study subjects agreed and signed the written informed consent for the use of their blood samples in research. All animal experiments were conducted in a Biosafety Level 3 (BSL-3) facility in accordance with the National University of Singapore (NUS) Institutional Animal Care and Use Committee (IACUC) (protocol no. R20-0504), and the NUS Institutional Biosafety Committee (IBC) and NUS Medicine BSL-3 Biosafety Committee (BBC) approved SOPs.

Cell Lines

HEK293T cells (ATCC, Manassas, VA, USA), HeLa cells expressing hACE2 orthologs (kindly provided by Dr. Qiang Ding), and Vero E6 cells (ATCC) were maintained at 37°C in 5% CO_2 in Dulbecco's minimal essential medium (DMEM) containing 10% (*v*/*v*) heat-inactivated fetal bovine serum (FBS) and 100 U/ml penicillin–streptomycin. FreeStyle 293F cells (R79007; Thermo Fisher Scientific, Waltham, MA, USA) were maintained at 37°C in 5% CO_2. Sf9 cells and Hi5 cells (ATCC) were maintained at 27°C in Sf-900 II SFM medium.

Recombinant Protein Expression and Purification

Recombinant SARS-CoV-2 RBD (residues R319–F541) and trimeric spike for SARS-CoV-2 (residues M1–Q1208) and the N-terminal peptidase domain of human ACE2 (residues S19–D615) were expressed using the Bac-to-Bac Baculovirus Expression System (Invitrogen, Carlsbad, CA, USA) as previously described (9, 47). The SARS-CoV-2 spike contains proline substitutes at residues 986 and 987, "GSAS" substituted at the furin cleavage site (residues 682–685), and C-terminal foldon trimerization motif, Strep-tag, and six-histidine tag. The SARS-CoV-2 RBD, RBD-3M, carrying K417N/E484K/N501Y mutations and ACE2 peptidase domain contains a C-terminal six-histidine tag. These recombinant protein genes were cloned into pFastBac-Dual vectors (Invitrogen) and transformed into DH10Bac component cells. The bacmid was extracted and transfected into Sf9 cells using Cellfectin II Reagent (Invitrogen). The recombinant baculoviruses were extracted from the transfected supernatant and amplified to generate high-titer virus stock. Viruses were then used to infect Hi5 cells for recombinant protein expression.

Antibody and Fab Production

Antibody and Fab production was conducted as previously described (47, 48). The published SARS-CoV-2 mAbs REGN10933, CB6, BD368-2, REGN10987, and 4A8 and the negative control antibody 2G4 against Ebola virus (EBOV) glycoprotein (GP) were synthesized according to the sequences released in Protein Data Bank (PDB) (26, 27, 32, 40, 49). Antibodies were produced by transient transfection of HEK 293F cells (Life Technologies, Carlsbad, CA, USA) using equal amounts of paired heavy- and light-chain plasmids by PEI (Sigma, St. Louis, MO, USA). After 5 days, the culture supernatant containing antibodies was collected and purified with protein A microbeads (GenScript, Piscataway, NJ, USA) according to the manufacturer's protocol. Beads were collected using the magnetic separation rack and the antibodies eluted from beads with an elution buffer (0.3 M glycine, pH 2.0) into a neutralization buffer (1 M Tris-HCl, pH 8.0), followed by dialyzing into phosphate-buffered saline (PBS). Concentrations were determined by BCA Protein Assay kits (Thermo Scientific, Waltham, MA, USA). To produce Fab fragments, the antibodies were cleaved using Protease Lys-C (Sigma) with an IgG/Lys-C ratio of 4000:1 (*w*/*w*) in 10 mM EDTA, 100 mM Tris-HCl, pH 8.5, at 37°C for 12 h. Fc fragments were removed using Protein A microbeads.

Isolation of Spike-Specific Single B Cells by FACS

Spike-specific single B cells were sorted as previously described (28). Peripheral blood mononuclear cells (PBMCs) from individuals infected with SARS-CoV-2 were collected and incubated with 500 nM SARS-CoV-2 spike for 30 min at 4°C, followed by antibody cocktail for the identification of spike-specific B cells. The cocktail consisted of CD3-PE-Cy5 (BD Biosciences, Franklin Lakes, NJ, USA) at a 1:25 dilution, CD14-PE-Cy5 (eBioscience, San Diego, CA, USA) at a 1:50 dilution, CD16-PE-Cy5 (BD Biosciences) at a 1:25 dilution, CD235a-PE-Cy5 (BD Biosciences) at a 1:100 dilution, CD20-PE-Cy7 (BD Biosciences) at a 1:200 dilution, CD27-BV421 (BD Biosciences) at a 1:50 dilution, IgG–fluorescein isothiocyanate (FITC) (BD Biosciences) at a 1:25 dilution, anti-His-APC (BioLegend, San Diego, CA, USA) at a 1:20 dilution, and streptavidin–phycoerythrin (PE) (eBioscience) at a 1:100 dilution. The

stained cells were washed with FACS buffer (PBS containing 2% FBS) and resuspended in 500 µl FACS buffer before being stained with propidium iodide (PI) (eBioscience). Spike-specific single B cells were gated as live$^+$CD3$^-$CD14$^-$CD16$^-$CD235a$^-$CD20$^+$ CD27$^+$IgG$^+$Spike$^+$ and sorted into 96-well PCR plates containing 2 µl of lysis buffer (1.9 µl 0.2% Triton X-100, 0.1 µl RNase inhibitor; Clontech, Mountain View, CA, USA) per well. The plates were then snap-frozen on dry ice and stored at −80°C until the reverse transcription reaction.

Single B-Cell PCR and Construction of Antibody Genes

The IgG heavy- and light-chain variable genes were amplified by nested PCR and cloned into linear expression cassettes or expression vectors to produce full IgG1 antibodies as previously described (28). Specifically, all second-round PCR primers containing tag sequences were used to produce the linear Ig expression cassettes by overlapping PCR. Separate primer pairs containing the specific restriction enzyme cutting sites (heavy chain, 5′-*Age*I/3′-*Sal*I; kappa chain, 5′-*Age*I/3′-*Bsi*WI; and lambda chain, 5′-*Age*I/3′-*Xho*I) were used to amplify the cloned PCR products. The PCR products were purified and cloned into the backbone of the antibody expression vectors containing the constant regions of human IgG1. Overlapping PCR products of paired heavy- and light-chain expression cassettes were co-transfected into HEK 293F cells.

Neutralization Activity of mAbs Against Pseudotyped SARS-CoV-2

WT and mutated SARS-CoV-2 pseudoviruses were generated by co-transfection of human immunodeficiency virus backbones expressing firefly luciferase (pNL43R-E-luciferase) and pcDNA3.1 (Invitrogen) expression vectors encoding the respective spike proteins into 293T cells (ATCC) (20). Viral supernatants were collected 48 h later. Viral titers were measured as the luciferase activity in relative light units (Bright-Glo Luciferase Assay Vector System; Promega Biosciences, WI, USA). Serial dilutions of mAbs were prepared with the highest concentration of 5 or 50 µg/ml. WT or mutated spike pseudoviruses were mixed with mAbs and incubated at 37°C for 1 h. HeLa-hACE2 cells (1.5×10^4 per well) were then added into the mixture and incubated at 37°C for 60 h before cell lysis for measuring the luciferase activity. The percent of neutralization was determined by comparing with the virus control.

Neutralization Activity of mAbs Against Infectious SARS-CoV-2

A plaque reduction neutralization test against infectious SARS-CoV-2 WT, shown in **Supplementary Figure S1A**, was performed in a Chinese certified BSL-3 laboratory. Neutralization assays against infectious SARS-CoV-2 WT were conducted using a clinical isolate (Beta/Shenzhen/SZTH-003/2020, EPI_ISL_406594 at GISAID) previously obtained from a nasopharyngeal swab of an infected patient (28). Serial dilutions of the test antibodies were conducted, mixed with 75 µl of SARS-CoV-2 [8×10^3 focus-forming units (FFU)/ml] in 96-well Microwell plates, and incubated for 1 h at 37°C. The mixtures were then transferred into 96-well plates, seeded with Vero E6 cells, and allowed absorption for 1 h at 37°C. The inocula were then removed before adding the overlay media (100 µl MEM containing 1.6% carboxymethyl cellulose). The plates were then incubated at 37°C, 5% CO_2 for 24 h. Cells were fixed in 4% formaldehyde solution for 30 min and the overlays removed. Cells were permeabilized with 0.2% Triton X-100 and incubated with cross-reactive rabbit anti-SARS-CoV-N IgG (Sino Biological, Beijing, China) for 1 h at room temperature before adding horseradish peroxidase (HRP)-conjugated goat anti-rabbit IgG (H+L) antibody (Jackson ImmunoResearch, West Grove, PA, USA). Cells were further incubated at room temperature. The reactions were developed with KPL TrueBlue Peroxidase substrates (Seracare Life Sciences, Milford, MA, USA). The numbers of SARS-CoV-2 foci were calculated using an EliSpot reader (Cellular Technology, Shaker Heights, OH, USA).

The plaque assay against infectious SARS-CoV-2 VOCs, shown in **Figure 1C**, was performed in the National University of Singapore certified BSL-3 laboratory. The infectious SARS-CoV-2 used in the neutralization belongs to GISAID lineage clade L (WT, B) (accession ID: EPI_ISL_574502), GRY (Alpha, B.1.1.7) (accession ID: EPI_ISL_754083), and GH (Beta, B.1.351.3) (accession ID: EPI_ISL_1173248). Serial dilutions of the test antibodies were conducted, mixed with 50 PFU infectious SARS-CoV-2 in 12-well plates, and incubated for 1 h at 37°C. The mixtures were then transferred into 12-well plates, seeded with Vero E6 cells, and allowed absorption for 1 h at 37°C. The inocula were then removed and the wells washed once with PBS before adding the overlay media [1 ml DMEM containing 1.2% microcrystalline cellulose (MCC)]. The plates were then incubated at 37°C, 5% CO_2 for 72 h for plaque formation. Cells were fixed in 10% formalin overnight before counterstaining with crystal violet. The virus titer of each dilution was determined through the number of plaques formed and expressed in neutralization percentage in comparison to positive control.

Antibody Binding Kinetics, Competition with Receptor ACE2, Epitope Mapping Measured by SPR

The binding kinetics of mAbs to SARS-CoV-2 RBD were analyzed using SPR (Biacore 8K; GE Healthcare, Chicago, IL, USA). Specifically, recombinant protein A (Sino Biological) or the anti-His antibody (Cytiva, Marlborough, MA, USA) was covalently immobilized to a CM5 sensor chip *via* amine groups in 10 mM sodium acetate buffer (pH 4.5) for a final RU (response units) around 7,000. The running buffer HBS-EP was composed of 0.01 M HEPES, pH 7.4, 0.15 M NaCl, and 0.05% (*v*/*v*) Tween-20. The IgG form of mAbs was captured by the sensor chip immobilized with recombinant protein A, and then serial dilutions of SARS-CoV-2 RBD flowed through the sensor chip system. The resulting data were fitted to a 1:1 binding model using the Biacore 8K Evaluation software (GE Healthcare).

To determine competition with the human ACE2, the SARS-CoV-2 RBD was immobilized to a CM5 sensor chip *via* the amine group for a final RU around 250. In the first round, antibodies (1 μM) were injected onto the chip for 120 s to reach binding steady state and HBS-EP was injected for 120 s. In the second round, antibodies (1 μM) were injected onto the chip for 120 s and ACE2 (2 μM) was then injected for 120 s. In the third round, HBS-EP was injected for 120 s and ACE2 (2 μM) was then injected for 120 s. The sensorgrams of the three rounds were aligned from 120 to 240 s in Biacore 8K Evaluation software (GE Healthcare). The blocking efficacy was determined by a comparison of the response units with and without prior antibody injection.

For epitope mapping, the SARS-CoV-2 RBD was immobilized to a CM5 sensor chip *via* the amine group for a final RU around 250. Two different mAbs were sequentially injected and monitored for binding activity to determine whether these two mAbs recognized separate or closely situated epitopes.

Binding of mAbs to Cell Surface-Expressed WT and Mutated Spikes

The entire procedure was conducted as previously described (20). HEK 293T cells were transfected with expression plasmids encoding either WT or mutated full-length spike of SARS-CoV-2, and incubated at 37°C for 36 h. Cells were removed from the plate using trypsin and distributed into 96-well plates for individual staining. Cells were washed twice with 200 μl staining buffer (PBS with 2% FBS) between each of the following. Firstly, cells were stained with 2 μg/ml testing mAb and 5 μg/ml S2-specific monoclonal antibody (MP Biomedicals, Santa Ana, CA, USA) at 4°C for 30 min in 100 μl staining buffer. Then, PE-labeled anti-human IgG Fc (BioLegend) at a 1:100 dilution and anti-mouse IgG FITC (Thermo Fisher Scientific) at a 1:200 dilution were added into 40 μl staining buffer at room temperature for 30 min. After extensive washes, the cells were resuspended and analyzed with BD LSRFortassa (BD Biosciences) and FlowJo v10 software (FlowJo). HEK 293T cells without transfection were also stained as a background control. The RBD-specific mAbs REGN10933, CB6, BD368-2, and REGN10987 were used as positive control mAbs, while 2G4 was used as a negative control mAb. HEK 293T cells with mock transfection were stained as a background control.

Antibody Protection in hACE2 Transgenic Mice

Eight-week-old female K18-hACE2 transgenic mice (InVivos Ptd Ltd, Lim Chu Kang, Singapore) were used for this study. The mice were housed and acclimatized in an ABSL-3 facility for 72 h prior to the start of the experiment.

K18-hACE2 transgenic mice were subjected to pretreatment of mAb P36-5D2 (10 μg/kg) delivered through IP injection a day prior to infection. The inoculation of mice was conducted through IN delivery with 25 μl, 10^3 PFU of the infectious SARS-CoV-2 Alpha or Beta variant. Baseline body weights were measured prior to infection and monitored daily by two personnel post-infection for the duration of the experiment. To assess the viral load, mice from each experimental group were sacrificed 4 dpi, with brain and lung tissues harvested. Each organ was halved for the plaque assay and histology, respectively. Tissues were homogenized with 0.5 ml DMEM supplemented with antibiotic and antimycotic (Gibco, Waltham, MA, USA) and titrated in Vero E6 cells using plaque assays.

For virus titer determination, supernatants from homogenized tissues were diluted 10-fold serially in DMEM supplemented with antibiotic and antimycotic. Of each serial diluted supernatant, 250 μl was added to Vero E6 cells into 12-well plates. After 1 h of incubation for virus adsorption, the inoculum was removed and washed once with PBS. About 1.2% MCC-DMEM supplemented with antibiotic and antimycotic overlay media was added to each well and incubated at 37°C, 5% CO_2 for 72 h for plaque formation. The cells were then fixed in 10% formalin overnight and counterstained with crystal violet. The number of plaques was determined and the virus titers of individual samples were expressed in logarithm of PFU per organ.

Histopathological Analyses

Left lung lobes were fixed in 3.7% formaldehyde solution prior to removal from BSL-3 containment. The tissues were routinely processed, embedded in paraffin blocks (Leica Surgipath Paraplast), sectioned at 5-μm thickness, and stained with H&E (Thermo Scientific) following standard histological procedures. The extent and severity of lung damage was qualitatively described as no infection, mild, moderate, or severe.

Crystal Analysis and Structural Determination

The antibody P36-5D2 Fab and RBD-3M were mixed at a molar ratio of 1:1.5 and incubated at 4°C for 60 min. The mixture was purified by gel filtration pre-equilibrated by 1× HBS buffer. The complex of P36-5D2 Fab and RBD-3M was concentrated to 11 mg/ml for crystallization. Crystal of the P36-5D2 Fab and RBD-3M complex was obtained after 5 days using the sitting drop method. The well solution was 0.1 M sodium HEPES 7.5, 10% (*w*/*v*) PEG 6000, and 5% (*v*/*v*) MPD. Diffraction data were collected at SSRFBL18U1 beam line of the Shanghai Synchrotron Research Facility (SSRF). The data were processed by HKL3000 and the structure was determined using the molecular replacement method with PHASER in the CCP4 suite (50). Model building and refinement were performed using COOT v.0.9.2 and PHENIX v.1.18.2, respectively (51, 52). The data processing statistics are listed in **Supplementary Table S1**.

Cryo-EM Sample Preparation and Data Collection

Aliquots of complex of SARS-CoV-2 spike ectodomains and P36-5D2 Fab (4 μl, 1.6 mg/ml, in buffer containing 20 mM Tris, pH 8.0, and 150 mM NaCl) were applied to glow-discharged holey carbon grids (Quantifoil grid, Au 300 mesh, R1.2/1.3). The grids were then blotted for 2 s and plunge-frozen into liquid ethane using Vitrobot Mark IV (Thermo Fisher Scientific).

Images for complex were recorded using the FEI Titan Krios microscope (Thermo Fisher Scientific) operating at 300 kV with a Gatan K3 Summit direct electron detector (Gatan Inc.,

Pleasanton, CA, USA) at Tsinghua University. The automated software AutoEMation2 (53) was used to collect 4,534 movies for complex of SARS-CoV-2 spike ectodomains and P36-5D2 Fab in super-resolution mode at a nominal magnification of ×29,000 and at a defocus range between −1.5 and −1.8 μm. Each movie has a total accumulated exposure of 50 e-/Å^2 fractionated in 32 frames of 2.13-s exposures. The final image was binned twofold to a pixel size of 0.97 Å. The data collection statistics are summarized in **Supplementary Table S3**.

Cryo-EM Data Processing

Motion correction (MotionCor2 v.1.2.6) (54), CTF estimation (GCTF v.1.18) (55), and non-templated particle picking (Gautomatch v.0.56; http://www.mrc-lmb.cam.ac.uk/kzhang/) were automatically executed using the TsingTitan.py program. Sequential data processing was carried out on RELION-3.1 (56). Initially, ~910,000 particles were subjected to 2D classification. After three additional 2D classifications, the best selected 480,469 particles were applied for the initial model and 3D classification. A subset of 242,871 particle images from state 1 (one RBD up and two RBDs down) and 225,216 particle images from state 2 (two RBDs up and one RBD down) were further subjected to 3D auto-refine and post-processing. The final resolutions for states 1 and 2 were 3.69 and 3.65 Å, respectively. The interface between the S protein of SARS-CoV-2 and Fab was subjected to focused refinement with mask on the region of the RBD–Fab complex to improve the map quality. The selected 480,469 particles were 3D classified focused on the RBD–Fab complex. Then, the good particles were selected for focused refinement and post-processing with a final resolution of 3.8 Å. The resolution was estimated with the gold-standard Fourier shell correlation 0.143 criterion. Details of the data collection and processing are shown in **Supplementary Figure S4** and **Table S3**.

Cryo-EM Model Building and Refinement

The initial model of complex of SARS-CoV-2 spike ectodomains and P36-5D2 Fab was generated using the models (PDB 7A94 and 7A97) and fit into the map using UCSF Chimera v.1.15 (57). Manual model rebuilding was carried out using COOT v.0.9.2 (51) and refined with PHENIX v.1.18.2 (52) real-space refinement. The quality of the final model was analyzed with PHENIX v.1.18.2 (52). The validation statistics of the structural models are summarized in **Supplementary Table S3**. All structural figures were generated using PyMOL 2.0 (58) and Chimera v.1.15 (57).

Quantification and Statistical Analysis

The technical and independent experiment replicates were indicated in the figure legends. The half-maximal inhibitory concentration (IC_{50}) and 90% inhibitory concentration (IC_{90}) of the mAbs were calculated using the four-parameter dose inhibition equation in Graphpad Prism 9.0. Percentages of the binding of mAbs to cell surface-expressed SARS-CoV-2 variants were calculated as the ratio between the mutated over WT mean fluorescence intensity (MFI) normalized relative to that of the S2-specific antibody. All MFI values were weighted by multiplying the number of positive cells in the selected gates. The fold change of the mutant spike relative to WT D614G in binding or neutralization was calculated by simple division of the respective IC_{50} or MFI values. In animal experiments, a two-tailed unpaired *t*-test was used to assess statistical significance. Statistical calculations were performed in GraphPad Prism 9.0. Differences with *p*-values less than 0.05 were considered to be statistically significant ($^*p < 0.05$, $^{**}p < 0.01$; n.s., not significant).

DATA AVAILABILITY STATEMENT

The datasets presented in this study can be found in online repositories. The names of the repository/repositories and accession number(s) can be found in the article/**Supplementary Material**.

ETHICS STATEMENT

The studies involving human participants were reviewed and approved by the Research Ethics Committee of Beijing Youan Hospital, China (LL-2020-039-K) and Shenzhen Third People's Hospital (2020-084). The patients/participants provided written informed consent to participate in this study. The animal study was reviewed and approved by the National University of Singapore (NUS) Institutional Animal Care and Use Committee (IACUC) and the NUS Institutional Biosafety Committee (IBC) and NUS Medicine BSL-3 Biosafety Committee (BBC).

AUTHOR CONTRIBUTIONS

LZ, JC, XW, and JW conceived, designed, and supervised the entire study. SS and JLi did antibody isolation and sequencing under the conduction of JW. SS and ZY did antibody binding analysis and pseudovirus neutralization. CM, ZA, and JC performed the antibody protection experiment in K18-hACE2 mice. SZ did the cryo-EM structure of the Fab-spike complex. JLa collected the crystal structure of the Fab-RBD complex. CM, ZA, LC, and ZZ carried out the infectious virus neutralization assays. JY provided the SARS-CoV-2 spike protein. ZZ, TZ, XS, QZ, and RW conducted the antibody evaluation, structural analysis, and animal experiment. SS, CM, SZ, JLa, JLi, and LZ had full access to the data in the study, generated the figures and tables, and took responsibility for the integrity and accuracy of the data presentation. LZ, SS, CM, XW, and ZA wrote the original draft. LZ, JC, XW, and JW reviewed and edited the manuscript. All authors contributed to the article and approved the submitted version.

FUNDING

This study was funded by the National Key Plan for Scientific Research and Development of China (2020YFC0848800 and 2020YFC0849900), the National Natural Science Foundation (81530065, 91442127, and 32000661), Beijing Municipal

Science and Technology Commission (D171100000517 and Z201100005420019), the Science and Technology Innovation Committee of Shenzhen Municipality (202002073000002), COVID-19 Science and Technology Project of Beijing Hospitals Authority (YGZX-C1), Beijing Advanced Innovation Center for Structural Biology, Tsinghua University Scientific Research Program (20201080053 and 2020Z99CFG004), Tencent Foundation, Shuidi Foundation, TH Capital, and the National Science Fund for Distinguished Young Scholars (82025022), Singapore National Medical Research Council Centre Grant Program (CGAug16M009).

ACKNOWLEDGMENTS

We acknowledge the work and contributions of all healthcare providers from Beijing Youan Hospital and Shenzhen Third People's Hospital. We also thank the affected individuals for their active participation. We thank the SSRF BL17U1 beamline for data collection and processing. We are grateful to the NUS Yong Loo Lin School of Medicine BSL-3 Core Facility for their support with this work.

SUPPLEMENTARY MATERIAL

The Supplementary Material for this article can be found online at: https://www.frontiersin.org/articles/10.3389/fimmu.2021.766821/full#supplementary-material

Supplementary Figure 1 | SARS-CoV-2 spike-specific neutralizing antibodies screening and evaluation. **(A)** Antibody neutralization against pseudotyped and infectious SARS-CoV-2. Antibodies included eight isolated neutralizing mAbs P33-1F1, P33-3C5, P36-1A3, P36-1B7, P36-1C5, P36-5D2, P36-8F2 and P74-6D2 from SARS-CoV-2 infected individuals, four RBD-specific representative mAbs REGN10933, CB6, BD368-2, REGN10987, one NTD-specific representative mAb 4A8 and one negative control mAb 2G4. Data are presented as the means ± SEM from three independent experiments. **(B)** Binding kinetics of the top four isolated neutralizing mAbs P36-1A3, P36-1B7, P36-5D2 and P74-6D2 with SARS-CoV-2 RBD measured by SPR. The black lines indicate the experimentally derived curves while the red lines represent fitted curves based on the experimental data. Results presented are representatives of two independent experiments. **(C)** Antibody competition with ACE2 for binding to SARS-CoV-2 RBD measured by SPR. The plots show distinct binding patterns of ACE2 to the RBD with (colored curve) or without (black curve) prior incubation with each tested mAb. The results are representative of two independent experiments and color-coded for each mAb. **(D)** Epitope mapping through competitive binding measured by SPR. Pairs of antibodies were sequentially applied to SARS-CoV-2 RBD immobilized sensor chip. The level of reduction in response unit comparing with or without prior antibody incubation is the criterion for determining the two antibodies recognize the separate or closely situated epitopes. **(E)** Summary of antibody competition in **(D)**, in which '+++' indicates >70% competition; '++' 50–70%; '+' 20–50%; and '–' <20%.

Supplementary Figure 2 | Neutralization of SARS-CoV-2 variants by each antibody, related to Figure. 1. Pseudoviruses bearing the indicated mutations were tested against serial dilutions of each mAb. Neutralizing activity was defined as the percent reduction in luciferase activities compared to no antibody controls. Levels of resistance were calculated as the -fold change in IC_{50} between each mutant and WT D614G, as presented in Figure. 1A. Results are presented as the mean value from three independent experiments.

Supplementary Figure 3 | Binding to cell surface expressed SARS-CoV-2 variants by each antibody, related to Figure. 1. Wildtype and mutated spike were expressed on the surface on HEK 293T, incubated with the mAbs, followed by staining with anti-human IgG Fc PE and analysed by FACS. The gated cell percentages are shown. The fold changes in antibody binding, as shown in Figure. 1B, was determined by comparing the total MFI in the selected gate between spike variants and WT D614G. S2 mAb is a positive control antibody used for spike expression normalization. 2G4 targeting EBOV GP is negative control antibody. NC is HEK 293T cells with mock transfection.

Supplementary Figure 4 | Cryo-EM data processing workflow. **(A)** Processing workflow of the P36-5D and SARS-CoV-2 spike complex cryo-EM data. Local resolution map and particle orientation distribution of the P36-5D/spike complex with 2 "down" and 1 "up" RBD **(B)** or with 1 "down" and 2 "up" RBD **(C)**. **(D, E)** The corrected, unmasked, masked and phase randomised FSC for the cryo-EM reconstructions of the density maps of P36-5D2/spike complex with C3 symmetry. The final resolution of the P36-5D/spike complex with 2 "down" and 1 "up" RBD is 3.69 Å **(D)**. The final resolution of the P36-5D/spike complex with 1 "down" and 2 "up" RBD is 3.65 Å **(E)**.

Supplementary Table 1 | Crystal structure data collection and refinement statistics.

Supplementary Table 2 | Contacts between SARS-CoV-2 RBD-3M and P36-5D2 (distance cutoff 4 Å).

Supplementary Table 3 | Cryo-EM data collection, refinement and validation statistics.

REFERENCES

1. Fujino T, Nomoto H, Kutsuna S, Ujiie M, Suzuki T, Sato R, et al. Novel SARS-CoV-2 Variant in Travelers From Brazil to Japan. *Emerg Infect Dis* (2021) 27 (4):1243–5. doi: 10.3201/eid2704.210138
2. Kupferschmidt K. Fast-Spreading U.K. Virus Variant Raises Alarms. *Science* (2021) 371(6524):9–10. doi: 10.1126/science.371.6524.9
3. Maggi F, Novazzi F, Genoni A, Baj A, Spezia PG, Focosi D, et al. Imported SARS-CoV-2 Variant P.1 in Traveler Returning From Brazil to Italy. *Emerg Infect Dis* (2021) 27(4):1249–51. doi: 10.3201/eid2704.210183
4. Tegally H, Wilkinson E, Giovanetti M, Iranzadeh A, Fonseca V, Giandhari J, et al. Detection of a SARS-CoV-2 Variant of Concern in South Africa. *Nature* (2021) 592(7854):438–43. doi: 10.1038/s41586-021-03402-9
5. Tegally H, Wilkinson E, Lessells RJ, Giandhari J, Pillay S, Msomi N, et al. Sixteen Novel Lineages of SARS-CoV-2 in South Africa. *Nat Med* (2021) 27 (3):440–6. doi: 10.1038/s41591-021-01255-3
6. European Centre for Disease Prevention and Control. *Threat Assessment Brief: Emergence of SARS-CoV-2 B.1.617 Variants in India and Situation in the EU/EEA* (2021). Available at: https://www.ecdc.europa.eu/en/publications-data/threat-assessment-emergence-sars-cov-2-b1617-variants.
7. Public Health England. *Investigation of Novel SARS-COV-2 Variant: Variant of Concern 202012/01: Technical Briefings* (2020). Available at: https://www.gov.uk/government/publications/investigation-of-novel-sars-cov-2-variant-variant- of-concern-20201201.
8. Barnes CO, Jette CA, Abernathy ME, Dam KA, Esswein SR, Gristick HB, et al. SARS-CoV-2 Neutralizing Antibody Structures Inform Therapeutic Strategies. *Nature* (2020) 588(7839):682–7. doi: 10.1038/s41586-020-2852-1
9. Lan J, Ge J, Yu J, Shan S, Zhou H, Fan S, et al. Structure of the SARS-CoV-2 Spike Receptor-Binding Domain Bound to the ACE2 Receptor. *Nature* (2020) 581(7807):215–20. doi: 10.1038/s41586-020-2180-5
10. Yuan M, Liu H, Wu NC, Lee CD, Zhu X, Zhao F, et al. Structural Basis of a Shared Antibody Response to SARS-CoV-2. *Science* (2020) 369(6507):1119–23. doi: 10.1126/science.abd2321
11. Abdool Karim SS, de Oliveira T. New SARS-CoV-2 Variants - Clinical, Public Health, and Vaccine Implications. *N Engl J Med* (2021) 384(19):1866–8. doi: 10.1056/NEJMc2100362

12. Corti D, Purcell LA, Snell G, Veesler D. Tackling COVID-19 With Neutralizing Monoclonal Antibodies. *Cell* (2021) 184(12):3086–108. doi: 10.1016/j.cell.2021.05.005
13. Garcia-Beltran WF, Lam EC, St Denis K, Nitido AD, Garcia ZH, Hauser BM, et al. Multiple SARS-CoV-2 Variants Escape Neutralization by Vaccine-Induced Humoral Immunity. *Cell* (2021) 184(9):2372–2383 e2379. doi: 10.1016/j.cell.2021.03.013
14. Harvey WT, Carabelli AM, Jackson B, Gupta RK, Thomson EC, Harrison EM, et al. SARS-CoV-2 Variants, Spike Mutations and Immune Escape. *Nat Rev Microbiol* (2021) 19(7):409–24. doi: 10.1038/s41579-021-00573-0
15. Hoffmann M, Arora P, Gross R, Seidel A, Hornich BF, Hahn AS, et al. SARS-CoV-2 Variants B.1.351 and P.1 Escape From Neutralizing Antibodies. *Cell* (2021) 184(9):2384–93.e2312. doi: 10.1016/j.cell.2021.03.036
16. McCallum M, De Marco A, Lempp FA, Tortorici MA, Pinto D, Walls AC, et al. N-Terminal Domain Antigenic Mapping Reveals a Site of Vulnerability for SARS-CoV-2. *Cell* (2021) 1842332-2347(9):e2316. doi: 10.1016/j.cell.2021.03.028
17. Planas D, Bruel T, Grzelak L, Guivel-Benhassine F, Staropoli I, Porrot F, et al. Sensitivity of Infectious SARS-CoV-2 B.1.1.7 and B.1.351 Variants to Neutralizing Antibodies. *Nat Med* (2021) 27(5):917–24. doi: 10.1038/s41591-021-01318-5
18. Tregoning JS, Flight KE, Higham SL, Wang Z, Pierce BF. Progress of the COVID-19 Vaccine Effort: Viruses, Vaccines and Variants Versus Efficacy, Effectiveness and Escape. *Nat Rev Immunol* (2021) 21(10):626–36. doi: 10.1038/s41577-021-00592-1
19. Wang P, Nair MS, Liu L, Iketani S, Luo Y, Guo Y, et al. Antibody Resistance of SARS-CoV-2 Variants B.1.351 and B.1.1.7. *Nature* (2021) 593(7857):130–5. doi: 10.1038/s41586-021-03398-2
20. Wang R, Zhang Q, Ge J, Ren W, Zhang R, Lan J, et al. Analysis of SARS-CoV-2 Variant Mutations Reveals Neutralization Escape Mechanisms and the Ability to Use ACE2 Receptors From Additional Species. *Immunity* (2021) 54 (7):1611–21.e1615. doi: 10.1016/j.immuni.2021.06.003
21. Zhang Q, Ju B, Ge J, Chan JF, Cheng L, Wang R, et al. Potent and Protective IGHV3-53/3-66 Public Antibodies and Their Shared Escape Mutant on the Spike of SARS-CoV-2. *Nat Commun* (2021) 12(1):4210. doi: 10.1038/s41467-021-24514-w
22. Chan KK, Tan TJC, Narayanan KK, Procko E. An Engineered Decoy Receptor for SARS-CoV-2 Broadly Binds Protein S Sequence Variants. *Sci Adv* (2021) 7 (8):eabf1738. doi: 10.1126/sciadv.abf1738
23. Laffeber C, de Koning K, Kanaar R, Lebbink JHG. Experimental Evidence for Enhanced Receptor Binding by Rapidly Spreading SARS-CoV-2 Variants. *J Mol Biol* (2021) 433(15):167058. doi: 10.1016/j.jmb.2021.167058
24. Wang Z, Schmidt F, Weisblum Y, Muecksch F, Barnes CO, Finkin S, et al. mRNA Vaccine-Elicited Antibodies to SARS-CoV-2 and Circulating Variants. *Nature* (2021) 592(7855):616–22. doi: 10.1038/s41586-021-03324-6
25. Madhi SA, Baillie V, Cutland CL, Voysey M, Koen AL, Fairlie L, et al. Efficacy of the ChAdOx1 Ncov-19 Covid-19 Vaccine Against the B.1.351 Variant. *N Engl J Med* (2021) 384(20):1885–98. doi: 10.1056/NEJMoa2102214
26. Cao Y, Su B, Guo X, Sun W, Deng Y, Bao L, et al. Potent Neutralizing Antibodies Against SARS-CoV-2 Identified by High-Throughput Single-Cell Sequencing of Convalescent Patients' B Cells. *Cell* (2020) 182(1):73–84.e16. doi: 10.1016/j.cell.2020.05.025
27. Hansen J, Baum A, Pascal KE, Russo V, Giordano S, Wloga E, et al. Studies in Humanized Mice and Convalescent Humans Yield a SARS-CoV-2 Antibody Cocktail. *Science* (2020) 369(6506):1010–4. doi: 10.1126/science.abd0827
28. Ju B, Zhang Q, Ge J, Wang R, Sun J, Ge X, et al. Human Neutralizing Antibodies Elicited by SARS-CoV-2 Infection. *Nature* (2020) 584(7819):115–9. doi: 10.1038/s41586-020-2380-z
29. Liu L, Wang P, Nair MS, Yu J, Rapp M, Wang Q, et al. Potent Neutralizing Antibodies Against Multiple Epitopes on SARS-CoV-2 Spike. *Nature* (2020) 584(7821):450–6. doi: 10.1038/s41586-020-2571-7
30. Robbiani DF, Gaebler C, Muecksch F, Lorenzi JCC, Wang Z, Cho A, et al. Convergent Antibody Responses to SARS-CoV-2 in Convalescent Individuals. *Nature* (2020) 584(7821):437–42. doi: 10.1038/s41586-020-2456-9
31. Rogers TF, Zhao F, Huang D, Beutler N, Burns A, He WT, et al. Isolation of Potent SARS-CoV-2 Neutralizing Antibodies and Protection From Disease in a Small Animal Model. *Science* (2020) 369(6506):956–63. doi: 10.1126/science.abc7520
32. Shi R, Shan C, Duan X, Chen Z, Liu P, Song J, et al. A Human Neutralizing Antibody Targets the Receptor-Binding Site of SARS-CoV-2. *Nature* (2020) 584(7819):120–4. doi: 10.1038/s41586-020-2381-y
33. Wec AZ, Wrapp D, Herbert AS, Maurer DP, Haslwanter D, Sakharkar M, et al. Broad Neutralization of SARS-Related Viruses by Human Monoclonal Antibodies. *Science* (2020) 369(6504):731–6. doi: 10.1126/science.abc7424
34. Zost SJ, Gilchuk P, Case JB, Binshtein E, Chen RE, Nkolola JP, et al. Potently Neutralizing and Protective Human Antibodies Against SARS-CoV-2. *Nature* (2020) 584(7821):443–9. doi: 10.1038/s41586-020-2548-6
35. Zost SJ, Gilchuk P, Chen RE, Case JB, Reidy JX, Trivette A, et al. Rapid Isolation and Profiling of a Diverse Panel of Human Monoclonal Antibodies Targeting the SARS-CoV-2 Spike Protein. *Nat Med* (2020) 26(9):1422–7. doi: 10.1038/s41591-020-0998-x
36. Chen RE, Winkler ES, Case JB, Aziati ID, Bricker TL, Joshi A, et al. *In Vivo* Monoclonal Antibody Efficacy Against SARS-CoV-2 Variant Strains. *Nature* (2021) 596(7870):103–8. doi: 10.1038/s41586-021-03720-y
37. Martinez DR, Schaefer A, Gobeil S, Li D, de la Cruz G, Parks R, et al. A Broadly Neutralizing Antibody Protects Against SARS-CoV, Pre-Emergent Bat CoVs, and SARS-CoV-2 Variants in Mice. *bioRxiv* (2021) 2021.04.27.441655. doi: 10.1101/2021.04.27.441655
38. Planas D, Veyer D, Baidaliuk A, Staropoli I, Guivel-Benhassine F, Rajah MM, et al. Reduced Sensitivity of SARS-CoV-2 Variant Delta to Antibody Neutralization. *Nature* (2021) 596(7871):276–80. doi: 10.1038/s41586-021-03777-9
39. Tortorici MA, Czudnochowski N, Starr TN, Marzi R, Walls AC, Zatta F, et al. Broad Sarbecovirus Neutralization by a Human Monoclonal Antibody. *Nature* (2021) 597(7874):103–8. doi: 10.1038/s41586-021-03817-4
40. Chi X, Yan R, Zhang J, Zhang G, Zhang Y, Hao M, et al. A Neutralizing Human Antibody Binds to the N-Terminal Domain of the Spike Protein of SARS-CoV-2. *Science* (2020) 369(6504):650–5. doi: 10.1126/science.abc6952
41. Pinto D, Park YJ, Beltramello M, Walls AC, Tortorici MA, Bianchi S, et al. Cross-Neutralization of SARS-CoV-2 by a Human Monoclonal SARS-CoV Antibody. *Nature* (2020) 583(7815):290–5. doi: 10.1038/s41586-020-2349-y
42. McCray PB Jr, Pewe L, Wohlford-Lenane C, Hickey M, Manzel L, Shi L, et al. Lethal Infection of K18-Hace2 Mice Infected With Severe Acute Respiratory Syndrome Coronavirus. *J Virol* (2007) 81(2):813–21. doi: 10.1128/jvi.02012-06
43. Zheng J, Wong LR, Li K, Verma AK, Ortiz ME, Wohlford-Lenane C, et al. COVID-19 Treatments and Pathogenesis Including Anosmia in K18-Hace2 Mice. *Nature* (2021) 589(7843):603–7. doi: 10.1038/s41586-020-2943-z
44. Hastie KM, Li H, Bedinger D, Schendel SL, Dennison SM, Li K, et al. Defining Variant-Resistant Epitopes Targeted by SARS-CoV-2 Antibodies: A Global Consortium Study. *Science* (2021) 374(6566):472–8. doi: 10.1126/science.abh2315
45. Schmidt T, Klemis V, Schub D, Mihm J, Hielscher F, Marx S, et al. Immunogenicity and Reactogenicity of Heterologous ChAdOx1 Ncov-19/mRNA Vaccination. *Nat Med* (2021) 27(9):1530–5. doi: 10.1038/s41591-021-01464-w
46. Stamatatos L, Czartoski J, Wan YH, Homad LJ, Rubin V, Glantz H, et al. mRNA Vaccination Boosts Cross-Variant Neutralizing Antibodies Elicited by SARS-CoV-2 Infection. *Science* (2021) eabg9175. doi: 10.1126/science.abg9175
47. Ge J, Wang R, Ju B, Zhang Q, Sun J, Chen P, et al. Antibody Neutralization of SARS-CoV-2 Through ACE2 Receptor Mimicry. *Nat Commun* (2021) 12 (1):250. doi: 10.1038/s41467-020-20501-9
48. Jiang L, Wang N, Zuo T, Shi X, Poon KM, Wu Y, et al. Potent Neutralization of MERS-CoV by Human Neutralizing Monoclonal Antibodies to the Viral Spike Glycoprotein. *Sci Transl Med* (2014) 6(234):234ra259. doi: 10.1126/scitranslmed.3008140
49. Audet J, Wong G, Wang H, Lu G, Gao GF, Kobinger G, et al. Molecular Characterization of the Monoclonal Antibodies Composing ZMAb: A Protective Cocktail Against Ebola Virus. *Sci Rep* (2014) 4:6881. doi: 10.1038/srep06881
50. McCoy AJ, Grosse-Kunstleve RW, Adams PD, Winn MD, Storoni LC, Read RJ. Phaser Crystallographic Software. *J Appl Crystallogr* (2007) 40(Pt 4):658–74. doi: 10.1107/S0021889807021206

51. Emsley P, Cowtan K. Coot: Model-Building Tools for Molecular Graphics. *Acta Crystallogr D Biol Crystallogr* (2004) 60(Pt 12 Pt 1):2126–32. doi: 10.1107/S0907444904019158
52. Adams PD, Afonine PV, Bunkoczi G, Chen VB, Davis IW, Echols N, et al. PHENIX: A Comprehensive Python-Based System for Macromolecular Structure Solution. *Acta Crystallogr D Biol Crystallogr* (2010) 66(Pt 2):213–21. doi: 10.1107/S0907444909052925
53. Lei J, Frank J. Automated Acquisition of Cryo-Electron Micrographs for Single Particle Reconstruction on an FEI Tecnai Electron Microscope. *J Struct Biol* (2005) 150(1):69–80. doi: 10.1016/j.jsb.2005.01.002
54. Zheng SQ, Palovcak E, Armache JP, Verba KA, Cheng Y, Agard DA. MotionCor2: Anisotropic Correction of Beam-Induced Motion for Improved Cryo-Electron Microscopy. *Nat Methods* (2017) 14(4):331–2. doi: 10.1038/nmeth.4193
55. Zhang K. Gctf: Real-Time CTF Determination and Correction. *J Struct Biol* (2016) 193(1):1–12. doi: 10.1016/j.jsb.2015.11.003
56. Zivanov J, Nakane T, Scheres SHW. Estimation of High-Order Aberrations and Anisotropic Magnification From Cryo-EM Data Sets in RELION-3.1. *IUCrJ* (2020) 7(Pt 2):253–67. doi: 10.1107/S2052252520000081
57. Pettersen EF, Goddard TD, Huang CC, Couch GS, Greenblatt DM, Meng EC, et al. UCSF Chimera–a Visualization System for Exploratory Research and Analysis. *J Comput Chem* (2004) 25(13):1605–12. doi: 10.1002/jcc.20084
58. Janson G, Zhang C, Prado MG, Paiardini A. PyMod 2.0: Improvements in Protein Sequence-Structure Analysis and Homology Modeling Within PyMOL. *Bioinformatics* (2017) 33(3):444–6. doi: 10.1093/bioinformatics/btw638

Conflict of Interest: The authors declare that the research was conducted in the absence of any commercial or financial relationships that could be construed as a potential conflict of interest.

Publisher's Note: All claims expressed in this article are solely those of the authors and do not necessarily represent those of their affiliated organizations, or those of the publisher, the editors and the reviewers. Any product that may be evaluated in this article, or claim that may be made by its manufacturer, is not guaranteed or endorsed by the publisher.

frontiers in Immunology

SYSTEMATIC REVIEW
published: 07 February 2022
doi: 10.3389/fimmu.2022.817829

Convalescent Plasma Treatment in Patients with Covid-19: A Systematic Review and Meta-Analysis

*Anselm Jorda[1], Manuel Kussmann[2], Nebu Kolenchery[3], Jolanta M. Siller-Matula[4,5], Markus Zeitlinger[1], Bernd Jilma[1] and Georg Gelbenegger[1]**

[1] Department of Clinical Pharmacology, Medical University of Vienna, Vienna, Austria, [2] Division of Infectious Diseases and Tropical Medicine, Department of Medicine I, Medical University of Vienna, Vienna, Austria, [3] Department of Public Health, Saint Louis County, St. Louis, MO, United States, [4] Division of Cardiology, Department of Medicine II, Medical University of Vienna, Vienna, Austria, [5] Department of Experimental and Clinical Pharmacology, Center for Preclinical Research and Technology (CEPT), Medical University of Warsaw, Warsaw, Poland

Convalescent plasma is a suggested treatment for Coronavirus disease 2019 (Covid-19), but its efficacy is uncertain. We aimed to evaluate whether the use of convalescent plasma is associated with improved clinical outcomes in patients with Covid-19.In this systematic review and meta-analysis, we searched randomized controlled trials investigating the use of convalescent plasma in patients with Covid-19 in Medline, Embase, Web of Science, Cochrane Library, and medRxiv from inception to October 17th, 2021. Two reviewers independently extracted the data. The primary efficacy outcome was all-cause mortality. The Cochrane Risk of Bias Tool and GRADE (Grading of Recommendations Assessment, Development and Evaluation) method were used. This study was registered with PROSPERO, CRD42021284861. Of the 8874 studies identified in the initial search, sixteen trials comprising 16 317 patients with Covid-19 were included. In the overall population, the all-cause mortality was 23.8% (2025 of 8524) with convalescent plasma and 24.4% (1903 of 7769) with standard of care (risk ratio (RR) 0.97, 95% CI 0.90-1.04) (high-certainty evidence). All-cause mortality did not differ in the subgroups of noncritically ill (21.7% [1288 of 5929] vs. 22.4% [1320 of 5882]) and critically ill (36.9% [518 of 1404] vs. 36.4% [455 of 1247]) patients with Covid-19. The use of convalescent plasma in patients who tested negative for anti-SARS-CoV-2 antibodies at baseline was not associated with significantly improved survival (RR 0.94, 95% CI 0.87-1.02). In the overall study population, initiation of mechanical ventilation (RR 0.97, 95% CI 0.88-1.07), time to clinical improvement (HR 1.09, 95% CI 0.91-1.30), and time to discharge (HR 0.95, 95% CI 0.89-1.02) were similar between the two groups. In patients with Covid-19, treatment with convalescent plasma, as compared with control, was not associated with lower all-cause mortality or improved disease progression, irrespective of disease severity and baseline antibody status.

Systematic Review Registration: https://www.crd.york.ac.uk/prospero/, identifier PROSPERO (CRD42021284861).

Keywords: antibodies, passive immunization, SARS-CoV-2, convalescent plasma (CP) therapy, coronavirus – COVID-19, serotherapy, hyperimmune globulin

OPEN ACCESS

Edited by:
Raymund Razonable, Mayo Clinic, United States

Reviewed by:
Javier Carbone, Gregorio Marañón Hospital, Spain
Anita Chandra, University of Cambridge, United Kingdom

****Correspondence:***
Georg Gelbenegger
georg.gelbenegger@meduniwien.ac.at

Specialty section:
This article was submitted to Vaccines and Molecular Therapeutics, a section of the journal Frontiers in Immunology

Received: *18 November 2021*
Accepted: *17 January 2022*
Published: *07 February 2022*

Citation:
Jorda A, Kussmann M, Kolenchery N, Siller-Matula JM, Zeitlinger M, Jilma B and Gelbenegger G (2022) Convalescent Plasma Treatment in Patients with Covid-19: A Systematic Review and Meta-Analysis. Front. Immunol. 13:817829. doi: 10.3389/fimmu.2022.817829

INTRODUCTION

Coronavirus disease 2019 (Covid-19) is an acute illness caused by the severe acute respiratory syndrome coronavirus 2 (SARS-CoV-2) that is associated with severe inflammation and organ dysfunction. Immunomodulatory treatments for Covid-19 remain elusive with only a few strategies (glucocorticoids and tocilizumab) showing a clear survival benefit. Therapeutic use of plasma from individuals who have recovered from Covid-19 has been hypothesized to show clinical benefits, particularly in immunocompromised patients and when used early in the course of the disease (1). The treatment rationale behind the use of convalescent plasma is to bridge the critical time period until a sufficient immune response is established in the infected patient (2). The use of convalescent plasma for the treatment of patients with Covid-19 has attracted widespread attention, yet definitive evidence of its efficacy is missing.

Observational data showed that convalescent plasma may have a role for patients who are immunocompromised and unable to adequately produce antibodies (3, 4). Further data suggested some benefits of targeting selected patient populations (non-intubated patients, age under 80 years) and using high-titer plasma (5–7). However, clinical data from randomized controlled trials were unable to reproduce these findings in an overall Covid-19 patient population.

With this systematic review we aimed to summarize all available data from published randomized controlled trials and discuss potential clinical implications. In the meta-analysis, we investigated whether convalescent plasma is associated with improved survival and disease progression.

METHODS

Search Strategy and Selection Criteria

This meta-analysis has been reported in accordance with the Preferred Reporting Items for Systematic Review and Meta-analysis and performed according to established methods, as described previously (8). This meta-analysis was registered at PROSPERO under the registration number CRD42021284861. We employed a systematic search strategy in Medline, Embase, Web of Science, Cochrane Library and the preprint server medRxiv from database inception through October 17th, 2021 by searching for Covid-19 (and related terms) and convalescent plasma (and related terms) (9). The exact search strategies can be found in **Appendix Table 1**. Retrieved articles were assessed for their eligibility by reading the title and abstract and, if necessary, the full text. References of identified articles and previous meta-analysis or systematic reviews were searched for additional literature. There were no restrictions on language, publication date, publication status restrictions, or geographic region.

Only full-text articles were included in this meta-analysis. We included trials that (i) were randomized controlled trials (RCTs), (ii) compared convalescent plasma with standard of care or placebo, and (iii) reported on at least one of our outcomes of interest (all-cause mortality, requirement of mechanical ventilation, time to clinical improvement, time to hospital discharge). Ongoing, retrospective, other non-RCTs, and duplicate studies were excluded. Studies were excluded from the analysis if one could determine, from the title, abstract, or both that the study did not meet the inclusion criteria. If an article could not be excluded with certainty, the full text of the study in question was acquired and evaluated. The literature search and study selection were independently carried out by two reviewers (A.J. and G.G.). Any discrepancies were resolved with personal discussion and author consensus.

Data Analysis

Selected trials included patients with Covid-19, that were being randomly allocated to convalescent plasma, standard-of-care treatment, or placebo and standard-of-care treatment. Randomized controlled trials were included regardless of the level of plasma titer (high or low antibody titer), number of patients included or healthcare setting (inpatient or outpatient). We extracted the following information for each RCT: trial design characteristics, number of patients included, patient demographics, convalescent plasma treatment details and regimen.

High antibody titer was defined as S-protein receptor-binding domain-specific IgG antibody titer of 1:640 or higher or serum neutralization titer of 1:40 or higher, according to previously used definitions (10).

The primary efficacy outcome was all-cause mortality. Secondary outcomes included requirement of mechanical ventilation after enrollment, time to clinical improvement, and time to hospital discharge. Due to variable endpoint definitions and study designs of the included trials, the pooling of other relevant endpoints was not feasible. We performed predefined subgroup analyses for all-cause mortality comparing critically ill and noncritically ill patients and patients with and without anti-SARS-CoV-2 antibodies at baseline. The definition of critically ill patients included those with shock or organ failure requiring admission to an intensive care unit (ICU), invasive mechanical ventilation, and/or vasopressors. Noncritically ill patients were those with moderate to severe Covid-19 not admitted to an ICU and without organ failure or shock. Sensitivity analyses were performed by removing each trial from the overall analyses and testing the impact of fixed- versus random-effect models of each outcome. Another sensitivity analysis involved the removal of preprint studies from the overall analysis. All reports eligible for analysis were assessed using the Cochrane Risk of Bias Tool. Publication bias was assessed by preparing funnel plots based on fixed-effect models of the key outcomes of the meta-analysis. Finally, the overall certainty of evidence for the primary and secondary outcomes was assessed according to the GRADE recommendations (11).

The data was extracted from full-text publications and, if available, supplementary files. Categorical variables are reported as frequencies and percentages. Results were pooled according to the inverse variance model. Risk ratios (RR) with 95% confidence intervals (95% CI) or hazard ratios (HR) with 95% CIs of each study and of pooled data are reported. Unadjusted p values are reported throughout, with hypothesis testing set at the two-tailed significance level of below 0.05. Heterogeneity between studies was assessed by inconsistency testing (I^2). Percentages lower than

25% (I^2 < 25%), between 25% and 50% (25% ≥ I^2 < 50%), or 50% or higher (I^2 ≥ 50%) correspond to low, medium and high heterogeneity, respectively. Due to high clinical heterogeneity of the included trials, a random-effect model was used. The statistical analysis was carried out using Review Manager (Version 5.4 Copenhagen: The Nordic Cochrane Centre, The Cochrane Collaboration, 2014).

Role of Funding Source

There was no funding source for this study. G.G. is supported by a grant from the Austrian Science Funds (SFB54-P04) and by the Federal Ministry of Education, Science and Research for performing the ACOVACT trial.

RESULTS

The literature search identified a total of 8874 records (**Figure 1**). After removal of duplicates and articles that were not randomized controlled trials, 27 articles were assessed for eligibility. Of these, eleven articles were excluded because they were retrospective studies (n=3), investigated other treatments (n=3), were study protocols (n=2), or because of other reasons (n=3). One trial was excluded because it was not a randomized trial (12). The final analysis included sixteen trials with a total of 16 317 patients. Twelve studies were published in peer-reviewed journals (13–24) and four were published on the preprint server medRxiv (25–28). Included trials were performed in North and South America, Europe, Asia and Australia (**Appendix Table 2**). Seven trials were terminated early, because of futility or poor recruitment. One trial was stopped early after emergency use authorization was granted for convalescent plasma in the United States (23). Four included trials were double-blind, placebo-controlled trials (20–23); one trial was single-blind (24), and the remaining trials were all open-label. The trials only included patients with confirmed Covid-19, except for the RECOVERY trial, which also included patients with suspected SARS-CoV-2 infection (18). Only one trial included outpatients (20). In one trial, patients were randomly allocated to either convalescent plasma or fresh frozen plasma in addition to the standard of care (26). Patients received a single infusion of convalescent plasma in eight trials and were given two infusions 24 hours apart in seven trials. Plasma antibody titers ranged from 1:100 to 1:1000. Five trials did not provide plasma titers (13, 14, 24, 26, 28). Eleven of the sixteen trials reported on the time from symptom onset to enrolment. Of these, nine trials had median durations from symptom onset to enrolment between 7 and 10 days (**Table 1**). The longest median duration was reported by the ChiCTR trial (median [IQR], 27 [22-39] vs.30 [19-38] days), and the shortest mean duration was reported by the INFANT-COVID-19 trial (mean ± SD, 1.7 ± 0.6 vs. 1.6 ± 0.6 days). Six trials assessed the anti-SARS-CoV-2 antibody status at baseline. In the convalescent plasma group, 56% of patients (3986 of 7120) had pre-existing antibodies and 33% (2417 of 7120) had no antibodies at baseline. In the control group, 52% of patients (3467 of 6690) had pre-existing antibodies and 29% (1992 of 6690) had no antibodies at baseline. The serologic status of the remaining patients was unknown.

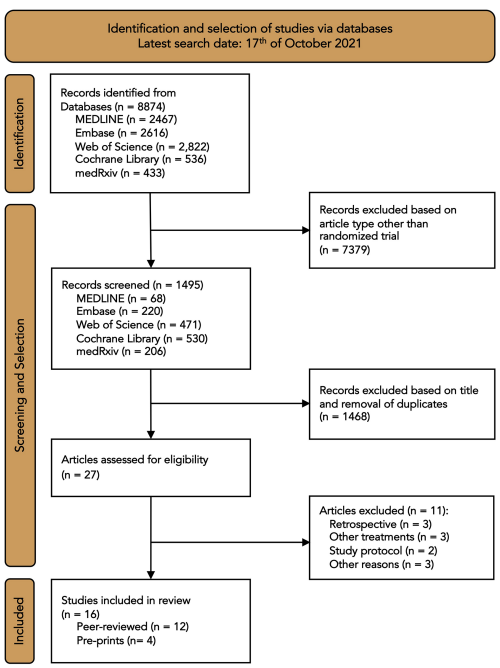

FIGURE 1 | Flow diagram of search and selection process.

Using the Cochrane Risk of Bias Tool, the risk of bias of the key outcomes of this meta-analysis was assessed as low for most of the trials (**Appendix Table 3**). In two trials, some concerns were associated with the risk of bias arising from the randomization process (14, 25). The risk of bias was deemed high in one trial because of incomplete reporting on randomization and treatment allocation and adherence (28). Funnel plots did not show obvious asymmetry, indicating no clear evidence of publication bias (**Appendix Figure 1**).

The primary endpoint all-cause mortality was assessed in all sixteen trials. All-cause mortality was assessed from 15 to 30 days after randomization in fourteen trials. Two trials assessed all-cause mortality 60 days after randomization (17, 24), and one trial did not provide the length of follow-up (14). Five trials only included noncritically ill patients (13, 14, 20, 25, 28), and one trial included only critically ill patients with Covid-19 (16). Of the remaining ten trials, two trials provided subgroup analyses for all-cause mortality in noncritically and critically ill patients (18, 19). Two trials performed a subgroup analysis of all-cause mortality according to the anti-SARS-CoV-2 antibody status at baseline (16, 18).

Data on the use of mechanical ventilation were available in seven trials (six peer-reviewed and one preprint). Time to hospital discharge was assessed in eight trials, only one of which was published as a preprint. All trials reporting on time to hospital discharge provided hazard ratios. Similarly, four trials

TABLE 1 | Characteristics of the included trials.

Study	Status	Illness severity	Symptom onset to enrolment (median days)	Blinding	Dose description	Titer	Control arm	N (n vs. n)
AlQahtani et al., 2021 (14)	Completed	Noncritical	Not reported	Open label	Two transfusions of 200 mL administered 24 h apart	Not specified	SOC	40 (20 vs. 20)
CONCOR-1, 2021 (15)	Terminated early	Noncritical and critical	8 (5–10) vs.8 (5–10)	Open label	Single transfusion of 500 mL	Low (>1:100 RBD)	SOC	921 (614 vs. 307)
ConCOVID, 2021 (17)	Terminated early	Noncritical and critical	9 (7–13) vs. 11 (6–16)	Open label	Single transfusion of 300 mL	Low (≥1:400 RBD)	SOC	86 (43 vs. 43)
ChiCTR, 2020 (19)	Terminated early	Noncritical and critical	27 (22-39) vs. 30 (19-38)	Open label	Single transfusion of 4 to 13 mL/kg body weight	High (not specified)	SOC	103 (52 vs. 51)
O'Donnell, 2021 (21)	Completed	Noncritical and critical	10 (7–13) vs. 9 (7–11)	Double-blind	Single transfusion of 200 to 250 mL	Low (1:400)	SOC + placebo	223 (150 vs. 73)
PLACID, 2020 (13)	Completed	Noncritical	8 (6-11) vs. 8 (6-11)	Open label	Two transfusions of 200 mL administered 24 h apart	Not specified	SOC	464 (235 vs. 229)
RECOVERY, 2021 (18)	Completed	Noncritical and critical	9 (6–12) vs. 9 (6–12)	Open label	Two transfusions of 200 to 350 mL administered 12 h apart	High (neutralizing titers of 1:100)	SOC	11 558 (5795 vs. 5763)
REMAP-CAP, 2021 (16)	Terminated according to protocol	Critical	Not reported	Open label	Two transfusions of 550 ± 150 mL	High (not specified)	SOC	2000 (1084 vs. 916)
PlasmAr, 2021 (22)	Completed	Noncritical and critical	8 (5–10) vs. 8 (5–10)	Double-blind	Single transfusion of 5 to 10 mL/kg body weight	High (≥1:800 RBD)	SOC + placebo	333 (228 vs. 105)
Bennett-Guerrero et al., 2021 (23)	Terminated early	Noncritical and critical	9 (6–18) vs. 9 (6–15)	Double-blind	Two transfusions of 480 mL	≥145 reflectance light units for IgG	SOC + placebo	74 (59 vs. 15)
Pouladzadeh et al., 2021 (24)	Completed	Noncritical and critical	Not reported	Single-blind	One or two transfusions of 500mL	Not specified	SOC	60 (30 vs. 30)
INFANT-COVID-19, 2021 (20)	Terminated early	Noncritical	1.7 ± 0.6 vs. 1.6 ± 0.6*	Double-blind	Single transfusion of 250mL	High (IgG titer > 1:1000)	SOC + placebo	160 (80 vs. 80)
ConPlas-19 (preprint) (25)	Terminated early	Noncritical	8 (7–9) vs. 8 (6-9)	Open label	Single transfusion of 250 to 300 mL	High (VMNT-ID50: all titers >1:80)	SOC	81 (38 vs. 43)
PICP19 (preprint) (28)	Not reported	Noncritical	Not reported	Open label	Two transfusions of 200mL	Not specified	SOC	80 (40 vs. 40)
CAPSID (preprint) (27)	Not reported	Noncritical and critical	7 (2-9) vs. 7 (5-10.5)	Open label	Three transfusions on day 1, 3, 5	Median PRNT50 titer 1:160 IQR: 1:80 to 1:320	SOC	105 (53 vs. 52)
ILBS-COVID-02 (preprint) (26)	Not reported	Noncritical and critical	Not reported	Open label	Two transfusions of 500 mL administered 24 h apart	Not specified	SOC + FFP	29 (14 vs. 15)

IgG, immunoglobulin G; PRNT50, concentration of serum to reduce the number of plaques by 50%; RBD, receptor-binding domain; SOC, standard of care; VMNT-ID50 virus microneutralization test - ID50% assay.
**mean ± standard deviation.*

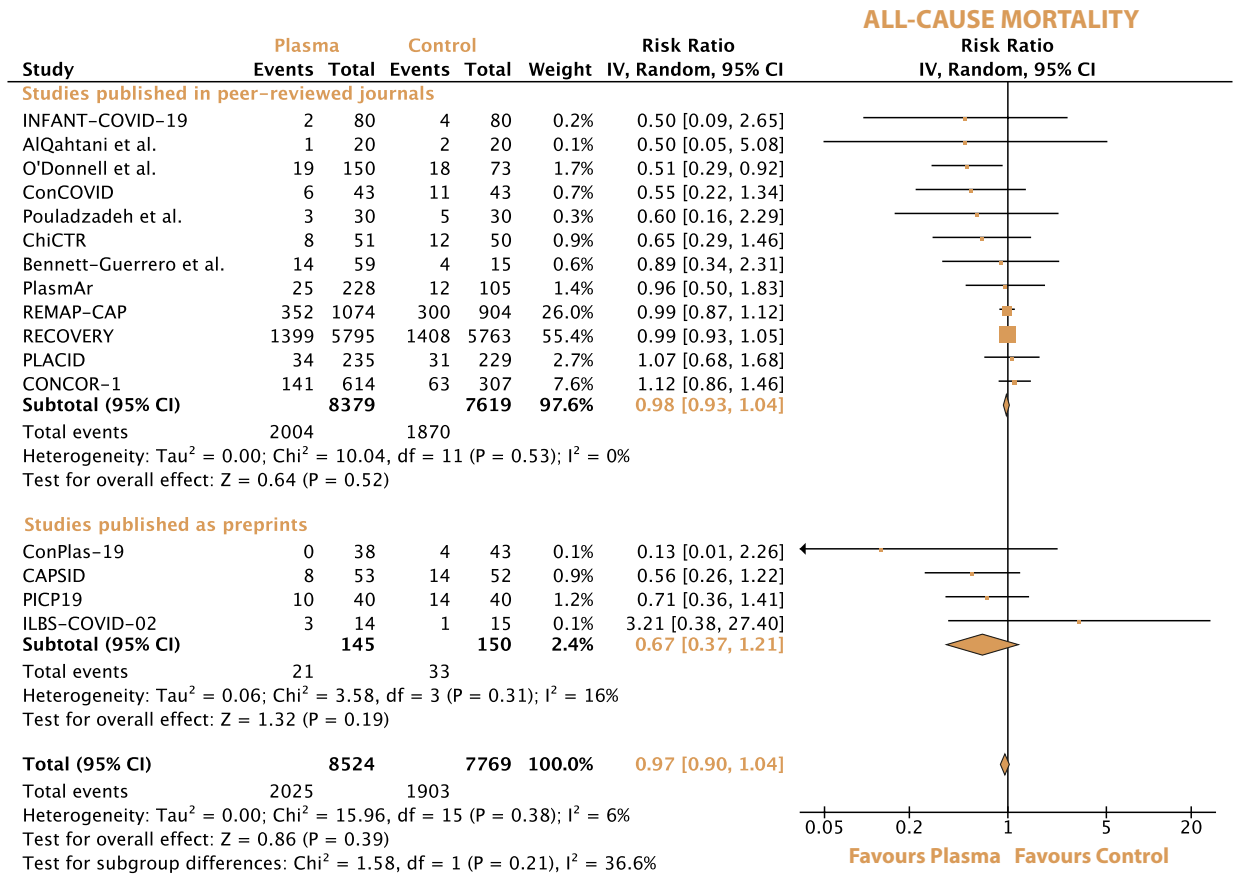

FIGURE 2 | Forrest plot depicting the risk ratio of all-cause mortality between treatment with convalescent plasma and standard of care alone.

provided data on time to clinical improvement (three published in peer-reviewed journals, one as a preprint) using hazard ratios.

In the overall population, the all-cause mortality was 23.8% (2025 of 8524) with convalescent plasma and 24.4% (1903 of 7769) with standard of care. The risk ratio for all-cause mortality between convalescent plasma and standard of care was 0.97 (95% CI 0.90-1.04, p = 0.39) (**Figure 2**). After excluding the preprints, the all-cause mortality was 23.9% (2004 of 8379) with convalescent plasma and 24.5% (1870 of 7619) with standard of care alone, resulting in a risk ratio of 0.98 (95% CI 0.93-1.04, p = 0.53).

Convalescent plasma neither decreased the risk for all-cause mortality in noncritically ill patients (21.7% [1288 of 5929] vs. 22.4% [1320 of 5882]) nor in critically ill patients with Covid-19 (36.9% [518 of 1404] vs. 36,4% [455 of 1247]). The risk ratios for all-cause mortality were 0.97 (95% CI 0.91-1.04, p = 0.38) in noncritically ill patients and 1.04 (95% CI 0.93-1.16, p = 0.49) in critically ill patients (**Appendix Figure 2**).

All-cause mortality did not differ significantly in patients with or without preexisting anti-SARS-CoV-2 antibodies at baseline (20.8% [765 of 3675] vs. 19.8% [636 of 3219]) and 33.8% [772 of 2286] vs. 35.2% [636 of 1808]), respectively) (**Appendix Figure 3**). The respective risk ratios for all-cause mortality were 1.03 (95% CI 0.93-1.12, p = 0.6) in patients with preexisting anti-SARS-CoV-2 antibodies and 0.94 (95% CI 0.87-1.02, p = 0.16) in patients without antibodies.

Initiation of mechanical ventilation was required in 11.8% (734 of 6236) of patients with convalescent plasma and in 12.2% (734 of 5993) of patients with standard of care (RR 0.97, 95% CI 0.88-1.07, p = 0.54) (**Appendix Figure 4**).

The time to clinical improvement was reported by four trials. The definitions of clinical improvement varied among the trials and were specified as improvement of one or two points on similar but not identical ordinal outcome scales (**Appendix Table 4**). The median days to clinical improvement are provided in **Appendix Table 4**. Overall, the time to clinical improvement was similar between patients receiving convalescent plasma and the control group (HR 1.09, 95% CI 0.91-1.30, p = 0.37) (**Appendix Figure 5**).

Given the different levels of illness severity, the median time to hospital discharge varied considerably among the seven trials included in this analysis. The REMAP-CAP trial (16) reported the longest median time to hospital discharge between convalescent plasma and control (44 vs. 39 days, HR 0.95, 95% CI 0.86-1.06), and the trial by Pouladzadeh at al. (24). reported the shortest mean hospital stay (8.7 ± 3.9 vs. 6.7 ± 4.3 days, HR

0.37, 95% CI 0.02-6.84) (**Appendix Table 5**). Overall, the use of convalescent plasma, as compared with control, was not associated with a reduced time to hospital discharge (HR 0.95, 95% CI 0.89-1.02, p = 0.19) (**Appendix Figure 6**).

The sequential exclusion of each trial from the overall analyses did not change the pooled risk ratios and hazard ratios for any of the outcomes significantly. The exclusion of the preprints also did not change any of the pooled outcomes. For all-cause mortality, there was no statistically significant subgroup difference and a medium level of heterogeneity between peer-reviewed articles and preprints (Chi^2 = 1.58, I^2 = 36.6%, p = 0.21) (**Figure 2**). For all-cause mortality between noncritically and critically ill patients, there was no statistically significant subgroup difference and a low level of heterogeneity (Chi^2 = 1.09, I^2 = 8.2%, p = 0.3) (**Appendix Figure 2**). No statistically significant subgroup difference was observed between seronegative and seropositive patients in terms of all-cause mortality (Chi^2 = 1.79, I^2 = 44.1%, p = 0.18). Switching from a random-effect model to a fixed-effect model did not influence the outcomes of the meta-analyses significantly.

According to the GRADE assessment, the evidence for the observed effect of convalescent plasma on all-cause mortality is high (**Appendix Table 6**). The width of the 95% confidence interval (0.93-1.04 without preprints and 0.90-1.04 with preprints) makes substantial clinical effects on mortality unlikely in the given patient population. Further factors contributing to the high level of certainty of evidence include the large sample size (over 16 000 patients), the objective endpoint death, the low level of heterogeneity (I^2 = 6%) and the robustness to sensitivity analyses. Similarly, the certainty of evidence for the use of mechanical ventilation was rated as high. The evidence for the effect of convalescent plasma on the time to hospital discharge was downgraded to moderate because of moderate concerns regarding the risk of bias, which might have been introduced by incomplete reporting and the subjectiveness of the endpoint. The evidence for the time of clinical improvement was downgraded to very low because of serious concerns regarding the risk of bias, incomplete reporting, heterogenous endpoint definitions, and imprecision (95% CI 0.91-1.30).

DISCUSSION

In this meta-analysis that included sixteen RCTs with over 16 000 patients with Covid-19, there was no significant difference in all-cause mortality or any other clinical outcomes between treatment with convalescent plasma and control (standard of care alone or standard of care and placebo) (**Figure 3**). Similarly, there was no difference in all-cause mortality between convalescent plasma and control in the subgroups of critically ill or noncritically ill patients and in patients without anti-SARS-CoV-2 antibodies at baseline. This meta-analysis confirms the results of previous analyses which did not support the routine use of convalescent plasma.

So far, very few immunomodulatory agents, glucocorticoids and interleukin-6 antagonists, have been shown to significantly reduce mortality in patients hospitalized with Covid-19 (29, 30). Failure of RCTs to show a significant survival benefit of convalescent plasma could be due to a number of reasons: (i) In contrast to other pharmacological treatments against Covid-19, convalescent plasma is not artificially produced but collected from patients who recovered from a SARS-CoV-2 infection. Although the U.S. Food and Drug Administration provides guidance on the collection and use of convalescent plasma (31), it is inherently variable, which may confound the evidence of its potential benefits. In the sixteen included trials, six titer cut-offs using different SARS-CoV-2 antibody detection assays were defined, six trials did not specify any thresholds, and almost all trials administered different plasma volumes (**Table 1**); (ii) most patients were included more than seven days after symptom onset. Delayed patient inclusion might have concealed potential therapeutic effects of convalescent plasma; (iii) the type of SARS-CoV-2 variant of the infected individual may also affect the patient's clinical response to treatment with convalescent plasma. SARS-CoV-2 variant types, of both the infected patient and the infused convalescent plasma, were not reported; (iv) cumulatively, more than 50% of patients in the treatment group tested positive for preexisting anti-SARS-CoV-2 antibodies at baseline, while around 30% of patients in the treatment group tested negative. Considering that the anticipated treatment effect of convalescent plasma is the highest in patients without adequate immune response, the vast inclusion of immunocompetent patients might have confounded the results. The question remains whether the absence of baseline anti-SARS-CoV-2 antibodies may potentially be helpful to guide the appropriate use of convalescent plasma. Our subgroup analysis, although possibly underpowered, showed no significant survival benefit of convalescent plasma over control in patients who tested negative for anti-SARS-CoV-2 antibodies at baseline.

In light of these uncertainties, it is unclear whether different plasma products, given at different stages of disease progression, may convey therapeutic benefits. The expected - but to this day undetected - treatment benefit might only apply for selected populations, such as immunocompromised patients. Clinical trials have included an overall patient population with Covid-19, irrespective of immunocompetency, and were therefore unable to determine the efficacy of convalescent plasma in immunocompromised patients. Treatment advantages of convalescent plasma have been observed in immuno-compromised patients (32, 33) but lack of data from prospective RCTs precludes clear recommendations for this particular patient population. One larger trial, although only of observational nature, investigating the efficacy and safety of convalescent plasma in immunocompromised patients is currently underway (NCT04884477).

No formal analysis was performed on the safety profile or serious adverse events because of limited data availability and inadequate quality of data. The use of convalescent plasma is deemed safe, with a low incidence of serious adverse events (5).

The RECOVERY trial was the only study that was powered for the primary endpoint all-cause mortality. The remaining trials were potentially susceptible to biased adjudication of

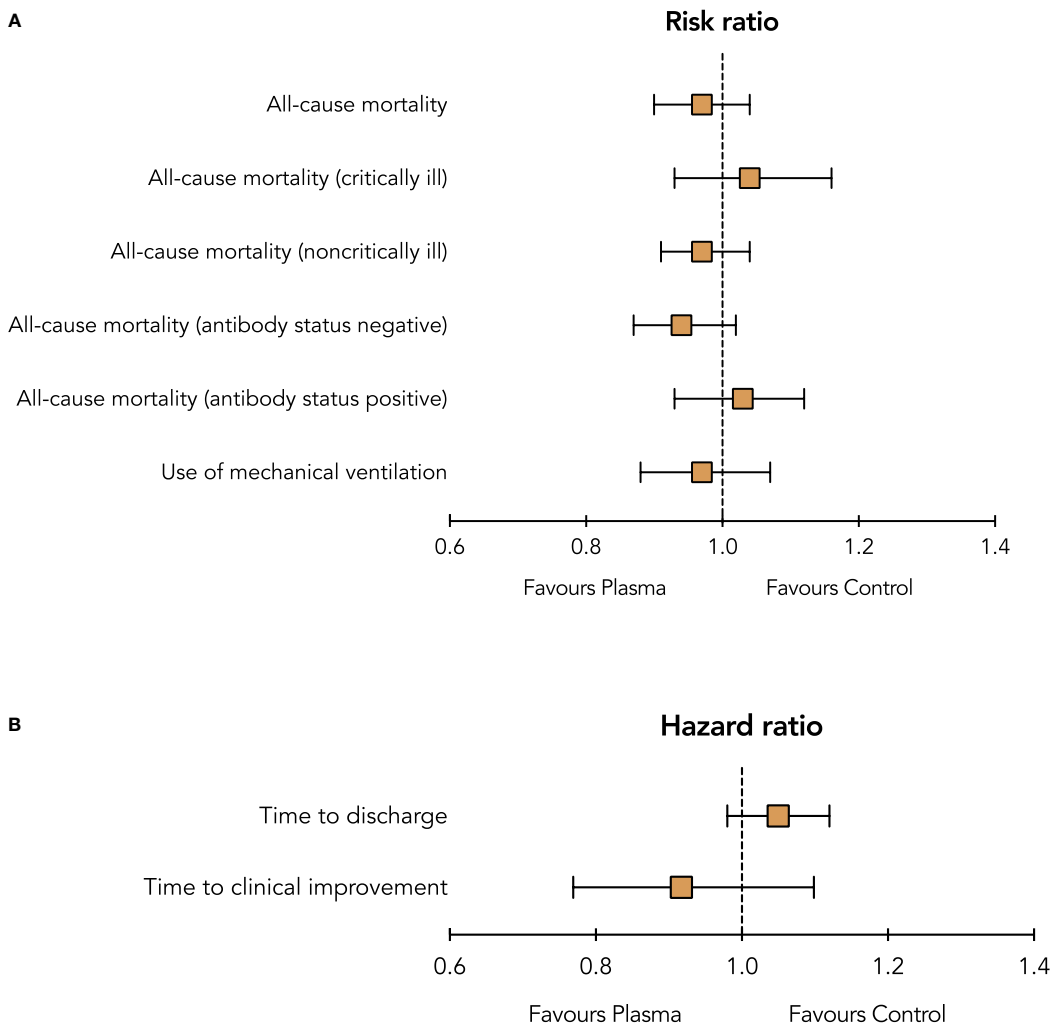

FIGURE 3 | Summary risk ratios **(A)** and hazard ratios **(B)** of outcomes between treatment with convalescent plasma and control (standard of care with or without placebo).

primary and secondary outcomes (use of ventilation, time to clinical improvement, time to hospital discharge, clinical status, or disease progression) due to their open-label design (34).

The current guidelines from the National Institute of Health already recommend against the use of convalescent plasma in patients without impaired immunity but acknowledge insufficient evidence to recommend either for or against the use of convalescent plasma in immunocompromised patients with Covid-19 (35). Considering the overall lack of evidence for convalescent plasma in patients with Covid-19, the associated high treatment costs (36), and tenuous supply (especially when only high-titer plasma is sought) may contribute to a negative cost-effectiveness balance and may not warrant routine clinical use. In addition, the recent emergence of neutralizing monoclonal antibodies against SARS-CoV-2, having already shown a good clinical efficacy and safety profile, may render the use of convalescent plasma obsolete in the future (37–40).

The main strength of this meta-analysis is the large sample size of over 16 000 patients and the low heterogeneity of all-cause mortality among the trials. Considering the high quality of most of the included RCTs, the results of this meta-analysis provide a high certainty of evidence and should assist physician and health care providers in their decision-making in the current pandemic.

This study has several limitations. First, data from four studies were only available as preprint versions, which have not yet been peer-reviewed. However, they only contributed a small proportion of the patient population, and sensitivity analyses showed that the results were not changed by these preprints. Second, treatment regimens of convalescent plasma varied significantly between trials. Nine trials did not define the time window of symptom onset to treatment. Third, time of outcome assessment of the primary endpoint was not the same between trials. Fourth, twelve of the sixteen trials were open-label trials, which may have influenced the assessment of clinical outcomes. Fifth, contrary to the overall analysis, the

subgroup analyses were possibly underpowered and should be interpreted with caution. Sixth, except for one trial (20), the results of this meta-analysis only apply to patients hospitalized with moderate or severe Covid-19. The efficacy of convalescent plasma in mild Covid-19 remains unclear. Seventh, the RECOVERY trial contributed to 71% of patients (11 558 of 16 293) and 55% of the weight of the meta-analysis in the random-effects model. Notably, the results of the RECOVERY trial were consistent with the pooled outcomes of the remaining studies. Eighth, trials did not provide sufficient data to assess the potential therapeutic benefit of convalescent plasma in patients with Covid-19 and impaired immunity or increased inflammatory markers.

In conclusion, convalescent plasma treatment compared with control was not associated with a significant decrease in all-cause mortality or with any improvement of other clinical outcomes in the overall patient population, consisting of critically ill and noncritically ill patients with Covid-19. Considering the high certainty of evidence, these results do not support the routine clinical use of convalescent plasma in patients with Covid-19.

DATA AVAILABILITY STATEMENT

The raw data supporting the conclusions of this article will be made available by the authors, without undue reservation.

AUTHOR CONTRIBUTIONS

GG conceived the idea. AJ and GG performed the research, interpreted the results, and drafted the manuscript. All authors critically revised the manuscript and approved the final version for publication.

SUPPLEMENTARY MATERIAL

The Supplementary Material for this article can be found online at: https://www.frontiersin.org/articles/10.3389/fimmu.2022.817829/full#supplementary-material

REFERENCES

1. Chen L, Xiong J, Bao L, Shi Y. Convalescent Plasma as a Potential Therapy for COVID-19. *Lancet Infect Dis* (2020) 20(4):398–400. doi: 10.1016/S1473-3099(20)30141-9
2. Luke TC, Kilbane EM, Jackson JL, Hoffman SL. Meta-Analysis: Convalescent Blood Products for Spanish Influenza Pneumonia: A Future H5N1 Treatment? *Ann Intern Med* (2006) 145(8):599–609. doi: 10.7326/0003-4819-145-8-200610170-00139
3. Clark E, Guilpain P, Filip IL, Pansu N, Le Bihan C, Cartron G, et al. Convalescent Plasma for Persisting COVID-19 Following Therapeutic Lymphocyte Depletion: A Report of Rapid Recovery. *Br J Haematol* (2020) 190(3):e154–e6. doi: 10.1111/bjh.16981
4. Thompson MA, Henderson JP, Shah PK, Rubinstein SM, Joyner MJ, Choueiri TK, et al. Association of Convalescent Plasma Therapy With Survival in Patients With Hematologic Cancers and COVID-19. *JAMA Oncol* (2021) 7(8):1167–75. doi: 10.1101/2021.02.05.21250953
5. Joyner MJ, Bruno KA, Klassen SA, Kunze KL, Johnson PW, Lesser ER, et al. Safety Update: COVID-19 Convalescent Plasma in 20,000 Hospitalized Patients. *Mayo Clin Proc* (2020) 95(9):1888–97. doi: 10.1016/j.mayocp.2020.06.028
6. Joyner MJ, Senefeld JW, Klassen SA, Mills JR, Johnson PW, Theel ES, et al. Effect of Convalescent Plasma on Mortality Among Hospitalized Patients With COVID-19: Initial Three-Month Experience. *medRxiv* (2020). doi: 10.1101/2020.08.12.20169359
7. Joyner MJ, Carter RE, Senefeld JW, Klassen SA, Mills JR, Johnson PW, et al. Convalescent Plasma Antibody Levels and the Risk of Death From Covid-19. *N Engl J Med* (2021) 384(11):1015–27. doi: 10.1056/NEJMoa2031893
8. Page MJ, McKenzie JE, Bossuyt PM, Boutron I, Hoffmann TC, Mulrow CD, et al. The PRISMA 2020 Statement: An Updated Guideline for Reporting Systematic Reviews. *BMJ* (2021) 372:n71. doi: 10.1136/bmj.n71
9. McGowan J, Sampson M, Salzwedel DM, Cogo E, Foerster V, Lefebvre C. PRESS Peer Review of Electronic Search Strategies: 2015 Guideline Statement. *J Clin Epidemiol* (2016) 75:40–6. doi: 10.1016/j.jclinepi.2016.01.021
10. Janiaud P, Axfors C, Schmitt AM, Gloy V, Ebrahimi F, Hepprich M, et al. Association of Convalescent Plasma Treatment With Clinical Outcomes in Patients With COVID-19: A Systematic Review and Meta-Analysis. *JAMA* (2021) 325(12):1185–95. doi: 10.1001/jama.2021.2747
11. Guyatt GH, Oxman AD, Vist GE, Kunz R, Falck-Ytter Y, Alonso-Coello P, et al. GRADE: An Emerging Consensus on Rating Quality of Evidence and Strength of Recommendations. *BMJ* (2008) 336(7650):924–6. doi: 10.1136/bmj.39489.470347.AD
12. Abolghasemi H, Eshghi P, Cheraghali AM, Imani Fooladi AA, Bolouki Moghaddam F, Imanizadeh S, et al. Clinical Efficacy of Convalescent Plasma for Treatment of COVID-19 Infections: Results of a Multicenter Clinical Study. *Transfus Apher Sci* (2020) 59(5):102875. doi: 10.1016/j.transci.2020.102875
13. Agarwal A, Mukherjee A, Kumar G, Chatterjee P, Bhatnagar T, Malhotra P. Convalescent Plasma in the Management of Moderate Covid-19 in Adults in India: Open Label Phase II Multicentre Randomised Controlled Trial (PLACID Trial). *Bmj* (2020) 371:m3939. doi: 10.1136/bmj.m3939
14. AlQahtani M, Abdulrahman A, Almadani A, Alali SY, Al Zamrooni AM, Hejab AH, et al. Randomized Controlled Trial of Convalescent Plasma Therapy Against Standard Therapy in Patients With Severe COVID-19 Disease. *Sci Rep* (2021) 11(1):9927. doi: 10.1038/s41598-021-89444-5
15. Bégin P, Callum J, Jamula E, Cook R, Heddle NM, Tinmouth A, et al. Convalescent Plasma for Hospitalized Patients With COVID-19: An Open-Label, Randomized Controlled Trial. *Nat Med* (2021) 27(11):2012–24. doi: 10.1038/s41591-021-01488-2
16. Estcourt LJ, Turgeon AF, McQuilten ZK, McVerry BJ, Al-Beidh F, Annane D, et al. Effect of Convalescent Plasma on Organ Support-Free Days in Critically Ill Patients With COVID-19: A Randomized Clinical Trial. *JAMA* (2021) 326(17):1690–702. doi: 10.1001/jama.2021.18178
17. Gharbharan A, Jordans CCE, GeurtsvanKessel C, den Hollander JG, Karim F, Mollema FPN, et al. Effects of Potent Neutralizing Antibodies From Convalescent Plasma in Patients Hospitalized for Severe SARS-CoV-2 Infection. *Nat Commun* (2021) 12(1):3189. doi: 10.1038/s41467-021-23469-2
18. RECOVERY Collaborative Group. Convalescent Plasma in Patients Admitted to Hospital With COVID-19 (RECOVERY): A Randomised Controlled, Open-Label, Platform Trial. *Lancet* (2021) 397(10289):2049–59. doi: 10.1016/S0140-6736(21)00897-7
19. Li L, Zhang W, Hu Y, Tong X, Zheng S, Yang J, et al. Effect of Convalescent Plasma Therapy on Time to Clinical Improvement in Patients With Severe and Life-Threatening COVID-19: A Randomized Clinical Trial. *JAMA* (2020) 324(5):460–70. doi: 10.1001/jama.2020.10044
20. Libster R, Perez Marc G, Wappner D, Coviello S, Bianchi A, Braem V, et al. Early High-Titer Plasma Therapy to Prevent Severe Covid-19 in Older Adults. *N Engl J Med* (2021) 384(7):610–8. doi: 10.1056/NEJMoa2033700
21. O'Donnell MR, Grinsztejn B, Cummings MJ, Justman JE, Lamb MR, Eckhardt CM, et al. A Randomized Double-Blind Controlled Trial of Convalescent Plasma in Adults With Severe COVID-19. *J Clin Invest* (2021) 131(13):e150646. doi: 10.1172/JCI150646

22. Simonovich VA, Burgos Pratx LD, Scibona P, Beruto MV, Vallone MG, Vázquez C, et al. A Randomized Trial of Convalescent Plasma in Covid-19 Severe Pneumonia. *N Engl J Med* (2021) 384(7):619–29. doi: 10.1056/NEJMoa2031304
23. Bennett-Guerrero E, Romeiser JL, Talbot LR, Ahmed T, Mamone LJ, Singh SM, et al. Severe Acute Respiratory Syndrome Coronavirus 2 Convalescent Plasma Versus Standard Plasma in Coronavirus Disease 2019 Infected Hospitalized Patients in New York: A Double-Blind Randomized Trial. *Crit Care Med* (2021) 49(7):1015–25. doi: 10.1097/CCM.0000000000005066
24. Pouladzadeh M, Safdarian M, Eshghi P, Abolghasemi H, Bavani AG, Sheibani B, et al. A Randomized Clinical Trial Evaluating the Immunomodulatory Effect of Convalescent Plasma on COVID-19-Related Cytokine Storm. *Intern Emerg Med* (2021) 16(8):2181–91. doi: 10.1007/s11739-021-02734-8
25. Avendaño-Solà C, Ramos-Martínez A, Muñez-Rubio E, Ruiz-Antorán B, de Molina RM, Torres F, et al. Convalescent Plasma for COVID-19: A Multicenter, Randomized Clinical Trial. *medRxiv* (2020) 2020.08.26.20182444. doi: 10.1101/2020.08.26.20182444
26. Bajpai M, Kumar S, Maheshwari A, Chhabra K, kale P, Gupta A, et al. Efficacy of Convalescent Plasma Therapy Compared to Fresh Frozen Plasma in Severely Ill COVID-19 Patients: A Pilot Randomized Controlled Trial. *medRxiv* (2020) 2020.10.25.20219337. doi: 10.1101/2020.10.25.20219337
27. Körper S, Weiss M, Zickler D, Wiesmann T, Zacharowski K, M.Corman V, et al. High Dose Convalescent Plasma in COVID-19: Results From the Randomized Trial CAPSID. *medRxiv* (2021) 2021.05.10.21256192. doi: 10.1101/2021.05.10.21256192
28. Ray Y, Paul SR, Bandopadhyay P, D'Rozario R, Sarif J, Lahiri A, et al. Clinical and Immunological Benefits of Convalescent Plasma Therapy in Severe COVID-19: Insights From a Single Center Open Label Randomised Control Trial. *medRxiv* (2020) 2020.11.25.20237883. doi: 10.1101/2020.11.25.20237883
29. WHO Rapid Evidence Appraisal for COVID-19 Therapies (REACT) Working Group, Shankar-Hari M, Vale CL, Godolphin PJ, Fisher D, Higgins JPT, Spiga F, et al. Association Between Administration of IL-6 Antagonists and Mortality Among Patients Hospitalized for COVID-19: A Meta-Analysis. *JAMA* (2021) 326(6):499–518. doi: 10.1001/jama.2021.11330
30. WHO Rapid Evidence Appraisal for COVID-19 Therapies (REACT) Working Group, Sterne JAC, Murthy S, Diaz JV, Slutsky AS, Villar J, Angus DC, et al. Association Between Administration of Systemic Corticosteroids and Mortality Among Critically Ill Patients With COVID-19: A Meta-Analysis. *JAMA* (2020) 324(13):1330–41. doi: 10.1001/jama.2020.17023
31. U.S. Food and Drug Administration. *Investigational COVID-19 Convalescent Plasma: Guidance for Industry*. Maryland, United States: Silver Spring (2021).
32. Hueso T, Pouderoux C, Pere H, Beaumont AL, Raillon LA, Ader F, et al. Convalescent Plasma Therapy for B-Cell-Depleted Patients With Protracted COVID-19. *Blood* (2020) 136(20):2290–5. doi: 10.1182/blood.2020008423
33. Rodionov RN, Biener A, Spieth P, Achleitner M, Holig K, Aringer M, et al. Potential Benefit of Convalescent Plasma Transfusions in Immunocompromised Patients With COVID-19. *Lancet Microbe* (2021) 2(4):e138. doi: 10.1016/S2666-5247(21)00030-6
34. Zeitlinger M, Idzko M. Inhaled Budesonide for Early Treatment of COVID-19. *Lancet Respir Med* (2021) 9(7):e59. doi: 10.1016/S2213-2600(21)00215-0
35. *COVID-19 Treatment Guidelines Panel 2021*. (2021). Available at: https://www.covid19treatmentguidelines.nih.gov/on.
36. Health Technology Wales. (2021). Available at: https://www.healthtechnology.wales/covid-19/on.
37. Ledford H. COVID Antibody Treatments Show Promise for Preventing Severe Disease. *Nature* (2021) 591(7851):513–4. doi: 10.1038/d41586-021-00650-7
38. RECOVERY Collaborative Group, Horby PW, Mafham M, Peto L, Campbell M, Pessoa-Amorim G, et al. Casirivimab and Imdevimab in Patients Admitted to Hospital With COVID-19 (RECOVERY): A Randomised, Controlled, Open-Label, Platform Trial. *medRxiv* (2021) 2021.06.15.21258542. doi: 10.1101/2021.06.15.21258542
39. Dougan M, Nirula A, Azizad M, Mocherla B, Gottlieb RL, Chen P, et al. Bamlanivimab Plus Etesevimab in Mild or Moderate Covid-19. *N Engl J Med* (2021) 385(15):1382–92. doi: 10.1056/NEJMoa2102685
40. Gupta A, Gonzalez-Rojas Y, Juarez E, Crespo Casal M, Moya J, Falci DR, et al. Early Treatment for Covid-19 With SARS-CoV-2 Neutralizing Antibody Sotrovimab. *N Engl J Med* (2021) 385(21):1941–50. doi: 10.1101/2021.05.27.21257096

Conflict of Interest: The authors declare that the research was conducted in the absence of any commercial or financial relationships that could be construed as a potential conflict of interest.

Publisher's Note: All claims expressed in this article are solely those of the authors and do not necessarily represent those of their affiliated organizations, or those of the publisher, the editors and the reviewers. Any product that may be evaluated in this article, or claim that may be made by its manufacturer, is not guaranteed or endorsed by the publisher.

frontiers in Immunology

ORIGINAL RESEARCH
published: 22 February 2022
doi: 10.3389/fimmu.2022.816159

Is Better Standardization of Therapeutic Antibody Quality in Emerging Diseases Epidemics Possible?

Sanda Ravlić[1,2†], Ana Hećimović[3†], Tihana Kurtović[1,2], Jelena Ivančić Jelečki[1,2], Dubravko Forčić[1,2], Anamarija Slović[1,2], Ivan Christian Kurolt[2,4], Željka Mačak Šafranko[2,4], Tatjana Mušlin[3], Dina Rnjak[5], Ozren Jakšić[6], Ena Sorić[6], Gorana Džepina[7], Oktavija Đaković Rode[8,9], Kristina Kujavec Šljivac[10], Tomislav Vuk[3], Irena Jukić[3], Alemka Markotić[2,4,11,12] and Beata Halassy[1,2]*

[1] Centre for Research and Knowledge Transfer in Biotechnology, University of Zagreb, Zagreb, Croatia, [2] Center of Excellence for Virus Immunology and Vaccines (CERVirVac), Zagreb, Croatia, [3] Croatian Institute of Transfusion Medicine, Zagreb, Croatia, [4] Research Department, University Hospital for Infectious Diseases "Dr. Fran Mihaljević", Zagreb, Croatia, [5] Clinics for Pulmonary Diseases, University Hospital Centre Zagreb, Zagreb, Croatia, [6] Department of Hematology, University Hospital Dubrava, Zagreb, Croatia, [7] Department for Transfusion Medicine, University Hospital Dubrava, Zagreb, Croatia, [8] Department for Clinical Microbiology, University Hospital for Infectious Diseases "Dr. Fran Mihaljević", Zagreb, Croatia, [9] School of Dental Medicine, University of Zagreb, Zagreb, Croatia, [10] Clinical Institute for Transfusion Medicine, Clinical University Hospital Centre Osijek, Osijek, Croatia, [11] School of Medicine, Catholic University of Croatia, Zagreb, Croatia, [12] Faculty of Medicine, University of Rijeka, Rijeka, Croatia

OPEN ACCESS

Edited by:
Raymund Razonable,
Mayo Clinic, United States

Reviewed by:
Mike Joyner,
Mayo Clinic, United States
Stella Joan Berendam,
Duke University, United States

***Correspondence:**
Beata Halassy
bhalassy@unizg.hr

[†]These authors have contributed equally to this work

Specialty section:
This article was submitted to Vaccines and Molecular Therapeutics, a section of the journal Frontiers in Immunology

Received: 01 December 2021
Accepted: 02 February 2022
Published: 22 February 2022

Citation:
Ravlić S, Hećimović A, Kurtović T, Ivančić Jelečki J, Forčić D, Slović A, Kurolt IC, Mačak Šafranko Z, Mušlin T, Rnjak D, Jakšić O, Sorić E, Džepina G, Đaković Rode O, Kujavec Šljivac K, Vuk T, Jukić I, Markotić A and Halassy B (2022) Is Better Standardization of Therapeutic Antibody Quality in Emerging Diseases Epidemics Possible? Front. Immunol. 13:816159. doi: 10.3389/fimmu.2022.816159

During the ongoing COVID-19 epidemic many efforts have gone into the investigation of the SARS-CoV-2–specific antibodies as possible therapeutics. Currently, conclusions cannot be drawn due to the lack of standardization in antibody assessments. Here we describe an approach of establishing antibody characterisation in emergent times which would, if followed, enable comparison of results from different studies. The key component is a reliable and reproducible assay of wild-type SARS-CoV-2 neutralisation based on a banking system of its biological components - a challenge virus, cells and an anti-SARS-CoV-2 antibody in-house standard, calibrated to the First WHO International Standard immediately upon its availability. Consequently, all collected serological data were retrospectively expressed in an internationally comparable way. The neutralising antibodies (NAbs) among convalescents ranged from 4 to 2869 IU mL^{-1} in a significant positive correlation to the disease severity. Their decline in convalescents was on average 1.4-fold in a one-month period. Heat-inactivation resulted in 2.3-fold decrease of NAb titres in comparison to the native sera, implying significant complement activating properties of SARS-CoV-2 specific antibodies. The monitoring of NAb titres in the sera of immunocompromised COVID-19 patients that lacked their own antibodies evidenced the successful transfusion of antibodies by the COVID-19 convalescent plasma units with NAb titres of 35 IU mL^{-1} or higher.

Keywords: passive antibody therapy, convalescent plasma, COVID-19, SARS-CoV-2, wild-type virus neutralization assay

INTRODUCTION

Passive immunotherapy is a century-old practice of administering pathogen-specific antibodies to prevent or treat a disease caused by the same pathogen (1). Specific immunoglobulins (pooled, purified and concentrated immunoglobulin preparations), some even sourced from animals, have an important role in the prophylactic or therapeutic treatment of various clinical conditions, including viral diseases (hepatitis A and B, rabies, varicella, infections with respiratory syncytial virus, cytomegalovirus, measles). However, in situations with insufficient time or resources to generate the immunoglobulin preparations, such as during emerging infections and pandemics (influenza, SARS-CoV-1, MERS, Ebola), convalescent plasma can be collected from recovered donors and employed to treat the infectious disease in question (2). In 2020, the worldwide spread of a previously unknown virus named SARS-CoV-2 caused the global COVID-19 pandemic. Experience from prior outbreaks with other coronaviruses (SARS-CoV-1) showed that convalescent sera contained neutralising antibodies (NAbs) against the virus and that their use was beneficial to the treated patients (3, 4). Therapy with antibody-laden blood of those who have recovered from SARS-CoV-2 infection is currently used and investigated worldwide (5–18).

Although convalescent plasma therapy has been considered generally beneficial due to multiple examples, both historical and recent (1, 19, 20), scientific medical community lacks definitive proof of its efficacy coming from carefully designed randomized clinical trials (2). When such trials were undertaken, they were unable to demonstrate a beneficial effect of plasma over placebo (21). The reasons lay mostly in the specific circumstances of its usage. Namely, the time frame of convalescent plasma usage is short. It is used only during epidemics caused by a new and insufficiently known pathogen, in a period when pathogen-specific therapy and vaccines are lacking. During this period, methods for plasma neutralisation potency determination are usually lacking or if they exist, they are neither standardized nor validated. This results in variability within the individual trials and renders comparison between different case studies, case series or trials difficult. Further, convalescent plasma is a complex, non-standardized medicine varying in NAb titre, as well as in the content of non-specific immunomodulators between units collected from different individuals. The inability to demonstrate convalescent plasma effectiveness might be linked to variation in the concentration of NAbs and the subsequent lack of standardized doses between patients (22, 23).

We describe here the Croatian approach to the establishing of prerequisites for the COVID-19 convalescent plasma (CCP) usage in a manner that enables comparison between different countries and studies. The approach includes several steps: (i) development of a reproducible wild-type SARS-CoV-2 neutralisation potency assay; (ii) establishment and continuous usage of an anti-SARS-CoV-2 in-house standard; (iii) finding the best fitting correlation function between the results of commercial assays used by Croatian transfusion centres and the results of neutralisation assay, thus enabling that the neutralisation potencies of plasma units can be expressed in the same way and in the same units in the whole country; and (iv) finally, and most importantly, recalculation of all neutralisation potencies of plasma units used in Croatia in relation to the first WHO international standard once it was established and available to the scientific community, by calibrating our own in-house standard (24).

MATERIALS AND METHODS

Cell Media, Buffers and Solutions

Minimum Essential Medium (MEM; GIBCO, Thermo Fisher Scientific, MA USA) supplemented with penicillin (100 IU mL^{-1}), streptomycin (100 µg mL^{-1}), and L-glutamine (2 mM) (all from Capricorn Scientific, Germany) was used. Foetal bovine serum (PAN-Biotech, Germany) was inactivated at 56°C for 60 minutes prior the use. For the Vero E6 cell propagation and maintenance medium with 10% FBS was used. In SARS-CoV-2 titration ($CCID_{50}$ assay) and SARS-CoV-2 neutralisation (ED_{50}) assays medium was supplemented with 2.5% FBS.

Cell Culture

Vero E6 cells, an epithelial cell line from the kidney of an African green monkey (*Ceropithecus aethiops*), were acquired from the American Type Culture Collection (ATCC – CRL 1587). The working cell bank was prepared, aliquoted and stored in liquid nitrogen. After thawing, cells were cultivated in cell cultivation flasks in the medium with 10% FBS in a 5% CO_2 environment at 37°C, and maintained by subcultivations every 3-4 days, according to ATCC instructions.

SARS-CoV-2 Working Stock

SARS-CoV-2 isolate was derived from the PCR positive oro- and nasopharyngeal swab designated 297/20 Zagreb taken from a patient in Zagreb, Croatia. It was propagated four times in Vero E6 cells. The virus was subcultivated one more time at m.o.i. 0.001 in Vero E6 maintained in MEM supplemented with 10% FBS, penicillin, streptomycin, and L-glutamine in a 5% CO_2 environment at 37°C, to obtain SARS-CoV-2 working stock. Two days post infection virus-infected Vero E6 cell culture supernatant was centrifuged for 10 minutes at 1500×*g*, formulated in 20% FBS, aliquoted and stored at -75°C. It has been used throughout as a challenge virus in neutralisation assay, and as a reference in a virus microtitration assay.

Next Generation Sequencing (NGS)

RNA vas isolated from 400 µL of virus-infected Vero E6 cell culture supernatants using Quick-RNA Viral kit (Zymo Research, USA). Reverse transcription and PCR amplification were performed following nCoV-2019 sequencing protocol for Illumina V.3 (available at https://www.protocols.io/), using LunaScript RT SuperMix kit (New England Biolabs, Germany) and Q5 Hot-Start High-Fidelity DNA polymerase (New England Biolabs) with primers from ARTIC nCoV-2019 V3 Panel (Integrated DNA Technologies, USA). Libraries were prepared with NEBNext Ultra II FS DNA Library prep kit (New England Biolabs), their quality was checked on 2100 Bioanalyser (Agilent, USA) using High Sensitivity DNA Kit (Agilent). Libraries were pooled and sequenced on

Illumina MiniSeq instrument (Illumina, USA) using MiniSeq Mid Output Kit (2 × 150 paired-end reads; Illumina). Quality of raw reads was assessed with FastQC v0.11.8 and subjected to trimming, adapter removal and removal of short reads using BBDuk within BBTools package. Paired-end reads were aligned to hCoV-19/Wuhan/WIV04/2019 (GISAID accession ID EPI_ISL_402124) using Bowtie2 v2.4.2 (25). Geneious Prime® 2019.2.3 software was used for construction of consensus sequences. The epidemiological lineage was attributed by the GISAID database, software version v.3.1.7 2021-07-09.

Neutralisation Assay

Infective virus-neutralisation assay followed the general principles already described for other viruses (26, 27), but was adapted specifically to the SARS-CoV-2, as follows. SARS-CoV-2 neutralisation assay was performed in 96-well tissue culture microplates (TPP, Switzerland). Octaplicates of two-fold serial dilutions of the patient's sera or the plasma donor's serum (50 µL) were preincubated with approximately 20 $CCID_{50}$/50 µL per well of SARS-CoV-2 working stock at 37°C and 5% CO_2 for 90 minutes. Plasma of known neutralising capacity (anti-SARS-CoV-2 in-house standard) was used as a positive control (in duplicate). After adding 100 µL/well of Vero E6 cells (3×10^5 mL^{-1}), the plates were incubated at 37°C and 5% CO_2. Wells with cell suspension without the virus served as cell growth control. After four days of incubation cell layers in all wells were inspected by an inverted optical microscope and wells with cytopathic effect (CPE) counted. The effective dose 50 (ED_{50}), the amount of undiluted serum that inhibits CPE in 50% of infected wells, was calculated according to Spearman-Kärber method. Neutralisation titre (NT) was expressed as number of ED_{50} doses in 1 mL of plasma/serum. NTs of experimental samples in each assay were corrected for the deviation of anti-SARS-CoV-2 in-house standard from its nominal NT value. The quantity of SARS-CoV-2 working stock used as a challenge in each neutralisation assay was determined using 50% cell culture infective dose ($CCID_{50}$) assay in 96-well format. Octaplicates of three-fold serial dilutions of virus suspension (100 µL) were mixed with Vero E6 cell suspension (3×10^5 mL^{-1}; 100 µL). After four days of incubation at 37°C and 5% CO_2, wells with CPE were counted and $CCID_{50}$ mL^{-1} calculated using Spearman-Kärber method. Anti-SARS-CoV-2 in-house standard was calibrated to the 1st WHO International Standard for anti-SARS-CoV-2 (NIBSC, UK; https://www.nibsc.org/products/brm_product_catalogue/detail_page.aspx?catid=20/136), upon its availability, enabling expression of NT in IU mL^{-1}.

Commercial Serological Assays

Human IgG antibodies specific for SARS-CoV-2 spike (S) protein were determined by several commercial assays. Anti-SARS-CoV-2 ELISA (Euroimmun Medizinische Labordiagnostika AG, Germany) for determination of S-specific IgG uses S1 domain recombinantly produced in HEK 293 cells as a coating antigen. The VIDAS® SARS-CoV-2 IgG (BioMerieux, France) is an automated ELFA assay, which uses recombinant receptor binding domain (RBD) of the S protein as the coating agent. The VIDAS® SARS-COV-2 IgG test was performed on a VIDAS® instrument. The LIAISON® SARS-CoV-2 CLIA (DiaSorin Inc., USA) uses magnetic beads coated with recombinant S1 and S2 antigens and was performed on a Liaison XL analyser. Architect SARS-CoV-2 IgG II quant (Abbott, Ireland) is an automated assay using CMIA technique, in which receptor RBD of the S protein is used as a coating antigen. The assay was performed using Architect i2000SR instrument. Human IgG antibodies specific for nucleoprotein of the SARS-CoV-2 virus were measured by Abbott's SARS-CoV-2 IgG assay, which uses recombinant nucleoprotein as a coating agent. We also measured human IgM and IgA antibodies specific for S protein, by BioMerieux's VIDAS® SARS-CoV-2 IgM and Euroimmun's anti-SARS-CoV-2 ELISA (IgA) assays, respectively.

Convalescent Plasma Samples

COVID-19 convalescent plasma (CCP) was obtained by apheresis using the Amicus (Fenwal, USA) and MCS+ (Haemonetics, USA) devices. Each donor had a documented history of laboratory-confirmed SARS-CoV-2 infection (positive RT-PCR test, positive SARS-CoV-2 antigen test, and/or SARS-CoV-2 specific antibodies). All plasma units were donated by recovered and healthy COVID-19 patients who had been asymptomatic for ≥ 28 days. If eligible according to standard blood donor criteria, donors were enrolled in a plasmapheresis program. Sera from eligible plasma donors were analysed by virus neutralisation assay for quantification of SARS-CoV-2 NAbs. Sera were analysed in native form and after inactivation by heating at 56°C for an hour. Collected plasma was used for therapy from donors having NT in heat-inactivated sample above 700 ED_{50} mL^{-1} (which equals 35 IU mL^{-1}).

CCP-Treated Patients

Demonstrated here are the NAb changes during the CCP therapy in the blood of three representative immunocompromised COVID-19 patients, who lacked their own antibodies. The first patient was diagnosed with nasopharyngeal diffuse large C-cell lymphoma and treated with R-CHOP/R-DHAP chemotherapy protocols (containing rituximab, cyclophosphamide, doxorubicin, vincristine and prednisone/rituximab, dexamethasone, cytarabine and cisplatin), followed by autologous stem cell transplantation, radiotherapy of Waldeyer's ring, and finally maintenance therapy with the anti-CD-20 monoclonal antibody rituximab. At the start of CCP therapy a nasopharyngeal swab showed persistent RT-PCR positivity for SARS-CoV-2 for 45 days and he had a fever, respiratory insufficiency and lung infiltrates (28). The second patient had history of chronic lymphocytic leukaemia and was treated with rituximab and bendamustine. At the start of CCP therapy on the 57th day of the disease, he had no anti-SARS-CoV-2 antibodies and was respiratory insufficient (dependent on low flow of oxygen therapy). The third patient had a history of follicular lymphoma treated with G-CHOP chemotherapy protocol (containing 2nd generation anti-CD20 monoclonal antibody obinutuzumab, cyclophosphamide, doxorubicin, vincristine and prednisone), with the last cycle administered around the time of his infection with SARS-CoV-2 virus. He was diagnosed with COVID-19 pneumonia and treated with remdesivir and high flow oxygen therapy on several occasions. He lacked SARS-CoV-2 specific

antibodies before the CCP transfusion, which was received on the 102nd day of the disease.

Data Analysis

NT values expressed as ED_{50} mL^{-1} or IU mL^{-1} were linearized by calculating logarithmic values and then used for statistical analysis. When average value from the set of *n* data was calculated, 95% confidence interval was provided as an indicator of measurement uncertainty. To assess a relationship of the antibody level with the donor disease severity and the time period from recovery to collection of CCP, Kruskal-Wallis test was performed. To assess a difference between heat inactivated and native sera a two tailed *t*-test for paired samples was used with *p* and *t* values, as well as degrees of freedom (DF) provided. Relationship between neutralisation assay results and results of other serological assays was assessed by Pearson's correlation coefficient (*r*). MedCalc v20.011 was used for statistical analysis.

Study Approval

Collection of COVID-19 convalescent plasma (CCP) was approved by the Croatian Ministry of Health (023-03/20-01/235; permission No. 534-04-3-2/2-20-11). The approval was based on the positive opinion of the Ethical Committee of Croatian Institute of Transfusion Medicine (003-06/20-04/02, opinion No.251-541-06/6-20-2). Immunocompromised COVID-19 patients were treated with COVID-19 plasma according to periodically updated FDA and EC guidelines (https://www.fda.gov/media/141477/download; https://ec.europa.eu/health/sites/default/files/blood_tissues_organs/docs/guidance_plasma_covid19_en.pdf). All COVID-19 convalescent plasma donors and all included patients (or their representatives) were informed about the study and gave written informed consent.

RESULTS

Characterisation of SARS-CoV-2 Working Stock

The infectivity of SARS-CoV-2 working stock (the fifth (P5) subcultivation of 297/20 Zagreb SARS-CoV-2 isolate) was determined to be 6.83 ± 0.15 $CCID_{50}$ mL^{-1} (*n*=8). Its complete genomic sequence was determined by NGS and compared to the sequence of the same virus isolate from the second subcultivation (P2), which is the closest one to the original clinical sample. Obtained genome coverage was 99.75% for both P2 and P5 samples. Sequences were submitted to GISAID database, accession IDs are EPI_ISL_3013040 and EPI_ISL_3013041 for P2 and P5, respectively. The virus belongs to the lineage B.1.1.1. Their consensus sequences were identical, except for nucleotides 4402 (ORF1ab gene) and 23607 (S gene). The difference stems from P5 ambiguity at both positions (C4402Y and G23607R in reference to P2; **Figure S1**). Both C and T at the position 4402 lead to the same amino acid in nsp3. The nucleotide 23607 is located in the S gene. Its ambiguity causes an amino acid substitution in a portion of the virus population (**Figure S1**). This amino acid is located within S1 protein subunit, but outside the RBD. In comparison to S protein of hCoV-19/Wuhan/WIV04/2019 [the sequence that represents the consensus of early submissions of SARS-CoV-2 sequences (29)] two differences were observed: G23607R (present only in P5) and A23402G (present in both P2 and P5). The latter difference is a well-known D614G mutation which occurred in early February 2020 (30) and is characteristic for nearly all strains detected since late spring 2020. The list of all nucleotide and amino acid differences between P5 and hCoV-19/Wuhan/Wiv04/2019 is presented in the **Table S1**.

Overall, we concluded that the virus has not substantially changed on its way from the clinical sample to the SARS-CoV-2 working stock, and can be considered as having the wild-type phenotype.

Neutralisation Assay Development and Characterisation

Although there were plenty of different assays available on the market, none were sufficiently characterised to provide the information on the antibody quality and functionality. We focused on the establishment of stable and reproducible wild-type SARS-CoV-2 neutralisation assay, as the most relevant assay for estimation of the ability of antibodies to neutralise the virus infectivity. To gain reproducible and reliable results, we established laboratory working banks of Vero E6 cells, SARS-CoV-2 and anti-SARS-CoV-2 antibodies, aliquoted and stored in liquid nitrogen, at -60°C or below, and at -16°C or below, respectively.

After thawing, Vero E6 cells were used for the assay from the 3rd up to the 28th subcultivation. The number of subcultivations did not significantly impact the titre of SARS-CoV-2 working stock, which was quantified in each assay run (**Figure 1A**). Linear function describing dependence of virus titre and "cell age" expressed as a number of subcultivations indicates a slight, negligible rise in titre value if cells for the assays were from 3rd or 28th subcultivation. In contrast, the titre of SARS-CoV-2 working stock has been continuously slowly dropping down with the increase of the storage period. Within the period of 9.3 months of storage at -60°C and below, the titre decreased from nominal 6.83 log $CCID_{50}$ mL^{-1} to 6.21 log $CCID_{50}$ mL^{-1}, resulting in overall drop of approx. 0.61 log $CCID_{50}$ mL^{-1}, or 0.09 log $CCID_{50}$ mL^{-1} per month (**Figure 1B**). This decrease was considered when preparing a working dilution of a challenge virus for the assay. Knowing that the results of the neutralisation assay inversely correlate with the titre of the challenge virus (26), we targeted 20 $CCID_{50}$ per well (400 $CCID_{50}$ mL^{-1}), the estimated lowest amount ensuring 100% infectivity in all wells, which at the same time enables highest sensitivity of the neutralisation assay.

Anti-SARS-CoV-2 in-house standard was prepared by selecting one of the convalescent plasma samples, having a medium high NT in the preliminary assays. It was heat-inactivated, aliquoted and stored. Its nominal titre was determined to be 3.50 ± 0.04 log ED_{50} mL^{-1} (*n*=14). The NAb titre was stable throughout the 6-month period of its usage (**Figure 1C**). When the First WHO International Standard for anti-SARS-CoV-2 became available (NIBSC, UK, beginning of 2021) having nominal NT of 1000 IU mL^{-1} (4.32 ± 0.11 log ED_{50}

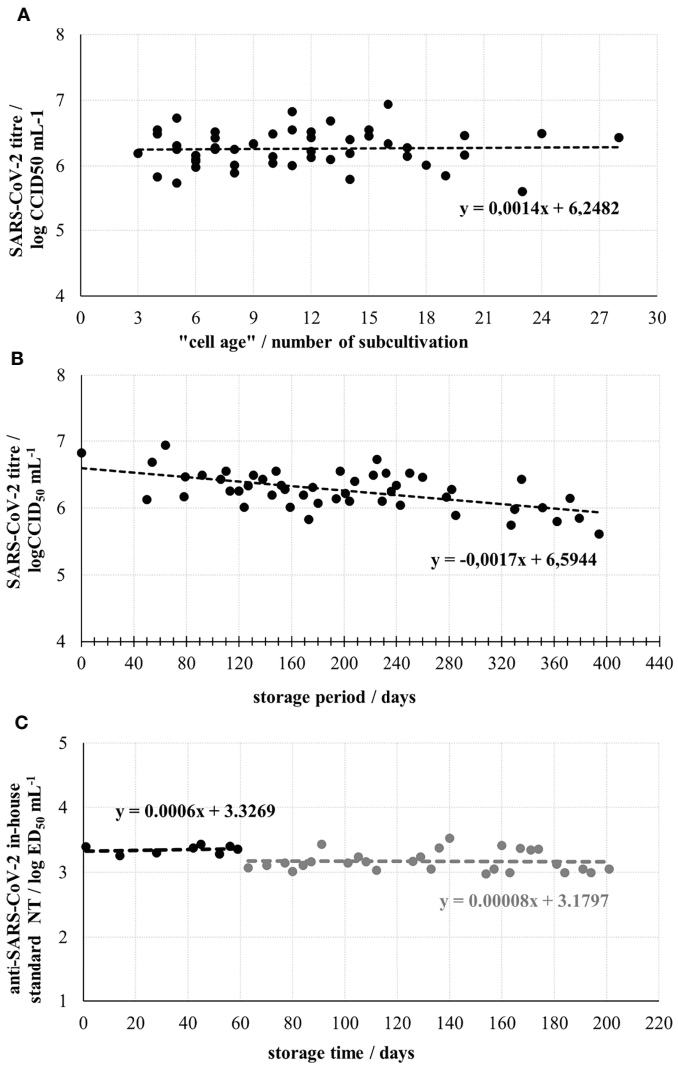

FIGURE 1 | Optimization and control parameters of the neutralisation assay performance. **(A)** SARS-CoV-2 working stock titre determined in assay runs using Vero E6 cells from different subcultivations. **(B)** SARS-CoV-2 working stock stability during the storage at -60°C or below. **(C)** Stability of anti-SARS-CoV-2 in-house standard during 6-month storage. The break in line indicates the start of two times lower dilution of SARS-CoV-2 working stock usage as a challenge virus, due to the drop of its infectivity.

mL^{-1} (n=11) in our assay), we calibrated our in-house standard to it. Several independently performed simultaneous analyses of both standards indicated that WHO International Standard, with 1000 IU mL^{-1} had 6.6 times higher neutralising activity than our in-house standard, to which 152 IU mL^{-1} was assigned accordingly. This enabled recalculation of all previously collected results and their expression in both ED_{50} mL^{-1} and IU mL^{-1}, the units of the WHO International Standard.

The Role of Complement in SARS-CoV-2 Neutralisation

Analysis of 69 convalescent sera samples in native and heat inactivated form revealed 2.37 ± 0.30 (average ± 95% CI) times higher neutralisation potency of native samples (**Figure 2A**). The difference was statistically significant (p<0.0001; t=12.809; DF=68), indicating complement activation properties of convalescents' SARS-CoV-2-specific antibodies. Moreover, the factor of neutralisation potency decrease upon complement inactivation was highest in samples with low neutralisation potency in comparison to the high titre sera (**Figure 2B**). This difference could be explained by the properties of the assay itself, since low titre samples are analysed in low dilutions in the assay, while high titre samples had to be highly diluted for analysis. In such situation, complement components and factors are also highly diluted, and their effect cannot be expressed equally as in low titre samples, analysed in low dilutions. So, it would be correctly to estimate complement activation properties of NAbs from the data obtained for low titre sera only (n=52), showing

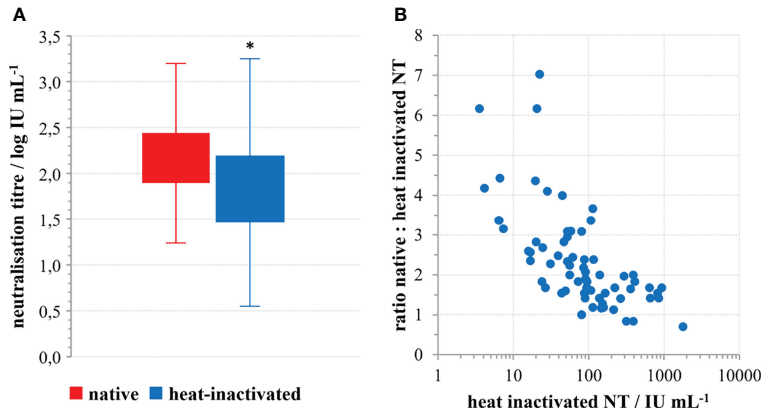

FIGURE 2 | The role of complement in SARS-CoV-2 neutralisation. **(A)** Decrease of SARS-CoV-2 neutralisation power of convalescent sera upon heat inactivation; *p<0.0001 (n=69) according to the two-tailed t-test for paired samples; (t=12.809; DF=68), **(B)** Factor of neutralisation titre decrease in relation to the quantity of neutralising antibodies in the convalescents' sera.

that neutralisation potency of specific antibodies is increased 2.67 ± 0.30 (average ± 95% CI) times, probably through classical activation of human complement. No complement activity against the SARS-CoV-2 was detected in the native human sera collected from people who were not infected or vaccinated.

Neutralisation Potency of COVID-19 Convalescents' Sera

Learning that the complement is activated by virus-specific antibodies and that it increases neutralisation potency, differently in high- and low-titre sera due to assay inherent properties, only heat-inactivated sera were tested to assess SARS-CoV-2 specific humoral immunity. We analysed in total 124 sera samples of COVID-19 convalescents by SARS-CoV-2 neutralisation assay who had a documented COVID-19 history and who successfully recovered. The time frame of plasma donation ranged between 1 to 7 months after recovery from the illness. Only four donors had unmeasurable quantities of NAbs in their blood, all four reported only mild symptoms and all four donated plasma within 3 months from the illness. The range of neutralisation potencies in positive sera was from 73 to 59452 ED_{50} mL^{-1} (1.87 to 4.77 log ED_{50} mL^{-1}), which equals 4 to 2869 IU mL^{-1} (0.55 to 3.46 log IU mL^{-1}). However, the median value was 1631 ED_{50} mL^{-1} (3.21 log ED_{50} mL^{-1}) or 79 IU mL^{-1} (1.90 log IU mL^{-1}).

For 113 samples we had complete data on the disease severity and the time of onset of their illness and used them to analyse the impact of these two factors on the NT level. NTs were highest in the group of sera taken within the first two months after the illness onset, then slowly decreased. However, measurable, even high levels of NTs were determined in samples taken 4-7 months after the illness onset (**Figure 3A**). If longer periods passed and antibodies were still high, it was highly probable that donors faced contact with the virus again which boosted their response, while having no symptoms due to the pre-existing immunity. To avoid such situations that might mislead our conclusion, only samples taken within first three months (n=77) were considered in the analysis of the impact of disease severity on NT. Disease severity was classified as asymptomatic (0), mild (1), moderate (2) and severe (3), on the basis of the donor's report and on medical documentation (**Table 1**). Donors that reported the most severe clinical picture also had the highest levels of NTs (**Figure 4**) and this increase was statistically significant (p<0.002). However, most of them were not found eligible for donation due to their comorbidities. Furthermore, if their recovery was not complete for months after the illness, they were not considered for donation. Consequently, NAb titres in collected CCP units were not higher than 600 IU mL^{-1}.

Population picture (**Figure 3A**) implied that high NAb titres in convalescents persist for several months, and that their decrease is slow. This was proven by the analysis of duration of antibodies in six individual convalescents, showing that their neutralising antibodies were indeed persistent (**Figure 3B**). Slopes of lines describing the relationship between NT and the time after the first donation were in the range from -0.0117 to 0.0023, with an average value of -0.0042 log IU mL^{-1} per day.

Relationship Between Neutralisation Potency and Commercial Assays for SARS-CoV2-Specific Antibody Determination

COVID-19 convalescent plasma collection was initiated at the Croatian Institute of Transfusion Medicine in Zagreb. In parallel with the neutralisation potency determination of CCP plasma samples, several commercial assays compatible with instrumentation at this transfusion centre were also screened. We found high correlation (r=0.93; n=49) between the in-house neutralisation potency results of heat inactivated convalescent sera and the VIDAS SARS-CoV-2 IgG determining IgG specific for receptor binding domains of the SARS-CoV-2 S protein (**Figure 5A**). Due to the low throughput properties of the neutralisation potency assay, further characterisation of CCP

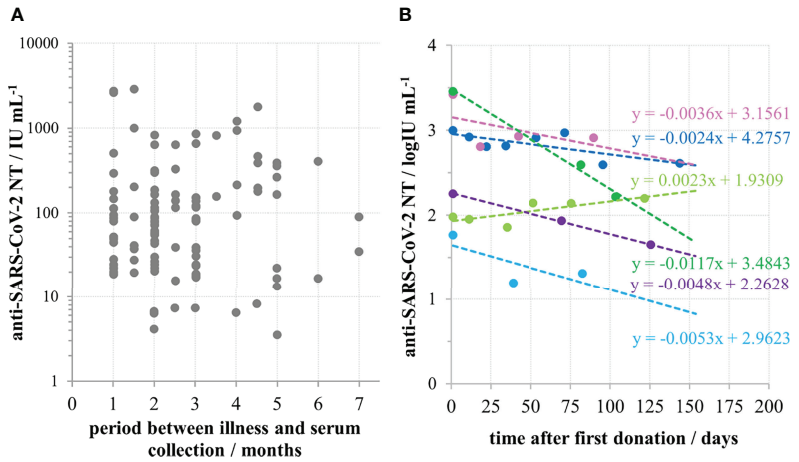

FIGURE 3 | Persistence of anti-SARS-CoV-2 neutralizing antibodies in convalescent sera. **(A)** Neutralisation titre in convalescent donors' sera (n=113) in relation to the time period between the illness and serum collection. **(B)** Longitudinal monitoring of neutralisation titre in sera of six convalescents.

TABLE 1 | Categories of COVID-19 disease severity.

Category	Designation	Symptoms
ASYMPTOMATIC	0	positive PCR test, no symptoms
MILD	1	short-term fever up to 38.5°C, anosmia, ageusia, runny nose, cough
MODERATE	2	short-term fever over 38.5°C, accompanied with several or all of the following: headache, mialgia, general weakness, vertigo and anosmia, ageusia, runny nose, cough
SEVERE	3	prolonged, persistent fever over 38.5°C, accompanied with the most of symptoms 2, involving also pneumonia in some cases; patients that seeked medical help, but without the need for hosptalization

samples was performed only by VIDAS SARS-CoV-2 IgG, and the results expressed in IgG index have been converted to NTs expressed in log IU mL^{-1} according to the inverse formula: y = 0.3477ln(x) + 1.4259, where x is IgG index. After the international standard became available, Biomerieux calibrated VIDAS SARS-CoV-2 IgG accordingly to it and their previous cut off value of 1.0 was replaced with 20 IU mL^{-1}. Using the above formula describing the relationship between the NT and the SARS-CoV-2 IgG VIDAS assay results, we calculated similarly that the IgG index value of 1.0 equals 26.7 IU mL^{-1}. This confirms that the correlation between VIDAS SARS-CoV-2 IgG and NT in COVID-19 convalescent sera is strong and that the transformation of ED_{50} mL^{-1} results to IU mL^{-1} is accurate.

NTs also significantly (p<0.0001) correlated to the results of several other commercially available serological assays that are used in other Croatian transfusion centres. A high correlation was found between NT of heat-inactivated convalescent sera and the results of Euroimmun's anti-SARS-CoV-2 IgG (**Figure 5B**), DiaSorin's anti-SARS-CoV-2 IgG (**Figure 5C**) and Abbott's anti-SARS-CoV-2 IgG (**Figure 5D**), with Pearson's coefficients of correlation being 0.87 (n=36), 0.93 (n=25) and 0.90 (n=27), respectively.

Results of commercial assay measuring IgG directed to the nucleoprotein of SARS-CoV-2 virus as well as of those measuring antibodies of IgM or IgA class specific for S protein did not correlate with the neutralisation potency results (data not shown).

Convalescent Plasma Usage for COVID-19 Therapy

In Croatia, the collection of convalescent plasma started in July 2020 and its use for COVID-19 therapy started in December 2020. A regularly updated document (last on 23/06/2020) "An EU programme of COVID-19 convalescent plasma collection and transfusion - Guidance on collection, testing, processing, storage, distribution and monitored use" was used as the main guidance document (https://www.isbtweb.org/fileadmin/user_upload/guidance_plasma_covid19_en.pdf). This most recent version still does not provide a cut-off value of NAb titre for the release of CCP for transfusion, due to lack of robust scientific evidence. When deciding which plasma units to provide to the hospitals the following assumptions were considered: (1) the lowest NT measured in sera of COVID-19 convalescents was around 4 IU mL^{-1}, implying that such quantities might also be beneficial; (2) if the volume of one plasma unit is 200 mL and the average volume of human blood is 5-6 L, 25–30x dilution of NAbs is expected during transfusion; (3) the recruitment of convalescents for plasma donations was slow; (4) the median level of NT in convalescent plasma is closer to the lowest then to the highest measured value among the convalescents; (5) plasma units have to be given only to ABO compatible patients, which

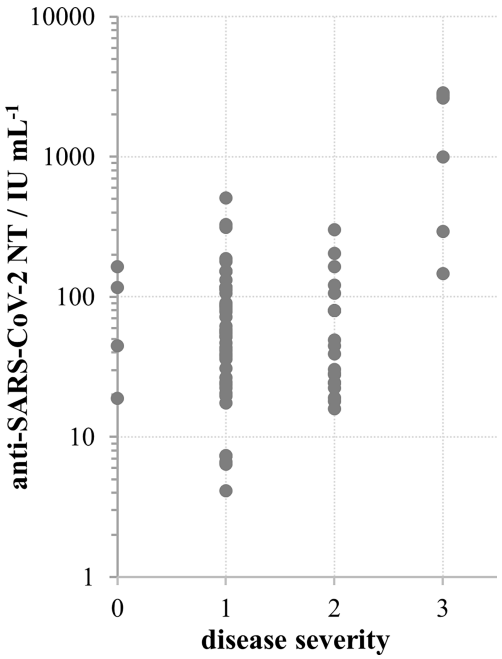

FIGURE 4 | SARS-CoV-2 neutralisation titre in convalescent donors' sera in relation to disease severity according to scale: 0 – no symptoms, 1 – mild, 2 – moderate, 3 – severe; *$p < 0.002$ in comparison to other groups, calculated by Kruskal-Wallis test.

together with (3) and (4) would contribute to the insufficiency of units for the high needs during epidemics. The final decision was to consider plasma units with titres of 35 IU mL^{-1} and greater as suitable for transfusion, with a recommendation to provide the compatible plasma with the highest titre available at the moment and, if plasma units were of the lower titres, to provide several of them. COVID-19 convalescent plasma was given mostly to patients immunocompromised due to the different haematological malignancies or their treatment. Those lacking B-cell branch of immune system and immunoglobulins had no NAb before the CCP therapy and were excellent experimental systems to test the appropriateness of the above described recommendations. The increase of NAb levels in their serum samples after transfusion was successfully monitored, and measured quantities were in accordance to theoretical expectation, proving our decisions on plasma unit cut-off value and multiple units administration correct. Waves of NAbs were detected in the patients' blood in quantities equal to the ones measured in some successfully recovered convalescents (three examples in **Figure 6**), proving that the here described approach indeed provided SARS-CoV-2 neutralising immunoglobulins to patients incapable of mounting these by themselves. Transfused NAbs were cleared from systemic circulation within the period of 3 weeks, after which plasma was given again if needed. NAbs induced improvement of clinical symptoms, either permanently or just transiently (28). Results on the effectiveness of COVID-19 convalescent plasma treatment of COVID-19 patients with underlying haematological malignancies will be reported separately.

DISCUSSION

Convalescent plasma (CP) usage to treat infectious diseases is limited to short periods of epidemics, when other treatment options are not available. These are the only times when clinical studies on CP application can be conducted, but in circumstances of inadequate characterisation of plasma units used for the treatment. In regular times drug investigated in clinical trials should be characterised by fully validated methods. In epidemics the methods are just being developed, with no calibration to international standards (because none exists) so CP is characterised in different, incomparable ways and sometimes used without any antibody characterisation. All this aggravates the assessment of clinical trial results (15). Currently, there is a growing number of trials on CCP usage for the treatment of COVID-19 hospitalized immunocompetent patients that have been completed or the interim results have been published and reviewed (31, 15). Most of them demonstrated no effectiveness of CCP over placebo, which is in line with the general principles of passive antibody therapy, based on a century long experience (3). Namely, antibodies have been considered more effective in prevention of infection diseases than in their treatment. If used for the treatment, they are more effective if provided before the onset of symptoms. Also, it has already been known that high antibody concentrations are required. Thus, the lack of evidence that CCP is beneficial in the treatment of COVID-19 severe patients should not come as a surprise, since the antibodies from a plasma unit (200 mL) are being diluted 25-30 times considering the full volume of human blood (cca 8% of human body weight). In addition, evidence is growing (including our work) that the quantity of SARS-CoV-2 specific antibodies is correlated with the severity of disease, highest in the most severe cases (32), implying that a small additional infusion cannot provide significant benefit. However, there are trials reporting beneficial outcomes of CCP usage for COVID-19 treatment (17, 33, 34), particularly those attributed to the high-titre CCP usage early in the course of the illness (13, 15, 16, 23). Currently collected data on the CCP treatment of COVID-19 in patients with innate or acquired immunosuppression have been promising and warrant further investigation (14, 18). It would be highly important to ensure that the plethora of available clinical data is comparable between different studies to correctly assess available results and make reliable conclusions for the future. This is currently not possible. For example, Li et al. reported the usage of CCP with S-RBD-specific antibody titre of at least 1:640 (not specifying assay and producer), which correlated to neutralisation titre (also not specifying the details of the assay) to some extent (r=0.622) (9). They reported that a serum NT of 1:80 is approximately equivalent to a titre of 1:1280 for S-RBD-specific IgG. Agarwal et al. treated patients with CCP without determining the antibody titre, but assayed them in a stored plasma samples at the end of the trial. They reported that 2/3 of donated plasmas had NT higher than 1:20, without stating many details of the assay itself (8). They also stated that most of their donors had only mild symptoms, implying low levels of antibodies in the blood given for transfusion. Simonovich et al. reported that infused plasma had median titre

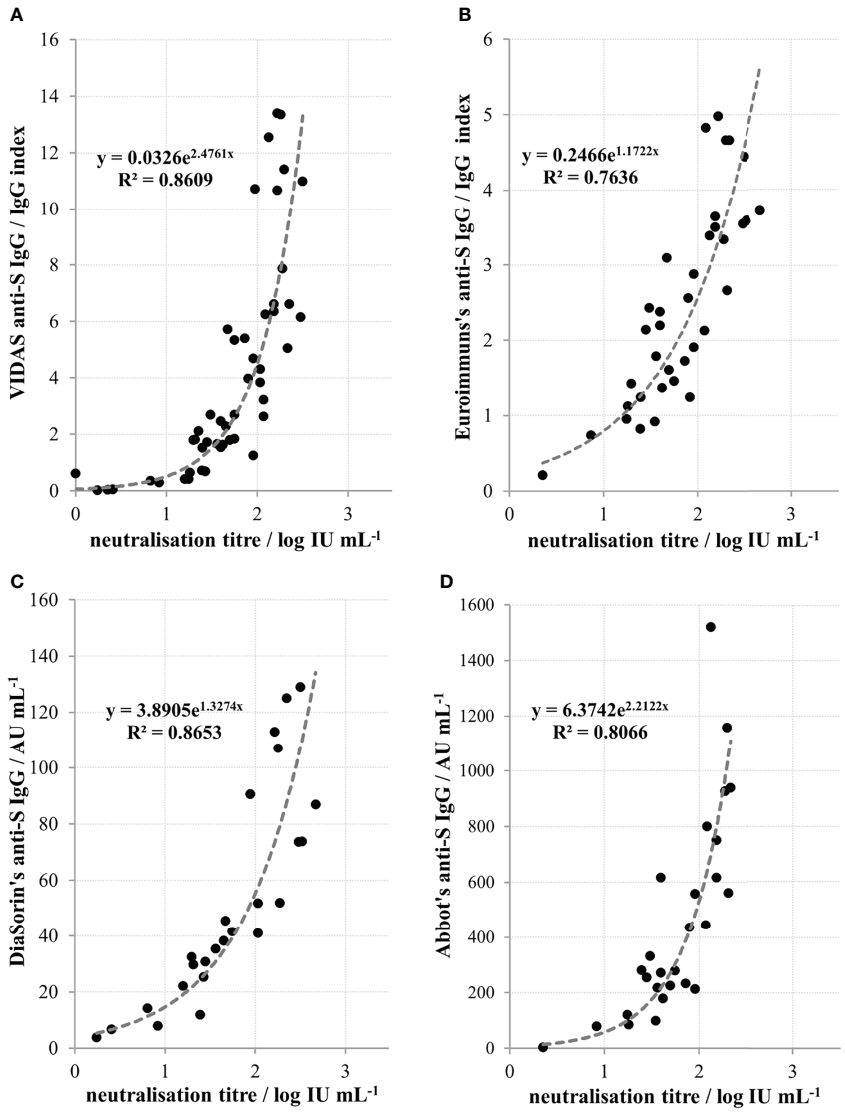

FIGURE 5 | Relationship between neutralisation titres of convalescent sera and quantity of anti-spike protein (anti-S) IgGs determined by **(A)** Biomerieux's VIDAS (*r*=0.93, *n*=49), **(B)** Euroimmun's (*r*=0.87*; n*=36), **(C)** DiaSorin's (*r*=0.93; *n*=25) and **(D)** Abbott's (*r*=0.90; *n*=27) commercial assays. Coefficient *r* denotes Pearson's coefficient of correlation from the *n* number of measurements.

of 1:3200 obtained in COVIDAR ELISA measuring IgG specific for RBD of S protein. They demonstrated a certain, though not a high degree of correlation between this assay and the neutralising activity in a pseudotyped particle system (*r*=0.52) (10). Joyner et al. characterised antibody content in the plasma by the VITROS anti-SARS-CoV-2 enzyme immunoassay providing results in signal-to-cut off ratios. They categorized plasma units to low, medium and high, and observed the beneficial effect in patients treated with high antibody units (23). Obviously, COVID-19 convalescent plasma was used globally, but characterised by different assays, so the results cannot be compared.

In Croatia we established the wild-type virus neutralisation assay as the most reliable indicator of protective humoral immunity and used it in the screening of convalescent plasma units. ED_{50} assay format using 8 replicates of each two-fold dilution was preferred over plaque reduction neutralization assay due to its better resolution. Here we provide a detailed demonstration on the establishment of a highly controlled SARS-CoV-2 neutralisation assay. For the reduction of assay variability, the banking system of the main biological components of the assay – virus, cells and in-house antibody standard was used and they have been constantly controlled **Figure 1**). Involvement of the in-house standard in each assay and its use for the correction of experimental samples results ensured the assay's reproducibility. Calibration of the in-house standard to the international standard as soon as it became available (24), enabled recalculation of all gained results for transfused

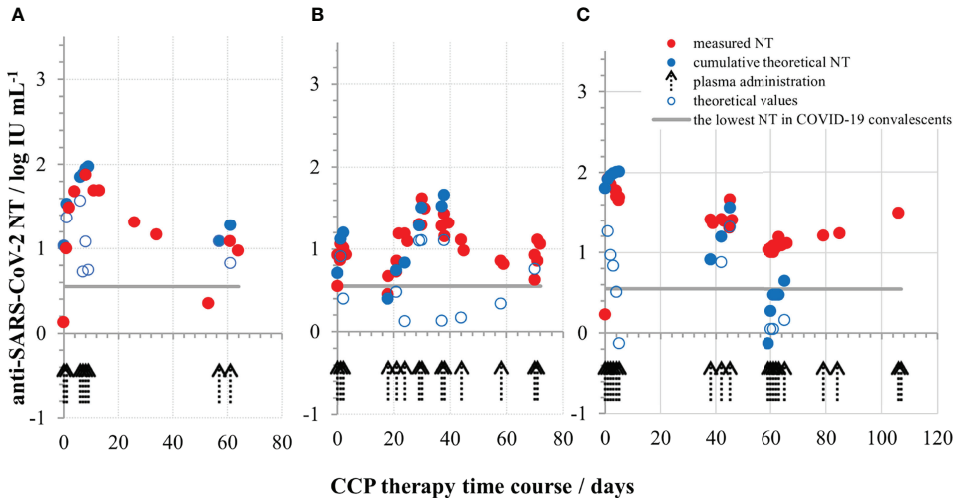

FIGURE 6 | Neutralising SARS-CoV-2 antibody titres (in IU mL^{-1}) during COVID-19 convalescent plasma therapy in the first **(A)**, second **(B)** and the third **(C)** representative COVID-19 patient, all three completely lacking their own immunoglobulins due to the underlying haematological malignancy and its treatment. The quantities of measured NAbs were above the lowest NT detected in successfully recovered persons.

plasmas to the units of the international standard, therefore expressing the results from our country in an internationally comparable way.

We demonstrate here that NAb level in plasma of COVID-19 convalescents (not including hospitalized patients) was in the range from 4 to 2869 IU mL^{-1} (0.55 to 3.46 log IU mL^{-1}). We observed significant positive correlation between SARS-CoV-2 NTs in convalescents and the disease severity (**Figure 4**), already noticed by others (32, 35, 36). We also observed a slow decline of NAbs in COVID-19 recovered persons (**Figure 3A**), the kinetics of which were calculated from the data of longitudinal monitoring of NT levels in six individual patients (**Figure 3B**). Neutralising antibodies declined on average 1.4-times during one-month period, or *cca* 3-times during 3 months, which is in line with the estimation of Crawford et al. of 4-fold decline from 1 to 4 months after the symptom onset (37). Complement activity in COVID-19 has so far been addressed mainly from the pathology-inducing aspect (38, 39). Kang et al. also investigated the role of antibodies directed to SARS-CoV-2 nucleoprotein (40), based on the pre-printed hypothesis of Gao et al. that complement hyperactivation is induced *via* N-protein, and its binding to mannan-binding lectin-associated serine protease 2 (41). We demonstrated here that complement activation in convalescent sera is probably initiated by SARS-CoV-2 antibodies (**Figure 2**), resulting in titres 2.7 times higher in native than in heat-inactivated sera. High correlation between NTs in convalescent sera and results of several widely used serological assays determining IgGs specific to S protein was clearly demonstrated (**Figure 5**) corroborating the results of Šimanek et al. (42), while no correlation was found with assays determining other antibody classes or different antibody specificities. The cut-off value for the release of convalescent plasma to therapy was set to 35 IU mL^{-1}. Food and Drug Administration authorized the emergency use of high titre COVID-19 convalescent plasma for the treatment of hospitalized patients with COVID-19 early in the course of disease and those hospitalized with impaired humoral immunity (August 23, 2020; revision on March 09, 2021; https://www.fda.gov/media/141477/download). High titre COVID-19 plasma, according to the current version, is the one with anti-SARS-CoV-2 IgG ratio in Euroimmun's ELISA ≥ 3.5 or Abbott's SARS-CoV-2 IgG result ≥ 840 AU mL^{-1}. These values correspond to 144 and 131 IU mL^{-1}, respectively, according to here determined relationships between the results of these two assays and neutralisation titres (**Figures 5B, D**). We can indirectly conclude that the value of high titre plasma expressed in units of the First WHO International Standard for anti-SARS-CoV-2 would be approx. 140 IU mL^{-1}. In comparison to FDA recommendations, our limit for plasma usage was four-fold lower. However, patients were always given several units, thus multiplying the quantity of NAbs received. In RECOVERY trial plasma donations with a sample to cut-off ratio of 6.0 or more on the Euroimmun IgG ELISA were used for the treatment (7). We could estimate from the function describing significantly correlating relationship between NTs and Euroimmun's results (**Figure 5B**) that plasmas of 323 IU mL^{-1} or more were used, but this is only estimation. True determination should be performed by assessing international standard in the Euroimmun's assay, used in this particular trial.

In conclusion, a high amount of currently incomparable data has been generated during the previous two years. We should put our efforts to validate all different assays used in different studies and calibrate them to the First WHO International Standard as to enable conclusions on quantities of antibodies providing or not providing benefit in the treatment of COVID-19 immunocompetent and particularly immunocompromised patients.

DATA AVAILABILITY STATEMENT

The datasets presented in this study can be found in online repositories. The name of the repository and accession numbers can be found below: Global Initiative on Sharing Avian Influenza Data (GISAID) database, https://www.gisaid.org/, EPI_ISL_3013040 and EPI_ISL_3013041. All users of GISAID databases are issued personal access credentials after having provided their identity and agreed to terms of use that govern the GISAID sharing mechanism.

ETHICS STATEMENT

The studies involving human participants were reviewed and approved by Croatian Ministry of Health (023-03/20-01/235; permission No. 534-04-3-2/2-20-11). The approval was based on the positive opinion of the Ethical Committee of Croatian Institute of Transfusion Medicine (003-06/20-04/02, opinion No.251-541-06/6-20-2). Immunocompromised COVID-19 patients were treated with COVID-19 plasma according to periodically updated FDA and EC guidelines (https://www.fda.gov/media/141477/download; https://ec.europa.eu/health/sites/default/files/blood_tissues_organs/docs/guidance_plasma_covid19_en.pdf). All COVID-19 convalescent plasma donors and all included patients (or their representatives) were informed about the study and gave written informed consent. The patients/participants provided their written informed consent to participate in this study.

AUTHOR CONTRIBUTIONS

SR established and performed the SARS-CoV-2 neutralisation assay. AH organized the convalescent plasma collection and its characterisation by different commercial serological assays, and managed distribution of plasma units toward clinicians. TK, OĐR, TM, and KK determined the anti-S antibodies using different commercial serological assays. TV and IJ were responsible for legislation connected to the plasma collection and usage. DR, OJ, GD, and ES treated COVID-19 patients using CCP. ŽMŠ isolated the wild-type SARS-CoV-2 virus from the clinical sample and subcultivated it. IK and AM ensured the continuous availability of BSL3 resources. JIJ, DF, and AS performed the NGS analysis of SARS-CoV-2 virus used in this study. BH orchestrated the whole work, collected and analysed the data and wrote the manuscript. The whole team participated in its shaping. All authors contributed to the article and approved the submitted version.

FUNDING

The research was funded by the Croatian Science Foundation (grant IP-CORONA-04-2053 to BH) and by the European Regional Development Fund, grant number KK.01.1.1.01.0006, "Strengthening the capacity of CerVirVac for research in virus immunology and vaccinology".

ACKNOWLEDGMENTS

The authors are grateful to Mrs. Renata Jug for the excellent technical assistance. The authors thank Marta Špoljar for proofreading and editing the manuscript. Particular gratitude goes to volunteers who provided plasma for CCP collection and/or research.

SUPPLEMENTARY MATERIAL

The Supplementary Material for this article can be found online at: https://www.frontiersin.org/articles/10.3389/fimmu.2022.816159/full#supplementary-material

REFERENCES

1. Graham BS, Ambrosino DM. History of Passive Antibody Administration for Prevention and Treatment of Infectious Diseases. *Curr Oppinion HIV AIDS* (2015) 10(13):129–34. doi: 10.1097/COH.0000000000000154.History
2. Bloch EM, Shoham S, Casadevall A, Sachais BS, Shaz B, Winters JL, et al. Deployment of Convalescent Plasma for the Prevention and Treatment of COVID-19. *J Clin Invest* (2020) 130(6):2757–65. doi: 10.1172/JCI138745
3. Casadevall A, Pirofski LA. The Convalescent Sera Option for Containing COVID-19. *J Clin Invest* (2020) 130(4):1545–8. doi: 10.1172/JCI138003
4. Cheng Y, Wong R, Soo YOY, Wong WS, Lee CK, Ng MHL, et al. Use of Convalescent Plasma Therapy in SARS Patients in Hong Kong. *Eur J Clin Microbiol Infect Dis* (2005) 24(1):44–6. doi: 10.1007/s10096-004-1271-9
5. Barreira DF, Lourenço RA, Calisto R, Moreira-Gonçalves D, Santos LL, Videira PA. Assessment of the Safety and Therapeutic Benefits of Convalescent Plasma in COVID-19 Treatment: A Systematic Review and Meta-Analysis. *Front Med* (2021) 8:660688(April). doi: 10.3389/fmed.2021.660688
6. Cohn CS, Estcourt L, Grossman BJ, Pagano MB, Allen ES, Bloch EM, et al. COVID-19 Convalescent Plasma: Interim Recommendations From the AABB. *Transfusion* (2021) 61(4):1313–23. doi: 10.1111/trf.16328
7. Abani O, Abbas A, Abbas F, Abbas M, Abbasi S, Abbass H, et al. Convalescent Plasma in Patients Admitted to Hospital With COVID-19 (RECOVERY): A Randomised Controlled, Open-Label, Platform Trial. *Lancet* (2021) 397 (10289):2049–59. doi: 10.1016/S0140-6736(21)00897-7
8. Agarwal A, Mukherjee A, Kumar G, Chatterjee P, Bhatnagar T, Malhotra P. Convalescent Plasma in the Management of Moderate Covid-19 in Adults in India: Open Label Phase II Multicentre Randomised Controlled Trial (PLACID Trial). *BMJ* (2020) 371:1–10. doi: 10.1136/bmj.m3939
9. Li L, Zhang W, Hu Y, Tong X, Zheng S, Yang J, et al. Effect of Convalescent Plasma Therapy on Time to Clinical Improvement in Patients With Severe and Life-Threatening COVID-19: A Randomized Clinical Trial. *JAMA - J Am Med Assoc* (2020) 324(5):460–70. doi: 10.1001/jama.2020.10044
10. Simonovich VA, Burgos Pratx LD, Scibona P, Beruto MV, Vallone MG, Vazquez C, et al. A Randomized Trial of Convalescent Plasma in Covid-19 Severe Pneumonia. *N Engl J Med* (2021) 384(7):619–29. doi: 10.1056/nejmoa2031304
11. Katz LM. (A Little) Clarity on Convalescent Plasma for Covid-19. *N Engl J Med* (2021) 384(7):666–8. doi: 10.1056/nejme2035678
12. Libster R, Pérez Marc G, Wappner D, Coviello S, Bianchi A, Braem V, et al. Early High-Titer Plasma Therapy to Prevent Severe Covid-19 in Older Adults. *N Engl J Med* (2021) 384(7):610–8. doi: 10.1056/nejmoa2033700
13. Körper S, Weiss M, Zickler D, Wiesmann T, Zacharowski K, Corman VM, et al. Results of the CAPSID Randomized Trial for High-Dose Convalescent Plasma in Patients With Severe COVID-19. *J Clin Invest* (2021) 131(20): e152264. doi: 10.1172/JCI152264

14. Senefeld JW, Klassen SA, Ford SK, Senese KA, Wiggins CC, Bostrom BC, et al. Use of Convalescent Plasma in COVID-19 Patients With Immunosuppression. *Transfusion* (2021) 61(8):2503–11. doi: 10.1111/trf.16525
15. Klassen SA, Senefeld JW, Senese KA, Johnson PW, Wiggins CC, Baker SE, et al. Convalescent Plasma Therapy for COVID-19: A Graphical Mosaic of the Worldwide Evidence. *Front Med* (2021) 8:684151(June). doi: 10.3389/fmed.2021.684151
16. Franchini M, Corsini F, Focosi D, Cruciani M. Safety and Efficacy of Convalescent Plasma in COVID-19: An Overview of Systematic Reviews. *Diagnostics* (2021) 11:1663. doi: 10.3390/diagnostics11091663
17. Avendaño-Solá C, Ramos-Martínez A, Muñez-Rubio E, Ruiz-Antoran B, Malo de Molina R, Torres F, et al. A Multicenter Randomized Open-Label Clinical Trial for Convalescent Plasma in Patients Hospitalized With COVID-19 Pneumonia. *J Clin Invest* (2021) 131(20):e152740. doi: 10.1172/JCI152740
18. Biernat MM, Kolasińska A, Kwiatkowski J, Urbaniak-Kujda D, Biernat P, Janocha-Litwin J, et al. Early Administration of Convalescent Plasma Improves Survival in Patients With Hematological Malignancies and COVID-19. *Viruses* (2021) 13(3):436. doi: 10.3390/v13030436
19. Luke TC, Kilbane EM, Jackson JL, Hoffman SL. Meta-Analysis : Convalescent Blood Products for Spanish Influenza. *Ann Intern Med* (2006) 145(8):599–609. doi: 10.7326/0003-4819-145-8-200610170-00139
20. Casadevall A, Scharff MD. Return to the Past: The Case for Antibody-Based Therapies in Infectious Diseases. *Clin Infect Dis* (1995) 21(1):150–61. doi: 10.1093/clinids/21.1.150
21. Subbarao K, Mordant F, Rudraraju R. Convalescent Plasma Treatment for COVID-19: Tempering Expectations With the Influenza Experience. *Eur J Immunol* (2020) 50(10):1447–53. doi: 10.1002/eji.202048723
22. Hurt AC, Wheatley AK. Neutralizing Antibody Therapeutics for Covid-19. *Viruses* (2021) 13(4):1–15. doi: 10.3390/v13040628
23. Joyner MJ, Carter RE, Senefeld JW, Klassen SA, Mills JR, Johnson PW, et al. Convalescent Plasma Antibody Levels and the Risk of Death From Covid-19. *N Engl J Med* (2021) 384(11):1015–27. doi: 10.1056/nejmoa2031893
24. Kristiansen PA, Page M, Bernasconi V, Mattiuzzo G, Dull P, Makar K, et al. WHO International Standard for Anti-SARS-CoV-2 Immunoglobulin. *Lancet* (2021) 397(10282):1347–8. doi: 10.1016/S0140-6736(21)00527-4
25. Langmead B, Salzberg SL. Fast Gapped-Read Alignment With Bowtie 2. *Nat Methods* (2012) 9(4):357–9. doi: 10.1038/nmeth.1923
26. Brgles M, Kurtović T, Lang Balija M, Hećimović A, Mušlin T, Halassy B. Impact of Complement and Difference of Cell-Based Assay and ELISA in Determination of Neutralization Capacity Against Mumps and Measles Virus. *J Immunol Methods* (2021) 490:112957. doi: 10.1016/j.jim.2021.112957
27. Halassy B, Kurtović T, Brgles M, Lang Balija M, Forčić D. Factors Influencing Preclinical *In Vivo* Evaluation of Mumps Vaccine Strain Immunogenicity. *Hum Vaccines Immunother* (2015) 11(10):2446–54. doi: 10.1080/21645515.2015.1062191
28. Rnjak D, Ravlić S, Šola AM, Halassy B, Šemnički J, Šuperba M, et al. COVID-19 Convalescent Plasma as Long-Term Therapy in Immunodeficient Patients? *Transfus Clin Biol* (2021) 28(3):264–70. doi: 10.1016/j.tracli.2021.04.004
29. Okada P, Buathong R, Phuygun S, Thanadachakul T, Parnmen S, Wongboot W, et al. Early Transmission Patterns of Coronavirus Disease 2019 (COVID-19) in Travellers From Wuhan to Thailand, January 2020. *Eurosurveillance* (2020) 25(8):2000097. doi: 10.2807/1560-7917.ES.2020.25.8.2000097
30. Korber B, Fischer WM, Gnanakaran S, Yoon H, Theiler J, Abfalterer W, et al. Tracking Changes in SARS-CoV-2 Spike: Evidence That D614G Increases Infectivity of the COVID-19 Virus. *Cell* (2020) 182(4):812–27.e19. doi: 10.1016/j.cell.2020.06.043
31. Prati D, Fiorin F, Berti P, De Silvestro G, Accorsi P, Ostuni A. Position Paper on the Use of COVID-19 Convalescent Plasma: An Update. *Blood Transfus* (2021) 19:277–80. doi: 10.2450/2021.0150-21
32. Wang P, Liu L, Nair MS, Yin MT, Luo Y, Wang Q, et al. SARS-CoV-2 Neutralizing Antibody Responses Are More Robust in Patients With Severe Disease. *Emerg Microbes Infect* (2020) 9(1):2091–3. doi: 10.1080/22221751.2020.1823890
33. Estcourt LJ, Turgeon AF, McQuilten ZK, McVerry BJ, Al-Beidh F, Annane D, et al. Effect of Convalescent Plasma on Organ Support-Free Days in Critically Ill Patients With COVID-19: A Randomized Clinical Trial. *JAMA - J Am Med Assoc* (2021) 326(17):1690–702. doi: 10.1001/jama.2021.18178
34. Tobian A, Cohn C, Shaz B. COVID-19 Convalescent Plasma. *Blood* (2021) 61:1313–23. doi: 10.1182/blood.2021012248
35. Seow J, Graham C, Merrick B, Acors S, Pickering S, Steel KJA, et al. Longitudinal Observation and Decline of Neutralizing Antibody Responses in the Three Months Following SARS-CoV-2 Infection in Humans. *Nat Microbiol* (2020) 5(12):1598–607. doi: 10.1038/s41564-020-00813-8
36. Hashem AM, Algaissi A, Almahboub SA, Alfaleh MA, Abujamel TS, Alamri SS, et al. Early Humoral Response Correlates With Disease Severity and Outcomes in Covid-19 Patients. *Viruses* (2020) 12(12):1–13. doi: 10.3390/v12121390
37. Crawford KHD, Dingens AS, Eguia R, Wolf CR, Wilcox N, Logue JK, et al. Dynamics of Neutralizing Antibody Titers in the Months After Severe Acute Respiratory Syndrome Coronavirus 2 Infection. *J Infect Dis* (2021) 223(2):197–205. doi: 10.1093/infdis/jiaa618
38. Yu J, Gerber GF, Chen H, Yuan X, Chatuvedi S, Vraunstein EM, et al. Complement Dysregulation Is Associated With Severe COVID-19 Illness. *Haematologica* (2021). doi: 10.3324/haematol.2021.279155
39. Wilk CM. Coronaviruses Hijack the Complement System. *Nat Rev Immunol* (2020) 20(6):350. doi: 10.1038/s41577-020-0314-5
40. Kang S, Yang M, He S, Wang Y, Chen X, Chen Y-Q, et al. A SARS-CoV-2 Antibody Curbs Viral Nucleocapsid Protein-Induced Complement Hyperactivation. *Nat Commun* (2021) 12(1):1–11. doi: 10.1038/s41467-021-23036-9
41. Preprint, Gao T, Hu M, Li H, Zhu L, Liu H, et al. Highly Pathogenic Coronavirus N Protein Aggravates Lung Injury by MASP-2-Mediated Complement Over-Activation. *medRxiv* (2020). doi: 10.1101/2020.03.29.20041962
42. Šimánek V, Pecen L, Krátká Z, Fuerst T, Rezačkova H, Topolčan O, et al. Five Commercial Immunoassays for Sars-Cov-2 Antibody Determination and Their Comparison and Correlation With the Virus Neutralization Test. *Diagnostics* (2021) 11(4):1–14. doi: 10.3390/diagnostics11040593

Conflict of Interest: The authors declare that the research was conducted in the absence of any commercial or financial relationships that could be construed as a potential conflict of interest.

frontiers in Immunology

ORIGINAL RESEARCH
published: 24 February 2022
doi: 10.3389/fimmu.2022.822159

Single-Domain Antibodies Efficiently Neutralize SARS-CoV-2 Variants of Concern

Irina A. Favorskaya[1], Dmitry V. Shcheblyakov[2], Ilias B. Esmagambetov[2], Inna V. Dolzhikova[3], Irina A. Alekseeva[2], Anastasia I. Korobkova[2], Daria V. Voronina[2], Ekaterina I. Ryabova[2], Artem A. Derkaev[2], Anna V. Kovyrshina[3], Anna A. Iliukhina[3], Andrey G. Botikov[3], Olga L. Voronina[2], Daria A. Egorova[2], Olga V. Zubkova[2], Natalia N. Ryzhova[2], Ekaterina I. Aksenova[2], Marina S. Kunda[2], Denis Y. Logunov[1], Boris S. Naroditsky[2] and Alexandr L. Gintsburg[2]*

[1] Medical Microbiology Department, Federal State Budget Institution "National Research Center for Epidemiology and Microbiology Named after Honorary Academician N.F. Gamaleya" of the Ministry of Health of the Russian Federation, Moscow, Russia, [2] Department of Genetics and Molecular Biology of Bacteria, Federal State Budget Institution "National Research Centre for Epidemiology and Microbiology Named after Honorary Academician N.F. Gamaleya" of the Ministry of Health of the Russian Federation, Moscow, Russia, [3] Department of the National Virus Collection, Federal State Budget Institution "National Research Centre for Epidemiology and Microbiology Named after Honorary Academician N.F. Gamaleya" of the Ministry of Health of the Russian Federation, Moscow, Russia

OPEN ACCESS

Edited by:
Peter Chen,
Cedars-Sinai Medical Center,
United States

Reviewed by:
Serge Muyldermans,
Vrije University Brussel, Belgium
Matias Gutiérrez-González,
Ragon Institute, United States

***Correspondence:**
Dmitry V. Shcheblyakov
sdmitryv@yahoo.com

Specialty section:
This article was submitted to Vaccines and Molecular Therapeutics, a section of the journal Frontiers in Immunology

Received: 25 November 2021
Accepted: 28 January 2022
Published: 24 February 2022

Citation:
Favorskaya IA, Shcheblyakov DV, Esmagambetov IB, Dolzhikova IV, Alekseeva IA, Korobkova AI, Voronina DV, Ryabova EI, Derkaev AA, Kovyrshina AV, Iliukhina AA, Botikov AG, Voronina OL, Egorova DA, Zubkova OV, Ryzhova NN, Aksenova EI, Kunda MS, Logunov DY, Naroditsky BS and Gintsburg AL (2022) Single-Domain Antibodies Efficiently Neutralize SARS-CoV-2 Variants of Concern. Front. Immunol. 13:822159. doi: 10.3389/fimmu.2022.822159

Virus-neutralizing antibodies are one of the few treatment options for COVID-19. The evolution of SARS-CoV-2 virus has led to the emergence of virus variants with reduced sensitivity to some antibody-based therapies. The development of potent antibodies with a broad spectrum of neutralizing activity is urgently needed. Here we isolated a panel of single-domain antibodies that specifically bind to the receptor-binding domain of SARS-CoV-2 S glycoprotein. Three of the selected antibodies exhibiting most robust neutralization potency were used to generate dimeric molecules. We observed that these modifications resulted in up to a 200-fold increase in neutralizing activity. The most potent heterodimeric molecule efficiently neutralized each of SARS-CoV-2 variant of concern, including Alpha, Beta, Gamma, Delta and Omicron variants. This heterodimeric molecule could be a promising drug candidate for a treatment for COVID-19 caused by virus variants of concern.

Keywords: SARS-CoV-2, COVID-19, single-domain antibodies, VHH, VOC, neutralizing antibodies, nanobodies

INTRODUCTION

The COVID-19 pandemic, caused by severe acute respiratory syndrome coronavirus 2 (SARS-CoV-2), has resulted in over 340 million of infections and over 5 million deaths worldwide (January 2022, WHO). These numbers are still rising and COVID-19 disease remains a great challenge to public health system. The development of safe and effective treatment together with vaccination is a highly important goal for scientists and health care professionals over the world.

One of the approaches to the development of an effective therapeutic agent is the isolation of monoclonal antibodies that efficiently neutralize SARS-CoV-2 virus. Currently, several monoclonal antibodies already received emergency use authorization for COVID-19 treatment and post-exposure prophylaxis. These antibodies are bamlanivimab plus etesevimab, casirivimab plus imdevimab, sotrovimab and regdanvimab (1–4).

Along with conventional antibodies, camelid single-domain antibodies (also called nanobodies or VHHs) are promising candidates for the development of antibody-based therapies (5, 6). Camelids have unique heavy-chain antibodies that are devoid of light chains (7). Nanobodies are the minimal antigen-binding domains of these heavy-chain antibodies. They have several advantages, including the ability to recognize epitopes that are not accessible to conventional antibodies, increased stability of nanobodies, simplicity of generation of multivalent forms and low cost bacterial production (8). Currently, several nanobodies to SARS-COV-2 have been isolated showing neutralizing activity in *in vitro* and *in vivo* studies, which confirms their promising potential as therapeutic agents (9–15).

The evolution of SARS-CoV-2 virus has resulted in emergence of virus variants that have become more transmissible and less sensitive to neutralizing antibodies. The spread of these new virus variants has reduced the efficacy of vaccines and some therapeutic antibodies. The list of these variants of concern (VOCs) consist of B.1.1.7 (Alpha), B.1.351 (Beta), B.1.1.28/P.1 (Gamma), B.1.617.2 (Delta) and B.1.1.529 (Omicron) variants (January 2022, WHO). The reduction of neutralization by antibodies is caused by mutations in S glycoprotein, including K417N/T, L452R, T478K, E484K and N501Y substitutions (16, 17). Recently appeared Omicron variant has more than 30 mutations in S glycoprotein that provide considerable escape from neutralization by antibodies (18, 19). In this regard, it became necessary to isolate antibodies, the neutralizing activity of which will not be affected due to observed mutations, therefore, these antibodies or their cocktails will retain activity against each of VOCs.

Here we identified and characterized a panel of single-domain antibodies isolated from immune VHH library that specifically bind RBD of S glycoprotein. We assessed the neutralizing activity of the isolated antibodies in a microneutralization assay with live SARS-CoV-2 and selected three most potent antibodies. To increase the therapeutic potential, these clones were modified to homodimeric and heterodimeric forms, and the neutralizing activity against SARS-CoV-2 VOCs was investigated. The most potent heterodimeric form, P2C5-P5F8, exhibited activity against all tested virus variants at low concentration. These results indicate that P2C5-P5F8 heterodimer is a promising candidate for further research to develop COVID-19 antibody-based therapy.

RESULTS

To identify SARS-CoV-2 neutralizing single-domain antibodies we immunized one Bactrian camel with SARS-CoV-2 RBD. The recombinant RBD protein was previously produced in CHO-S cells and purified. Immunization was performed using five sequential injections (**Figure 1A**). Blood was collected 5 days after final immunization and the serum RBD-specific antibodies titer was detected by ELISA. Post-immunization serum demonstrated potent binding to SARS-CoV-2 RBD with titer more than 1/200 000 (**Figure 1B**). The neutralizing activity of antibodies in the immunized serum was measured by the microneutralization assay using live SARS-CoV-2 B.1.1.1, the neutralizing antibodies titer was 1/1280.

To isolate monoclonal RBD-specific nanobodies, we constructed a VHH phage display library by cloning VHH sequences from B cells of immunized camel into a phagmid vector. We performed one round of phage display followed by ELISA-based screening of individual clones to identify RBD-specific binders.

We used monoclonal phage-ELISA together with monoclonal ELISA to identify RBD binders with high expression levels and high solubility. A total of 212 clones showing positive phage-ELISA and ELISA signals were selected for sequencing (**Figure 1C**), which lead to the identification of 39 unique clones of nanobodies. After sequence alignment and phylogenetic analysis we selected 16 antibodies with highly diverse sequences for further research (**Figure 1D**). These nanobodies were expressed and purified, and the RBD binding activity of each antibody was analyzed by ELISA. We confirmed the binding of 14 clones with ELISA EC50 values ranged from 1.1 to 313.3 nM (**Figure 2A**). Most of the antibodies (13 out of 14) displayed strong positive signals with EC50 below 22 nM.

To examine the capacity of selected RBD binders to neutralize live SARS-CoV-2 virus we performed a microneutralization assay with inhibition of the cytopathic effect of virus as a marker of neutralization. We found that 10 of 14 nanobodies efficiently neutralized SARS-CoV-2 virus (B.1.1.1) at concentrations ranging from 12 nM to 1540 nM (**Figure 2A**). The three most potent antibodies were P2C5, P2G1 and P5F8, which completely inhibited the cytopathic effect of the virus at 24 nM, 12 nM and 48 nM, respectively.

We investigated the binding kinetics of P2C5, P2G1 and P5F8 neutralizing nanobodies *via* surface plasmon resonance (SPR). All antibodies tested bound RBD with high affinity, dissociation constants (K_D) were 3.97 nM, 5.36 nM and 1.94 nM for P2C5, P2G1 and P5F8, respectively (**Figure 2B**).

To explore whether the isolated antibodies bound to distinct epitopes we performed epitope binning immunoassay using SPR. Two groups of nanobodies were identified; antibodies from the first group have overlapping or competing epitopes with P2C5, and antibodies from the second group with P2G1 (**Figure 2C**). We also revealed that P2C5 competes with class I anti-RBD antibody casirivimab and P2G1 competes with class III antibody imdevimab.

Since the capacity of an antibody to neutralize SARS-CoV-2 virus is frequently associated with blocking the interaction between S glycoprotein and ACE2 receptor, we analyzed the ability of isolated nanobodies to block the RBD binding to ACE2 by competitive ELISA (**Figure 2D**). We revealed a decrease in ELISA signal for most of neutralizing nanobodies indicating

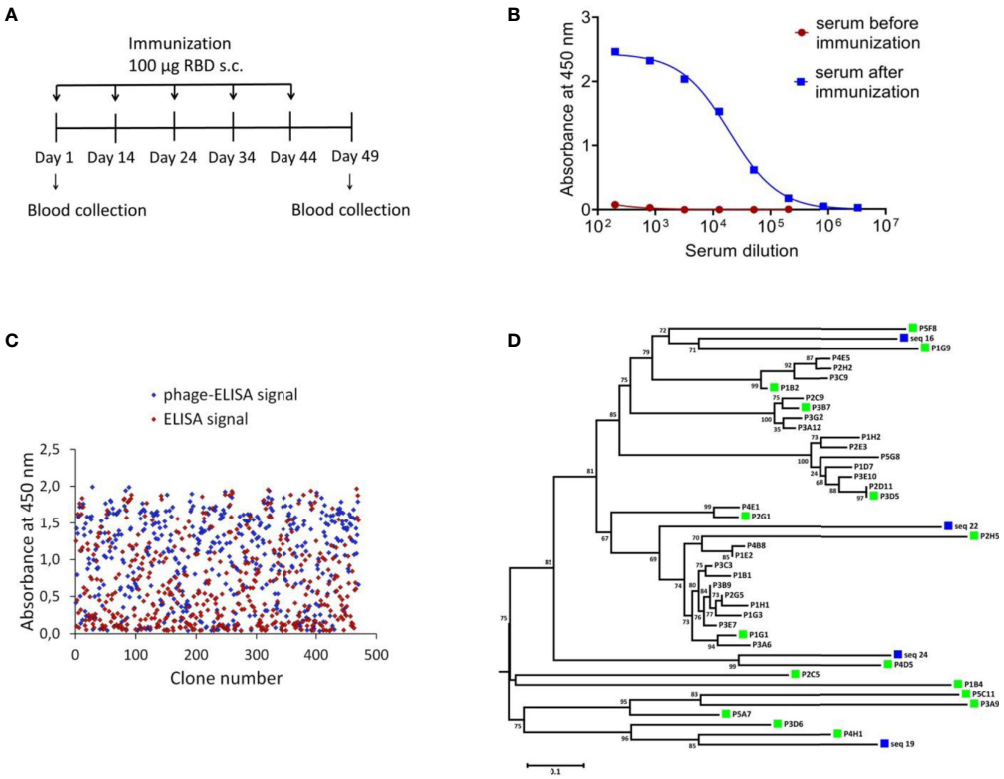

FIGURE 1 | Isolation of RBD-specific nanobodies. **(A)** Immunization schedule. Bactrian camel was immunized with 100 µg RBD subcutaneously (with complete Freund`s adjuvant), followed by four consecutive immunization with 100 µg RBD subcutaneously (with incomplete Freund`s adjuvant). Blood samples were collected before immunization and five days after the last immunization. **(B)** RBD-specific antibodies in camel serum before and after immunization, detected by ELISA. The assay reveals a strong positive RBD-specific serological activity 5 days after the last immunization. **(C)** ELISA-based RBD-binders screening. A total of 212 individual clones with a strong positive ELISA signal were selected for sequencing. **(D)** Phylogenetic tree showing sequence diversity of 39 unique VHH clones from this study and four previously described single-domain antibodies of C. bactrianus (20), blue squares –previously described single-domain antibodies of C. bactrianus, green squares – the clones selected for further analysis.

antibodies competition with ACE2 for RBD binding. We observed that one of the most potent neutralizing antibodies, P2C5, blocked the ACE2-RBD interaction with an inhibition rate greater than 90% at 0.5 µg/ml.

In order to improve the antiviral property of antibodies we produced homodimer and heterodimer forms of P2C5, P2G1 and P5F8 clones. Monomers were fused using a flexible GS-linker $(Gly4Ser)_4$ for dimerization. The binding of generated dimeric molecules to the recombinant RBD protein was confirmed by ELISA. Analysis of the neutralization capacity in the microneutralization assay revealed a pronounced improvement in the neutralizing activity of several dimeric forms (**Table 1**). Notable, P2C5 homodimer inhibited cytopathic effect of the virus at 89 pM, thus the homodimer activity increased more than 200-fold compared to the monomer activity. We also observed that P2C5-P5F8 heterodimer form was up to 100 times more active than the monomeric forms, this molecule exhibited neutralization activity at 178 pM.

With the emergence and spread of new variants of SARS-CoV-2 with increased transmissibility and reduced neutralization by antibodies it became necessary to isolate antibodies with a broad spectrum of neutralizing activity. We assessed the neutralizing activity of isolated antibodies against variants of concern (VOCs), including B.1.1.7 (Alpha), B.1.351 (Beta), B.1.1.28/P.1 (Gamma), B.1.617.2 (Delta) and B.1.1.529 (Omicron) variants (**Table 1**). P2C5 monomer neutralized B.1.1.7, B.1.351, B.1.1.28/P.1 and B.1.1.529 but was unable to neutralize B.1.617.2. P5F8 and P2G1 monomeric forms remained active against all tested VOCs (inhibited CPE at 12-96 nM) except Omicron variant. P5F8 monomer showed a 2-fold decrease in activity against B.1.351 and B.1.1.28/P.1. P2G1 showed a 2-4-fold decrease against VOCs. The most potent heterodimeric molecule P2C5-P5F8 exhibited activity against all VOCs neutralizing B.1.1.7, B.1.351, B.1.1.28/P.1, B.1.617.2 and B.1.1.529 variants at 89 pM, 356 pM, 356 pM, 2.85 nM and 709 pM, respectively. The most active P2C5 homodimer neutralized each of VOC except B.1.617.2 at a concentration 356 pM and lower, depending on the virus variant. Overall, P2C5-P5F8 heterodimer showed neutralizing activity against each of the tested VOCs and was a promising candidate for further investigations as a potential therapeutic agent.

A

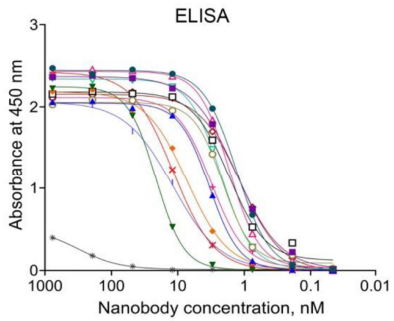

Nanobody	ELISA EC50, nM	Minimal neutralizing concentration, nM
P1G1	1.31	192
P1G9	1.32	>1540
P2C5	3.35	24
P2G1	21.39	12
P3D6	7.30	384
P4D5	2.10	769
P5C11	1.70	1540
P1B2	1.68	769
P1B4	2.26	>1540
P5A7	1.14	769
P5F8	11.73	48
P3B7	11.91	>1540
P3A9	313.3	>1540
P4H1	3.15	384

B

Nanobody	k_{on} (1/Ms)	k_{off} (1/s)	R_{max} (RU)	K_A (1/M)	K_D (M)	Chi^2
P2C5	$1.2x10^5$	$4.74x10^{-4}$	135	$2.52x10^8$	$3.97x10^{-9}$	8.5
P5F8	$1.13x10^5$	$2.18x10^{-5}$	90.7	$5.16x10^8$	$1.94x10^{-9}$	6.17
P2G1	$1.06x10^5$	$5.94x10^{-4}$	97.2	$1.86x10^8$	$5.36x10^{-9}$	1.74

C

Nanobody	P2C5	P2G1
P2C5		
P1G9		
P3D6		
P4D5		
P5C11		
P1B2		
P5A7		
P3B7		
P4H1		
P2G1		
P1G1		
P1B4		
P5F8		
P3A9		
Casirivimab		
Imdevimab		

Competing antibodies
Non-competing antibodies
Not tested

D

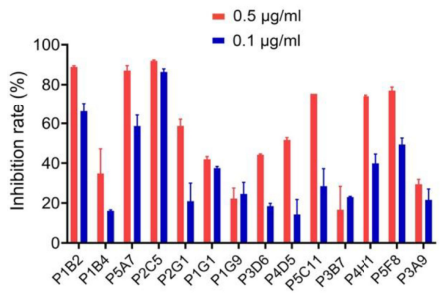

FIGURE 2 | Characterization of the selected nanobodies. **(A)** RBD-binding activity of nanobodies by ELISA and neutralization activity of nanobodies by microneutralization assay using live SARS-CoV-2 virus. The minimal neutralizing concentration was defined as the lowest antibody concentration (highest antibody dilution) that completely inhibited the cytopathic effect of the virus in two or three from the three replicable wells. **(B)** Kinetic parameters of nanobodies interaction with RBD by SPR. Association (k_{on}), dissociation (k_{off}), maximal analyte binding capacity (R_{max}), equilibrium association constants (K_A), equilibrium dissociation constants (K_D) and Chi^2 for VHHs binding to RBD. **(C)** SPR-based epitope binning experiments, in-tandem format. The first saturating antibody indicated on the top row, the second competing antibody indicated on the left column. **(D)** Blocking of ACE2-RBD interaction measured by competitive ELISA.

DISCUSSION

The SARS-CoV-2 virus gave rise to ongoing pandemic, which continues to claim lives and poses a threat to public health. Along with vaccination to prevent COVID-19, therapeutic antiviral agents are urgently needed to treat the infection.

One of the promising approaches for the viral infection treatment is an antibody-based therapy. Antibodies administration approved for immunoprophylaxis and treatment of viral infections caused by respiratory syncytial virus and ebolavirus (21, 22). Today, several monoclonal antibodies are already in use for COVID-19 treatment (bamlanivimab plus etesevimab, casirivimab plus imdevimab and sotrovimab). It was shown that the administration of these antibodies to nonhospitalized patients with symptomatic COVID-19 and risk factors for disease progression reduced the risk of hospitalization and death (1–4).

In addition to conventional antibodies, single-domain antibodies or nanobodies from camelid heavy-chain antibodies are being actively investigated as a potential therapeutic agent

TABLE 1 | Neutralizing activity of the most potent monomers of nanobodies, homodimeric and heterodimeric forms of nanobodies in a microneutralization assay against live SARS-CoV-2 variants of concern.

Antibody		Minimal neutralizing concentration of antibody, nM					
		B.1.1.1	Alpha (B.1.1.7)	Beta (B.1.351)	Gamma (B.1.1.28/P.1)	Delta (B.1.617.2)	Omicron (B.1.1.529)
Monomers	P2C5	24.04	48.08	96.15	48.08	>1500	24.04
	P2G1	12.02	48.08	96.15	48.08	24.04	>1500
	P5F8	48.08	48.08	96.15	96.15	48.08	>1500
Homodimers	(P2C5)2	0.089	0.178	0.356	0.356	>1500	0.089
	(P2G1)2	11.36	22.73	45.45	45.45	45.45	>1500
	(P5F8)2	5.68	5.68	22.72	22.72	11.36	>1500
Heterodimers	P2C5-P2G1	0.709	0.356	2.84	2.84	11.36	0.709
	P2C5-P5F8	0.178	0.089	0.356	0.356	2.85	0.709
	P2G1-P2C5	2.84	2.84	11.36	5.68	45.45	2.84
	P2G1-P5F8	45.45	45.45	181.82	45.45	90.91	>1500
	P5F8-P2C5	5.68	11.36	22.73	22.72	90.91	5.68
	P5F8-P2G1	11.36	22.72	90.91	22.72	22.73	>1500

with a number of advantages. The small size and single-domain nature of nanobodies allow them to bind epitopes that are not available for conventional antibodies, in particular concave epitopes such as grooves and clefts (23–25). Nanobodies show strong binding affinities and also are highly stable across wide range of temperatures and pH (26). The production of nanobodies in bacteria is less expensive than classical antibody production. All this allows the use of single-domain antibodies for many of applications, including research, diagnostics and therapy (6, 8).

The main mechanism of virus-neutralizing activity of antibodies is associated with the prevention of viral entry into host cells. The entry of SARS-CoV-2 virus occurs after the interaction of S glycoprotein with cell receptor angiotensin-converting enzyme 2 (ACE2). Therefore, S glycoprotein, in particular its receptor-binding domain (RBD), is an attractive target for the development of neutralizing antibodies.

In our work, we immunized a Bactrian camel with the recombinant RBD protein for following isolation of effective neutralizing antibodies against SARS-CoV-2 virus. We generated a VHH phage display library and selected a panel of RBD-specific nanobodies. Using an *in vitro* microneutralization assay we identified three clones (P2C5, P5F8 and P2G1) of the most potent antibodies that completely inhibited the cytopathic effect of SARS-CoV-2 virus at minimal concentrations from 12 nM to 48 nM.

At the next stage, to enhance the neutralization potential of isolated nanobodies we generated homodimeric and heterodimeric forms of the most active antibodies. It was previously shown that multivalent forms of nanobodies are characterized by increased functionality by improving antigen-binding through avidity effect (27). For example, the dimeric form of anti-TNF VHH was up to 500 times more active than the monovalent form in rheumatoid arthritis model *in vivo* (28), homotrimeric molecule of anti-SARS-CoV-2 nanobody $Nb21_3$ were 30-fold more potent in pseudovirus neutralization (14), dimeric forms of nanobodies to botulinum neurotoxin showed a higher protective activity *in vivo* (29). In our study, we revealed a 200-fold improvement of neutralization potential after dimerization of P2C5 nanobody. The bivalent molecule effectively neutralized SARS-CoV-2 virus at 89 pM. We also observed a pronounced increase in neutralizing activity in the case of P2C5-P5F8 heterodimeric form, which inhibited SARS-CoV-2 virus at 178 pM. In the case of the bivalent form of P5F8 we observed only a slight increase in activity. We assume that this may be due to the monovalent binding of P5F8 dimer to the S glycoprotein, for example as a result of the insufficient linker length to span the distance between epitopes in the trimeric S glycoprotein.

The emergence of SARS-CoV-2 variants with mutations in their RBD epitopes leads to the viral escape from neutralizing antibodies. It was shown that the virus-neutralization activity of sera samples obtained from individuals vaccinated with Pfizer/BNT162b2, Moderna/mRNA-1273 or Sputnik V decreased in the case of the B.1.351, B.1.1.28/P.1 and B.1.617.2 variants compared to wild-type virus (30–33). The most pronounced decrease of the virus-neutralization activity of sera observed in case of the B.1.1.529 (Omicron) variant (34–36). Escape mutations are also a challenge for antibody-based therapy development. Some therapeutic antibodies have become ineffective against VOCs, for example, the activity of bamlanivimab against Delta is reduced, the activity of etesevimab and casivimab against Beta variant is reduced (37). The activity of most neutralizing antibodies is escaped by the Omicron variant. Several monoclonal antibodies completely lost inhibitory activity against Omicron, including bamlanivimab, etesevimab, casirivimab, imdevimab and regdanvimab (18, 38). The activity of some previously isolated nanobodies also altered by escape mutations. The Beta strain drastically reduced the efficacy of the high-affinity nanobodies Nb20 and Nb21 (39). Thereby, it is urgently needed to identify nanobodies or their combinations that retain activity against SARS-CoV-2 variants of concern.

We investigated the activity of isolated potent nanobodies and their dimeric forms using a microneutralization assay against live SARS-CoV-2 VOCs. We found that P2C5-P5F8 heterodimer effectively neutralized all tested virus variants at low concentration, including Delta and Omicron VOCs. In particular it was observed that this dimeric molecule completely inhibited the cytopathic effect of the Alpha, Beta,

Gamma, Delta and Omicron variants at concentrations 89 pM, 356 pM, 356 pM, 2.85 nM and 709 pM, respectively.

For the improvement of antiviral efficacy of obtained P2C5-P5F8 molecule further modifications may include the fusion of the heterodimer to human IgG1 Fc domain. Fc modifications are often used to increase serum half-life of nanobodies, as well as to involve Fc-mediated effector functions (antibody-dependent cell-mediated cytotoxicity, complement-dependent cytotoxicity, etc.) (29, 40).

Overall, we produced heterodimeric form of nanobodies that possess a broad spectrum of activity, overcoming escape mutations in VOCs. This heterodimeric molecule is a promising candidate for the further development of an effective antiviral agent for COVID-19 treatment especially for patients with risk factors for progression to severe COVID-19.

MATERIALS AND METHODS

Cell Lines and Viruses

CHO-S cells were obtained from Thermo Fisher Scientific (USA), cat. no. R80007. Vero E6 cells (ATCC CRL 1586) was obtained from Russian collection of vertebrate cell lines.

SARS-CoV-2 strains B.1.1.1 (hCoV-19/Russia/Moscow_PMVL-1/2020), B.1.351 (hCoV-19/Russia/SPE-RII-27029S/2021), B.1.617.2 (hCoV-19/Russia/SPE-RII-32758S/2021) and B.1.1.529 (hCoV-19/Russia/MOW-Moscow_PMVL-O16/2021) were isolated from nasopharyngeal swabs.

SARS-CoV-2 strains B.1.1.7 (hCoV-19/Netherlands/NoordHolland_20432/2020) and B.1.1.28/P.1 (hCoV-19/Netherlands/NoordHolland_10915/2021) were obtained from European Virus Archive Global.

Cloning, Expression and Purification of Recombinant SARS-CoV-2 RBD Protein

The RBD nucleotide sequence of SARS-CoV-2 Wuhan-Hu-1 isolate (Genbank accession number MN908947, from 319 to 545 aa) was synthesized (Evrogen, Russia) and cloned into the pCEP4 mammalian expression vector (Thermo Fisher Scientific, USA). The signal peptide of alkaline phosphatase SEAP was inserted before RBD coding sequence, the His tag was fused to the end of the sequence. The obtained recombinant vector was transfected into CHO-S cells using CHOgro High Yield Expression System (Mirus Bio, USA). The culture supernatant containing the RBD protein was harvested after 10 days, the recombinant RBD protein was purified by IMAC using an AKTA start system (Cytiva, USA) and a HisTrap column (Cytiva, USA). The protein expression and purity was confirmed with SDS-PAGE.

Bactrian Camel Immunization

Bactrian camel was immunized with recombinant SARS-CoV-2 RBD protein at a dose of 100 μg with complete Freund`s adjuvant subcutaneously followed by four booster immunizations with 100 μg RBD with incomplete Freund`s adjuvant. The interval between the first and second injections was 14 days; the intervals between all subsequent injections were 10 days. Before immunization, a small blood sample (5 ml) was collected as a control. 50 ml blood was collected 5 days after the last immunization and was used for peripheral blood mononuclear cells (PBMC) isolation and VHH phage display library construction.

Phage Display Library Construction

The library construction was performed as described earlier (29). Briefly, total RNA was isolated from PBMCs and then reverse transcribed to cDNA. VHHs coding sequences were PCR amplified and cloned into a pHEN1 phagmid vector (41). Recombinant phagmids were electroporated into TG1 cells (Lucigen, USA). A VHH library of 7.3 x 10^6 individual clones was obtained. 98% of the clones harbored the vector with the right insert size.

Phage Preparation and Biopanning

Phage preparation was performed according to the previous description (29). To select RBD-specific nanobodies one round of biopanning was performed. 5 μg of recombinant SARS-CoV-2 RBD protein were immobilized in the well of microtiter plate. After rinsing three times with PBS with 0.1% Tween 20 (TPBS), the well was blocked with blocking buffer (5% non-fat dried milk in TPBS) at 37°C for 1 h. A total of ~10^{11} phage particles in blocking buffer were added to the well and the plate was incubated at 37°C for 1 h. Unbound phages were removed by washing with TPBS. The bound phages were eluted by trypsin (1 mg/ml). The eluted phage particles were used for infection of TG1 cells.

ELISA

Screening for RBD-specific binders was performed using monoclonal phage ELISA and monoclonal ELISA. For monoclonal phage ELISA, individual clones were inoculated in 1 ml of 2xYT (Sigma, USA) containing 100 μg/ml ampicillin in 96-deep-well plates. Bacterial cells were infected with KM13 helper phage and incubated overnight at 30°C. The plates were centrifuged, 50 μl of the supernatant were used for phage ELISA. For monoclonal ELISA, individual clones were cultured in 96-deep-well plates at 30°C overnight. The next day, the cells were lysed by the freeze-thaw method, and then the plates were centrifuged. 50 μl of the supernatant were used for monoclonal ELISA. Immunoplates (Nunc MaxiSorp, Thermo Fisher Scientific, USA) were coated with recombinant RBD protein (100 ng per well) at 4°C overnight. The plates were rinsed three times with TPBS and the wells were blocked with blocking buffer at 37°C for 1 h. 50 μl of bacterial supernatants containing monoclonal recombinant phages (monoclonal phage ELISA) or monoclonal nanobodies (monoclonal ELISA) were added to the wells. After 1 h incubation at 37°C, the wells were rinsed five times with TPBS. Bound phages were detected by HRP-conjugated anti-M13 antibody (Sino Biological, China), bound VHH were detected by HRP-conjugated anti-Myc-tag antibody (Abcam, UK) followed by the addition of 3,3`5,5`-tetramethylbenzidine (TMB) (Bio-Rad, USA) as a substrate. The reaction was stopped by 1M H_2SO_4, the absorbance at 450

nm was read using a Varioskan LUX (Thermo Fisher Scientific, USA).

To confirm RBD-specific binding of the selected nanobodies immunoplates (Nunc MaxiSorp, Thermo Fisher Scientific, USA) were coated with RBD (100 ng per well). Serial two-fold dilutions of antibodies were made, starting from 10 μg/ml to 0.6 ng/ml. 100 μl of each concentration was added to the wells. Bound VHHs were detected by HRP-conjugated anti-Myc-tag antibody and TMB substrate. EC50 values were calculated using four-parameter logistic regression using GraphPad Prism 9 (GraphPad Software Inc., USA).

For competitive ELISA recombinant hACE2 protein were immobilized (400 ng per well) on immunoplates (Nunc MaxiSorp, Thermo Fisher Scientific, USA). RBD-specific nanobodies were mixed with HRP-conjugated recombinant RBD protein (0.2 μg/ml) to two final concentrations of antibodies (0.5 μg/ml and 0.1 μg/ml) and incubated at 37°C for 30 min. Nanobody to C. difficile Toxin B was used as a negative control. After incubation samples (100 μl) were transferred to hACE2 coated plates and incubated at 37°C for 30 min. The TMB solution was added for 15 min, the reaction was stopped by the addition of 1M H_2SO_4. The inhibition rate of ACE2-RBD binding was calculated by comparing the signals in the sample and the negative control wells.

Expression and Purification of Nanobodies

Phagmids encoding the sequences of the selected nanobodies were transformed into BL21 cells (NEB, USA) for expression and purification. The cells were cultured in 100 ml 2xYT (containing 100 μg/ml ampicillin) overnight at 30°CC. The cells were harvested by centrifugation and lysed by a BugBuster Protein Extraction Reagent (Novagen, USA). Nanobodies were purified by IMAC using an AKTA start system and a HisTrap column, dialyzed against PBS and sterile filtered. Protein expression and purity was confirmed with SDS-PAGE.

Microneutralization Assay With Live SARS-CoV-2

Nanobodies were two-fold serially diluted starting from 20 μg/ml to 1.2 ng/ml in complete Dulbecco`s modified Eagle medium (DMEM) supplemented with 2% heat-inactivated fetal bovine serum (HI-FBS). Triplicates of each dilution were mixed with 100 TCID50 (median tissue culture infectious doses) of SARS-CoV-2 and incubated at 37°C for 1 h. After incubation samples were added to a monolayer of Vero E6 cells and incubated in a 5% CO_2 incubator at 37°C for 96-120 h. The cytopathic effect (CPE) of the virus was assessed visually. The minimal neutralizing concentration was defined as the lowest antibody concentration (highest antibody dilution) that completely inhibited CPE of the virus in two or three of the three replicable wells.

The following SARS-CoV-2 strains were used in the assay: B.1.1.1, B.1.1.7, B.1.351, B.1.1.28/P.1, B.1.617.2 and B.1.1.529.

All experiments were performed in a Biosafety Level 3 facility (BSL-3).

Binding Kinetics Measurements and Epitope Binning Assay

The affinity of nanobodies was measured by surface plasmon resonance (Biacore 3000, GE Healthcare Bio-Sciences AB, Sweden). Recombinant RBD protein at a concentration 20 μg/ml in 10 mM acetate buffer (pH 4.5) was immobilized on the surface of a CM5 sensor chip using a Amine Coupling Kit (GE Healthcare Bio-Sciences AB, Sweden). VHHs were serial 4-fold diluted from 417 nM to 0 nM and flowed over the captured RBD surface at 15 μl/min for 3 minutes. Dissociation time was 10 minutes. Working buffer was HBS-EP (0.01 M HEPES pH 7.4, 0.15 M NaCl, 2 mM EDTA, 0.005% v/v Surfactant P20). After each injection, the chip surface was regenerated with 10 mM Tris-HCl, pH 1.5 for 40 s at a flow rate 30 μl/min. Calculations were performed using the BIAEvaluation software (GE Healthcare Bio-Sciences AB, Sweden).

For epitope binning recombinant RBD protein was immobilized on CM5 sensor chip as described above. The first antibody (10 μg/ml in working buffer) was flowed over the captured RBD surface at 15 μl/min for 2 minutes to achieve saturation. Then the injection of second antibody at the same concentration and conditions was performed. After each experiment, the chip surface was regenerated.

Generation of Homodimeric and Heterodimeric Forms of Nanobodies

Homodimeric and heterodimeric forms of nanobodies were generated using two rounds of PCR followed by cloning PCR products into a pHEN1 vector. VHHs in dimeric forms were fused by GS-linker $(Gly4Ser)_4$. In the first round of PCR, VHH monomers were amplified using Q5 High-fidelity DNA polymerase (NEB, UK) and the primers listed in **Table 2**. In the second round PCR nanobodies sequences were assembled together and amplified using pHEN1-F and pHEN1-R primers. PCR products and the pHEN1 vector were digested with SfiI and NotI restriction enzymes (Thermo Fisher Scientific, USA) and ligated using T4 ligase (Thermo Fisher Scientific, USA). Recombinant vectors were used for TG1 cells transformation.

TABLE 2 | Primers used for generation of dimeric molecules.

Primer	Sequence
PHEN1-F	CACACAGGAAACAGCTATGAC
VHH-GS-R	CCCAGGTCACTGTCTCCTCAGGTGGTGGCGGATCAGGTGGAGGTGGATCTGGCGGCGGCGGCTCAGGC
VH1-GS-F	TCTGGCGGCGGCGGCTCAGGCGGAGGAGGTTCCCAGGTGCAGCTGGTGCAGTCT
VH3-GS-F	TCTGGCGGCGGCGGCTCAGGCGGAGGAGGTTCCGAGGTGCAGCTGGTGGAGTCT
PHEN1-R	ACAACTTTCAACAGTCTAGCTCC

DNA Isolation and Sequencing

Phagemid DNA was isolated from bacterial cells using the Plasmid miniprep kit (Evrogen, Russia). VHH-coding sequences were sequenced with Lac-prom (5'-CTTTATGCTTCCGGCTCGTATG-3') and pIII-R (5` CTTTCCAGACGTTAGTAAATG 3`) primers according to the protocol of the BigDyeTerminator 3.1 Cycle Sequencing kit for the Genetic Analyzer 3500 Applied Biosystems (Waltham, MA, USA). The electrophoretic DNA separation was performed in 50-cm capillaries with POP7 polymer. MEGA X was used for the generation of the single consensus sequences by assembling of the forward and reverse sequences (42).

Phylogenetic Tree Analysis

A phylogenetic tree of isolated VHHs was constructed to display the sequence diversity of single-domain antibodies. The analysis comprised the following traditional steps: alignment, phylogeny and tree rendering. Sequences were aligned with MUSCLE (v3.8.31) (43). The phylogenetic tree was reconstructed using the maximum likelihood method implemented in the PhyML program (v3.1/3.0 aLRT) (44). The WAG substitution model was selected assuming an estimated proportion of invariant sites (of 0.000) and 4 gamma-distributed rate categories to account for rate heterogeneity across sites. The gamma shape parameter was estimated directly from the data (gamma=0.448). Reliability for internal branch was assessed using the aLRT test (SH-Like) (45). Graphical representation and edition of the phylogenetic tree were performed with MEGA X (42).

DATA AVAILABILITY STATEMENT

The data analyzed in this study is subject to the following licenses/restrictions: This article utilizes proprietary sequencing data. Requests to access these datasets should be directed to Dmitry V. Shcheblyakov, sdmitryv@yahoo.com.

ETHICS STATEMENT

The animal study was reviewed and approved by Bioethics Committee of FSBI National Research Center for Epidemiology and Microbiology named after the honorary academician N. F. Gamaleya of the Russian Ministry of Health.

AUTHOR CONTRIBUTIONS

Conception and design of the experiments: IF, DS, IE, and ID. Library construction, phage display, cloning, production, purification and characterization of VHH and their dimeric forms: IF, IA, AIK, IE, ER, AD, and OZ. Production and purification of recombinant proteins: IE, ER, AD. SARS-CoV-2 culture and microneutralization assay: ID, AVK, AI, and AB. SRP kinetic measurements: DV. Camel immunization and blood collection: DE. DNA sequencing, phylogenetic tree construction: OV, NR, EA, and MK. Data analysis and interpretation, figures preparation: IF and DS. Drafting the manuscript: IF. Revision the manuscript: DS, IE, ID, and OV. Approval of the final version for submission: DS, DL, BN, and AG. All authors contributed to the article and approved the submitted version.

FUNDING

This work received funding from Sberbank Charitable Foundation "Investment to the Future", donation agreement no. BM-03/2020.

ACKNOWLEDGMENTS

We would like to thank Y.S. Lebedin who kindly provided us with the recombinant hACE2 protein and the HRP conjugated recombinant RBD protein.

REFERENCES

1. Dougan M, Nirula A, Azizad M, Mocherla B, Gottlieb RL, Chen P, et al. Bamlanivimab Plus Etesevimab in Mild or Moderate Covid-19. *N Engl J Med* (2021) 385:1382–92. doi: 10.1056/NEJMoa2102685
2. Gupta A, Gonzalez-Rojas Y, Juarez E, Crespo Casal M, Moya J, Falci DR, et al. Early Treatment for Covid-19 With SARS-CoV-2 Neutralizing Antibody Sotrovimab. *N Engl J Med* (2021). doi: 10.1056/NEJMoa2107934
3. Weinreich DM, Sivapalasingam S, Norton T, Ali S, Gao H, Bhore R, et al. REGEN-COV Antibody Combination and Outcomes in Outpatients With Covid-19. *N Engl J Med* (2021). doi: 10.1056/NEJMoa2108163
4. Lee JY, Lee JY, Ko JH, Hyun M, Kim HA, Cho S, et al. Effectiveness of Regdanvimab Treatment in High-Risk COVID-19 Patients to Prevent Progression to Severe Disease. *Front Immunol* (2021). doi: 10.3389/fimmu.2021.772320
5. Bessalah S, Jebahi S, Mejri N, Salhi I, Khorchani T, Hammadi M. Perspective on Therapeutic and Diagnostic Potential of Camel Nanobodies for Coronavirus Disease-19 (COVID-19). *3 Biotech* (2021) 11:89. doi: 10.1007/s13205-021-02647-5
6. Jovčevska I, Muyldermans S. The Therapeutic Potential of Nanobodies. *BioDrugs* (2020) 34:11–26. doi: 10.1007/s40259-019-00392-z
7. Muyldermans S. Single Domain Camel Antibodies: Current Status. *J Biotechnol* (2001) 74:277–302. doi: 10.1016/s1389-0352(01)00021-6
8. Muyldermans S. Nanobodies: Natural Single-Domain Antibodies. *Annu Rev Biochem* (2013) 82:775–97. doi: 10.1146/annurev-biochem-063011-092449
9. Dong J, Huang B, Wang B, Titong A, Gallolu Kankanamalage S, Jia Z, et al. Development of Humanized Tri-Specific Nanobodies With Potent Neutralization for SARS-CoV-2. *Sci Rep* (2020) 10:17806. doi: 10.1038/s41598-020-74761-y
10. Huo J, Mikolajek H, Le Bas A, Clark JJ, Sharma P, Kipar A, et al. A Potent SARS-CoV-2 Neutralising Nanobody Shows Therapeutic Efficacy in the Syrian Golden Hamster Model of COVID-19. *Nat Commun* (2021) 12:5469. doi: 10.1038/s41467-021-25480-z
11. Lu Q, Zhang Z, Li H, Zhong K, Zhao Q, Wang Z, et al. Development of Multivalent Nanobodies Blocking SARS-CoV-2 Infection by Targeting RBD of Spike Protein. *J Nanobiotechnol* (2021) 19:33. doi: 10.1186/s12951-021-00768-w
12. Pymm P, Adair A, Chan L-J, Cooney JP, Mordant FL, Allison CC, et al. Nanobody Cocktails Potently Neutralize SARS-CoV-2 D614G N501Y Variant and Protect Mice. *Proc Natl Acad Sci USA* (2021) 118(19):e2101918118. doi: 10.1073/pnas.2101918118
13. Schoof M, Faust B, Saunders RA, Sangwan S, Rezelj V, Hoppe N, et al. An Ultrapotent Synthetic Nanobody Neutralizes SARS-CoV-2 by

Stabilizing Inactive Spike. *Science* (2020) 370:1473–9. doi: 10.1126/science.abe3255
14. Xiang Y, Nambulli S, Xiao Z, Liu H, Sang Z, Duprex WP, et al. Versatile and Multivalent Nanobodies Efficiently Neutralize SARS-CoV-2. *Science* (2020) 370:1479–84. doi: 10.1126/science.abe4747
15. Xu J, Xu K, Jung S, Conte A, Lieberman J, Muecksch F, et al. Multimeric Nanobodies From Camelid Engineered Mice and Llamas Potently Neutralize SARS-CoV-2 Variants. *bioRxiv* (2021). doi: 10.1101/2021.03.04.433768
16. Harvey WT, Carabelli AM, Jackson B, Gupta RK, Thomson EC, Harrison EM, et al. SARS-CoV-2 Variants, Spike Mutations and Immune Escape. *Nat Rev Microbiol* (2021) 19:409–24. doi: 10.1038/s41579-021-00573-0
17. Hastie KM, Li H, Bedinger D, Schendel SL, Dennison SM, Li K, et al. Defining Variant-Resistant Epitopes Targeted by SARS-CoV-2 Antibodies: A Global Consortium Study. *Science* (2021) 374:472–8. doi: 10.1126/science.abh2315
18. Planas D, Saunders N, Maes P, Guivel-Benhassine F, Planchais C, Buchrieser J, et al. Considerable Escape of SARS-CoV-2 Variant Omicron to Antibody Neutralization. *Biorxiv: Preprint Server Biol* (2021). doi: 10.1101/2021.12.14.472630
19. Cao Y, Wang J, Jian F, Xiao T, Song W, Yisimayi A, et al. B.1.1.529 Escapes the Majority of SARS-CoV-2 Neutralizing Antibodies of Diverse Epitopes. *Biorxiv: Preprint Server Biol* (2021). doi: 10.1101/2021.12.07.470392
20. Tillib SV, Vyatchanin AS, Muyldermans S. Molecular Analysis of Heavy Chain-Only Antibodies of Camelus Bactrianus. *Biochem (Mosc)* (2014) 79:1382–90. doi: 10.1134/S000629791412013X
21. Markham A. REGN-EB3: First Approval. *Drugs* (2021) 81:175–8. doi: 10.1007/s40265-020-01452-3
22. Rocca A, Biagi C, Scarpini S, Dondi A, Vandini S, Pierantoni L, et al. Passive Immunoprophylaxis Against Respiratory Syncytial Virus in Children: Where Are We Now? *Int J Mol Sci* (2021) 22:3703. doi: 10.3390/ijms22073703
23. de Genst E, Silence K, Decanniere K, Conrath K, Loris R, Kinne J, et al. Molecular Basis for the Preferential Cleft Recognition by Dromedary Heavy-Chain Antibodies. *Proc Natl Acad Sci USA* (2006) 103:4586–91. doi: 10.1073/pnas.0505379103
24. Muyldermans S. Applications of Nanobodies. *Annu Rev Anim Biosci* (2021) 9:401–21. doi: 10.1146/annurev-animal-021419-083831
25. Zavrtanik U, Lukan J, Loris R, Lah J, Hadži S. Structural Basis of Epitope Recognition by Heavy-Chain Camelid Antibodies. *J Mol Biol* (2018) 430:4369–86. doi: 10.1016/j.jmb.2018.09.002
26. van der Linden RH, Frenken LG, de Geus B, Harmsen MM, Ruuls RC, Stok W, et al. Comparison of Physical Chemical Properties of Llama VHH Antibody Fragments and Mouse Monoclonal Antibodies. *Biochim Biophys Acta* (1999) 1431:37–46. doi: 10.1016/s0167-4838(99)00030-8
27. Saerens D, Ghassabeh GH, Muyldermans S. Single-Domain Antibodies as Building Blocks for Novel Therapeutics. *Curr Opin Pharmacol* (2008) 8:600–8. doi: 10.1016/j.coph.2008.07.006
28. Coppieters K, Dreier T, Silence K, de Haard H, Lauwereys M, Casteels P, et al. Formatted Anti-Tumor Necrosis Factor Alpha VHH Proteins Derived From Camelids Show Superior Potency and Targeting to Inflamed Joints in a Murine Model of Collagen-Induced Arthritis. *Arthritis Rheum* (2006) 54:1856–66. doi: 10.1002/art.21827
29. Godakova SA, Noskov AN, Vinogradova ID, Ugriumova GA, Solovyev AI, Esmagambetov IB, et al. Camelid VHHs Fused to Human Fc Fragments Provide Long Term Protection Against Botulinum Neurotoxin A in Mice. *Toxins (Basel)* (2019) 11. doi: 10.3390/toxins11080464
30. Choi A, Koch M, Wu K, Dixon G, Oestreicher J, Legault H, et al. Serum Neutralizing Activity of mRNA-1273 Against SARS-CoV-2 Variants. *J Virol* (2021) 95:e0131321. doi: 10.1128/JVI.01313-21
31. Gushchin VA, Dolzhikova IV, Shchetinin AM, Odintsova AS, Siniavin AE, Nikiforova MA, et al. Neutralizing Activity of Sera From Sputnik V-Vaccinated People Against Variants of Concern (VOC: B.1.1.7, B.1.351, P.1, B.1.617.2, B.1.617.3) and Moscow Endemic SARS-CoV-2 Variants. *Vaccines (Basel)* (2021) 9. doi: 10.3390/vaccines9070779
32. Hoffmann M, Arora P, Groß R, Seidel A, Hörnich BF, Hahn AS, et al. SARS-CoV-2 Variants B.1.351 and P.1 Escape From Neutralizing Antibodies. *Cell* (2021) 184:2384–93.e12. doi: 10.1016/j.cell.2021.03.036
33. Hoffmann M, Hofmann-Winkler H, Krüger N, Kempf A, Nehlmeier I, Graichen L, et al. SARS-CoV-2 Variant B.1.617 Is Resistant to Bamlanivimab and Evades Antibodies Induced by Infection and Vaccination. *Cell Rep* (2021) 36:109415. doi: 10.1016/j.celrep.2021.109415
34. Dolzhikova IV, Iliukhina AA, Kovyrshina AV, Kuzina AV, Gushchin VA, Siniavin AE, et al. Sputnik Light Booster After Sputnik V Vaccination Induces Robust Neutralizing Antibody Response to B.1.1.529 (Omicron) SARS-CoV-2 Variant. *MedRxiv: Preprint Server Health Sci* (2021). doi: 10.1101/2021.12.17.21267976
35. Rossler A, Riepler L, Bante D, von Laer D, Kimpel J. SARS-CoV-2 B.1.1.529 Variant (Omicron) Evades Neutralization by Sera From Vaccinated and Convalescent Individuals. *MedRxiv: Preprint Server Health Sci* (2021). doi: 10.1101/2021.12.08.21267491
36. Doria-Rose NA, Shen X, Schmidt SD, O`Dell S, McDanal C, Feng W, et al. Booster of mRNA-1273 Vaccine Reduces SARS-CoV-2 Omicron Escape From Neutralizing Antibodies. *MedRxiv: Preprint Server Health Sci* (2021). doi: 10.1101/2021.12.15.21267805
37. Planas D, Veyer D, Baidaliuk A, Staropoli I, Guivel-Benhassine F, Rajah MM, et al. Reduced Sensitivity of SARS-CoV-2 Variant Delta to Antibody Neutralization. *Nature* (2021) 596:276–80. doi: 10.1038/s41586-021-03777-9
38. VanBlargan LA, Errico JM, Halfmann PJ, Zost SJ, Crowe JE Jr, Purcell LA, et al. An Infectious SARS-CoV-2 B.1.1.529 Omicron Virus Escapes Neutralization by Several Therapeutic Monoclonal Antibodies. *Biorxiv: Preprint Server Biol* (2021). doi: 10.1101/2021.12.15.472828
39. Sun D, Sang Z, Kim YJ, Xiang Y, Cohen T, Belford AK, et al. Potent Neutralizing Nanobodies Resist Convergent Circulating Variants of SARS-CoV-2 by Targeting Diverse and Conserved Epitopes. *Nat Commun* (2021) 12:4676. doi: 10.1038/s41467-021-24963-3
40. Günaydın G, Yu S, Gräslund T, Hammarström L, Marcotte H. Fusion of the Mouse IgG1 Fc Domain to the VHH Fragment (ARP1) Enhances Protection in a Mouse Model of Rotavirus. *Sci Rep* (2016) 6:30171. doi: 10.1038/srep30171
41. Hoogenboom HR, Griffiths AD, Johnson KS, Chiswell DJ, Hudson P, Winter G. Multi-Subunit Proteins on the Surface of Filamentous Phage: Methodologies for Displaying Antibody (Fab) Heavy and Light Chains. *Nucleic Acids Res* (1991) 19:4133–7. doi: 10.1093/nar/19.15.4133
42. Kumar S, Stecher G, Li M, Knyaz C, Tamura K. MEGA X: Molecular Evolutionary Genetics Analysis Across Computing Platforms. *Mol Biol Evol* (2018) 35:1547–9. doi: 10.1093/molbev/msy096
43. Edgar RC. MUSCLE: Multiple Sequence Alignment With High Accuracy and High Throughput. *Nucleic Acids Res* (2004) 32:1792–7. doi: 10.1093/nar/gkh340
44. Guindon S, Gascuel O. A Simple, Fast, and Accurate Algorithm to Estimate Large Phylogenies by Maximum Likelihood. *Syst Biol* (2003) 52:696–704. doi: 10.1080/10635150390235520
45. Anisimova M, Gascuel O. Approximate Likelihood-Ratio Test for Branches: A Fast, Accurate, and Powerful Alternative. *Syst Biol* (2006) 55:539–52. doi: 10.1080/10635150600755453

Conflict of Interest: The authors declare that the research was conducted in the absence of any commercial or financial relationships that could be construed as a potential conflict of interest.

frontiers | Frontiers in Immunology

REVIEW
published: 27 April 2022
doi: 10.3389/fimmu.2022.814365

Considerations for the Feasibility of Neutralizing Antibodies as a Surrogate Endpoint for COVID-19 Vaccines

Jianyang Liu[1,2,3†], Qunying Mao[1,2,3†], Xing Wu[1,2,3], Qian He[1,2,3], Lianlian Bian[1,2,3], Yu Bai[1,2,3], Zhongfang Wang[4], Qian Wang[1,2,3], Jialu Zhang[1,2,3], Zhenglun Liang[1,2,3] and Miao Xu[1,2,3*]*

[1] National Institutes for Food and Drug Control, Beijing, China, [2] NHC Key Laboratory of Research on Quality and Standardization of Biotech Products, Beijing, China, [3] NMPA Key Laboratory for Quality Research and Evaluation of Biological Products, Beijing, China, [4] Guangzhou Laboratory, Guangzhou, China

OPEN ACCESS

Edited by:
Raymund Razonable,
Mayo Clinic, United States

Reviewed by:
Helen Baxendale,
Royal Papworth Hospital NHS Foundation Trust, United Kingdom
Xionglin Fan,
Huazhong University of Science and Technology, China

***Correspondence:**
Miao Xu
xumiaobj@126.com
Zhenglun Liang
lzhenglun@126.com

[†]These authors have contributed equally to this work and share first authorship

Specialty section:
This article was submitted to Vaccines and Molecular Therapeutics, a section of the journal Frontiers in Immunology

Received: 13 November 2021
Accepted: 31 March 2022
Published: 27 April 2022

Citation:
Liu J, Mao Q, Wu X, He Q, Bian L, Bai Y, Wang Z, Wang Q, Zhang J, Liang Z and Xu M (2022) Considerations for the Feasibility of Neutralizing Antibodies as a Surrogate Endpoint for COVID-19 Vaccines. Front. Immunol. 13:814365. doi: 10.3389/fimmu.2022.814365

To effectively control and prevent the pandemic of coronavirus disease 2019 (COVID-19), suitable vaccines have been researched and developed rapidly. Currently, 31 COVID-19 vaccines have been approved for emergency use or authorized for conditional marketing, with more than 9.3 billion doses of vaccines being administered globally. However, the continuous emergence of variants with high transmissibility and an ability to escape the immune responses elicited by vaccines poses severe challenges to the effectiveness of approved vaccines. Hundreds of new COVID-19 vaccines based on different technology platforms are in need of a quick evaluation for their efficiencies. Selection and enrollment of a suitable sample of population for conducting these clinical trials is often challenging because the pandemic so widespread and also due to large scale vaccination. To overcome these hurdles, methods of evaluation of vaccine efficiency based on establishment of surrogate endpoints could expedite the further research and development of vaccines. In this review, we have summarized the studies on neutralizing antibody responses and effectiveness of the various COVID-19 vaccines. Using this data we have analyzed the feasibility of establishing surrogate endpoints for evaluating the efficacy of vaccines based on neutralizing antibody titers. The considerations discussed here open up new avenues for devising novel approaches and strategies for the research and develop as well as application of COVID-19 vaccines.

Keywords: COVID-19 Vaccines, surrogate endpoints, neutralizing antibody, standard neutralization test assay, national standard

INTRODUCTION

The current coronavirus disease 2019 (COVID-19) pandemic caused by the severe acute respiratory syndrome coronavirus 2 (SARS–CoV–2) is a disaster of unprecedented magnitude in modern times. On the other hand, the rapid research and development (R&D) and application of COVID-19 vaccines in response to the pandemic can be regarded as a miracle in the history of

vaccine development. Over a span of less than 2 years, a total of 31 different types of COVID-19 vaccines around the world have been granted Emergency Use Authorizations (EUAs) or marketing approvals (1–3). As of January 15, 2022, more than 9.3 billion doses of COVID-19 vaccines have been administered worldwide (4), but vaccination rates remain low in many regions and countries. The current lots of vaccines are far from perfect. Reduction in immunity over a period of time and lower efficiency against variants seem to be the major concerns. However, vaccines do offer a means to combat the pandemic. The R&D and application of vaccines with superior immunogenicity and universal effectiveness against all SARS–CoV−2 variants, are of utmost priority in addition to increasing vaccination coverage and administrating of a third (booster) COVID-19 vaccine dose (5–7).

Phase III clinical trials are the main rate-limiting steps in vaccine R&D and application. In countries with high COVID-19 vaccination coverage or viral prevalence, it is difficult to conduct trials on the clinical efficacy of vaccines. The search for methods to rapidly and effectively evaluate vaccine's effectiveness has, therefore, become a bottleneck in subsequent vaccine R&D efforts. Surrogate endpoints may effectively save clinical time and are compliant with ethical standards. There has been a successful history of using antibodies as surrogate endpoints for other licensed viral vaccines. The key to establishing surrogate endpoints relies on finding a correlationship between vaccine-induced immune responses and the level of protection (8). The cellular and humoral immunity induced by the vaccine synergistically protects the human body from viral infection (9, 10). Antibodies, especially neutralizing antibodies, are key immunological markers that signal the elicitation of defense responses for the prevention and control of viral infections and disease onset. Consequently, the respective protective antibody levels have been used as surrogate endpoints for many viral vaccines such as influenza virus vaccine, measles vaccine, Japanese encephalitis vaccine, rabies vaccine, polio virus vaccine, hepatitis A vaccine, enterovirus 71 (EV71) vaccine, varicella vaccine and hepatitis B vaccine (**Table 1**) (11–21). In the case of measles, a pre-exposure neutralizing antibodies level in serum samples was positively correlated with clinical protection. Based on this finding, neutralizing antibodies titers of >120 mIU/mL were considered as a reliable surrogate endpoint for measles vaccine (12, 22). Similarly, a titer of ≥ 20 mIU/mL was defined as seroconversion level for hepatitis A vaccine. This seroconversion rate showed a high level of agreement with clinical efficacy data of hepatitis A vaccine. Subsequently, in 2012, hepatitis A virus (HAV) IgG ≥ 20 mIU/mL was included as the antibody threshold level for clinical effectiveness in the World Health Organization (WHO) technical reports on hepatitis A vaccines (17, 23–25). A neutralizing antibody titer of 1:32 for EV71 vaccine has been recommended as the immunological surrogate endpoint because of its association with protection against EV71 (18, 19). Previous clinical studies have confirmed that COVID-19 vaccine-induced humoral immunity generates effective neutralization antibodies against SARS-CoV-2 (26, 27). The studies by Khoury et al. and Earle et al. demonstrated that there is a correlation between the level of neutralizing antibodies responses to SARS-CoV-2 and the protection level of the vaccine, which raises the possibility for the establishment of

TABLE 1 | Recommended immunological surrogate endpoints for licensed viral vaccines.

Vaccine name	Vaccine type	Route of virus transmission	Recommended clinical surrogate endpoint for vaccine	Ref
Influenza vaccines	Inactivated vaccines Split virus vaccines Subunit vaccines	Respiratory tract	1. Significant increase in seroconversion factor or hemagglutination inhibition (HI) antibody titer of > 40%; 2. Increase in GMT of > 2.5; 3. Proportion of subjects with HI titer ≥ 1:40 or single radial hemolysis (SRH) area > 25 mm^2 > 70%	(11)
Measles vaccines	Live attenuated vaccines	Respiratory tract	Hemagglutinin (H)- and fusion protein (F)-specific neutralizing antibody titer > 120 mIU/mL in the plaque reduction neutralization test (PRNT)	(12)
Japanese encephalitis vaccines	Live attenuated vaccines	Mosquito vectors	Baseline negative: $PRNT_{50}$ ≥ 1:10 Baseline positive: 4-fold increase in $PRNT_{50}$	(13)
Rabies vaccines	Inactivated and live attenuated vaccines	Animals	The WHO states that vaccines with a potency of 2.5 IU/dose can induce adequate immunogenicity and provide protective effects with the generation of antibody concentrations of > 0.5 IU	(14)
Polio vaccines	Inactivated and live attenuated vaccines	Gastrointestinal tract	Oral live attenuated vaccine: neutralizing antibody titer of 1:4–1:8 or 4-fold increase in antibody titer; inactivated vaccine: neutralizing antibody titer of 1:8 or 4-fold increase in antibody titer	(15, 16)
Hepatitis A vaccines	Inactivated and live attenuated vaccines	Gastrointestinal tract	Anti-hepatitis A virus (HAV) IgG ≥ 20 mIU/mL	(17)
Enterovirus 71 (EV71) vaccines	Inactivated vaccines	Gastrointestinal tract	Neutralizing antibody titer of 1:32	(18, 19)
Varicella vaccines	Live attenuated vaccines	Contact	Titer of antibodies to the varicella-zoster virus (VZV) glycoprotein measured by ELISA ≥ 5 gpELISA units	(20)
Hepatitis B vaccines	Recombinant vaccines	Blood	Percentage of subjects with hepatitis B surface antibody (anti-HB) titer ≥10 mIU/mL	(21)

surrogate endpoint (28, 29). T cell response is essential in inducing high-affinity antibodies and immune memory (30). SARS-CoV-2 specific responsive T cell numbers are associated with protection against COVID-19 and accelerated viral clearance (31, 32). In fact, mRNA vaccination induced early $CD4^+$ T cell responses have been shown to correlate well with long-term humoral immunity. Robust cellular immune memory to SARS-CoV-2 and its variants persist for at least 6 months after mRNA vaccination (33). However, the correlation between the T cell immunity and the protection level of COVID-19 vaccines is not very clear. In addition, compared to T cell immunity, antibody threshold levels are commonly used as surrogate endpoints for viral vaccines due to the ease of establishment of standardized test methods.

At present, a large number of ongoing clinical trials of COVID-19 vaccines have not reported the threshold antibody levels of protection of their respective study populations. In addition, a lack of standardized neutralizing antibody detection methods and the effects of variants on the serum neutralizing activity of vaccines also pose challenges to the establishment of surrogate endpoints (5). This present paper provides a review of the current status of research on neutralizing antibody responses and their utility in gauging the effectiveness of the various COVID-19 vaccines. An analysis of the feasibility of establishing surrogate endpoints based on neutralizing antibody levels in the hope of opening up new horizons for the R&D of an efficient and expedited application of COVID-19 vaccines.

CURRENT STATUS OF R&D AND APPLICATION OF COVID-19 VACCINES

The R&D and application of COVID-19 vaccines have progressed at an unparalleled pace in a global effort to control the ongoing pandemic. **Figure 1A** shows the major milestones in

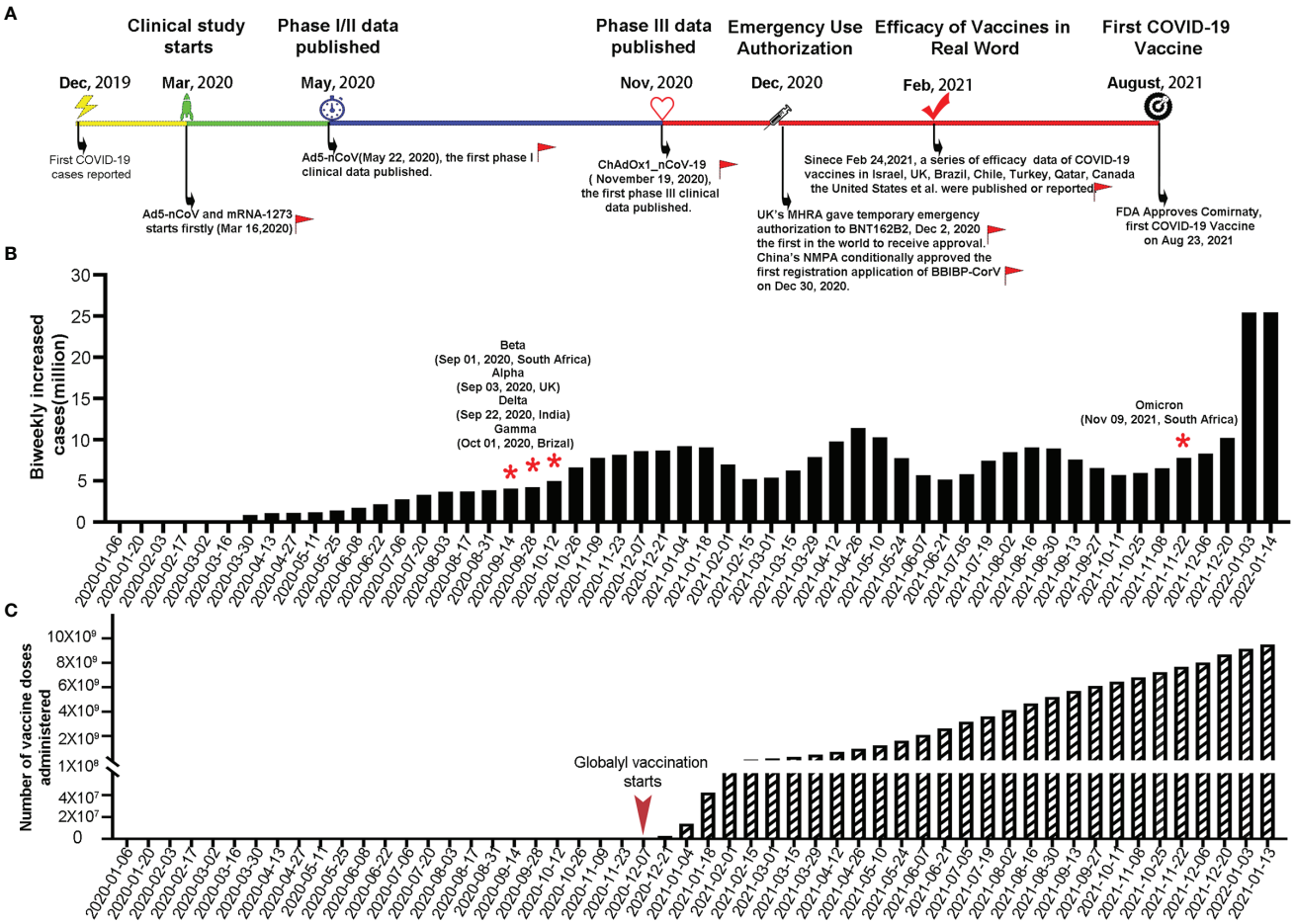

FIGURE 1 | Key milestones in COVID-19 vaccine R&D, biweekly increases in COVID-19 cases worldwide, and total number of COVID-19 vaccine doses administered worldwide. **(A)** Timeline of the R&D of COVID-19 vaccines. Red flags indicate the key milestones in global COVID-19 vaccine R&D and vaccination with the corresponding dates indicated in parentheses. **(B)** Biweekly increases in COVID-19 cases worldwide with red stars denoting the time points of emergence of SARS–CoV–2 variants (data source: https://covid19.who.int/, https://cov-lineages.org/index.html). **(C)** Total number of COVID-19 vaccine doses administered worldwide (data source: https://github.com/owid/covid-19-data/blob/master/public/data/README.md).

COVID-19 vaccine R&D and application. In December 2020, merely 1 year after the first report of COVID-19, the BNT162b2 vaccine jointly developed by Pfizer and BioNTech was granted the first-ever EUA in the United Kingdom (UK) (34). This marked the start of large-scale, rapid vaccinations around the world (**Figure 1C**). Currently, 31 vaccines have received EUAs or conditional marketing authorizations, including two mRNA, eleven inactivated viruses, five adenoviral vectors, twelve recombinant subunits, and one DNA vaccine (1–3). As of January 15, 2022, eight COVID-19 vaccines have been approved for emergency use by the World Health Organization; namely, BNT162b2, AZD1222, Ad26.COV2.S, mRNA-1273, BBIBP-CorV, Coronavac, NVX-CoV2373 and Covaxin (35, 36).

At present, the percentage of fully vaccinated people who have received all recommended doses of a COVID-19 vaccine has exceeded 50% in the United States of America (USA), Canada, and many developed countries of the European Union. In the two most populous countries in the world (China and India), the number of COVID-19 vaccine doses administered has reached 2.93 billion and 1.56 billion, respectively, which jointly account for approximately half of the total doses administered globally (37, 38). With rapid vaccination efforts, the number of new COVID-19 cases worldwide showed a significant decrease between January and March 2021 (**Figure 1B**). However, the emergence of the Alpha, Beta, Gamma, Delta and Omicron variants with high transmissibility and an immune evasion ability has resulted in new waves of the pandemic, with the fourth wave caused by the Omicron variant on the rapid upswing (**Figure 1B**). In particular, the highly divergent Omicron variant, carrying over 30 mutations in the spike protein, has a substantial growth advantage over previous variant and has been identified in 149 countries since November 2021 (39–41). Neutralization titer against Omicron is significantly reduced in convalescent sera from previous SARS-CoV-2 patient, sera after vaccination and therapeutic monoclonal antibodies (42–44). The combined effects of the spread of the Delta and Omicron variants and decrease in neutralizing antibody titers with time after vaccination, have led to an increase in breakthrough infection rates in the real world. Therefore, current vaccines are no longer capable of effectively preventing breakthrough infections and the transmission of variants. The goal of vaccination seems to have shifted from preventing disease onset to reducing the number of critically ill patients and deaths (38, 45–47).

To cope with the aforementioned situation, booster vaccination has become the strategy of choice for certain countries. Studies have indicated that a 5–25-fold increase in neutralizing antibody titer could be achieved after the administration of a third vaccine dose, which indicates a significant increase in efficacy compared with two vaccine doses (48–51). Real-world data from Israel showed that 12 days after the booster dose, the rate of confirmed infection was lower in the booster group than in the non-booster group by a factor of 11.3 (95% confidence interval (CI): 10.4 to 12.3), and the rate of severe illness decreased by a factor of 19.5 (95% CI: 12.9 to 29.5) (9). On October 21, 2021, Pfizer and BioNTech announced the first phase 3 clinical trial data of a booster dose of their COVID-19 vaccine. When Delta is the prevalent strain, the protection rate of booster vaccine is as high as 95.6% (52). Compared with prime COVID-19 vaccination, a homologous and heterologous booster dose elicits potent neutralization titers against Omicron variant, which increasing vaccine effectiveness (28, 53–57). Currently, some countries, including Israel, the USA, the UK, Switzerland, Germany, and China, have already launched booster vaccination campaigns (58–60). However, research data on booster vaccination are relatively scarce. In particular, the duration of retention of adequate neutralizing antibody levels and mechanisms of titer decline after the booster shot remain unclear. Importantly, the safety of this approach has also not been adequately demonstrated yet (61). Considering that infectious diseases know no borders and the vaccination coverage rates worldwide remain low, the WHO has repeatedly called for developed countries to refrain from the widespread rollout of booster shots until the percentage of fully vaccinated people of other nations have been adequately increased because the vaccination of a high percentage of the world's population may serves as the most effective pandemic prevention and control strategy (62, 63). On October 26, 2021, the WHO Emergency Committee acknowledged that the COVID-19 pandemic is far from over, calling for the development of vaccines, diagnostic tools and therapeutics for long-term control of the pandemic (7). To curb the spread of variants, institutions and companies around the world have embarked on the R&D of multi-variant COVID-19 vaccines (64–66).

STUDIES ON THE CORRELATION BETWEEN NEUTRALIZING ANTIBODY LEVELS AND IMMUNOLOGICAL PROTECTION

The establishment of immunological surrogate endpoints is aimed at finding relevant indicators of vaccine protection through animal or human challenge experiments, and then using clinical data to obtain the relationship between immune protection indicators and clinical protection through different data statistical analysis models. Such an exercise produces the initial surrogate endpoints. Neutralizing antibody levels are generally used as the primary surrogate endpoint of the immunological protection of viral vaccines. Results of animal challenge models, efficacy of monoclonal antibodies, data from clinical trials of different vaccines, and real-world data of COVID-19 vaccines in many countries, have demonstrated the existence of a certain correlation between neutralizing antibody levels and an vaccine's effectiveness (5, 28, 67–71).

Immunological Protection in Nonhuman Primates

Data from preclinical nonhuman primates challenge studies investigating the correlation between neutralizing antibody levels and vaccine effectiveness have indicated that vaccines developed using various technologies are capable of inducing the production of neutralizing antibodies in nonhuman primates. The

neutralizing antibody titers induced in nonhuman primates by the vast majority of vaccine candidates tested in Phase III clinical trials are within the range of 100–5000. Despite significant differences in neutralizing antibody levels, all of these vaccines are capable of reducing the pathological response and viral load in the bronchoalveolar lavage or lungs to a certain extent (**Table 2**). Studies on the effectiveness of adenoviral vector vaccines (Johnson & Johnson) (76) and DNA vaccines (80) have revealed that the viral load in lungs is negatively correlated with the neutralizing antibody titer (R values: −0.5714−−0.7702) and that the neutralizing antibody titer must not be lower than 100–250 for the vaccine in order to provide full protection.

Phase III Clinical Trials Data

In recent months, vaccine manufacturers have published phase III COVID-19 vaccine clinical trial data, which have indicated vaccine efficacies consistent with those reported in phase I/II clinical trials. Although differences exist among specific vaccines, the various vaccines have exhibited good effects in the prevention of disease onset and critical illness (**Table 3**). At present, data related to the correlation between efficacy and neutralizing antibody titer in phase III clinical trials have not yet been reported. A meta-analysis that compared the correlations between efficacy and neutralization titer in recovering subjects across several phase III clinical trials revealed the presence of a strong nonlinear relationship between mean neutralization level and efficacy, which is in agreement with results obtained from animal challenge models (28). However, inconsistencies in the selected serum samples of the recovery phase may reduce the credibility of this relationship. In addition, large differences exist in the neutralizing antibody titers induced by similarly efficacious vaccines developed by different manufacturers. This may be attributed to differences in the sample population, test methods, tested variants, and dominant variant in the country of residence of the subjects, among phase III clinical trials conducted by different vaccine manufacturers (**Table 3**). In a recent study, Feng et al. analyzed the clinical data of the ChAdOx1 nCoV-19 (AZD1222) vaccine in the UK and found that the vaccine efficacy was associated with antibody levels (especially those of neutralizing antibodies). Measurements of neutralizing antibody titers revealed values of 938 international units (IU)/mL was associated with 90% VE against symptomatic infection at 28 days post-vaccination (71). A study on breakthrough infections in vaccinated healthcare workers at the largest medical center in Israel predicted that breakthrough infections could only be effectively prevented when the geometric mean titer (GMT) exceeded 533.7 (95% CI: 408.1 to 698.0) (98).

Real-World Data

With the publication of real-world data, it is apparent that current COVID-19 vaccines that have been granted EUAs or conditional marketing authorizations, achieve different efficacies in individuals of different age groups, ethnicities, and countries. However, all vaccines have met the minimum efficacy requirement of 50% set by the WHO for EUAs and demonstrated high efficacies against progression towards severe disease or death (**Table 4**) (26, 99–102). The effectiveness of the vaccines is positively correlated with the level of neutralizing antibodies (**Table 3**), which is consistent with Knory's and Earle's studies (28, 29). Although the efficacies of current vaccines against the SARS−CoV−2 variants of concern (VOC) have decreased significantly compared to the preclinical stage, these vaccines still provide certain protective effects, especially against critical illness and disease-related death (27, 102, 103).

The decrease in the efficacy of current vaccines has mainly been caused by the following: (1) Neutralizing antibodies generated after vaccination with current vaccines providing weaker neutralizing effects against newly emerged variants, resulting in

TABLE 2 | Protective effects of neutralizing antibodies in nonhuman primates challenge studies.

Vaccines	Immunization procedure			Challenge dose	Neutralizing antibodies		Viral load (copies/ml) in BAL fluid		Ref
	Dosage	Doses	Interval (weeks)		Method	geometric mean titer (GMT)	Control	Vaccine	
mRNA-1273	100 μg	2	4	7.6×10^5 PFU	PV	1862	D4: ~7×10^5	D4: < LLOD	(72)
BNT162b2	100 μg	2	3	1.05×10^6 PFU	PV	310	D3: ~1×10^6	D4: < LLOD	(73)
Ad26.COV2.S	5×10^{10} vp	2	8	1×10^5 TCID50	PV	~1000	D4: ~1×10^5	D4: < LLOD	(74)
ChAdOx1 nCoV19	2.5×10^{10} vp	1	_	2.6×10^6 TCID50	Live-CPE	~20 (5–40)	D3: ~1×10^5	D3: < LLOD	(75)
	2.5×10^{10} vp	2	4	2.6×10^6 TCID50	Live-CPE	10–160	_	_	(76)
BBIBP-CorV	2/8 μg	2	2	10^6 TCID50	Live-CPE	215/256	~1×10^3-1×10^6 (lung)	< LLOD (lung)	(77)
PiCoVacc	6 μg	3	1	10^6 TCID50	Live-CPE	~50	~1×10^3-1×10^6 (lung)	< LLOD (lung)	(78)
BBV152	3 μg	2	2	$1.25 \times 10^{6.5}$ TCID50	Live-PRNT	~3100	D3: ~1×10^6	< LLOD	(79)
INO-4800	1 mg	1/2	4	5×10^6 PFU	Live-PRNT	2199	1×10^6	1×10^4	(80)
NVX-Cov2373	50 μg	2	3	1.1×10^4 PFU	Live-CPE	23040	sgRNA ~ < 1E4	< LLOD	(81)
SCB-2019	30 μg	2	3	2.6×10^6 TCID50	Live-CPE	2700/35047	D2: 1×10^4	< LLOD	(82)

vp, viral particles; PFU, plaque-forming units; $TCID_{50}$, tissue culture infective dose 50; CPE, cytophatic effect detection assay; PRNT, plaque reduction neutralisation test; LLOD, lower limits of detection; BAL, Bronchoalveolar lavage.

TABLE 3 | Neutralizing antibody titer and protection efficacy of COVID-19 vaccines for emergency use in Phase III clinical trials.

Vaccine	Clinical trial No.	Country	No. of participants	Age	Efficacy (%) (95% CI)	Neutralizing antibodies titer to live SARS-CoV-2 Geometric mean ratio (95% CI) (SARS-CoV-2 strain)	Ref
BBIBP-CorV	NCT04510207	UAE, Bahrain	40382	≥ 18	78.1 (64.8–86.3)	68.7 (65.5–72.1) [19nCoVCDC-Tan-Strain04 (QD01)]	(83)
Inactivated (Wuhan, Sinopharm)	NCT04510207	UAE, Bahrain	40382	≥ 18	72.8 (58.1–82.4)	41.0 (38.9–43.2) (19nCoVCDC-Tan-Strain04 (QD01))	(83)
CoronaVac	NCT04456595	Brazil	9823	≥ 18	50.7 (36.0–62.0)	64.4 (B.1.128 (SARS-CoV-2/human/(BRA/SP02/2020 strain MT126808.1) 46.8 (SARS-CoV-2-P.1 MAN 87201 strain) 45.8 (SARS-CoV-2-P.2 LMM38019 strain)	(84)
CoronaVac	NCT04582344	Turkey	10214	18–59	83.5 (65.4–92.1)	–	(85)
ChAdOx1 (AZD1222)	NCT04324606 NCT04400838 NCT04444674 ISRCTN89951424	UK, Brazil, South Africa	11636	≥ 18	62.1 (41.0–75.7)	51 (32–103)*	(86, 87)
Sputnik V	NCT04530396	Russia	21977	≥ 18	91.6 (85.6–95.2)	44.5 (31.8–62.2) (hCoV-19/Russia/Moscow_PMVL-1/2020)	(88)
BBV152	NCT04641481	India	25798	18–98	77.8 (65.2–86.4)	125.6 (111.2-141.8)	(89)
mRNA-1273	NCT04470427	United States	30420	≥ 18	94.1 (89.3–96.8)	654.3(460.1–930.5)*	(90, 91)
BNT162b2	NCT04368728	United States, Argentina, Brazil, South Africa Germany, Turkey	43448	≥ 16	95.0 (90.3–97.6).	363*	(92, 93)
Ad26.COV2.S	NCT04505722	Argentina, Brazil, Chile, Colombia, Mexico, Peru, South Africa, United States	39321	≥ 18	66.9 (59.0–73.4)	827 (508–1183)* (Victoria/1/2020 SARSCoV-2 strain)	(94, 95)
NVX-CoV2373	EudraCT number, 2020-004123-16	United Kingdom	14039	18–84	89.7 (80.2–94.6)	3906*	(96, 97)

**Represents that these data were reported in phase I or II clinical trials.*

decreased vaccine efficacy (104, 105); (2) Neutralizing antibody levels starting to decrease gradually at a certain point of time after vaccination, resulting in the occurrence of breakthrough infection. Consequently, populations that have been vaccinated earlier are more susceptible to breakthrough infection than those vaccinated later (106–108). Studies have found that booster vaccination leads to increased neutralizing antibody levels against variants and enhances vaccine efficacy (49, 50, 52). Both clinical and real-world data demonstrate the presence of a positive correlation between neutralizing antibody level and vaccine effectiveness,

TABLE 4 | Efficacy of COVID-19 vaccines in real word.

Vaccine	Country	No. of participants	Age	Efficacy (%) (95%CI)				Ref
				prevention of Covid-19	prevention of hospital	prevention of severe disease	prevention of death	
CoronaVac	Chile	10,187,720	≥16	65.9 (65.2- 66.6)	87.5 (86.7-88.2)	90.3 (89.1-91.4)	86.3 (84.5- 87.9)	(26)
BNT162b2, mRNA-1273	Canada	324 033	≥16	91 (89- 93)	98 (88- 100) (hospital or death)			(99)
BNT162b2	Israel	119,236	≥16	92 (88- 95)	87 (55-100)	92 (75- 100)	–	(100)
BNT162b2	Qatar	–	–	–	–	97.4 (92.2- 99.5)		(101)
BNT162b2*	Unite States	51,738	≥18	76 (69-81)	85 (73-93)	–	–	(102)
mRNA-1273*	Unite States	51,738	≥18	86 (81-90.6)	91. (81-97)	–	–	(102)

**Alpha or Delta variant was highly prevalent in this region in this study.*

which provides a scientific basis for further data collection and analysis, to validate the use of neutralizing antibody threshold values as surrogate endpoints.

Application of Neutralizing Antibody Immunobridging for COVID-19 Vaccine

In recent clinical studies of two COVID-19 vaccines that were performed around the world, neutralizing antibody immune bridging was used to assess vaccine's effectiveness. The two co-primary endpoint criteria used were: 1. The neutralizing antibody titer is higher compared to active comparator vaccine AZD1222 (ChAdOx1-S); 2. The seroconversion rate of neutralizing antibody is more than the set threshold of 50% or 95% (109, 110). After full immunization schedule, seroconversion of SARS-CoV-2-specific neutralizing antibodies is defined as 4-fold increase from baseline in the phase III clinical of VLA2011 (111). The Phase II clinical results of MVC-COV1901 showed that the geometric mean serum neutralizing antibody titer at 28 days after receiving the second recommended dose (i.e. Day 57) against wild type SARS-CoV-2 virus was 408.5 IU/mL. The neutralizing antibody GMT induced by MVC-COV1901 was 3.4 times that of AZD1222, and the seroconversion rate was 99.8% (109, 112–114). On July 19, 2021, without providing clinical research data on vaccine protection, MVC-COV1901 was approved by the EUA of Taiwan, China, becoming the first approved COVID-19 vaccine based on neutralizing antibody bridging experiments to evaluate immune protection (109, 114). Phase III clinical results of the AZD1222 vaccine showed an efficacy of 62.1%. Based on the study of the relationship between the level of neutralizing antibody and vaccine immunity by Feng et al., it can be inferred that the protection rate of the MVC-COV1901 vaccine is between 80% and 90% (71, 86). On October 18, 2021, Valneva reported positive phase 3 results for VLA2001. The neutralizing antibody titer at two weeks after the second receiving the second recommended dose (i.e. Day 43) in adults aged 30 years and older of VLA2001 is 1.39 times that of AZD1222 (VLA2001 GMT 803.5, AZD1222 GMT 576.6), and the neutralizing antibody seroconversion rate is more than 95% (110, 115). The efficacies of MVC-COV1901 and VLA2001 vaccines will be evaluated based on real-world vaccination data. This will be the direct and effective verification of the feasibility of using neutralizing antibodies as surrogate endpoints for COVID-19 vaccines.

Neutralizing Antibody Test Methods

Neutralizing antibody testing can be performed using live virus, pseudovirus neutralization assays and lateral flow immunoassay (116). A report by the WHO revealed the presence of differences in the experimental methods, variants, and calculation methods used for neutralizing antibody testing among different laboratories around the world, which resulted in significant biases in the measured neutralizing antibody levels of the same sample. In the collaborative calibration of the First WHO International Standard and Reference Panel for the anti-SARS-CoV-2 antibody, live virus neutralization assays performed by 15 laboratories [including live virus plaque reduction neutralisation assay (Live-PRNT), live virus foci reduction neutralisation assay (Live-FRNT), live virus cytophatic effect detection assay (Live-CPE), and live virus microneutralization assay (Live-MN)] and pseudovirus neutralization assays performed by 12 laboratories [including pseudotyped virus - lentiviral (HIV) vector (PV-LVV) and pseudotyped virus - vesicular stomatitis virus (PV-VSV)] were adopted (117). Results indicated that with the exception of two low-titer samples and one negative sample for which the titers could not be easily calculated, the total GMTs of seven collaborative calibration samples determined by Live-PRNT, Live-FRNT, Live-CPE, and Live-MN were 317.1, 445.3, 93.9, and 239.6, respectively. When the same assay was used, the average fold (the ratio of the maximum value to the minimum value) in GMT across different laboratories were 14.7-, 12.9-, 19.5-, and 4.5-fold, respectively. Total GMTs determined by PV-LVV and PV-VSV were 371.8 and 519.2, respectively; average fold in GMT across different laboratories when the same method was used were 908.7- and 10.9-fold, respectively.

During the collaborative calibration of the first Chinese national standards for SARS-CoV-2 neutralizing antibody, live virus neutralization assays performed by four laboratories (including Live-PRNT and Live-CPE), with one laboratory adopting two types of assays for testing and the remaining three laboratories using the CPE assay, and pseudovirus neutralization assays performed by 10 laboratories (all PV-VSV) were adopted. As shown in **Table 5**, the GMTs of four collaborative calibration samples determined by different assays are significantly inconsistent. When the same assay was used, the fold (the ratio of the maximum value to the minimum value) in GMT across different laboratories are more than 4.7 at least. These results indicate the presence of considerable differences among different laboratories and methods (**Table 5**) (118).

TABLE 5 | Comparison of geometric mean of SARS-CoV-2 neutralising antibodies reported in ref. (118).

Type	No. of lab	Sample							
		22		44		77		99	
		GMT	Fold	GMT	Fold	GMT	Fold	GMT	Fold
Live-CPE	4	176.6	36.9	728.2	6.0	38.7	10.7	469.4	7.6
Live-PRNT	1	1063	–	2308	–	183	–	1463	–
PV-VSV	10	1938	4.8	3973	4.7	162	23.1	2064	10.5

Fold, the ratio of the maximum value to the minimum value; FRNT, foci reduction neutralization assay; PV, pseudotyped virusbased neutralization assay; VSV, vesicular stomatitis virus.

Studies have shown that differences in neutralizing antibody test results among different laboratories were significantly decreased with the use of the WHO International Standard and the Chinese National Standards (117, 118). When the International Standard was adopted, the total geometric coefficients of variation (GCVs) of five high- and medium-titer samples were reduced from 249%, 179%, 231%, 281%, and 161% to 94%, 95%, 119%, 67%, and 93%, and the upper quartile/lower quartile (UQ/LQ) values were reduced by 1.432-, 1.978-, 2.206-, 6.511-, and 2.348-fold. However, a low-titer sample did not exhibit a significant decrease in GCV and only showed a 0.97-fold decrease in UQ/LQ compared with the pre-standardization value, which may be related to the fact that the low neutralizing antibody titer was close to the threshold value (117). In the collaborative calibration of the Chinese national standards, the GCV values of three collaborative calibration samples measured by different laboratories using an authentic virus neutralization assay were 129%, 266%, and 146%. When standards with a titer of 1000 U/mL were used, the total GCVs among laboratories were reduced to 107%, 18%, and 90% (118).

The standardization of neutralizing antibody test methods directly affects the establishment of immunological surrogate endpoints and has become a major influencing factor of COVID-19 vaccine R&D and evaluation. With the establishment of the first standard pseudovirus neutralization assay by Chinese researchers (119) and WHO's subsequent approval of the First International Standard for anti-SARS-CoV-2 immunoglobulin (human), methods for measuring neutralizing antibody titer can be standardized and the comparability of cross-platform test results can be effectively enhanced (120).

ACTIONS TO DEVELOP NEUTRALIZING ANTIBODIES AS ENDPOINT FOR VACCINES OF WHO AND MORE NATIONAL LEVELS OF DIFFERENT COUNTRIES TO PRACTICAL APPLICATION

As trials on the clinical effectiveness of vaccines constitute the main rate-limiting step in vaccine R&D, the current status of COVID-19 vaccine application and R&D urgently require the establishment of immunogenicity surrogate endpoints for testing vaccine's effectiveness. Recently, a number of reports on clinical and real-word effectiveness of COVID-19 vaccines have been published, and two COVID19 vaccines have reported positive comparative immunogenicity trial results (109–114). We are beginning to harness the potential utility of these data for establishing surrogate endpoints. However, the current guidance documents on immunological surrogate endpoints are not systematic and comprehensive. There are obstacles to sharing and analyzing large amounts of clinical data among vaccines manufactures. In addition, the lack of a standardized neutralizing antibody test assay and continuously emerging variants further complicate the comparisons. The robustness of immunological surrogate endpoints will largely depend on how we address these issues.

Guidance Documents on Surrogate Endpoints for COVID-19 Vaccines Promptly Issued by the WHO and National Regulatory Agencies

The pandemic of COVID-19 requires the WHO and national regulatory agencies to quickly assess the protective effectiveness of vaccines. Recently, the WHO and pharmaceutical regulatory agencies of the USA, UK, and China have indicated the need for studies investigating the relationships between vaccine-induced neutralizing antibody levels and vaccine's effectiveness (**Table 6**). In particular, the Medicines and Healthcare products Regulatory Agency (MHRA) of the UK has announced that neutralizing antibody surrogate endpoints established using the WHO standard units can be applied to immunobridging studies in the R&D of vaccines against SARS–CoV–2 variants (121–124).

Guidelines issued by the Center for Drug Evaluation (CDE) of the National Medical Products Administration (NMPA) of China state that the correlation between immunological markers and protection should be investigated in COVID-19 vaccine clinical trials, and the establishment of surrogate endpoints requires the provision of evidence for five different aspects, which include the correlations of immune response mechanisms and antibody levels (particularly those of neutralizing antibodies) with protection (123). Considering the fact that the current global outbreaks are caused by SARS–CoV–2 variants, the Unite States Food and Drug Administration (USFDA) has indicated the need to assess the neutralization of the virus from which the prototype vaccine was derived, as well as variants of concern with clinical serology samples obtained from persons immunized with vaccines against variants, when investigating the effectiveness of newly developed vaccines against variants (124). Guidance provided by the WHO recommends the approach of looking for concordance of neutralization data and vaccine effectiveness results for VOCs to estimate the effectiveness of vaccines against new variants (121). The MHRA considers that the weight of evidence from studies with authorized vaccines is sufficient to support the use of neutralizing antibody titers as a primary endpoint in cross-platform immunobridging trials. Therefore, neutralizing antibody titers may be justified as an immune marker to predict vaccine effectiveness, but they should be standardized using the WHO reference standards and expressed in terms of IU (125). To guide deliberations regarding vaccines against variants, the European Medicines Agency (EMA) requires the evaluation of the neutralizing antibody levels elicited by the vaccines against variants and the parent strain under standardized conditions to serve as a secondary endpoint (122).

Analysis of the Use of Phase III Clinical and Real-World Data as Surrogate Endpoints

Currently, 31 different types of COVID-19 vaccines have received EUAs or conditional marketing authorizations, and preclinical,

TABLE 6 | Guidance for COVID-19 vaccine R&D.

Regulatory agency	Guidance document	Date of issue	Requirements for surrogate endpoints	Ref
WHO	Guidance on conducting vaccine effectiveness evaluations in the setting of new SARS-CoV-2 variants: Interim guidance	2021.07.22	An approach to better estimate the vaccine effectiveness for new variants is looking for concordance of neutralization data and vaccine effectiveness results for new variants, which would add credibility to the vaccine effectiveness estimate.	(121)
EMA	Reflection paper on the regulatory requirements for vaccines intended to provide protection against variant strain (s) of SARS-CoV-2	2021.02.23	In the absence of an immune correlate of protection, the evaluation of the neutralizing antibody levels elicited by the vaccines against variants and the parent strain under standardized test conditions is required to serve as a secondary endpoint.	(122)
CDE (China)	Technical guidelines for the development of novel coronavirus preventive vaccines (trial)	2020.08.14	1. The investigation of correlations between immunogenicity markers and protection in the evaluation of clinical efficacies of vaccines is recommended. 2. Surrogate endpoints should be explored, and the investigation of correlations between vaccine immunogenicity and effectiveness, and reasonable immunological surrogate endpoints are encouraged during clinical R&D of vaccines. 3. The use of neutralizing antibody levels as surrogate endpoints requires evidence in the following five aspects: (1) Viral pathogenesis and mechanisms underlying immune response to the virus; (2) Relationships of viral infection-induced serum antibody levels with disease onset, progression, and outcome; (3) Relationship of the serum antibody level with vaccine efficacy and the predicted values; (4) Immune response after vaccination, production/non-production of neutralizing antibodies, and neutralizing antibody levels; (5) Neutralizing antibody levels during the effective period of protection and correlation with vaccine efficacy.	(123)
FDA (USA)	Emergency use authorization for vaccines to prevent COVID-19; Guidance for industry	2021.05.25	When evaluating vaccines targeted against new variants, the neutralizing antibody may be considered a relevant measure of immunogenicity. Data demonstrating the ability of new COVID-19 vaccines to induce a neutralizing antibody response are needed, which may be derived by assessing the neutralization of SARS-CoV-2 viruses (including the virus from which the prototype vaccine was derived as well as variants of interest) with clinical serology samples.	(124)
MHRA (UK)	Decision: Access consortium: Alignment with ICMRA consensus on immunobridging for authorizing new COVID-19 vaccines	2021.09.15	1. Based on the specifics of the product under consideration, a neutralizing antibody titer may be justified as an immune marker to predict vaccine effectiveness. However, neutralizing antibody titers should be determined using the WHO-certified reference standards. 2. The weight of evidence from studies with authorized COVID-19 vaccines is sufficient to support the use of a neutralizing antibody titer as a primary endpoint in cross-platform immunobridging trials.	(125)

clinical, and real-world data on efficacy and neutralizing antibody levels are available for many of these vaccines. However, inadequacies exist in the openness and correlation analyses of the efficacy and neutralizing antibody data of current vaccines (28, 71).The clinical studies of MVC-COV1901 and VLA2001 vaccines provide the results of immune bridging of neutralizing antibodies, but there is a lack of data on the protection rate of vaccines. These data could be jointly analyzed by vaccine manufacturers and regulatory agencies, and coordination efforts could be made by international health organizations for the standardized formulation of scientific surrogate endpoints. These will be greatly beneficial to the screening of high-immunogenicity vaccines from the immense number of vaccines being subjected to preclinical and clinical testing worldwide, maximization of the protection of participants and saving various resources. On the basis of existing clinical data, statistical tools may be utilized to investigate the relationships between neutralizing antibody level and vaccine efficacy, changes in neutralizing antibody level with time, and threshold levels of neutralizing antibody protection against different variants (28, 71). However, neutralizing antibodies are likely not the only mechanism of protection (126). Further clinical and real-world data are required to determine the ability of neutralizing antibody levels to accurately evaluate the effectiveness of COVID-19 vaccines when used as surrogate endpoints.

Standardization of Laboratory Serological Test Methods and the Establishment of Secondary National Standards

There are a number of neutralizing antibody test methods available for the estimation of antibodies against SARS-CoV2 (116). Standardized laboratory serological test methods are a prerequisite for the realization of data comparability among different laboratories and platforms for surrogate endpoint establishment. The standardization of test methods has become the main rate-limiting step in the R&D of COVID-19 vaccines. On the basis of the WHO antibody standard, countries and regions are advised to expedite the establishment of secondary national standards to specify requirements for the use of IU in

test methods. This will enable the comparison of neutralizing antibody test results across different studies for the accurate analysis and determination of correlations between neutralizing antibody levels and vaccine efficiencies.

New Variants Pose Challenges to the Establishment of Surrogate Endpoints

SARS−CoV−2 is highly prone to mutations. To date, several hundreds of lineages have already emerged and new lineages are still appearing on a continuous basis. In particular, lineages with immune evasion abilities exert greater effects on vaccine protection (127). Serum neutralizing capacity has been used as an efficient indicator to quickly assess the protective effect of vaccines on emerging variants. Results of these studies show that compared with the early strains, the neutralizing antibody titer against new variants has been significantly decreased (5, 128, 129). Surrogate endpoints established using current clinical data will inevitably face challenges posed by continuously emerging variants. Therefore, continuous endpoint revisions may be required based on changes in variant dominance with time and the R&D status of vaccines (130).

In addition, SARS-CoV-2 specific T cell immunity acquired by COVID-19 vaccines or previous infection still remain broadly robust and long-term protection against VOCs, including Omicron variant (131–134). A standardized measurement of T cells immunity may be served as an potential surrogate endpoint to better assess the protective effect of COVID-19 vaccines on emerging variants subsequently (135).

CONCLUSION

The global scale of the pandemic, high vaccination coverage rates and ethical requirements, pose challenges to the effectiveness of subsequently developed COVID-19 vaccines in clinical trials. The establishment of immunological surrogate endpoints is of great significance to the acceleration of efficacy evaluations of vaccines. Current studies have indicated that vaccine-induced neutralizing antibody levels are correlated with clinical protection, and predictable clinical progression have tried to assess clinical protection through neutralizing antibody immunobridging experiments (109, 110). Research efforts on surrogate endpoints should focus on the establishment and application of standardized test methods, and adoption of the WHO international standard to express titers in terms of IU and reduce measurement errors. In addition, it should also analyze the threshold levels of neutralization antibody protection against different variants based on current clinical data, and appropriate endpoint adjustments based on changes in variant circulation and vaccine R&D. Due to the rapid waning of neutralization tier, it is critial to assess quality and durability of the neutralization antibody in conjunction with standardization of time lines after vaccination (28). During the use of COVID-19 vaccines in clinical trials of booster and sequential vaccination, the threshold levels of new vaccines' neutralization antibody should be significantly superior to those of the primary vaccines. Higher titers of neutralization antibody will serve as an indication of the superior effectiveness of these new vaccines.

AUTHOR CONTRIBUTIONS

ZL and MX conceived the framework and main text of this review article. JL, QM, XW, QH, and LB wrote the draft. ZL, MX, ZW and QW reviewed the manuscript. JL, YB, and JZ searched the literature. All authors contributed to the article and approved the submitted version.

FUNDING

This work was supported by the Emergency Key Program (NO. EKPG21-30-1) of Guangzhou Laboratory, China.

REFERENCES

1. World Health Organization. *COVID-19 Vaccine Tracker and Landscape* (2021). Available at: https://www.who.int/publications/m/item/draft-landscape-of-covid-19-candidate-vaccines (Accessed January 15, 2022).
2. Shenzhen Kangtai Biological Products Co. *Ltd. Indicative Announcement on the Authorization of the Inactivated COVID-19 Vaccine for Emergency Use* (2021). Available at: http://www.szse.cn/disclosure/listed/bulletinDetail/index.html?d3c250ff-42f9-4a8b-87ce-41ad63495776 (Accessed May 14, 2021).
3. Zydus Cadila. *Zydus Receives EUA From DCGI for ZyCoV-D, the Only Needle-Free COVID Vaccine in the World* (2021). Available at: https://www.zyduscadila.com/public/pdf/pressrelease/Press%20Release-Zydus-receives-EUA-from-DCGI-for-ZyCoV-D.pdf (Accessed August 20, 2021).
4. World Health Organization. *WHO Coronavirus (COVID-19) Dashboard* (2021). Available at: https://covid19.who.int/ (Accessed January 15, 2022).
5. Planas D, Veyer D, Baidaliuk A, Staropoli I, Guivel-Benhassine F, Rajah MM, et al. Reduced Sensitivity of SARS-CoV-2 Variant Delta to Antibody Neutralization. *Nature* (2021) 596(7871):276–80. doi: 10.1038/s41586-021-03777-9
6. Callaway E, Ledford H. How to Redesign COVID Vaccines So They Protect Against Variants. *Nature* (2021) 590:15–6. doi: 10.1038/d41586-021-00241-6
7. World Health Organization. *Statement on the Ninth Meeting of the International Health Regulations (2005) Emergency Committee Regarding the Coronavirus Disease (COVID-19) Pandemic* (2021). Available at: https://www.who.int/news/item/26-10-2021-statement-on-the-ninth-meeting-of-the-international-health-regulations-(2005)-emergency-committee-regarding-the-coronavirus-disease-(covid-19)-pandemic (Accessed October 26, 2021).
8. Krammer F. A Correlate of Protection for SARS-CoV-2 Vaccines is Urgently Needed. *Nat Med* (2021) 27(7):1147–8. doi: 10.1038/s41591-021-01432-4
9. Amanna IJ, Slifka MK. Contributions of Humoral and Cellular Immunity to Vaccine-Induced Protection in Humans. *Virology* (2011) 411(2):206–15. doi: 10.1016/j.virol.2010.12.016
10. Zellweger RM, Miller R, Eddy WE, White LJ, Johnston RE, Shresta S. Role of Humoral Versus Cellular Responses Induced by a Protective Dengue Vaccine Candidate. *PloS Pathog* (2013) 9(10):e1003723. doi: 10.1371/journal.ppat.1003723

11. World Health Organization. *Recommendations for the Production and Control of Influenza Vaccine (Inactivated). Annex 3 of WHO TRS No. 927*. (2005). Available at: https://www.who.int/publications/m/item/influenza-vaccine-inactivated-annex-3-trs-no-927. (Accessed January 1, 2005)
12. World Health Organization. *WHO Position Papers on Measles* (2017). Available at: https://www.who.int/teams/immunization-vaccines-and-biologicals/policies/position-papers/measles (Accessed April 28, 2017).
13. World Health Organization. *Recommendations to Assure the Quality, Safety and Efficacy of Japanese Encephalitis Vaccines (Live, Attenuated) for Human Use. Annex 7 of WHO TRS No. 980* (2014). Available at: https://www.who.int/publications/m/item/japanese-encephalitisvaccines-live-attenuated-annex-7-trs-no-980 (Accessed May 15,2014).
14. World Health Organization. *Recommendations for Inactivated Rabies Vaccine for Human Use Produced in Cell Substrates and Embryonated Eggs. Annex 2. Of WHO TRS No. 941*. (2007) Available at: https://www.who.int/publications/m/item/inactivated-rabies-vaccine-for-human-use-annex-2-trs-no-941 (Accessed January 1, 2007).
15. World Health Organization. *Recommendations to Assure the Quality, Safety and Efficacy of Poliomyelitis Vaccines (Oral, Live, Attenuated). WHO Expert Committee on Biological Standardization. Annex 2 of WHO TRS No. 980*. (2014). Available at: https://www.who.int/publications/m/item/oral-live-attenuated-poliomyelitis-vaccine-annex-2-trs-no-980 (Accessed November 6, 2014).
16. World Health Organization. *Recommendations to Assure the Quality, Safety and Efficacy of Poliomyelitis Vaccines (Inactivated). Annex3 of WHO TRS No. 1024*. (2020) Available at: https://www.who.int/publications/m/item/poliomyelitis-vaccines-annex-3-trs-no-1024 (Accessed November 6, 2020).
17. World Health Organization. *WHO Position Paper on Hepatitis A Vaccines* (2016). Available at: https://www.who.int/teams/immunization-vaccines-and-biologicals/policies/position-papers/hepatitis-a (Accessed June 16, 2016).
18. Zhu FC, Meng FY, Li JX, Li XL, Mao QY, Tao H, et al. Efficacy, Safety, and Immunology of an Inactivated Alum-Adjuvant Enterovirus 71 Vaccine in Children in China: A Multicentre, Randomised, Double-Blind, Placebo-Controlled, Phase 3 Trial. *Lancet* (2013) 381(9882):2024–32. doi: 10.1016/s0140-6736(13)61049-1
19. Zhu F, Xu W, Xia J, Liang Z, Liu Y, Zhang X, et al. Efficacy, Safety, and Immunogenicity of an Enterovirus 71 Vaccine in China. *N Engl J Med* (2014) 370(9):818–28. doi: 10.1056/NEJMoa1304923
20. Li S, Chan IS, Matthews H, Heyse JF, Chan CY, Kuter BJ, et al. Inverse Relationship Between Six Week Postvaccination Varicella Antibody Response to Vaccine and Likelihood of Long Term Breakthrough Infection. *Pediatr Infect Dis J* (2002) 21(4):337–42. doi: 10.1097/00006454-200204000-00014
21. World Health Organization. *Recommendations to Assure the Quality, Safety and Efficacy of Recombinant Hepatitis B Vaccines. Annex 4 of WHO TRS No. 978*. (2013). Available at: https://www.who.int/publications/m/item/recombinant-hep-b-A4-trs-978 (Accessed May 25, 2013).
22. Chen RT, Markowitz LE, Albrecht P, Stewart JA, Mofenson LM, Preblud SR, et al. Measles Antibody: Reevaluation of Protective Titers. *J Infect Dis* (1990) 162(5):1036–42. doi: 10.1093/infdis/162.5.1036
23. Lemon SM, Binn LN. Serum Neutralizing Antibody Response to Hepatitis A Virus. *J Infect Dis* (1983) 148(6):1033–9. doi: 10.1093/infdis/148.6.1033
24. André FE, D'Hondt E, Delem A, Safary A. Clinical Assessment of the Safety and Efficacy of an Inactivated Hepatitis A Vaccine: Rationale and Summary of Findings. *Vaccine* (1992) 10 Suppl 1:S160–168. doi: 10.1016/0264-410x(92)90576-6
25. Clemens R, Safary A, Hepburn A, Roche C, Stanbury WJ, André FE. Clinical Experience With an Inactivated Hepatitis A Vaccine. *J Infect Dis* (1995) 171 Suppl 1:S44–49. doi: 10.1093/infdis/171.supplement_1.s44
26. Jara A, Undurraga EA, González C, Paredes F, Fontecilla T, Jara G, et al. Effectiveness of an Inactivated SARS-CoV-2 Vaccine in Chile. *N Engl J Med* (2021) 385(10):875–84. doi: 10.1056/NEJMoa2107715
27. Chemaitelly H, Yassine HM, Benslimane FM, Al Khatib HA, Tang P, Hasan MR, et al. mRNA-1273 COVID-19 Vaccine Effectiveness Against the B.1.1.7 and B.1.351 Variants and Severe COVID-19 Disease in Qatar. *Nat Med* (2021) 27(9):1614–21. doi: 10.1038/s41591-021-01446-y
28. Khoury DS, Cromer D, Reynaldi A, Schlub TE, Wheatley AK, Juno JA, et al. Neutralizing Antibody Levels Are Highly Predictive of Immune Protection From Symptomatic SARS-CoV-2 Infection. *Nat Med* (2021) 27(7):1205–11. doi: 10.1038/s41591-021-01377-8
29. Earle KA, Ambrosino DM, Fiore-Gartland A, Goldblatt D, Gilbert PB, Siber GR, et al. Evidence for Antibody as a Protective Correlate for COVID-19 Vaccines. *Vaccine* (2021) 39(32):4423–8. doi: 10.1016/j.vaccine.2021.05.063
30. Dörner T, Radbruch A. Antibodies and B Cell Memory in Viral Immunity. *Immunity* (2007) 27(3):384–92. doi: 10.1016/j.immuni.2007.09.002
31. Wyllie D, Jones HE, Mulchandani R, Trickey A, Taylor-Phillips S, Brooks T, et al. SARS-CoV-2 Responsive T Cell Numbers and Anti-Spike IgG Levels are Both Associated With Protection From COVID-19: A Prospective Cohort Study in Keyworkers. *medRxiv* (2021) 2020.2011.2002.20222778. doi: 10.1101/2020.11.02.20222778
32. Tan AT, Linster M, Tan CW, Le Bert N, Chia WN, Kunasegaran K, et al. Early Induction of Functional SARS-CoV-2-Specific T Cells Associates With Rapid Viral Clearance and Mild Disease in COVID-19 Patients. *Cell Rep* (2021) 34(6):108728. doi: 10.1016/j.celrep.2021.108728
33. Goel RR, Painter MM. mRNA Vaccines Induce Durable Immune Memory to SARS-CoV-2 and Variants of Concern. *Science* (2021) 374(6572):abm0829. doi: 10.1126/science.abm0829
34. Medicines & Healthcare products Regulatory Agency. *Vaccine BNT162b2 – Conditions of Authorisation Under Regulation 174*. (2020). Available at: https://www.gov.uk/government/publications/regulatoryapproval-of-pfizer-biontech-vaccine-for-covid-19/conditionsof-authorisation-for-pfizerbiontech-covid-19-vaccine (Accessed December 30, 2020).
35. World Health Organization. *Regulation and Prequalification* (2020). Available at: https://www.who.int/teams/regulation-prequalification/eul/covid-19 (Accessed January 15, 2022).
36. U.S. Food and Drug Administration. *FDA Approves First COVID-19 Vaccine* (2021). Available at: https://www.fda.gov/news-events/press-announcements/fda-approves-first-covid-19-vaccine (Accessed August 23, 2021).
37. Our World in Data. *COVID-19 Vaccine Doses Administered* (2021). Available at: https://ourworldindata.org/grapher/cumulative-covid-vaccinations (Accessed January 15, 2022).
38. National Health Commission of the Peoples's Republic of China. *Novel Coronavirus Vaccination Status* (2021). Available at: http://www.nhc.gov.cn/xcs/yqfkdt/202111/5e687b673afa480da56c01be4259675a.shtml (Accessed January 15, 2022).
39. Viana R, Moyo S, Amoako DG, Tegally H, Scheepers C, Althaus CL, et al. Rapid Epidemic Expansion of the SARS-CoV-2 Omicron Variant in Southern Africa. *medRxiv* (2021) 2012:201921268028. doi: 10.1101/2021.12.19.21268028
40. World Health Organization. *Enhancing Response to Omicron SARS-CoV-2 Variant* (2022). Available at: https://www.who.int/publications/m/item/enhancing-readiness-for-omicron-(b.1.1.529)-technical-brief-and-priority-actions-for-member-states (Accessed January 19, 2022).
41. U.S. Centers for Disease Control and Prevention. *Potential Rapid Increase of Omicron Variant Infections in the United States* (2022). Available at: https://www.cdc.gov/coronavirus/2019-ncov/science/forecasting/mathematical-modeling-outbreak.html (Accessed January 19, 2022).
42. Ikemura N, Hoshino A, Higuchi Y, Taminishi S, Inaba T, Matoba S. SARS-CoV-2 Omicron Variant Escapes Neutralization by Vaccinated and Convalescent Sera and Therapeutic Monoclonal Antibodies. *medRxiv* (2021) 2021.2012.2013.21267761. doi: 10.1101/2021.12.13.21267761
43. VanBlargan LA, Errico JM, Halfmann PJ, Zost SJ, Crowe JE, Purcell LA, et al. An Infectious SARS-CoV-2 B.1.1.529 Omicron Virus Escapes Neutralization by Several Therapeutic Monoclonal Antibodies. *bioRxiv* (2021) 2021.2012.2015.472828. doi: 10.1101/2021.12.15.472828
44. Planas D, Saunders N, Maes P, Guivel-Benhassine F, Planchais C, Buchrieser J, et al. Considerable Escape of SARS-CoV-2 Omicron to Antibody Neutralization. *Nature* (2021) 602(7898):671–5. doi: 10.1038/s41586-021-04389-z

45. Wall EC, Wu M, Harvey R, Kelly G, Warchal S, Sawyer C, et al. AZD1222-Induced Neutralising Antibody Activity Against SARS-CoV-2 Delta VOC. *Lancet* (2021) 398:207–9. doi: 10.1016/S0140-6736(21)01462-8
46. Thompson MG, Burgess JL, Naleway AL, Tyner H, Yoon SK, Meece J, et al. Prevention and Attenuation of Covid-19 With the BNT162b2 and mRNA-1273 Vaccines. *N Engl J Med* (2021) 385(4):320–9. doi: 10.1056/NEJMoa2107058
47. Andrews N, Stowe J, Kirsebom F, Toffa S, Rickeard T, Gallagher E, et al. Effectiveness of COVID-19 Vaccines Against the Omicron (B.1.1.529) Variant of Concern. *medRxiv* (2021) 2021.2012.2014.21267615. doi: 10.1101/2021.12.14.21267615
48. Wang K, Cao Y, Zhou Y, Wu J, Jia Z, Hu Y, et al. A Third Dose of Inactivated Vaccine Augments the Potency, Breadth, and Duration of Anamnestic Responses Against SARS-CoV-2. *medRxiv* (2021) 2021.2009.2002.21261735. doi: 10.1101/2021.09.02.21261735
49. Bar-On YM, Goldberg Y, Mandel M, Bodenheimer O, Freedman L, Kalkstein N, et al. Protection of BNT162b2 Vaccine Booster Against Covid-19 in Israel. *N Engl J Med* (2021) 385(15):1393–400. doi: 10.1056/NEJMoa2114255
50. U.S. Centers for Disease Control and Prevention. *Evidence to Recommendation Framework: Pfizer-BioNTech COVID-19 Booster Dose* (2021). Available at: https://www.cdc.gov/vaccines/acip/meetings/downloads/slides-2021-9-23/03-COVID-Oliver.pdf (Accessed September 23, 2021).
51. Falsey AR, Frenck RW, Walsh EE, Kitchin N, Absalon J, Gurtman A, et al. SARS-CoV-2 Neutralization With BNT162b2 Vaccine Dose 3. *N Engl J Med* (2021) 385(17):1627–9. doi: 10.1056/NEJMc2113468
52. Pfizer. *Pfizer And BioNTech Announce Phase 3 Trial Data Showing High Efficacy Of A Booster Dose Of Their COVID-19 Vaccine* (2021). Available at: https://www.pfizer.com/news/press-release/press-release-detail/pfizer-and-biontech-announce-phase-3-trial-data-showing (Accessed October 21, 2021).
53. Yu X, Wei D, Xu W, Li Y, Li X, Zhang X, et al. Pseudotyped SARS-CoV-2 Omicron Variant Exhibits Significant Escape From Neutralization Induced by a Third Booster Dose of Vaccination. *medRxiv* (2021) 2021.2012.2017.21267961. doi: 10.1101/2021.12.17.21267961
54. Doria-Rose NA, Shen X, Schmidt SD, O'Dell S, McDanal C, Feng W, et al. Booster of mRNA-1273 Vaccine Reduces SARS-CoV-2 Omicron Escape From Neutralizing Antibodies. *medRxiv* (2021) 2021.2012.2015.21267805. doi: 10.1101/2021.12.15.21267805
55. Garcia-Beltran WF, St Denis KJ, Hoelzemer A, Lam EC, Nitido AD, Sheehan ML, et al. mRNA-Based COVID-19 Vaccine Boosters Induce Neutralizing Immunity Against SARS-CoV-2 Omicron Variant. *Cell* (2022) 185(3):457–66.e4. doi: 10.1016/j.cell.2021.12.033
56. Nemet I, Kliker L, Lustig Y, Zuckerman N, Erster O, Cohen C, et al. Third BNT162b2 Vaccination Neutralization of SARS-CoV-2 Omicron Infection. *N Engl J Med* (2022) 386(5):492–4. doi: 10.1056/NEJMc2119358
57. Schmidt F, Muecksch F, Weisblum Y, Da Silva J, Bednarski E, Cho A, et al. Plasma Neutralization of the SARS-CoV-2 Omicron Variant. *N Engl J Med* (2022) 386(6):599–601. doi: 10.1056/NEJMc2119641
58. U.S. Food and Drug Administration. *FDA Authorizes Booster Dose of Pfizer-BioNTech COVID-19 Vaccine for Certain Populations* (2021). Available at: https://www.fda.gov/news-events/press-announcements/fda-authorizes-booster-dose-pfizer-biontech-covid-19-vaccine-certain-populations (Accessed September 22, 2021).
59. Our World in Data. *COVID-19 Vaccine Booster Doses Administered* (2021). Available at: https://ourworldindata.org/covid-vaccinations (Accessed October 02, 2021).
60. The State Council. *The People's Republic of China* (2021). Available at: http://www.gov.cn/xinwen/gwylflkjz165/index.htm (Accessed August 27, 2021).
61. Krause PR, Fleming TR, Peto R, Longini IM, Figueroa JP, Sterne JAC, et al. Considerations in Boosting COVID-19 Vaccine Immune Responses. *Lancet*. (2021) 398(10308):1377–80. doi: 10.1016/S0140-6736(21)02046-8
62. Consumer News and Business Channel. *WHO Reiterates Warning Against Covid Boosters for Healthy People as U.S. Weighs Wide Distribution of Third Shots* (2021). Available at: https://www.cnbc.com/2021/09/21/who-repeats-warning-against-covid-booster-shots-for-healthy-people-.html (Accessed November 02, 2021).
63. World Health Organization. *WHO, UN Set Out Steps to Meet World COVID Vaccination Targets* (2021). Available at: https://www.who.int/news/item/07-10-2021-who-un-set-out-steps-to-meet-world-covid-vaccination-targets (Accessed October 07, 2021).
64. *Sinopharm* (2021). Available at: http://www.sinopharm.com/s/1223-3769-39691.html (Accessed September 08, 2021).
65. ClinicalTrials.gov. *Safety, Reactogenicity and Immunogenicity Study of ReCOV* (2021). Available at: https://clinicaltrials.gov/ct2/show/NCT04818801 (Accessed November 02, 2021).
66. Clinical Trials Arena. *Gritstone Starts Phase I Dosing of Second-Gen mRNA Covid-19 Vaccine* (2021). Available at: https://www.clinicaltrialsarena.com/news/gritstone-covid-vaccine-uk-phasei/ (Accessed September 21, 2021).
67. Chen P, Nirula A, Heller B, Gottlieb RL, Boscia J, Morris J, et al. SARS-CoV-2 Neutralizing Antibody LY-CoV555 in Outpatients With Covid-19. *N Engl J Med* (2020) 384(3):229–37. doi: 10.1056/NEJMoa2029849
68. Huang AT, Garcia-Carreras B, Hitchings MDT, Yang B, Katzelnick LC, Rattigan SM, et al. A Systematic Review of Antibody Mediated Immunity to Coronaviruses: Kinetics, Correlates of Protection, and Association With Severity. *Nat Commun* (2020) 11(1):4704. doi: 10.1038/s41467-020-18450-4
69. McMahan K, Yu J, Mercado NB, Loos C, Tostanoski LH, Chandrashekar A, et al. Correlates of Protection Against SARS-CoV-2 in Rhesus Macaques. *Nature* (2021) 590(7847):630–4. doi: 10.1038/s41586-020-03041-6
70. Lilly Investors. *Lilly"s Neutralizing Antibody Bamlanivimab (LY-CoV555) Prevented COVID-19 at Nursing Homes in the BLAZE-2 Trial, Reducing Risk by Up to 80 Percent for Residents* (2021). Available at: https://investor.lilly.com/news-releases/news-release-details/lillys-neutralizing-antibody bamlanivimab-ly-cov555-prevented (Accessed January 21, 2021).
71. Feng S, Phillips DJ, White T, Sayal H, Aley PK, Bibi S, et al. Correlates of Protection Against Symptomatic and Asymptomatic SARS-CoV-2 Infection. *Nat Med* (2021) 27(11):2032–40. doi: 10.1038/s41591-021-01540-1
72. Corbett KS, Flynn B, Foulds KE, Francica JR, Boyoglu-Barnum S, Werner AP, et al. Evaluation of the mRNA-1273 Vaccine Against SARS-CoV-2 in Nonhuman Primates. *N Engl J Med* (2020) 383(16):1544–55. doi: 10.1056/NEJMoa2024671
73. Vogel AB, Kanevsky I, Che Y, Swanson KA, Muik A, Vormehr M, et al. A Prefusion SARS-CoV-2 Spike RNA Vaccine is Highly Immunogenic and Prevents Lung Infection in non-Human Primates. *bioRxiv* (2020). doi: 10.1101/2020.09.08.280818
74. Solforosi L, Solforosi L, Kuipers H, Jongeneelen M, Rosendahl Huber SK, van der Lubbe JEM, et al. Immunogenicity and Efficacy of One and Two Doses of Ad26.COV2.S COVID Vaccine in Adult and Aged NHP. *J Exp Med* (2021) 218(7):e20202756. doi: 10.1084/jem.20202756
75. van Doremalen N, Lambe T, Spencer A, Belij-Rammerstorfer S, Purushotham JN, Port JR, et al. ChAdOx1 Ncov-19 Vaccination Prevents SARS-CoV-2 Pneumonia in Rhesus Macaques. *bioRxiv* (2020) 2020.2005.2013.093195. doi: 10.1101/2020.05.13.093195
76. van Doremalen N, Lambe T, Spencer A, Belij-Rammerstorfer S, Purushotham JN, Port JR, et al. ChAdOx1 Ncov-19 Vaccine Prevents SARS-CoV-2 Pneumonia in Rhesus Macaques. *Nature* (2020) 586 (7830):578–82. doi: 10.1038/s41586-020-2608-y
77. Wang H, Zhang Y, Huang B, Deng W, Quan Y, Wang W, et al. Development of an Inactivated Vaccine Candidate, BBIBP-CorV, With Potent Protection Against SARS-CoV-2. *Cell* (2020) 182(3):713–21.e719. doi: 10.1016/j.cell.2020.06.008
78. Gao Q, Bao L, Mao H, Wang L, Xu K, Yang M, et al. Development of an Inactivated Vaccine Candidate for SARS-CoV-2. *Science* (2020) 369 (6499):77–81. doi: 10.1126/science.abc1932
79. Yadav PD, Ella R, Kumar S, Patil DR, Mohandas S, Shete AM, et al. Immunogenicity and Protective Efficacy of Inactivated SARS-CoV-2 Vaccine Candidate, BBV152 in Rhesus Macaques. *Nat Commun* (2021) 12 (1):1386. doi: 10.1038/s41467-021-21639-w
80. Gooch KE, Smith TRF, Salguero FJ, Fotheringham SA, Watson RJ, Dennis MJ, et al. One or Two Dose Regimen of the SARS-CoV-2 Synthetic DNA Vaccine INO-4800 Protects Against Respiratory Tract Disease Burden in Nonhuman Primate Challenge Model. *Vaccine* (2021) 39(34):4885–94. doi: 10.1016/j.vaccine.2021.06.057
81. Guebre-Xabier M, Patel N, Tian J-H, Zhou B, Maciejewski S, Lam K, et al. NVX-CoV2373 Vaccine Protects Cynomolgus Macaque Upper and Lower

Airways Against SARS-CoV-2 Challenge. *Vaccine* (2020) 38(50):7892–6. doi: 10.1016/j.vaccine.2020.10.064
82. Liang JG, Su D, Song T-Z, Zeng Y, Huang W, Wu J, et al. S-Trimer, a COVID-19 Subunit Vaccine Candidate, Induces Protective Immunity in Nonhuman Primates. *Nat Commun* (2021) 12(1):1346. doi: 10.1038/s41467-021-21634-1
83. Al Kaabi N, Zhang Y, Xia S, Yang Y, Al Qahtani MM, Abdulrazzaq N, et al. Effect of 2 Inactivated SARS-CoV-2 Vaccines on Symptomatic COVID-19 Infection in Adults: A Randomized Clinical Trial. *JAMA* (2021) 326(1):35–45. doi: 10.1001/jama.2021.8565
84. Palacios R, Batista AP, Albuquerque CSN, Patiño EG, Santos J, do P, et al. Efficacy and Safety of a COVID-19 Inactivated Vaccine in Healthcare Professionals in Brazil: The PROFISCOV Study. *SSRN* (2021). doi: 10.2139/ssrn.3822780
85. Tanriover MD, Doğanay HL, Akova M, Güner HR, Azap A, Akhan S, et al. Efficacy and Safety of an Inactivated Whole-Virion SARS-CoV-2 Vaccine (CoronaVac): Interim Results of a Double-Blind, Randomised, Placebo-Controlled, Phase 3 Trial in Turkey. *Lancet* (2021) 398(10296):213–22. doi: 10.1016/S0140-6736(21)01429-X
86. Voysey M, Clemens S, Madhi SA, Weckx LY, Folegatti PM, Aley PK, et al. Safety and Efficacy of the ChAdOx1 Ncov-19 Vaccine (AZD1222) Against SARS-CoV-2: An Interim Analysis of Four Randomised Controlled Trials in Brazil, South Africa, and the UK. *Lancet* (2021) 397(10269):99–111. doi: 10.1016/S0140-6736(20)32661-1
87. Folegatti PM, Ewer KJ, Aley PK, Angus B, Becker S, Belij-Rammerstorfer S, et al. Safety and Immunogenicity of the ChAdOx1 Ncov-19 Vaccine Against SARS-CoV-2: A Preliminary Report of a Phase 1/2, Single-Blind, Randomised Controlled Trial. *Lancet* (2020) 396(10249):467–78. doi: 10.1016/S0140-6736(20)31604-4
88. Logunov DY, Dolzhikova IV, Shcheblyakov DV, Tukhvatulin AI, Zubkova OV, Dzharullaeva AS, et al. Safety and Efficacy of an Rad26 and Rad5 Vector-Based Heterologous Prime-Boost COVID-19 Vaccine: An Interim Analysis of a Randomised Controlled Phase 3 Trial in Russia. *Lancet* (2021) 397(10275):671–81. doi: 10.1016/S0140-6736(21)00234-8
89. Ella R, Reddy S, Blackwelder W, Potdar V, Yadav P, Sarangi V, et al. Efficacy, Safety, and Lot to Lot Immunogenicity of an Inactivated SARS-CoV-2 Vaccine (BBV152): A Double-Blind, Randomised, Controlled Phase 3 Trial. *medRxiv* (2021) 2021.2006.2030.21259439. doi: 10.1101/2021.06.30.21259439
90. Baden LR, El Sahly HM, Essink B, Kotloff K, Frey S, Novak R, et al. Efficacy and Safety of the mRNA-1273 SARS-CoV-2 Vaccine. *N Engl J Med* (2020) 384(5):403–16. doi: 10.1056/NEJMoa2035389
91. Jackson LA, Anderson EJ, Rouphael NG, Roberts PC, Makhene M, Coler RN, et al. An mRNA Vaccine Against SARS-CoV-2 - Preliminary Report. *N Engl J Med* (2020) 383(20):1920–31. doi: 10.1056/NEJMoa2022483
92. Polack FP, Thomas SJ, Kitchin N, Absalon J, Gurtman A, Lockhart S, et al. Safety and Efficacy of the BNT162b2 mRNA Covid-19 Vaccine. *N Engl J Med* (2020) 383(27):2603–15. doi: 10.1056/NEJMoa2034577
93. Walsh EE, Frenck RWJr., Falsey AR, Kitchin N, Absalon J, Gurtman A, et al. Safety and Immunogenicity of Two RNA-Based Covid-19 Vaccine Candidates. *N Engl J Med* (2020) 383(25):2439–50. doi: 10.1056/NEJMoa2027906
94. Sadoff J, Gray G, Vandebosch A, Cárdenas V, Shukarev G, Grinsztejn B, et al. Safety and Efficacy of Single-Dose Ad26.Cov2.S Vaccine Against Covid-19. *N Engl J Med* (2021) 384(23):2187–201. doi: 10.1056/NEJMoa2101544
95. Sadoff J, Le Gars M, Shukarev G, Heerwegh D, Truyers C, de Groot AM, et al. Interim Results of a Phase 1-2a Trial of Ad26.COV2.S Covid-19 Vaccine. *N Engl J Med* (2021) 384(19):1824–35. doi: 10.1056/NEJMoa2034201
96. Heath PT, Galiza EP, Baxter DN, Boffito M, Browne D, Burns F, et al. Safety and Efficacy of NVX-CoV2373 Covid-19 Vaccine. *N Engl J Med* (2021) 385 (13):1172–83. doi: 10.1056/NEJMoa2107659
97. Keech C, Albert G, Cho I, Robertson A, Reed P, Neal S, et al. Phase 1-2 Trial of a SARS-CoV-2 Recombinant Spike Protein Nanoparticle Vaccine. *N Engl J Med* (2020) 383(24):2320–32. doi: 10.1056/NEJMoa2026920
98. Bergwerk M, Gonen T, Lustig Y, Amit S, Lipsitch M, Cohen C, et al. Covid-19 Breakthrough Infections in Vaccinated Health Care Workers. *N Engl J Med* (2021) 9(12):1396–406. doi: 10.1056/NEJMoa2109072
99. Chung H, He S, Nasreen S, Sundaram ME, Buchan SA, Wilson SE, et al. Effectiveness of BNT162b2 and mRNA-1273 Covid-19 Vaccines Against Symptomatic SARS-CoV-2 Infection and Severe Covid-19 Outcomes in Ontario, Canada: Test Negative Design Study. *BMJ* (2021) 374:n1943. doi: 10.1136/bmj.n1943
100. Dagan N, Barda N, Kepten E, Miron O, Perchik S, Katz MA. BNT162b2 mRNA Covid-19 Vaccine in a Nationwide Mass Vaccination Setting. *N Engl J Med* (2021) 384(15):1412–23. doi: 10.1056/NEJMoa2101765
101. Abu-Raddad LJ, Chemaitelly H, Butt AANational Study Group for COVID-19 Vaccination. Effectiveness of the BNT162b2 Covid-19 Vaccine Against the B.1.1.7 and B.1.351 Variants. *N Engl J Med* (2021) 385(2):187–9. doi: 10.1056/NEJMc2104974
102. Puranik A, Lenehan PJ, Silvert E, Niesen MJM, Corchado-Garcia J, O'Horo JC, et al. Comparison of Two Highly-Effective mRNA Vaccines for COVID-19 During Periods of Alpha and Delta Variant Prevalence. *medRxiv* (2021). doi: 10.1101/2021.08.06.21261707
103. Souza WM, Amorim MR, Sesti-Costa R, Coimbra LD, Brunetti NS, Toledo-Teixeira DA, et al. Neutralisation of SARS-CoV-2 Lineage P.1 by Antibodies Elicited Through Natural SARS-CoV-2 Infection or Vaccination With an Inactivated SARS-CoV-2 Vaccine: An Immunological Study. *Lancet Microbe* (2021) 2(10):e527–35. doi: 10.1016/S2666-5247(21)00129-4
104. Lopez Bernal J, Andrews N, Gower C, Gallagher E, Simmons R, Thelwall S, et al. Effectiveness of Covid-19 Vaccines Against the B.1.617.2 (Delta) Variant. *N Engl J Med* (2021) 385(7):585–94. doi: 10.1056/NEJMoa2108891
105. Pouwels KB, Pritchard E, Matthews PC, Stoesser N, Eyre DW, Vihta K-D, et al. Impact of Delta on Viral Burden and Vaccine Effectiveness Against New SARS-CoV-2 Infections in the UK. *medRxiv* (2021) 2021.2008.2018.21262237. doi: 10.1101/2021.08.18.21262237
106. Widge AT, Rouphael NG, Jackson LA, Anderson EJ, Roberts PC, Makhene M, et al. Durability of Responses After SARS-CoV-2 mRNA-1273 Vaccination. *N Engl J Med* (2020) 384(1):80–2. doi: 10.1056/NEJMc2032195
107. Zhang H, Jia Y, Ji Y, Cong X, Liu Y, Yang R, et al. Studies on the Level of Neutralizing Antibodies Produced by Inactivated COVID-19 Vaccines in the Real World. *medRxiv* (2021) 2021.2008.2018.21262214. doi: 10.1101/2021.08.18.21262214
108. Goldberg Y, Mandel M, Bar-On YM, Bodenheimer O, Freedman L, Haas EJ, et al. Waning Immunity of the BNT162b2 Vaccine: A Nationwide Study From Israel. *medRxiv* (2021) 2021:2008.2024.21262423. doi: 10.1101/2021.08.24.21262423
109. Medigen Vaccine Biologics Corp. *MVC COVID-19 Vaccine Obtains Taiwan EUA Approval* (2021). Available at: https://www.medigenvac.com/public/en/news/detail/83?from_sort=2 (Accessed July 19, 2021).
110. Valneva. *Valneva Reports Positive Phase 3 Results for Inactivated, Adjuvanted COVID-19 Vaccine Candidate Vla2001* (2021). Available at: https://valneva.com/press-release/valneva-reports-positive-phase-3-results-for-inactivated-adjuvanted-covid-19-vaccine-candidate-vla2001/ (Accessed October 18, 2021).
111. ClinicalTrials.gov. *Study To Compare The Immunogenicity Against COVID-19, Of VLA2001 Vaccine To AZD1222 Vaccine (COV-COMPARE)* (2021). Available at: https://clinicaltrials.gov/ct2/show/NCT04864561 (Accessed October 29, 2021).
112. Hsieh S-M, Liu M-C, Chen Y-H, Lee W-S, Hwang S-J, Cheng S-H, et al. Safety and Immunogenicity of CpG 1018 and Aluminium Hydroxide-Adjuvanted SARS-CoV-2 S-2P Protein Vaccine MVC-COV1901: Interim Results of a Large-Scale, Double-Blind, Randomised, Placebo-Controlled Phase 2 Trial in Taiwan. *Lancet Respir Med* (2021) 9(12):1396-406. doi: 10.1016/S2213-2600(21)00402-1
113. Hsieh S-M, Liu W-D, Huang Y-S, Lin Y-J, Hsieh E-F, Lian W-C, et al. Safety and Immunogenicity of a Recombinant Stabilized Prefusion SARS-CoV-2 Spike Protein Vaccine (MVC COV1901) Adjuvanted With CpG 1018 and Aluminum Hydroxide in Healthy Adults: A Phase 1, Dose-Escalation Study. *EClinicalMedicine* (2021) 38:100989. doi: 10.1016/j.eclinm.2021.100989
114. Available at: https://geneonline.news/eua-medigen-vaccine (Accessed August 02, 2021).
115. Valneva. *Valneva Reports Positive Phase 1/2 Data for Its Inactivated, Adjuvanted COVID-19 Vaccine Candidate, Vla2001* (2021). Available at: https://valneva.com/press-release/valneva-reports-positive-phase-1-2-data-

for-its-inactivated-adjuvanted-covid-19-vaccine-candidate-vla2001/ (Accessed April 6, 2021).
116. Banga Ndzouboukou J-L, Zhang Y-d, Fan X-l. Recent Developments in SARS-CoV-2 Neutralizing Antibody Detection Methods. *Curr Med Sci* (2021) 41(6):1052–64. doi: 10.1007/s11596-021-2470-7
117. World Health Organization. *WHO/BS.2020.2403 Establishment of the WHO International Standard and Reference Panel for Anti-SARS-CoV-2 Antibody* (2020). Available at: https://www.who.int/publications/m/item/WHO-BS-2020.2403 (Accessed November 18, 2020).
118. Guan L, Yu Y, Wu X, Nie J, Zhang J, Wang Z, et al. The First Chinese National Standards for SARS-CoV-2 Neutralizing Antibody. *Vaccine* (2021) 39(28):3724–30. doi: 10.1016/j.vaccine.2021.05.047
119. Nie J, Li Q, Wu J, Zhao C, Hao H, Liu H, et al. Establishment and Validation of a Pseudovirus Neutralization Assay for SARS-CoV-2. *Emerg Microbes Infect* (2020) 9(1):680–6. doi: 10.1080/22221751.2020.1743767
120. Kristiansen PA, Page M, Bernasconi V, Mattiuzzo G, Dull P, Makar K, et al. WHO International Standard for Anti-SARS-CoV-2 Immunoglobulin. *Lancet* (2021) 397(10282):1347–8. doi: 10.1016/S0140-6736(21)00527-4
121. World Health Organization. *Guidance on Conducting Vaccine Effectiveness Evaluations in the Setting of New SARS-CoV-2 Variants* (2021). Available at: https://www.who.int/publications/i/item/WHO-2019-nCoV-vaccine_effectiveness-variants-2021.1 (Accessed July 23, 2021).
122. European Medicines Agency. *Regulatory Requirements for Vaccines Intended to Provide Protection Against Variant Strain(s) of SARS-CoV-2* (2021). Available at: https://www.ema.europa.eu/en/regulatory-requirements-vaccines-intended-provide-protection-against-variant-strains-sars-cov-2 (Accessed February 25, 2021).
123. National Medical Products Administration. *Technical Guidelines for the Development of Novel Coronavirus Preventive Vaccines (Trial)* (2020). Available at: https://www.nmpa.gov.cn/xxgk/ggtg/qtggtg/20200814230916157.html (Accessed August 14, 2020).
124. U.S. Food and Drug Administration. *GUIDANCE DOCUMENT Emergency Use Authorization for Vaccines to Prevent COVID-19 Guidance for Industry* (2021). Available at: https://www.fda.gov/regulatory-information/search-fda-guidance-documents/emergency-use-authorization-vaccines-prevent-covid-19 (Accessed May 25, 2021).
125. Medicines & Healthcare products Regulatory Agency. *Decision Access Consortium: Alignment With ICMRA Consensus on Immunobridging for Authorising New COVID-19 Vaccines* (2021). Available at: https://www.gov.uk/government/publications/access-consortium-alignment-with-icmra-consensus-on-immunobridging-for-authorising-new-covid-19-vaccines/access-consortium-alignment-with-icmra-consensus-on-immunobridging-for-authorising-new-covid-19-vaccines (Accessed September 15, 2021).
126. Cevik M, Grubaugh ND, Iwasaki A, Openshaw P. COVID-19 Vaccines: Keeping Pace With SARS-CoV-2 Variants. *Cell* (2021) 184(20):5077–81. doi: 10.1016/j.cell.2021.09.010
127. Aggarwal A, Stella AO, Walker G, Akerman A, Milogiannakis V, Brilot F, et al. SARS-CoV-2 Omicron: Evasion of Potent Humoral Responses and Resistance to Clinical Immunotherapeutics Relative to Viral Variants of Concern. *medRxiv* (2021) 2021.2012.2014.21267772. doi: 10.1101/2021.12.14.21267772
128. Cov-lineages.org. *Lineage List* (2021). Available at: https://cov-lineages.org/lineage_list.html (Accessed October 02, 2021).
129. Yadav PD, Sapkal GN, Ella R, Sahay RR, Nyayanit DA, Patil DY, et al. Neutralization of Beta and Delta Variant With Sera of COVID-19 Recovered Cases and Vaccinees of Inactivated COVID-19 Vaccine BBV152/Covaxin. *J Travel Med* (2021) 28(7):taab104. doi: 10.1093/jtm/taab104
130. Gómez-Carballa A, Pardo-Seco J, Bello X, Martinón-Torres F, Salas A. Superspreading in the Emergence of COVID-19 Variants. *Trends Genet* (2021). doi: 10.1016/j.tig.2021.09.003
131. Ahmed SF, Quadeer AA, McKay MR. SARS-CoV-2 T Cell Responses Elicited by COVID-19 Vaccines or Infection Are Expected to Remain Robust Against Omicron. *Viruses* (2022) 14(1):79. doi: 10.3390/v14010079
132. Tarke A, Sidney J, Methot N, Yu ED, Zhang Y, Dan JM, et al. Impact of SARS-CoV-2 Variants on the Total CD4(+) and CD8(+) T Cell Reactivity in Infected or Vaccinated Individuals. *Cell Rep Med* (2021) 2(7):100355. doi: 10.1016/j.xcrm.2021.100355
133. Adamo S, Michler J, Zurbuchen Y, Cervia C, Taeschler P, Raeber ME, et al. Signature of Long-Lived Memory CD8+ T Cells in Acute SARS-CoV-2 Infection. *Nature* (2021) 602(7895):148–55. doi: 10.1038/s41586-021-04280-x
134. Kundu R, Narean JS, Wang L, Fenn J, Pillay T, Fernandez ND, et al. Cross-Reactive Memory T Cells Associate With Protection Against SARS-CoV-2 Infection in COVID-19 Contacts. *Nat Commun* (2022) 13(1):80. doi: 10.1038/s41467-021-27674-x
135. World Health Organization. *Correlates of Protection - Will Emerging Data Allow Increased Reliance on Vaccine Immune Responses for Public Health and Regulatory Decision-Making?* (2022). Available at: https://www.who.int/news-room/events/detail/2021/09/03/default-calendar/save-the-date—will-emerging-data-allow-increased-reliance-on-vaccine-immune-responses-for-public-health-and-regulatory-decision-making (Accessed January 19, 2022).

Conflict of Interest: The authors declare that the research was conducted in the absence of any commercial or financial relationships that could be construed as a potential conflict of interest.

Publisher's Note: All claims expressed in this article are solely those of the authors and do not necessarily represent those of their affiliated organizations, or those of the publisher, the editors and the reviewers. Any product that may be evaluated in this article, or claim that may be made by its manufacturer, is not guaranteed or endorsed by the publisher.

frontiers | Frontiers in Immunology

ORIGINAL RESEARCH
published: 11 May 2022
doi: 10.3389/fimmu.2022.833085

Humoral Immune Response Diversity to Different COVID-19 Vaccines: Implications for the "Green Pass" Policy

Immacolata Polvere[1†], Alfredina Parrella[2,3†], Lucrezia Zerillo[1,4], Serena Voccola[2,4], Gaetano Cardinale[2,3], Silvia D'Andrea[1,4], Jessica Raffaella Madera[1], Romania Stilo[1], Pasquale Vito[1,4] and Tiziana Zotti[1,4*]*

[1] Department of Science and Technology, University of Sannio, Benevento, Italy, [2] Consorzio Sannio Tech, Apollosa, Italy, [3] Tecno Bios srl, Apollosa, Italy, [4] Genus Biotech srls, University of Sannio, Benevento, Italy

OPEN ACCESS

Edited by:
Raymund Razonable,
Mayo Clinic, United States

Reviewed by:
Alfred Hyoungju Kim,
Washington University in St. Louis, United States
Doug Lake,
Arizona State University, United States

***Correspondence:**
Pasquale Vito
vito@unisannio.it
Tiziana Zotti
tzotti@unisannio.it

†These authors have contributed equally to this work and share first authorship

Specialty section:
This article was submitted to Vaccines and Molecular Therapeutics, a section of the journal Frontiers in Immunology

Received: 10 December 2021
Accepted: 31 March 2022
Published: 11 May 2022

Citation:
Polvere I, Parrella A, Zerillo L, Voccola S, Cardinale G, D'Andrea S, Madera JR, Stilo R, Vito P and Zotti T (2022) Humoral Immune Response Diversity to Different COVID-19 Vaccines: Implications for the "Green Pass" Policy. Front. Immunol. 13:833085. doi: 10.3389/fimmu.2022.833085

In the COVID-19 pandemic year 2021, several countries have implemented a vaccine certificate policy, the "Green Pass Policy" (GPP), to reduce virus spread and to allow safe relaxation of COVID-19 restrictions and reopening of social and economic activities. The rationale for the GPP is based on the assumption that vaccinated people should maintain a certain degree of immunity to SARS-CoV-2. Here we describe and compare, for the first time, the humoral immune response to mRNA-1273, BNT162b2, Ad26.COV2.S, and ChAdOx1 nCoV-19 vaccines in terms of antibody titer elicited, neutralizing activity, and epitope reactogenicity among 369 individuals aged 19 to 94 years. In parallel, we also considered the use of a rapid test for the determination of neutralizing antibodies as a tool to guide policymakers in defining booster vaccination strategies and eligibility for Green Pass. Our analysis demonstrates that the titer of antibodies directed towards the receptor-binding domain (RBD) of SARS-CoV-2 Spike is significantly associated with age and vaccine type. Moreover, natural COVID-19 infection combined with vaccination results, on average, in higher antibody titer and higher neutralizing activity as compared to fully vaccinated individuals without prior COVID-19. We also found that levels of anti-Spike RBD antibodies are not always strictly associated with the extent of inhibition of RBD-ACE2 binding, as we could observe different neutralizing activities in sera with similar anti-RBD concentrations. Finally, we evaluated the reactivity to four synthetic peptides derived from Spike protein on a randomly selected serum sample and observed that similar to SARS-CoV-2 infection, vaccination elicits a heterogeneous antibody response with qualitative individual features. On the basis of our results, the use of rapid devices to detect the presence of neutralizing antibodies, even on a large scale and repeatedly over time, appears helpful in determining the duration of the humoral protection elicited by vaccination. These aspects and their implications for the GPP are discussed.

Keywords: vaccine, neutralizing antibodies, anti-RBD antibody titer, SARS-CoV-2, humoral immune response, Green Pass Policy

INTRODUCTION

Many companies have developed COVID-19 vaccines simultaneously in an exceptionally short time. So far, over a plethora of more than 300 candidates, 18 have been approved for use (1). In the European Union (EU), the European Medicines Agency authorized two mRNA-based vaccines, the mRNA-1273 from Moderna and the BNT162b2 from Pfizer/BioNTech, and two adenoviral DNA-based vaccines, the Ad26.COV2.S from Johnson & Johnson and the ChAdOx1 nCoV-19 from Oxford-AstraZeneca (2). In the United States, the Food and Drug Administration has approved the emergency use of mRNA-1273 and Ad26.COV2.S and licensed BNT162b2 (3). After more than a year after the start of the vaccination campaign, several studies have reported the analysis of the immune system response to natural infection and/or vaccine inoculation (1, 4, 5). Thanks to the efficacy demonstrated by the approved vaccines, on July 1, 2021, the European Commission introduced a Digital COVID Certificate Regulation (*Green Pass*), with the purpose of facilitating the free movement of citizens inside the EU with no restrictions (6). Originally, several European governments proposed a standard acceptance period of 12 months for vaccination certificates issued following the completion of the primary vaccination series. However, due to uncertainty about the length of the protective coverage provided by the approved vaccines, on November 25, 2021, the European Commission introduced a standard acceptance period of 9 months (6). Both humoral and cellular adaptive immunities are crucial to protect against infection, prevent severe disease induced by SARS-CoV-2, and, more generally, limit virus spread, alleviating pressure on hospitals and intensive care. The most commonly used approach to evaluate the elicited response to vaccine inoculation is the serological determination of antibodies raised against SARS-CoV-2 Spike protein (7, 8). Among them, anti-SARS-CoV-2 neutralizing antibodies are of particular importance, as they can physically prevent the "entry complex" formed by the receptor-binding domain (RBD) of virus Spike and the human angiotensin-converting enzyme 2 (ACE2) expressed on target cells, thereby limiting infection spread and disease symptoms (9–11). Testing assays aimed at detecting neutralizing antibodies are diverse and include micro-neutralization assays (MNA), plaque reduction neutralization tests (PRNT), and pseudotyped virus neutralization assays (PNA) (12). Some of them have high costs, require trained personnel, and can only be carried out in a Biosafety Safety Level 3-equipped laboratory, whereas others, such as the cPass surrogate virus neutralization test (sVNT) (GenScript, Piscataway, NJ, USA) used in this work, are ELISA-based assays and only require optical density readers. The development of immunocapture-based rapid diagnostic tests that determine the levels of neutralizing antibodies in serum and/or whole capillary blood provides an inexpensive, simple, and highly portable tool that could be helpful on a large scale and, outside of the lab, in immuno-surveillance settings (13–15). In this study, we aimed at investigating the antibody response of a large cohort of individuals who received different types of vaccines in terms of anti-RBD antibody titer and neutralizing activity, measured with both an sVNT and a rapid test. So far, many reports have shown that both RNA- and DNA-based vaccines, as well as heterologous vaccination, are efficient in inducing antibody production towards the RBD of Spike proteins and that the antibody titer decreases over time from last inoculation (16–24). We also have correlated anti-RBD antibody titer with age and compared the humoral immune response between COVID-19-naïve vaccinated individuals and those who have recovered from COVID-19. Interestingly, our study demonstrates that, due to polyclonal response to vaccination, anti-RBD levels and inhibition of ACE2-RBD binding are not always strictly associated, suggesting that the concentration of serum antibodies against the RBD of Spike protein alone may be misleading in identifying a correlate to vaccine protection, with important implications for green pass validity policy. Moreover, we show that rapid devices could be useful in monitoring the vaccine efficacy in terms of humoral protection on a global scale, supporting policymakers and governments in defining appropriate vaccination strategies and pandemic containment measures.

Abbreviations: COVID-19, coronavirus disease 2019; SARS-CoV-2, severe acute respiratory syndrome coronavirus 2; ACE2, angiotensin-converting enzyme 2; RBD, receptor-binding domain; ECLIA, electrochemiluminescence immunoassay; AbNeu, neutralizing antibodies.

MATERIAL AND METHODS

Population and Informed Consent

A serological screening addressing the adult population was carried out in the town of Foglianise (Benevento, Italy) on September 18 and 25, 2021, in order to evaluate the titer of antibodies raised against SARS-CoV-2 Spike protein following the vaccine campaign. The study was approved by the Institutional Review Board of Consorzio Sannio Tech (n. 02/2021) in compliance with all relevant ethical regulations. Participants declared age, sex, which type of vaccine and when they received it, if and when they had a diagnosed SARS-CoV-2 infection in the previous months, and signed informed consent for the anonymized use of the leftover blood sample.

Sample Collection

Capillary blood samples from 369 volunteers were collected in lithium-heparin vials by trained personnel and transported within 1 h to the testing laboratory in refrigerated biocarriers. Then, vials were centrifugated for 10 min at 1,400*g* to allow blood cell sedimentation. Aliquots of serum were stored in sterile tubes and stored at −80°C until analysis. Antibody titer was measured in all samples (n = 369), whereas neutralizing activity determination was carried out through a qualitative rapid test on 180 samples, 70 of which were assayed also through an ELISA-based kit detection for detection of neutralizing antibodies to SARS-CoV-2 (**Supplementary Figure 1**).

Anti-Receptor-Binding Domain Antibody Titer

Quantitative determination of specific antibodies directed towards the RBD of the Spike Protein of SARS-CoV-2 was

carried out on serum samples within 48 h from collection through the double-antigen sandwich electroluminescence immunoassay Elecsys® Anti-SARS-CoV-2S (Roche Diagnostics, Basel, Switzerland) according to manufacturer's instructions. The assay uses a recombinant protein representing the RBD of the Spike antigen and streptavidin-coated microparticles to separate bound from unbound antibodies prior to applying a voltage to the electrode (25). This assay has a detection range of 0.40 to 250 UI/ml and a positive threshold set at 0.8 UI/ml. Sera with anti-RBD antibody titers higher than 250 UI/ml have been appropriately diluted in Diluent Universal, and the resulting antibody titer was calculated according to the dilution factor and expressed in UI/ml. As declared by the manufacturer, the specificity and sensibility of the test were 99.98% (CI95 99.91%–100%) and 98.8% (CI95 98.10%–99.30%), respectively. As reported by Jochum et al. (26), Roche's UI/ml is almost equivalent to Binding Antibody Units (BAU)/ml (1 UI/ml = 1.029 BAU/ml) as defined by First WHO International Standard for anti-SARS-CoV-2 human immunoglobulin (NIBSC code: 20/136) (27). Therefore, no conversion of UI/ml is required, and our data can be compared to other studies reporting data in BAU/ml.

Antibody Neutralizing Activity

Qualitative direct detection of total neutralizing antibodies to SARS-CoV-2 in human serum was performed with an ELISA-based cPass™ SARS-CoV-2 Neutralization Antibody Detection Kit (GenScript Biotech Corporation, Piscataway, NJ, USA), according to the manufacturer's instructions. Briefly, serum samples were diluted 1:10 with the sample dilution buffer and mixed with an equal volume of horseradish peroxidase (HRP)-conjugated recombinant SARS-CoV-2 RBD fragment solution diluted in RBD dilution buffer. Subsequently, 100 µl of this solution have been added to a human ACE2-coated 96-well plate and incubated for 30 min at 37°C. The plate was automatically washed four times with the provided wash buffer. Then, 3,3′,5,5′-tetramethylbenzidine (TMB) was added to each well and incubated for 15 min in the dark. The reaction was stopped by the addition of the stop solution. Optical density at 450 nm was measured and compared to that of the control wells. For each serum sample, the percentage of signal inhibition was calculated, and samples were considered positive for neutralizing antibodies when ≥30% inhibition was measured.

IgG/Neutralizing Antibody Rapid Test

In vitro qualitative detection of human IgG antibodies against SARS-CoV-2 and neutralizing antibodies was performed with the immunocapture-based FAST-COVID SARS-CoV-2 IgG/Neutralizing Antibody Rapid Test Kit—Colloidal Gold (JOYSBIO Tianjin Biotechnology Co., Ltd, Tianjin, China). As declared by the manufacturer, the kit has been validated on 93 BNT162b2-vaccinated and 317 uninfected and unvaccinated individuals showing 92.47% sensitivity and 99.68% specificity. In the testing device, the nitrocellulose membrane was coated with mouse anti-human IgG antibody, human ACE2 receptor protein (hACE2), and goat anti-chicken IgY antibody. According to the manufacturer's instructions, when specimens (serum, whole blood, or plasma) are processed and added to the test device together with a diluent buffer, neutralizing antibodies present in the specimen will bind to the colloidal gold-labeled RBD and block the protein–protein interaction between RBD and hACE2. The unbound colloidal gold-labeled RBD as well as any colloidal gold-labeled RBD bound to a non-neutralizing antibody will be captured on the test line (T2 line). Human IgG antibodies against SARS-CoV-2 will combine with colloidal gold-labeled novel coronavirus antigen to form a complex, which is captured by the mouse anti-human IgG antibody coated on the test line (T1 line), forming a colored band. The colloidal gold-labeled chicken IgY antibody is bound to the goat anti-chicken IgY antibody coated on the test line (C line), which acts as a quality control line. The T2 line will get weaker with the increase in concentration of the neutralizing antibodies and disappear at a high concentration of the neutralizing antibodies (**Supplementary Figure 2**). Samples were scored according the following: 0 = IgG negative/Nab negative (colored line/lines: C and T2), 1 = IgG positive/Nab negative (colored line/lines: C, T1 and T2), 2 = IgG positive/Nab positive (colored line/lines: C, T1 and faint T2), 3 = IgG positive/Nab strongly positive (colored line/lines: C and T1). Autonomously and independently three different operators observed the cassettes and assigned a score. The scores given by at least two out of three operators were assigned to the samples with discordant attribution.

Enzyme-Linked Immunosorbent Assay

Peptide-based ELISA was performed on four synthetic peptides derived from the Spike protein of SARS-CoV-2 Hu-1 strain (GeneBank: MN908947) as published elsewhere (28–30). Peptide sequences are reported in **Supplementary Table 5**. Pep2_Spike, Pep5_Spike, Pep6_Spike, and Pep10_Spike were used as adsorbed phases on 96-well high-binding plates (NUNC Maxisorp, Thermo Fisher, Waltham, MA, USA). After being blocked with 5% bovine serum albumin (BSA) (Sigma, St. Louis, MO, USA) dissolved in TBS containing 0.05% Tween-20 (TBST) for 1 h, sera samples were diluted in blocking buffer and incubated for 1 h at room temperature with continuous agitation. Wells were washed three times with 300 µl/well of phosphate-buffered saline (PBS) containing 0.05% Tween-20 (PBST) and incubated with 90 µl of HRP-conjugated goat anti-human IgG diluted 1:50,000 in 2.5% BSA-TBST for 1 h at room temperature. Subsequently, an unbound antibody was removed by washing six times with 300 µl/well of PBST, and 70 µl of freshly prepared TMB substrate (Thermo Fisher) diluted 1:3 in PBS was added to every well and left for 15–30 min to allow the color to develop. The reaction was stopped with an equal volume of 0.3 M of H_2SO_4, and absorbance readings at 450 nm were taken using a microplate reader Seac-Sirio-S. Pre-pandemic human sera were used as negative controls, and the antibody response was measured as a $\log_2$-fold change with respect to negative control absorbances. Positivity was arbitrarily scored for fold changes higher than 1.

Statistical Analysis

All statistics were examined using GraphPad Prism 8.0.1. Parametricity tests were performed on antibody titers and age

to verify normal and/or lognormal distribution. Correlation analysis was carried out for non-parametric data distributions using Spearman's coefficient. One-way ANOVA was performed by the Kruskal–Wallis method for non-parametric data, followed by Dunn's multiple comparison test. Mean neutralizing activities were compared by using ordinary one-way ANOVA followed by Tukey's test or with an unpaired t-test. Test performances of FAST-COVID SARS-CoV-2 IgG/Neutralizing Antibody Rapid Test Kit—Colloidal Gold were evaluated with respect to the ELISA-based cPass™ SARS-CoV-2 Neutralization Antibody Detection Kit (GenScript Biotech Corporation, Piscataway, NJ, USA) by sensitivity and specificity parameters with the associated SE and 95% CI through MedCalc software (available from: https://www.medcalc.org/calc/diagnostic_test.php). Median antibody titers that resulted in positive or negative to IgG/Neutralizing Antibody Rapid Test were compared by using the Mann–Whitney method. p-values < 0.05 were considered statistically significant.

RESULTS

After written informed consent was obtained, about 200–300 µl of capillary blood was collected from 369 enrolled individuals, 209 female (57%) and 161 male (43%), aged from 19 to 94 years (mean age ± SD, 55.90 ± 18.34). The participants in the study underwent vaccination in the previous 9 months, and 87.3% of them (322 out of 369) completed their vaccination cycle between March and July 2021, with 140 individuals fully vaccinated in May 2021 (**Supplementary Tables 1, 2**). As reported in **Table 1**, out of 369 participants, 205 received 2 doses of BNT162b2 (Pfizer/BioNTech), 86 received 2 doses of ChAdOx1-nCov19 (Oxford-AstraZeneca), 28 received a single dose of Ad26.COV2.S (Johnson & Johnson), 14 received 2 doses of mRNA-1273 (Moderna), 19 received vaccination and were COVID-19 convalescent ("COVID19 + vaccine"), 9 did not declare the type of vaccination ("Unknown"), 4 received heterologous vaccination ("Mixed Vaccines"), 2 were only COVID-19 convalescent ("COVID19"), and 2 received a single dose (1 of ChAdOx1-nCov19 and 1 of BNT162b2).

The titer of specific antibodies towards the RBD of SARS-CoV-2 Spike was evaluated in all sera through an *in vitro* diagnostic (IVD)-validated electrochemiluminescence immunoassay (ECLIA). All tested samples resulted positive for anti-RBD (≥0.80 UI/ml), with a median antibody level of 710.0 UI/ml (interquartile range (IQR) 330.0–1695 UI/ml), ranging from a minimum titer of 8.6 UI/ml to a maximum of 73,150 UI/ml (**Table 1**). A parametricity test was used to verify the lognormal distribution of antibody titer values and the normal distribution of age in the study population (**Supplementary Figure 3**). Next, the distribution of antibody titer within individuals who received the same vaccine was evaluated and correlated to age (**Table 1**; **Figure 1**). Median antibody titers varied significantly among different vaccination groups as assessed by the Kruskal–Wallis test ($p < 0.0001$). As expected, the vaccination of COVID-19-convalescent patients notably enhances the amount of serum anti-Spike RBD, whereas, among all, the mRNA-1273 vaccine produces a higher antibody titer when compared to others, although multiple comparisons test reveals statistically significant differences only with respect to Ad26.COV2.S and ChAdOx1-nCov19 (respectively, $p < 0.0001$ and $p = 0.0009$) (**Figure 1A** and **Supplementary Table 3**). Conversely, Ad26.COV2.S vaccinated individuals show the lowest median IQR antibody titer (**Figure 1A** and **Supplementary Table 3**). In addition, we observed a moderate negative association between age and antibody levels on the whole dataset (Spearman's $r = -0.3305$, $p < 0.0001$) (**Figure 1B**), but when the correlation with age was evaluated within each vaccination group, it appeared variable ranging from negligible correlation, but not statistically significant, for ChAdOx1-nCov19-vaccinated individuals (Spearman's $r = -0.1575$, $p = 0.1474$) to a stronger negative correlation for BNT162b2- and Ad26.COV2.S-vaccinated patients (respectively, Spearman's $r = -0.5951$ and $r = -0.6776$, $p < 0.0001$) (**Figure 1C**).

Then, we asked whether an elevated concentration of anti-RBD is synonymous with high neutralizing activity, which

TABLE 1 | Median anti-RBD antibody titers and demographic details of tested population.

Vaccine type	N (%)	Age Mean ± SD (min-max)	Median UI/ml (IQR; min–max)
All	369 (100%)	55.90 ± 18.34 (19–94)	710.0 (330.0–1,695; 8.60–73,150)
BNT162b2	205 (55.60%)	58.21 ± 19.37 (19–94)	790.0 (362.5–1,780; 10.40–7,250)
ChAdOx1-nCov19	86 (23.30%)	60.74 ± 11.21 (27–80)	552.3 (290.0–918.8; 70.0–5,675)
Ad26.COV2.S	28 (7.60%)	38.57 ± 10.84 (21–62)	152.8 (53.75–351.3; 8.60–29,750)
mRNA-1273	14 (3.80%)	49.78 ± 23.17 (19–86)	3,118 (1,718–5,287; 195.0–11,055)
COVID19 + vaccine	19 (5.10%)	48.4 ± 19.27 (24–86)	2,184 (1,360–6,000; 505–73,150)
Mixed vaccines	4 (1.10%)	39.25 ± 16.39 (25–58)	1,653 (1,104–2,659; 990–2,925)
COVID19	2 (0.50%)	40.5 ± 3.53 (38–43)	797.0 (32–1,562; 32–1,562)
Unknown	9 (2.50)	51.37 ± 19.84 (19–73)	1,100 (640.0–3,908; 380–4,780)
BNT162b2 I dose	1 (0.30%)	47 (N/A)	19.80 (N/A)
ChAdOx1-nCov19 I dose	1 (0.30%)	30 (N/A)	55.00 (N/A)

RBD, receptor-binding domain; IQR, interquartile range.

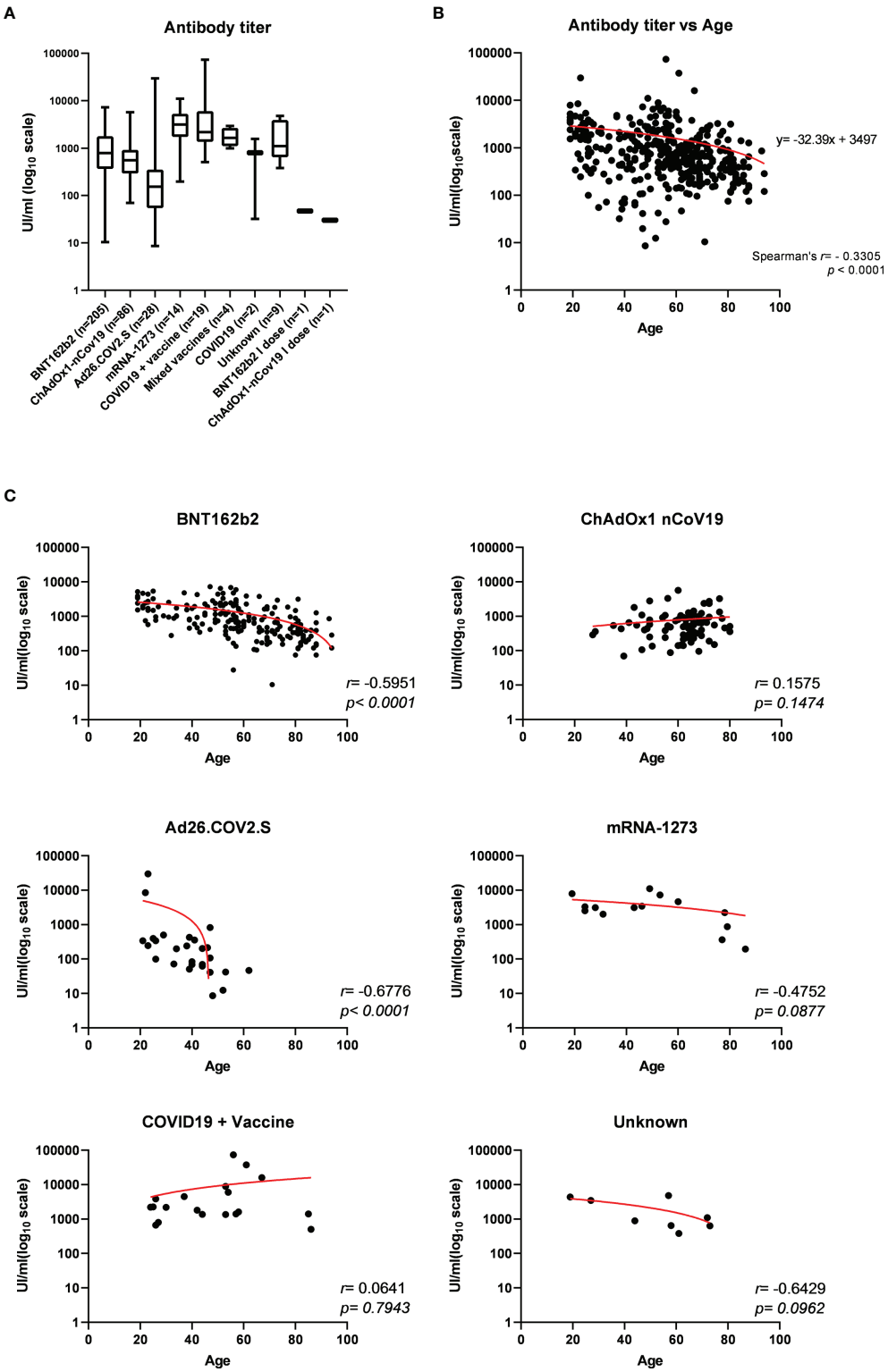

FIGURE 1 | **(A)** Electrochemiluminescence immunoassay (ECLIA)-based determination of the titer of specific antibodies towards the receptor-binding domain (RBD) of SARS-CoV-2 Spike expressed as median UI/ml ± IQR and represented on log10 scale, evaluated in serum from 369 individuals who received different vaccination. Statistically significant variations of medians were assessed by Kruskal–Wallis method for non-parametric data ($p < 0.0001$), followed by Dunn's multiple comparisons test. **(B)** Distribution of serum anti-RBD antibody titers according to age among the study population and **(C)** within each vaccination group. Spearman's correlation *r* and *p*-values have been calculated for each group (statistical significance for $p < 0.05$). Trendline is represented in red.

confers protection against virus infection and replication. To address this point, among the most abundant samples, we randomly and blindly selected 70 sera (22 sera from the BNT162b2 group, 27 from ChAdOx1-nCov19, 9 from Ad26.COV2.S, 9 from mRNA-1273, 1 from a COVID-19-convalescent patient, and 2 sera from mixed vaccines group) and compared total anti-RBD antibody titers to the neutralizing effectiveness. The neutralizing activity was evaluated both quantitatively with the cPass™ ELISA-based assay and qualitatively with an IgG/Neutralizing Antibody Rapid Test (**Table 2**). Interestingly, antibody titer and percentage of inhibition measured by the cPass™ ELISA-based test appear remarkably associated (Spearman's $r = 0.7500$, $p < 0.0001$) (**Figure 2A**), but when the correlation is evaluated between antibody levels and rapid test scores only, the strength of correlation increases ($r = 0.8034$, $p < 0.0001$) (**Figure 2B**). Nevertheless, the degree of correlation between total anti-RBD antibody titer and neutralizing activity appears variable depending on the vaccination group, as for the BNT162b2 group, Spearman's r is 0.7908, $p < 0.0001$; for ChAdOx1-nCov19, $r = 0.6702$, $p < 0.0001$; for Ad26.COV2.S, $r = 0.7667$, $p < 0.05$; and for mRNA-1273, $r = 0.7197$, $p < 0.05$ (**Supplementary Table 4**). As expected, correlation analysis confirmed a very strong association between rapid test scores and the percentage of inhibition assessed by the cPass™ ELISA-based kit ($r = 0.8626$, $p < 0.0001$) (**Figure 2C**; **Supplementary Figure 4**). When comparing neutralizing activity measured by the cPass™ ELISA-based test in patients that received different immunization types, we observed significant differences among mean percentages of inhibition as assessed by ANOVA ($p = 0.0009$) (**Figure 3A**). In particular, it could be noticed that the mRNA-1273 vaccine gives, on average, the strongest effect in inhibiting ACE2-RBD interaction (mean percentage of inhibition ± SD, 88.96% ± 16.35%) with respect to others (**Table 3**), showing nearly double effectiveness of ChAdOx1-nCov19 and Ad26.COV2.S in inducing a neutralizing antibody response (**Figure 3A**). Overall, samples selected from participants that received adenoviral DNA-based vaccines show a lower antibody-mediated inhibiting activity (53.39% ± 28.39%) when compared to individuals who received mRNA-based vaccines (75.59% ± 26.62%; **Figure 3B**).

Since we used an IgG/Neutralizing Antibody Rapid Test validated only on BNT162b2-vaccinated individuals, we have also analyzed its diagnostic performance on sera from differently vaccinated individuals in our study, by comparing the scores of the rapid test to the percentage of inhibition evaluated through the cPass™ ELISA-based test. We assumed that rapid scores ≥2 are indicative of positivity to neutralizing antibodies (AbNeu), whereas the reference neutralizing positivity threshold was set at different levels of inhibition measured by the cPass™ ELISA-based kit (**Supplementary Table 6**). By the comparison of the two neutralizing tests, we observed that the rapid kit is able to identify AbNeu-positive serum samples (i.e., samples in which the cPass™ ELISA-based test has detected a percentage of inhibition ≥30%) with a probability of 66.67% (sensitivity 66.67%, CI95 53.31%–78.31%; specificity 90.00%, CI95 55.50%–78.31%; accuracy 70.00%, CI95 57.87%–80.38%). When 55% inhibition is used as the cutoff value instead of 30%, the rapid test kit appears more accurate in identifying AbNeu-positive samples (sensitivity 90.48%, CI95 77.38%–97.34%; specificity 89.29%, CI95 71.77%–97.73%; accuracy 90.00%, CI95 80.48%–95.88%) and shows a higher agreement with respect to the cPass™ ELISA-based reference test (Cohen's K coefficient = 0.793, CI95 0.648–0.938). Altogether, this evidence demonstrates that the IgG-Neutralizing Antibody rapid test is less sensitive than the cPass™ ELISA-based test but is capable to score as "positive" serum samples with a neutralizing activity ≥55% with a likelihood higher than 90% (**Supplementary Table 6**).

To confirm the positive correlation between total anti-RBD antibody titer and qualitative neutralization test results, we further tested a total of 180 samples on rapid tests and compared data (**Supplementary Figure 5**; **Supplementary Table 7**). Interestingly, rapid scores and antibody titers appear associated in all samples tested ($r = 0.7557$ $p < 0.0001$) (**Table 4**; **Figure 4A**) and within each vaccination group (**Figures 4B–E, G**), indicating that high total anti-RBD antibody titers imply a higher probability of having an effective neutralizing activity. We did not observe a significant correlation between the anti-RBD levels and the rapid test score in COVID-19 patients (**Figure 4F**; **Table 4**), as 15 out of 17 serum samples from this group demonstrated strongly positive (rapid score = 3) on the rapid test, while the measured anti-RBD titers varied by a factor of 10^3 (**Figure 4F**).

In our hands, 68 (37.78%) samples resulted in AbNeu negative and 112 (62.22%) AbNeu positive to rapid test, with median anti-RBD antibody titers (281 and 1,193 UI/ml, respectively) that are significantly different (Mann–Whitney test, $p < 0.0001$) (**Figure 5A**; **Table 5**). Importantly, within each vaccination group, the positive rate for AbNeu varies considerably, ranging from 19.05% for Ad26.COV2.S to 85.71% for mRNA-1273 (**Figures 5B–F**). Likewise, the distribution of antibody levels in AbNeu-negative and AbNeu-positive samples appear disparate when comparing different vaccines, indicating that similar concentrations of antibodies towards Spike-RBD can confer with diverse neutralizing activities, depending on the type of vaccine that induced them (**Figures 5B–G**).

Finally, on the basis of previous data from BNT162b2-vaccinated patients, we asked whether antibody response elicited by specific vaccines is qualitatively individual by using an ELISA developed towards four synthetic peptides derived from the SARS-CoV-2 Spike protein (**Supplementary Table 5**) (28–30). We randomly tested 13 sera from the BNT162b2 group, 22 from the Ad26.COV2.S group, 20 from the ChAdOx1-nCov19 group, 11 from the mRNA-1273 group, 10 from the COVID19+ vaccine group, and 4 from the mixed vaccines group (**Supplementary Figure 6**). Interestingly, qualitative ELISA against synthetic Spike-derived peptides on differently vaccinated individuals shows that mRNA-based vaccines elicit a broader response compared to that elicited by adenoviral DNA-based vaccines. Indeed, reactivity to single peptides was more heterogeneous, particularly for the Ad26.COV2.S and the ChAdOx1-nCov19 groups, confirming that antibody response

TABLE 2 | Comparison of anti-RBD antibody titers and neutralizing activity determined qualitatively as percentage of inhibition by an ELISA and qualitatively by a rapid test (see *Materials and Methods*).

Vaccine type	Sample	% of inhibition	UI/ml	Rapid test score
ChAdOx 1 nCoV 19	FO1809 v031	52.58403	1,042	2
ChAdOx 1 nCoV 19	FO1809 v037	35.88724	510	1
ChAdOx 1 nCoV 19	FO1809 v039	23.16588	355	0
ChAdOx 1 nCoV 19	FO1809 v041	51.42754	549.5	1
ChAdOx 1 nCoV 19	FO1809 v042	54.5356	575	2
ChAdOx 1 nCoV 19	FO1809 n001	84.38742	1,090	2
ChAdOx 1 nCoV 19	FO1809 n010	57.06541	780	2
ChAdOx 1 nCoV 19	FO1809 n019	89.88074	800	3
ChAdOx 1 nCoV 19	FO1809 n027	34.22479	525	1
ChAdOx 1 nCoV 19	FO1809 v047	43.54897	290	1
ChAdOx 1 nCoV 19	FO1809 n053	40.73003	290	1
ChAdOx 1 nCoV 19	FO1809 n068	89.01337	230	2
ChAdOx 1 nCoV 19	FO1809 n072	92.26599	2,695	1
ChAdOx 1 nCoV 19	FO1809 n080	52.87315	290	1
ChAdOx 1 nCoV 19	FO1809 no87	28.00867	250	2
ChAdOx 1 nCoV 19	FO2509 v011	78.82183	1,270	1
ChAdOx 1 nCoV 19	FO2509 v048	94.43441	655	3
ChAdOx 1 nCoV 19	FO2509 v072	54.5356	272	1
ChAdOx 1 nCoV 19	FO2509 v076	20.92519	190	0
ChAdOx 1 nCoV 19	FO2509 v097	37.33285	310	1
ChAdOx 1 nCoV 19	FO2509 n003	85.11023	2,780	2
ChAdOx 1 nCoV 19	FO2509 n013	53.37911	399	1
ChAdOx 1 nCoV 19	FO2509 n040	9.577159	70	0
ChAdOx 1 nCoV 19	FO2509 n071	62.41417	555	2
ChAdOx 1 nCoV 19	FO2509 n086	80.84568	915	2
ChAdOx 1 nCoV 19	FO2509 n093	73.61764	530	1
ChAdOx 1 nCoV 19	FO2509 n131	67.40152	730	2
Ad26.COV2.S	FO1809 n002	−7.91471	12.4	0
Ad26.COV2.S	FO1809 n003	−11.8179	8.6	0
Ad26.COV2.S	FO1809 n013	76.87026	395	2
Ad26.COV2.S	FO1809 n014	27.14131	245	1
Ad26.COV2.S	FO1809 n043	18.10625	500	1
Ad26.COV2.S	FO1809 n081	88.65197	824	3
Ad26.COV2.S	FO2509 n008	42.10336	355	0
Ad26.COV2.S	FO2509 v009	60.75172	240	1
Ad26.COV2.S	FO2509 n012	79.97832	29,750	3
mRNA-1273	FO1809 v025	96.09686	11,055	3
mRNA-1274	FO1809 v038	96.09686	4,636	3
mRNA-1275	FO1809 n040	96.53054	7,240	3
mRNA-1276	FO1809 n056	45.78966	365	1
mRNA-1277	FO1809 n082	95.88001	73,150	3
mRNA-1278	FO1809 n085	92.41055	1,410	3
mRNA-1279	FO1809 n092	92.62739	870	2
mRNA-1280	FO2509 v018	89.73618	3,130	3
mRNA-1281	FO2509 v025	95.44633	1,360	3
Covid19	FO2509 n024	96.96422	1,562	3
Mixed vaccines	FO2509 n005	91.90459	1,860	2
Mixed vaccines	FO2509 v036	95.08493	2,925	3
BNT162b2	FO2509 v064	20.18272	19.8	0
BNT162b2	FO2509 n024	44.18605	115	0
BNT162b2	FO2509 n025	50.44311	75	0
BNT162b2	FO2509 n026	96.80964	1,690	3
BNT162b2	FO1809 v001	1.949663	10.4	0

(Continued)

TABLE 2 | Continued

Vaccine type	Sample	% of inhibition	UI/ml	Rapid test score
BNT162b2	FO1809 n005	49.02517	105	0
BNT162b2	FO1809 n006	96.80964	1,315	3
BNT162b2	FO1809 n060	92.98121	202	2
BNT162b2	FO2509 v040	55.68947	1,080	2
BNT162b2	FO1809 n064	93.12301	120	2
BNT162b2	FO1809 n061	57.60369	575	2
BNT162b2	FO1809 n062	61.7866	665	2
BNT162b2	FO1809 n063	42.36086	185	1
BNT162b2	FO2509 v049	93.12301	4,650	3
BNT162b2	FO2509 v050	97.23502	1,485	3
BNT162b2	FO2509 v039	97.23502	2,380	3
BNT162b2	FO2509 v030	96.80964	440	2
BNT162b2	FO2509 n076	97.23502	2,055	3
BNT162b2	FO2509 n077	74.68983	1,885	2
BNT162b2	FO2509 n075	72.9883	975	2
BNT162b2	FO2509 n074	97.51861	4,355	3
BNT162b2	FO2509 n078	52.92449	740	1

RBD, receptor-binding domain.

has qualitatively individual features even within the same vaccination group (**Supplementary Figure 6**).

DISCUSSION

In the last 2 years, the COVID-19 pandemic has forced many countries to impose lockdowns and restrictions on their residents to control the spread of the disease. The introduction of COVID-19 vaccines has allowed countries to relax some restrictions and reopen economic and social activities. To support the resumption of socioeconomic life, in July 2021, the European Commission introduced a vaccine passport to facilitate safe free movement within the EU for those who are vaccinated, recovered, or negatively tested (6). However, an essential element in making the rationale behind the green pass at least tenable is that certificate holders should be to some extent protected by the vaccine. In this work, we monitored the humoral response triggered by the inoculation of the four different anti-SARS-CoV-2 vaccines approved in Europe and used in Italy since the end of 2020, namely, mRNA-1273, BNT162b2, Ad26.COV2.S, and ChAdOx1 nCoV-19. Although others have reported a direct comparison of antibody response to different vaccines (5, 23, 24, 31, 32), this is one of the first reports where the effectiveness of the abovementioned vaccines is directly compared in terms of antibody titer and neutralizing activity. Indeed, while this manuscript was in peer-reviewing, Szczepanek et al. (33) have described substantial differences in the anti-Spike IgG levels from a cohort of 511 individuals vaccinated with mRNA-1273, BNT162b2, Ad26.COV2.S, and ChAdOx1 nCoV-19. Our study shows that all four approved vaccines in the European community are effective in stimulating a humoral response against SARS-CoV-2 Spike, and, as already reported (34), the magnitude of the total anti-RBD antibody decreases with age. Nevertheless, we observed different levels of correlation within each vaccination group and with equally variable statistical significance, presumably due to the fact that the groups are not homogeneous with each other in terms of number and age. Indeed, whereas mRNA-based vaccines were administered to patients aged 18 and over, only individuals under 60 had access to adenoviral-based DNA vaccines and only for a few months in 2021. Moreover, according to Szczepanek et al. (33), our data confirmed that natural COVID-19 infection combined with vaccination results, on average, in higher antibody titer and higher neutralizing activity with respect to fully vaccinated individuals without prior COVID-19, as reported elsewhere (35). Next, we investigated the correlation between total anti-RBD antibody and neutralizing capacity, finding that the concentration of serum antibodies against Spike is partially correlated with ACE2-RBD binding inhibition, as sera with lower antibody titer could show similar neutralizing activity to that observed in sera with higher antibody titer, consistently with previous reports (36). In this attempt, we also considered the usefulness of a rapid cassette test as a highly portable and inexpensive tool for measuring neutralizing antibodies from a capillary blood drop. In comparison with the cPass^{TM} ELISA-based SARS-CoV-2 Neutralization Antibody Detection Kit, we found that the IgG/Neutralizing Antibody Rapid Test is able to identify with an accuracy of 90% and with a sensitivity slightly greater than 90%, vaccine-induced serum antibodies whose neutralizing activity is greater than or equal to 55%. By comparing the antibody titer to the rapid test scores in different vaccination groups, we observed that among patients with a total anti-RBD antibody titer lower than 1,000 UI/ml, the probability of having a neutralizing capacity greater than 55% appears different if the individual has received the BNT162b2 vaccine or the Ad26.COV2.S vaccine. Indeed, whereas a high anti-RBD antibody titer

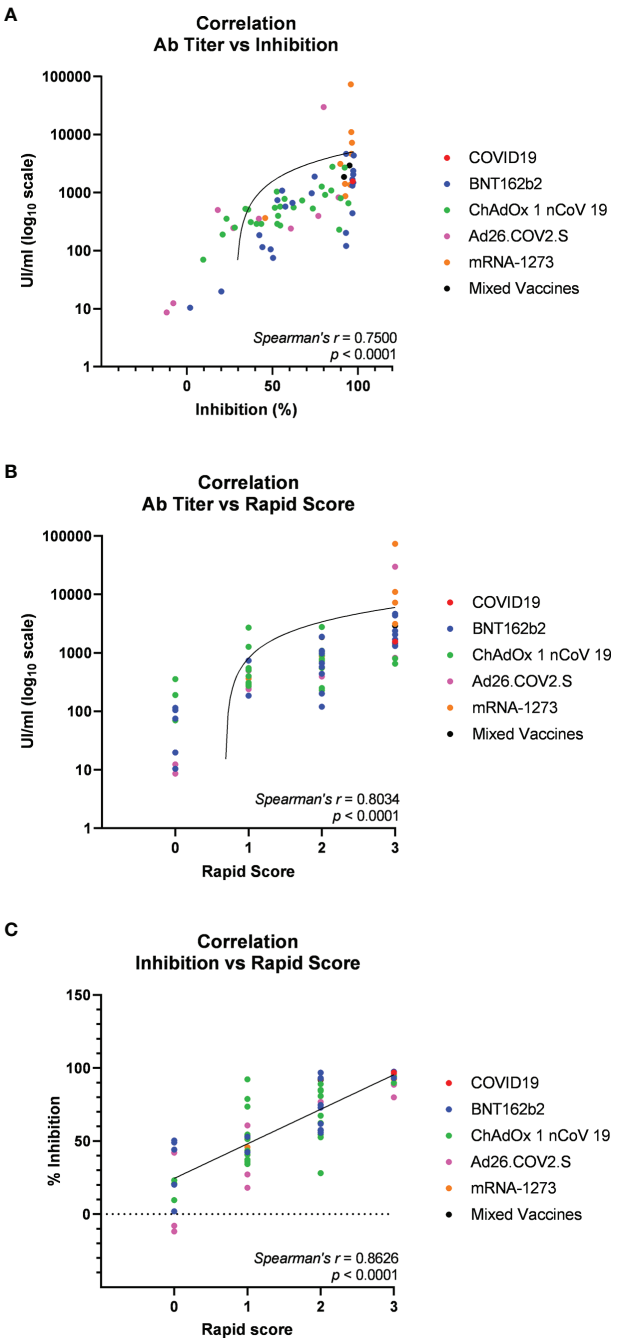

FIGURE 2 | Spearman's correlation analysis of serum anti-receptor-binding domain (anti-RBD) antibody titers and neutralizing activity in 70 participants in the study (22 vaccinated with BNT162b2, 9 with mRNA-1273, 27 with ChAdOx1 nCov19, 9 with Ad26.COV2.S, 1 COVID-19 convalescent, and 2 with mixed vaccines). **(A)** Correlation plot of anti-RBD antibody titers versus neutralizing activity (percentage inhibition of RBD-ACE2 binding) assessed through the cPass™ ELISA-based assay. **(B)** Correlation plot of anti-RBD antibody titers versus neutralizing activity assessed through IgG/Neutralizing Antibody Rapid Test. **(C)** Correlation plot of neutralizing activity evaluated through cPass™ ELISA-based assay and IgG/Neutralizing Antibody Rapid Test cassettes. Trendlines, Spearman's *r*, and *p*-values are also represented (statistical significance for $p < 0.05$).

implies a higher probability of having an effective neutralizing activity, we could see a remarkable association between the type of vaccine and the related serum neutralizing antibodies, with mRNA-based vaccines being overall more capable of producing antibody-mediated inhibiting activity respect to adenoviral DNA-based vaccines, as also reported by Szczepanek et al. (33). Together with the ELISA-based qualitative assessment of peptide reactogenicity in sera from study participants, our data show that the polyclonal response to vaccination confers different levels of protection and that the neutralizing activity cannot be recapitulated by the measurement of serum antibodies against Spike-RBD alone, in contrast with previous findings (37). Moreover, the assays for the analysis and description of immune protection against SARS-CoV-2 require adaptability and flexibility, so that the ability of vaccine-produced antibodies to recognize and neutralize new virus variants can be easily determined. In fact, all tested vaccines are based on the expression of the ancestral Spike protein and can, by consequence, stimulate the production of specific antibodies against primitive Spike. On the one hand, most of the assays that are routinely used to measure anti-Spike IgG (either neutralizing or not) have been developed by using ancestral RBD. On the other hand, new circulating variants are characterized by increased infectivity and have been shown to escape vaccine-induced neutralizing antibodies due to several mutations in the BD of the Spike protein (38). In the peptide-based ELISA described in our study (**Supplementary Figure 6**), we used four synthetic Spike-derived peptides whose sequences (**Supplementary Table 5**) have been generated from deposited Hu1 original strain: for this reason, such peptides are helpful tools to assess the reactogenicity of vaccine-induced antibodies. Nevertheless, it is worth noting that, among all, Pep6_Spike and Pep10_Spike display residues affected by mutations: D614 in Pep6_Spike is a G in both Delta and Omicron variants, and T547 in Pep10_Spike is a K in Omicron variant. Therefore, we cannot exclude that they may fail to detect any antibodies raised after natural infection with recent variants in further applications. However, the use of a degenerated Spike-derived peptide library could represent a valid and novel approach to assess antibody reactogenicity and effectiveness of administered vaccines and, also, to identify binding epitope determinants that drive immunogenicity.

The main limitations of our work are that the study population 1) is not uniform with respect to the number of individuals who received the different vaccines and 2) is not synchronized with respect to the vaccination period; therefore, fluctuations due to the decay of the anti-RBD antibody titer over time are underrated (32, 39, 40). It should also be noted that we classified patients based on self-reported data, and, as consequence, we did not verify whether there have been asymptomatic or undiagnosed SARS-CoV-2 previous infections or whether, along with the vaccine, patients have taken drugs or suffered comorbidities that interfere with the antibody response, biasing antibody titer data (41). In addition, our data derived from analyses on capillary blood samples, which are small but can be considered reliable for serological evaluation (42), do not allow specific tests for cell-mediated immunity. Indeed, in order

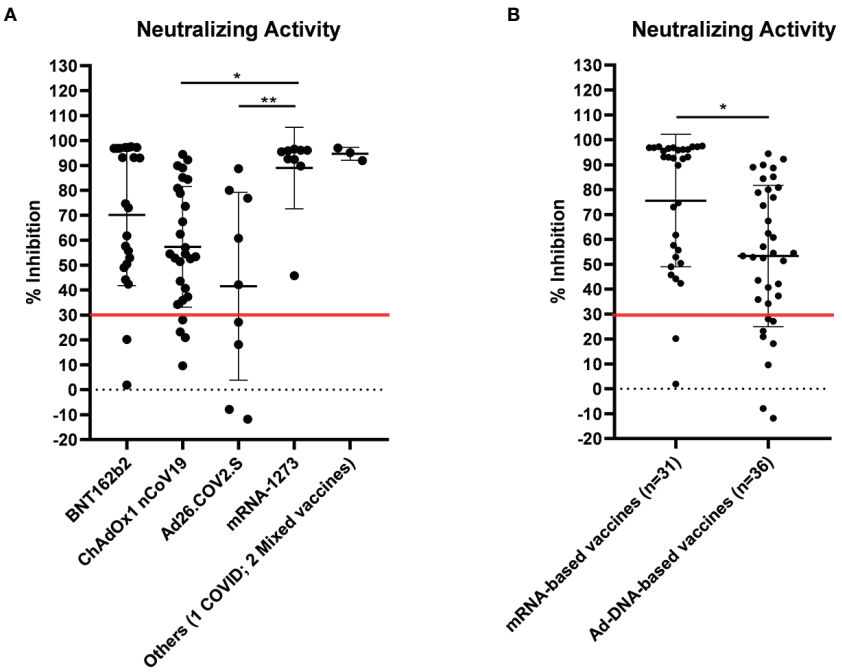

FIGURE 3 | Neutralizing activity evaluated by cPass™ ELISA-based SARS-CoV-2 Neutralization Antibody Detection Kit in 70 sera from differently vaccinated individuals. Serum samples were considered positive when ≥30% inhibition was measured, as shown by the red line in the graph. **(A)** Percentage inhibition of receptor-binding domain–angiotensin-converting enzyme 2 (RBD-ACE2) binding within different vaccination groups (see also **Table 3**). Statistical significance was assessed by ANOVA following Tukey's multiple comparisons test, $^{**}p < 0.005$, $^{*}p < 0.05$. **(B)** Comparison of neutralizing activity in sera from individuals who received adenoviral DNA-based vaccines and mRNA-based vaccines. Statistical significance was assessed by unpaired t-test, $^{*}p = 0.0016$.

TABLE 3 | Mean neutralizing activity measured by the cPass™ ELISA-based assay in sera from 70 individuals who received different vaccines.

Vaccine type	N (%)	Neutralizing activity* (mean ± SD)
All	70 (100%)	64.05% ± 31,12
BNT162b2	22 (31.43%)	70.12% ± 28.33%
ChAdOx1-nCov19	27 (38.57%)	57.33% ± 24.16%
Ad26.COV2.S	9 (12.86%)	41.54% ± 37.69%
mRNA-1273	9 (12.86%)	88.96% ± 16.35%**
Others§	3 (4.28%)	94.65% ± 2.56%

Significant differences among means were assessed by ordinary one-way ANOVA (p-value = 0.0009) followed by Tukey's multiple comparisons test.
***Tukey's comparison vs. ChAdOx1-nCov19 p < 0.05 and vs. Ad26.COV2.S p < 0.005.*
§*This group is formed by samples from 2 individuals receiving mixed vaccines and 1 COVID-19-convalescent patient.*

TABLE 4 | Spearman's correlation between rapid test score and anti-RBD antibody titers in individuals who received different vaccines.

Vaccine type	N (%)	Spearman's correlation between rapid test score and anti-RBD antibody titer	
		r	*p*-Value*
All	180 (100%)	0.7557	<0.0001
BNT162b2	62 (34.44%)	0.7793	<0.0001
ChAdOx1-nCov19	56 (31.11%)	0.6445	<0.0001
Ad26.COV2.S	21 (11.67%)	0.7541	<0.0001
mRNA-1273	14 (7.78%)	0.6892	0.0084
COVID19 + Vaccine	17 (9.44%)	0.2407	0.3824
Others§	10 (5.56%)	0.8136	0.0075

Significant p-value <0.05.
§*This group is formed by samples from 2 single-dose vaccinated individuals, 2 COVID-19-convalescent patients, 4 individuals receiving mixed vaccines, and 2 individuals declaring nothing.*

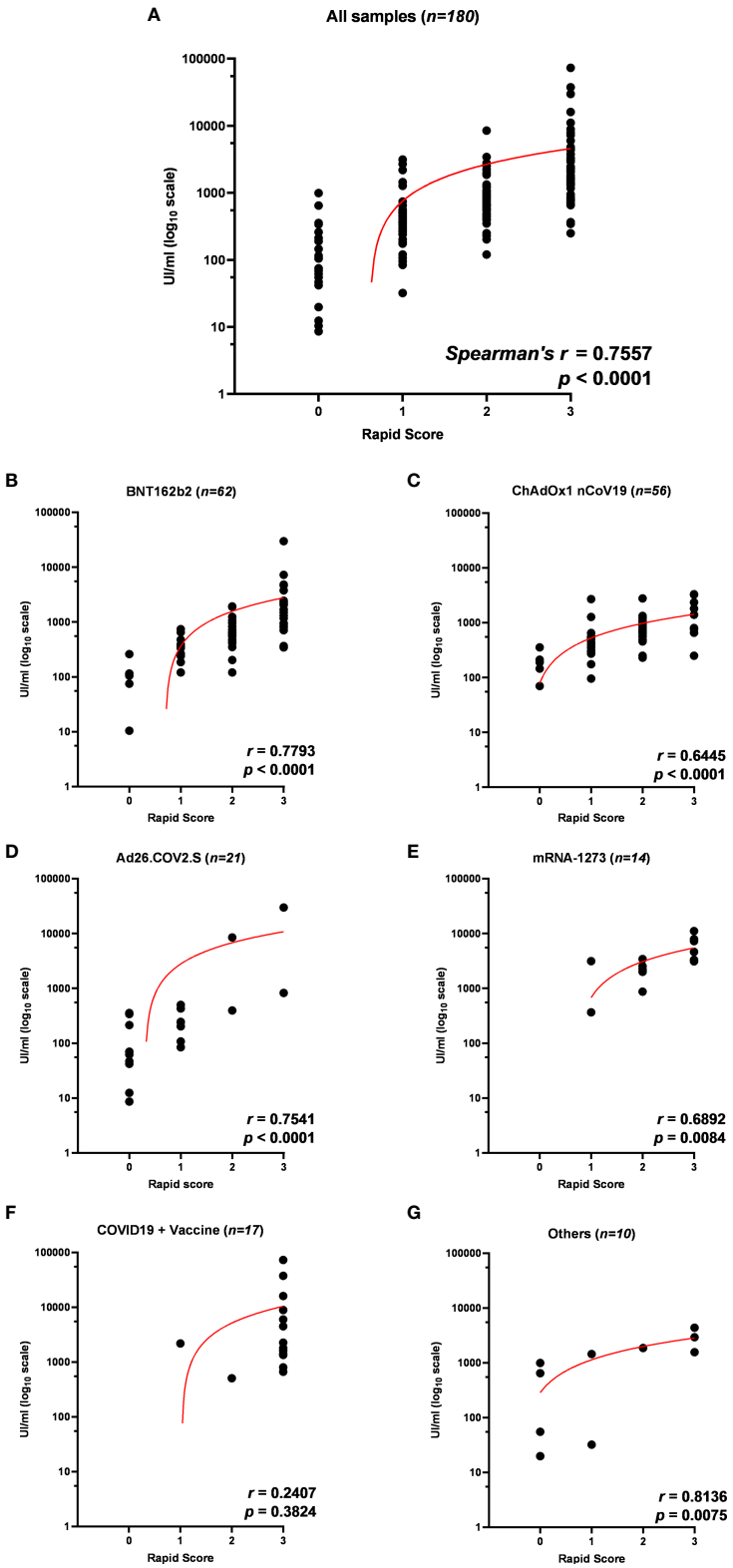

FIGURE 4 | **(A)** Correlation of anti-receptor-binding domain (anti-RBD) antibody titer to rapid test scores for IgG/Neutralizing antibodies in sera from 180 participants in the study and within each vaccination group: **(B)** BNT162b2, **(C)** ChAdOx1 nCov19, **(D)** Ad26.COV2.S, **(E)** mRNA-1273, **(F)** COVID19 + vaccine, and **(G)** others. Trendlines, Spearman's *r*, and *p*-values are also reported (statistical significance for $p < 0.05$).

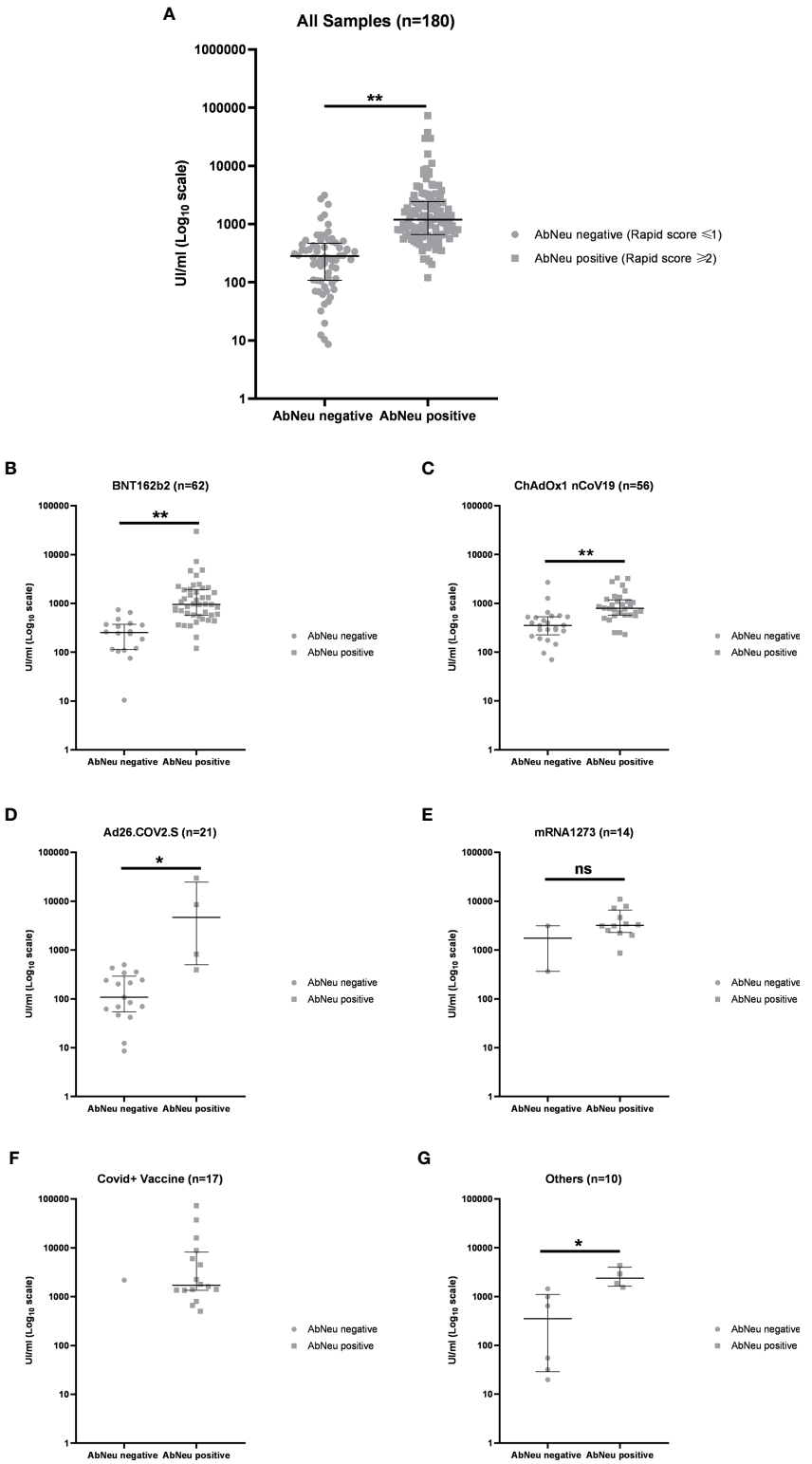

FIGURE 5 | **(A)** Distribution of anti-receptor-binding domain (anti-RBD) antibody titers in AbNeu-positive and AbNeu-negative sera from 180 participants in the study and within each vaccination group: **(B)** BNT162b2, **(C)** ChAdOx1 nCov19, **(D)** Ad26.COV2.S, **(E)** mRNA-1273, **(F)** COVID19 + vaccine, and **(G)** others. Data are represented as scatter plot with median UI/ml ± IQR on log10 scale. Mann–Whitney test was performed to assess statistical significance of differences between medians (see **Table 5**). ***p*-value <0.0001; **p*-value <0.01; ns, not specific.

TABLE 5 | Anti-RBD antibody titer distribution in AbNeu-positive and AbNeu-negative individuals who received different vaccines.

Vaccine type	AbNeu negative (rapid testscore ≤1) N; %	Median UI/ml (IQR)	AbNeu positive (rapid testscore ≥2) N; %	MedianUI/ml(IQR)	*p*-Value (Mann–Whitney test)
All	68; 37.78%	281.0 UI/ml (108.1–467.5)	112; 62.22%	1,193 UI/ml (657.5–2,429)	<0.0001
BNT162b2	18; 29.03%	252.5 UI/ml (113.8–375.0)	44; 70.97%	957.5 UI/ml (257.5–1,915)	<0.0001
ChAdOx1-nCov19	24; 42.86%	353.8 UI/ml (227.0–528.8)	32; 57.14%	790 UI/ml (575.0–1,185)	<0.0001
Ad26.COV2.S	17; 80.95%	107.5 UI/ml (54.30–292.5)	4; 19.05%	4,655 UI/ml (502.3–24,434)	0.0013
mRNA-1273	2; 14.29%	1,748 UI/ml (365–3,130)	12; 85.71%	3,218 UI/ml (2,300–6,589)	0.2857
COVID19 + Vaccine	1; 5.88%	2,184 UI/ml	16; 94.12%	1,708 UI/ml (1,353–8,175)	N/A
Others[§]	6; 60.00%	350.0 UI/ml (28.95–1,104)	4; 40.00%	2,393 UI/ml (1,637–3,998)	0.0095

§This group is formed by samples from 2 single-dose vaccinated individuals, 2 COVID-19-convalescent patients, 4 individuals receiving mixed vaccines, and 2 individuals declaring nothing.

to exhaustively compare the immune response induced by the four different types of vaccines authorized in Europe, further studies are required about the involvement of specific lymphocyte populations and the persistence over time of vaccine-induced cellular-mediated protection. Nevertheless, the present study provides important insights into vaccine-induced humoral protection in a real-world setting. Since the current discussion among policymakers is about when to inoculate the booster dose of the vaccine, it must be considered that the anti-Spike RBD IgG levels in the serum alone may be not sufficient to indicate protection against the virus and the disease. On the basis of our results, the use of rapid devices for the diagnosis of the neutralizing fraction, even on a large scale and repeatedly over time, appears more informative and can help to determine even individually the duration of protection offered by vaccine immunity, also against arising variants of concern (11, 43, 44).

DATA AVAILABILITY STATEMENT

The original contributions presented in the study are included in the article/**Supplementary Material**. Further inquiries can be directed to the corresponding authors.

ETHICS STATEMENT

The studies involving human participants were reviewed and approved by the Institutional Review Board of Consorzio Sannio Tech. The patients/participants provided their written informed consent to participate in this study.

AUTHOR CONTRIBUTIONS

IP performed ELISAs. IP and TZ carried out statistical analyses. AP performed antibody titer determination and neutralizing activity assay. LZ, SD'A, and SV collected and acquired demographic data. PV and GC provided resources. RS and JM revised the manuscript. IP, LZ, PV, and TZ conceived the study and wrote the draft of the manuscript. All authors listed have made a substantial, direct, and intellectual contribution to the work and approved it for publication.

FUNDING

This research was partially funded by the grant INBIOMED PON RI 2014-2020—MIUR—CUP F26C18000160005.

ACKNOWLEDGMENTS

We thank Mrs. Natalia Olivieri and Mr. Valerio Mattera for their technical support.

SUPPLEMENTARY MATERIAL

The Supplementary Material for this article can be found online at: https://www.frontiersin.org/articles/10.3389/fimmu.2022.833085/full#supplementary-material

Supplementary Figure 1 | Schematic representation of humoral response analysis on serum samples from participants to the study.

Supplementary Figure 2 | Schematic diagram of IgG/Neutralizing Antibody Rapid Test and result interpretation. (Upper panel) Specimens are added to the sample pad together with a diluent buffer and results are read within 30 minutes. The test is valid only if the control line C is clearly visible. (Lower panel) Samples where scored according the following: 0 = IgG negative/Nab negative (Coloured line/lines: C and T2); 1 = IgG positive/Nab negative (Coloured line/lines: C, T1 and T2); 2 = IgG positive/Nab positive (Coloured line/lines: C, T1 and faint T2); 3 = IgG positive/Nab strongly positive (Coloured line/lines: C and T1).

Supplementary Figure 3 | Parametricity test on anti-RBD antibody titers **(A)** and age **(B)** distribution in the population study. QQ plots indicate a log-normal distribution for antibody titers and a normal distribution for age.

Supplementary Figure 4 | Direct comparison of neutralizing activity measured by ELISA based- cPass™ SARS-CoV-2 Neutralization Antibody Detection Kit

and by IgG/Neutralizing Antibody Rapid Test in 70 sera from differently vaccinated individuals. According to manufacturer's instructions, samples were considered positive for neutralizing antibodies when ≥30% inhibition (see red line) was measured.

Supplementary Figure 5 | Assessment of neutralizing antibodies with rapid test cassettes in 180 participants to the study.

Supplementary Figure 6 | Immunoreactivity of IgG to four peptides (from top to bottom: Pep2-Spike, Pep5-Spike, Pep6-Spike, Pep10-Spike) derived from SARS-CoV-2 Spike in sera from individuals that received different vaccines: BNT162b2, ChAdOx1 nCov19; Ad26.COV2.S; mRNA-1273; COVID19 + vaccine; mixed vaccines. The antibody response is reported as a $\log_2$ fold-change (mean ± SD) compared to negative control sera. A positive response was arbitrarily scored for a $\log_2$ fold-change > 1 (see red line). Experiments were performed in duplicate.

REFERENCES

1. Tregoning JS, Flight KE, Higham SL, Wang Z, Pierce BF. Progress of the COVID-19 Vaccine Effort: Viruses, Vaccines and Variants Versus Efficacy, Effectiveness and Escape. *Nat Rev Immunol* (2021) 21(10):626–36. doi: 10.1038/s41577-021-00592-1
2. European Medicines Agency. *Authorized COVID-19 Vaccines*. Available at: https://www.ema.europa.eu/en/human-regulatory/overview/public-health-threats/coronavirus-disease-covid-19/treatments-vaccines/vaccines-covid-19/covid-19-vaccines-authorised#authorised-covid-19-vaccines-section (Accessed November, 23rd 2021).
3. Food and Drug Administration. *COVID-19 Vaccines Authorized for Emergency Use or FDA-Approved*. Available at: https://www.fda.gov/emergency-preparedness-and-response/coronavirus-disease-2019-covid-19/covid-19-vaccines (Accessed November, 23rd 2021).
4. Dong Y, Dai T, Wang B, Zhang L, Zeng LH, Huang J, et al. The Way of SARS-CoV-2 Vaccine Development: Success and Challenges. *Signal Transduct Target Ther* (2021) 6(1):387. doi: 10.1038/s41392-021-00796-w
5. Yu S, Chen K, Fang L, Mao H, Lou X, Li C, et al. Comparison and Analysis of Neutralizing Antibody Levels in Serum After Inoculating With SARS-CoV-2, MERS-CoV, or SARS-CoV Vaccines in Humans. *Vaccines (Basel)* (2021) 9 (6):588. doi: 10.3390/vaccines9060588
6. European Commission. *EU Digital COVID Certificate*. Available at: https://ec.europa.eu/info/live-work-travel-eu/coronavirus-response/safe-covid-19-vaccines-europeans/eu-digital-covid-certificate_en (Accessed December, 7th 2021).
7. Zheng J, Deng Y, Zhao Z, Mao B, Lu M, Lin Y, et al. Characterization of SARS-CoV-2-Specific Humoral Immunity and Its Potential Applications and Therapeutic Prospects. *Cell Mol Immunol* (2021) 13:1–8. doi: 10.1038/s41423-021-00774-w
8. Van Tilbeurgh M, Lemdani K, Beignon AS, Chapon C, Tchitchek N, Cheraitia L, et al. Predictive Markers of Immunogenicity and Efficacy for Human Vaccines. *Vaccines (Basel)* (2021) 9(6):579. doi: 10.3390/vaccines9060579
9. Premkumar L, Segovia-Chumbez B, Jadi R, Martinez DR, Raut R, Markmann A, et al. The Receptor Binding Domain of the Viral Spike Protein Is an Immunodominant and Highly Specific Target of Antibodies in SARS-CoV-2 Patients. *Sci Immunol* (2020) 5(48):eabc8413. doi: 10.1126/sciimmunol.abc8413
10. Shang J, Wan Y, Luo C, Ye G, Geng Q, Auerbach A, et al. Cell Entry Mechanisms of SARS-CoV-2. *Proc Natl Acad Sci USA* (2020) 117(21):11727–34. doi: 10.1073/pnas.2003138117
11. Khoury DS, Cromer D, Reynaldi A, Schlub TE, Wheatley AK, Juno JA, et al. Neutralizing Antibody Levels are Highly Predictive of Immune Protection From Symptomatic SARS-CoV-2 Infection. *Nat Med* (2021) 27(7):1205–11. doi: 10.1038/s41591-021-01377-8
12. Bewley KR, Coombes NS, Gagnon L, McInroy L, Baker N, Shaik I, et al. Quantification of SARS-CoV-2 Neutralizing Antibody by Wild-Type Plaque Reduction Neutralization, Microneutralization and Pseudotyped Virus Neutralization Assays. *Nat Protoc* (2021) 16(6):3114–40. doi: 10.1038/s41596-021-00536-y
13. Wang JJ, Zhang N, Richardson SA, Wu JV. Rapid Lateral Flow Tests for the Detection of SARS-CoV-2 Neutralizing Antibodies. *Expert Rev Mol Diagn* (2021) 21(4):363–70. doi: 10.1080/14737159.2021.1913123
14. Lake DF, Roeder AJ, Kaleta E, Jasbi P, Pfeffer K, Koelbela C, et al. Development of a Rapid Point-of-Care Test That Measures Neutralizing Antibodies to SARS-CoV-2. *J Clin Virol* (2021) 145:105024. doi: 10.1016/j.jcv.2021.105024
15. Jung BK, Yoon J, Bae JY, Kim J, Park MS, Lee SY, et al. Performance Evaluation of the BZ COVID-19 Neutralizing Antibody Test for the Culture-Free and Rapid Detection of SARS-CoV-2 Neutralizing Antibodies. *Diagnostics (Basel)* (2021) 11(12):2193. doi: 10.3390/diagnostics11122193
16. Payne RP, Longet S, Austin JA, Skelly DT, Dejnirattisai W, Adele S, et al. Immunogenicity of Standard and Extended Dosing Intervals of BNT162b2 mRNA Vaccine. *Cell* (2021) 184(23):5699–714.e11. doi: 10.1016/j.cell.2021.10.011
17. Barrett JR, Belij-Rammerstorfer S, Dold C, Ewer KJ, Folegatti PM, Gilbride C, et al. Phase 1/2 Trial of SARS-CoV-2 Vaccine ChAdOx1 Ncov-19 With a Booster Dose Induces Multifunctional Antibody Responses. *Nat Med* (2021) 27(2):279–88. doi: 10.1038/s41591-020-01179-4
18. Feng S, Phillips DJ, White T, Sayal H, Aley PK, Bibi S, et al. Correlates of Protection Against Symptomatic and Asymptomatic SARS-CoV-2 Infection. *Nat Med* (2021) 27(11):2032–40. doi: 10.1038/s41591-021-01540-1
19. Alter G, Yu J, Liu J, Chandrashekar A, Borducchi EN, Tostanoski LH, et al. Immunogenicity of Ad26.COV2.S Vaccine Against SARS-CoV-2 Variants in Humans. *Nature* (2021) 596(7871):268–72. doi: 10.1038/s41586-021-03681-2
20. Pegu A, O'Connell SE, Schmidt SD, O'Dell S, Talana CA, Lai L, et al. Durability of mRNA-1273 Vaccine-Induced Antibodies Against SARS-CoV-2 Variants. *Science* (2021) 373(6561):1372–7. doi: 10.1126/science.abj4176
21. Gilbert PB, Montefiori DC, McDermott AB, Fong Y, Benkeser D, Deng W, et al. Immune Correlates Analysis of the mRNA-1273 COVID-19 Vaccine Efficacy Clinical Trial. *Science* (2021) 375(6576):43–50. doi: 10.1126/science.abm3425
22. Ho TC, Chen YA, Chan HP, Chang CC, Chuang KP, Lee CH, et al. The Effects of Heterologous Immunization With Prime-Boost COVID-19 Vaccination Against SARS-CoV-2. *Vaccines (Basel)* (2021) 9(10):1163. doi: 10.3390/vaccines9101163
23. Steensels D, Pierlet N, Penders J, Mesotten D, Heylen L. Comparison of SARS-CoV-2 Antibody Response Following Vaccination With BNT162b2 and mRNA-1273. *JAMA* (2021) 326(15):1533–5. doi: 10.1001/jama.2021.15125
24. Barbeau DJ, Martin JM, Carney E, Dougherty E, Doyle JD, Dermody TS, et al. Comparative Analysis of Human Immune Responses Following SARS-CoV-2 Vaccination With BNT162b2, mRNA-1273, or Ad26.COV2.S. *medRxiv* (2021) 09:21.21262927. doi: 10.1101/2021.09.21.21262927
25. Roche Diagnostics GmbH, 2021; Elecsys®. *Anti-SARS-CoV-2 S Assay Method Sheet; 09289267501 V2.0*. Available at: https://www.fda.gov/media/144037/download (Accessed February, 10th 2022).
26. Jochum S, Kirste I, Hortsch S, Grunert VP, Legault H, Eichenlaub U, et al. Clinical Utility of Elecsys Anti-SARS-CoV-2 S Assay in COVID-19 Vaccination: An Exploratory Analysis of the mRNA-1273 Phase 1 Trial. *Front Immunol* (2022) 12:798117. doi: 10.3389/fimmu.2021.798117
27. Kristiansen PA, Page M, Bernasconi V, Mattiuzzo G, Dull P, Makar K, et al. WHO International Standard for Anti-SARS-CoV-2 Immunoglobulin. *Lancet* (2021) 397(10282):1347–8. doi: 10.1016/S0140-6736(21)00527-4
28. Polvere I, Voccola S, Cardinale G, Fumi M, Aquila F, Parrella A, et al. A Peptide-Based Assay Discriminates Individual Antibody Response to SARS-CoV-2. *Genes Dis* (2021) 9(1):275–81. doi: 10.1016/j.gendis.2021.01.008
29. Polvere I, Parrella A, Casamassa G, D'Andrea S, Tizzano A, Cardinale G, et al. Seroprevalence of Anti-SARS-CoV-2 IgG and IgM Among Adults Over 65 Years Old in the South of Italy. *Diagnostics (Basel)* (2021) 11(3):483. doi: 10.3390/diagnostics11030483
30. Polvere I, Voccola S, Parrella A, Cardinale G, Zerillo L, Varricchio R, et al. A Peptide-Based Assay Discriminates Individual Antibody Response to the COVID-19 Pfizer/BioNTech mRNA Vaccine. *Vaccines (Basel)* (2021) 9 (9):987. doi: 10.3390/vaccines9090987

31. Dashdorj NJ, Wirz OF, Röltgen K, Haraguchi E, Buzzanco AS3rd, Sibai M, et al. Direct Comparison of Antibody Responses to Four SARS-CoV-2 Vaccines in Mongolia. *Cell Host Microbe* (2021) 29(12):1738–43.e4. doi: 10.1016/j.chom.2021.11.004
32. Gray AN, Martin-Blais R, Tobin NH, Wang Y, Brooker SL, Li F, et al. Humoral Responses to SARS-CoV-2 mRNA Vaccines: Role of Past Infection. *PloS One* (2021) 16(11):e0259703. doi: 10.1371/journal.pone.0259703
33. Szczepanek J, Skorupa M, Goroncy A, Jarkiewicz-Tretyn J, Wypych A, Sandomierz D, et al. Anti-SARS-CoV-2 IgG Against the S Protein: A Comparison of BNT162b2, mRNA-1273, ChAdOx1 Ncov-2019 and Ad26.COV2.S Vaccines. *Vaccines (Basel)* (2022) 10(1):99. doi: 10.3390/vaccines10010099
34. Collier DA, Ferreira IATM, Kotagiri P, Datir RP, Lim EY, Touizer E, et al. Age-Related Immune Response Heterogeneity to SARS-CoV-2 Vaccine BNT162b2. *Nature* (2021) 596(7872):417–22. doi: 10.1038/s41586-021-03739-1
35. Dupont L, Snell LB, Graham C, Seow J, Merrick B, Lechmere T, et al. Neutralizing Antibody Activity in Convalescent Sera From Infection in Humans With SARS-CoV-2 and Variants of Concern. *Nat Microbiol* (2021) 6(11):1433–42. doi: 10.1038/s41564-021-00974-0
36. Criscuolo E, Diotti RA, Strollo M, Rolla S, Ambrosi A, Locatelli M, et al. Weak Correlation Between Antibody Titers and Neutralizing Activity in Sera From SARS-CoV-2 Infected Subjects. *J Med Virol* (2021) 93(4):2160–7. doi: 10.1002/jmv.26605
37. Dolscheid-Pommerich R, Bartok E, Renn M, Kümmerer BM, Schulte B, Schmithausen RM, et al. Correlation Between a Quantitantiative Anti-SARS-CoV-2 IgG ELISA and Neutralization Activity. *J Med Virol* (2022) 94 (1):388–92. doi: 10.1002/jmv.27287
38. Hu J, Peng P, Cao X, Wu K, Chen J, Wang K, et al. Increased Immune Escape of the New SARS-CoV-2 Variant of Concern Omicron. *Cell Mol Immunol* (2022) 19(2):293–5. doi: 10.1038/s41423-021-00836-z
39. Israel A, Shenhar Y, Green I, Merzon E, Golan-Cohen A, Schäffer AA, et al. Large-Scale Study of Antibody Titer Decay Following BNT162b2 mRNA Vaccine or SARS-CoV-2 Infection. *Vaccines (Basel)* (2021) 10(1):64. doi: 10.3390/vaccines10010064
40. Doria-Rose N, Suthar MS, Makowski M, O'Connell S, McDermott AB, Flach B, et al. Antibody Persistence Through 6 Months After the Second Dose of mRNA-1273 Vaccine for Covid-19. *N Engl J Med* (2021) 384(23):2259–61. doi: 10.1056/NEJMc2103916
41. Powelson I, Kaufmann RA, Chida NM, Shores JT. A New Consideration for Corticosteroid Injections: Severe Acute Respiratory Syndrome Coronavirus 2 (SARS-CoV-2/COVID-19) Vaccination. *J Handb Surg Am* (2022) 47(1):79–83. doi: 10.1016/j.jhsa.2021.07.002
42. Brown L, Byrne RL, Fraser A, Owen SI, Cubas-Atienzar AI, Williams CT, et al. Self-Sampling of Capillary Blood for SARS-CoV-2 Serology. *Sci Rep* (2021) 11 (1):7754. doi: 10.1038/s41598-021-86008-5
43. Garcia-Beltran WF, Lam EC, St Denis K, Nitido AD, Garcia ZH, Hauser BM, et al. Multiple SARS-CoV-2 Variants Escape Neutralization by Vaccine-Induced Humoral Immunity. *Cell* (2021) 184(9):2372–83.e9. doi: 10.1016/j.cell.2021.03.013
44. Hadj Hassine I. Covid-19 Vaccines and Variants of Concern: A Review. *Rev Med Virol* (2021) 9:e2313. doi: 10.1002/rmv.2313

Conflict of Interest: Authors SV, SD'A, and RV are employed by the spin-off Genus Biotech srl. Authors TZ and LZ were employed by the spin-off Genus Biotech srl. Authors AP and GC are employed by the company Tecno Bios srl.

The remaining authors declare that the research was conducted in the absence of any commercial or financial relationships that could be construed as a potential conflict of interest.

Publisher's Note: All claims expressed in this article are solely those of the authors and do not necessarily represent those of their affiliated organizations, or those of the publisher, the editors and the reviewers. Any product that may be evaluated in this article, or claim that may be made by its manufacturer, is not guaranteed or endorsed by the publisher.

Advantages of publishing in Frontiers

OPEN ACCESS
Articles are free to read for greatest visibility and readership

FAST PUBLICATION
Around 90 days from submission to decision

HIGH QUALITY PEER-REVIEW
Rigorous, collaborative, and constructive peer-review

TRANSPARENT PEER-REVIEW
Editors and reviewers acknowledged by name on published articles

Frontiers
Avenue du Tribunal-Fédéral 34
1005 Lausanne | Switzerland

Visit us: www.frontiersin.org
Contact us: frontiersin.org/about/contact

REPRODUCIBILITY OF RESEARCH
Support open data and methods to enhance research reproducibility

DIGITAL PUBLISHING
Articles designed for optimal readership across devices

FOLLOW US
@frontiersin

IMPACT METRICS
Advanced article metrics track visibility across digital media

EXTENSIVE PROMOTION
Marketing and promotion of impactful research

LOOP RESEARCH NETWORK
Our network increases your article's readership